ACR Announcements

AMERICAN COLLEGE OF RHEUMATOLOGY
2200 Lake Boulevard NE, Atlanta, Georgia 30319-5312
www.rheumatology.org

Kenneth G. Saag, MD, MSc, ACR President

Eighty-Fifth President of the ACR

At the annual business meeting of the American College of Rheumatology on November 9, 2021, Kenneth G. Saag, MD, MSc was installed as the eighty-fifth President of the College.

Dr. Saag is Professor of Medicine and holds the Jane Knight Lowe Endowed Chair in the Department of Medicine at the University of Alabama at Birmingham. At UAB he is also Director of the Division of Clinical Immunology and Rheumatology, Director of the Comprehensive Arthritis, Musculoskeletal, Bone, and Autoimmunity Center, and Director of the Center of Research Translation in Gout and Hyperuricemia.

Proud to have grown up in the diverse city of Evanston, Illinois, where he became an Eagle Scout and graduated third in his high school class of over 1,000 students, Dr. Saag was trained as a bioengineer at the University of Michigan, and received his MD from Northwestern University. As a medical resident at Evanston Hospital, he was recognized as Outstanding Intern of the Year and as a Chief Resident. While at the University of Iowa completing his fellowship in rheumatology, he simultaneously earned an MSc in epidemiology. At Iowa, he began his interest in and pursuit of clinical epidemiology and experimental therapeutics. Dr. Saag continued at the University of Iowa as an Assistant Professor until joining the University of Alabama at Birmingham, where he has been a practicing physician, educator, and research scientist since 1998.

Dr. Saag's research has advanced the field of implementation science and disparities research in the areas of osteoporosis and gout. His recent work has focused on methods to implement evidence into practice using novel study designs. Using cohorts and other large databases, he has contributed to an understanding of comparative effectiveness and safety of drugs in rheumatoid arthritis, osteoporosis, and gout. He has authored more than 400 peer-reviewed manuscripts, including 3 original first-author articles in the *New England Journal of Medicine* on treatment of glucocorticoid-induced osteoporosis and on fracture prevention in women with osteoporosis. He has also authored more than 100 reviews, editorials, and book chapters, as well as the first and second editions of the clinical handbook *Diagnosis and Management of Osteoporosis*. He has served on the editorial boards of *Arthritis Care & Research, Annals of Internal Medicine, Archives of Internal Medicine, Bone,* and other biomedical journals. As a research mentor, he has trained more than 20 postdoctoral fellows and junior faculty and has been principal investigator on several large program project grants at UAB. He directs the K and T training components for the UAB Center for Clinical and Translational Science. He served a term as a standing member on the NIH Neurologic Aging and Musculoskeletal Epidemiology (NAMES) study section and chaired the Arthritis Foundation Review Committee, Clinical Outcomes and Therapeutics Study Section in the past.

Dr. Saag has been frequently recognized for his contributions to research and research training. Among the honors he has received are the UAB Max Cooper Research Award in 2005, the UAB Department of Medicine Research Award (first place among professors) in 2012–2014, the 2017 UAB Dean's Excellence Award for Mentorship, and the 2021 European Calcified Tissue Society Excellence in Research Award. He was elected to the Association of American Physicians in 2015. In 2013 the ACR honored him with its Excellence in Investigative Mentoring Award. He has been listed in *Best Doctors* annually since 1996. Through his research pursuits he has been a very frequent lecturer in all continents except Antarctica and has particularly enjoyed his collaborations and visiting professorships in Latin America. Past lectureships and plenary presentations have included visits to EULAR, PANLAR, APLAR, the European Calcified Tissue Society, the International Osteoporosis Foundation, the Australian and New Zealand Bone and Mineral Society, as well as rheumatology and metabolic bone disease societies in 30 countries.

Throughout his career, Dr. Saag has served actively in numerous medical professional and patient advocacy organizations, and has been particularly focused on developing practice guidelines and quality of care indicators. In 1998–2002 he was a member of the Institute of Medicine Committee on Identifying Effective Treatment for Gulf War Veterans' Health Problems. In the early 2000s he served on the American Medical Association Osteoarthritis Performance Measures Physicians Workgroup, the National Center for Quality Assurance Musculoskeletal Workgroup, and the American Pain Society Low Back Pain Guidelines Committee. He was a member of the American Society for Bone and Mineral Research Advocacy Committee in 2010–2013 and Program Co-Chair of the organization's 2017 Meeting Planning Committee. He served on the National Osteoporosis Foundation Board of Trustees in 2008–2013 and was Vice-President of the organization in 2014–2016 and President in 2016–2018, during which time he also served as Co-Chair of the National Bone Health Alliance. He was a member of the American Gout Society Board of Directors in 2005–2020. In addition, he has served on the FDA Arthritis Drugs Advisory Committee and on numerous panels and working groups of the National Institute of Arthritis and Musculoskeletal and Skin Diseases, NIH, including delivering the keynote address on career journey for the NIAMS K-Trainees Forum in 2019.

A member of the American College of Rheumatology since 1992, Dr. Saag's active involvement with the ACR began early in his career. He served on the Atypical Connective Tissue Diseases

Classification Criteria Subcommittee and the Ad Hoc Committee to Revise Guidelines for Glucocorticoid-Induced Osteoporosis in 1998 and on the Professional Meetings Committee in 1998–2001. He was the senior author on 2 prior iterations of the ACR rheumatoid arthritis guidelines and he served as the American delegate to past EULAR rheumatoid arthritis guidelines. He also served as the senior author on the ACR COVID-19 treatment guidance document produced in 2020. He chaired the Summer Rheumatology Meeting Planning Committee in 2001 and was a member of the Educational Products Committee and the Academic Rheumatology Workforce Ad Hoc Committee in 2002. He served as Co-Chair of the ACR Quality Measures Subcommittee in 2007–2009, as Chair of the Committee on Quality of Care in 2009–2013, and as Chair of the Committee on Corporate Relations from 2018 to 2020. During his time on these committees he helped fashion new approaches to guideline development and advised the College on public–private partnerships during the start of the pandemic. Dr. Saag was appointed to the ACR Board of Directors in 2013 and to the ACR Finance Committee in 2016. He served as ACR Secretary in 2018–2020 and as President-Elect in 2020–2021.

Dr. Saag resides in Birmingham with his wife Leah. They have 3 daughters, Jenny (Christopher) Keshishian, Lauren (Yitzi) Peetluk, and Stefanie Saag, who work as a certified nurse anesthetist at UAB, an epidemiologist faculty member at Vanderbilt University, and a social work student in Chicago, respectively. Dr. Saag and his wife enjoy international travel, hiking, eclectic food and wine, and in particular, spending time with their children, granddaughter Clara Keshishian, parents Jim Saag and Marlene Waller, extended family/friends throughout the country, and a large cadre of family dogs.

ACR Board of Directors, 2021–2022

Executive Committee

President: Kenneth G. Saag, MD, MSc, Jane Knight Lowe Professor and Director, Division of Clinical Immunology and Rheumatology and Center of Research Translation in Gout and Hyperuricemia, University of Alabama at Birmingham, Birmingham, Alabama

President-Elect: Douglas White, MD, PhD, Chair, Department of Rheumatology, Gundersen Health System and Head, Rheumatology Research Laboratory, Gundersen Medical Foundation, La Crosse, Wisconsin; and Clinical Adjunct Assistant Professor, University of Wisconsin School of Medicine and Public Health, Madison, Wisconsin

Secretary: Deborah Dyett Desir, MD, Associate Professor of Clinical Medicine, Department of Medicine, Section of Rheumatology, Allergy & Immunology, Yale School of Medicine, New Haven, Connecticut; and Medical Director, YM Rheumatology, Hamden Site, Hamden, Connecticut

Treasurer: Carol Langford, MD, MHS, Professor of Medicine, Harold C. Schott Endowed Chair in Rheumatic and Immunologic Diseases, and Director, Center for Vasculitis Care and Research, Cleveland Clinic, Cleveland, Ohio

Foundation President: V. Michael Holers, MD, Smyth Professor of Rheumatology, Professor of Medicine and Immunology, and Director of Faculty Ventures within CU Innovations, University of Colorado School of Medicine, Aurora, Colorado

ARP President: Barbara A. Slusher, MSW, PA-C, DFAAPA, Advanced Practice Provider Supervisor, Regional–MD Anderson Cancer Center, League City and Galveston, Texas; and Genetics Clinic, Regional–MD Anderson Cancer Center, League City, Texas

Members

Anne Bass, MD, New York, New York
Marcy Bolster, MD, Boston, Massachusetts
Sean Fahey, MD, Mooresville, North Carolina
Norman Gaylis, MD, Aventura, Florida
Jane Kang, MD, New York, New York
Bharat Kumar, MD, Iowa City, Iowa
S. Sam Lim, MD, MPH, Atlanta, Georgia
Amanda Myers, MD, CCD, Evanston, Illinois
Tamar Rubinstein, MD, MS, Bronx, New York
Eric Ruderman, MD, Chicago, Illinois
John Varga, MD, Ann Arbor, Michigan
Swamy Venuturupalli, MD, Los Angeles, California
Angus Worthing, MD, Washington, DC

Arthritis & Rheumatology

An Official Journal of the American College of Rheumatology
www.arthritisrheum.org and wileyonlinelibrary.com

Editor
Daniel H. Solomon, MD, MPH, *Boston*

Deputy Editors
Richard J. Bucala, MD, PhD, *New Haven*
Mariana J. Kaplan, MD, *Bethesda*
Peter A. Nigrovic, MD, *Boston*

Co-Editors
Karen H. Costenbader, MD, MPH, *Boston*
David T. Felson, MD, MPH, *Boston*
Richard F. Loeser Jr., MD, *Chapel Hill*

Social Media Editor
Paul H. Sufka, MD, *St. Paul*

Journal Publications Committee
Amr Sawalha, MD, *Chair, Pittsburgh*
Susan Boackle, MD, *Denver*
Aileen Davis, PhD, *Toronto*
Deborah Feldman, PhD, *Montreal*
Donnamarie Krause, PhD, OTR/L, *Las Vegas*
Wilson Kuswanto, MD, PhD, *Stanford*
Michelle Ormseth, MD, *Nashville*
R. Hal Scofield, MD, *Oklahoma City*

Editorial Staff
Jane S. Diamond, MPH, *Managing Editor, Atlanta*
Lesley W. Allen, *Assistant Managing Editor, Atlanta*
Ilani S. Lorber, MA, *Assistant Managing Editor, Atlanta*
Jessica Hamilton, *Manuscript Editor, Atlanta*
Stefanie L. McKain, *Manuscript Editor, Atlanta*
Sara Omer, *Manuscript Editor, Atlanta*
Emily W. Wehby, MA, *Manuscript Editor, Atlanta*
Christopher Reynolds, MA, *Editorial Coordinator, Atlanta*
Brittany Swett, MPH, *Assistant Editor, Boston*

Associate Editors
Marta Alarcón-Riquelme, MD, PhD, *Granada*
Heather G. Allore, PhD, *New Haven*
Neal Basu, MD, PhD, *Glasgow*
Edward M. Behrens, MD, *Philadelphia*
Bryce Binstadt, MD, PhD, *Minneapolis*
Nunzio Bottini, MD, PhD, *San Diego*
John Carrino, MD, MPH, *New York*
Lisa Christopher-Stine, MD, MPH, *Baltimore*
Andrew Cope, MD, PhD, *London*
Nicola Dalbeth, MD, FRACP, *Auckland*
Brian M. Feldman, MD, FRCPC, MSc, *Toronto*
Richard A. Furie, MD, *Great Neck*
J. Michelle Kahlenberg, MD, PhD, *Ann Arbor*
Benjamin Leder, MD, *Boston*
Yvonne Lee, MD, MMSc, *Chicago*
Katherine Liao, MD, MPH, *Boston*
Bing Lu, MD, DrPH, *Boston*
Anne-Marie Malfait, MD, PhD, *Chicago*
Stephen P. Messier, PhD, *Winston-Salem*
Janet E. Pope, MD, MPH, *FRCPC, London, Ontario*
Christopher T. Ritchlin, MD, MPH, *Rochester*
William Robinson, MD, PhD, *Stanford*
Georg Schett, MD, *Erlangen*
Sakae Tanaka, MD, PhD, *Tokyo*
Maria Trojanowska, PhD, *Boston*
Betty P. Tsao, PhD, *Charleston*
Fredrick M. Wigley, MD, *Baltimore*
Edith M. Williams, PhD, MS, *Charleston*

Advisory Editors
Ayaz Aghayev, MD, *Boston*
Joshua F. Baker, MD, MSCE, *Philadelphia*
Bonnie Bermas, MD, *Dallas*
Jamie Collins, PhD, *Boston*
Kristen Demoruelle, MD, PhD, *Denver*
Christopher Denton, PhD, FRCP, *London*
Anisha Dua, MD, MPH, *Chicago*
John FitzGerald, MD, *Los Angeles*
Lauren Henderson, MD, MMSc, *Boston*
Monique Hinchcliff, MD, MS, *New Haven*
Hui-Chen Hsu, PhD, *Birmingham*
Mohit Kapoor, PhD, *Toronto*
Seoyoung Kim, MD, ScD, MSCE, *Boston*
Vasileios Kyttaris, MD, *Boston*
Carl D. Langefeld, PhD, *Winston-Salem*
Dennis McGonagle, FRCPI, PhD, *Leeds*
Julie Paik, MD, MHS, *Baltimore*
Amr Sawalha, MD, *Pittsburgh*
Julie Zikherman, MD, *San Francisco*

AMERICAN COLLEGE OF RHEUMATOLOGY

Kenneth G. Saag, MD, MSc, *Birmingham*, **President**
Douglas White, MD, PhD, *La Crosse*, **President-Elect**
Carol Langford, MD, MHS, *Cleveland,* **Treasurer**
Deborah Desir, MD, *New Haven*, **Secretary**
Steven Echard, IOM, CAE, *Atlanta*, **Executive Vice-President**

© 2021 American College of Rheumatology. All rights reserved. No part of this publication may be reproduced, stored or transmitted in any form or by any means without the prior permission in writing from the copyright holder. Authorization to copy items for internal and personal use is granted by the copyright holder for libraries and other users registered with their local Reproduction Rights Organization (RRO), e.g. Copyright Clearance Center (CCC), 222 Rosewood Drive, Danvers, MA 01923, USA (www.copyright.com), provided the appropriate fee is paid directly to the RRO. This consent does not extend to other kinds of copying such as copying for general distribution, for advertising or promotional purposes, for creating new collective works or for resale. Special requests should be addressed to: permissions@wiley.com.

Access Policy: Subject to restrictions on certain backfiles, access to the online version of this issue is available to all registered Wiley Online Library users 12 months after publication. Subscribers and eligible users at subscribing institutions have immediate access in accordance with the relevant subscription type. Please go to onlinelibrary.wiley.com for details.

The views and recommendations expressed in articles, letters, and other communications published in Arthritis & Rheumatology are those of the authors and do not necessarily reflect the opinions of the editors, publisher, or American College of Rheumatology. The publisher and the American College of Rheumatology do not investigate the information contained in the classified advertisements in this journal and assume no responsibility concerning them. Further, the publisher and the American College of Rheumatology do not guarantee, warrant, or endorse any product or service advertised in this journal.

Cover design: Todd Machen

This journal is printed on acid-free paper.

Arthritis & Rheumatology

An Official Journal of the American College of Rheumatology
www.arthritisrheum.org and wileyonlinelibrary.com

VOLUME 73 • December 2021 • NO. 12

In This Issue A15
Journal Club A16
Clinical Connections A17
ACR Announcements A29

Special Articles

American College of Rheumatology White Paper on Antimalarial Cardiac Toxicity
Julianna Desmarais, James T. Rosenbaum, Karen H. Costenbader, Ellen M. Ginzler, Nicole Fett, Susan Goodman, James O'Dell, Christian A. Pineau, Gabriela Schmajuk, Victoria P. Werth, Mark S. Link, and Richard Kovacs 2151

Editorial: Where There's Smoke, There's a Joint: Passive Smoking and Rheumatoid Arthritis
Milena A. Gianfrancesco, and Cynthia S. Crowson 2161

Editorial: Targeting the Myddosome in Systemic Autoimmunity: Ready for Prime Time?
Mariana J. Kaplan 2163

Review: A Decade of JAK Inhibitors: What Have We Learned and What May Be the Future?
Christine Liu, Jacqueline Kieltyka, Roy Fleischmann, Massimo Gadina, and John J. O'Shea 2166

COVID-19

Risk of COVID-19 in Rheumatoid Arthritis: A National Veterans Affairs Matched Cohort Study in At-Risk Individuals
Bryant R. England, Punyasha Roul, Yangyuna Yang, Andre C. Kalil, Kaleb Michaud, Geoffrey M. Thiele, Brian C. Sauer, Joshua F. Baker, and Ted R. Mikuls 2179

Clinical Images

Leukocytoclastic Vasculitis After Vaccination With a SARS–CoV-2 Vaccine
Anne Erler, John Fiedler, Anna Koch, Alexander Schütz, and Frank Heldmann 2188

Rheumatoid Arthritis

Incident Rheumatoid Arthritis in HIV Infection: Epidemiology and Treatment
Jennifer S. Hanberg, Evelyn Hsieh, Kathleen M. Akgün, Erica Weinstein, Liana Fraenkel, Amy C. Justice, and the VACS Project Team 2189

Brief Report: Identification of Novel, Immunogenic HLA–DR-Presented *Prevotella copri* Peptides in Patients With Rheumatoid Arthritis
Annalisa Pianta, Geena Chiumento, Kristina Ramsden, Qi Wang, Klemen Strle, Sheila Arvikar, Catherine E. Costello, and Allen C. Steere 2200

The Interleukin-1 Receptor–Associated Kinase 4 Inhibitor PF-06650833 Blocks Inflammation in Preclinical Models of Rheumatic Disease and in Humans Enrolled in a Randomized Clinical Trial
Aaron Winkler, Weiyong Sun, Saurav De, Aiping Jiao, M. Nusrat Sharif, Peter T. Symanowicz, Shruti Athale, Julia H. Shin, Ju Wang, Bruce A. Jacobson, Simeon J. Ramsey, Ken Dower, Tatyana Andreyeva, Heng Liu, Martin Hegen, Bruce L. Homer, Joanne Brodfuehrer, Mera Tilley, Steven A. Gilbert, Spencer I. Danto, Jean J. Beebe, Betsy J. Barnes, Virginia Pascual, Lih-Ling Lin, Iain Kilty, Margaret Fleming, and Vikram R. Rao 2206

Passive Smoking Throughout the Life Course and the Risk of Incident Rheumatoid Arthritis in Adulthood Among Women
Kazuki Yoshida, Jiaqi Wang, Susan Malspeis, Nathalie Marchand, Bing Lu, Lauren C. Prisco, Lily W. Martin, Julia A. Ford, Karen H. Costenbader, Elizabeth W. Karlson, and Jeffrey A. Sparks 2219

Prediction of the Progression of Undifferentiated Arthritis to Rheumatoid Arthritis Using DNA Methylation Profiling
Carlos de la Calle-Fabregat, Ellis Niemantsverdriet, Juan D. Cañete, Tianlu Li, Annette H. M. van der Helm-van Mil, Javier Rodríguez-Ubreva, and Esteban Ballestar 2229

Clinical Images

Cerebral Autosomal-Dominant Arteriopathy With Subcortical Infarcts and Leukoencephalopathy Syndrome, a Central Nervous System Vasculitis Mimic
Mithu Maheswaranathan, Anne F. Buckley, Andrew B. Cutler, Lisa Criscione-Schreiber, and Ankoor Shah 2239

Osteoarthritis

Subchondral Bone Length in Knee Osteoarthritis: A Deep Learning–Derived Imaging Measure and Its Association With Radiographic and Clinical Outcomes
Gary H. Chang, Lisa K. Park, Nina A. Le, Ray S. Jhun, Tejus Surendran, Joseph Lai, Hojoon Seo, Nuwapa Promchotichai, Grace Yoon, Jonathan Scalera, Terence D. Capellini, David T. Felson, and Vijaya B. Kolachalama 2240

Amelioration of Posttraumatic Osteoarthritis in Mice Using Intraarticular Silencing of Periostin via Nanoparticle-Based Small Interfering RNA
Xin Duan, Lei Cai, Christine T. N. Pham, Yousef Abu-Amer, Hua Pan, Robert H. Brophy, Samuel A. Wickline, and Muhammad Farooq Rai 2249

Osteoarthritis Care and Risk of Total Knee Arthroplasty Among Medicare Beneficiaries: A Population-Based Study of Regional Covariation
Michael M. Ward 2261

Psoriatic Arthritis

Targeting the CCR6/CCL20 Axis in Entheseal and Cutaneous Inflammation
Zhenrui Shi, Emma Garcia-Melchor, Xuesong Wu, Anthony E. Getschman, Mimi Nguyen, Douglas J. Rowland, Machelle Wilson, Flavia Sunzini, Moeed Akbar, Mindy Huynh, Timothy Law, Smriti K. Raychaudhuri, Siba P. Raychaudhuri, Brian F. Volkman, Neal L. Millar, and Sam T. Hwang 2271

Systemic Lupus Erythematosus

RNA Externalized by Neutrophil Extracellular Traps Promotes Inflammatory Pathways in Endothelial Cells
Luz P. Blanco, Xinghao Wang, Philip M. Carlucci, Jose Jiram Torres-Ruiz, Jorge Romo-Tena, Hong-Wei Sun, Markus Hafner, and Mariana J. Kaplan 2282
Neuropsychiatric Events in Systemic Lupus Erythematosus: Predictors of Occurrence and Resolution in a Longitudinal Analysis of an International Inception Cohort
John G. Hanly, Caroline Gordon, Sang-Cheol Bae, Juanita Romero-Diaz, Jorge Sanchez-Guerrero, Sasha Bernatsky, Ann E. Clarke, Daniel J. Wallace, David A. Isenberg, Anisur Rahman, Joan T. Merrill, Paul R. Fortin, Dafna D. Gladman, Murray B. Urowitz, Ian N. Bruce, Michelle Petri, Ellen M. Ginzler, M. A. Dooley, Rosalind Ramsey-Goldman, Susan Manzi, Andreas Jonsen, Graciela S. Alarcón, Ronald F. van Vollenhoven, Cynthia Aranow, Meggan Mackay, Guillermo Ruiz-Irastorza, S. Sam Lim, Murat Inanc, Kenneth C. Kalunian, Soren Jacobsen, Christine A. Peschken, Diane L. Kamen, Anca Askanase, and Vernon Farewell 2293
Lupus Susceptibility Region Containing *CDKN1B* rs34330 Mechanistically Influences Expression and Function of Multiple Target Genes, Also Linked to Proliferation and Apoptosis
Bhupinder Singh, Guru P. Maiti, Xujie Zhou, Mehdi Fazel-Najafabadi, Sang-Cheol Bae, Celi Sun, Chikashi Terao, Yukinori Okada, Kek Heng Chua, Yuta Kochi, Joel M. Guthridge, Hong Zhang, Matthew Weirauch, Judith A. James, John B. Harley, Gaurav K. Varshney, Loren L. Looger, and Swapan K. Nath 2303
Inositol-Requiring Enzyme 1α–Mediated Synthesis of Monounsaturated Fatty Acids as a Driver of B Cell Differentiation and Lupus-like Autoimmune Disease
Yana Zhang, Ming Gui, Yajun Wang, Nikita Mani, Shuvam Chaudhuri, Beixue Gao, Huabin Li, Yashpal S. Kanwar, Sarah A. Lewis, Sabrina N. Dumas, James M. Ntambi, Kezhong Zhang, and Deyu Fang 2314

Vasculitis

A Distinct Macrophage Subset Mediating Tissue Destruction and Neovascularization in Giant Cell Arteritis: Implication of the YKL-40/Interleukin-13 Receptor α2 Axis
Yannick van Sleen, William F. Jiemy, Sarah Pringle, Kornelis S. M. van der Geest, Wayel H. Abdulahad, Maria Sandovici, Elisabeth Brouwer, Peter Heeringa, and Annemieke M. H. Boots 2327

Systemic Sclerosis

Anticentromere Antibody Levels and Isotypes and the Development of Systemic Sclerosis
Nina M. van Leeuwen, Maaike Boonstra, Jaap A. Bakker, Annette Grummels, Suzana Jordan, Sophie Liem, Oliver Distler, Anna-Maria Hoffmann-Vold, Karin Melsens, Vanessa Smith, Marie-Elise Truchetet, Hans U. Scherer, René Toes, Tom W. J. Huizinga, and Jeska K. de Vries-Bouwstra 2338

Letters

Addressing Immeasurable Time Bias in an Observational Study: Comment on the Article by Suissa et al
Alanna Weisman, Gillian A. Hawker, and George A. Tomlinson 2348
Reply
Samy Suissa, Karine Suissa, and Marie Hudson 2349
Hypoxia-Induced Synovial Fibroblast Activation in Inflammatory Arthritis and the Role of Notch-1 and Notch-3 Signaling: Comment on the Article by Chen et al
Wang-Dong Xu and An-Fang Huang 2349
Reply
Jianhai Chen, Antonia Sun, Jian Li, Wenxiang Cheng, and Peng Zhang 2350
Disease Activity Assessment in Nonradiographic Axial Spondyloarthritis: Is It Time to Move Beyond the Bath Ankylosing Spondylitis Disease Activity Index or Ankylosing Spondylitis Disease Activity Score? Comment on the Article by Rusman et al
Debashish Mishra, B. V. Harish, Sudhish Gadde, and Pradeepta S. Patro 2351
Reply
Tamara Rusman, Mignon A. C. van der Weijden, Michael T. Nurmohamed, Carmella M. A. van der Bijl, Conny J. van der Laken, Pierre M. Bet, Robert B. M. Landewé, Janneke J. H. de Winter, Bouke J. H. Boden, and Irene E. van der Horst-Bruinsma 2352
Clinical and Methodologic Considerations With Regard to a Trial of Nintedanib in Patients With Systemic Sclerosis–Associated Interstitial Lung Disease: Comment on the Reanalysis by Maher et al
Markus Bredemeier 2353
Reply
Toby M. Maher, Maureen D. Mayes, Christian Stock, and Margarida Alves 2354
Suggested Considerations for the Treatment of Rheumatic Diseases in Adult Patients With COVID-19: Comment on the Article by Mikuls et al
Jeffrey Hsu, Chin-Hsiu Liu, and James C. Wei 2355

Erratum

Incorrect Frequency of Belimumab Infusions Reported in the Article by Atisha-Fregoso et al (Arthritis Rheumatol, January 2021) 2356

Reviewers 2357

Volume 73 Table of Contents 2361

Cover image: The figure on the cover (from Chang et al, pages 2240–2248) shows an example of an original magnetic resonance imaging slice in sagittal view, along with tracings of subchondral bone length on the femur and the tibia. Note the exclusion of the gap in cartilage coverage caused by a protruding central osteophyte. Subchondral bone length is shown as a red line on the femur and a blue line on the tibia.

In this Issue

Highlights from this issue of *A&R* | By Lara C. Pullen, PhD

Periostin-siRNA Ameliorates Posttraumatic OA in Mice

The growing understanding of the cellular and molecular pathways affected in osteoarthritis (OA) has yet to translate into new clinical therapeutic targets. New strategies are emerging, however, to target the joint, such as intraarticular (IA) administration of a small interfering RNA (siRNA) via nanoparticles. This approach has been used to deliver NF-κB siRNA to create an NF-κB knockdown that suppresses injury-induced chondrocyte death as well as early joint responses to injury. This therapeutic effect is linked to the suppression of matrix metalloproteinase 13 (MMP-13), an NF-κB-dependent gene, which is believed to be the major contributor to collagenase activity in OA.

p. 2249

In this issue, Duan et al (p. 2249) describe IA delivery of a periostin–siRNA nanoparticle complex in mice with posttraumatic OA. The investigators initiated their treatment of 10-week-old mice early, prior to injury-induced periostin-mediated cartilage degeneration, and found that the treatment mitigated cartilage degeneration, subchondral bone sclerosis, and heterotopic ossification. While the investigators were unable to identify a clear mechanism behind periostin's effects on the various tissues of the joint, the data suggest that periostin knockdown suppresses the activity of NF-κB.

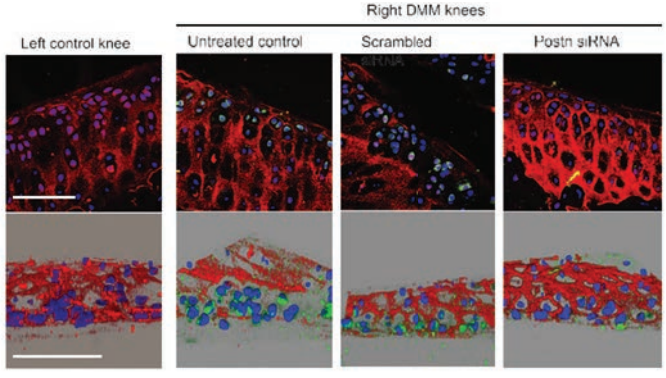

Figure 1. Immunofluorescence images show 2-dimensional views (top) and 3-dimensional views (bottom) of the mouse knee cartilage, indicating localization of p-p65 subunits in the cartilage adjacent to the destabilization of the medial meniscus injury site.

Consistent with this, the researchers found that periostin-induced MMP-13 expression was abrogated by the IκB kinase inhibitor SC-514, results that reinforce the link between periostin and NF-κB signaling. The authors note that future cartilage-specific gene-knockout strategies are needed to continue to illuminate the functional role of periostin in OA. These findings point to a promising clinical approach toward the mitigation of the severity of joint degeneration, and the authors recommend longitudinal studies as follow-up.

New Insights into a Lupus Susceptibility Region

A recent genome-wide association study (GWAS) in Han Chinese found a significant genetic association between rs34330 of CDKN1B and risk of systemic lupus erythematosus (SLE). *CDKN1B* encodes $p27^{Kip1}$, an inhibitor of cyclin/cyclin-dependent kinase (CDK) complexes, which are critical for cell cycle progression and development. Although intriguing, the GWAS data do not explain the mechanism behind how such a complex trait contributes to the pathologic processes of lupus. One hypothesis is that the dysregulated activation and proliferation of T cells and B cells that characterize patients with SLE may be affected by a disruption of the intricate balance of cyclins, CDKs, and CDK inhibitors (e.g., $p27^{Kip1}$).

p. 2303

In this issue, Singh et al (p. 2303) report the results of their efforts to identify target genes and mechanisms underlying the association between rs34330 and SLE. They propose a mechanism whereby the rs34330 risk allele (C) regulates expression of several target genes linked to proliferation and apoptosis and that the association of rs34330 with SLE occurs via its influence on the presence of histone marks, RNA polymerase II (Pol II), and the critical immune transcription factor (interferon regulatory factor 1 [IRF-1]). In particular, the rs34330 risk allele (C) exhibits increased binding with the IRF-1 transcriptional activator.

The investigators began their study by replicating the published genetic association between SLE and rs34330. They then performed a follow-up bioinformatics and expression quantitative trait locus analysis, which suggested that rs34330 is in active chromatin and potentially regulates several target genes. When they performed luciferase and chromatin immunoprecipitation–real-time quantitative polymerase chain reaction, they were able to demonstrate substantial allele-specific promoter and enhancer activity as well as allele-specific binding of 3 histone marks, Pol II, CCCTC-binding factor, and the critical IRF-1. The researchers then performed chromosome conformation capture, which revealed long-range chromatin interactions between rs34330 and the promoters of neighboring genes *APOLD1* and *DDX47*.

Identification of a Distinct Macrophage Subset That Drives Pathology in Giant Cell Arteritis

While rheumatologists know that macrophages are present in giant cell arteritis (GCA) lesions, scientists lack a clear understanding of the relationship between the functional heterogeneity of the macrophages and GCA pathology. One potential clue was the identification of YKL-40 (chitinase 3–like protein 1), an important biomarker of inflammation, on CD68+ macrophages located in the vascular media borders of GCA lesions. This finding suggests that the macrophages may be drivers of pathology. Additional studies have demonstrated that granulocyte–macrophage colony-stimulating factor (GM-CSF)–skewed macrophages derived from healthy donors produce higher levels of YKL-40 than do their macrophage colony-stimulating factor (M-CSF)–skewed counterparts. Despite these intriguing observations, up until now, few mechanistic studies have addressed the role of YKL-40 in autoinflammatory diseases such as GCA.

p. 2327

In this issue, van Sleen et al (p. 2327) report results that further support the hypothesis that YKL-40 is one of the upstream signals for the tissue-destructive protein matrix metalloproteinase 9 (MMP-9) production in macrophages. They found that, in patients with GCA, a GM-CSF–skewed, CD206+MMP-9+ macrophage subset expresses high levels of YKL-40, which appears to stimulate tissue destruction and angiogenesis via interleukin-13 receptor α2 (IL-13Rα2) signaling. The investigators also found that IL-13Rα2, a known receptor for YKL-40, was expressed by endothelial cells at the site of inflammation in GCA.

While previous studies have established that neovascularization fuels the inflammatory process in GCA, these new data suggest that production of YKL-40 by CD206+ is characteristic of GCA and may be an important mediator of not only tissue destruction, but also neovascularization. The authors describe GCA pathology as the result of a distinct macrophage subset that fuels media destruction, vasa vasorum neovascularization, and leukocyte invasion into the vessel wall, and they conclude by suggesting that YKL-40 may be a promising target for treatment of macrophage-driven diseases. They suggest that such an approach may inhibit GCA macrophages that cannot be sufficiently suppressed by glucocorticoids.

Journal Club

A monthly feature designed to facilitate discussion on research methods in rheumatology.

Incident RA in HIV Infection: Epidemiology and Treatment

Hanberg et al, *Arthritis Rheumatol* 2021;73:2189–2199

Patients with long-standing HIV infection exhibit persistent immune dysfunction and inflammation, even in the setting of successful viral suppression with antiretroviral therapy. Furthermore, recent investigations have demonstrated that new-onset autoimmune diseases among this population are more common than previously thought. In this study, the researchers evaluated the relative incidence of new-onset rheumatoid arthritis (RA) in patients with HIV infection versus those without HIV infection, as well as patterns of disease-modifying drug (DMARD) prescribing in these 2 groups. The authors identified cases from the Veterans Aging Cohort Study, a national cohort composed of ~56,000 individuals with HIV receiving care at the Veterans Administration clinic and age-, sex-, site-, and self-reported race–matched controls without HIV. They used International Classification of Diseases, Ninth Revision and Tenth Revision codes to identify patients with possible new RA, followed by chart review, both to confirm the diagnosis (based upon the American College of Rheumatology [ACR]/European Alliance of Associations for Rheumatology [EULAR] 2010 classification criteria) and to extract disease features and treatment details. Notable findings include the following: less robustly positive autoantibody levels among patients with HIV, a significantly lower rate of incident RA among patients with HIV compared to those without HIV, and a lower rate of non-hydroxychloroquine DMARD prescription among RA patients with HIV versus those without HIV.

Questions

1. **What other definitions of RA might have been used to identify cases?**
2. **How might the decision to use the ACR/EULAR 2010 classification criteria have affected the rate of detection of new RA in a retrospective, observational study?**
3. **How do these results speak to the process of evaluating a patient with chronic HIV for inflammatory arthritis? What special considerations might be needed?**
4. **Why might conventional synthetic DMARDs and biologics be prescribed to patients with HIV and RA at a lower rate than those without HIV? What literature exists to inform this decision-making?**

Clinical Connections

Prediction of the Progression of Undifferentiated Arthritis to RA Using DNA Methylation Profiling

De la Calle-Fabregat et al, *Arthritis Rheumatol* 2021;73:2229–2239

CORRESPONDENCE
Esteban Ballestar, PhD: eballestar@carrerasresearch.org

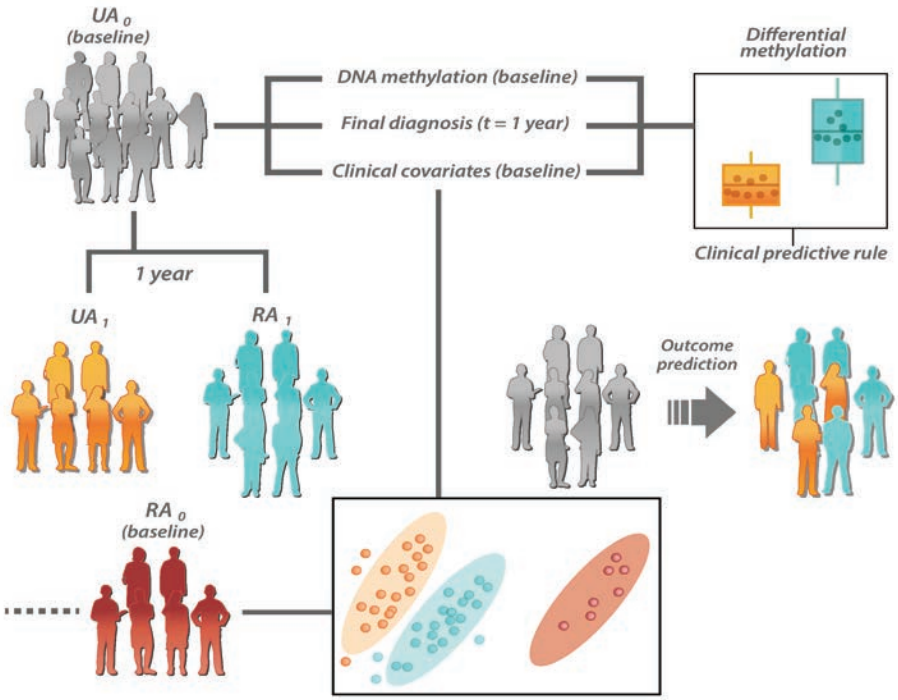

KEY POINTS

- DNA methylation alterations can be used to anticipate the evolution of UA to RA.
- DNA methylation data improve clinical parameter-driven outcome prediction.
- UA patients who eventually develop RA display RA-like DNA methylation signatures.

SUMMARY

Patients with undifferentiated arthritis (UA), who represent ~30% of all early arthritis cases, do not fit any definitive diagnostic criteria. A significant proportion of UA patients will eventually develop rheumatoid arthritis (RA) or another definite rheumatic disease, while others continue experiencing UA or achieve remission. In cases where a definite condition is developed, early treatment with disease-modifying antirheumatic drugs is essential to prevent disease progression and long-lasting sequelae. In a prospective study, de la Calle-Fabregat et al identified DNA methylation alterations in blood cells of UA patients with opposing outcomes (evolution to RA or continued classification of UA) after 1 year of follow-up. This epigenetic signature, which occurred in immune- and inflammation-associated genomic regions, was proposed as a novel prognostic marker. Along with clinical parameters, DNA methylation data appeared to improve the estimation of individual outcomes (RA or UA) in a validation cohort of UA patients. Additionally, the comparison of UA DNA methylation profiles to those of patients with RA revealed a higher similarity of RA patients and those with UA who will develop RA after 1 year. Taken together, these data suggest that DNA methylation is a good predictor of UA-to-RA progression and that it can be leveraged to determine treatment and improve clinical management.

RNA Externalized by Neutrophil Extracellular Traps Promotes Inflammatory Pathways in Endothelial Cells

Blanco et al, *Arthritis Rheumatol* 2021;73:2282–2292

CORRESPONDENCE
Mariana J. Kaplan, MD: mariana.kaplan@nih.gov

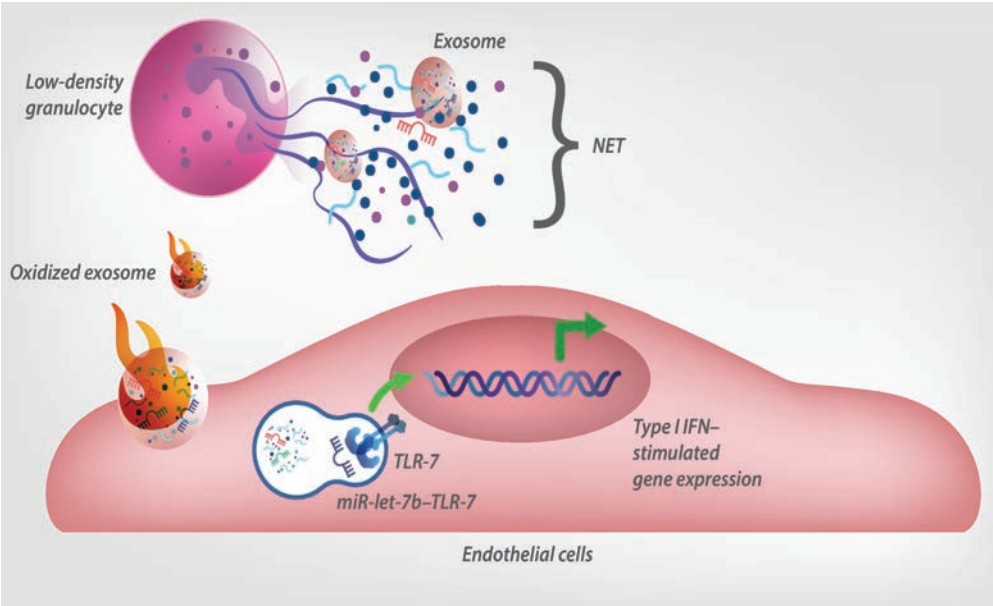

KEY POINTS

- NETs carry diverse types of RNAs that are taken up by endothelial cells. This is enhanced when NETs are generated by SLE LDGs and/or when the RNA is oxidized.
- Small RNAs derived from lupus NETs, particularly the TLR-7 agonist miR-let-7b, induce type I IFN responses in endothelial cells.
- NETs are a source of oxidized RNAs that may contribute to lupus vasculopathy.

SUMMARY

Two key pathogenic features of systemic lupus erythematosus (SLE) are the autoreactivity against nucleic acids (DNA and RNA) and the presence of a type I interferon (IFN) gene signature in blood and many organs. Both features have been associated with perturbed neutrophil extracellular trap (NET) formation and degradation in SLE. NETs are structures released by neutrophils upon exposure to danger signals, including microbes and sterile inflammatory stimuli, and, in certain conditions such as lupus, they can damage various cells including endothelial cells. Blanco et al now report that, in addition to DNA, NETs carry diverse types of RNA. The RNAs present in NETs can be internalized by endothelial cells in a process that is dependent on the degree of RNA oxidation. Internalization of NETs by endothelial cells requires endosomal Toll-like receptors (TLRs) and the actin cytoskeleton. Importantly, NETs generated by lupus low-density granulocytes (LDGs), a distinct subset of proinflammatory neutrophils with vasculopathic features, carry differential cargo of RNAs, and their content is more readily internalized than the content of NETs generated by healthy control neutrophils.

Among the most abundant RNAs present in SLE LDGs, the small microRNA let-7b (miR-let-7b), a TLR-7 agonist, triggers type I IFN stimulated gene expression in endothelial cells. These observations highlight NETs as messengers that deliver RNAs to target cells, inducing proinflammatory responses. The RNA-mediated endothelial cell activation induced by NETs could contribute to the deleterious effects on blood vessels, vasculopathy, and premature atherosclerosis characteristic of lupus, supporting the notion that targeting aberrant NET formation in this disease could have therapeutic benefits.

Arthritis & Rheumatology
Vol. 73, No. 12, December 2021, pp 2151–2160
DOI 10.1002/art.41934
© 2021, American College of Rheumatology

American College of Rheumatology
Empowering Rheumatology Professionals

SPECIAL ARTICLE

American College of Rheumatology White Paper on Antimalarial Cardiac Toxicity

Julianna Desmarais,[1] James T. Rosenbaum,[2] Karen H. Costenbader,[3] Ellen M. Ginzler,[4] Nicole Fett,[1] Susan Goodman,[5] James O'Dell,[6] Christian A. Pineau,[7] Gabriela Schmajuk,[8] Victoria P. Werth,[9] Mark S. Link,[10] and Richard Kovacs[11]

Hydroxychloroquine (HCQ) and chloroquine (CQ) are well-established medications used in treating systemic lupus erythematosus and rheumatoid arthritis, as well as skin conditions such as cutaneous lupus erythematosus. In rare cases, arrhythmias and conduction system abnormalities, as well as cardiomyopathy, have been reported in association with HCQ/CQ use. Recently, however, the corrected QT interval (QTc)–prolonging potential of these medications, and risk of torsade de pointes (TdP) in particular, have been highlighted in the setting of their experimental use for COVID-19 infection. This report was undertaken to summarize the current understanding of HCQ/CQ cardiac toxicity, describe QTc prolongation and TdP risks, and discuss areas of priority for future research. A working group of experts across rheumatology, cardiology, and dermatology performed a nonsystematic literature review and offered a consensus-based expert opinion. Current data clearly indicate that HCQ and CQ are invaluable medications in the management of rheumatic and dermatologic diseases, but they are associated with QTc prolongation by directly affecting cardiac repolarization. Prescribing clinicians should be cognizant of this small effect, especially in patients taking additional medications that prolong the QTc interval. Long-term use of HCQ/CQ may lead to a cardiomyopathy associated with arrhythmias and heart failure. Risk and benefit assessment should be considered prior to initiation of any medication, and both initial and ongoing risk–benefit assessments are important with regard to prescription of HCQ/CQ. While cardiac toxicity related to HCQ/CQ treatment of rheumatic diseases is rarely reported, it can be fatal. Awareness of the potential adverse cardiac effects of HCQ and CQ can increase the safe use of these medications. There is a clear need for additional research to allow better understanding of the cardiovascular risk and safety profile of these therapies used in the management of rheumatic and cutaneous diseases.

Introduction

Both hydroxychloroquine (HCQ) and chloroquine (CQ) are commonly used medications for the treatment of specific rheumatic and dermatologic diseases. HCQ and CQ were initially developed for treating malaria and have been in use since 1955 and 1935, respectively. The most frequent rheumatic diseases for which these medications have long been used include systemic lupus erythematous (SLE) (1) and rheumatoid arthritis (RA) (2). They are also used to treat discoid and subacute cutaneous lupus erythematosus, as well as dermatomyositis and other autoimmune skin conditions. Based on actual body

[1]Julianna Desmarais, MD, Nicole Fett, MD: Oregon Health & Science University, Portland; [2]James T. Rosenbaum, MD: Oregon Health & Science University and Legacy Devers Eye Institute, Portland, Oregon; [3]Karen H. Costenbader, MD, MPH: Brigham and Women's Hospital, Boston, Massachusetts; [4]Ellen M. Ginzler, MD, MPH: State University of New York Downstate Health Sciences University, Brooklyn; [5]Susan Goodman, MD: Hospital for Special Surgery, Weill Cornell Medicine, New York, New York; [6]James O'Dell, MD: University of Nebraska Medical Center and Omaha VA Hospital, Omaha, Nebraska; [7]Christian A. Pineau, MD: McGill University, Montreal, Quebec, Canada;[8]Gabriela Schmajuk, MD: University of California San Francisco, San Francisco VA Medical Center, and Philip R. Lee Institute for Health Policy, San Francisco, California; [9]Victoria P. Werth, MD: University of Pennsylvania and Corporal Michael J. Crescenz VAMC, Philadelphia, Pennsylvania; [10]Mark S. Link, MD: University of Texas Southwestern Medical Center, Dallas; [11]Richard Kovacs, MD: Indiana University School of Medicine, Indianapolis.

Author disclosures are available at https://onlinelibrary.wiley.com/action/downloadSupplement?doi=10.1002%2Fart.41934&file=art41934-sup-0001-Disclosureform.pdf.

Address correspondence to Julianna Desmarais, MD, 3181 SW Sam Jackson Park Road, Mail Code OP09, Portland, OR 97239. Email: desmaraj@ohsu.edu.

Submitted for publication April 1, 2021; accepted in revised form July 22, 2021.

weight, recommended HCQ and CQ dosing in rheumatic disease patients is ≤5 mg/kg/day and ≤2.3 mg/kg/day, respectively, as higher doses are associated with increased retinal toxicity (3).

Utilization of HCQ and CQ increased in early 2020 as a result of initial reports of potential anti-coronavirus activity (4). Randomized controlled trials quickly revealed that these treatments were not effective against COVID-19 (5,6). In addition, in the setting of HCQ/CQ use for the treatment of COVID-19 infection, prolonged corrected QT interval (QTc) and cardiac arrhythmias were reported, increasing concern about the cardiovascular safety of these drugs (7).

The US Food and Drug Administration (FDA) approves drugs based on rigorous testing for safety and efficacy and continues to monitor for postmarketing signals of adverse events. Cardiac safety of noncardiovascular drugs has been an area of emphasis. In a 2001 FDA report, it was noted that the most common reason for withdrawal of a drug from the US market between 1997 and 2000 was torsade de pointes (TdP) arrhythmia, with women at higher risk for this drug toxicity (https://www.gao.gov/assets/100/90642.pdf). In 2005, the FDA issued guidance regarding the evaluation of all new drugs for risk of QTc prolongation because of the association between drug-induced prolonged QTc and TdP (https://www.fda.gov/media/71372/download). Currently, any drug with systemic bioavailability undergoes a randomized, double-blind, placebo- and active-control study in healthy subjects who are administered doses of the test medication, including supratherapeutic doses. These studies are often referred to as "thorough QT studies." Cancer drugs and drugs for psychiatric disorders are generally not administered to healthy controls; accordingly, alternative assessments of QT liability (i.e., the totality of risk as assessed by in vitro testing, animal testing, and clinical data that inform clinicians of pro-arrhythmia risk) have been proposed (8).

However, since HCQ and CQ were in use prior to a requirement for routine QTc testing in drug development, no such studies on these medications have been performed. In order to provide information to prescribers and the public on this risk, the Arizona Center for Education and Research on Therapeutics reviews drug safety data and uses a panel of experts to rate the risk that a drug will prolong the QTc interval. This not-for-profit organization, founded in 2000 as one of 14 federally funded Centers for Education and Research on Therapeutics, has published 2 up-to-date lists: one list of 253 drugs with QT liability for all patients, and a second list of 293 drugs that present a risk for patients with underlying inherited long QT syndromes (www.crediblemeds.org) (9). Both HCQ and CQ are listed as having a known risk of TdP. In 2017 the FDA also issued warnings on the potential cardiovascular toxicities of HCQ (Figure 1).

The goals of this white paper were to review and summarize the current understanding of HCQ/CQ cardiac toxicity, to describe factors that may increase the risk of HCQ/CQ-associated QTc prolongation, to discuss cardiomyopathy and conduction system abnormalities, and to outline potential research strategies to address outstanding questions about HCQ/CQ cardiac toxicity.

Data ascertainment and evaluation

A committee representing diverse US geographic locations and specialties was formed. The committee comprises 8 rheumatologists, 2 dermatologists, and 2 expert electrophysiology cardiologists; its members are the authors of this white paper. Members of the American College of Rheumatology, the American College of Cardiology, and the American Academy of Dermatology were purposefully included. Iterative group discussions and consensus-building were supplemented by literature review. A non-systematic literature review was performed by one of the authors (JD) on September 6, 2020, searching PubMed with terms "hydroxychloroquine cardiac toxicity" with no limits on year or language. Through this literature search 61 abstracts were identified, all of which were reviewed. A broader PubMed search for "antimalarial cardiac toxicity" was done by the same author on September 6, 2020, yielding 386 abstracts, all of which were reviewed. Another

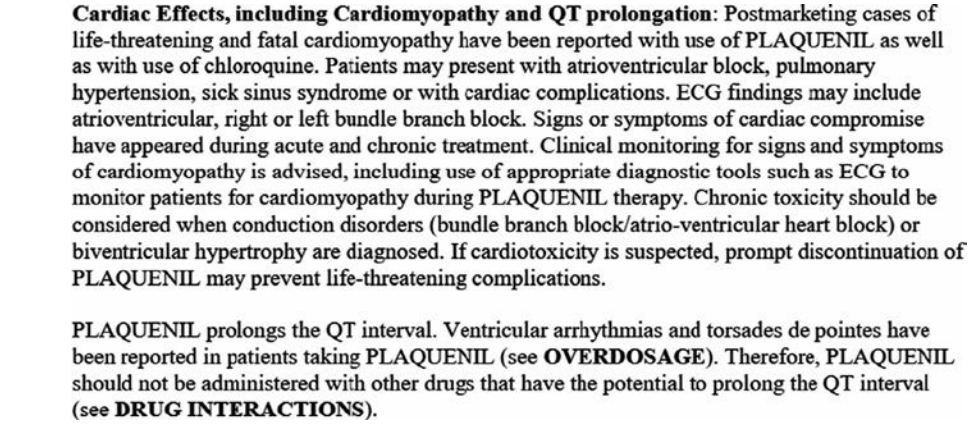

Cardiac Effects, including Cardiomyopathy and QT prolongation: Postmarketing cases of life-threatening and fatal cardiomyopathy have been reported with use of PLAQUENIL as well as with use of chloroquine. Patients may present with atrioventricular block, pulmonary hypertension, sick sinus syndrome or with cardiac complications. ECG findings may include atrioventricular, right or left bundle branch block. Signs or symptoms of cardiac compromise have appeared during acute and chronic treatment. Clinical monitoring for signs and symptoms of cardiomyopathy is advised, including use of appropriate diagnostic tools such as ECG to monitor patients for cardiomyopathy during PLAQUENIL therapy. Chronic toxicity should be considered when conduction disorders (bundle branch block/atrio-ventricular heart block) or biventricular hypertrophy are diagnosed. If cardiotoxicity is suspected, prompt discontinuation of PLAQUENIL may prevent life-threatening complications.

PLAQUENIL prolongs the QT interval. Ventricular arrhythmias and torsades de pointes have been reported in patients taking PLAQUENIL (see **OVERDOSAGE**). Therefore, PLAQUENIL should not be administered with other drugs that have the potential to prolong the QT interval (see **DRUG INTERACTIONS**).

Figure 1. US Food and Drug Administration recommendations regarding possible cardiac effects of hydroxychloroquine (https://www.accessdata.fda.gov/drugsatfda_docs/label/2017/009768s037s045s047lbl.pdf). ECG = electrocardiography.

author (MSL) performed a Medline and Google Scholar search on September 3, 2020 by searching for "hydroxychloroquine and QT and rheumatology" limited to the year 2020, identifying 533 results by title and abstract. Reference lists of selected articles were reviewed as well. Types of articles reviewed included systematic reviews, randomized controlled trials, meta-analyses, and observational studies (including case reports and small case series).

Authors participated in 2 in-depth virtual conferences, at which time the strengths and weaknesses of the existing data were discussed. Consensus regarding the format and content of this white paper was reached among authors. It was decided that this report would include the following information of which clinicians who prescribe HCQ/CQ should be aware: 1) a brief scientific background on QTc prolongation and TdP; 2) known risk factors for QTc prolongation in the non–COVID-19 setting; 3) available data regarding QTc prolongation with use of HCQ or CQ; 4) available data regarding cardiac deposition disease with long-term HCQ or CQ use; and 5) areas for future research.

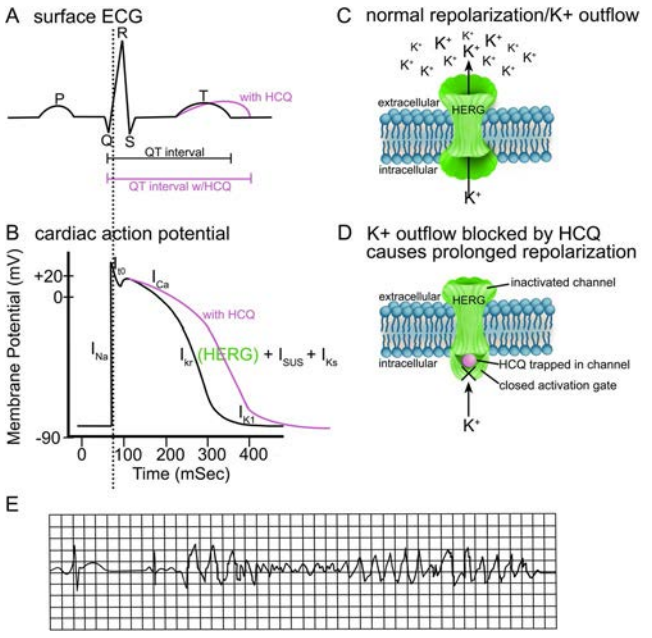

Figure 2. QT-prolonging effect of hydroxychloroquine (HCQ) or chloroquine (CQ) as seen on surface electrocardiography (**A**), which occurs due to prolongation of the action potential of the ventricular myocytes (**B**). The dotted line corresponds to rapid depolarization of the ventricular myocardium via fast sodium channels (I_{Na}). A transient outward current (I_{to}) ends depolarization. The plateau phase of the action, corresponding to the ST segment of the surface ECG, is due to the slow inward calcium current (I_{Ca}). Outward flow of potassium is largely responsible for the repolarization of ventricular myocytes via a variety of potassium currents, including the genetically determined potassium current (I_{Kr}) (human ether-a-go-go–related gene [hERG] channel) (80) and is reflected on the surface ECG as the T wave. Normal myocyte repolarization occurs due to potassium efflux from the cell through the hERG channel (**C**), which is blocked by HCQ or CQ (18) (**D**). This leads to prolongation of the corrected QT interval with risk for torsade de pointes (**E**). I_{Ks} = slow potassium channel; I_{SUS} = sum of the currents through other potassium channels.

QTc and torsades de pointes

The QT interval is an electrocardiographic (ECG) measurement from the beginning of the QRS complex to the end of the T wave, reflecting the time required for ventricular depolarization and repolarization (Figure 2). It is dependent on heart rate and thus needs to be corrected for heart rate (QTc), especially if a comparison needs to be made in an individual exhibiting different heart rates at different points in time. As there are different formulas available, the same formula should be used across ECG studies (10). Ranges considered prolonged for the commonly used Bazett-corrected QTc intervals include >450 ms in adult men and >470 ms in adult women (10).

A prolonged QTc as defined above increases the risk of sudden cardiac death (11), possibly related to the association of prolonged QTc with torsades de pointes ("twisting of the points"), an uncommon type of polymorphic ventricular tachycardia (12,13). In addition to QTc-prolonging medications there are other known risks for prolonged QTc, some of which are modifiable (Table 1).

HCQ and CQ are known to interact with cardiac ventricular myocytes by blocking potassium efflux channels, potentially leading to QTc prolongation (14). While this effect has been reported to occur in healthy subjects as soon as 2 days after starting HCQ and CQ (15), it takes 6 months for HCQ to reach steady-state blood concentration in healthy subjects (16). However, there is variability in HCQ blood levels even among subjects receiving similar dosing (in mg/kg/day) (17). HCQ and CQ inhibit the potassium channel in a concentration-dependent manner (18,19).

The COVID-19 pandemic enhanced awareness and recognition of the QT-prolonging effects of HCQ/CQ, but data demonstrate that HCQ and/or CQ prolong QT intervals independent of COVID-19 infection (for a list of studies see Supplementary Table 1, on the *Arthritis & Rheumatology* website at http://onlinelibrary.wiley.com/doi/10.1002/art.41934/abstract). It should be noted as well that COVID-19 viral infection has been associated with prolonged QTc and pro-arrhythmic state (14,20) (see Supplementary text, http://onlinelibrary.wiley.com/doi/10.1002/art.41934/abstract).

SLE patients with anti-SSA (anti–Ro 52) antibody may have an increased risk of QTc prolongation (21). Patients with higher levels of anti-SSA were found to have a higher degree of QTc prolongation (22). Of interest, anti-SSA has been found to interact with the potassium channel in a dose-dependent manner (23,24).

Clinical experience with HCQ/CQ, the QT interval, and torsade de pointes

Recent studies (25–28), as well as earlier case reports (29,30), have shown QTc prolongation with HCQ or CQ at conventional doses used to treat rheumatic disease. In a Veterans Administration study of >800 patients with rheumatic disease (90% male and 10% female) seen between 2000 and early 2020 who were taking HCQ and had available ECG data, HCQ was associated with QTc

Table 1. Risk factors for prolonged QTc*

Risk factor	Ref.
Female sex	81
Older age (especially >68 years)	81
Heart disease (including recent MI or CHF)	81
Use of >1 QTc-prolonging medication	81
Severe acute illness (sepsis, ICU admission, potentially COVID-19)	14, 20, 81, 82
Congenital long QT syndrome (estimated prevalence of 1/2,500)	80, 83, 84
Electrolyte abnormalities (hypokalemia, hypomagnesemia, hypocalcemia)	81, 85
Alcoholic liver disease	86
Hypothyroidism	87, 88
Obesity	89
Diabetes mellitus (due to cardiac autonomic neuropathy)	90, 91
Anti–Ro 52 positivity	21, 22

* QTc = corrected QT interval; MI = myocardial infarction; CHF = congestive heart failure; ICU = intensive care unit.

prolongation in 8.5% (7% with QTc 470–500 ms and 1.5% with QTc >500 ms) (25). Among 591 patients in this study who had paired ECG data before and after starting HCQ, 23 patients (3.9%) had either a >15% increase in QTc or a QTc of >500 ms with HCQ treatment. Chronic kidney disease, atrial fibrillation history, and heart failure were independent risks for QTc prolongation with HCQ use in the study. While QTc >470 ms with HCQ therapy was associated with long-term mortality in a univariate Cox regression analysis, this increased mortality risk was no longer apparent after adjustment for age, sex, and comorbidities. In patients with paired ECG data, change in QTc was not associated with mortality (hazard ratio 1.001 [95% confidence interval (95% CI) 0.998–1.005], $P = 0.51$) (25). In a Danish study (published in preprint form) evaluating data from 3 registries of patients with RA, SLE, or Sjögren's syndrome paired with controls, there was a mean prolongation of the QTc of 5.5 ms with the use of CQ (26). A review of the World Health Organization (WHO) pharmacovigilance database from 1967 through March 1, 2020 showed increased reports of QTc prolongation with both HCQ and azithromycin, with more frequent reporting of prolonged QTc and/or TdP/ventricular tachycardia with the combination of these 2 medications (odds ratio 2.48 [95% CI 1.28-4.79]) (27). In a commercial claims database analysis of events from 2001 through 2017, after 5 days of HCQ therapy the incidence of cardiac events (including myocardial infarction [MI], cerebrovascular accident/transient ischemic attack, sudden death, and arrhythmia) in 2001–2017 among women ages 60–79 years was 0.92 per 1,000 (28). Among those receiving both HCQ and azithromycin, the rate was 4.78 per 1,000 patients (28).

Other studies suggest that QTc prolongation has not been a substantial problem among rheumatic disease patients receiving HCQ or CQ. An FDA Adverse Event Reporting System (FAERS) review was conducted from 1969 through 2019, evaluating reports of prolonged QT/TdP and death. For HCQ and CQ the proportional reporting ratio (PRR) was 1.43 (95% CI 1.29–2.59), which was below the accepted meaningful safety signal of >2.0 (31). With the addition of azithromycin treatment the PRR became clinically meaningful (3.77 [95% CI 1.80–7.87]) (31). Other studies have shown that with higher cumulative exposure to antimalarial therapy the incidence of conduction abnormalities, including prolonged QTc, was decreased (32,33).

In a majority-female population with connective tissue disease, 85 unselected patients had normal ECG results after ≥1 year of HCQ therapy (34). While one study demonstrated a significant increase in the QTc in RA patients treated with HCQ versus other disease-modifying antirheumatic drugs (DMARDs) (mean ± SD 420.3 ± 30.8 ms versus 410.6 ± 28.7 ms), the QTc even with this prolongation remained within the normal range (35). It was reported in abstract form that in a population of RA and SLE patients (all without any known cardiovascular disease [CVD]), there was no significant difference in QTc among those treated with HCQ (n = 368) and those not treated with HCQ (n = 313) (36). Likewise, in a second abstract it was reported that rates of arrhythmia did not differ between RA patients who took HCQ and those who did not (37). A WHO Evidence Review Group found very few cases of documented arrhythmia due to prolonged QTc among patients treated for malaria with higher doses of HCQ (1 dose of 800 mg orally, followed by 3 doses [at 6, 24, and 48 hours] of 400 mg orally) despite 2.2 billion courses of HCQ and CQ administered worldwide, although arrhythmia monitoring was not routinely performed (38).

Antimalarial-induced cardiomyopathy

Both HCQ and CQ accumulate in mammalian lysosomes to cause a more alkaline pH (39). HCQ and CQ concentrate in the eyes (particularly in the melanin-containing retinal pigment epithelium), adrenal and pituitary glands, kidney, bone marrow, lung, liver, and cardiac tissue (40–42). This lysosomal accumulation may confer efficacy in the treatment of rheumatic and cutaneous conditions, but also may be responsible for toxicities such as atrioventricular (AV) conduction defects and cardiomyopathy. While channel blockade tends to be dose dependent and more immediate (18,19), cardiac toxicities related to HCQ/CQ deposition in cardiac myocytes to cause cardiomyopathy typically requires a longer duration of treatment (43,44).

Accumulation of HCQ/CQ in lysosomes of cardiac myocytes leading to arrhythmias and infiltrative cardiomyopathy has been

reported (45). A 2018 systematic review of rheumatologic use of HCQ/CQ identified 127 published cases of conduction system diseases and structural myocardial changes (43). Long-term use of HCQ/CQ is known to cause AV conduction system disease, including bundle branch block, fascicular blocks, and third-degree AV block (45–48). While the AV conduction disease is permanent once it occurs, there is evidence that there can be improvement in the cardiomyopathy upon cessation of these medications (43,49). Endomyocardial biopsy is often necessary for diagnosis, and the classic histologic findings of curvilinear bodies and lysosomal inclusions are similar to those in Fabry's disease (44,50). Hypertrophic, dilated, restrictive cardiomyopathy and/or biventricular endomyocardial fibrosis are all possible, though classically the cardiomyopathy associated with HCQ/CQ use is that of a biventricular concentric hypertrophy with restrictive physiology (44). Duration of drug use and daily dose appear to be the main risks for this cardiac toxicity, although endomyocardial biopsy–proven cases described in the literature occurred after as little as 2 (and as long as 35) years of use, with mean treatment durations of 7–12 years (43,44). Cardiomyopathy can develop more quickly in those receiving higher-than-recommended daily doses of CQ (51–53).

Cardiomyopathy was thought to be a rare occurrence since there were few biopsy-proven cases reported in the literature (54), but it may be both underrecognized and underreported. Serious Individual Case Safety Reports (ICSRs) for HCQ registered in the Vigibase data system between 2010 and 2019 showed cardiomyopathy in 3.3% of all reported ICSR cases (55). The FAERS pharmacovigilance database for HCQ/CQ showed a cardiomyopathy reporting odds ratio of 29.9 (95% CI 23.3–35.9) in 2004–2019 (56). Review of the WHO pharmacovigilance database showed that HCQ use was associated with heart failure (27).

For cardiac arrhythmias, ICSRs for HCQ registered in the Vigibase data system in 2010–2019 reported arrhythmias in 3.4% of reported events (this specifically does not include QTc prolongation or TdP) (55). The FAERS pharmacovigilance database reporting odds ratio for bradyarrhythmia in 2004–2019 was 5.1 (95% CI 3.9–6.7) (56). Review of the WHO pharmacovigilance database demonstrated that HCQ was associated with AV and bundle branch block (27).

Rheumatic autoimmune diseases, antimalarial agents, and atherosclerotic disease

It should be recognized that RA and SLE are themselves established independent risk factors for atherosclerotic CVD, especially with high disease activity (57–60). RA patients are more likely to be hospitalized for acute MI or to have an unrecognized MI, and disease duration of >10 years confers higher MI risk (61,62). Among patients with SLE, the relative risks of nonfatal MI and of death due to CVD have been estimated to be 10.1 (95% CI 5.8–15.6) and 17.0, respectively (60,63). Traditional risk factors further increase CVD risk in individuals with RA or SLE (64,65).

In observational studies, HCQ use has been associated with lower CVD risk in RA and SLE populations. In RA, a retrospective study showed a 72% lower CVD risk among HCQ-treated compared to non–HCQ-treated patients (66). A population-based study with propensity score matching showed an adjusted CVD hazard ratio for HCQ-treated versus non–HCQ-treated patients of 0.32 (95% CI 0.18–0.56, $P < 0.01$), with an even stronger relationship demonstrated among patients under age 50 years (67). A 2018 meta-analysis of HCQ use among RA patients demonstrated improved lipid profiles and a lower incidence of diabetes in those who had taken HCQ versus those who had never received this treatment (68). In retrospective studies of SLE, antimalarial therapy has been associated with improved dyslipidemia and lower CVD risk, though confounding by indication remains possible in all of these retrospective uncontrolled studies as treatment with HCQ may be a marker of better care or milder rheumatic disease (69–71). It is interesting to note, however, that in a multinational retrospective study of 14 international health databases prior to March 27, 2020, with >950,000 patients receiving HCQ monotherapy, HCQ (compared to sulfasalazine) administered long-term in patients with RA was associated with increased cardiovascular mortality (hazard ratio 1.65 [95% CI 1.12–2.44]) (72).

Cardiac monitoring considerations

The FDA HCQ label contains warnings and monitoring guidance, commenting on risk of heart failure due to cardiomyopathy and conduction abnormalities, as well as on the QT prolongation and risk of TdP (Figure 1). However, ECG monitoring is not part of the current standard practice when HCQ or CQ is prescribed for the treatment of rheumatologic or dermatologic conditions, and there is currently insufficient evidence on which to base specific monitoring recommendations across all patient populations prescribed HCQ/CQ. Practice considerations could include obtaining a baseline ECG in patients with additional risk factors for QT prolongation, such as those listed in Table 1, and avoidance,

Table 2. Selected QTc-prolonging medications that rheumatologists and dermatologists may see used in their patients with autoimmune conditions*

Class	Examples
Analgesics/sedatives	Propofol, hydrocodone
Antibiotics	Fluoroquinolones, macrolides, HIV antiretrovirals
Antiemetics	Ondansetron, droperidol
Antihistamines	Hydroxyzine
Beta-2-agonists	Albuterol, salmeterol
Diuretics	Furosemide (under conditions of electrolyte deficiencies)
Immunosuppressants	Tacrolimus
Psychotropic medications	Antipsychotics (haloperidol, ziprasidone), TCAs, SSRIs

* For more specific information on corrected QT interval (QTc)–prolonging medications, see www.crediblemeds.org. TCAs = tricyclic antidepressants; SSRIs = selective serotonin reuptake inhibitors.

when possible, of concomitant medications also known to prolong the QTc interval (Table 2). Patients should be educated and involved in shared decision-making about the potential for HCQ/CQ cardiac effects as well as the effect of other medications that prolong the QTc (Table 2). If patients do have symptoms suggestive of an arrhythmia such as syncope, presyncope, or unexplained dizziness, a cardiac evaluation including an ECG should be performed as per FDA label recommendations. Providers should also maintain a high index of suspicion for cardiomyopathy in patients who have received long-term HCQ/CQ treatment and present with new cardiac symptoms. If a restrictive cardiomyopathy is found and no other cause is identified, an endomyocardial biopsy should be considered.

By including FDA label recommendations, we do not wish to imply that we unequivocally endorse the FDA recommendation to never administer other drugs with the potential to prolong the QTc interval. As with all approved drugs, prescribers may deviate from the label directions using their clinical judgment. These decisions are best made with a discussion of the risks and benefits of combining medications. Though we focus on the HCQ label, this also applies to CQ. Some data suggest that CQ has a higher rate of adverse cardiac outcomes (56).

CVD is the leading cause of death worldwide (73). Both RA and SLE increase the risk of CVD by severalfold (61–63). The tragedies of the COVID-19 pandemic should not be underestimated, but one positive outcome is that it led to the discovery of previously underrecognized and potentially lethal cardiac side effects of what is generally held to be a truly safe medication. Many prescribers correctly assert that despite years of practice, they have never encountered arrhythmia in a patient receiving antimalarial treatment. The precise incidence of serious arrhythmia in patients taking HCQ for rheumatic disease is unknown; let us assume for the sake of argument that it is one per one thousand. At this rate, indeed the majority of prescribers would never have a patient in whom sudden cardiac death occurs. Since prescribers are unlikely to ascribe sudden death to HCQ, this might also contribute to a potentially mistaken assumption that antimalarials are not an important cause of arrhythmia. But even if the rate is as low as one per thousand, an ECG—a relatively inexpensive screening tool that is also indicated by virtue of the increased cardiac risk secondary to inflammatory disease—could save hundreds of lives.

The importance of antimalarial therapy in diseases such as SLE cannot be overstated. These medications have been found to lead to a decreased need for glucocorticoid treatment, lowered risk of thrombosis (74), improved dyslipidemia (69), lowered risk of CVD (70), and reduced organ damage (75) and risk of disease flares (76). Ultimately the low risk of cardiac toxicity in the setting of the benefits of these medications should be weighed appropriately, as the benefits far outweigh the risks. Furthermore, in terms of side effects and laboratory abnormalities, HCQ is well-tolerated compared to other DMARDs (77).

Limitations

There are several limitations to the studies we have reviewed here. The pre–COVID-19 published studies on cardiac toxicity were smaller retrospective studies or case reports. Safety data historically have been based on clinical experience and spontaneous reporting of adverse events, both of which have been shown to be ineffective methods of assessing drug safety in practice compared to randomized trials or active surveillance (78). Since the start of the COVID-19 pandemic, larger studies from databases have emerged, though data from large prospective trials in rheumatic disease patients are lacking. While administrative database studies are powerful in providing large sample sizes and many person-years of exposure, it is not possible to correctly identify the underlying causes of outcomes such as "cardiovascular mortality" and whether deaths were due to atherosclerotic disease and thrombosis, infiltrative cardiomyopathy, or arrhythmias associated with QTc prolongation. Data from patients with COVID-19 should not be extrapolated directly to patients with RA or SLE. There is evidence of cardiotoxicity with COVID-19 itself, and HCQ doses used for treatment of COVID-19 were much higher than the usual dosing for autoimmune diseases (for examples of HCQ dosing see Supplementary text, http://onlinelibrary.wiley.com/doi/10.1002/art.41934/abstract). Additionally, patients may have received other QTc-prolonging medications along with HCQ/CQ treatment (79).

Future studies

There is a lack of strong prospective data on the risk of QTc prolongation from HCQ/CQ and the true incidence of the cardiac toxicity from drug accumulation in cardiac myocytes in cohorts of patients with autoimmune diseases. Cross-sectional and retrospective observational studies have many limitations, which include confounding by indication, as well as immortal time, surveillance, and survival biases. Prospective studies should be designed to evaluate QTc intervals in patients with rheumatic disease before and after treatment with HCQ or CQ, although it may take several years and extremely large populations for any safety signals to be observed. Other long-term studies with regular cardiac monitoring including ECG should be undertaken to evaluate the association between cumulative HCQ/CQ exposure and the risk of ECG abnormalities (both TdP and AV conduction system disease), sudden cardiac death, as well as heart failure and cardiomyopathy.

Studies free of confounding by indication and biases related to retrospective, uncontrolled, observational data will be very challenging to perform, however. Sudden cardiac death due to TdP may be an extremely rare outcome and often misreported or difficult to capture. It would also be helpful to have studies that include assessment of economic cost-benefit and quality-adjusted life years gained from performing ECG monitoring. We

look forward to better data informing recommendations and to more accurate estimates of the true number needed to harm in our patient population, which is thought to be very low.

Key points

HCQ and CQ are important medications used in SLE and RA with known clinical benefits, and patients should not stop taking them without talking to their prescriber. The risk of cardiac toxicity is considered to be low in comparison to the benefits of these medications. There is risk of TdP with the use of HCQ/CQ that is thought to be low. Current data do not support institution of specific recommendations regarding how to avoid these adverse effects; options include baseline ECG in patients with multiple risk factors and follow-up ECG in patients with prolonged QTc or those receiving HCQ/CQ in combination with other QTc-prolonging therapies. Cardiomyopathy and conduction blocks are reported with long-term use, and providers should be vigilant to screen for cardiac symptoms in their patients.

Conclusions

Prescribers of HCQ and CQ should be aware of the potential cardiac toxicity of these medications, especially in high-risk populations. There is considerable clinical overlap between patients who are at high risk for cardiac complications and those who are likely to be treated by rheumatologists. The COVID-19 pandemic has focused attention on the potential cardiac toxicity of these drugs with the risk for prolonged QTc and TdP. However, existing studies of patients with autoimmune disease are retrospective with lower-quality data. Risk factor assessment and performance of baseline ECG in patients with risk factors can help identify those at higher risk of QTc prolongation when starting antimalarial therapy, as well as screening for long-term toxicity including cardiomyopathy. Increased clinical awareness of the potential for cardiac toxicity, both pro-arrhythmic and associated with long-term use, is essential as HCQ and CQ remain foundational medications in the treatment of autoimmune rheumatic diseases, and their proven benefits should be weighed along with these risks.

ACKNOWLEDGMENTS

We would like to thank Sasha Bernatsky (Research Institute of the McGill University Health Centre), Murray Urowitz (University of Toronto, Toronto, Ontario, Canada), and Ann Clarke (University of Calgary, Calgary, Alberta, Canada) for their input and expertise. We also appreciate the assistance of Paige Herman in the design of Figure 2.

AUTHOR CONTRIBUTIONS

All authors were involved in drafting the article or revising it critically for important intellectual content, and all authors approved the final version to be published. Dr. Desmarais had full access to all of the data in the study and takes responsibility for the integrity of the data and the accuracy of the data analysis.

Study conception and design. Desmarais, Rosenbaum, Costenbader, Kovacs.
Acquisition of data. Desmarais, Link.
Analysis and interpretation of data. Ginzler, Fett, Goodman, O'Dell, Pineau, Schmajuk, Werth, Link, Kovacs.

REFERENCES

1. Mullins JF, Kirk JM, Shapiro EM. Chloroquine treatment of lupus erythematosus. South Med J 1955;48:732–6.
2. Popert AJ, Meijers KA, Sharp J, Bier F. Chloroquine diphosphate in rheumatoid arthritis: a controlled trial. Ann Rheum Dis 1961;20:18–35.
3. Marmor MF, Kellner U, Lai TY, Melles RB, Mieler WF. Recommendations on screening for chloroquine and hydroxychloroquine retinopathy (2016 revision). Ophthalmology 2016;123:1386–94.
4. Shehab N, Lovegrove M, Budnitz DS. US hydroxychloroquine, chloroquine, and azithromycin outpatient prescription trends, October 2019 through March 2020. JAMA Intern Med 2020;180:1384–6.
5. Rosenberg ES, Dufort EM, Udo T, Wilberschied LA, Kumar J, Tesoriero J, et al. Association of treatment with hydroxychloroquine or azithromycin with in-hospital mortality in patients with COVID-19 in New York State. JAMA 2020;323:2493–502.
6. Self WH, Semler MW, Leither LM, Casey JD, Angus DC, Brower RG, et al. Effect of hydroxychloroquine on clinical status at 14 days in hospitalized patients with COVID-19: a randomized clinical trial. JAMA 2020;324:2165–76.
7. US Food and Drug Administration. Drug safety communication: FDA cautions against use of hydroxychloroquine or chloroquine for COVID-19 outside of the hospital setting or a clinical trial due to risk of heart rhythm problems. 2020.
8. Rock EP, Finkle J, Fingert HJ, Booth BP, Garnett CE, Grant S, et al. Assessing proarrhythmic potential of drugs when optimal studies are infeasible [review]. Am Heart J 2009;157:827–36.
9. CredibleMeds. QTDrugs List. 2020. URL: https://www.crediblemeds.org.
10. Goldenberg I, Moss AJ, Zareba W. QT interval: how to measure it and what is "normal". J Cardiovasc Electrophysiol 2006;17:333–6.
11. Straus SM, Kors JA, De Bruin ML, van der Hooft CS, Hofman A, Heeringa J, et al. Prolonged QTc interval and risk of sudden cardiac death in a population of older adults. J Am Coll Cardiol 2006;47:362–7.
12. Postema PG, De Jong JS, van der Bilt IA, Wilde AA. Accurate electrocardiographic assessment of the QT interval: teach the tangent. Heart Rhythm 2008;5:1015–8.
13. Dessertenne F. Ventricular tachycardia with 2 variable opposing foci. Arch Mal Coeur Vaiss 1966;59:263–72. In French.
14. Toraih EA, Elshazli RM, Hussein MH, Elgaml A, Amin M, El-Mowafy M, et al. Association of cardiac biomarkers and comorbidities with increased mortality, severity, and cardiac injury in COVID-19 patients: a meta-regression and decision tree analysis. J Med Virol 2020;92:2473–2488.
15. Bustos MD, Gay F, Diquet B, Thomare P, Warot D. The pharmacokinetics and electrocardiographic effects of chloroquine in healthy subjects. Trop Med Parasitol 1994;45:83–6.
16. Tett SE, Cutler DJ, Day RO, Brown KF. Bioavailability of hydroxychloroquine tablets in healthy volunteers. Br J Clin Pharmacol 1989;27:771–9.
17. Petri M, Elkhalifa M, Li J, Magder LS, Goldman DW. Hydroxychloroquine blood levels predict hydroxychloroquine retinopathy. Arthritis Rheumatol 2020;72:448–53.
18. Traebert M, Dumotier B, Meister L, Hoffmann P, Dominguez-Estevez M, Suter W. Inhibition of hERG K+ currents by antimalarial drugs in stably transfected HEK293 cells. Eur J Pharmacol 2004;484:41–8.

19. Borsini F, Crumb W, Pace S, Ubben D, Wible B, Yan GX, et al. In vitro cardiovascular effects of dihydroartemisin-piperaquine combination compared with other antimalarials. Antimicrob Agents Chemother 2012;56:3261–70.
20. Mercuro NJ, Yen CF, Shim DJ, Maher TR, McCoy CM, Zimetbaum PJ, et al. Risk of QT interval prolongation associated with use of hydroxychloroquine with or without concomitant azithromycin among hospitalized patients testing positive for coronavirus disease 2019 (COVID-19). JAMA Cardiol 2020;5:1036–41.
21. Bourré-Tessier J, Clarke AE, Huynh T, Bernatsky S, Joseph L, Belisle P, et al. Prolonged corrected QT interval in anti-Ro/SSA–positive adults with systemic lupus erythematosus. Arthritis Care Res (Hoboken) 2011;63:1031–7.
22. Lazzerini PE, Capecchi PL, Acampa M, Morozzi G, Bellisai F, Bacarelli MR, et al. Anti-Ro/SSA–associated corrected QT interval prolongation in adults: the role of antibody level and specificity. Arthritis Care Res (Hoboken) 2011;63:1463–70.
23. Yue Y, Castrichini M, Srivastava U, Fabris F, Shah K, Li Z, et al. Pathogenesis of the novel autoimmune-associated long-QT syndrome. Circulation 2015;132:230–40.
24. Nakamura K, Katayama Y, Kusano KF, Haraoka K, Tani Y, Nagase S, et al. Anti-KCNH2 antibody-induced long QT syndrome: novel acquired form of long QT syndrome. J Am Coll Cardiol 2007;50:1808–9.
25. Hooks M, Bart B, Vardeny O, Westanmo A, Adabag S. Effects of hydroxychloroquine treatment on QT interval. Heart Rhythm 2020;17:1930–5.
26. Isaksen J, Holst A, Pietersen A, Nielsen J, Graff C, Kanters J. Chloroquine, but not hydroxychlorquine, prolongs the QT interval in a primary care population [preprint]. MedRxiv 2020. doi: https://doi.org/10.1101/2020.06.19.20135475. E-pub ahead of print.
27. Nguyen LS, Dolladille C, Drici MD, Fenioux C, Alexandre J, Mira JP, et al. Cardiovascular toxicities associated with hydroxychloroquine and azithromycin: an analysis of the World Health Organization pharmacovigilance database. Circulation 2020;142:303–5.
28. Simmering JE, Polgreen LA, Polgreen PM, Teske RE, Comellas AP, Carter BL. The cardiovascular effects of treatment with hydroxychloroquine and azithromycin. Pharmacotherapy 2020;40:978–83.
29. Morgan ND, Patel SV, Dvorkina O. Suspected hydroxychloroquine-associated QT-interval prolongation in a patient with systemic lupus erythematosus. J Clin Rheumatol 2013;19:286–8.
30. Chen CY, Wang FL, Lin CC. Chronic hydroxychloroquine use associated with QT prolongation and refractory ventricular arrhythmia. Clin Toxicol (Phila) 2006;44:173–5.
31. Sarayani A, Cicali B, Henriksen CH, Brown JD. Safety signals for QT prolongation or torsades de pointes associated with azithromycin with or without chloroquine or hydroxychloroquine. Res Social Adm Pharm 2020;17:483–6.
32. McGhie TK, Harvey P, Su J, Anderson N, Tomlinson G, Touma Z. Electrocardiogram abnormalities related to anti-malarials in systemic lupus erythematosus. Clin Exp Rheumatol 2018;36:545–51.
33. Touma Z. HCQ and the heart. CRAJ 2020;30:29.
34. Costedoat-Chalumeau N, Hulot JS, Amoura Z, Leroux G, Lechat P, Funck-Brentano C, et al. Heart conduction disorders related to antimalarials toxicity: an analysis of electrocardiograms in 85 patients treated with hydroxychloroquine for connective tissue diseases. Rheumatology (Oxford) 2007;46:808–10.
35. Erre GL, Ferraccioli ES, Piga M, Mangoni A, Passiu G, Gremese E, et al. Antimalarial use and arrhythmias in COVID-19 and rheumatic patients: a matter of dose and inflammation? Ann Rheum Dis 2020. doi: https://doi.org/10.1136/annrheumdis-2020-217828. E-pub ahead of print.
36. Park E, Giles J, Perez-Recio T, Pina P, Depender C, Bathon J, et al. Hydroxychloroquine use was not associated with QTc length in a large cohort of SLE and RA patients [abstract]. Arthritis Rheumatol 2020;72 Suppl 10. URL: https://acrabstracts.org/abstract/hydroxychloroquine-use-was-not-associated-with-qtc-length-in-a-large-cohort-of-sle-and-ra-patients/.
37. Restrepo J, Escalante A, Battafarano D, Lorenzo C, Del Rincon I. Hydroxychloroquine is not cardiotoxic in patients with rheumatoid arthritis [abstract]. Arthritis Rheumatol 2020;72 Suppl 10. URL: https://acrabstracts.org/abstract/hydroxychloroquine-is-not-cardiotoxic-in-patients-with-rheumatoid-arthritis/.
38. World Health Organization. The cardiotoxicity of antimalarials:WHO evidence review group meeting. 2016. URL: https://www.who.int/malaria/mpac/mpac-mar2017-erg-cardiotoxicity-report-session2.pdf.
39. Ohkuma S, Poole B. Fluorescence probe measurement of the intralysosomal pH in living cells and the perturbation of pH by various agents. Proc Natl Acad Sci U S A 1978;75:3327–31.
40. Mackenzie AH. Pharmacologic actions of 4-aminoquinoline compounds. Am J Med 1983;75:5–10.
41. Larsson B, Tjälve H. Studies on the mechanism of drug-binding to melanin. Biochem Pharmacol 1979;28:1181–7.
42. De Sisternes L, Hu J, Rubin DL, Marmor MF. Localization of damage in progressive hydroxychloroquine retinopathy on and off the drug: inner versus outer retina, parafovea versus peripheral fovea. Invest Ophthalmol Vis Sci 2015;56:3415–26.
43. Chatre C, Roubille F, Vernhet H, Jorgensen C, Pers YM. Cardiac complications attributed to chloroquine and hydroxychloroquine: a systematic review of the literature. Drug Saf 2018;41:919–31.
44. Yogasundaram H, Putko BN, Tien J, Paterson DI, Cujec B, Ringrose J, et al. Hydroxychloroquine-induced cardiomyopathy: case report, pathophysiology, diagnosis, and treatment [review]. Can J Cardiol 2014;30:1706–15.
45. Tönnesmann E, Kandolf R, Lewalter T. Chloroquine cardiomyopathy: a review of the literature. Immunopharmacol Immunotoxicol 2013;35:434–42.
46. Ladipo GO, Essien EE, Andy JJ. Complete heart block in chronic chloroquine poisoning. Int J Cardiol 1983;4:198–200.
47. Ratliff NB, Estes ML, Myles JL, Shirey EK, McMahon JT. Diagnosis of chloroquine cardiomyopathy by endomyocardial biopsy. N Engl J Med 1987;316:191–3.
48. Reuss-Borst M, Berner B, Wulf G, Müller GA. Complete heart block as a rare complication of treatment with chloroquine. J Rheumatol 1999;26:1394–5.
49. Costedoat-Chalumeau N, Hulot JS, Amoura Z, Delcourt A, Maisonobe T, Dorent R, et al. Cardiomyopathy related to antimalarial therapy with illustrative case report [review]. Cardiology 2007;107:73–80.
50. Roos JM, Aubry MC, Edwards WD. Chloroquine cardiotoxicity: clinicopathologic features in three patients and comparison with three patients with Fabry disease. Cardiovasc Pathol 2002;11:277–83.
51. Freihage JH, Patel NC, Jacobs WR, Picken M, Fresco R, Malinowska K, et al. Heart transplantation in a patient with chloroquine-induced cardiomyopathy. J Heart Lung Transplant 2004;23:252–5.
52. Azimian M, Gultekin SH, Hata JL, Atkinson JB, Ely KA, Fuchs HA, et al. Fatal antimalarial-induced cardiomyopathy: report of 2 cases. J Clin Rheumatol 2012;18:363–6.
53. Pieroni M, Smaldone C, Camporeale A, Ierardi C, Dell'Antonio G, Bellocci F, et al. Chloroquine-induced transition from dilated to restrictive cardiomyopathy. J Am Coll Cardiol 2011;57:515.
54. Tselios K, Deeb M, Gladman DD, Harvey P, Urowitz MB. Antimalarial-induced cardiomyopathy: a systematic review of the literature. Lupus 2018;27:591–9.
55. Montastruc JL, Rousseau V, Durrieu G, Bagheri H. Serious adverse drug reactions with hydroxychloroquine: a pharmacovigilance study in Vigibase. Eur J Clin Pharmacol 2020;76:1479–80.

56. Goldman A, Bomze D, Dankner R, Hod H, Meirson T, Boursi B, et al. Cardiovascular adverse events associated with hydroxychloroquine and chloroquine: a comprehensive pharmacovigilance analysis of pre-COVID-19 reports. Br J Clin Pharmacol 2020;87:1432–42.
57. Avina-Zubieta JA, Thomas J, Sadatsafavi M, Lehman AJ, Lacaille D. Risk of incident cardiovascular events in patients with rheumatoid arthritis: a meta-analysis of observational studies. Ann Rheum Dis 2012;71:1524–9.
58. Solomon DH, Reed GW, Kremer JM, Curtis JR, Farkouh ME, Harrold LR, et al. Disease activity in rheumatoid arthritis and the risk of cardiovascular events. Arthritis Rheumatol 2015;67:1449–55.
59. Manzi S, Meilahn EN, Rairie JE, Conte CG, Medsger TA Jr, Jansen-McWilliams L, et al. Age-specific incidence rates of myocardial infarction and angina in women with systemic lupus erythematosus: comparison with the Framingham Study. Am J Epidemiol 1997;145:408–15.
60. Lin CY, Shih CC, Yeh CC, Chou WH, Chen TL, Liao CC. Increased risk of acute myocardial infarction and mortality in patients with systemic lupus erythematosus: two nationwide retrospective cohort studies. Int J Cardiol 2014;176:847–51.
61. Maradit-Kremers H, Crowson CS, Nicola PJ, Ballman KV, Roger VL, Jacobsen SJ, et al. Increased unrecognized coronary heart disease and sudden deaths in rheumatoid arthritis: a population-based cohort study [review]. Arthritis Rheum 2005;52:402–11.
62. Solomon DH, Karlson EW, Rimm EB, Cannuscio CC, Mandl LA, Manson JE, et al. Cardiovascular morbidity and mortality in women diagnosed with rheumatoid arthritis. Circulation 2003;107:1303–7.
63. Esdaile JM, Abrahamowicz M, Grodzicky T, Li Y, Panaritis C, du Berger R, et al. Traditional Framingham risk factors fail to fully account for accelerated atherosclerosis in systemic lupus erythematosus. Arthritis Rheum 2001;44:2331–7.
64. Sandoo A, Chanchlani N, Hodson J, Smith JP, Douglas KM, Kitas GD. Classical cardiovascular disease risk factors associate with vascular function and morphology in rheumatoid arthritis: a six-year prospective study. Arthritis Res Ther 2013;15:R203.
65. Fernández-Nebro A, Rúa-Figueroa Í, López-Longo FJ, Galindo-Izquierdo M, Calvo-Alén J, Olivé-Marqués A, et al. Cardiovascular events in systemic lupus erythematosus: a nationwide study in Spain from the RELESSER registry. Medicine (Baltimore) 2015;94:e1183.
66. Sharma TS, Wasko MC, Tang X, Vedamurthy D, Yan X, Cote J, et al. Hydroxychloroquine use is associated with decreased incident cardiovascular events in rheumatoid arthritis patients. J Am Heart Assoc 2016;5:e002867.
67. Hung YM, Wang YH, Lin L, Wang PY, Chiou JY, Wei JC. Hydroxychloroquine may be associated with reduced risk of coronary artery diseases in patients with rheumatoid arthritis: a nationwide population-based cohort study. Int J Clin Pract 2018;72:e13095.
68. Rempenault C, Combe B, Barnetche T, Gaujoux-Viala C, Lukas C, Morel J, et al. Metabolic and cardiovascular benefits of hydroxychloroquine in patients with rheumatoid arthritis: a systematic review and meta-analysis [review]. Ann Rheum Dis 2018;77:98–103.
69. Rahman P, Gladman DD, Urowitz MB, Yuen K, Hallett D, Bruce IN. The cholesterol lowering effect of antimalarial drugs is enhanced in patients with lupus taking corticosteroid drugs. J Rheumatol 1999;26:325–30.
70. Liu D, Li X, Zhang Y, Kwong JS, Li L, Zhang Y, et al. Chloroquine and hydroxychloroquine are associated with reduced cardiovascular risk: a systematic review and meta-analysis [review]. Drug Des Devel Ther 2018;12:1685–95.
71. Yang DH, Leong PY, Sia SK, Wang YH, Wei JC. Long-term hydroxychloroquine therapy and risk of coronary artery disease in patients with systemic lupus erythematosus. J Clin Med 2019;8:796.
72. Lane JC, Weaver J, Kostka K, Duarte-Salles T, Abrahao MT, Alghoul H, et al. Risk of hydroxychloroquine alone and in combination with azithromycin in the treatment of rheumatoid arthritis: a multinational, retrospective study. Lancet Rheumatol 2020.
73. World Health Organization. Global health estimates 2016. 2018.
74. Petri M. Hydroxychloroquine use in the Baltimore Lupus Cohort: effects on lipids, glucose and thrombosis [review]. Lupus 1996;5 Suppl 1:S16–22.
75. Bruce IN, O'Keeffe AG, Farewell V, Hanly JG, Manzi S, Su L, et al. Factors associated with damage accrual in patients with systemic lupus erythematosus: results from the Systemic Lupus International Collaborating Clinics (SLICC) inception cohort. Ann Rheum Dis 2015;74:1706–13.
76. Canadian Hydroxychloroquine Study Group. A randomized study of the effect of withdrawing hydroxychloroquine sulfate in systemic lupus erythematosus. N Engl J Med 1991;324:150–4.
77. Fries JF, Williams CA, Ramey D, Bloch DA. The relative toxicity of disease-modifying antirheumatic drugs. Arthritis Rheum 1993;36:297–306.
78. Sarganas G, Garbe E, Klimpel A, Hering RC, Bronder E, Haverkamp W. Epidemiology of symptomatic drug-induced long QT syndrome and torsade de pointes in Germany. Europace 2014;16:101–8.
79. The RECOVERY Collaborative Group. Effect of hydroxychloroquine in hospitalized patients with Covid-19. N Engl J Med 2020;383:2030–40.
80. Sanguinetti MC, Jiang C, Curran ME, Keating MT. A mechanistic link between an inherited and an acquired cardiac arrhythmia: HERG encodes the IKr potassium channel. Cell 1995;81:299–307.
81. Tisdale JE, Jaynes HA, Kingery JR, Mourad NA, Trujillo TN, Overholser BR, et al. Development and validation of a risk score to predict QT interval prolongation in hospitalized patients. Circ Cardiovasc Qual Outcomes 2013;6:479–87.
82. Pickham D, Helfenbein E, Shinn JA, Chan G, Funk M, Weinacker A, et al. High prevalence of corrected QT interval prolongation in acutely ill patients is associated with mortality: results of the QT in Practice (QTIP) Study. Crit Care Med 2012;40:394–9.
83. Vincent GM, Timothy KW, Leppert M, Keating M. The spectrum of symptoms and QT intervals in carriers of the gene for the long-QT syndrome. N Engl J Med 1992;327:846–52.
84. Crotti L, Celano G, Dagradi F, Schwartz PJ. Congenital long QT syndrome [review]. Orphanet J Rare Dis 2008;3:18.
85. Moss AJ. Prolonged QT-interval syndromes. JAMA 1986;256:2985–7.
86. Day CP, James OF, Butler TJ, Campbell RW. QT prolongation and sudden cardiac death in patients with alcoholic liver disease. Lancet 1993;341:1423–8.
87. Sarma JS, Venkataraman K, Nicod P, Polikar R, Smith J, Schoenbaum MP, et al. Circadian rhythmicity of rate-normalized QT interval in hypothyroidism and its significance for development of class III antiarrhythmic agents. Am J Cardiol 1990;66:959–63.
88. Bakiner O, Ertorer ME, Haydardedeoglu FE, Bozkirli E, Tutuncu NB, Demirag NG. Subclinical hypothyroidism is characterized by increased QT interval dispersion among women. Med Princ Pract 2008;17:390–4.
89. Frank S, Colliver JA, Frank A. The electrocardiogram in obesity: statistical analysis of 1,029 patients. J Am Coll Cardiol 1986;7:295–9.
90. Gonin JM, Kadrofske MM, Schmaltz S, Bastyr EJ III, Vinik AI. Corrected Q-T interval prolongation as diagnostic tool for assessment of cardiac autonomic neuropathy in diabetes mellitus. Diabetes Care 1990;13:68–71.

91. Ewing DJ, Neilson JM. QT interval length and diabetic autonomic neuropathy. Diabet Med 1990;7:23–6.
92. Yu CM, Wong RS, Wu EB, Kong SL, Wong J, Yip GW, et al. Cardiovascular complications of severe acute respiratory syndrome. Postgrad Med J 2006;82:140–4.
93. Lang JP, Wang X, Moura FA, Siddiqi HK, Morrow DA, Bohula EA. A current review of COVID-19 for the cardiovascular specialist. Am Heart J 2020;226:29–44.
94. Shi S, Qin M, Shen B, Cai Y, Liu T, Yang F, et al. Association of cardiac injury with mortality in hospitalized patients with COVID-19 in Wuhan, China. JAMA Cardiol 2020;5:802–10.
95. Kochi AN, Tagliari AP, Forleo GB, Fassini GM, Tondo C. Cardiac and arrhythmic complications in patients with COVID-19 [review]. J Cardiovasc Electrophysiol 2020;31:1003–8.
96. Bessière F, Roccia H, Delinière A, Charrière R, Chevalier P, Argaud L, et al. Assessment of QT intervals in a case series of patients with coronavirus disease 2019 (COVID-19) infection treated with hydroxychloroquine alone or in combination with azithromycin in an intensive care unit. JAMA Cardiol 2020;5:1067–9.
97. Borba MG, Val FF, Sampaio VS, Alexandre MA, Melo GC, Brito M, et al. Effect of high vs low doses of chloroquine diphosphate as adjunctive therapy for patients hospitalized with severe acute respiratory syndrome coronavirus 2 (SARS-CoV-2) infection: a randomized clinical trial. JAMA Netw Open 2020;3:e208857.
98. Saleh M, Gabriels J, Chang D, Fishbein J, Qiu M, Mountantonakis SE, et al. Safely administering potential QTc prolonging therapy across a large healthcare system in the COVID-19 era. Circ Arrhythm Electrophysiol 2020;13:e008937.
99. Jankelson L, Karam G, Becker ML, Chinitz LA, Tsai MC. QT prolongation, torsades de pointes, and sudden death with short courses of chloroquine or hydroxychloroquine as used in COVID-19: a systematic review. Heart Rhythm 2020;17:1472–9.
100. Tleyjeh IM, Kashour Z, AlDosary O, Riaz M, Tlayjeh H, Garbati MA, et al. The cardiac toxicity of chloroquine or hydroxychloroquine in COVID-19 patients: a systematic review and meta-regression analysis. Mayo Clin Proc Innov Qual Outcomes 2021;5:137–50.
101. Oren O, Yang EH, Gluckman TJ, Michos ED, Blumenthal RS, Gersh BJ. Use of chloroquine and hydroxychloroquine in COVID-19 and cardiovascular implications: understanding safety discrepancies to improve interpretation and design of clinical trials [review]. Circ Arrhythm Electrophysiol 2020;13:e008688.

Arthritis & Rheumatology
Vol. 73, No. 12, December 2021, pp 2161–2162
DOI 10.1002/art.41940
© 2021, American College of Rheumatology

American College of Rheumatology
Empowering Rheumatology Professionals

EDITORIAL

Where There's Smoke, There's a Joint: Passive Smoking and Rheumatoid Arthritis

Milena A. Gianfrancesco[1] and Cynthia S. Crowson[2]

Among the established risk factors associated with developing rheumatoid arthritis (RA), smoking remains one of the leading environmental exposures associated with disease onset. One meta-analysis of 10 studies found that the risk of developing RA increased by 26% among those who smoked 1–10 pack-years, and nearly doubled among those who smoked more than 20 pack-years, compared to never smokers (1). Studies that closely examine smoking and the development of RA continue to be important, as smoking is a modifiable risk factor and its reduction can significantly decrease the burden of disease in the population.

Despite the extensive body of literature on smoking and RA, less is known regarding the impact of passive and active smoking throughout the life course on the development of incident RA. Ideally, examining this research question requires longitudinal data captured in disease-free individuals with sufficient follow-up time, which is not commonly available. Additionally, detailed information beyond "ever" versus "never" smoking is valuable in that the window of exposure susceptibility can be assessed, offering insight into how different exposures accumulate over the life course, since these are not singular risk factors, but rather are correlated variables that may contribute both directly and indirectly to the development of RA through various pathways.

In this issue of *Arthritis & Rheumatology*, Yoshida et al (2) report the findings of their analysis using the Nurses' Health Study II (n = ~90,000) and a life-course epidemiology approach to examine the effect of 3 passive smoking exposures on RA onset: 1) maternal smoking during pregnancy, 2) parental smoking during childhood, and 3) adulthood passive smoking. Analyses also accounted for personal (active) smoking, since earlier-life experiences of passive smoking could potentially influence the uptake of later-life personal smoking, which itself is a risk factor for RA onset. The life-course epidemiology approach is appropriate given how correlated the smoking variables are to each other, which can potentially accumulate to increase the risk of disease in adulthood and act through a number of pathways. Therefore, the analysis calculated both the direct and indirect effect of passive smoking, accounting for the time ordering of variables across the lifespan and controlling for time-varying covariates. Results demonstrated that early-life inhaled exposures, such as passive cigarette smoking, were associated with adult-onset seropositive RA, even after controlling for later-life personal smoking. Further, the effect of childhood passive smoking exposure was especially pronounced among "ever" adult smokers, similar to the findings of previous studies (3).

The study by Yoshida et al is unique in that it teases apart smoking exposure with the use of multiple variables and utilizes robust statistical analyses, including an inverse probability–weighted controlled direct effect model (a type of marginal structural model) (4,5). These models were developed to account for confounding in observational studies and have demonstrated the ability to mimic randomized clinical trial results. Since a clinical trial of exposure to passive smoking in childhood as a risk factor for the development of RA in adulthood is not feasible or ethical, investigation of this issue must use observational data. The life-course epidemiology approach and the state-of-the-art statistical models used in the study by Yoshida et al provide the best evidence to date regarding the association between passive smoking and RA development.

While a role for passive smoking aligns with previous work and the mucosal paradigm of RA pathogenesis (6), several unknowns remain. For example, residual confounding of factors such as socioeconomic status and/or other social determinants of health (e.g., poverty, poor diet) that are correlated with active and passive smoking may increase the risk of autoimmune disease and cannot be ruled out. Smoking also increases the risk of infections (7,8) and periodontal disease (9), which in turn could increase the risk of RA (10). As the authors note, smoking may also induce epigenetic

The content of this article is solely the responsibility of the authors and does not necessarily represent the official views of the NIH.

Dr. Gianfrancesco's work was supported the National Institute of Arthritis and Musculoskeletal and Skin Diseases, NIH (grant K01-AR-075085).

[1]Milena A. Gianfrancesco, PhD, MPH: University of California, San Francisco; [2]Cynthia S. Crowson, PhD: Mayo Clinic, Rochester, Minnesota.

Author disclosures are available at https://onlinelibrary.wiley.com/action/downloadSupplement?doi=10.1002%2Fart.41940&file=art41940-sup-0001-Disclosureform.pdf.

Address correspondence to Cynthia S. Crowson, PhD, 200 First Street Southwest, Rochester, MN 55905. Email: crowson@mayo.edu.

Submitted for publication July 13, 2021; accepted in revised form July 29, 2021.

changes years before symptoms develop in individuals genetically susceptible to RA. Lastly, there may be interaction effects with other factors, such as anti–citrullinated protein antibodies and rheumatoid factor, which were not explored in this analysis.

Although the specific mechanism remains unexplained, the research by Yoshida et al adds evidence to the literature suggesting that reducing exposure to passive smoking during early years may reduce the risk of RA in adulthood. Looking forward, interventions should focus on reducing not only personal smoking habits, but also secondhand smoke exposure in children, especially those at risk for autoimmune conditions (e.g., with familial susceptibility). Smoking harms nearly every organ of the body, and remains the leading cause of preventable disease, disability, and death in the US (11). Additionally, >40% of US children ages 3–11 years are exposed to secondhand smoke (12). Intervening on this important public health issue will not only potentially reduce the risk of RA, but also reduce the impact of other debilitating chronic diseases.

AUTHOR CONTRIBUTIONS

Drs. Gianfrancesco and Crowson drafted the article, revised it critically for important intellectual content, and approved the final version to be published.

REFERENCES

1. Giuseppe DD, Discacciati A, Orsini N, Wolk A. Cigarette smoking and risk of rheumatoid arthritis: a dose-response meta-analysis. Arthritis Res Ther 2014;16:R61.
2. Yoshida K, Wang J, Malspeis S, Marchand N, Lu B, Prisco LC, et al. Passive smoking throughout the life course and the risk of incident rheumatoid arthritis in adulthood among women. Arthritis Rheumatol 2021;73:2219–28.
3. Seror R, Henry J, Gusto G, Aubin HJ, Boutron-Ruault MC, Mariette X. Passive smoking in childhood increases the risk of developing rheumatoid arthritis. Rheumatology (Oxford) 2019;58:1154–62.
4. De Stavola BL, Daniel RM. Marginal structural models: the way forward for life-course epidemiology? [editorial]. Epidemiology 2012;23:233–7.
5. Cole SR, Hernán MA. Constructing inverse probability weights for marginal structural models. Am J Epidemiol 2008;168:656–64.
6. Sparks JA, Karlson EW. The roles of cigarette smoking and the lung in the transitions between phases of preclinical rheumatoid arthritis [review]. Curr Rheumatol Rep 2016;18:15.
7. US Department of Health and Human Services. The health consequences of involuntary exposure to tobacco smoke: a report of the surgeon general. 2006. URL: https://www.ncbi.nlm.nih.gov/books/NBK44324/.
8. US Department of Health and Human Services. A report of the surgeon general: how tobacco smoke causes disease: what it means to you. 2010. URL: https://www.cdc.gov/tobacco/data_statistics/sgr/2010/consumer_booklet/pdfs/consumer.pdf.
9. Ishikawa Y, Terao C. The impact of cigarette smoking on risk of rheumatoid arthritis: a narrative review. Cells 2020;9:475.
10. Joo YB, Lim YH, Kim K, Park K, Park Y. Respiratory viral infections and the risk of rheumatoid arthritis. Arthritis Res Ther 2019;21:199.
11. US Department of Health and Human Services. The health consequences of smoking—50 years of progress: a report of the surgeon general [review]. 2014. URL: https://www.ncbi.nlm.nih.gov/books/NBK179276/.
12. Homa DM, Neff LJ, King BA, Caraballo RS, Bunnell RE, Babb SD, et al. Vital signs: disparities in nonsmokers' exposure to secondhand smoke—United States, 1999–2012. MMWR Morb Mortal Wkly Rep 2015;64:103–8.

Arthritis & Rheumatology
Vol. 73, No. 12, December 2021, pp 2163–2165
DOI 10.1002/art.41951
© 2021, American College of Rheumatology

American College of Rheumatology
Empowering Rheumatology Professionals

EDITORIAL

Targeting the Myddosome in Systemic Autoimmunity: Ready for Prime Time?

Mariana J. Kaplan

Innate immune responses play key roles in the initiation and perpetuation of a variety of systemic autoimmune diseases, including rheumatoid arthritis (RA) and systemic lupus erythematosus (SLE) (1). While effective biologic agents and small molecules targeting innate and adaptive immune responses in these diseases are currently available, there are still significant gaps in the development of therapies that can hamper innate immune dysregulation in certain subgroups of patients in whom this pathway may play crucial pathogenic roles. Cellular receptors belonging to the Toll-like receptor (TLR)/interleukin-1 receptor (IL-1R) superfamily play fundamental roles in innate immune responses. TLRs sense pathogen-associated molecular patterns but are also implicated in detecting endogenous stimuli involved in immune dysregulation in autoimmune diseases, while members of the IL-1R family are stimulated by cytokines such as IL-1α and IL-1β (2). TLRs share with IL-1R a carboxyterminal intracellular domain that acts as a platform to recruit downstream signaling molecules. Upon activation with respective ligands, the intracellular Toll/IL-1R domains of TLR dimers initiate oligomerization of a multiprotein signaling platform comprising myeloid differentiation factor 88 and members of the interleukin-1 receptor–associated kinase (IRAK) family (3). Formation of this so-called myddosome complex initiates signal transduction pathways, leading to the activation of transcription factors and the production of various important inflammatory cytokines (4).

In this context, IRAK4 has a pivotal role as the master IRAK in TLR/IL-1R–triggered responses, as it functions upstream of other IRAK molecules. It serves as both a structural protein and a kinase, and both functions are required for myddosome complex formation. Switching on IRAK4 promotes the activation of NF-κB, interferon regulatory factor 5 (IRF-5), and the signaling pathways that lead to MAPK activity. Therefore, proper activation of this pathway leads to the synthesis of interferons (IFNs) and various proinflammatory cytokines including tumor necrosis factor (TNF), IL-1, and IL-6. While IRAK4 has been implicated in the pathogenesis of several autoimmune diseases, clinical development of IRAK4 inhibitors has been difficult due to conflicting effects on downstream inflammatory pathways related to inhibition of kinase activity versus scaffolding functions, as well as differences among species studied in the investigation of responses to the inhibitory effects of these compounds. Indeed, the selective utilization of IRAK kinases has been reported to differ substantially in mouse and human cells (5).

In this issue of *Arthritis & Rheumatology*, Winkler et al report that PF-06650833, an IRAK4-specific inhibitor, suppresses inflammation in preclinical models of RA and SLE and in phase I studies of healthy volunteers (6). The authors showed that PF-06650833 is highly selective as an inhibitor of the kinase activity of IRAK4. In in vitro experiments, it blocked specific downstream effects of disease-relevant stimuli in RA (inflammatory responses in synovial fibroblasts and immune complex–induced TNF production in macrophages) and in SLE (nucleic acid release from neutrophils and nuclear localization/activation of IRF-5 in monocytes, in response to TLR-7 agonists and/or lupus sera). Also relevant to SLE, PF-06650833 inhibited B cell cytokine synthesis and differentiation into plasma cells in response to IFNs and/or TLR-7 agonists and hampered type I IFN release by plasmacytoid dendritic cells and PBMCs in response to immune complexes. In in vivo systems, it inhibited various clinical and immunologic features in the rat collagen-induced arthritis model of RA and in 2 lupus models (pristane-induced lupus and the genetically prone MRL/*lpr* mouse model). In 2 previous studies, PF-06650833 had been well tolerated and induced a sustained decrease in serum high-sensitivity C-reactive protein levels in healthy volunteers (7).

Moving further into human in vivo studies, Winkler and colleagues performed 2 randomized, double-blind, ascending-dose phase I studies to assess the safety of PF-06650833 in healthy volunteers. The compound was well tolerated and induced a decrease of almost one-third in the type I IFN gene signature. As this inhibitory effect was tested in healthy subjects under

Mariana J. Kaplan, MD: National Institute of Arthritis and Musculoskeletal and Skin Diseases, NIH, Bethesda, Maryland.

Author disclosures are available at https://onlinelibrary.wiley.com/action/downloadSupplement?doi=10.1002%2Fart.41951&file=art41951-sup-0001-Disclosureform.docx.

Address correspondence to Mariana J. Kaplan, MD, Systemic Autoimmunity Branch, National Institute of Arthritis and Musculoskeletal and Skin Diseases, NIH, 10 Center Drive, 12N248C, Bethesda, MD 20892. Email: mariana.kaplan@nih.gov.

Submitted for publication July 26, 2021; accepted in revised form August 17, 2021.

steady-state conditions, it will be important to determine whether a significant inhibitory effect on the type I IFN gene signature that is enhanced in many SLE patients (1) can be achieved, and how the degree of inhibition will compare to that achieved with other currently used anti–type I IFN strategies (8).

Overall, this multimodal assessment of the potential efficacy of targeting IRAK4 activity in RA and SLE demonstrates promising effects on multiple innate inflammatory pathways relevant to a variety of chronic inflammatory conditions. These observations are supported by previously reported findings that indicate an antiinflammatory role of IRAK4 inhibition in crucial aspects of RA and SLE disease pathogenesis. These include end-organ complications, such as bone damage in the context of RA (9), as well as previous evidence from murine systems that IRAK4 is essential for autoimmune traits in various lupus-prone mouse models (10–12).

Although the study by Winkler et al presents many provocative findings, there are some limitations to the interpretation of the results. The renal phenotype in the pristane-induced lupus model on a BALB/c background was surprisingly mild and did not allow for full assessment of the role of an IRAK4 inhibitor in clinical kidney involvement in lupus, although the findings in the MRL/*lpr* mouse model do support the notion that IRAK4 inhibition could target lupus nephritis. The assessment of IRAK4 inhibition on the IFN signature in healthy volunteers under conditions of homeostasis is unlikely to adequately reflect the potential effects on dysregulated IFN pathways in SLE and other autoimmune diseases, which may not be entirely TLR dependent (13).

Safety will be a key issue to monitor in future studies in humans. Animals that lack IRAK4 are resistant to lipopolysaccharide challenge, display severe impairments in ability to synthesize proinflammatory cytokines, and are more susceptible to certain viral and bacterial infections (14). Of interest, despite the fundamental role of IRAK4 in innate immune signaling and danger sensing, patients with autosomal-recessive amorphic mutations in *IRAK4* display an immunologic syndrome with defective immunity in response to IL-1, IL-8, and various TLR ligands and effects on B cell subsets and IgM synthesis (15), but restricted effects on increased susceptibility to certain bacterial pyogenic infections that occur earlier, but not later, in life (16). These observations may suggest that, especially in adults, IRAK4 inhibition might provide benefits in autoimmune disorders without significantly hampering antimicrobial responses. Future studies will need to assess the safety effects of longer-term treatment with this compound in individuals with systemic autoimmunity.

Over the last few years an increased number of IRAK4 inhibitors have been developed and tested (5). While phase II and III studies will be needed to assess the role of these compounds in inhibiting various chronic inflammatory diseases, the results of the study by Winkler et al suggest a promising novel avenue that may be added to the armamentarium of drugs involved in hampering innate immune dysregulation in the context of systemic autoimmune disease. It will also be important to assess whether targeting of IRAK4 could be used in combination with other treatments (disease-modifying antirheumatic drugs or biologics) in patients whose disease may be resistant to more limited immunomodulatory therapy. Overall, identifying those patients with systemic autoimmunity in whom myddosome activation is a key dysregulated pathway in their specific syndrome and clinical presentation will be crucial in selecting those who may be more likely to benefit from such a targeted therapy.

AUTHOR CONTRIBUTIONS

Dr. Kaplan drafted the article, revised it critically for important intellectual content, and approved the final version to be published.

REFERENCES

1. Gupta S, Kaplan MJ. Bite of the wolf: innate immune responses propagate autoimmunity in lupus [review]. J Clin Invest 2021;131: e144918.
2. Lind NA, Rael VE, Pestal K, Liu B, Barton GM. Regulation of the nucleic acid-sensing Toll-like receptors [review]. Nat Rev Immunol 2021;16:1–12.
3. Huang YS, Misior A, Li LW. Novel role and regulation of the interleukin-1 receptor associated kinase (IRAK) family proteins [review]. Cell Mol Immunol 2005;2:36–9.
4. Bahia MS, Kaur M, Silakari P, Silakari O. Interleukin-1 receptor associated kinase inhibitors: potential therapeutic agents for inflammatory- and immune-related disorders [review]. Cell Signal 2015;27:1039–55.
5. Wiese MD, Manning-Bennett AT, Abuhelwa AY. Investigational IRAK-4 inhibitors for the treatment of rheumatoid arthritis [review]. Expert Opin Investig Drugs 2020;29:475–82.
6. Winkler A, Sun W, De S, Jiao A, Sharif MN, Symanowicz PT, et al. The interleukin-1 receptor–associated kinase 4 inhibitor PF-06650833 blocks inflammation in preclinical models of rheumatic disease and in humans enrolled in a randomized clinical trial. Arthritis Rheumatol 2021;73:2206–18.
7. Danto SI, Shojaee N, Singh RS, Li C, Gilbert SA, Manukyan Z, et al. Safety, tolerability, pharmacokinetics, and pharmacodynamics of PF-06650833, a selective interleukin-1 receptor-associated kinase 4 (IRAK4) inhibitor, in single and multiple ascending dose randomized phase 1 studies in healthy subjects. Arthritis Res Ther 2019;21:269.
8. Thorlacius GE, Wahren-Herlenius M, Ronnblom L. An update on the role of type I interferons in systemic lupus erythematosus and Sjogren's syndrome [review]. Curr Opin Rheumatol 2018;30:471–81.
9. Umar S, Palasiewicz K, van Raemdonck K, Volin MV, Romay B, Amin MA, et al. IRAK4 inhibition: a promising strategy for treating RA joint inflammation and bone erosion. Cell Mol Immunol 2021;18:2199–210.
10. Celhar T, Lu HK, Benso L, Rakhilina L, Lee HY, Tripathi S, et al. TLR7 protein expression in mild and severe lupus-prone models is regulated in a leukocyte, genetic, and IRAK4 dependent manner. Front Immunol 2019;10:1546.
11. Murphy M, Pattabiraman G, Manavalan TT, Medvedev AE. Deficiency in IRAK4 activity attenuates manifestations of murine Lupus. Eur J Immunol 2017;47:880–91.
12. Dudhgaonkar S, Ranade S, Nagar J, Subramani S, Prasad DS, Karunanithi P, et al. Selective IRAK4 inhibition attenuates disease in murine lupus models and demonstrates steroid sparing activity. J Immunol 2017;198:1308–19.

13. Lood C, Blanco LP, Purmalek MM, Carmona-Rivera C, De Ravin SS, Smith CK, et al. Neutrophil extracellular traps enriched in oxidized mitochondrial DNA are interferogenic and contribute to lupus-like disease. Nat Med 2016;22:146–53.
14. Suzuki N, Suzuki S, Duncan GS, Millar DG, Wada T, Mirtsos C, et al. Severe impairment of interleukin-1 and Toll-like receptor signalling in mice lacking IRAK-4. Nature 2002;416:750–6.
15. Maglione PJ, Simchoni N, Black S, Radigan L, Overbey JR, Bagiella E, et al. IRAK-4 and MyD88 deficiencies impair IgM responses against T-independent bacterial antigens. Blood 2014;124:3561–71.
16. Picard C, Casanova JL, Puel A. Infectious diseases in patients with IRAK-4, MyD88, NEMO, or IκBα deficiency [review]. Clin Microbiol Rev 2011;24:490–7.

Arthritis & Rheumatology
Vol. 73, No. 12, December 2021, pp 2166–2178
DOI 10.1002/art.41906
© 2021 American College of Rheumatology. This article has been contributed to by US Government employees and their work is in the public domain in the USA.

American College of Rheumatology
Empowering Rheumatology Professionals

REVIEW

A Decade of JAK Inhibitors: What Have We Learned and What May Be the Future?

Christine Liu,[1] Jacqueline Kieltyka,[1] Roy Fleischmann,[2] Massimo Gadina,[1] and John J. O'Shea[1]

The discovery of cytokines and their role in immune and inflammatory disease led to the development of a plethora of targeted biologic therapies. Later, efforts to understand mechanisms of cytokine signal transduction led to the discovery of JAKs, which themselves were quickly identified as therapeutic targets. It has been a decade since the first JAK inhibitors (jakinibs) were approved, and there are now 9 jakinibs approved for the treatment of rheumatic, dermatologic, hematologic, and gastrointestinal indications, along with emergency authorization for COVID-19. In this review, we will summarize relevant discoveries that led to first-generation jakinibs and review their efficacy and safety as demonstrated in pivotal clinical studies. We will discuss the next generation of more selective jakinibs, along with agents that target kinase families beyond JAKs. Finally, we will reflect on both the opportunities and challenges ahead as we enter the second decade of the clinical use of jakinibs.

Introduction

Cytokines serve as critical means of intercellular communication among immune and other cells, controlling many aspects of normal immune responses. However, their aberrant production results in the loss of immune homeostasis and exaggerated immune responses that underlie pathologies from autoimmunity to "cytokine storm."

The introduction of targeted anticytokine biologic (protein) therapies at the end of the 20th century led to dramatic improvements in our ability to treat many diseases, including rheumatoid arthritis (RA), psoriatic arthritis (PsA), ankylosing spondylitis (AS), psoriasis, atopic dermatitis, and inflammatory bowel disease (IBD). Their clinical success was largely driven by our understanding of the cells and molecules that drive these pathologies, which allowed the production of effective, generally safe, molecules that inhibit relevant inflammatory pathways. The development of biologic disease-modifying antirheumatic drugs (bMARDs)—namely, engineered proteins capable of selectively binding cytokines or their cognate receptors that include tumor necrosis factor (TNF), interleukin-1 (IL-1), IL-4/IL-13, IL-6, IL-17, and IL-12/23—was the capstone of years of research.

Many, but not all, of the cytokines that drive immunopathology act via type I or type II cytokine receptors. Cytokine binding to these receptors activates phosphotransferases (kinases) associated with the intracellular portion of these receptors. These kinases belong to a small family termed JAKs, comprising 4 members: JAK1, JAK2, JAK3, and TYK2. Different receptors are coupled with different JAKs working in pairs, either in a heterodimeric or homodimeric complex. Following receptor engagement, the JAKs phosphorylate themselves and tyrosine residues on the receptor chains that recruit the STAT family of DNA binding proteins. These factors are phosphorylated by the JAKs, resulting in their dimerization, translocation to the nucleus, and subsequent regulation of gene expression (Figure 1).

A series of mutant cell lines revealed the essential functions of JAKs in cytokine signaling (1), but identification of *JAK3* mutations in patients with severe combined immunodeficiency (SCID) revealed a critical role of JAK in vivo (2), as did various knockout mice. These insights led to the proposition that JAK inhibitors

Supported by the National Institute of Arthritis and Musculoskeletal and Skin Diseases Intramural Research Program.

[1]Christine Liu, BS, Jacqueline Kieltyka, BS, Massimo Gadina, PhD, John J. O'Shea, MD: National Institute of Arthritis and Musculoskeletal and Skin Diseases, NIH, Bethesda, Maryland; [2]Roy Fleischmann, MD: University of Texas Southwestern Medical Center, Dallas.

Drs. Gadina and O'Shea contributed equally to this work.

Author disclosures are available at https://onlinelibrary.wiley.com/action/downloadSupplement?doi=10.1002%2Fart.41906&file=art41906-sup-0001-Disclosureform.pdf.

Address correspondence to Massimo Gadina, PhD, Translational Immunology Section, Office of Science and Technology, Building 10, Room 10N311G, 10 Center Drive, Bethesda, MD 20892 (email: gadinama@mail.nih.gov); or to John J. O'Shea, MD, National Institute of Arthritis and Musculoskeletal and Skin Diseases, NIH, Building 10, Room 13C103, 10 Center Drive, Bethesda, MD 20892 (email: osheajo@mail.nih.gov).

Submitted for publication February 25, 2021; accepted in revised form June 23, 2021.

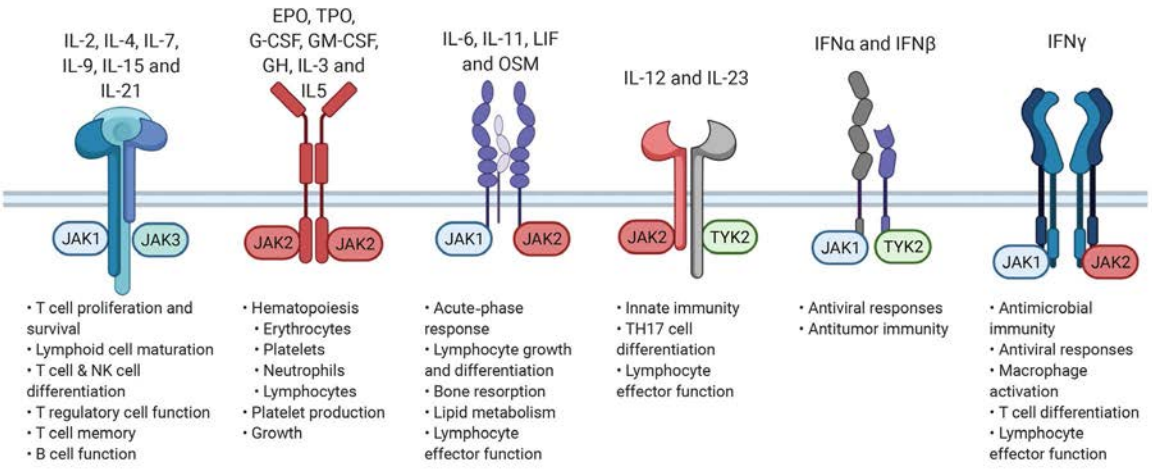

Pan-jakinibs Tofacitinib Delgocitinib Oclacitinib Gusacitinib Peficitinib	×	×	×	×	×	×
JAK1/JAK2-selective Baricitinib Cerdulatinib Ruxolitinib Momelotinib CTP-543	×	×	×	×	×	×
JAK1-selective Filgotinib Itacitinib Upadacitinib ARQ-252 Abrocitinib	×		×		×	×
JAK2-selective Gandotinib Fedratinib Pacritinib		×	×	×		×
JAK1/TYK2-selective Brepocitinib	×		×	×	×	×
JAK3-selective Ritlecitinib	×					
TYK2-selective BMS-986165				×	×	

Figure 1. Physiologic impact of JAK inhibitor (jakinib) targeting. Pan-jakinibs and jakinibs specific for the indicated JAK family members are listed. Type I and type II cytokine receptors (illustrations) associate with different members of the JAK family (JAK1, JAK2, JAK3, and TYK2) in order to transduce intracellular signals. Selective blockade of specific JAK molecules should inhibit specific biologic actions while allowing other JAK-dependent cytokines to signal normally. For example, by selectively inhibiting JAK1, the adverse events related to JAK2 inhibition, such as anemia and neutropenia, should be avoided. JAK3-mediated signaling, which is associated exclusively with the common γ-chain receptor, should also be unaffected, sparing T cell, B cell, and natural killer (NK) cell function. IL-2 = interleukin-2; EPO = erythropoietin; TPO = thrombopoietin; G-CSF = granulocyte colony-stimulating factor; GM-CSF = granulocyte–macrophage colony-stimulating factor; GH = growth hormone; LIF = leukemia inhibitory factor; OSM = oncostatin M; IFNα = interferon-α.

could represent a new class of immunomodulatory drugs (3). Recognition of *JAK2* gain-of-function mutations in myeloproliferative neoplasms (4) provided further rationale for JAK inhibition as an attractive therapeutic option. *TYK2* mutations in humans result in primary immunodeficiency (5), and *TYK2* variants are linked to a wide range of autoimmune diseases. Specifically, *TYK2* coding variants (e.g., rs34536443, P1104A) provide protection against multiple sclerosis, RA, psoriasis, and systemic lupus erythematosus (SLE) (5,6).

The development of jakinibs has accelerated over the past decade, with the subsequent approval of multiple agents and more candidates under investigation in various diseases. In this review, we will briefly discuss the efficacy of the approved jakinibs and their associated adverse events (AEs). Though these jakinibs are relatively specific for JAK family kinases, several inhibit multiple members of the family; other jakinibs demonstrate improved in vitro selectivity, which is influenced by a number of factors that will be discussed. We will also discuss the role of this class of drugs in the management of COVID-19.

Efficacy of approved jakinibs

The initially developed group of inhibitory molecules exert their effect by blocking the ATP-binding pocket of the JAK catalytic domain. Although these compounds are relatively selective, with limited off-target effects compared to other kinases, these jakinibs block the activity of multiple JAKs both in vitro and in vivo. Nonetheless, the promising results of these jakinibs in a wide range of preclinical disease models quickly led to investigation in multiple clinical settings and for diverse

Table 1. Approved JAK inhibitors and their current indications*

Drug	Target	Indication
Tofacitinib	JAK1/JAK2/JAK3	RA, PsA, UC, polyarticular course JIA
Baricitinib	JAK1/JAK2	RA, atopic dermatitis (approved in EU), COVID-19 (EUA)
Upadacitinib	JAK1	RA
Filgotinib	JAK1	RA (approved in EU, Japan)
Peficitinib	Multiple JAKs	RA (approved in Japan, Korea, Taiwan)
Ruxolitinib	JAK1/JAK2	Myeloproliferative neoplasms , acute GVHD
Fedratinib	JAK2/FLT3/RET/BRD-4	Myeloproliferative neoplasms
Delgocitinib (topical)	Multiple JAKs	Atopic dermatitis (approved in Japan)
Oclacitinib	Multiple JAKs	Atopic dermatitis (in dogs)

* RA = rheumatoid arthritis; PsA = psoriatic arthritis; UC = ulcerative colitis; JIA = juvenile idiopathic arthritis; EU = European Union; EUA = emergency use authorization; GVHD = graft-versus-host disease; BRD-4 = bromodomain-containing protein 4.

pathologies; regulatory agencies have now approved 9 jakinibs (Table 1).

The first jakinib to enter clinical trials, initially for renal transplantation, was tofacitinib, which inhibits JAK1/JAK2/JAK3; however, ruxolitinib, a JAK1/JAK2 inhibitor, was the first agent to receive approval, as a treatment for myeloproliferative neoplasms that often exhibit gain-of-function *JAK2* mutations. Ruxolitinib is also approved for steroid-refractory acute graft-versus-host disease (GVHD).

Tofacitinib was the first jakinib to be approved for the treatment of a rheumatic disease, specifically for patients with RA with an incomplete response to a conventional synthetic DMARD (csDMARD), either as tofacitinib monotherapy or in combination with a csDMARD (7–11). Subsequently, tofacitinib has been approved for PsA (12,13) and ulcerative colitis (UC) (14).Tofacitinib has also been approved for the treatment of polyarticular course juvenile idiopathic arthritis (JIA) in the US.

Baricitinib, a JAK1/JAK2 inhibitor, is approved for patients with RA in the US, with a dosage limited to 2 mg every day in combination with a csDMARD, or as monotherapy in patients with RA refractory to a bDMARD, based on phase III trial results. In many other countries, both 2 mg and 4 mg doses are approved for patients with an incomplete response to csDMARDs (15–18). Baricitinib is also approved for the treatment of atopic dermatitis in Europe.

Peficitinib, a pan-JAK inhibitor, is approved in Japan, Republic of Korea, and Taiwan for the treatment of RA in patients with an incomplete response to csDMARDs (19,20). Tofacitinib, baricitinib, and peficitinib have shown clinical, functional, and radiographic efficacy, after failure of a csDMARD, prior to treatment with a bDMARD, or after treatment with a bDMARD. Broadly speaking, with the exception of peficitinib, jakinibs have been documented to be more effective than methotrexate (MTX) (7,18).

Selective targeting of JAK1 should block the broadest cytokine profile compared to targeting of other JAKs, while avoiding a negative impact on hematopoiesis by sparing erythropoietin, thrombopoietin, and granulocyte colony-stimulating factor (G-CSF) signaling. Two jakinibs with relative JAK1 selectivity have been approved in RA: upadacitinib in many countries, including the US, the European Union (EU), Canada, and Japan, and filgotinib in the EU and Japan. Phase III trials demonstrated clinical, functional, and radiographic efficacy both in combination with a csDMARD or as monotherapy in patients with incomplete response to a csDMARD or a bDMARD (21–27). Upadacitinib monotherapy has also been shown to be more effective than MTX in MTX-naive patients with RA (24). Both upadacitinib and filgotinib have been referred to as "second-generation jakinibs" since they both preferentially inhibit JAK1 in vitro but their clinical efficacy and safety, to a large extent, is similar to pan-jakinibs in RA, although anemia and herpes zoster are seen less often with filgotinib.

The clinical responses to jakinibs are more rapid than clinical responses to bDMARDs, with a clinical effect shown as early as the first week of jakinib therapy, as well as more rapid and deeper pain alleviation. Of clinical interest, tofacitinib, baricitinib, upadacitinib, and filgotinib were all at least as effective as a bDMARD in those with an incomplete response to MTX, which suggests that after an incomplete response to a csDMARD, one can utilize a jakinib prior to a bDMARD. Additionally, if a patient does not respond adequately to a jakinib (upadacitinib), they may respond to a TNF inhibitor (adalimumab) (17,25,26,28,29).

Whether greater selectivity of JAK inhibition will lead to different outcomes remains unclear, and there is currently a lack of well-designed clinical studies evaluating the efficacy or safety of one jakinib compared to another. Determination of selectivity is not simple and is dependent upon the nature of the assay, whether the assay is done in whole blood, and exactly what is being measured. Evaluation of the in vitro cellular selectivity of baricitinib, tofacitinib, upadacitinib, and filgotinib has shown that all 4 agents inhibit IL-6 and interferon-α (IFNα) signaling; upadacitinib and tofacitinib were more potent inhibitors of JAK1/JAK3-dependent cytokines (IL-2, IL-4, IL-15, and IL-21) than baricitinib and filgotinib; and baricitinib, tofacitinib, and upadacitinib, but not filgotinib, inhibited the JAK2/JAK2 and JAK2/TYK2 cytokines IL-3, GM-CSF, and G-CSF but to varying degrees (30,31). Upadacitinib was the most potent inhibitor of the JAK2/JAK2-dependent cytokines IL-3 and GM-CSF, followed by baricitinib and tofacitinib; filgotinib was the least potent JAK2 inhibitor. Tofacitinib was

Table 2. Selected ongoing clinical trials of first-generation JAK inhibitors*

Agent, specificity and indication	ClinicalTrials.gov identifier
Tofacitinib, JAK1/JAK2/JAK3	
Down syndrome	NCT04246372
COVID-19	NCT04332042, NCT04415151, NCT04390061, and NCT04469114
Inflammatory eye disease (uveitis and scleritis)	NCT03580343
Sjögren's syndrome	NCT04496960
SLE	NCT03288324
Ruxolitinib, JAK1/JAK2†	
COVID-19	NCT04348071, NCT04477993, NCT04414098, NCT04359290, NCT04377620, NCT04348695, NCT04374149, NCT04424056, NCT04338958, NCT04403243, and NCT04334044
Vitiligo	NCT04530344, NCT04057573, NCT04052425, and NCT03099304
Thrombocythemia and polycythemia vera	NCT04644211, NCT04116502, NCT02962388, NCT03669965, NCT02577926, NCT03952039, and NCT04455841
Hypereosinophilic syndrome or primary eosinophilic disorders	NCT03801434 and NCT00044304
Atopic dermatitis	NCT03745638
Hidradenitis suppurativa	NCT04414514
Baricitinib, JAK1/JAK2	
COVID-19	NCT04340232, NCT04320277, NCT04399798, NCT04421027, NCT04393051, NCT04373044, NCT04640168, and NCT04321993
Alopecia areata	NCT03570749 and NCT03899259
JIA	NCT03773965, NCT04088396, and NCT03773978
SLE	NCT03843125, NCT03616964, and NCT03616912
Atopic dermatitis	NCT03559270, NCT03952559, NCT03435081, NCT03334435, and NCT03428100
GVHD	NCT02759731
Giant cell arteritis	NCT03026504
Uveitis	NCT04088409
Aicardi-Goutières syndrome	NCT03921554
Idiopathic inflammatory myopathies	NCT04208464
PMR	NCT04027101
Fedratinib	
Myelofibrosis/polycythemia vera	NCT03755518, NCT03952039, NCT04282187, NCT04446650, NCT04629508, NCT04562870, and NCT04370301
Delgocitinib, JAK1/JAK2/JAK3/TYK2	
Atopic dermatitis	NCT03826901 and NCT03725722
Chronic hand eczema	NCT03683719
CTP-543, JAK1/JAK2	
Alopecia areata	NCT03898479 and NCT04518995

* SLE = systemic lupus erythematosus; JIA = juvenile idiopathic arthritis; GVHD = graft-versus-host disease; PMR = polymyalgia rheumatica.
† Trials for cancer and/or malignancies were excluded.

the most potent inhibitor of the JAK2/TYK2-dependent cytokine G-CSF, followed by upadacitinib and baricitinib (31).

A common measure of JAK inhibition is the assessment of cytokine-induced STAT phosphorylation, and a nuanced aspect of the assay is exactly what STAT is being measured; measurement of different STATs can give different answers. Thus, interpretation of selectivity appears to also be influenced by the cytokine and STAT being assessed. Most receptors use JAKs in pairs, but the importance of one JAK versus the other in signaling is still not fully understood and will require more basic research and likely more specific agents. Perhaps most important in terms of safety and efficacy is that no jakinib mediates sustained reduction in cell signaling throughout the dosing interval—a high degree of JAK inhibition is very transient. This is likely to be relevant for side effects. Nonetheless, while the clinical relevance of these differences is unclear, jakinibs all appear to have similar efficacy and safety with the exception of fewer cases of anemia and herpes zoster with filgotinib.

Ongoing trials are investigating the efficacy of jakinibs in a wide range of additional indications. Phase III studies involving patients with active AS demonstrated promising efficacy and improvement with tofacitinib (32) and upadacitinib (33). Efficacy of upadacitinib in PsA has also recently been reported, with 30 mg upadacitinib shown to be superior to adalimumab (34,35). Upadacitinib has been evaluated in dose-ranging trials assessing efficacy in Crohn's disease (CD) and UC and has shown efficacy in both (36,37). Upadacitinib was found to be more effective than placebo in atopic dermatitis (38), and phase III trials are ongoing. Although phase II studies of filgotinib in PsA, AS, CD, and UC had positive results, these clinical development programs have been

Table 3. Major side effects of JAK inhibitors

Infections
Serious and opportunistic infections
Herpes zoster
Hematologic side effects
Anemia
Leukopenia
Thrombocytopenia
Venous thrombosis*
Hyperlipidemia

* Studies have shown conflicting results (34,46,55–57).

halted subsequent to the complete response letter from the US Food and Drug Administration (FDA) denying approval for filgotinib at present (39–41).

An open-label trial of subjects with refractory dermatomyositis receiving tofacitinib and a trial of tofacitinib in combination with glucocorticoids in subjects with amyopathic dermatomyositis-associated interstitial lung disease both suggested efficacy and reasonable safety profiles (42,43). In a compassionate use program for patients with refractory juvenile dermatomyositis, preliminary data indicated clinically significant improvements with baricitinib treatment (44). Other indications being investigated include alopecia areata, SLE, interferonopathies including Down syndrome, relapsing giant cell arteritis, GVHD, myasthenia gravis, and vitiligo (Table 2). Delgocitinib (JTE-052) is a topical jakinib approved in Japan for atopic dermatitis and oclacitinib, a JAK1/JAK2/JAK3 inhibitor, is approved for canine allergic dermatitis.

Safety of approved jakinibs

Jakinibs have been confirmed to be reasonably safe, with an AE profile that is similar to bDMARDs, although the specific AEs are somewhat different (Table 3). Many of the AEs seen with jakinibs could have been predicted based on their mechanism of action, while others could not. Common side effects are infections, including serious and opportunistic infections and herpes zoster (45–47). Vaccination with recombinant adjuvanted herpes zoster subunit is generally safe in patients with autoimmune disease, although flares are not uncommon (48,49). Investigation of the serologic response to the recombinant vaccine in RA patients treated with jakinibs suggests satisfactory antibody responses and acceptable tolerability (50). In contrast to herpes zoster, the rates of influenza AEs in an RA clinical program were comparable in the tofacitinib, adalimumab, MTX, and placebo groups (51).

Cytopenias such as neutropenia and anemia are also common AEs, likely due to JAK2 inhibition. Upadacitinib, a relatively JAK1-selective molecule, has similar effects as pan-jakinibs with regard to anemia, whereas anemia appears to occur less frequently in patients treated with filgotinib. Jakinibs can also result in lymphopenia, in particular a reduction in natural killer (NK) cells, related to JAK3 inhibition. Jakinib administration has been associated with elevated serum lipid levels due to reduced cholesterol ester catabolism, increasing cholesterol levels toward those in healthy volunteers, and improvement in markers of antiatherogenic high-density lipoprotein function (52).

The FDA requested a long-term safety study after the approval of tofacitinib in 2012, evaluating the safety of tofacitinib 5 mg and 10 mg twice daily versus a TNF inhibitor (TNFi), all in combination with MTX, in subjects with RA who were 50 years of age or older and had at least one additional cardiovascular risk factor (ORAL-Surveillance). The coprimary end points were noninferiority of the combined tofacitinib doses (5 mg and 10 mg twice a day) compared to the TNFi (etanercept or adalimumab) regarding 1) major adverse cardiovascular events (MACE) and 2) malignancies. Noninferiority was defined by the upper bound of the confidence interval not being greater than 1.8 (lower bound not calculated). The top-line results have been reported. Although the incidence rates for both end points for both mechanisms were <1.2 per 100/patient-years, with the differences between tofacitinib and TNFi being 0.25–0.35, the prespecified noninferiority criteria were not met for the primary comparison of the combined tofacitinib doses to TNFi. As seen for tofacitinib in the general RA population, the most frequently reported MACE was myocardial infarction, and the most frequently reported malignancy was lung cancer. Of note, most of the events with both mechanisms occurred in subjects with a higher prevalence of known risk factors for MACE and malignancy (e.g., older age, smoking) and one can only conclude that there is probably a slight advantage of TNFi over tofacitinib for avoiding such events but cannot conclude that tofacitinib increases these events (53,54).

A concern that the incidence of venous thromboembolism (VTE), including pulmonary embolism, would be increased was originally raised with regard to baricitinib. During the placebo-controlled portion of the phase III studies, there was an imbalance in the development of VTEs, which occurred only in the 4 mg group and not in the 2 mg or placebo groups. However, in a report of >8 years of follow-up, the incidence rate of VTE was comparable between the 2 mg and 4 mg groups and similar to what has been observed in RA patients treated with agents with other mechanisms of action (46). No disparity was seen in the clinical trials of tofacitinib (34) and upadacitinib (55).

Other studies have shown that there is no evidence of short-term risk of MACE or VTEs in RA patients initiating jakinibs (56). However, the situation has been confused because of the results of ORAL-Surveillance. Prior to completion of the study, data were released suggesting that, while there was not a statistically significant difference in the risk of VTE or pulmonary embolism between the tofacitinib 5 mg twice a day and TNFi groups, there was a significantly increased risk in the tofacitinib 10 mg twice a day a group, and a numerical difference favoring TNFi over 5 mg tofacitinib twice a day. For that reason, the European Medicines Agency placed severe restrictions on the use of tofacitinib, while the FDA strengthened its guidance and has proposed that a jakinib should be utilized after failure of a TNFi.

Table 4. Selected ongoing clinical trials of JAK inhibitors*

Agent, specificity, indication	ClinicalTrials.org identifier
Upadacitinib, JAK1	
Atopic dermatitis	NCT03569293, NCT03738397, NCT03568318, NCT03661138, NCT04195698, NCT03607422, and NCT04666675
Hidradenitis suppurativa	NCT04430855
Spondyloarthritis	NCT04169373
PsA	NCT03104374 and NCT03104400
AS	NCT03178487
SLE	NCT03978520 and NCT04451772
UC	NCT03653026, NCT03006068, and NCT02819635
CD	NCT03345836, NCT03345823, NCT02782663, and NCT02365649
Takayasu arteritis	NCT04161898
Giant cell arteritis	NCT03725202
Filgotinib, JAK1	
RA	NCT02065700 and NCT03025308
PsA	NCT03320876, NCT04115839, and NCT04115748
CD	NCT02914600, NCT02914561, and NCT03077412
AS	NCT04483700 and NCT04483687
UC	NCT02914535
IBD	NCT03201445
Noninfectious uveitis	NCT03207815
Abrocitinib, JAK1	
Atopic dermatitis	NCT04345367, NCT03422822, and NCT03915496
Itacitinib, JAK1	
Acute GVHD	NCT03846479
Chronic GVHD	NCT04200365, NCT03584516, and NCT04446182
Prophylaxis for GVHD and immune effector cell therapy (prevention of cytokine release syndrome)	NCT04071366 and NCT04339101
Asthma	NCT04129931
Myeloproliferative neoplasms/myelofibrosis	NCT04640025, NCT03144687, NCT01633372, and NCT04629508
Non–small cell lung cancer	NCT03425006 and NCT02917993
ARQ-252, JAK1	
Hand eczema	NCT04378569
BMS-986165, TYK2	
SLE	NCT03252587 and NCT03920267
Lupus nephritis	NCT03943147
CD	NCT03599622
UC	NCT03934216 and NCT04613518
PsA	NCT03881059
Plaque psoriasis	NCT03624127, NCT03611751, and NCT04167462
Psoriasis	NCT04036435 and NCT03924427
Brepocitinib (PF-06700841), TYK2/JAK1	
Psoriasis	NCT03850483
Acne inversa	NCT04092452
Hidradenitis suppurativa	NCT04092452
Non-segmental vitiligo	NCT03715829
PsA	NCT03963401
SLE	NCT03845517
CD	NCT03395184
UC	NCT02958865
Ritlecitinib, JAK3/TEC kinases	
RA	NCT02969044
CD	NCT03395184
UC	NCT02958865
Non-segmental vitiligo	NCT03715829
Alopecia areata	NCT03732807, NCT04006457, and NCT04517864
Cerdulatinib, JAK1/JAK2/Syk†	
Vitiligo	NCT04103060
Momelotinib, JAK1/JAK2/ALK1	
Myeloproliferative neoplasms	NCT04173494
Pacritinib, JAK2/IRAK1†	
GVHD	NCT02891603
Myeloproliferative neoplasms	NCT03645824 and NCT03165734
COVID-19	NCT04404361
Gusacitinib (ASN002), JAK1/JAK2/JAK3/TYK2/Syk†	
Chronic hand dermatitis	NCT03728504
Atopic dermatitis	NCT03531957

* PsA = psoriatic arthritis; AS = ankylosing spondylitis; SLE = systemic lupus erythematosus; UC = ulcerative colitis; CD = Crohn's disease; RA = rheumatoid arthritis; IBD = inflammatory bowel disease; GVHD = graft-versus-host disease; ALK1 = activin receptor–like kinase 1.
† Trials for cancer and/or malignancies have been excluded.

In further analysis and meta-analyses in patients treated with jakinibs compared to placebo, no clear evidence of jakinib-associated VTE could be found; therefore, longer-term data are needed to assess the risk of these events (57). To complicate matters further, there has been no clear mechanism that explains an increased risk of VTE with jakinibs, and thus, this is an area that requires further exploration. Regarding the risk of developing malignancies in RA, patients treated with jakinibs revealed higher rates of malignancy in the treated groups versus controls in a meta-analysis of 36 trials, but these differences did not reach statistical significance (58).

A long-term safety study of tofacitinib integrating data from phase I, II, IIIb/IV, and long-term extension studies in adult patients with RA (n = 7,061) found that AEs were stable over time and that incident rates were consistent with previous reports. No new safety risks were observed over the span of 9.5 years of cumulative tofacitinib exposure, and rates of safety events were comparable to those observed for bDMARDs and other jakinibs (59).

Filgotinib, but not other jakinibs, produced defects in spermatogenesis in rodent models, which prompted a safety study in male patients to investigate whether the 200 mg dose would have similar effects in humans. The top-line results have been reported: 8.3% of the patients receiving placebo and 6.7% of the patients receiving filgotinib had a ≥50% decline in sperm concentration at week 13. The study is ongoing, and results indicating whether the decrease will persist or affect more patients receiving filgotinib over time are still pending (60).

In summary, multiple trials support the conclusion that in RA, jakinibs are at least equivalent to or are superior to TNFi when used with a csDMARD in inducing a rapid response, with a reduction in pain observed in as early as 1 week. Jakinibs have safety profiles generally comparable to biologics, with the exceptions of an increased frequency of herpes zoster infection and hematologic side effects, and a slightly higher risk of MACE and malignancy in older patients with a history of smoking.

Next-generation jakinibs

The success of jakinibs has motivated the development of yet more jakinibs (Table 4). CTP-543, a deuterium-modified form of ruxolitinib, has received breakthrough and fast-track designation from the FDA and is currently being assessed in phase II and III studies of alopecia areata. Deuterated compounds have the potential advantage of improved pharmacokinetics with lower rates of metabolism, and hence a longer half-life.

Another JAK1-selective jakinib, abrocitinib, has been evaluated in phase III trials in atopic dermatitis and plaque psoriasis (61,62), showing efficacy in both diseases. AEs included herpes simplex and herpes zoster infection, appendicitis, pancreatitis, and IBD. No cases of VTEs, malignancies, MACE, or deaths were observed. Decreased platelet counts were noted with no decrease in hemoglobin. The JAK1-selective inhibitor, itacitinib, is currently being assessed in multiple clinical trials for oncologic indications as well as for chronic and acute GVHD, including GVHD prophylaxis. ARQ-252 is a selective topical JAK1 inhibitor, and a phase I/IIb trial in adults with chronic hand eczema is underway.

Inhibition of TYK2 would be expected to impact type I and type III IFNs, IL-10 family cytokines, IL-12, and IL-23, but not other cytokines. The success of monoclonal antibodies targeting IL-12 and IL-23 with acceptable AEs, along with *TYK2* coding variants being associated with reduced incidence of autoimmunity (63,64), support the potential efficacy of TYK2 inhibition. Deucravacitinib (BMS-986165) has shown efficacy in a psoriasis trial (65) and significantly greater American College of Rheumatology 20% improvement rates compared to placebo in patients with PsA. No anemia, cytopenias, serious infections, herpes zoster, opportunistic infections, or thrombotic events were observed (66). Trials are ongoing in SLE, including lupus nephritis, and in CD and UC. Unlike other jakinibs, deucravacitinib binds to the kinase-like domain (67). Since the kinase-like domain is a relatively unique feature of JAKs, in principle, this strategy could provide increased kinome selectivity.

PF-06826647 is a TYK2-selective jakinib (68) currently in trials for the treatment of psoriasis, UC, and hidradenitis suppurativa; brepocitinib is a TYK2/JAK1 inhibitor that was assessed in a phase II trial of psoriasis where clinical responses were seen with all doses (69). Ongoing investigations of either oral or topical brepocitinib include trials in atopic dermatitis, SLE, CD, UC, alopecia areata, hidradenitis suppurativa, and vitiligo.

Though the goal of JAK1- and TYK2-selective inhibitor use is to minimize JAK2 signaling interference and subsequent cytopenias, specifically targeting JAK2 can offer a treatment advantage for myeloproliferative neoplasms and potentially other hematologic malignancies. Fedratinib is a selective JAK2 inhibitor approved for primary and secondary myelofibrosis. An important AE observed with fedratinib is Wernicke's encephalopathy, which has been observed in patients taking the highest daily dosage (500 mg) (70). Fedratinib exerts off-target inhibitory activity against bromodomain-containing protein 4 and is effective regardless of JAK2 mutational status. Phase III trials are ongoing to assess fedratinib for long-term safety, efficacy, and its effects on overall survival (71).

Gandotinib is a JAK2-selective inhibitor that has potential increased potency for the $JAK2^{V617F}$ mutant kinase and has shown efficacy in myeloproliferative neoplasm (72), although there are currently no ongoing clinical investigations of gandotinib.

Within the JAK family, the action of JAK3 is seemingly most restricted because of its exclusive association with the common γ-chain, a shared subunit used by IL-2, IL-4, IL-7, IL-19, IL-15, and IL-21. Mutations of either the γ-chain (encoded by *IL2RG*) or *JAK3* lead to the complete absence of signaling of these cytokines and the consequent development of SCID, characterized by depletion of T, B, and NK cells, but with no other defects. Thus, JAK3 has been identified as a potential target to treat various inflammatory and autoimmune diseases.

Developed to target the kinase domain of JAK3, decernotinib (VX-509) showed selective in vitro inhibition of JAK3 over the other JAKs and efficacy in RA (73,74). However, a CYP3A4-mediated drug–drug interaction was also described, potentially limiting the use of decernotinib; development of this molecule has currently been halted (75).

Beyond just JAKs

Despite the effort to search for drugs with greater specificity, there may be advantages in efficacy in targeting JAKs along with kinases involved in other signaling pathways (Table 4). Ritlecitinib is an irreversible covalent inhibitor that binds to a distinct cysteine residue in the JAK3 catalytic domain, which other JAK family members lack. However, TEC family kinases possess this cysteine residue in their kinase catalytic domains. The TEC family consists of 5 members: Bruton's tyrosine kinase, bone marrow

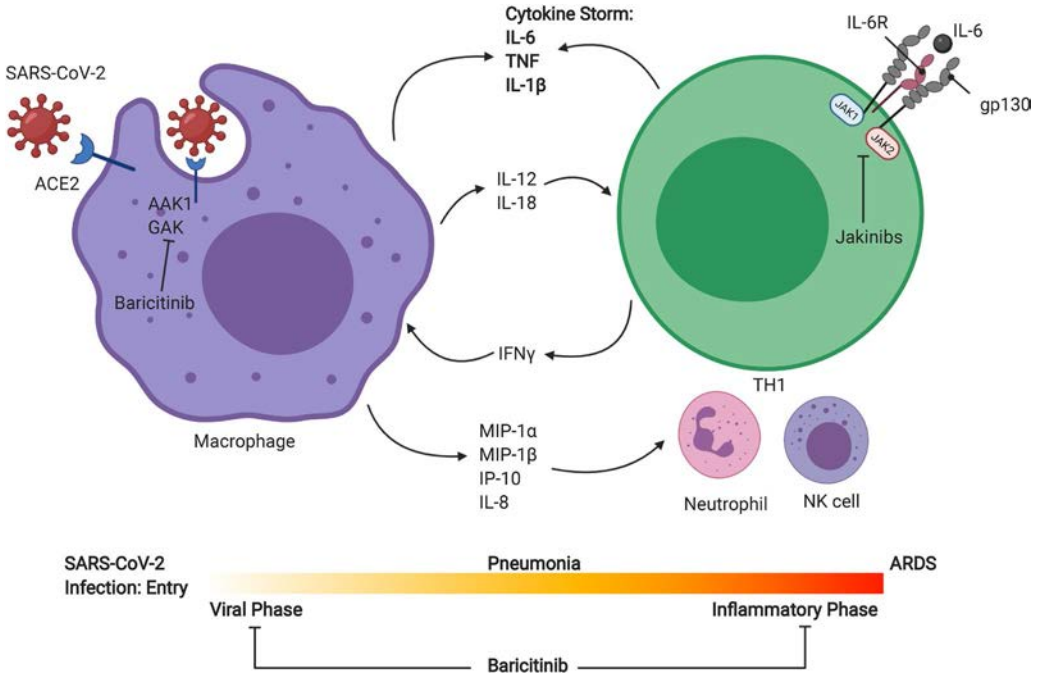

Figure 2. Potential mechanisms of JAK inhibitors (jakinibs) in blocking SARS–CoV-2 viral invasion and suppressing cytokine storm syndrome. SARS–CoV-2 entry is mediated by angiotensin-converting enzyme 2 (ACE-2), a receptor widely expressed in the lungs, heart, vasculature, kidneys, and gastrointestinal tract. The primary site of infection is alveolar epithelial cells in the lungs, and rapid replication of virus can lead to a hyperimmune response. Macrophage activation and chemokine release for neutrophil, Th1, and natural killer (NK) cell recruitment can lead to a massive cytokine release responsible for the clinical evolution to acute respiratory distress syndrome (ARDS). Jakinibs such as baricitinib can potentially block viral entry by inhibiting numb-associated kinase family proteins AP2-associated protein kinase 1 (AAK1) and cyclin G–associated kinase (GAK). During the inflammatory phase, many of the cytokines elevated in COVID-19 (interleukin-6 [IL-6], IL-12, and interferon-γ [IFNγ]) signal via JAKs, and therefore, jakinibs are being considered as potential therapeutics in severe SARS–CoV-2. TNF = tumor necrosis factor; MIP-1α = macrophage inflammatory protein 1α; IP-10 = IFNγ-inducible 10-kd protein; IL-6R = IL-6 receptor.

tyrosine kinase on chromosome X, IL-2–inducible T cell kinase, resting lymphocyte kinase, and TEC protein tyrosine kinase. These kinases are important mediators of signaling for T cell antigen receptors, B cell antigen receptors (BCR), and chemokine receptors. Thus, ritlecitinib targets more than just type I/II cytokine receptor signaling. Ritlecitinib was found to be superior to placebo in a phase II study in RA patients with an inadequate response to MTX (76). AEs included lymphopenia and infections such as herpes simplex. Ritlecitinib is currently in phase II trials for CD, UC, alopecia areata, and vitiligo.

Spleen tyrosine kinase (Syk) is highly expressed in hematopoietic cells and plays important and varied roles in immune cell signaling from BCR and FcR to lectins and integrins. Thus, simultaneous targeting of Syk along with JAKs could have utility in the treatment of immune and inflammatory disease. Gusacitinib (ASN002) is an oral JAK/Syk inhibitor that showed clinical efficacy, associated with decreased expression of inflammatory biomarkers, in a phase II trial in atopic dermatitis (77). Another JAK/Syk inhibitor, cerdulatinib (PRT062070), has been tested in several trials for the treatment of leukemia and lymphoma, and a topical formulation is being tested in phase II trials in patients with vitiligo.

Momelotinib is a JAK1/JAK2 inhibitor as well as an activin receptor–like kinase (ALK1) inhibitor. Because ALK1 is a receptor for bone morphogenic proteins, momelotinib is undergoing testing for the treatment of myelofibrosis (78). Pacritinib is a JAK2 and IL-1 receptor–associated kinase 1 inhibitor also being evaluated for the treatment of myelofibrosis. Blocking IL-1 and Toll receptor signaling might offer some interesting opportunities for autoimmune disease treatment.

Jakinibs in COVID-19

The emergence of a pandemic due to the novel coronavirus SARS–CoV-2 with its associated severe systemic immune hyperactivation has motivated the search for novel therapeutics to treat COVID-19 cytokine release syndrome, also termed cytokine storm (Figure 2). The extremely elevated levels of multiple cytokines are associated with pulmonary and endothelial disease, myocardial damage, and mortality. Consequently, the search for effective drugs to manage COVID-19 has focused on the modulation of cytokines. While dexamethasone has shown efficacy for the treatment of COVID-19 in the Randomized Evaluation of Covid-19 Therapy (RECOVERY) trial (79), the use of biologics has not consistently demonstrated efficacy.

Many of the cytokines elevated in COVID-19, including IL-2, IL-6, IL-12, IFNγ, and GM-CSF, signal via JAKs. For this reason,

jakinibs were considered potential therapeutic candidates. However, an obvious argument against the use of jakinibs is the risk of increased infection. While jakinibs generally have a reasonable degree of kinome selectivity, baricitinib additionally inhibits the Numb-associated kinase (NAK) family, AP2-associated protein kinase 1, and cyclin G–associated kinase (80,81) involved in viral entry of SARS–CoV-2. Several small trials have shown efficacy of ruxolitinib in the context of severe SARS–CoV-2 (82,83).

Baricitinib has shown utility in small trials in COVID-19 (84,85). Adaptive Covid-19 Treatment Trial 2 (ACTT-2) (86) is a double-blind, randomized, placebo-controlled trial testing remdesivir plus 4 mg baricitinib daily versus remdesivir plus placebo. This study enrolled 1,033 hospitalized adults with COVID-19 in 67 sites in 8 countries, and assessed the outcomes of time to recovery and clinical status at day 15. The results showed that baricitinib plus remdesivir was safe and superior to remdesivir alone for patients with COVID-19–associated pneumonia. The observed benefit of combination treatment was most evident in patients receiving supplemental oxygen, high-flow oxygen, or noninvasive ventilation. Overall, patients receiving baricitinib had a median time to recovery of 7 days compared to 8 days for control patients, whereas the time to recovery for patients receiving oxygen or noninvasive ventilation was 10 days for those treated with baricitinib plus remdesivir versus 18 days for those treated with remdesivir plus placebo. The benefit of the combination treatment was less evident in patients who did not require oxygen or in patients who required mechanical oxygenation or extracorporeal membrane oxygenation. Importantly and perhaps surprisingly, serious AEs, including infection, were less frequent in the combination group than in the control group.

ACTT-4, the fourth adaptive COVID-19 treatment trial, randomized patients to receive either remdesivir, intravenous (IV) dexamethasone, and placebo tablets or remdesivir, baricitinib tablets, and IV placebo. The goal was to assess which combination was more effective at preventing adults hospitalized with COVID-19 and receiving supplemental oxygen from progressing to requiring mechanical ventilation or death. Upon review of the current data, the Data Safety Monitoring Board determined that it is unlikely that the study will show a significant difference between these 2 arms even if the trial continued to full enrollment of 1,500 participants. As a result, enrollment in the trial was closed after slightly more than 1,000 participants were enrolled. Thus, at present, the 2 strategies appear to be equivalent (87).

An important outstanding question is the relevance of the potential antiviral activity of baricitinib via its inhibition of the NAK family. The Study of Baricitinib (LY3009104) in Participants With COVID-19 (COV-BARRIER) examined the addition of baricitinib versus placebo to standard of care. The results have been announced but not yet published. The primary end points were progression to noninvasive or invasive mechanical ventilation or death, which was not statistically significant in the baricitinib group, although a reduction in mortality was seen without additional AEs (88).

Many other trials with a variety of jakinibs are underway and will hopefully assess the utility of baricitinib versus other jakinibs. Beyond COVID-19, the data beg the question as to whether jakinibs have broad use in sepsis and acute respiratory distress syndrome.

Conclusions and challenges ahead

The year 2011 witnessed the approval of the first jakinib, ruxolitinib. Since that time, it has been remarkable to see the rapid development of multiple jakinibs and their approval for use in a broad range of indications, crossing multiple clinical specialties. We now know that jakinibs are generally as safe and effective as biologics, albeit with some differences in safety, and exert their effect more rapidly. Not surprisingly, they are being tested for the treatment of a plethora of disorders, from genetic interferonopathies to COVID-19. Despite the impressive advances, many questions remain.

In RA, should jakinibs be used prior to MTX, assuming equal patient access and affordability? Tofacitinib, baricitinib, and upadacitinib have been shown to be more efficacious than MTX, but there are some differences in safety and tolerability—some of which favor MTX while others favor jakinibs. Should jakinibs be used prior to bDMARDs considering that each jakinib has been shown to be at least as effective as bDMARDs and that jakinibs have the advantage of oral administration with rapid benefit? It has been shown that each jakinibs is more effective in combination with a csDMARD in RA, although monotherapy is effective in many patients. If a jakinib is added to a csDMARD and sustained control of the disease is achieved, should the jakinib or csDMARD be tapered or discontinued first? Many patients are initially treated with glucocorticoids as "bridge therapy," but in many, the "bridge" lasts for a prolonged time. Can jakinibs decrease the total exposure to glucocorticoids and thus prevent their significant toxicity? Importantly, what is the real risk of VTE, MACE, and malignancy with the use of a jakinib versus a treatment with another mechanism of action? As discussed above, issues surrounding specificity are not straightforward; do different in vitro specificities, measured by various assays, correlate with differences in efficacy and safety among the jakinibs? Well-designed head-to-head trials will need to be performed to answer all of these questions. Many of the same questions lack answers in PsA and AS, such as initial versus later use, monotherapy versus combination therapy, and treatment with a second jakinib after failure of the first. The question regarding glucocorticoids is not as relevant; however, we do not know the efficacy of jakinibs compared to non-TNF bDMARDs, such as the inhibitors of IL-17 or IL-23.

The use of jakinibs in combination with other inhibitors, whether intracellular or bDMARDs, or with potent immunosuppressants such as azathioprine and cyclosporine, is currently not recommended. However, it is conceivable that there are combinations which are more efficacious and/or safer; obviously, this too will need to be assessed in the setting of a rigorous randomized controlled trial—again, not a trivial undertaking. Mechanistic

studies have been performed that elucidate relevant aspects of jakinib action in terms of efficacy (89–92); however, more work is needed to understand how transient blockade of signaling by jakinibs versus sustained blockade of cytokines by biologics impacts relevant cell populations and immunopathogenesis.

In disorders such as lupus nephritis or vasculitis, aggressive approaches are warranted. Use of jakinibs has the potential for reducing toxicities of other agents, but as was clear in transplant trials, they also have the potential to lead to overimmunosuppression (93). We now know that jakinibs have utility in COVID-19 cytokine storm; remarkably, these agents are safe in patients with severe, life-threatening infectious disease. However, it is by no means clear that we have identified the right dose and the right combination of agents. Also remarkable is that a parenteral jakinib has yet to be generated. An advantage of this class of drugs is their rapid onset of action and short half-life, but it is not clear that that the current doses and formulations are optimal to interdict inflammatory responses quickly and effectively in severely ill patients.

The utility of jakinibs in COVID-19 cytokine storm suggests that these agents may be useful in additional clinical scenarios. Cytokine storm associated with chimeric antigen receptor T cell therapies is one possible setting. A concern, of course, would be that first-generation jakinibs might be toxic for the engineered T cells; however, this is a setting in which a selective JAK2 inhibitor might be advantageous. Similarly, in autoimmune disease associated with checkpoint blockade inhibitors, jakinibs might also have utility in dampening immune responses (94). On the one hand, jakinibs are being studied as therapy for a number of cancers, many of which are driven by a cytokine/STAT signature (95). On the other hand, jakinibs have the capacity to block IFNs and limit the ability of immune cells to kill cancer cells. However, there is an additional wrinkle here—by attenuating the action of IFNs, jakinibs have the capacity to reverse T cell exhaustion and promote elimination of tumors (96).

These reflections are certainly not an exhaustive list of challenges and opportunities in the jakinib arena. We present a few ideas of issues that will need to be addressed by thoughtful clinical studies, the need for which will likely increase as generic forms of jakinibs become available and jakinibs are more accessible to more patients. Considering a decade in, especially for those of us in the specialty, the advances in the jakinib field have been astonishing; however, we hope we have made the case that, in many respects, we are still at the beginning of what needs to be understood.

AUTHOR CONTRIBUTIONS

All authors drafted the article, revised it critically for important intellectual content, and approved the final version to be published.

REFERENCES

1. Darnell JE Jr, Kerr IM, Stark GR. Jak-STAT pathways and transcriptional activation in response to IFNs and other extracellular signaling proteins [review]. Science 1994;264:1415–21.
2. Russell SM, Tayebi N, Nakajima H, Riedy MC, Roberts JL, Aman MJ, et al. Mutation of Jak3 in a patient with SCID: essential role of Jak3 in lymphoid development. Science 1995;270:797–800.
3. Changelian PS, Flanagan ME, Ball DJ, Kent CR, Magnuson KS, Martin WH, et al. Prevention of organ allograft rejection by a specific janus kinase 3 inhibitor. Science 2003;302:875–8.
4. Kralovics R, Passamonti F, Buser AS, Teo SS, Tiedt R, Passweg JR, et al. A gain-of-function mutation of JAK2 in myeloproliferative disorders. N Engl J Med 2005;352:1779–90.
5. Kreins AY, Ciancanelli MJ, Okada S, Kong XF, Ramírez-Alejo N, Kilic SS, et al. Human TYK2 deficiency: mycobacterial and viral infections without hyper-IgE syndrome. J Exp Med 2015;212:1641–62.
6. Hainzl E, Stockinger S, Rauch I, Heider S, Berry D, Lassnig C, et al. Intestinal epithelial cell tyrosine kinase 2 transduces IL-22 signals to protect from acute colitis. J Immunol 2015;195:5011–24.
7. Lee EB, Fleischmann R, Hall S, Wilkinson B, Bradley JD, Gruben D, et al. Tofacitinib versus methotrexate in rheumatoid arthritis. N Engl J Med 2014;370:2377–86.
8. Fleischmann R, Kremer J, Cush J, Schulze-Koops H, Connell CA, Bradley JD, et al. Placebo-controlled trial of tofacitinib monotherapy in rheumatoid arthritis. N Engl J Med 2012;367:495–507.
9. Kremer J, Li ZG, Hall S, Fleischmann R, Genovese M, Martin-Mola E, et al. Tofacitinib in combination with nonbiologic disease-modifying antirheumatic drugs in patients with active rheumatoid arthritis: a randomized trial. Ann Intern Med 2013;159:253–61.
10. Van Vollenhoven RF, Fleischmann R, Cohen S, Lee EB, Meijide JA, Wagner S, et al. Tofacitinib or adalimumab versus placebo in rheumatoid arthritis. N Engl J Med 2012;367:508–19.
11. Burmester GR, Blanco R, Charles-Schoeman C, Wollenhaupt J, Zerbini C, Benda B, et al. Tofacitinib (CP-690,550) in combination with methotrexate in patients with active rheumatoid arthritis with an inadequate response to tumour necrosis factor inhibitors: a randomised phase 3 trial. Lancet 2013;381:451–60.
12. Mease P, Hall S, FitzGerald O, van der Heijde D, Merola JF, Avila-Zapata F, et al. Tofacitinib or adalimumab versus placebo for psoriatic arthritis. N Engl J Med 2017;377:1537–50.
13. Gladman D, Rigby W, Azevedo VF, Behrens F, Blanco R, Kaszuba A, et al. Tofacitinib for psoriatic arthritis in patients with an inadequate response to TNF inhibitors. N Engl J Med 2017;377:1525–36.
14. Sandborn WJ, Su C, Panes J. Tofacitinib as induction and maintenance therapy for ulcerative colitis. N Engl J Med 2017;377:496–7.
15. Genovese MC, Kremer J, Zamani O, Ludivico C, Krogulec M, Xie L, et al. Baricitinib in patients with refractory rheumatoid arthritis. N Engl J Med 2016;374:1243–52.
16. Dougados M, van der Heijde D, Chen YC, Greenwald M, Drescher E, Liu J, et al. Baricitinib in patients with inadequate response or intolerance to conventional synthetic DMARDs: results from the RA-BUILD study. Ann Rheum Dis 2017;76:88–95.
17. Taylor PC, Keystone EC, van der Heijde D, Weinblatt ME, Del Carmen Morales L, Gonzaga JR, et al. Baricitinib versus placebo or adalimumab in rheumatoid arthritis. N Engl J Med 2017;376:652–62.
18. Fleischmann R, Schiff M, van der Heijde D, Ramos-Remus C, Spindler A, Stanislav M, et al. Baricitinib, methotrexate, or combination in patients with rheumatoid arthritis and no or limited prior disease-modifying antirheumatic drug treatment. Arthritis Rheumatol 2017;69:506–17.
19. Tanaka Y, Takeuchi T, Tanaka S, Kawakami A, Iwasaki M, Song YW, et al. Efficacy and safety of peficitinib (ASP015K) in patients with rheumatoid arthritis and an inadequate response to conventional DMARDs: a randomised, double-blind, placebo-controlled phase III trial (RAJ3). Ann Rheum Dis 2019;78:1320–32.
20. Takeuchi T, Tanaka Y, Tanaka S, Kawakami A, Iwasaki M, Katayama K, et al. Efficacy and safety of peficitinib (ASP015K) in patients with rheumatoid arthritis and an inadequate response to methotrexate:

results of a phase III randomised, double-blind, placebo-controlled trial (RAJ4) in Japan. Ann Rheum Dis 2019;78:1305–19.

21. Genovese MC, Fleischmann R, Combe B, Hall S, Rubbert-Roth A, Zhang Y, et al. Safety and efficacy of upadacitinib in patients with active rheumatoid arthritis refractory to biologic disease-modifying anti-rheumatic drugs (SELECT-BEYOND): a double-blind, randomised controlled phase 3 trial. Lancet 2018;391:2513–24.
22. Burmester GR, Kremer JM, Van den Bosch F, Kivitz A, Bessette L, Li Y, et al. Safety and efficacy of upadacitinib in patients with rheumatoid arthritis and inadequate response to conventional synthetic disease-modifying anti-rheumatic drugs (SELECT-NEXT): a randomised, double-blind, placebo-controlled phase 3 trial. Lancet 2018;391:2503–12.
23. Smolen JS, Pangan AL, Emery P, Rigby W, Tanaka Y, Vargas JI, et al. Upadacitinib as monotherapy in patients with active rheumatoid arthritis and inadequate response to methotrexate (SELECT-MONOTHERAPY): a randomised, placebo-controlled, double-blind phase 3 study. Lancet 2019;393:2303–11.
24. Van Vollenhoven R, Takeuchi T, Pangan AL, Friedman A, Mohamed MF, Chen S, et al. Efficacy and safety of upadacitinib monotherapy in methotrexate-naive patients with moderately-to-severely active rheumatoid arthritis (SELECT-EARLY): a multicenter, multi-country, randomized, double-blind, active comparator–controlled trial. Arthritis Rheumatol 2020;72:1607–20.
25. Fleischmann R, Pangan AL, Song IH, Mysler E, Bessette L, Peterfy C, et al. Upadacitinib versus placebo or adalimumab in patients with rheumatoid arthritis and an inadequate response to methotrexate: results of a phase III, double-blind, randomized controlled trial. Arthritis Rheumatol 2019;71:1788–800.
26. Westhovens R, Rigby WF, van der Heijde D, Ching DW, Stohl W, Kay J, et al. Filgotinib in combination with methotrexate or as monotherapy versus methotrexate monotherapy in patients with active rheumatoid arthritis and limited or no prior exposure to methotrexate: the phase 3, randomised controlled FINCH 3 trial. Ann Rheum Dis 2021;80:727–38.
27. Genovese MC, Kalunian K, Gottenberg JE, Mozaffarian N, Bartok B, Matzkies F, et al. Effect of filgotinib vs placebo on clinical response in patients with moderate to severe rheumatoid arthritis refractory to disease-modifying antirheumatic drug therapy: the FINCH 2 randomized clinical trial. JAMA 2019;322:315–25.
28. Fleischmann R, Mysler E, Hall S, Kivitz AJ, Moots RJ, Luo Z, et al. Efficacy and safety of tofacitinib monotherapy, tofacitinib with methotrexate, and adalimumab with methotrexate in patients with rheumatoid arthritis (ORAL Strategy): a phase 3b/4, double-blind, head-to-head, randomised controlled trial. Lancet 2017;390:457–68.
29. Fleischmann RM, Blanco R, Hall S, Thomson GT, Van den Bosch FE, Zerbini C, et al. Switching between janus kinase inhibitor upadacitinib and adalimumab following insufficient response: efficacy and safety in patients with rheumatoid arthritis. Ann Rheum Dis 2020;80:432–9.
30. Traves PG, Murray B, Campigotto F, Galien R, Meng A, Di Paolo JA. JAK selectivity and the implications for clinical inhibition of pharmacodynamic cytokine signalling by filgotinib, upadacitinib, tofacitinib and baricitinib. Ann Rheum Dis 2021;80:865–75.
31. McInnes IB, Byers NL, Higgs RE, Lee J, Macias WL, Na S, et al. Comparison of baricitinib, upadacitinib, and tofacitinib mediated regulation of cytokine signaling in human leukocyte subpopulations. Arthritis Res Ther 2019;21:183.
32. Deodhar A, Sliwinska-Stanczyk P, Xu H, Baraliakos X, Gensler L, Fleishaker D, et al. Tofacitinib for the treatment of adult patients with ankylosing spondylitis: primary analysis of a phase 3, randomized, double-blind, placebo-controlled study [abstract]. Arthritis Rheumatol 2020;72 Suppl 10. URL: https://acrabstracts.org/abstract/tofacitinib-for-the-treatment-of-adult-patients-with-ankylosing-spondylitis-primary-analysis-of-a-phase-3-randomized-double-blind-placebo-controlled-study/.
33. Van der Heijde D, Song IH, Pangan AL, Deodhar A, Van den Bosch F, Maksymowych WP, et al. Efficacy and safety of upadacitinib in patients with active ankylosing spondylitis (SELECT-AXIS 1): a multicentre, randomised, double-blind, placebo-controlled, phase 2/3 trial. Lancet 2019;394:2108–17.
34. Mease PJ, Lertratanakul A, Anderson JK, Papp K, Van den Bosch F, Tsuji S, et al. Upadacitinib for psoriatic arthritis refractory to biologics: SELECT-PsA 2. Ann Rheum Dis 2020;80:312–20.
35. McInnes IB, Anderson JK, Magrey M, Merola JF, Liu Y, Kishimoto M, et al. Trial of upadacitinib and adalimumab for psoriatic arthritis. N Engl J Med 2021;384:1227–39.
36. Sandborn WJ, Feagan BG, Loftus EV, Peyrin-Biroulet L, Van Assche G, D'Haens G, et al. Efficacy and safety of upadacitinib in a randomized trial of patients with Crohn's disease. Gastroenterology 2020;158:2123–38.
37. Sandborn WJ, Ghosh S, Panes J, Schreiber S, D'Haens G, Tanida S, et al. Efficacy of upadacitinib in a randomized trial of patients with active ulcerative colitis. Gastroenterology 2020;158:2139–49.
38. Guttman-Yassky E, Thaçi D, Pangan AL, Hong HC, Papp KA, Reich K, et al. Upadacitinib in adults with moderate to severe atopic dermatitis: 16-week results from a randomized, placebo-controlled trial. J Allergy Clin Immunol 2020;145:877–84.
39. Mease P, Coates LC, Helliwell PS, Stanislavchuk M, Rychlewska-Hanczewska A, Dudek A, et al. Efficacy and safety of filgotinib, a selective janus kinase 1 inhibitor, in patients with active psoriatic arthritis (EQUATOR): results from a randomised, placebo-controlled, phase 2 trial. Lancet 2018;392:2367–77.
40. Van der Heijde D, Baraliakos X, Gensler LS, Maksymowych WP, Tseluyko V, Nadashkevich O, et al. Efficacy and safety of filgotinib, a selective janus kinase 1 inhibitor, in patients with active ankylosing spondylitis (TORTUGA): results from a randomised, placebo-controlled, phase 2 trial. Lancet 2018;392:2378–87.
41. Vermeire S, Schreiber S, Petryka R, Kuehbacher T, Hebuterne X, Roblin X, et al. Clinical remission in patients with moderate-to-severe Crohn's disease treated with filgotinib (the FITZROY study): results from a phase 2, double-blind, randomised, placebo-controlled trial. Lancet 2017;389:266–75.
42. Paik J, Albayda J, Tiniakou E, Purwin G, Koenig A, Christopher-Stine L. Long term open label extension of study of tofacitinib in refractory dermatomyositis [abstract]. Arthritis Rheumatol 2020;72 Suppl 10. URL: https://acrabstracts.org/abstract/long-term-open-label-extension-of-study-of-tofacitinib-in-refractory-dermatomyositis/.
43. Chen Z, Wang X, Ye S. Tofacitinib in amyopathic dermatomyositis-associated interstitial lung disease. N Engl J Med 2019;381:291–3.
44. Kim H, Dill S, O'Brien M, Vian L, Li X, Manukyan M, et al. Janus kinase (JAK) inhibition with baricitinib in refractory juvenile dermatomyositis. Ann Rheum Dis 2020 doi: 10.1136/annrheumdis-2020-218690. E-pub ahead of print.
45. Wollenhaupt J, Lee EB, Curtis JR, Silverfield J, Terry K, Soma K, et al. Safety and efficacy of tofacitinib for up to 9.5 years in the treatment of rheumatoid arthritis: final results of a global, open-label, long-term extension study. Arthritis Res Ther 2019;21:89.
46. Genovese MC, Smolen JS, Takeuchi T, Burmester GR, Deberdt W, Schlichting D, et al. Safety profile of baricitinib for the treatment of rheumatoid arthritis up to 8.4 years: an updated integrated safety analysis [abstract]. Ann Rheum Dis 2020;79:642–3.
47. Cohen SB, Van Vollenhoven R, Curtis JR, Calabrese L, Zerbini C, Tanaka Y, et al. Safety profile of upadacitinib up to 3 years of exposure in patients with rheumatoid arthritis [abstract]. Ann Rheum Dis 2020;79:319–20.
48. Stevens E, Weinblatt ME, Massarotti E, Griffin F, Emani S, Desai S. Safety of the zoster vaccine recombinant adjuvanted in rheumatoid arthritis and other systemic rheumatic disease patients: a single center's experience with 400 patients. ACR Open Rheumatol 2020;2:357–61.

49. Lenfant T, Jin Y, Kirchner E, Hajj-Ali RA, Calabrese LH, Calabrese C. Safety of recombinant zoster vaccine: a retrospective study of 622 rheumatology patients. Rheumatology (Oxford) 2021 doi: 10.1093/rheumatology/keab139. E-pub ahead of print.
50. Källmark H, Gullstrand B, Nagel J, Einarsson J, Jönsson G, Kahn F, et al. Immunogenicity of adjuvanted herpes zoster subunit vaccine in rheumatoid arthritis patients treated with janus kinase inhibitors and controls: preliminary results [abstract]. Arthritis Rheumatol 2020;72 Suppl 10. URL: https://acrabstracts.org/abstract/immunogenicity-of-adjuvanted-herpes-zoster-subunit-vaccine-in-rheumatoid-arthritis-patients-treated-with-janus-kinase-inhibitors-and-controls-preliminary-results/.
51. Winthrop K, Yndestad A, Henrohn D, Jo H, Marsal S, Galindo M, et al. Influenza adverse events in patients with rheumatoid arthritis in the tofacitinib clinical program [abstract]. Arthritis Rheumatol 2020;72 Suppl 10. URL: https://acrabstracts.org/abstract/influenza-adverse-events-in-patients-with-rheumatoid-arthritis-in-the-tofacitinib-clinical-program/.
52. Charles-Schoeman C, Fleischmann R, Davignon J, Schwartz H, Turner SM, Beysen C, et al. Potential mechanisms leading to the abnormal lipid profile in patients with rheumatoid arthritis versus healthy volunteers and reversal by tofacitinib. Arthritis Rheumatol 2015;67:616–25.
53. US Food and Drug Administration. Initial safety trial results find increased risk of serious heart-related problems and cancer with arthritis and ulcerative colitis medicine Xeljanz, Xeljanz XR (tofacitinib). February 2021. URL: https://www.fda.gov/drugs/drug-safety-and-availability/initial-safety-trial-results-find-increased-risk-serious-heart-related-problems-and-cancer-arthritis?utm_medium=email&utm_source=govdelivery.
54. Xie W, Huang Y, Xiao S, Sun X, Fan Y, Zhang Z. Impact of janus kinase inhibitors on risk of cardiovascular events in patients with rheumatoid arthritis: systematic review and meta-analysis of randomised controlled trials. Ann Rheum Dis 2019;78:1048–54.
55. Cohen SB, van Vollenhoven RF, Winthrop KL, Zerbini CA, Tanaka Y, Bessette L, et al. Safety profile of upadacitinib in rheumatoid arthritis: integrated analysis from the SELECT phase III clinical programme. Ann Rheum Dis 2020;80:304–11.
56. Malaurie M, Constantin A, Degboé Y, Ruyssen-Witrand A, Barnetche T. Short-term risk of major adverse cardiovascular events or venous thrombo-embolic events in patients with rheumatoid arthritis initiating a janus kinase inhibitor: a meta-analysis of randomised controlled trials [abstract]. Arthritis Rheumatol 2019;71 Suppl 10. URL: https://acrabstracts.org/abstract/short-term-risk-of-major-adverse-cardiovascular-events-or-venous-thrombo-embolic-events-in-patients-with-rheumatoid-arthritis-initiating-a-janus-kinase-inhibitor-a-meta-analysis-of-randomised-control/.
57. Bilal J, Riaz IB, Naqvi SA, Bhattacharjee S, Obert MR, Sadiq M, et al. Janus kinase inhibitors and risk of venous thromboembolism: a systematic review and meta-analysis. Mayo Clin Proc 2021;96:1861–73.
58. Lopez-Olivo MA, Tayar J, Zamora N, Pratt G, Suarez-Almazor M. Malignancies and serious infections in randomized controlled trials of janus kinase inhibitors in patients with rheumatoid arthritis: a systematic review and meta-analysis [abstract]. Arthritis Rheumatol 2018;70 Suppl 10. URL: https://acrabstracts.org/abstract/malignancies-and-serious-infections-in-randomized-controlled-trials-of-janus-kinase-inhibitors-in-patients-with-rheumatoid-arthritis-a-systematic-review-and-meta-analysis/.
59. Cohen SB, Tanaka Y, Mariette X, Curtis JR, Lee EB, Nash P, et al. Long-term safety of tofacitinib up to 9.5 years: a comprehensive integrated analysis of the rheumatoid arthritis clinical development programme. RMD Open 2020;6:e001395.
60. Galapagos. Galapagos reports primary endpoint for the ongoing filgotinib MANTA and MANTA-RAy safety studies. March 2021. URL: https://www.globenewswire.com/news-release/2021/03/04/2186756/0/en/galapagos-reports-primary-endpoint-for-the-ongoing-filgotinib-manta-and-manta-ray-safety-studies.html.
61. Simpson EL, Sinclair R, Forman S, Wollenberg A, Aschoff R, Cork M, et al. Efficacy and safety of abrocitinib in adults and adolescents with moderate-to-severe atopic dermatitis (JADE MONO-1): a multicentre, double-blind, randomised, placebo-controlled, phase 3 trial. Lancet 2020;396:255–66.
62. Silverberg JI, Simpson EL, Thyssen JP, Gooderham M, Chan G, Feeney C, et al. Efficacy and safety of abrocitinib in patients with moderate-to-severe atopic dermatitis: a randomized clinical trial. JAMA Dermatol 2020;156:863–73.
63. Sigurdsson S, Nordmark G, Göring HH, Lindroos K, Wiman AC, Sturfelt G, et al. Polymorphisms in the tyrosine kinase 2 and interferon regulatory factor 5 genes are associated with systemic lupus erythematosus. Am J Hum Genet 2005;76:528–37.
64. Graham DS, Morris DL, Bhangale TR, Criswell LA, Syvänen AC, Rönnblom L, et al. Association of NCF2, IKZF1, IRF8, IFIH1, and TYK2 with systemic lupus erythematosus. PLoS Genet 2011;7:e1002341.
65. Papp K, Gordon K, Thaçi D, Morita A, Gooderham M, Foley P, et al. Phase 2 trial of selective tyrosine kinase 2 inhibition in psoriasis. N Engl J Med 2018;379:1313–21.
66. Mease P, Deodhar A, van der Heijde D, Behrens F, Kivitz A, Kim J, et al. Efficacy and safety of deucravacitinib (BMS-986165), an oral, selective tyrosine kinase 2 inhibitor, in patients with active psoriatic arthritis: results from a phase 2, randomized, double-blind, placebo-controlled trial [abstract]. Arthritis Rheumatol 2020;72 Suppl 10. URL: https://acrabstracts.org/abstract/efficacy-and-safety-of-deucravacitinib-bms-986165-an-oral-selective-tyrosine-kinase-2-inhibitor-in-patients-with-active-psoriatic-arthritis-results-from-a-phase-2-randomized-double-blind-plac/.
67. Burke JR, Cheng L, Gillooly KM, Strnad J, Zupa-Fernandez A, Catlett IM, et al. Autoimmune pathways in mice and humans are blocked by pharmacological stabilization of the TYK2 pseudokinase domain. Sci Transl Med 2019;11:eaaw1736.
68. Gerstenberger BS, Ambler C, Arnold EP, Banker ME, Brown MF, Clark JD, et al. Discovery of tyrosine kinase 2 (TYK2) inhibitor (PF-06826647) for the treatment of autoimmune diseases. J Med Chem 2020;63:13561–77.
69. Forman SB, Pariser DM, Poulin Y, Vincent MS, Gilbert SA, Kieras EM, et al. TYK2/JAK1 inhibitor PF-06700841 in patients with plaque psoriasis: phase IIa, randomized, double-blind, placebo-controlled trial. J Invest Dermatol 2020;140:2359–70.
70. Pardanani A, Harrison C, Cortes JE, Cervantes F, Mesa RA, Milligan D, et al. Safety and efficacy of fedratinib in patients with primary or secondary myelofibrosis: a randomized clinical trial. JAMA Oncol 2015;1:643–51.
71. Talpaz M, Kiladjian JJ. Fedratinib, a newly approved treatment for patients with myeloproliferative neoplasm-associated myelofibrosis [review]. Leukemia 2020;35:1–17.
72. Berdeja J, Palandri F, Baer MR, Quick D, Kiladjian JJ, Martinelli G, et al. Phase 2 study of gandotinib (LY2784544) in patients with myeloproliferative neoplasms. Leuk Res 2018;71:82–8.
73. Fleischmann RM, Damjanov NS, Kivitz AJ, Legedza A, Hoock T, Kinnman N. A randomized, double-blind, placebo-controlled, twelve-week, dose-ranging study of decernotinib, an oral selective JAK-3 inhibitor, as monotherapy in patients with active rheumatoid arthritis. Arthritis Rheumatol 2015;67:334–43.
74. Genovese MC, van Vollenhoven RF, Pacheco-Tena C, Zhang Y, Kinnman N. VX-509 (decernotinib), an oral selective JAK-3 inhibitor, in combination with methotrexate in patients with rheumatoid arthritis. Arthritis Rheumatol 2016;68:46–55.
75. Zetterberg C, Maltais F, Laitinen L, Liao S, Tsao H, Chakilam A, et al. VX-509 (decernotinib)-mediated CYP3A time-dependent inhibition:

an aldehyde oxidase metabolite as a perpetrator of drug-drug interactions. Drug Metab Dispos 2016;44:1286–95.

76. Robinson MF, Damjanov N, Stamenkovic B, Radunovic G, Kivitz A, Cox L, et al. Efficacy and safety of PF-06651600 (ritlecitinib), a novel JAK3/TEC inhibitor, in patients with moderate-to-severe rheumatoid arthritis and an inadequate response to methotrexate. Arthritis Rheumatol 2020;72:1621–31.
77. Bissonnette R, Maari C, Forman S, Bhatia N, Lee M, Fowler J, et al. The oral janus kinase/spleen tyrosine kinase inhibitor ASN002 demonstrates efficacy and improves associated systemic inflammation in patients with moderate-to-severe atopic dermatitis: results from a randomized double-blind placebo-controlled study. Br J Dermatol 2019;181:733–42.
78. Harrison CN, Vannucchi AM, Platzbecker U, Cervantes F, Gupta V, Lavie D, et al. Momelotinib versus best available therapy in patients with myelofibrosis previously treated with ruxolitinib (SIMPLIFY 2): a randomised, open-label, phase 3 trial. Lancet Haematol 2018;5:e73–81.
79. RECOVERY Collaborative Group, Horby P, Lim WS, Emberson JR, Mafham M, Bell JL, et al. Dexamethasone in hospitalized patients with Covid-19. N Engl J Med 2021;384:693–704.
80. Sorrell FJ, Szklarz M, Abdul Azeez KR, Elkins JM, Knapp S. Family-wide structural analysis of human numb-associated protein kinases. Structure 2016;24:401–11.
81. Eberl HC, Werner T, Reinhard FB, Lehmann S, Thomson D, Chen P, et al. Chemical proteomics reveals target selectivity of clinical Jak inhibitors in human primary cells. Sci Rep 2019;9:14159.
82. Cao Y, Wei J, Zou L, Jiang T, Wang G, Chen L, et al. Ruxolitinib in treatment of severe coronavirus disease 2019 (COVID-19): a multicenter, single-blind, randomized controlled trial. J Allergy Clin Immunol 2020;146:137–46.
83. Giudice V, Pagliano P, Vatrella A, Masullo A, Poto S, Polverino BM, et al. Combination of ruxolitinib and eculizumab for treatment of severe SARS-CoV-2-related acute respiratory distress syndrome: a controlled study. Front Pharmacol 2020;11:857.
84. Cantini F, Niccoli L, Nannini C, Matarrese D, Natale ME, Lotti P, et al. Beneficial impact of Baricitinib in COVID-19 moderate pneumonia; multicentre study. J Infect 2020;81:647–79.
85. Stebbing J, Nievas GS, Falcone M, Youhanna S, Richardson P, Ottaviani S, et al. JAK inhibition reduces SARS-CoV-2 liver infectivity and modulates inflammatory responses to reduce morbidity and mortality. Sci Adv 2020;7:eabe4724.
86. Kalil AC, Patterson TF, Mehta AK, Tomashek KM, Wolfe CR, Ghazaryan V, et al. Baricitinib plus remdesivir for hospitalized adults with Covid-19. N Engl J Med 2021;384:795–807.
87. National Institutes of Health. NIH closes enrollment in trial comparing COVID-19 treatment regimens. April 2021. URL: https://www.nih.gov/news-events/news-releases/nih-closes-enrollment-trial-comparing-covid-19-treatment-regimens.
88. Eli Lilly and Company. Lilly and Incyte announce results from the Phase 3 COV-BARRIER study of baricitinib in hospitalized COVID-19 patients. April 2021. URL: https://investor.lilly.com/news-releases/news-release-details/lilly-and-incyte-announce-results-phase-3-cov-barrier-study.
89. Gao W, McGarry T, Orr C, McCormick J, Veale DJ, Fearon U. Tofacitinib regulates synovial inflammation in psoriatic arthritis, inhibiting STAT activation and induction of negative feedback inhibitors. Ann Rheum Dis 2016;75:311–5.
90. McGarry T, Orr C, Wade S, Biniecka M, Wade S, Gallagher L, et al. JAK/STAT blockade alters synovial bioenergetics, mitochondrial function, and proinflammatory mediators in rheumatoid arthritis. Arthritis Rheumatol 2018;70:1959–70.
91. Hanlon MM, Rakovich T, Cunningham CC, Ansboro S, Veale DJ, Fearon U, et al. STAT3 mediates the differential effects of oncostatin M and TNFα on RA synovial fibroblast and endothelial cell function. Front Immunol 2019;10:2056.
92. Marzaioli V, Canavan M, Floudas A, Wade SC, Low C, Veale DJ, et al. Monocyte-derived dendritic cell differentiation in inflammatory arthritis is regulated by the JAK/STAT axis via NADPH oxidase regulation. Front Immunol 2020;11:1406.
93. Busque S, Leventhal J, Brennan DC, Steinberg S, Klintmalm G, Shah T, et al. Calcineurin-inhibitor-free immunosuppression based on the JAK inhibitor CP-690,550: a pilot study in de novo kidney allograft recipients. Am J Transplant 2009;9:1936–45.
94. Murray K, Floudas A, Murray C, Fabre A, Crown J, Fearon U, et al. First use of tofacitinib to treat an immune checkpoint inhibitor-induced arthritis. BMJ Case Rep 2021;14:e238851.
95. Chan LN, Murakami MA, Robinson ME, Caeser R, Sadras T, Lee J, et al. Signalling input from divergent pathways subverts B cell transformation. Nature 2020;583:845–51.
96. Benci JL, Xu B, Qiu Y, Wu TJ, Dada H, Victor CT, et al. Tumor interferon signaling regulates a multigenic resistance program to immune checkpoint blockade. Cell 2016;167:1540–54.

Arthritis & Rheumatology
Vol. 73, No. 12, December 2021, pp 2179–2188
DOI 10.1002/art.41800
© 2021 American College of Rheumatology. This article has been contributed to by US Government employees and their work is in the public domain in the USA.

American College of Rheumatology
Empowering Rheumatology Professionals

Risk of COVID-19 in Rheumatoid Arthritis: A National Veterans Affairs Matched Cohort Study in At-Risk Individuals

Bryant R. England,[1] Punyasha Roul,[2] Yangyuna Yang,[2] Andre C. Kalil,[2] Kaleb Michaud,[3] Geoffrey M. Thiele,[1] Brian C. Sauer,[4] Joshua F. Baker,[5] and Ted R. Mikuls[1]

Objective. Rheumatoid arthritis (RA) and its treatments are associated with an increased risk of infection, but it remains unclear whether these factors have an impact on the risk or severity of COVID-19. The present study was undertaken to assess the risk and severity of COVID-19 in a US Department of Veterans Affairs (VA) cohort of patients with RA and those without RA.

Methods. A matched cohort study using national VA data was conducted. Patients diagnosed as having RA were identified among nondeceased individuals who were active in the VA health care system as of January 1, 2020 and who had received care in a VA medical center in 2019; patients for whom no RA diagnostic code was indicated were matched to the RA patients (1:1) by age, sex, and VA site (non-RA controls). Patients diagnosed as having COVID-19 and those with severe COVID-19 (defined as requiring hospitalization or leading to death) were ascertained from a national VA COVID-19 surveillance database through December 10, 2020. Multivariable Cox models were used to compare the risk of COVID-19 and COVID-19 hospitalization or death between RA patients and non-RA controls, after adjusting for demographic characteristics, comorbidities, health care utilization and access, and county-level COVID-19 incidence rates.

Results. This VA cohort of RA patients and non-RA controls (n = 33,886 subjects per group) predominantly comprised male patients (84.5%), and the mean age was 67.8 years. During follow-up, 1,503 patients in the cohort were diagnosed as having COVID-19; among them, 388 patients had severe COVID-19 (hospitalization or death), while in 228 patients, the deaths were not related to COVID-19. In the multivariable model, RA was associated with a higher risk of COVID-19 (adjusted hazard ratio [HR] 1.25 [95% confidence interval (95% CI) 1.13–1.39]) and a higher risk of COVID-19 hospitalization or death (adjusted HR 1.35 [95% CI 1.10–1.66]) as compared to non-RA controls. Use of disease-modifying antirheumatic drugs and prednisone, as well as self-reported Black race, self-reported Hispanic ethnicity, and presence of several chronic conditions, but not seropositivity for RA autoantibodies, were each associated with risk of COVID-19 and severe COVID-19 (hospitalization or death).

Conclusion. Patients with RA are at higher risk of developing COVID-19 and severe COVID-19 (leading to hospitalization or death) compared to those without RA. With a risk of COVID-19 that approaches that of other recognized chronic conditions, these findings suggest that RA patients should be prioritized for COVID-19 prevention and management strategies.

The views expressed in this article are those of the authors and do not necessarily reflect the position or policy of the US Department of Veterans Affairs or the US government.

Supported by the University of Nebraska Medical Center, College of Medicine. Drs. England and Mikuls' work was supported by the US Department of Veterans Affairs (grant IK2-CX-002203 to Dr. England and grant I01-BX-004660 to Dr. Mikuls), the Rheumatology Research Foundation (Scientist Development Award to Dr. England and Innovative Research Award to Dr. Mikuls), and the National Institute of General Medical Sciences, NIH (grant U54-GM-115458 to Dr. England and grant U54-GM-115458 to Dr. Mikuls). Dr. Baker's work was supported by the US Department of Veterans Affairs (grant I01-CX-001703).

[1]Bryant R. England, MD, PhD, Geoffrey M. Thiele, PhD, Ted R. Mikuls, MD, MSPH: VA Nebraska-Western Iowa Health Care System and University of Nebraska Medical Center, Omaha; [2]Punyasha Roul, MS, Yangyuna Yang, MBBS, PhD, Andre C. Kalil, MD, MPH: University of Nebraska Medical Center, Omaha; [3]Kaleb Michaud, PhD: University of Nebraska Medical Center, Omaha, and FORWARD—The National Databank for Rheumatic Diseases, Wichita, Kansas; [4]Brian C. Sauer, PhD, MS: VA Salt Lake City Health Care System and University of Utah; [5]Joshua F. Baker, MD, MSCE: Corporal Michael J. Crescenz VAMC and University of Pennsylvania, Philadelphia.

Dr. England has received consulting fees from Boehringer Ingelheim (less than $10,000). Dr. Thiele has received consulting fees, speaking fees, and/or honoraria from Sanofi (less than $10,000). Dr. Baker has received consulting fees from Bristol Myers Squibb, Pfizer, and Gilead (less than $10,000 each). Dr. Mikuls has received consulting fees from Pfizer, Sanofi, Gilead, and Horizon (less than $10,000 each) and research support from Bristol Myers Squib and Horizon. No other disclosures relevant to this article were reported.

Address correspondence to Bryant R. England, MD, PhD, 986270 Nebraska Medical Center, Omaha, NE 68198. Email: Bryant.england@unmc.edu.

Submitted for publication April 9, 2021; accepted in revised form May 4, 2021.

INTRODUCTION

Despite marked improvements in the long-term outcomes observed in patients with rheumatoid arthritis (RA) (1), infections frequently complicate the natural course of the disease and are likely overrepresented in this patient population; this could be attributable to several mechanisms. An increased risk of infection or serious infection in patients with RA is associated with the immune dysregulation inherent to RA itself, but also could be associated with RA treatments, such as disease-modifying antirheumatic drugs (DMARDs) and glucocorticoids, and with chronic conditions that often develop in conjunction with RA (2,3). However, most of the research in RA has focused on bacterial, and not viral, etiologies.

COVID-19 appears to yield a disproportionate impact among vulnerable populations, particularly among the elderly and those with chronic diseases (4,5). With the rapid development of effective vaccines for COVID-19, individuals with select chronic conditions that predispose the individual to a more severe COVID-19 disease course have been prioritized for vaccine administration (6). High-risk chronic conditions and lifestyle factors specified in these recommendations include cancer, chronic kidney disease, cardiovascular disease, prior solid organ transplantation, sickle cell disease, type 2 diabetes mellitus, obesity, smoking, and pregnancy (6). RA and other rheumatic diseases that require immunosuppressive therapies for management have not been prioritized. While the vaccine supply is increasing in the US, the need, timing, and prioritization of subsequent booster vaccination is unknown.

Few observational studies have evaluated whether rheumatic diseases and related immunosuppressive therapies are associated with COVID-19 outcomes. Findings from an international registry of rheumatic disease patients identified links between the severity of rheumatic disease, use of prednisone, and use of select immunosuppressive therapies with a higher risk of mortality, specifically among those with RA (7). Results of subsequent analyses have suggested that confounding by indication may explain the association between prednisone treatment and worse COVID-19 outcomes (8). Moreover, these observations have also been noted in the general population, including an association of certain ethnic groups and comorbidities with the development of severe COVID-19 or COVID-19–related death (7,9).

In a multicenter study utilizing electronic health records, patients with COVID-19 and systemic autoimmune rheumatic diseases had a higher risk of severe outcomes compared with matched comparators, although this appeared largely related to accompanying comorbidities (10). Similarly, a separate study in a multicenter health care system found that the association of rheumatic diseases with mechanical ventilation in COVID-19 was attenuated by the presence of comorbidities (11). In a study using a national sample of primary care patients from the UK, patients diagnosed as having RA, lupus, or psoriasis were found to have a 19% higher risk of COVID-19–related death (12). Although these findings, along with evidence from other investigators, are beginning to shed light on the outcomes experienced by patients with COVID-19, the aforementioned studies are prone to selection bias, which could be related to the approach taken for patient enrollment and/or to the fact that patient selection may be conditioned on a positive SARS–CoV-2 test finding. Moreover, prior studies have focused on heterogeneous populations, comprising patients with a number of different rheumatic conditions and treatments; this is likely to reduce the precision of the risk estimates generated.

Recognizing these gaps in our understanding and the significant limitations of prior study designs, the objective of the present study was to compare the risk of SARS–CoV-2 infection and the development of severe COVID-19 between patients with RA and matched comparator patients in an at-risk population. We hypothesized that patients with RA would have a higher risk of acquiring a SARS–CoV-2 infection, and would be more likely to require hospitalization or to die after having been diagnosed with COVID-19.

PATIENTS AND METHODS

Study design. We conducted a retrospective, matched cohort study within the US Department of Veterans Affairs (VA) Health Administration database. Patients who were active in the VA system as of January 1, 2020 were identified as having RA based on administrative algorithms, which searched for a record of multiple RA diagnostic codes, a rheumatologist's diagnosis of RA, treatment with a DMARD, or a positive test finding for RA autoantibodies (rheumatoid factor [RF] and/or anti–cyclic citrullinated peptide [anti-CCP] antibodies). Such algorithms have a >90% positive predictive value for the diagnosis of RA (13). Patients who had received care (outpatient or inpatient encounter) during the 2019 calendar year at the same VA medical center and for whom no RA diagnostic code was assigned were matched 1:1 to the RA patients by age, sex, and site (non-RA controls). Patients with other autoimmune conditions (rheumatic or nonrheumatic diseases) and those who were receiving immunosuppressant drugs were not excluded from the non-RA control group; this ensured that the control group was fully reflective of the VA non-RA population. For study eligibility, both RA patients and non-RA controls had to be alive as of January 1, 2020. Patients were subsequently followed up from January 1, 2020 to the first diagnosis of COVID-19, occurrence of death, or end of the study period (December 10, 2020). This study received institutional review board approval.

Identification of COVID-19. Among this VA cohort of RA patients and non-RA controls, a diagnosis of COVID-19 and information on related outcomes were obtained through the VA COVID-19 shared data resource. This is a national VA COVID-19 surveillance database that captures testing for COVID-19, clinical

results, severity of the disease, and patient outcomes, for the purposes of secondary research studies (14–16). In addition to capturing molecular SARS–CoV-2 test results and COVID-19 diagnoses within the VA health care system, natural language processing and medical record validation are performed to identify COVID-19 cases that are diagnosed outside the VA system (17). However, a negative SARS–CoV-2 test result that is determined outside the VA system is not captured in this resource.

The primary definition of COVID-19 included positive test results within or outside the VA health care system. We also identified patients with severe COVID-19, defined as COVID-19 that required hospitalization or that resulted in death within 30 days of infection. In sensitivity analyses, respiratory illnesses that could be attributed to SARS–CoV-2 infection but which lacked confirmation of the diagnosis (according to the VA COVID-19 shared data resource case definition) were also classified as COVID-19 (17). Data on death were collected from the VA COVID-19 shared data resource and from vital status records maintained by the VA.

Covariates. Data on covariates were obtained from the VA Corporate Data Warehouse. The covariates included race, ethnicity, body mass index (BMI), urban versus rural residence, presence of a VA service–connected condition (i.e., a condition directly related to military service for which the individual receives VA benefits), private insurance status, smoking status (current, former, or never), comorbidities, number of hospitalizations in the prior year, and county-level COVID-19 rates as of November 16, 2020. Demographic characteristics (race, ethnicity) were obtained from administrative VA data collected at the time of enrollment in the VA. BMI was calculated from the nearest visit preceding January 1, 2020, using vital signs data obtained from VA clinic encounters, as previously described (18,19). Smoking status was assessed by selecting and coding health factors recorded in the VA electronic medical record (20).

Comorbid conditions were assessed using scores on the Elixhauser Comorbidity Index (21) (excluding RA and collagen vascular diseases). In addition, we identified specific conditions within the Elixhauser Comorbidity Index that are recognized to portend a higher risk of COVID-19, including heart failure, chronic lung disease, diabetes, hypertension, cancer, chronic kidney disease, and liver disease (21). We required a record of at least 1 diagnostic code from outpatient or inpatient encounters during 2019 for one of these comorbid conditions to be considered present. International Classification of Diseases, Tenth Revision codes for each of the comorbidities were obtained from the Healthcare Cost and Utilization Project Elixhauser Comorbidity Software database (https://www.hcup-us.ahrq.gov/toolssoftware/comorbidityicd10/comorbidity_icd10.jsp). Cumulative county-level incidence rates of COVID-19 since the start of the pandemic were obtained from the COVID-19 Data Repository by the Center for Systems Science and Engineering at Johns Hopkins University (https://github.com/cssegisanddata/covid-19; accessed November 16, 2020) (22).

Medications and RA autoantibody status. We assessed recent treatments based on medical records noting a dispensing or infusion of DMARDs and prednisone in the 180 days prior to and including January 1, 2020, except for rituximab, which we assessed during an infusion period up to 365 days prior to January 1, 2020. The noted medications included conventional synthetic DMARDs (csDMARDs) (methotrexate, hydroxychloroquine, sulfasalazine, and leflunomide), and biologic or targeted synthetic DMARDs (bDMARDs/tsDMARDs) (tumor necrosis factor inhibitors [etanercept, adalimumab, certolizumab, golimumab, and infliximab], abatacept and interleukin-6 inhibitors [tocilizumab and sarilumab], rituximab, and JAK inhibitors [tofacitinib, baricitinib, and upadacitinib]). Prior work has shown that RA patients in the VA system rarely obtain DMARDs from non-VA sources (23). RA autoantibody status was determined based on laboratory data from the VA Corporate Data Warehouse database, with patients classified as either seronegative or seropositive for RF and anti-CCP antibodies.

Statistical analysis. Descriptive statistics were used to compare demographic and clinical characteristics between the RA patients and non-RA controls. We used multivariable Cox regression models to assess the incidence and risk of COVID-19 in RA patients compared to non-RA controls, censoring for non–COVID-19–related death or end of the study period. Models were clustered by matched pair, and included all of the aforementioned covariates. Similar models and covariates were used to compare the risk of severe COVID-19 (hospitalization or death) between RA patients and non-RA controls.

Sensitivity analyses were performed to 1) additionally include in the COVID-19 case definition respiratory illnesses that may have been related to SARS–CoV-2 infection but which lacked testing confirmation as evidence of COVID-19, and 2) model the effect of individual comorbidities, rather than the overall Elixhauser Comorbidity Index, on the risk of COVID-19. Secondary analyses included those that stratified RA patients and non-RA controls according to RA-specific autoantibody status (seropositive, seronegative, and unknown), recent DMARD use (none, csDMARDs, and bDMARDs/tsDMARDs), prednisone use (yes versus no), and use of combination treatment with DMARDs and prednisone. To address missing covariate data, we used multiple imputation with 10 imputations. Each imputed covariate (race, ethnicity, smoking status, BMI, urban/rural residence, and insurance status) was missing for <7% of patients.

Recognizing that COVID-19 outcomes began to improve later in the pandemic among both patients with rheumatic diseases and those without rheumatic diseases (24,25), we assessed time-dependent differences in the risk of COVID-19

Table 1. Baseline characteristics of the RA patients and non-RA controls*

	RA patients (n = 33,886)	Non-RA controls (n = 33,886)	*P*
Age, years	67.8 ± 11.1	67.8 ± 11.1	ND
Male sex, %	84.5	84.5	ND
Race, %			0.01
White	74.4	73.7	
Black	17.3	17.2	
Other	3.3	2.9	
Unknown	5.1	6.2	
Ethnicity, %			<0.001
Non-Hispanic	90.7	91.0	
Hispanic	6.1	5.0	
Unknown	3.2	3.9	
Smoking status, %			<0.001
Current	50.0	40.8	
Former	31.8	31.3	
Never	15.7	21.4	
Unknown	2.5	6.6	
BMI category, %			<0.001
<18.5 kg/m^2	0.7	0.6	
18.5–25 kg/m^2	8.4	9.0	
25–30 kg/m^2	28.8	30.8	
30–35 kg/m^2	31.1	31.1	
>35 kg/m^2	31.0	27.9	
Unknown	0.1	0.7	
Elixhauser Comorbidity Index	3.0 ± 2.2	2.5 ± 2.0	<0.001
Type of residence, %			0.33
Urban	63.5	64.0	
Rural	34.9	34.4	
Highly rural	1.5	1.5	
Unknown	0.1	0.1	
RF or anti-CCP antibody status, %			<0.001
Seropositive	60.5	0.9	
Seronegative	25.7	3.8	
Unknown	13.9	95.4	
DMARDs in prior 180 days, %†			<0.001
None	27.4	98.9	
csDMARDs	37.6	0.5	
bDMARDs/tsDMARDs	34.2	0.5	
Prednisone in prior 180 days, %	24.7	3.6	<0.001
Number of hospitalizations in prior year	0.2 ± 0.8	0.1 ± 0.6	<0.001
Insurance beneficiary, %	80.9	78.7	<0.001
Service-connected condition, %	62.6	58.7	<0.001

* Patients who were not assigned a diagnostic code for rheumatoid arthritis (RA) were matched to each RA patient by age, sex, and site (non-RA controls). Except where indicated otherwise, values are the mean ± SD. ND = no difference; BMI = body mass index; RF = rheumatoid factor; anti-CCP = anti–cyclic citrullinated peptide.
† Disease-modifying antirheumatic drugs (DMARDs), which included conventional synthetic DMARDs (csDMARDs) and biologic or targeted synthetic DMARDs (bDMARDs/tsDMARDs), were assessed 180 days prior to and including January 1, 2020, except for rituximab, which was assessed during an infusion period up to 365 days prior to January 1, 2020.

through proportional hazards testing. Schoenfeld residuals and interactions between RA status and log(time) were not significant (all $P > 0.3$). Similarly, log–log survival rates and Schoenfeld residual plots indicated that there was no violation of the proportional hazards assumption (data not shown). All analyses were completed using Stata MP software, version 15.1 (StataCorp).

RESULTS

Characteristics of the study patients. In this study cohort, we identified 33,886 patients with RA and 33,886 non-RA controls who were age-, sex-, and site-matched to each RA patient. Compared to controls, RA patients were more likely to be current smokers and to have a higher BMI, greater comorbidity burden according to the Elixhauser Comorbidity Index, and more hospitalizations in the prior year (Table 1). The majority of patients with RA were seropositive for RF or anti-CCP antibodies (60.5%). DMARDs were dispensed within the prior 180 days (i.e., recent DMARD treatment) in 73% of the patients with RA, with 34.2% having received a bDMARD or tsDMARD. The frequency of recent use of each individual DMARD is provided in Supplementary Table 1 (available on the *Arthritis & Rheumatology* website at http://onlinelibrary.wiley.com/doi/10.1002/art.41800/abstract).

Incidence rates of COVID-19. In analyses spanning 62,894 patient-years of follow-up among patients assessed according to the primary case definition of COVID-19 (i.e., confirmed SARS–CoV-2 infection), we identified 1,503 patients with COVID-19. Among these, the diagnosis was categorized as severe in 388 cases, of which 345 required hospitalization and 84 resulted in death. During the same period of observation, there were 288 non–COVID-related deaths.

When a more sensitive case definition of COVID-19 was applied to the cohort (i.e., additional inclusion of patients with respiratory illnesses possibly attributable to COVID-19 but lacking testing confirmation), we identified 2,037 patients with COVID-19, with 468 cases resulting in either hospitalization or death. Crude incidence rates of COVID-19 and severe COVID-19 (hospitalization or death), both in the primary analysis and in the sensitivity analysis, were higher in RA patients compared to matched non-RA controls (Table 2).

Risk of COVID-19 in RA patients. In unadjusted multivariable Cox regression models assessing RA patients compared to non-RA matched controls, as well as adjusted models that further accounted for demographic characteristics, comorbidities, health care utilization and access, and county-level COVID-19 incidence rates, the risk of COVID-19 was found to be significantly

Table 2. Crude incidence rates of COVID-19 and severe COVID-19 in patients with RA and non-RA controls*

	Number of events	Person-years of follow-up	Incidence rate per 1,000 person-years (95% CI)
Primary analysis			
All COVID-19			
Non-RA	647	31,552	20.5 (19.0–22.1)
RA	856	31,342	27.3 (25.5–29.2)
Severe COVID-19†			
Non-RA	153	31,552	4.8 (4.1–5.7)
RA	235	31,342	7.5 (6.6–8.5)
Sensitivity analysis‡			
All COVID-19			
Non-RA	863	31,465	27.4 (25.7–29.3)
RA	1,174	31,217	37.6 (35.5–39.8)
Severe COVID-19†			
Non-RA	181	31,465	5.8 (5.0–6.7)
RA	287	31,217	9.2 (8.2–10.3)

* RA = rheumatoid arthritis; 95% CI = 95% confidence interval.
† Severe COVID-19 was defined as COVID-19 requiring hospitalization or resulting in death.
‡ Sensitivity analyses additionally included patients with respiratory illnesses that were suspected to be attributable to COVID-19 but lacked confirmation.

higher in RA patients compared to non-RA controls. Specifically, the risk of COVID-19 in RA patients was 25% higher (adjusted hazard ratio [HR] 1.25 [95% confidence interval (95% CI) 1.13–1.39]) and the risk of COVID-19 hospitalization or death was 35% higher (adjusted HR 1.35 [95% CI 1.10–1.66]) when compared to non-RA controls (Table 3). Results of the sensitivity analysis, in which possible COVID-19 cases were included, were consistent with those of the primary analysis (Table 3).

In addition to the association with RA, other factors that were significantly associated with a higher risk of COVID-19 were self-reported Black race, self-reported Hispanic ethnicity, a higher Elixhauser Comorbidity Index, lack of insurance, presence of a military service–connected condition, a BMI categorized as either underweight or obese, a greater number of hospitalizations in the prior year, and higher county-level incidence rates of COVID-19 (Table 4). Fewer factors were significantly associated with a higher risk of severe COVID-19 (resulting in hospitalization or death). These factors included a higher Elixhauser Comorbidity Index, lack of insurance, a greater number of hospitalizations in the prior year, and higher county-level COVID-19 incidence rates.

In sensitivity analyses that incorporated individual comorbidities rather than the overall Elixhauser Comorbidity Index, both the risk of COVID-19 and the risk of severe COVID-19 (hospitalization or death) were elevated to a similar extent as that seen in patients with RA in patients with individual comorbidities, specifically among patients with heart failure (adjusted HRs for COVID-19 and severe COVID-19 of 1.30 and 1.70, respectively), those with chronic lung disease (adjusted HRs of 1.28 and 1.32, respectively), those with diabetes (adjusted HRs of 1.29 and 1.85, respectively), those with liver disease (adjusted HRs of 1.35 and 1.52, respectively), and those with chronic kidney disease (adjusted HRs of 1.14 and 1.76, respectively) (Table 5).

Risk of COVID-19 by RA autoantibody status and medication usage. In secondary analyses, we compared the risk of COVID-19 and severe COVID-19 (resulting in hospitalization or death) between RA patients and non-RA controls based on RA autoantibody status and use of medications. The risk of COVID-19 and of severe COVID-19 (hospitalization or death) was similar between patients with seronegativity for RA autoantibodies

Table 3. Risk of COVID-19 and severe COVID-19 in RA patients relative to non-RA controls*

	Unadjusted HR (95% CI)	Adjusted HR (95% CI)
Primary analysis		
All COVID-19		
Non-RA	1 (Referent)	1 (Referent)
RA	1.34 (1.21–1.48)	1.25 (1.13–1.39)
Severe COVID-19†		
Non-RA	1 (Referent)	1 (Referent)
RA	1.55 (1.26–1.90)	1.35 (1.10–1.66)
Sensitivity analysis‡		
All COVID-19		
Non-RA	1 (Referent)	1 (Referent)
RA	1.38 (1.26–1.50)	1.29 (1.18–1.41)
Severe COVID-19†		
Non-RA	1 (Referent)	1 (Referent)
RA	1.60 (1.33–1.93)	1.39 (1.15–1.68)

* Results are the hazard ratio (HR) with 95% confidence interval (95% CI) for the risk of developing COVID-19 or severe COVID-19 in patients with rheumatoid arthritis (RA) relative to matched non-RA controls, as determined in unadjusted models and models adjusted for race, ethnicity, smoking status, Elixhauser Comorbidity Index, private insurance status, urban/rural residence, number of hospitalizations in prior year, military service–connected condition, and county-level COVID-19 incidence rates.
† Severe COVID-19 was defined as COVID-19 requiring hospitalization or resulting in death.
‡ Sensitivity analyses additionally included patients with respiratory illnesses that were suspected to be attributable to COVID-19 but lacked confirmation.

Table 4. Fully adjusted models evaluating potential risk factors for COVID-19 and severe COVID-19 in the study cohort*

	All COVID-19	Severe COVID-19
RA, vs. non-RA	1.25 (1.13–1.39)†	1.35 (1.10–1.66)†
Race		
White	1 (Referent)	1 (Referent)
Black	1.22 (1.07–1.39)†	1.25 (0.97–1.60)
Other	1.29 (0.99–1.68)	1.23 (0.71–2.11)
Ethnicity		
White	1 (Referent)	1 (Referent)
Hispanic	1.48 (1.23–1.78)†	1.25 (0.85–1.86)
Smoking status		
Current	0.78 (0.68–0.90)	1.09 (0.80–1.50)
Former	0.90 (0.78–1.04)	1.31 (0.94–1.82)
Never	1 (Referent)	1 (Referent)
Elixhauser Comorbidity Index, per 1-unit increase	1.12 (1.09–1.15)†	1.24 (1.20–1.30)†
Insurance (no, vs. yes)	1.40 (1.24–1.58)†	1.88 (1.49–2.37)†
Service-connected condition	1.22 (1.10–1.37)†	1.08 (0.87–1.34)
BMI category		
<18.5 kg/m^2	1.78 (1.01–3.15)†	1.30 (0.38–4.47)
18.5–25 kg/m^2	1 (Referent)	1 (Referent)
25–30 kg/m^2	1.21 (0.96–1.54)	1.29 (0.79–2.11)
30–35 kg/m^2	1.36 (1.08–1.72)†	1.42 (0.88–2.31)
>35 kg/m^2	1.51 (1.19–1.90)†	1.59 (0.98–2.57)
Urban/rural status		
Urban	1 (Referent)	1 (Referent)
Rural	0.90 (0.80–1.01)	0.98 (0.78–1.22)
Highly rural	1.06 (0.70–1.61)	0.79 (0.29–2.14)
No. of hospitalizations in prior year	1.11 (1.05–1.16)†	1.13 (1.06–1.21)†
County COVID-19 incidence rate per 100,000	1.00 (1.00–1.00)†	1.00 (1.00–1.00)†

* Values are the hazard ratio (95% confidence interval) for the risk of developing COVID-19 or severe COVID-19 (requiring hospitalization or resulting in death) based on each factor assessed. RA = rheumatoid arthritis; BMI = body mass index.
† $P < 0.05$.

and those with a seropositive status, independent of potential confounders (Figures 1A and B).

Moreover, compared to non-RA controls, a higher risk of COVID-19 and of severe COVID-19 (hospitalization or death) was observed among RA patients who had received treatment with csDMARDs, bDMARDs/tsDMARDs, and prednisone (Figures 1A and B). RA patients treated with both bDMARDs/tsDMARDs and prednisone had the highest risk of COVID-19 (adjusted HR 1.66 [95% CI 1.36–2.03]) and the highest risk of COVID-19 hospitalization or death (adjusted HR 2.12 [95% CI 1.48–3.03]), relative to non-RA controls.

DISCUSSION

In this large, national VA at-risk cohort of RA patients and matched non-RA controls, we found that patients with RA were at a significantly higher risk of developing SARS–CoV-2 infection and having severe COVID-19 leading to hospitalization or death. Those treated with DMARDs and prednisone were at the highest risk of COVID-19 and more severe disease. This was independent of potential confounders, including demographic characteristics, comorbidities, health care utilization and access, and county-level COVID-19 incidence rates. Strikingly, the heightened risk of COVID-19 related to RA was consistent with the risk posed by other chronic conditions that receive priority vaccination status. Thus, the immediate implication of our findings is the suggestion that similar consideration for vaccine prioritization should be given to patients with RA receiving immunosuppressive therapies.

After adjusting for potential confounders, we estimated that RA was associated with a 25% increased risk of COVID-19 and a

Table 5. Sensitivity analysis of fully adjusted models evaluating potential risk factors for COVID-19 and severe COVID-19 in the study cohort*

	All COVID-19	Severe COVID-19
RA, vs. non-RA	1.27 (1.14–1.41)†	1.39 (1.13–1.71)†
Race		
White	1 (Referent)	1 (Referent)
Black	1.25 (1.09–1.42)†	1.24 (0.97–1.59)
Other	1.26 (0.97–1.65)	1.18 (0.67–2.08)
Ethnicity		
White	1 (Referent)	1 (Referent)
Hispanic	1.50 (1.24–1.80)†	1.30 (0.88–1.92)
Smoking status		
Current	0.78 (0.68–0.90)	1.15 (0.84–1.57)
Former	0.90 (0.78–1.04)	1.30 (0.93–1.80)
Never	1 (Referent)	1 (Referent)
Chronic condition		
Heart failure	1.30 (1.09–1.15)†	1.70 (1.25–2.32)†
Chronic lung disease	1.28 (1.13–1.44)†	1.32 (1.04–1.67)†
Diabetes mellitus	1.29 (1.16–1.45)†	1.85 (1.47–2.33)†
Hypertension	0.96 (0.86–1.08)	1.18 (0.91–1.52)
Liver disease	1.35 (1.11–1.63)†	1.52 (1.09–2.12)†
Cancer	1.16 (0.98–1.37)	1.35 (1.00–1.82)†
Renal disease	1.14 (0.97–1.34)	1.76 (1.34–2.32)†
Insurance (no, vs. yes)	1.40 (1.24–1.59)†	2.01 (1.59–2.56)†
Service-connected condition	1.24 (1.11–1.38)†	1.12 (0.90–1.38)
BMI category		
<18.5 kg/m^2	1.85 (1.04–3.27)†	1.32 (0.39–4.52)
18.5–25 kg/m^2	1 (Referent)	1 (Referent)
25–30 kg/m^2	1.21 (0.96–1.54)	1.22 (0.74–2.00)
30–35 kg/m^2	1.38 (1.10–1.74)†	1.32 (0.81–2.15)
>35 kg/m^2	1.57 (1.24–1.98)†	1.49 (0.91–2.45)
Urban/rural status		
Urban	1 (Referent)	1 (Referent)
Rural	0.89 (0.80–1.00)	0.95 (0.76–1.18)
Highly urban	1.04 (0.68–1.58)	0.72 (0.26–2.00)
Number of hospitalizations in prior year	1.17 (1.12–1.22)†	1.23 (1.16–1.30)†
County COVID-19 incidence rate per 100,000	1.00 (1.00–1.00)†	1.00 (1.00–1.00)†

* Values are the hazard ratio (95% confidence interval) for the risk of developing COVID-19 or severe COVID-19 (requiring hospitalization or resulting in death) in sensitivity analyses of fully adjusted models, in which individual comorbidities, rather than the overall Elixhauser Comorbidity Index, were incorporated in the model. RA = rheumatoid arthritis; BMI = body mass index.
† $P < 0.05$.

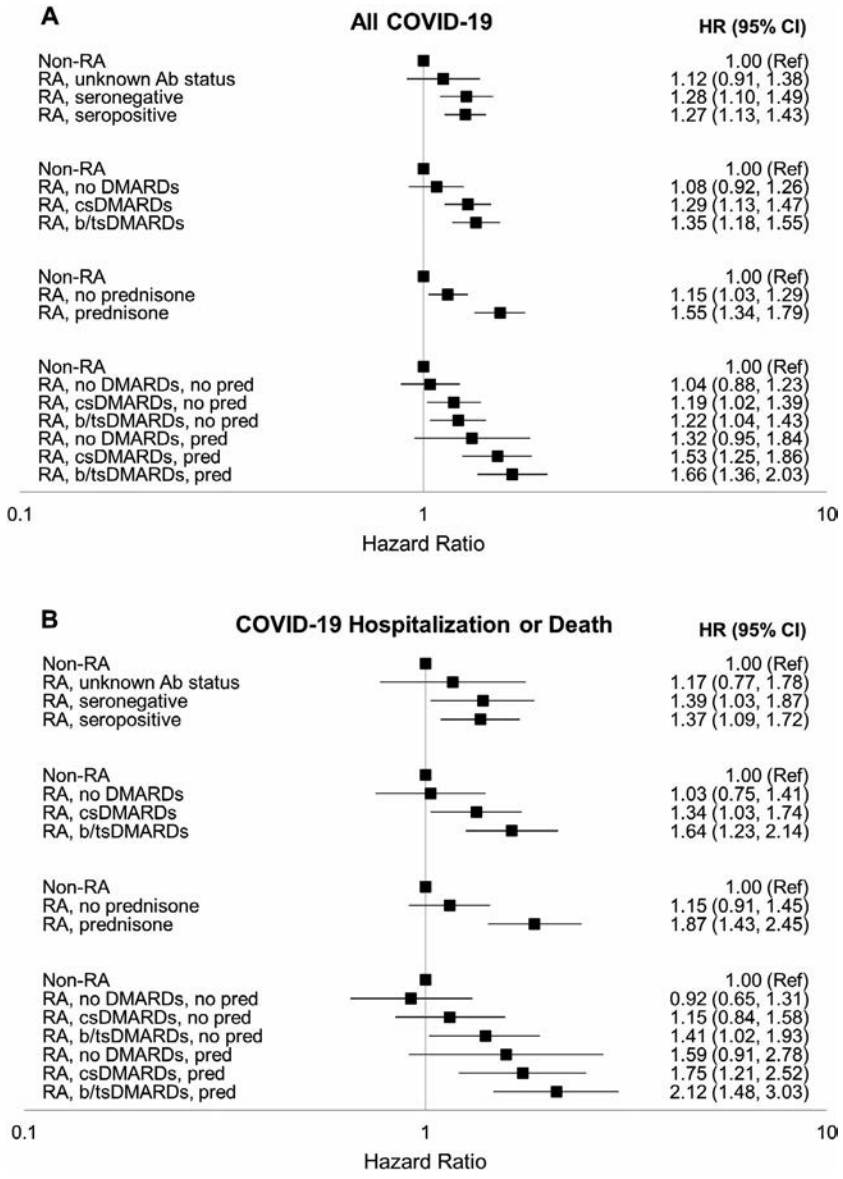

Figure 1. Risk of COVID-19 (**A**) and severe COVID-19 (requiring hospitalization or leading to death) (**B**) in subgroups of patients with rheumatoid arthritis (RA) and age-, sex-, and site-matched non-RA controls. RA patients were stratified according to antibody (Ab) status, treatment with disease-modifying antirheumatic drugs (DMARDs), treatment with prednisone (pred), and combination treatment with DMARDs and prednisone. Values are the hazard ratio (HR) with 95% confidence interval (95% CI) for the risk of COVID-19 or severe COVID-19, adjusted for race, ethnicity, smoking status, body mass index, Elixhauser Comorbidity Index, insurance status, urban/rural residence, number of hospitalizations in prior year, presence of a military service–connected condition, and county-level COVID-19 incidence rates. Ref = referent; csDMARDs = conventional synthetic DMARDs; b/tsDMARDs = biologic/targeted synthetic DMARDs.

35% increased risk of COVID-19 hospitalization or death. These are among the first data to link RA with a higher risk of COVID-19. Moreover, our results linking RA with a higher risk of viral infection is an important contribution to our understanding of how RA may affect the risk of developing other viral infections, since prior literature has focused on bacterial infections (3). Our findings of a higher risk of a more severe COVID-19 disease course in RA are consistent with results from a UK study of at-risk patients with RA, psoriasis, or lupus, in whom a 19% higher risk of COVID-19–associated death was observed (12), and also consistent with results from another study of COVID-19 patients in which a 14% higher risk of hospitalization in those with a rheumatic disease was observed (10). Our findings are also in line with prior estimates of the risk of serious infection (bacterial or nonbacterial) in RA patients relative to those without RA, with one study of patients in the FORWARD registry showing a 50% increased risk of serious infection (26).

In our study, RA patients receiving csDMARDs, those receiving bDMARDs/tsDMARDs, and those receiving prednisone had a higher risk of COVID-19 and higher risk of a severe COVID-19

disease course. Although we are not aware of prior literature describing a link between these therapies and COVID-19 risk in RA, others have similarly found that select immunosuppressive therapies, specifically rituximab and prednisone, were associated with a more severe disease course among patients with COVID-19, including those with RA (7,10,27). The highest-risk RA subgroup in our study was those who were receiving both bDMARDs/tsDMARDs and prednisone. These individuals had a >2-fold higher risk of COVID-19 hospitalization or death compared to non-RA controls. Similar risks have been identified in RA patients who were receiving bDMARDs/tsDMARDs and prednisone for non–COVID-19–related severe infections (28,29).

While there has been hope that some of these therapies might suppress the hyperinflammatory features of COVID-19 and improve outcomes, findings in this study highlight the notion that the timing of immunosuppressive therapies (preceding or at the time of exposure, early infection, or severe infection stages) may be crucial for measuring their potential impact on disease outcomes. Use of immunosuppressive medications may predispose an individual to COVID-19 infection or a more severe disease course early, but during the hyperinflammatory phase of severe COVID-19 (30), select immunosuppressive therapies may become beneficial. Our findings, and those of others, also raise concerns that patients with other medical conditions receiving these immunosuppressive therapies may be at higher risk of COVID-19 and severe COVID-19. Importantly, confounding by indication is recognized as a complicating factor in such observational studies of therapies and COVID-19, and therefore causal conclusions cannot be drawn (8). Further study is warranted.

Our findings have clear relevance to health policy surrounding COVID-19 prevention and management. Risk stratification for vaccination, for example, has primarily been established on the basis of age, occupational risks, and the presence of several chronic conditions. RA or the use of immunosuppressive therapies outside the setting of prior organ transplantation are not considered chronic conditions that would receive priority vaccination status (6). Our results suggest that RA patients receiving DMARDs and/or prednisone should be considered for priority status in these prevention efforts, including priority for receiving initial and booster vaccination. The 35% increased risk of COVID-19 hospitalization or death related to RA falls within the range we estimated for other conditions that receive priority status (adjusted HR ranging from 1.18 to 1.85). With <1.0% of the population having RA (31), the inclusion of RA as a priority group is unlikely to drastically impact vaccine or treatment supplies for other individuals, and the vulnerable population would remain protected. Moreover, since treatment with DMARDs and/or prednisone was linked to more severe COVID-19 in both our study (RA only) and other studies (including those with other rheumatic diseases [7,10]), prioritization may be warranted for any medical conditions requiring long-term immunosuppressive medications.

Consistent with other studies in the general population and in patients with rheumatic diseases, we found that race and ethnicity were major determinants of SARS–CoV-2 infection and severe COVID-19 (9,32). Black patients had a 22% higher risk of SARS–CoV-2 infection and a 25% higher risk of COVID-19 hospitalization or death. Similarly, patients with Hispanic ethnicity had a 48% higher risk of SARS–CoV-2 infection and a 25% increased risk of COVID-19 hospitalization or death, though the latter did not reach statistical significance. Importantly, the associations of race and ethnicity with COVID-19 were independent of other factors, including demographic characteristics, comorbidity burden and individual chronic conditions, health care utilization and insurance, and county-level COVID-19 incidence rates, all of which may mediate or confound such associations. Our findings therefore suggest that additional factors may contribute to the racial and ethnic disparities in the incidence and severity of COVID-19, such as differences in the severity of comorbid chronic conditions, community or occupational risks, time to receiving care, access during surges, or immune responses to SARS–CoV-2 (32); these factors will require further study.

There are limitations to this study. There is a potential for misclassification of RA status with the use of administrative algorithms. This is most likely to occur in RA patients who were not receiving DMARDs. Misclassification of non-RA patients as having RA should only bias the findings toward the null, resulting in an underestimation of the risk of COVID-19 in RA. Our study was designed to compare the risk of COVID-19 between RA patients and non-RA controls, rather than comparing the risk between specific medications or medication doses. To generate valid data for such comparisons and avoid the misinformation that has plagued the pandemic (33), alternative study designs would be required. DMARD and prednisone doses were not available for these analyses. In addition, misclassification of COVID-19 may have occurred, and the sensitivity of the standardized process utilized in the VA system for capturing non-VA COVID-19 cases has not been established. Our study population was composed primarily of older male patients (although >10,000 female patients were included), consistent with the demographics of the VA health care system, but findings may not be generalizable to other populations. While male sex has been associated with more severe COVID-19 (34), it is not expected that the impact of RA and RA therapies on COVID-19 risk would be differential between men and women. Finally, because of the observational nature of our study, unmeasured confounding may be present.

In conclusion, we observed that patients with RA in this VA cohort had a 25% increased risk of COVID-19 and a 35% increased risk of severe COVID-19 (leading to hospitalization or death), independent of several potential confounders. RA patients who had recently received DMARDs and prednisone were at the highest risk of COVID-19 and more severe COVID-19, risks that rivaled those accompanying other chronic conditions. Consideration should be given to the establishment of RA, and potentially other conditions that require treatment with similar immunosuppressive medications, as a chronic condition that should receive prioritization for COVID-19 prevention and management strategies.

ACKNOWLEDGMENTS

This study was supported by access to data from the VA COVID-19 Shared Data Resource, and by the resources and facilities of the VA Informatics and Computing Infrastructure (VA HSR RES 13-457).

AUTHOR CONTRIBUTIONS

All authors were involved in drafting the article or revising it critically for important intellectual content, and all authors approved the final version to be published. Dr. England had full access to all of the data in the study and takes responsibility for the integrity of the data and the accuracy of the data analysis.

Study conception and design. England, Mikuls.
Acquisition of data. England, Roul, Yang, Sauer, Baker, Mikuls.
Analysis and interpretation of data. England, Roul, Yang, Kalil, Michaud, Thiele, Sauer, Baker, Mikuls.

REFERENCES

1. Sparks JA. Rheumatoid arthritis. Ann Intern Med 2019;170: ITC1–16.
2. Jani M, Barton A, Hyrich K. Prediction of infection risk in rheumatoid arthritis patients treated with biologics: are we any closer to risk stratification? [review]. Curr Opin Rheumatol 2019;31:285–92.
3. Listing J, Gerhold K, Zink A. The risk of infections associated with rheumatoid arthritis, with its comorbidity and treatment [review]. Rheumatology (Oxford) 2013;52:53–61.
4. Wu C, Chen X, Cai Y, Xia J, Zhou X, Xu S, et al. Risk factors associated with acute respiratory distress syndrome and death in patients with coronavirus disease 2019 pneumonia in Wuhan, China. JAMA Intern Med 2020;180:934–43.
5. Zhou F, Yu T, Du R, Fan G, Liu Y, Liu Z, et al. Clinical course and risk factors for mortality of adult inpatients with COVID-19 in Wuhan, China: a retrospective cohort study. Lancet 2020;395:1054–62.
6. Oliver SE, Gargano JW, Marin M, Wallace M, Curran KG, Chamberland M, et al. The Advisory Committee on Immunization Practices' updated interim recommendation for allocation of COVID-19 vaccine—United States, December 2020. MMWR Morb Mortal Wkly Rep 2021;69:1657–60.
7. Strangfeld A, Schafer M, Gianfrancesco MA, Lawson-Tovey S, Liew JW, Ljung L, et al. Factors associated with COVID-19-related death in people with rheumatic diseases: results from the COVID-19 Global Rheumatology Alliance physician-reported registry. Ann Rheum Dis 2021;80:930–42.
8. Schafer M, Strangfeld A, Hyrich KL, Carmona L, Gianfrancesco M, Lawson-Tovey S, et al. Response to: 'Correspondence on 'Factors associated with COVID-19-related death in people with rheumatic diseases: results from the COVID-19 Global Rheumatology Alliance physician reported registry" by Mulhearn et al. Ann Rheum Dis 2021. doi: 10.1136/annrheumdis-2021-220134. E-pub ahead of print.
9. Gianfrancesco MA, Leykina LA, Izadi Z, Taylor T, Sparks JA, Harrison C, et al. Association of race and ethnicity with COVID-19 outcomes in rheumatic disease: data from the COVID-19 Global Rheumatology Alliance physician registry. Arthritis Rheumatol 2021;73:374–80.
10. D'Silva KM, Jorge A, Cohen A, McCormick N, Zhang Y, Wallace ZS, et al. COVID-19 outcomes in patients with systemic autoimmune rheumatic diseases compared to the general population: a US multicenter, comparative cohort study. Arthritis Rheumatol 2021;73:914–20.
11. Serling-Boyd N, D'Silva KM, Hsu TY, Wallwork R, Fu X, Gravallese EM, et al. Coronavirus disease 2019 outcomes among patients with rheumatic diseases 6 months into the pandemic. Ann Rheum Dis 2021;80:660–66.
12. Williamson EJ, Walker AJ, Bhaskaran K, Bacon S, Bates C, Morton CE, et al. Factors associated with COVID-19-related death using OpenSAFELY. Nature 2020;584:430–6.
13. Chung CP, Rohan P, Krishnaswami S, McPheeters ML. A systematic review of validated methods for identifying patients with rheumatoid arthritis using administrative or claims data. Vaccine 2013;31 Suppl 10:K41–61.
14. Donnelly JP, Wang XQ, Iwashyna TJ, Prescott HC. Readmission and death after initial hospital discharge among patients with COVID-19 in a large multihospital system. JAMA 2021;325:304–6.
15. Bowe B, Cai M, Xie Y, Gibson AK, Maddukuri G, Al-Aly Z. Acute kidney injury in a national cohort of hospitalized US veterans with COVID-19. Clin J Am Soc Nephrol 2020;16:14–25.
16. Luo J, Jeyapalina S, Stoddard GJ, Kwok AC, Agarwal JP. Coronavirus disease 2019 in veterans receiving care at Veterans Health Administration facilities. Ann Epidemiol 2021;55:10–4.
17. US Department of Veterans Affairs. VA informatics and computing infrastructure: updates to the VA COVID-19 Shared Data Resource and its use for research. June 2020. URL: https://www.hsrd.research.va.gov/for_researchers/cyber_seminars/archives/video_archive.cfm?SessionID=3834.
18. Baker JF, Billig E, Michaud K, Ibrahim S, Caplan L, Cannon GW, et al. Weight loss, the obesity paradox, and the risk of death in rheumatoid arthritis. Arthritis Rheumatol 2015;67:1711–7.
19. England BR, Baker JF, Sayles H, Michaud K, Caplan L, Davis LA, et al. Body mass index, weight loss, and cause-specific mortality in rheumatoid arthritis. Arthritis Care Res (Hoboken) 2018;70:11–8.
20. McGinnis KA, Brandt CA, Skanderson M, Justice AC, Shahrir S, Butt AA, et al. Validating smoking data from the Veteran's Affairs Health Factors dataset, an electronic data source. Nicotine Tob Res 2011;13:1233–9.
21. Elixhauser A, Steiner C, Harris DR, Coffey RM. Comorbidity measures for use with administrative data. Med Care 1998;36:8–27.
22. Dong E, Du H, Gardner L. An interactive web-based dashboard to track COVID-19 in real time [letter]. Lancet Infect Dis 2020;20:533–4.
23. Schwab P, Sayles H, Bergman D, Cannon GW, Michaud K, Mikuls TR, et al. Utilization of care outside the Veterans Affairs health care system by US veterans with rheumatoid arthritis. Arthritis Care Res (Hoboken) 2017;69:776–82.
24. Dennis JM, McGovern AP, Vollmer SJ, Mateen BA. Improving survival of critical care patients with coronavirus disease 2019 in England: a national cohort study, March to June 2020. Crit Care Med 2021;49:209–14.
25. Jorge A, D'Silva KM, Cohen A, Wallace ZS, McCormick N, Zhang Y, et al. Temporal trends in severe COVID-19 outcomes in patients with rheumatic disease: a cohort study. Lancet Rheumatol 2021;3:e131–7.
26. Mehta B, Pedro S, Ozen G, Kalil A, Wolfe F, Mikuls T, et al. Serious infection risk in rheumatoid arthritis compared with non-inflammatory rheumatic and musculoskeletal diseases: a US national cohort study. RMD Open 2019;5:e000935.
27. Ungaro RC, Agrawal M, Park S, Hirten R, Colombel JF, Twyman K, et al. Autoimmune and chronic inflammatory disease patients with COVID-19. ACR Open Rheumatol 2021;3:111–5.
28. Singh JA, Cameron C, Noorbaloochi S, Cullis T, Tucker M, Christensen R, et al. Risk of serious infection in biological treatment of patients with rheumatoid arthritis: a systematic review and meta-analysis. Lancet 2015;386:258–65.
29. George MD, Baker JF, Winthrop K, Hsu JY, Wu Q, Chen L, et al. Risk for serious infection with low-dose glucocorticoids in patients with rheumatoid arthritis: a cohort study. Ann Intern Med 2020;173:870–8.
30. Cao X. COVID-19: immunopathology and its implications for therapy [review]. Nat Rev Immunol 2020;20:269–70.
31. Cross M, Smith E, Hoy D, Carmona L, Wolfe F, Vos T, et al. The global burden of rheumatoid arthritis: estimates from the

Global Burden of Disease 2010 study. Ann Rheum Dis 2014;73:1316–22.
32. Price-Haywood EG, Burton J, Fort D, Seoane L. Hospitalization and mortality among black patients and white patients with Covid-19. N Engl J Med 2020;382:2534–43.
33. Kim AH, Sparks JA, Liew JW, Putman MS, Berenbaum F, Duarte-Garcia A, et al. A rush to judgment? Rapid reporting and dissemination of results and its consequences regarding the use of hydroxychloroquine for COVID-19 [editorial]. Ann Intern Med 2020;172:819–21.
34. Peckham H, de Gruijter NM, Raine C, Radziszewska A, Ciurtin C, Wedderburn LR, et al. Male sex identified by global COVID-19 meta-analysis as a risk factor for death and ITU admission. Nat Commun 2020;11:6317.

DOI 10.1002/art.41910

Clinical Images: Leukocytoclastic vasculitis after vaccination with a SARS–CoV-2 vaccine

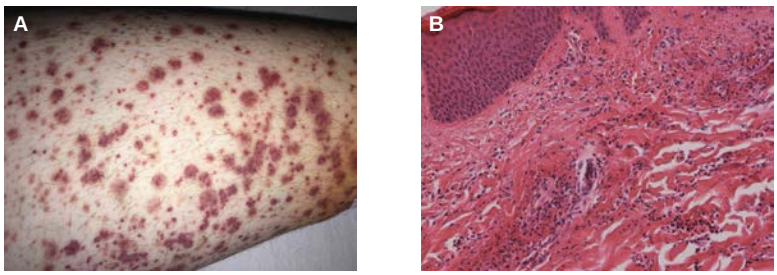

The patient, a 42-year-old White woman, presented to the emergency room with a 1-week history of rash on the lower legs, which had first appeared 4 days after vaccination with the BioNTech/Pfizer SARS–CoV-2 vaccine. The rash—with the typical appearance of cutaneous small vessel vasculitis (SVV)—spread from the lower limbs up to the gluteal area over the course of a few days (**A**). Application of topical steroids did not lead to improvement. Physical examination showed no other conditions, except for hypertension and severe obesity (body mass index 47 kg/m^2). Typical causes of cutaneous SVV (1) were considered, and concomitant medication or infection could be ruled out as possible triggers. Besides slightly elevated levels of inflammation markers, laboratory test results for complement components C3 and C4, CH50, IgM, IgA, immunofixation, and renal and liver parameters were normal. IgG and thyroid-stimulating hormone were slightly elevated (20.3 gm/liter and 8.3 μU/liter, respectively). Chest radiography, echocardiography, and ultrasound examination of the abdomen revealed normal results, as did serologic tests for autoimmune antibodies (classic/perinuclear antineutrophil cytoplasmic antibody, rheumatoid factor, anti–citrullinated protein antibody, antinuclear antibody [titer 1:160 with nuclear fine speckled pattern] and negativity for a panel of extractable nuclear antigen antibodies [including Jo-1, U1 RNP, Scl-70, Sm, and Ro/La antibodies]), and screening for viral infections (hepatitis B and C, cytomegalovirus, Epstein-Barr virus, coxsackievirus, and HIV) and cryoglobulins. Following analysis of a skin biopsy sample from the patient's left ankle (**B**), leukocytoclastic vasculitis was diagnosed. The skin tissue was also assessed by immunostaining, but results were not evaluable. Prednisolone treatment was started, at an initial dose of 30 mg/day which was later increased to 60 mg/day due to poor response. With this treatment the rash resolved over the next 5 days. Leukocytoclastic vasculitis is typically found to be idiopathic in up to 50% of cases; however, due to its emergence in this patient shortly after she had received the SARS–Cov-2 vaccination, we think a possible connection to the vaccine should be considered. To our knowledge, this might be the first case of the development of leukocytoclastic vasculitis after vaccination against SARS–CoV-2, whereas cutaneous SVV has been described in a patient following SARS–CoV-2 infection (2), and also SVV has been observed in patients after various other vaccinations, such as those against influenza or pneumococci (3). Since experience with the new COVID-19 vaccines is limited—as they have been in use for <1 year—further investigations and observations are essential.

Author disclosures are available at https://onlinelibrary.wiley.com/action/downloadSupplement?doi=10.1002%2Fart.41910&file=art41910-sup-0001-Disclosureform.docx.

1. Gota CE, Calabrese LH. Diagnosis and treatment of cutaneous leukocytoclastic vasculitis [review]. Int J Clin Rheumatol 2013;8:49–60.
2. Gottlieb M, Long B. Dermatologic manifestations and complications of COVID-19 [review]. Am J Emerg Med 2020;38:1715–21.
3. Cao S, Sun D. Leucocytoclastic vasculitis following influenza vaccination. BMJ Case Rep 2017;2017:bcr-2016-217755.

Anne Erler, MD
John Fiedler
Anna Koch
Frank Heldmann, MD
Zeisigwaldkliniken Bethanien Chemnitz
Chemnitz, Germany
Alexander Schütz, MD
Institute of Pathology at Elsapark
Leipzig, Germany

Arthritis & Rheumatology
Vol. 73, No. 12, December 2021, pp 2189–2199
DOI 10.1002/art.41802
Published 2021. This article is a U.S. Government work and is in the public domain in the USA.

American College of Rheumatology
Empowering Rheumatology Professionals

Incident Rheumatoid Arthritis in HIV Infection: Epidemiology and Treatment

Jennifer S. Hanberg,[1] Evelyn Hsieh,[1] Kathleen M. Akgün,[1] Erica Weinstein,[2] Liana Fraenkel,[1] Amy C. Justice,[1] and the VACS Project Team

Objective. To assess the incidence, presentation, and management of rheumatoid arthritis (RA) in patients with HIV, including the use of disease-modifying antirheumatic drugs (DMARDs) in this immunosuppressed population.

Methods. Patients included in this study were from the Veterans Aging Cohort Study, a longitudinal cohort of veterans with HIV and age-, race-, and site-matched uninfected veterans. We identified all patients who had ≥1 rheumatologist-generated International Classification of Diseases, Ninth Revision (ICD-9) or Tenth Revision (ICD-10) code for RA and whose serum samples were tested for rheumatoid factor (RF) and anti–cyclic citrullinated peptide (anti-CCP) antibodies. To further confirm the diagnosis of RA, medical charts were reviewed to verify whether patients met the American College of Rheumatology/European Alliance of Associations for Rheumatology 2010 criteria for RA. We recorded DMARD use and adverse effects during the first contiguous course of treatment (i.e., >6 months of no interruption in DMARD treatment).

Results. This study included 56,250 patients with HIV and 116,944 uninfected individuals over 2,384,541 person-years. Of the 2,748 individuals in this cohort who were reviewed for a diagnosis of RA based on ICD-9 or ICD-10 codes, incident RA was identified in 215 individuals, including 21 patients with HIV. The incidence rate ratio of RA for patients with HIV compared to uninfected individuals was 0.29 (95% confidence interval 0.19–0.48). Most of the patients diagnosed as having RA (88%) were seropositive for RA-associated autoantibodies (RF and/or anti-CCP). However, high autoantibody titers were less frequent in RA patients with HIV compared to RA patients without HIV. In total, 5% of RA patients with HIV (1 of 21) had both high titers of anti-CCP and high titers of RF, compared to 41% of uninfected individuals (81 of 194). DMARDs were prescribed in 71% of RA patients with HIV (15 of 21) compared to 94% of RA patients without HIV (183 of 194). There was no indication that the DMARD safety profile was worse among RA patients with HIV who were prescribed DMARDs (n = 10 assessed) compared to RA patients without HIV who were prescribed DMARDs (n = 158 assessed).

Conclusion. In this cohort, incident RA was less common in patients with HIV compared to uninfected individuals. Moreover, compared to RA patients without HIV, the seropositivity rate and titers of RA-specific autoantibodies were lower among RA patients with HIV, and those with HIV were prescribed DMARDs less frequently than those without HIV.

INTRODUCTION

HIV infection affects >37 million individuals worldwide. In the era of modern antiretroviral therapy (ART), the care of patients with HIV has moved beyond the management of opportunistic infections to encompass the management of a lifelong, viral, proinflammatory infection that is associated with increased risk of multiple chronic diseases, as well as accelerated mortality (1,2). Although HIV was initially regarded as a purely immunosuppressive condition, mounting evidence among patients with HIV receiving

Presented in abstract form at the American College of Rheumatology Convergence 2020.

Supported by the NIH (National Institute on Alcohol Abuse and Alcoholism grants U24-AA-020794, U01-AA-020790, and U10-AA-013566 and National Heart, Lung, and Blood Institute grant T35-HL-007649), the US Department of Veterans Affairs, and the Rheumatology Research Foundation Medical and Pediatric Resident Research Award.

[1]Jennifer S. Hanberg, MD, Evelyn Hsieh, MD, PhD, Kathleen M. Akgün, MD, MS, Liana Fraenkel, MD, MPH, Amy C. Justice, MD, PhD: Yale University, New Haven, Connecticut, and VA Connecticut Healthcare System, West Haven, Connecticut; [2]Erica Weinstein, MD: University of Pennsylvania Perelman School of Medicine, Philadelphia.

No potential conflicts of interest relevant to this article were reported.

Address correspondence to Amy C. Justice, MD, PhD, VA Connecticut Healthcare System, 950 Campbell Avenue, West Haven, CT 06516. Email: amy.justice2@va.gov.

Submitted for publication January 21, 2021; accepted in revised form May 4, 2021.

ART suggests that it is associated with chronic inflammation and immune dysfunction, and a wide variety of autoinflammatory and autoimmune conditions have been described in patients with HIV (3–5). Among these, rheumatoid arthritis (RA) is of particular interest, given the shared tendency toward autoantibody development, the shared increased risk of chronic inflammation–driven end-organ disease, and the relatively high population-level prevalence of RA (0.5–2% in the general population) (6–11).

There is evidence to suggest that RA may interfere in the diagnosis of HIV (due to false-positive enzyme-linked immunosorbent assay findings in RA patients) and HIV may interfere in the diagnosis of RA (due to the presence of autoantibodies and nonspecific inflammatory arthritis in both conditions) (12). Increased frequency of autoantibodies and impaired immune tolerance are shared features of RA and HIV: ~80% of patients with RA have detectable levels of autoantibodies (including rheumatoid factor [RF], anti–cyclic citrullinated peptide [anti-CCP] antibodies, or both) (12–15). For comparison, 10–47% of patients with HIV were reported to be positive for RF. While anti-CCP antibodies are rarer, both types of autoantibodies are less prevalent in patients with HIV receiving ART (12,16). Additionally, hepatitis C virus (HCV) infection, a common coinfection among patients with HIV, can cause an individual to be positive for RF. Finally, multiple types of inflammatory arthritic conditions have been reported in HIV, including, but not limited to, RA. These conditions range from suspected "HIV arthritis" in 0.4–13.8% of patients, to reactive arthritis in 0–11% of patients with HIV, to RA in 0.1–5% of patients with HIV (7,16–18).

Formal estimates of the incidence of RA among patients with HIV compared to uninfected individuals are lacking. With the improved prognosis and life expectancy among patients with HIV, it is crucial to understand the epidemiology and clinical features of RA in HIV patients, since RA is one of the most prevalent autoimmune conditions in adults and since these have not been described to date. Furthermore, given that patients with HIV have underlying immune dysfunction, and RA is often treated with immunosuppression, clinicians often struggle with treating these opposing yet overlapping diseases. Current clinical practices, treatments, and outcomes of RA among patients with HIV have not been well described. Additionally, there is a paucity of data on the prescribing practices, safety, and efficacy of disease-modifying antirheumatic drugs (DMARDs), which include the core immunomodulatory and immunosuppressive medications, to treat RA in patients with HIV.

To address these knowledge gaps, we utilized a large database of patients with HIV and age-, race-, and site-matched HIV-negative individuals with the following aims: 1) to compare the incidence and presentation of RA in patients with HIV to individuals without HIV, 2) to assess DMARD prescribing patterns in RA patients with HIV, and 3) to evaluate the safety and tolerability of these regimens in patients with HIV.

PATIENTS AND METHODS

We conducted a prospective cohort study using data from the Veterans Aging Cohort Study (VACS), which has been described in detail previously (19,20). Briefly, the VACS is a prospective, longitudinal observational study of patients with HIV within the Veterans Health Administration. The cohort comprises ~56,000 patients with HIV and 117,000 HIV-negative individuals. In the present study, for each patient with HIV, 2 HIV-negative individuals were matched to the patients by age, race, and site. The institutional review boards associated with the participating sites, as well as the coordinating center for the study, approved use of the VACS, and written informed consent was obtained from each subject. The RA cohort was drawn from the overall VACS cohort, which we defined as our population at risk of RA. Within the VACS, we aimed to identify patients who may have RA, based on a recorded International Classification of Diseases, Ninth Revision (ICD-9) or Tenth Revision (ICD-10) code for RA and clinical findings from rheumatology clinic visits (according to clinic stop codes) between 1997 and 2017.

Identification of patients with HIV, and classification of RA within the cohort. Patients with HIV were identified based on the presence of 2 outpatient or 1 inpatient ICD-9 or ICD-10 codes for HIV (20). ICD-based algorithms used for the identification of patients with RA have been published. In particular, Kim et al reported that 2 rheumatologist-based diagnoses ≥6 weeks apart, in conjunction with a DMARD prescription, had a positive predictive value of 89%, making it the gold standard for RA diagnosis by a rheumatologist observable on chart review (21). However, in preliminary analyses, we found a significant discrepancy in the rates of DMARD use in ICD-coded RA patients with HIV versus those without HIV (28% [158 of 556] versus 42% [923 of 2,200], respectively), which led to concerns that this algorithm may not be as sensitive in patients with HIV. Therefore, we used an alternative approach to identify patients for inclusion (Supplementary Figure 1, available on the *Arthritis & Rheumatology* website at http://onlinelibrary.wiley.com/doi/10.1002/art.41802/abstract), which consisted of a sensitive algorithm to identify potential RA patients, followed by manually reviewing charts to confirm all identified cases.

Given the findings above, we used the following algorithm to identify patients for inclusion (Supplementary Figure 1, available on the *Arthritis & Rheumatology* website at http://onlinelibrary.wiley.com/doi/10.1002/art.41802/abstract). First, individuals with at least one ICD-9 (714.x) or ICD-10 (M05.x, M06.x) diagnosis code for RA were identified. Of these, we excluded those who did not have a diagnosis from a rheumatologist (required for documentation of a thorough, standardized joint examination with documentation of swelling, tenderness, and synovitis). We then excluded individuals without serologic assessment of RA-associated antibodies

(which are required for classification in the 2010 American College of Rheumatology [ACR]/European Alliance of Associations for Rheumatology [EULAR] criteria for RA) (22). After applying these requirements, we manually reviewed charts to identify only cases fulfilling the 2010 RA classification criteria (Figure 1).

In accordance with the ACR/EULAR criteria, points were assigned for the following features: duration of symptoms (1 point = disease duration of ≥6 weeks), presence of elevated markers of inflammation (1 point), serologic status (i.e., absence of RF and/or anti-CCP antibodies versus presence and titers of RF and/or anti-CCP antibodies; 0 points = absence of RF and anti-CCP, 2 points = low-positive titers [defined as ≥1 value above the upper limit of normal (ULN)], and 3 points = high-positive titers [defined as ≥1 value ≥3 times the ULN]). In addition, points were assigned for the extent of joint involvement (excluding the first carpometacarpal joints and distal interphalangeal joints of the hands), as follows: 0 points = 1 large joint involved, 1 point = 2–10 large joints involved, 2 points = 1–3 small joints involved, 3 points = 4–10 small joints involved, and 5 points = >10 small joints involved (22). In accordance with the criteria, we required a score of ≥6 or the presence of radiographic erosions, with no alternative diagnosis to explain the symptoms, to classify a patient as having "definite" RA. If criteria were not fulfilled at the first visit, all subsequent rheumatology visits were reviewed to determine if the patient fulfilled criteria at a later date, which is consistent with the intended use of the criteria as published. Any patients who eventually fulfilled the criteria were considered to have incident RA, with the date of onset recorded as the date that they fulfilled the criteria.

Since the criteria listed above do not specifically address some situations that arise during chart review, we used the following additional decision rules. For example, if a clinician indicated that the metacarpophalangeal (MCP) joints were swollen, a score of 2 was assigned; if the clinician indicated swelling in all MCPs, then a score of 3 was assigned, consistent with the involvement of 8 small joints. Patients were classified as having prevalent RA if there was documentation of a medical history of RA or a prior diagnosis of RA.

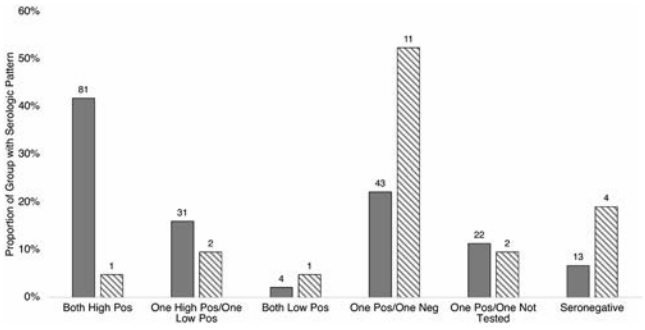

Figure 1. Distribution of rheumatoid factor and anti–cyclic citrullinated peptide autoantibody patterns in rheumatoid arthritis patients (RA) with HIV (cross-hatched bar) compared to RA patients without HIV (shaded bar). High-positive (High Pos) was defined as a titer of ≥3 times the upper limit of normal (ULN), in accordance with the 2010 American College of Rheumatology/European Alliance of Associations for Rheumatology criteria for RA. Low-positive (Low Pos) was defined as a titer of above the ULN but lower than 3 times the ULN or any autoantibody recorded as "positive" without quantification of the titer. Values above the bars represent the number of RA patients with HIV or RA patients without HIV in each serologic pattern group.

Baseline demographic and clinical data. Demographic data, including age, sex, and race or ethnicity, were extracted as categorical variables from the VACS database. Smoking status was evaluated by determining the most common smoking status designation between all visits (never, former, or current smoker) (23). The presence of HCV in the VACS database was determined based on assessment of HCV serologic test results, genotype, and viral loads. We classified patients as HCV positive if they had either HCV antibody positivity or a positive genotype or were viral load–positive (24).

Additional clinical variables of interest, including CD4 cell counts and HIV viral load data at diagnosis of RA and at the beginning of follow-up or first measurement, serologic results indicating positivity for RF and anti-CCP antibodies, and the presence of radiographic erosions, were collected during manual chart review. Radiologist reports were used to determine the presence of erosions, since we did not have access to radiographic images.

Outcomes. Primary outcomes included incident RA, DMARD prescription among RA patients with HIV, and safety/tolerability events during DMARD therapy in RA patients with HIV who are new users. To evaluate tolerability and safety, events in the first course of contiguous DMARD therapy, defined as a period of >6 months with no interruption in DMARD treatment, were identified during manual review of charts. We recorded medications used to treat RA for at least the first 5 years after diagnosis or until the end of follow-up (December 31, 2019). In patients whose first course of DMARD therapy was >5 years, all medications used in that course were recorded. We excluded hydroxychloroquine (HCQ) from this analysis, since it has been shown to be more tolerable, with studies showing that its immunosuppressive effects in the bone marrow are less intense than those observed with other DMARDs. Records from rheumatology clinic visits were evaluated to determine changes in therapy and the reasons for these changes, including loss of efficacy and adverse effects. We evaluated trends in HIV disease control after the initiation of DMARD therapy using viral load data and CD4 cell percentage. We used CD4 cell percentage rather than absolute CD4 cell counts due to the anticipated treatment effects on total leukocyte counts.

To determine the occurrence of serious infections in patients receiving DMARD therapy (and those not receiving DMARD therapy, as a comparator group), we utilized previously validated discharge diagnosis ICD-9 codes for infectious pneumonia, meningitis/encephalitis, skin/soft tissue infections, bacteremia/sepsis, septic arthritis, and pyelonephritis (25). We also utilized

their ICD-10 counterpart codes with Crosswalk (also known as General Equivalence Mappings, a process that translates ICD codes between versions, such as translating ICD-9 codes to ICD-10; more details available at www.icd10codesearch.com and www.icd10data.com).

Statistical analysis. Measures of central tendency were reported as the mean ± SD or the median (interquartile range [IQR]). Between-group differences in terms of the distribution of categorical variables were assessed using chi-square test, except where values were <5, in which case Fisher's exact test was used.

Table 1. Characteristics of the overall study population*

	HIV patients (n = 56,250)	HIV-negative individuals (n = 116,944)
Demographic characteristic		
Age at study initiation, mean ± SD years	45 ± 11	44 ± 11
Sex, male	54,772 (97)	113,642 (97)
Race or ethnicity		
White	22,253 (40)	47,334 (40)
Black	26,757 (48)	54,282 (46)
Hispanic	4,519 (8)	9,686 (8)
Other	2,712 (5)	5,612 (5)
HCV status		
Negative (by antibody or RNA test)	32,340 (57)	74,570 (64)
Positive (by antibody or RNA test or ICD code)	16,062 (29)	16,200 (14)
Never tested	7,848 (14)	26,174 (22)
Smoking status†		
Current	26,214 (56)	53,281 (51)
Former	7,619 (16)	20,133 (19)
Never	13,288 (28)	32,002 (30)
CD4 cell count at cohort entry, cells/mm^3		
≥500	14,794 (33)	–
350–499	8,489 (19)	–
300–349	3,082 (7)	–
100–299	11,598 (26)	–
50–99	2,590 (6)	–
<50	4,373 (10)	–
HIV-1 RNA, copies/ml		
<500	18,479 (41)	–
500–10,000	8,077 (18)	–
>10,000	18,938 (42)	–
RA status‡		
Only ICD code present	108 (76)	376 (51)
Prevalent RA	14 (10)	168 (23)
Incident RA	21 (15)	194 (26)
Serology		
No antibody testing	48,528 (86)	96,202 (82)
Anti-CCP, no.	1,449	4,460
High-positive	83 (6)	447 (10)
Low-positive	113 (8)	250 (6)
Negative	1,253 (86)	3,763 (84)
RF, no.	7,510	20,229
High-positive	319 (4)	938 (5)
Low-positive	1,202 (16)	3,082 (15)
Negative	5,989 (80)	16,209 (80)
Serologic pattern, no.§	1,636	4,338
Both high-positive	32 (2)	241 (6)
1 high-positive/1 low-positive	32 (2)	83 (2)
Both low-positive	17 (1)	55 (1)
1 positive/1 negative	371 (23)	1,065 (25)
1 positive/1 not tested	1,184 (72)	2,894 (67)

* Except where indicated otherwise, values are the number (%) of subjects. HCV = hepatitis C virus; HIV-1 = HIV type 1; anti-CCP = anti–cyclic citrullinated peptide; RF = rheumatoid factor.
† Data on smoking status were collected from 47,121 HIV patients and 105,416 HIV-negative individuals.
‡ Of those with an International Classification of Diseases (ICD) code for rheumatoid arthritis (RA).
§ Of those with ≥1 positive antibody test finding.

Differences in the distribution of continuous variables between >2 groups were assessed using the Kruskal-Wallis test. Incidence rate ratios with corresponding 95% confidence intervals (95% CIs) for incidence rates were estimated using generalized linear modeling and Poisson regression. Logistic regression analyses were used to evaluate the association between the dependent variable of treatment with DMARDs and independent covariates, including HIV infection, HCV infection, and the presence of radiographic erosions. These covariates were chosen based on the clinical relevance of parameters to disease severity and treatment options (e.g., severe liver disease may be a contraindication for certain DMARDs, whereas the presence of radiographic erosions may indicate more severe disease that is more likely to require therapy).

Statistical analysis was performed using Stata software version 14 (StataCorp), SAS software version 9.4 (SAS Institute), and R software (R Core Team). *P* values less than 0.05 (2-tailed) were considered significant.

RESULTS

Sociodemographic and clinical characteristics of the overall cohort. The VACS Cohort includes 56,250 patients with HIV and 116,944 individuals without HIV, comprising a total of 2,384,541 person-years of observation. Most patients with HIV were men (97%), and the median age of patients with HIV at the initiation of the study was 45 years (44 years in uninfected individuals) (Table 1). HCV infection was more common among patients with HIV (29%) than among individuals without HIV (14%), although any type of testing for HCV was more frequently performed among patients with HIV (86% versus 78% among uninfected individuals).

Among the entire cohort, 16% of patients underwent serologic testing for RA (Table 1). The distribution of individuals in each RF and/or anti-CCP serologic category was similar between patients with HIV and individuals without HIV. High-positive titers (≥3 times the ULN) were observed in 4% of patients with HIV and 5% of HIV-negative individuals ($P = 0.13$). Low-positive titers were observed in 15–16% of individuals in each group. In total, 80% of individuals were seronegative for RF and/or anti-CCP antibodies (Table 1). The percentage of individuals with high titers of anti-CCP (≥3 times the ULN) was lower in patients with HIV than in individuals without HIV (6% [83 of 1,449] versus 10% [447 of 4,460]; $P < 0.0001$). Despite similar rates of antibody positivity overall, the false-positive rates for a diagnosis of RA based on RF testing (i.e., positive for RF in the absence of RA) was higher in patients with HIV than in individuals without HIV. That is, among patients positive for RF, 14 of 1,521 patients with HIV (0.9%) were classified as having incident RA compared to 145 of 4,020 individuals without HIV (3.6%). Furthermore, among the whole cohort, the known association of HCV with autoantibody positivity was observed. Any seropositivity was present in 19% of both patients with HIV without HCV and HIV-negative individuals without HCV, compared to 25% of HIV patients with HCV and 31% of HIV-negative individuals with HCV ($P < 0.0001$).

Prevalence and incidence of RA among patients with HIV and uninfected individuals. Of 2,748 patients (547 patients with HIV, 2,201 uninfected individuals) with an ICD-9 or ICD-10 code for RA, 1,609 had ≥1 rheumatologist-generated ICD-9 or ICD-10 code (305 patients with HIV, 1,304 uninfected individuals). The rates of ICD-based RA diagnoses by a rheumatologist were comparable between groups (55% in patients with HIV versus 59% in uninfected individuals; $P = 0.14$). We excluded patients without documentation of serologic testing for RA (n = 728) (Supplementary Figure 1, available on the *Arthritis & Rheumatology* website at http://onlinelibrary.wiley.com/doi/10.1002/art.41802/abstract). This left us with 881 charts to review. After reviewing the charts of these remaining cases (143 patients with HIV, 738 uninfected individuals), 182 cases of prevalent RA (14 patients with HIV, 168 uninfected individuals) and 215 cases of incident RA (21 patients with HIV, 194 uninfected individuals) were identified (Tables 1 and 2).

The median time from first observation at the Veterans Administration clinic recorded in the electronic medical records to fulfilment of RA criteria was 10 years in patients with HIV (IQR 6–15) and 10 years in individuals without HIV (IQR 7–15). The crude incidence of RA was 0.33 cases per 10,000 person-years in patients with HIV (95% CI 0.21–0.51) compared to 1.11 cases per 10,000 person-years in individuals without HIV (95% CI 0.96–1.28). The incidence rate ratio of RA in individuals without HIV compared to patients with HIV was 0.29 (95% CI 0.19–0.48; $P < 0.0001$).

Clinical and serologic features of RA patients. Most patients classified as having RA were seropositive (Table 2). However, high antibody titers were found less frequently in patients with HIV: among patients with HIV with incident RA, 5% had both high anti-CCP titers and high RF titers, compared to 41% of uninfected individuals with incident RA (Figure 1). Among patients with HIV, the most common serologic pattern observed was a positive/negative mixed autoantibody pattern (52% of patients showing this mixed pattern); the proportion of patients who were positive for RF/negative for anti-CCP and the proportion of patients who were negative for RF/positive for anti-CCP was roughly equally divided (Figure 1). This further confirms the association between HIV infection and less robust RA serologic profiles among those with prevalent RA (i.e., RA diagnosed before HIV is diagnosed); serologic profiles were at least as strongly positive as those of uninfected individuals. The occurrence of both high titers of anti-CCP and high titers of RF was in fact more frequently observed among patients with HIV (43%) than individuals without HIV (29%).

The median time from the diagnosis of HIV to the diagnosis of incident RA was 13.7 years (IQR 9.3–19.7). At diagnosis, the median CD4 cell count in patients with HIV was 487 cells/

Table 2. Baseline characteristics of the patients with incident RA, separated by HIV status*

Characteristic	Patients with HIV (n = 21)	Patients without HIV (n = 194)	*P*
Demographic			
Age at diagnosis, mean ± SD years	58 ± 11	56 ± 10	0.38
Sex, male	20 (95)	181 (93)	0.73
Race or ethnicity			0.67
White	8 (42)	73 (40)	
Black	9 (47)	73 (40)	
Hispanic	2 (11)	26 (14)	
Other	0 (0)	11 (6)	
Smoking status			0.47
Current	9 (43)	98 (51)	
Former	8 (38)	49 (26)	
Never	4 (19)	45 (23)	
HCV status			0.004
Negative	12 (57)	162 (84)	
Positive†	9 (43)	28 (14)	
Never tested	0 (0)	4 (2)	
Time from first observation to RA criteria fulfilment, median (IQR) years	10 (6–15)	10 (7–15)	
Time since HIV diagnosis, median (IQR) years	14 (10–20)	–	
Time since ART initiated, median (IQR) years	8 (1–10)	–	
CD4 cells cells/mm^3‡			
≥500	11 (52)	–	
350–499	6 (29)	–	
300–349	2 (10)	–	
100–299	1 (5)	–	
50–99	0 (0)	–	
<50	1 (5)	–	
HIV-1 RNA, copies/ml‡			
≤500	16 (80)	–	
501–10,000	4 (20)	–	
>10,000	0 (0)	–	
Joint involvement§			0.07
One large joint	0 (0)	1 (1)	
2–10 large joints	1 (5)	12 (6)	
1–4 small joints	9 (42)	103 (53)	
5–10 small joints	7 (33)	54 (28)	
>10 small joints	4 (19)	24 (12)	
Elevated inflammation markers	12 (67)	140 (73)	0.55
Radiographic erosions			
Present within 1 year of RA diagnosis	5 (24)	51 (26)	0.81
Ever present	7 (33)	91 (47)	0.18
Treatments			
None	6 (29)	11 (6)	0.0002
Glucocorticoids	15 (71)	127 (65)	0.58
HCQ	12 (57)	119 (61)	0.71
SSZ	4 (19)	61 (31)	0.24
MTX	7 (33)	127 (66)	0.004
LEF	0 (0)	23 (12)	0.01
AZA	0 (0)	7 (4)	0.38
Biologics and JAK inhibitors	2 (10)	68 (35)	0.02
Other¶	0 (0)	7 (4)	0.38
Serology			
RF status			0.0002
High positive	6 (29)	116 (60)	
Low positive	5 (24)	47 (24)	
Negative	9 (43)	19 (10)	
Not tested	1 (5)	12 (6)	
Anti-CCP status			0.01
High positive	5 (24)	116 (60)	
Low positive	5 (24)	18 (9)	
Negative	9 (43)	44 (23)	
Not tested	2 (10)	16 (8)	
Serologic pattern			0.002
Both high-positive	1 (5)	81 (42)	
1 high-positive/1 low-positive	2 (10)	31 (16)	
Both low-positive	1 (5)	4 (2)	
1 positive/1 negative	11 (52)	43 (22)	
1 positive/1 not tested	2 (10)	22 (11)	
Seronegative	4 (19)	13 (7)	

* Except where indicated otherwise, values are the number (%) of subjects. Due to missing data, some values are not percentages of the total patient populations. IQR = interquartile range; ART = antiretroviral therapy; HIV-1 = type 1 HIV; HCQ = hydroxychloroquine; SSZ = sulfasalazine; MTX = methotrexate; LEF = leflunomide; AZA = azathioprine; RF = rheumatoid factor; anti-CCP = anti–cyclic citrullinated peptide.
† Hepatitis C virus (HCV)–positive status was determined by antibody test or International Classification of Diseases code.
‡ Values were obtained at rheumatoid arthritis (RA) diagnosis.
§ Joint involvement is defined as tenderness and swelling.
¶ Other drugs include oral gold and tetracyclines.

mm^3 (range 367–650), and 81% of patients with recent (within 1 year) type 1 HIV viral titer measurements had <500 copies/ml.

Among individuals with RA, HCV infection was more prevalent in patients with HIV than individuals without HIV (43% versus 14%; $P < 0.0001$). The incidence of RA in patients with HIV and HCV was 0.46 cases per 10,000 person-years (95% CI 0.23–0.91) compared to an incidence of RA of 0.30 cases per 10,000 person-years (95% CI 0.17–0.53) in HIV patients without HCV ($P = 0.35$). Among these groups, HIV status appeared to be a more powerful determinant of serologic status than was HCV status (Table 2), since seronegativity was present in 22–25% of HIV patients with or without HCV compared to 7% of HIV-negative individuals ($P = 0.02$ for the differences in serologic patterns across the 4 groups).

Erosive disease (at any time point) developed in 47% of patients with HIV compared to 33% of individuals without HIV

(P = 0.18). Of all patients with HIV, 24% had developed radiographic erosions within 1 year of the RA diagnosis compared to 26% of individuals without HIV (P = 0.81) (Table 2). Subgroup analyses stratified by HCV status did not demonstrate any differences in terms of the presence of erosions in RA patients with HIV or individuals without HIV according to the presence or absence of HCV (P = 0.18).

Use of DMARDs and other RA therapies. Among those with RA, 29% of patients with HIV compared to 6% of RA patients without HIV (P = 0.0002) did not receive targeted DMARD therapy. The most commonly used DMARD among RA patients with HIV was HCQ (57%), while methotrexate (MTX) was more common in RA patients without HIV (66%) (Table 2). Compared to RA patients without HIV, RA patients with HIV were significantly less likely to be prescribed MTX (33% versus 66%; P = 0.004), leflunomide (0% versus 12%; P = 0.01), and biologic agents or JAK inhibitors (10% versus 35%; P = 0.02) (Table 2). Rates of prednisone use were similar between RA patients with HIV and RA patients without HIV (71% versus 65%, respectively; P = 0.58).

In a logistic regression model incorporating the presence of erosive disease, HIV status, and HCV status, HIV infection was associated with lower odds of being prescribed DMARD therapy other than HCQ (OR 0.21 [95% CI 0.08–0.52]; P = 0.002). In the same model, as expected, the presence of erosions was associated with higher odds of being prescribed DMARD therapy (OR 2.1 [95% CI 1.01–4.24]; P = 0.047). In a sensitivity analysis incorporating an interaction term of HIV and the presence of erosions, the presence of erosions was not found to be an effect modifier in the relationship between an RA patient having HIV and receiving a DMARD prescription (P = 0.85).

DMARD tolerability and safety. Among the 10 RA patients with HIV who received non-HCQ DMARD therapy, 7 patients required changes in their treatment regimen due to adverse effects, and 2 patients required changes in their treatment regimen due to a lack or loss of efficacy (Tables 3 and 4). In comparison, the 158 RA patients without HIV who received DMARD therapy were more likely to require changes in their treatment regimen due to a lack of efficacy (49% in RA patients without HIV versus 20% in RA patients with HIV; P = 0.08) and less likely to require changes due to adverse effects (38% in RA patients without HIV versus 70% in RA patients with HIV; P = 0.04). Most treatment-limiting side effects occurred between 5 months and 1 year after the initial DMARD treatment had been started.

Among RA patients with HIV treated with non-HCQ DMARDs, CD4 cell percentages stayed stable. The CD4 cell percentages and viral load trajectories of 9 of 10 RA patients with HIV treated with DMARDs are shown in Figure 2. Data on CD4 cell percentages and viral load trajectories were missing for 1 of the RA patients with HIV who were treated with DMARDs. It is notable that 2 of the 9 patients with available data experienced significant increases in viral load (defined as a log fold change from baseline of 2–3-fold) after treatment with DMARDs (patients 7 and 9) (Figure 2). At the time, patient 7 was determined to be a long-term nonprogressor and did not receive antiretroviral therapy at any point during the study. While patient 9 experienced a viral load increase during the use of a biologic agent, patient 9 did not have a prior history of sustained viral suppression.

Table 3. Frequency of adverse effects occurring in RA patients with HIV compared to RA patients without HIV during the first contiguous course of disease-modifying antirheumatic drug therapy other than hydroxychloroquine among those with newly diagnosed RA*

	Patients with HIV (n = 10)	Patients without HIV (n = 158)
Adverse effect		
General malaise	0 (0)	10 (6)
Infections	1 (10)	8 (5)
Increased liver enzyme levels	2 (20)	14 (9)
Hematologic abnormalities	2 (20)	9 (6)
GI side effects	2 (20)	13 (8)
Rash or oral ulcers	0 (0)	5 (3)
Worsening renal function	0 (0)	1 (1)
Pulmonary complications	2 (20)	8 (5)

* Except where indicated otherwise, values are the number (%) of subjects. RA = rheumatoid arthritis; GI = gastrointestinal.

Among the 10 RA patients with HIV receiving DMARD therapy, no serious infections requiring hospitalization occurred. Similarly, among RA patients with HIV with an ICD-9 or ICD-10 code for RA but no confirmed incident RA, the overall hospitalized infection rate during follow-up was 24% compared to 21% in RA patients with HIV without an ICD-9 or ICD-10 code for RA.

DISCUSSION

In a large cohort of patients with HIV and uninfected individuals, we investigated the incidence of RA using established classification criteria, as well as presenting features of RA in both groups. We found that incident RA was less common in patients with HIV than in age-, race-, and site-matched HIV-negative individuals. In terms of presentation, RA-associated autoantibodies were present less frequently and at lower titers in RA patients with HIV than in RA patients without HIV, but with respect to the variables we evaluated, clinical presentation of RA was otherwise similar between the 2 groups. Additionally, we provide evidence that prescribing patterns differed between RA patients with HIV and RA patients without HIV, with DMARDs prescribed less frequently in RA patients with HIV.

Given that RA is generally considered to be a state of immune system overactivation, while HIV is associated with immunodeficiency and immune dysregulation, the interplay and comparative incidence between these 2 diseases provides an interesting opportunity to investigate their pathophysiology. Our finding that RA was 3.4 times less common in patients with HIV than in HIV-negative individuals is unsurprising: it has been well established

Table 4. Clinical course of DMARD therapy in 10 HIV patients with incident RA*

Clinical features at RA diagnosis							Details of DMARD treatment course			
Patient/age (in years)	Duration of ART, years	Years since HIV diagnosis	CD4 cell count, cells/mm^3†	Viral load†	RF	Anti-CCP	Medications in first course (length of first course, in years)	First DMARD	Adverse effects (associated treatment, time at onset)	Ineffective drugs
1/40–49	8.6	10	680	ND	Negative	Low-positive	MTX, HCQ (5.7)	MTX	GI intolerance (MTX, 15 months); anemia (MTX, treatment-limiting, 5 years)	–
2/50–59	6.6	20	360	ND	Low-positive	High-positive	Pred., MTX, and HCQ (0.9)	MTX	Pneumonia without hospitalization (MTX, treatment-limiting, within 1 year)	–
3/50–59	6.7	16	911	ND	High-positive	Low-positive	MTX (2.8)	MTX	–	–
4/60–69	0.1	29	515	ND	High-positive	Negative	MTX and HCQ (0.7)	MTX	Cough (MTX, treatment-limiting, 8 months)	–
5/70–79	5.0	11	520	ND	High-positive	Negative	SSZ and Pred. (3.2)	SSZ	–	–
6/50–59	–	6	559	Positive	Low-positive	Negative	HCQ, Pred., NSAIDs, and SSZ (0.4)	SSZ	Thrombocytopenia (SSZ, treatment-limiting, 5 months)	–
7/50–59	–	8	339	ND	High-positive	High-positive	HCQ, Pred., and MTX (5.7)	MTX	Increased liver enzyme levels (MTX, 2.5 years)	–
8/30–39	7.7	15	885	ND	Negative	High-positive	Pred. and ETN (3.6)	ETN	–	–
9/50–59	1.0	12	459	Positive	Negative	Low-positive	SSZ, HCQ, Pred., MTX, ADA, ETN, and HCQ (12.9)	SSZ	Increased liver enzyme levels (SSZ, 15 months; MTX, 2 months), nausea (ETN)	ETN
10/50–59	–	5	346	Positive	Negative	Negative	SSZ, Pred., MTX, and HCQ (3.8)	SSZ	Nausea (SSZ, 5 months after dose increase)	SSZ

* DMARD = disease-modifying antirheumatic drug; ART = antiretroviral therapy; RF = rheumatoid factor; anti-CCP = anti–cyclic citrullinated peptide; ND = not detectable; MTX = methotrexate; HCQ = hydroxychloroquine; GI = gastrointestinal; Pred. = prednisone; SSZ = sulfasalazine; NSAIDs = nonsteroidal antiinflammatory drugs; ETN = etanercept; ADA = adalimumab.
† These data were obtained around the time of diagnosis of rheumatoid arthritis (RA).

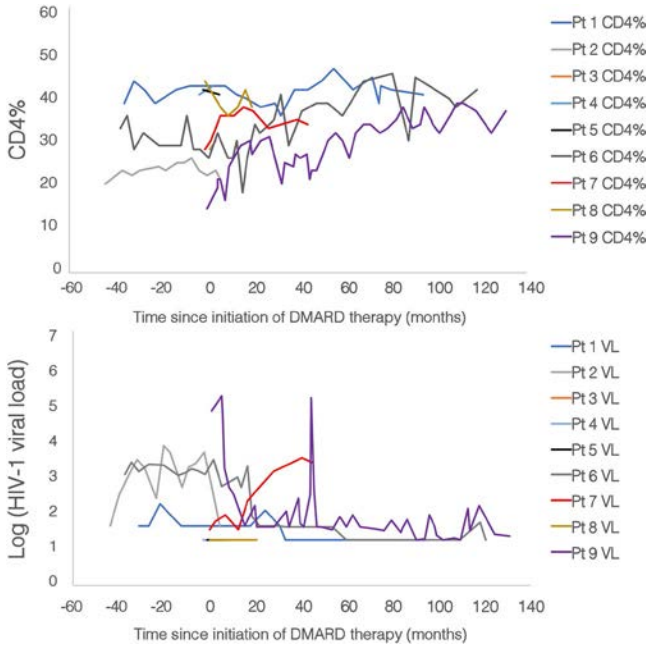

Figure 2. CD4 cell percentages and viral load (VL) trajectories among 9 of 10 rheumatoid arthritis (RA) patients (Pt) with HIV treated with disease-modifying antirheumatic drugs (DMARDs) other than hydroxychloroquine. Data on CD4 cell percentages and viral load trajectories were missing for 1 RA patient with HIV treated with DMARDs.

that in patients with HIV, levels and function of memory B cells are decreased, whereas in RA patients, memory B cell levels are elevated and the sites of abnormal cell expression differ from those in HIV patients (14,26). Furthermore, cell-mediated immunity plays a significant role in the development and progression of RA, whereas a defect in cell-mediated immunity is central to the pathogenesis of HIV (15). From a clinical perspective, our findings are consistent with prior studies demonstrating decreased incidence of RA in patients with HIV taking ART compared to the overall population (27).

With respect to the humoral immune system, we observed differences in autoantibody profiles among patients with HIV compared to individuals without HIV. Prior studies of RF in HIV have demonstrated conflicting results depending on when they were performed, and these studies have been limited by small sample sizes. As a result, some studies have shown elevated frequencies of RF and/or anti-CCP positivity in patients with HIV, while other studies have shown no difference in terms of autoantibody levels between patients with HIV and HIV-negative individuals (12,28–30). In our overall population, we found that low titers of RF occurred more commonly in patients with HIV, but that this appeared to be attributable to the presence of HCV coinfection. In patients with HIV without HCV, the rate of RF positivity was equivalent to that in individuals without HIV who are HCV-negative. Among patients with HIV with incident RA, positive autoantibody titers tended to be less robust. The clinical implication of this finding is that in patients with HIV in whom a diagnosis of RA is suspected, low-positive serologic test results could be considered normal, rather than the exception. Therefore, in the right clinical setting, an RA diagnosis should be strongly considered even if autoantibody titers are negative or only mildly positive.

We identified differences in antirheumatic drug prescribing patterns between RA patients with HIV and RA patients without HIV. Specifically, while the majority of both groups received HCQ, more potent immunosuppressant treatment was less frequently prescribed in RA patients with HIV, and RA patients with HIV were more likely to be treated with expectant management or glucocorticoids alone. This was true even when controlling for a measure of disease severity (presence of radiographic joint erosions). There are many possible explanations for this trend, the simplest being understandable concern on the part of the clinician regarding the risk of infection in patients with already suppressed immune function. There may also be concerns on the part of patients who fear experiencing the same rate or a higher rate of comorbidities or who are concerned about the baseline pill burden or anticipated drug interactions, which could result in hesitancy to change their existing medical treatment regimens. Additionally, higher rates of HCV coinfection in RA patients with HIV may preclude the use of MTX or leflunomide due to cytopenias or liver toxicity. This is a concerning trend, since RA-related outcomes are worse among patients not receiving appropriate DMARD therapy, and both patients with RA and patients with HIV have a higher risk of comorbidities related to systemic inflammation (9,31,32).

When addressing safety and tolerability, our very small sample of RA patients with HIV receiving non-HCQ DMARDs (n = 10) was a limiting factor in our analysis. Due to the sample size, we were unable to control for health care exposure, attendance to follow-up visits, or adherence to laboratory monitoring, which may have influenced our rates of detection of adverse effects, such as increases in liver enzyme levels. With this caveat, we did not observe any hospitalizations for serious infections, and we did not observe any indications that would suggest that DMARD therapy in clinically selected patients receiving antiretroviral therapy interfered with the management of HIV in these patients. It is, however, notable that intolerance or adverse effects were more common in RA patients with HIV than in RA patients who were HIV-negative, and it is not clear whether this is due to drug interactions, the presence of viral comorbidities (i.e., HCV) predisposing the patient to drug-induced liver injury, or other factors (18,33).

Our study was primarily limited by the small number of cases of incident RA among patients with HIV (n = 21). This was despite our use of a sensitive algorithm to identify potential RA patients. Although a score of ≥6 indicated definite RA according to the 2010 RA classification criteria, post hoc analyses have shown that these criteria are much more sensitive than they are specific, since they are designed to identify a population with early high-risk RA that may benefit from DMARD therapy (34). However, the level of detail used when documenting clinical joint examinations, even

by board-certified rheumatologists, was highly variable, and our interpretation of ambiguous findings may have led to the underestimation of incident RA cases in this cohort.

Inconsistent documentation also limited our analysis of RA clinical presentation, since we were unable to systematically assess validated disease activity scores, such as the Disease Activity Score in 28 joints (35) or Clinical Disease Activity Index (36) scores, in our cohort. Our study population was also almost entirely male, which limits generalizability to female patients. Additionally, our definition of HCV positivity included those with only a positive antibody, which may only reflect past infection. Since this was an observational study, the results should be regarded as hypothesis-generating and are susceptible to uncontrolled confounding variables. Although we took several steps to minimize the risk of misclassification bias in this study, a lack of diagnostic certainty remains for this population of patients with HIV diagnosed as having RA, due to the prevalence of low titers of antibodies and atypical inflammatory arthritis among patients with HIV. Finally, this investigation was primarily limited to the presentation and frequency of incident RA in patients with HIV. Further research is required to fully characterize the impact of incident HIV in patients with established RA.

In a large cohort of patients with HIV and age-, race-, and site-matched HIV-negative individuals, the incidence of RA was lower in the patients with HIV compared to those who were HIV-negative. Incident RA in patients with HIV, compared to those without HIV, was characterized by less robust autoantibody titers but otherwise similar clinical features. DMARDs were less frequently prescribed in RA patients with HIV than in RA patients without HIV. Future research is needed to characterize RA-related outcomes and optimal management of RA in patients with HIV.

AUTHOR CONTRIBUTIONS

All authors were involved in drafting the article or revising it critically for important intellectual content, and all authors approved the final version to be published. Dr. Justice had full access to all of the data in the study and takes responsibility for the integrity of the data and the accuracy of the data analysis.

Study conception and design. Hanberg, Fraenkel, Justice.
Acquisition of data. Hanberg, Justice.
Analysis and interpretation of data. Hanberg, Hsieh, Akgün, Weinstein, Fraenkel, Justice.

REFERENCES

1. Deeks SG, Lewin SR, Havlir DV. The end of AIDS: HIV infection as a chronic disease [review]. Lancet 2013;382:1525–33.
2. Justice AC, McGinnis KA, Skanderson M, Chang CC, Gibert CL, Goetz MB, et al. Towards a combined prognostic index for survival in HIV infection: the role of 'non-HIV' biomarkers. HIV Med 2010;11:143–51.
3. Iordache L, Launay O, Bouchaud O, Jeantils V, Goujard C, Boue F, et al. Autoimmune diseases in HIV-infected patients: 52 cases and literature review. Autoimmun Rev 2014;13:850–7.
4. Lebrun D, Hentzien M, Cuzin L, Rey D, Joly V, Cotte L, et al. Epidemiology of autoimmune and inflammatory diseases in a French nationwide HIV cohort. AIDS 2017;31:2159–66.
5. Virot E, Duclos A, Adelaide L, Miailhes P, Hot A, Ferry T, et al. Autoimmune diseases and HIV infection: a cross-sectional study. Medicine (Baltimore) 2017;96:e5769.
6. Hunter TM, Boytsov NN, Zhang X, Schroeder K, Michaud K, Araujo AB. Prevalence of rheumatoid arthritis in the United States adult population in healthcare claims databases, 2004–2014. Rheumatol Int 2017;37:1551–7.
7. Zandman-Goddard G, Shoenfeld Y. HIV and autoimmunity [review]. Autoimmun Rev 2002;1:329–37.
8. Dougados M. Comorbidities in rheumatoid arthritis [review]. Curr Opin Rheumatol 2016;28:282–8.
9. Urman A, Taklalsingh N, Sorrento C, McFarlane IM. Inflammation beyond the joints: rheumatoid arthritis and cardiovascular disease. Scifed J Cardiol 2018;2:1000019.
10. England BR, Thiele GM, Anderson DR, Mikuls TR. Increased cardiovascular risk in rheumatoid arthritis: mechanisms and implications. BMJ 2018;361:k1036.
11. Crowson CS, Rollefstad S, Ikdahl E, Kitas GD, van Riel PL, Gabriel SE, et al. Impact of risk factors associated with cardiovascular outcomes in patients with rheumatoid arthritis. Ann Rheum Dis 2018;77:48–54.
12. Cunha BM, Mota LM, Pileggi GS, Safe IP, Lacerda MV. HIV/AIDS and rheumatoid arthritis [review]. Autoimmun Rev 2015;14:396–400.
13. Savige JA, Chang L, Horn S, Crowe SM. Anti-nuclear, anti-neutrophil cytoplasmic and anti-glomerular basement membrane antibodies in HIV-infected individuals. Autoimmunity 1994;18:205–11.
14. Bugatti S, Vitolo B, Caporali R, Montecucco C, Manzo A. B cells in rheumatoid arthritis: from pathogenic players to disease biomarkers [review]. Biomed Res Int 2014;2014:681678.
15. Mellado M, Martinez-Munoz L, Cascio G, Lucas P, Pablos JL, Rodriguez-Frade JM. T cell migration in rheumatoid arthritis [review]. Front Immunol 2015;6:384.
16. Fox C, Walker-Bone K. Evolving spectrum of HIV-associated rheumatic syndromes [review]. Best Pract Res Clin Rheumatol 2015;29:244–58.
17. Roszkiewicz J, Smolewska E. Kaleidoscope of autoimmune diseases in HIV infection [review]. Rheumatol Int 2016;36:1481–91.
18. Adizie T, Moots RJ, Hodkinson B, French N, Adebajo AO. Inflammatory arthritis in HIV positive patients: a practical guide [review]. BMC Infect Dis 2016;16:100.
19. Justice AC, Dombrowski E, Conigliaro J, Fultz SL, Gibson D, Madenwald T, et al. Veterans Aging Cohort Study (VACS): overview and description. Med Care 2006;44 Suppl 2:S13–24.
20. Fultz SL, Skanderson M, Mole LA, Gandhi N, Bryant K, Crystal S, et al. Development and verification of a "virtual" cohort using the National VA Health Information System. Med Care 2006;44 Suppl 2:S25–30.
21. Kim SY, Servi A, Polinski JM, Mogun H, Weinblatt ME, Katz JN, et al. Validation of rheumatoid arthritis diagnoses in health care utilization data. Arthritis Res Ther 2011;13:R32.
22. Aletaha D, Neogi T, Silman AJ, Funovits J, Felson DT, Bingham CO III, et al. 2010 rheumatoid arthritis classification criteria: an American College of Rheumatology/European League Against Rheumatism collaborative initiative. Arthritis Rheum 2010;62:2669–81.
23. McGinnis KA, Brandt CA, Skanderson M, Justice AC, Shahrir S, Butt AA, et al. Validating smoking data from the Veteran's Affairs Health Factors dataset, an electronic data source. Nicotine Tob Res 2011;13:1233–9.
24. Hanberg JS, Freiberg MS, Goetz MB, Rodriguez-Barradas MC, Gibert C, Oursler KA, et al. Neutrophil-to-lymphocyte and platelet-to-lymphocyte ratios as prognostic inflammatory biomarkers in human immunodeficiency virus (HIV), hepatitis C

virus (HCV), and HIV/HCV coinfection. Open Forum Infect Dis 2019;6:ofz347.

25. Wiese AD, Griffin MR, Stein CM, Schaffner W, Greevy RA, Mitchel EF Jr, et al. Validation of discharge diagnosis codes to identify serious infections among middle age and older adults. BMJ Open 2018;8:e020857.
26. Moir S, Fauci AS. B cells in HIV infection and disease [review]. Nat Rev Immunol 2009;9:235–45.
27. Yen YF, Chuang PH, Jen IA, Chen M, Lan YC, Liu YL, et al. Incidence of autoimmune diseases in a nationwide HIV/AIDS patient cohort in Taiwan, 2000–2012. Ann Rheum Dis 2017;76:661–5.
28. Telles JP, Grande MA, Jurgensen A, Hecke JC, Skare T, Nisihara RM, et al. Rheumatic manifestations in brazilian patients with AIDS. Acta Reumatol Port 2014;39:143–5.
29. Du Toit R, Whitelaw D, Taljaard JJ, du Plessis L, Esser M. Lack of specificity of anticyclic citrullinated peptide antibodies in advanced human immunodeficiency virus infection. J Rheumatol 2011;38:1055–60.
30. Rowe IF, Forster SM, Seifert MH, Youle MS, Hawkins DA, Lawrence AG, et al. Rheumatological lesions in individuals with human immunodeficiency virus infection. Q J Med 1989;73:1167–84.
31. Singh JA, Saag KG, Bridges SL Jr, Akl EA, Bannuru RR, Sullivan MC, et al. 2015 American College of Rheumatology guideline for the treatment of rheumatoid arthritis. Arthritis Rheumatol 2016;68:1–26.
32. Sokoya T, Steel HC, Nieuwoudt M, Rossouw TM. HIV as a cause of immune activation and immunosenescence [review]. Mediators Inflamm 2017;2017:6825493.
33. Cepeda EJ, Williams FM, Ishimori ML, Weisman MH, Reveille JD. The use of anti-tumour necrosis factor therapy in HIV-positive individuals with rheumatic disease. Ann Rheum Dis 2008;67:710–2.
34. Kennish L, Labitigan M, Budoff S, Filopoulos MT, McCracken WA, Swearingen CJ, et al. Utility of the new rheumatoid arthritis 2010 ACR/EULAR classification criteria in routine clinical care. BMJ Open 2012;2.
35. Prevoo ML, van 't Hof MA, Kuper HH, van Leeuwen MA, van de Putte LB, van Riel PL. Modified disease activity scores that include twenty-eight–joint counts: development and validation in a prospective longitudinal study of patients with rheumatoid arthritis. Arthritis Rheum 1995;38:44–8.
36. Aletaha D, Nell VP, Stamm T, Uffmann M, Pflugbeil S, Machold K, et al. Acute phase reactants add little to composite disease activity indices for rheumatoid arthritis: validation of a clinical activity score. Arthritis Res Ther 2005;7:R796–806.

American College of Rheumatology
Empowering Rheumatology Professionals

Arthritis & Rheumatology
Vol. 73, No. 12, December 2021, pp 2200–2205
DOI 10.1002/art.41807
© 2021, American College of Rheumatology

BRIEF REPORT

Identification of Novel, Immunogenic HLA–DR-Presented *Prevotella copri* Peptides in Patients With Rheumatoid Arthritis

Annalisa Pianta,[1] Geena Chiumento,[1] Kristina Ramsden,[1] Qi Wang,[2] Klemen Strle,[1] Sheila Arvikar,[1] Catherine E. Costello,[2] and Allen C. Steere[1]

Objective. We previously identified HLA–DR-presented epitopes from a 27-kd protein of *Prevotella copri* (Pc) obtained from peripheral blood mononuclear cells (PBMCs) from 1 rheumatoid arthritis (RA) patient. Herein, we sought to identify other HLA–DR-presented Pc peptides and source proteins in PBMCs from additional patients to better understand Pc immune responses and RA disease pathogenesis.

Methods. Using tandem mass spectrometry, we searched for HLA–DR-presented Pc peptides in PBMCs from RA and Lyme arthritis (LA) patients. The identified peptides and source proteins were tested for reactivity in RA patients, those with other arthritides, and the general population. These results were assessed for correlation with clinical findings.

Results. Including Pc-p27, we identified 5 HLA–DR-presented Pc peptides, each derived from a different Pc protein, in 3 of 4 RA patients, but none in 2 LA patients. When tested in our RA cohort, 14 of 19 patients (74%) had T cell responses, and 47 of 89 patients (53%) had IgG or IgA responses to ≥1 of the 5 Pc peptides or proteins, most commonly IgA reactivity with Pc-p27. Additionally, 74% of RA patients with IgA antibodies to ≥1 Pc protein had anti–citrullinated protein antibodies (ACPAs) compared with 49% of patients who lacked IgA Pc antibody responses ($P = 0.05$), and IgA Pc antibody levels correlated with ACPA values.

Conclusion. The majority of the RA patients had Pc immune responses. The correlation of IgA Pc antibody responses, particularly to Pc-p27, with ACPA supports the hypothesis that specific microbial antigens in the mucosa have a role in shaping or amplifying immune responses in RA joints.

INTRODUCTION

There is increasing evidence that mucosal immune responses to microbial agents in the periodontium, lung, or intestine may shape immune responses in the joints of patients with rheumatoid arthritis (RA) (1,2). However, identification of microbial agents and immune responses that may connect mucosal and joint immunity remains incomplete. In a seminal study of the gut microbiota in RA patients, Scher et al reported an overabundance of *Prevotella* species, particularly *Prevotella copri* (Pc), in stool samples from patients with new-onset RA (3), which was the stimulus for our Pc immune response studies.

We developed a novel technique to identify HLA–DR-presented microbial peptides or self-peptides in synovial tissue, synovial fluid mononuclear cells (SFMCs), or peripheral blood mononuclear cells (PBMCs) from arthritis patients using

Supported by the NIH (National Institute of Allergy and Infectious Diseases grant R01-AI-144365 to Dr. Steere and National Institute of Arthritis and Musculoskeletal and Skin Diseases grant K01-AR-062098 to Dr. Strle, and grants P41-GM-104603, R24-GM-134210, S10-RR-020946, and S10-OD-010724 to Dr. Costello), a grant from the Within Our Reach program of the Rheumatology Research Foundation, the Ounsworth-Fitzgerald Foundation, the G. Harold and Leila Y. Mathers Foundation, the English-Bonter-Mitchell Foundation, the Lucius N. Littauer Foundation, the Lillian Butler Davey Foundation, and the Eshe Fund (awarded to Dr. Steere). Dr. Arvikar is recipient of a Scientist Development award from the Rheumatology Research Foundation.

[1]Annalisa Pianta, PhD (current address: Janssen Vaccines, Bern, Switzerland), Geena Chiumento, MPH (current address: Massachusetts Department of Public Health, Boston), Kristina Ramsden, BA, Klemen Strle, PhD (current address: Wadsworth Center, New York State Department of Health, Albany), Sheila Arvikar, MD, Allen C. Steere, MD: Massachusetts General Hospital, Harvard Medical School, Boston, Massachusetts; [2]Qi Wang, PhD (current address: Bristol Myers Squibb, Devens, Massachusetts), Catherine E. Costello, PhD: Boston University School of Medicine, Boston, Massachusetts.

Dr. Steere is an inventor on a patent for T cell testing for Pc-p27. No other disclosures relevant to this article were reported.

Address correspondence to Allen C. Steere, MD, Massachusetts General Hospital, CNY 149/8301, 55 Fruit Street, Boston, MA 02114. Email: asteere@mgh.harvard.edu.

Submitted for publication January 2, 2020; accepted in revised form May 6, 2021.

nano–liquid chromatography tandem mass spectrometry (nano-LC-MS/MS), followed by determination of the antigenicity of the peptides and their source proteins using patient samples (4). With this technique, we first searched for Pc peptides and self-peptides in 9 such samples (2 from PBMCs) from RA patients. In the PBMCs from 1 of the 2 patients, 1 HLA–DR-presented Pc peptide was identified, which was derived from a 27-kd Pc protein (Pc-p27) (5). Pc peptides were not identified in synovia or SFMCs. When testing was performed in our entire cohort of RA patients, 42% of 40 patients had Th1 responses to the Pc-p27 peptide, and 24% of 127 patients had IgG or IgA antibodies to the Pc-p27 protein.

Two novel, immunogenic HLA–DR-presented self-peptides (1 derived from *N*-acetylglucosamine-6-sulfatase and the other from filamin A) were identified in the synovial tissue from the same patient in whom the Pc peptide was identified (6). These 2 self-proteins have sequences homologous with *Prevotella* epitopes, and patients who had T cell reactivity with 1 or both self-peptides also had responses to the corresponding *Prevotella* peptides (6), implicating molecular mimicry between these microbial and self-proteins as a possible link between gut microbial immunity and autoimmunity in joints.

In the present study, we searched for HLA–DR-presented Pc peptides in PBMCs from 2 additional RA patients and, for comparison, from 2 Lyme arthritis (LA) patients. We identified 4 new HLA–DR-presented Pc peptides (T cell epitopes) in the 2 additional RA patients. When samples from our recent RA cohort were tested for reactivity with these 4 Pc proteins and the previously identified Pc-p27, the majority of patients had T cell and/or B cell responses to ≥1 of these 5 Pc antigens. Moreover, the correlation between IgA responses to Pc proteins and anti–citrullinated protein antibodies (ACPAs) supports the hypothesis that specific microbial antigens in the mucosa may shape immune responses in RA.

PATIENTS AND METHODS

Patients. This study was approved by the Human Investigations Committee at Massachusetts General Hospital (MGH). All subjects provided written informed consent. All RA patients fulfilled the 2010 American College of Rheumatology/European Alliance of Associations for Rheumatology criteria for RA (7). HLA–DR typing was performed at the American Red Cross in Dedham, Massachusetts.

Isolation and identification of HLA–DR-presented peptides. We have previously published methods for immunoprecipitation of HLA–DR molecules from patient samples, followed by the elution and identification of HLA–DR-presented peptides using nano-LC-MS/MS (4). Here, only PBMCs were analyzed, as we did not previously identify Pc proteins in synovia or SFMCs. Spectra-to-peptide assignments were made by searching each patient's MS/MS data set against a UniProt Pc database (assembled in-house) using 3 search engines: Mascot, OMSSA, and X!Tandem. A consensus match among ≥2 programs was required for identification of a peptide sequence, with a Mascot score of ≥20, OMSSA E-value of ≤0.01, and X!Tandem score of ≤10. To rule out erroneous assignment of a human sequence as a Pc sequence, each microbial sequence was screened against the most recent version of the UniProt human database.

Enzyme-linked immunospot (ELISpot) T cell assay. Each HLA–DR-presented candidate microbial antigen was synthesized and purified by high-performance liquid chromatography in the Core Proteomics Laboratory at MGH. Each peptide was used first to stimulate the matching patient's PBMCs in an interferon-γ (IFNγ) ELISpot assay. Immunogenic peptides were then tested in larger numbers of patients as previously described (5). A positive T cell response was defined as a value 3 SD above the mean value in healthy subjects.

Determination of Pc antibodies. Recombinant preparations of the 5 Pc proteins were made by GenScript using an *Escherichia coli* expression vector (pET30a). Target protein purity was estimated to be ~90% based on densitometric analysis with sodium dodecyl sulfate–polyacrylamide gel electrophoresis.

Enzyme-linked immunosorbent assays were performed, with modifications of previously described methods (5). After coating with each recombinant Pc protein (1 μg/ml) overnight at 4°C, the plates were incubated at room temperature with blocking buffer (phosphate buffered saline–Tween, 5% milk) for 1 hour. Depending on the Pc protein, each patient's serum sample (diluted at 1:50 or 1:100) was added for 2 hours, followed by horseradish peroxidase–conjugated goat anti-human IgG or IgA (Dako) (diluted at 1:2,000 or 1:3,000) for 1.5 hours and then tetramethylbenzidine substrate (BD Biosciences) for 10–15 minutes. A positive antibody response was defined as a value 2 SD above the mean value in the general population.

Statistical analysis. Quantitative data were analyzed using the Mann-Whitney test or *t*-test with Welch's correction, categorical data using Fisher's exact test, and correlations using Spearman's correlation test. All analyses were performed using GraphPad Prism 8. All *P* values were 2-tailed. *P* values less than 0.05 were considered significant.

RESULTS

Identification of naturally presented HLA–DR Pc peptides. When HLA–DR-presented peptides were eluted from PBMCs from 2 new RA patients and analyzed by nano-LC-MS/MS, 4 new Pc peptides were identified. When combined with the 2 previously described RA patients (5), 3 of the 4 RA patients tested had 1–3 HLA–DR-presented Pc peptides, and each of these 3 patients had Pc IgG or IgA antibodies. Pc peptides or antibodies were not identified in the remaining RA patient or in the 2 LA patients. Clinical data on all 6 RA and LA patients are presented in Supplementary

Table 1 (available on the *Arthritis & Rheumatology* website at http://onlinelibrary.wiley.com/doi/10.1002/art.41807/abstract).

The 5 HLA–DR-presented Pc peptides that have been identified to date were each derived from a different Pc protein: 27-kd protein (Pc-p27), ribonuclease HII protein (Pc-ribo), DNA binding protein (Pc-DNAbind), glutamate 5-kinase protein (Pc-glut), and type III restriction endonuclease protein (Pc-endo) (Supplementary Figure 1, http://onlinelibrary.wiley.com/doi/10.1002/art.41807/abstract). Peptide length ranged from 10 to 19 amino acids, which is typical of HLA–DR class II–presented peptides. Each peptide had 100% sequence homology with the corresponding Pc protein but had limited sequence homology with any human peptide, suggesting that they were not human peptides erroneously assigned with a microbial database.

T cell reactivity with Pc peptides. As previously reported (5), when PBMCs from 40 patients with new-onset RA were stimulated with the peptide sequence from Pc-p27, 17 patients (42%) secreted IFNγ levels that were >3 SD above the mean value in healthy controls (P = 0.0002) (Figure 1). To conserve cells, samples from these patients were not retested for Pc-p27 responses. However, the 4 new Pc peptides were tested for this study using PBMCs from 20 of the 40 patients with new-onset RA in whom enough cells remained.

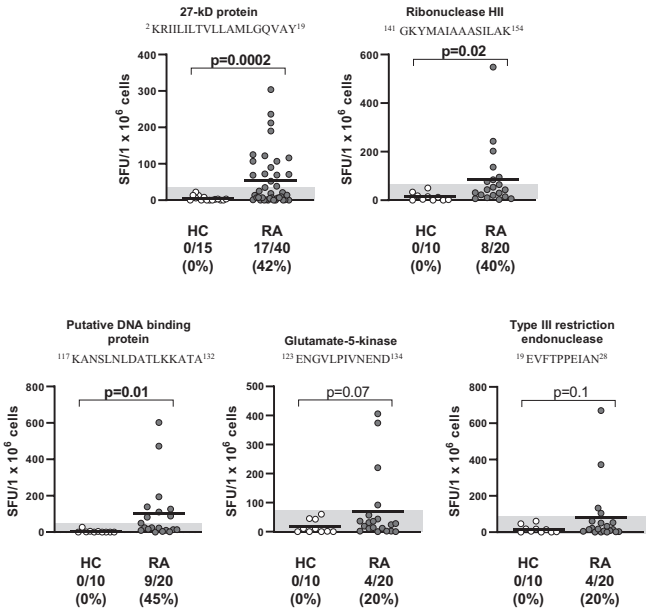

Figure 1. T cell responses to *Prevotella copri* (Pc) HLA–DR-presented peptides in rheumatoid arthritis (RA) patients. Five peptides derived from 5 Pc proteins were synthesized and used to stimulate peripheral blood mononuclear cells from RA patients by interferon-γ enzyme-linked immunospot assay. Using TEPITOPE, the Pc-p27, Pc–ribonuclease HII, and Pc–DNA binding peptides were predicted to be promiscuous binders of ≥20 of the 25 HLA–DR molecules modeled in the program. The predicted binding of the Pc–glutamate 5-kinase and Pc–type III restriction endonuclease peptides was restricted primarily to DRB1*04 molecules. The superscript numbers around each peptide sequence show the location of the amino acids within the source protein. Each symbol represents an individual subject. Bars show the mean, and the shaded areas show >3 SD above the mean value in healthy control (HC) subjects (hospital personnel). The groups were compared using unpaired *t*-tests with Welch's correction. SFU = spot-forming units per 1 × 10^6 cells.

Of the 20 patients with new-onset RA, 40% responded to the promiscuous binding Pc-ribo, and 45% reacted with the Pc-DNAbind peptide (Figure 1). A smaller percentage of patients (20%) responded to the 2 peptides with more restricted HLA–DR binding profiles (Pc-glut and Pc-endo). Of the 19 patients in whom testing was conducted with all 5 proteins, 14 patients (74%) had T cell reactivity with ≥1 of the 5 Pc peptides.

B cell reactivity with Pc proteins. IgG and IgA antibody responses to the 5 Pc proteins were determined in 89 RA patients, including 54 patients with new-onset RA and 35 patients with chronic RA (Figure 2). The 89 patients included 17 of the 20 patients in whom T cell testing was performed and 72 patients in our new RA cohort who were enrolled during the past 2 years. Because the results were similar in patients with new-onset RA and those with chronic RA, these data were combined for presentation here. For comparison, we tested serum samples from 37 patients with other chronic inflammatory arthritides (including spondyloarthritides, psoriatic arthritis, or sarcoidosis), from 80 patients with LA, and from 45 individuals in the general population, including hospital personnel and blood donors.

Of the 89 RA patients, 24 (27%) had IgA antibody responses to Pc-p27 that were >2 SD above the mean value in the general population (Figure 2). The number of patients with positive IgA responses to Pc-p27 and quantitative Pc-p27 values was significantly greater than in comparison groups. Although only small numbers of patients had positive IgA responses to the 4 new Pc proteins, quantitative values were frequently greater in the RA cohort than in other groups.

Among the 89 RA patients, 12% had positive IgG Pc-p27 responses, 10% had IgG Pc-ribo antibodies, and 10% had IgG Pc-endo antibodies, which tended to be higher than the percentages in the other groups, but the number of patients who had positive values was not significantly different among the groups. However, quantitative values for each Pc protein, except for Pc-DNAbind, were significantly greater in RA patients than in the inflammatory arthritides group. Surprisingly, 13 of the 80 LA patients (16%) had elevated IgG responses to Pc-DNAbind, which was a higher percentage than that in RA patients, raising the question of whether Pc-DNAbind has a cross-reactive antibody epitope with a spirochetal protein. Unlike RA patients, only a small number of LA patients had IgA responses to Pc-DNAbind or other Pc proteins.

Most patients in the RA or comparison groups had IgG or IgA responses to only a single Pc protein. Only 8 RA patients had positive IgG or IgA responses to >1 Pc protein, but none had both IgG and IgA responses to the same protein. Overall, 29 RA patients

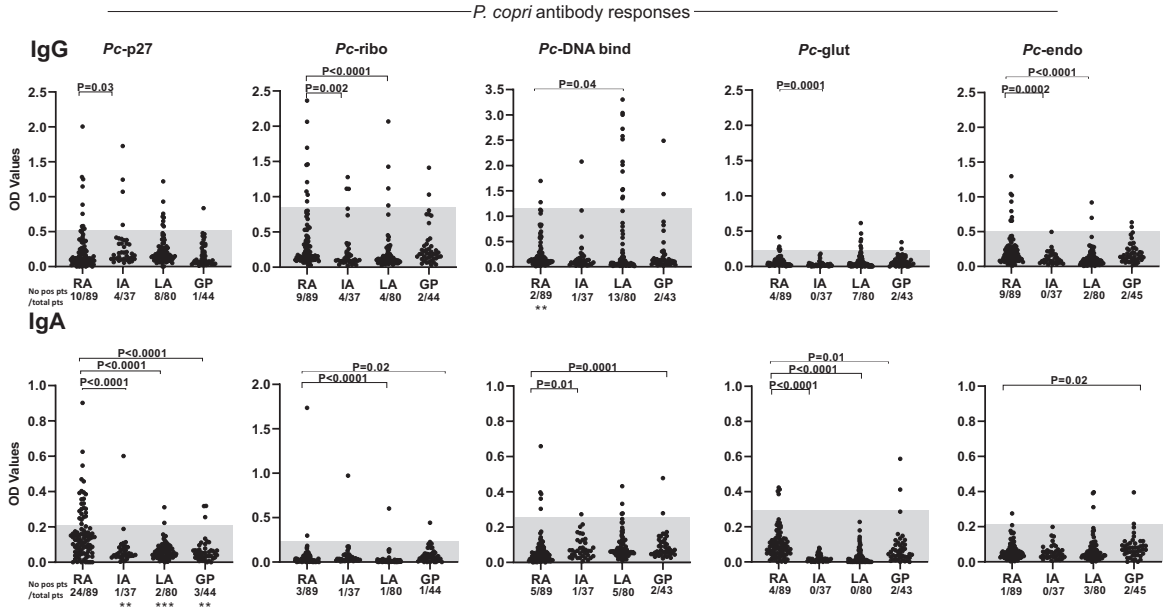

Figure 2. Antibody responses to *Prevotella copri* (Pc) proteins in rheumatoid arthritis (RA) patients, those with other forms of arthritis (e.g., inflammatory arthritides [IA] and Lyme arthritis [LA]), and those in the general population (GP). IgG and IgA antibody responses to the 5 Pc proteins, including Pc-p27, Pc–ribonuclease HII (Pc-ribo), Pc–DNA binding (Pc-DNAbind), Pc–glutamate 5-kinase (Pc-glut), and Pc–type III restriction endonuclease (Pc-endo) proteins, are shown. Each symbol represents an individual subject. The shaded areas show 2 SD above the mean value in the general population. Quantitative values were compared between RA patients and those in each of the other groups using the Mann-Whitney test, and these *P* values are shown above the data points. The number of individuals with positive responses in each group was compared between RA patients and those in each of the other groups by Fisher's exact test, and these *P* values are indicated with asterisks. ** = *P* = 0.001; *** = *P* = 0.0001. Only significant *P* values are shown.

(33%) had IgA responses to ≥1 of the 5 Pc proteins, compared with 18 of 161 patients (11%) in all other groups ($P < 0.0001$). Twenty-six of the 89 RA patients (29%) had IgG antibody responses to ≥1 of the 5 Pc proteins, compared with 39 of 161 patients (24%) in the other groups ($P = 0.45$). A total of 47 of 89 RA patients (53%) had IgG or IgA responses to ≥1 of the 5 Pc proteins.

Table 1. Demographic and clinical characteristics of the patients with rheumatoid arthritis according to presence versus absence of *Prevotella copri* (Pc) antibodies*

	Pc-p27 IgG (n = 10)	Pc-p27 IgA (n = 24)	No Pc-p27 IgG/IgA (n = 55)	Any Pc IgG (n = 26)	Any Pc IgA (n = 31)	No Pc IgG/IgA (n = 41)
Demographics						
Age, years	52 (24–75)	46 (19–91)	51 (19–80)	53 (24–75)	49 (19–91)	52 (19–75)
Female:male ratio	5:5†	20:4	46:9	17:9	25:6	34:7
Smoking, no. (%)						
Current	1 (10)	1 (4)	8 (15)	3 (12)	2 (7)	6 (15)
Former	2 (20)	5 (21)	16 (29)	5 (19)	7 (23)	14 (34)
Never	7 (70)	18 (75)	31 (56)	18 (69)	22 (71)	21 (51)
Autoantibodies						
RF positive, no. (%)	5 (50)	11 (46)	19 (35)	13 (50)	14 (45)	13 (32)
ACPA positive, no. (%)	7 (70)	18 (75)	30 (55)	18 (69)	23 (74)‡	20 (49)
HLA–DRB1 alleles						
SE, no. positive/no. tested (%)§	4/7 (57)	12/19 (63)	21/38 (55)	12/18 (67)	15/24 (63)	16/29 (55)
Disease activity						
ESR, mm/hour	22 (2–67)	23 (4–107)	14 (2–60)	21 (2–107)	23 (4–107)	12 (2–60)
CRP, mg/liter	16 (0.5–92)	3.7 (0.1–126)	4.7 (0.2–0.96)	9.6 (0.5–126)	7.7 (0.1–126)	4.3 (0.2–96)
DAS28-ESR	4.5 (2–7)	3.6 (1.3–8.2)	3.3 (1–7)	3.7 (1.6–8.2)	3.7 (1.3–8.2)	3.17 (1–7)
DAS28-CRP	3.8 (2–7)	3.1 (1.5–7.6)	3.2 (1.1–6.8)	3.5 (1.3–7.6)	3.5 (1.3–7.6)	3.17 (1.1–6.8)

* Except where indicated otherwise, values are the median (range). RF = rheumatoid factor; ACPA = anti–citrullinated protein antibody; SE = shared epitope; DAS28-ESR = Disease Activity Score in 28 joints using the erythrocyte sedimentation rate; DAS28-CRP = DAS28 using the C-reactive protein level.
† $P = 0.03$ versus patients with neither Pc-p27 IgA or IgG antibodies.
‡ $P = 0.05$ versus patients with neither Pc IgA or IgG antibodies.
§ Alleles *0101, 0102, 0401, 0404, 0405, 0408, and 1001.

Table 2. Correlation of rheumatoid arthritis autoantibodies with Pc antibodies*

	ACPA		RF	
	r	*P*	r	*P*
Pc antibody IgG				
Pc-p27 IgG	0.116	0.3	0.086	0.4
Pc-ribo IgG	0.172	0.1	0.135	0.2
Pc-DNAbind	0.098	0.4	0.026	0.8
IgG				
Pc-glut IgG	0.051	0.6	−0.0752	0.5
Pc-endo IgG	−0.137	0.2	−0.0631	0.6
Pc antibody IgA				
Pc-p27 IgA	0.283	0.008	0.194	0.07
Pc-ribo IgA	0.251	0.018	0.245	0.02
Pc-DNAbind	0.006	0.95	0.087	0.42
IgA				
Pc-glut IgA	0.271	0.01	0.260	0.014
Pc-endo IgA	0.112	0.3	0.212	0.047

* Correlations were calculated using Spearman's test. Pc-ribo = Pc-ribonuclease HII protein; Pc-DNAbind = Pc-DNA binding protein; Pc-glut = Pc-glutamate 5-kinase protein; Pc-endo = Pc-type III restriction endonuclease protein (see Table 1 for other definitions).

Clinical correlations. Among the 89 RA patients, the majority (60%) had new-onset RA, the female:male ratio was 4:1, 60% were positive for ACPA, 38% were positive for rheumatoid factor (RF), and 62% were positive for ACPA or RF, percentages typical of cohorts of early RA patients (8). Among patients with IgA Pc-p27 antibodies, 75% had ACPA compared with 55% of those without IgA/IgG Pc-p27 antibodies ($P = 0.1$), and there was a similar trend for RF (Table 1). Moreover, IgA antibody responses to Pc-p27, Pc-ribo, or Pc-glut correlated directly with ACPA levels, and IgA antibody responses to Pc-ribo, Pc-glut, or Pc-endo correlated with RF levels (Table 2). Overall, ACPAs were found in 74% of those who had IgA responses to ≥1 of 5 Pc proteins, compared with 49% of those who lacked such responses ($P = 0.05$). Conversely, among the 34 patients who lacked ACPA or RF, 6 patients (18%) had IgA Pc-p27 antibodies, and 3 patients (9%) had IgG Pc-p27 antibodies. Finally, patients with Pc tended to have higher levels of inflammatory markers and a higher frequency of shared epitope HLA–DRB1 alleles than patients without Pc antibodies, but the differences were not statistically significant.

DISCUSSION

Using a novel approach in which HLA–DR-presented peptides were identified directly from patient samples, we have now identified 5 immunogenic HLA–DR-presented Pc peptides from PBMCs in 3 of 4 RA patients tested. The large sample volumes and the complexity of the technique precluded evaluation of large numbers of patients. However, when serum samples from our current RA cohort and comparison groups were tested for IgG or IgA reactivity with each of the 5 Pc proteins, the most robust difference between the groups was IgA Pc-p27 reactivity. Of the 89 RA patients, 24 (27%) had IgA responses to this protein, a significantly higher percentage compared with the other groups, making it an attractive diagnostic target. However, in contrast to findings from our initial study (5), the number of patients with positive IgG Pc responses was not significantly greater in RA patients, though quantitative values were often higher in the RA group than in the other groups.

Because of the importance of ACPAs in RA (9,10), we searched our MS/MS spectra carefully for evidence of peptides with the 1-dalton gain that could indicate an arginine-to-citrulline conversion. Of the 5 Pc T cell epitopes examined here, only Pc-p27 contained an arginine, and that peptide was not citrullinated. However, ACPA levels correlated significantly with Pc-p27 antibodies, suggesting that another portion of the protein may become citrullinated. Moreover, when we previously citrullinated 2 autoantigens, *N*-acetylglucosamine-6-sulfatase and filamin A, which had T cell epitopes with sequence similarity with *Prevotella* species, RA patients had higher antibody responses to citrullinated *N*-acetylglucosamine-6-sulfatase than to its noncitrullinated proteoform (6), suggesting that the *N*-acetylglucosamine-6-sulfatase self-protein may be citrullinated in vivo.

In the current study, the correlation of IgA Pc responses with ACPA values supports a central hypothesis in RA pathogenesis that specific microbial antigens in the mucosa, which may cross-react with like self-proteins (6), could shape immune responses in RA joints (1). ACPAs appear to be beneficial in controlling microbes in the mucosa but may become detrimental in joints (1). In addition, we previously found *Prevotella* DNA in joint fluid in 3 of 5 patients with IgG Pc antibody responses (5), suggesting that Pc or their products may sometimes reach joints where they may further amplify inflammatory responses. There is provocative, emerging literature about the distant spread of commensal organisms resulting not only in autoimmunity, but also in malignancies and adverse treatment outcomes (11,12).

Limitations of this study include the small number of patients in whom it was possible to test for HLA–DR-presented Pc peptides. However, this initial assessment shows that nano-LC-MS/MS is now sensitive enough to identify immunogenic in vivo HLA–DR-presented microbial peptides directly from PBMCs, which can then be tested in large numbers of patients. Second, the reasons for gut dysbiosis and mucosal Pc immunoreactivity are not yet defined in RA patients. However, in a recent analysis of ileal biopsies in 50 HLA–B27-positive patients with ankylosing spondylitis, adherent, invading rod-shaped bacteria, identified primarily as *E coli* or *Prevotella* species, were often seen in the epithelial layer of the gut mucosa along with significant down-regulation of tight junction proteins, resulting in a loosening of the epithelial and gut vascular barriers (13). A similar process may occur in RA patients.

Greater understanding of the interactions between gut commensals and joint autoimmunity will likely influence the diagnosis and treatment of RA. In addition to disease-modifying antirheumatic drugs, adjunctive treatment aimed at the control of gut "pathobionts," such as targeted nonabsorbable antibiotic therapy, probiotic

strategies, dietary changes, or fecal matter transplants, may prove to be effective and safe. Moreover, the identification of T cell epitopes to microbial and related self-proteins may lead to therapies with blocking peptides. Animal models have shown that blocking peptides may ameliorate pathogenic responses (14), and reestablishment of tight junctions in the gut restores gut homeostasis, which may reverse autoimmune processes (15). In the future, biomarkers, such as those identified here, may contribute to the diagnosis and treatment of patients with gut-associated RA.

ACKNOWLEDGMENTS

We thank Dr. John Branda, Judith M. Holden, and Gail McHugh for help with microbial cultures, Robert Seward and Chunxiang Yao for help with mass spectrometry analyses, and Drs. Deborah Collier and Marcy Bolster for help with patient care.

AUTHOR CONTRIBUTIONS

All authors were involved in drafting the article or revising it critically for important intellectual content, and all authors approved the final version to be published. Dr. Steere had full access to all of the data in the study and takes responsibility for the integrity of the data and the accuracy of the data analysis.

Study conception and design. Pianta, Strle, Costello, Steere.
Acquisition of data. Pianta, Chiumento, Ramsden, Wang, Arvikar.
Analysis and interpretation of data. Pianta, Chiumento, Wang, Strle, Arvikar, Costello, Steere.

REFERENCES

1. Holers VM, Demoruelle MK, Kuhn KA, Buckner JH, Robinson WH, Okamoto Y, et al. Rheumatoid arthritis and the mucosal origins hypothesis: protection turns to destruction [review]. Nat Rev Rheumatol 2018;14:542–57.
2. Zhang X, Zhang D, Jia H, Feng Q, Wang D, Liang D, et al. The oral and gut microbiomes are perturbed in rheumatoid arthritis and partly normalized after treatment. Nat Med 2015;21:895–905.
3. Scher JU, Sczesnak A, Longman RS, Segata N, Ubeda C, Bielski C, et al. Expansion of intestinal Prevotella copri correlates with enhanced susceptibility to arthritis. Elife 2013;2:e01202.
4. Wang Q, Drouin EE, Yao C, Zhang J, Huang Y, Leon DR, et al. Immunogenic HLA–DR-presented self-peptides identified directly from clinical samples of synovial tissue, synovial fluid, or peripheral blood in patients with rheumatoid arthritis or Lyme arthritis. J Proteome Res 2017;16:122–36.
5. Pianta A, Arvikar S, Strle K, Drouin EE, Wang Q, Costello CE, et al. Evidence of the immune relevance of Prevotella copri, a gut microbe, in patients with rheumatoid arthritis. Arthritis Rheumatol 2017;69:964–75.
6. Pianta A, Arvikar SL, Strle K, Drouin EE, Wang Q, Costello CE, et al. Two rheumatoid arthritis-specific autoantigens correlate microbial immunity with autoimmune responses in joints. J Clin Invest 2017;127:2946–56.
7. Aletaha D, Neogi T, Silman AJ, Funovits J, Felson DT, Bingham CO III, et al. 2010 rheumatoid arthritis classification criteria: an American College of Rheumatology/European League Against Rheumatism collaborative initiative. Arthritis Rheum 2010;62:2569–81.
8. Kuriya B, Xiong J, Boire G, Haraoui B, Hitchon C, Pope J, et al. Earlier time to remission predicts sustained clinical remission in early rheumatoid arthritis: results from the Canadian Early Arthritis Cohort (CATCH). J Rheumatol 2014;41:2161–6.
9. De Rycke L, Nicholas AP, Cantaert T, Kruithof E, Echols JD, Vandekerckhove B, et al. Synovial intracellular citrullinated proteins colocalizing with peptidyl arginine deiminase as pathophysiologically relevant antigenic determinants of rheumatoid arthritis–specific humoral autoimmunity. Arthritis Rheum 2005;52:2323–30.
10. Kuhn KA, Kulik L, Tomooka B, Braschler KJ, Arend WP, Robinson WH, et al. Antibodies against citrullinated proteins enhance tissue injury in experimental autoimmune arthritis. J Clin Invest 2006;116:961–73.
11. Vieira SM, Hiltensperger M, Kumar V, Zegarra-Ruiz D, Dehner C, Khan N, et al. Translocation of a gut pathobiont drives autoimmunity in mice and humans. Science 2018;359:1156–61.
12. Rubinstein MR, Wang X, Liu W, Hao Y, Cai G, Han YW. Fusobacterium nucleatum promotes colorectal carcinogenesis by modulating E-cadherin/β-catenin signaling via its FadA adhesin. Cell Host Microbe 2013;14:195–206.
13. Ciccia F, Guggino G, Rizzo A, Alessandro R, Luchetti MM, Milling S, et al. Dysbiosis and zonulin upregulation alter gut epithelial and vascular barriers in patients with ankylosing spondylitis. Ann Rheum Dis 2017;76:1123–32.
14. Larché M, Wraith DC. Peptide-based therapeutic vaccines for allergic and autoimmune diseases [review]. Nat Med 2005;11:S69–76.
15. Fasano A. Leaky gut and autoimmune diseases [review]. Clin Rev Allergy Immunol 2012;42:71–8.

Arthritis & Rheumatology
Vol. 73, No. 12, December 2021, pp 2206–2218
DOI 10.1002/art.41953
© 2021 The Authors. *Arthritis & Rheumatology* published by Wiley Periodicals LLC on behalf of American College of Rheumatology.
This is an open access article under the terms of the Creative Commons Attribution-NonCommercial-NoDerivs License, which permits use and distribution in any medium, provided the original work is properly cited, the use is non-commercial and no modifications or adaptations are made.

American College of Rheumatology
Empowering Rheumatology Professionals

The Interleukin-1 Receptor–Associated Kinase 4 Inhibitor PF-06650833 Blocks Inflammation in Preclinical Models of Rheumatic Disease and in Humans Enrolled in a Randomized Clinical Trial

Aaron Winkler,[1] Weiyong Sun,[1] Saurav De,[2] Aiping Jiao,[1] M. Nusrat Sharif,[1] Peter T. Symanowicz,[1] Shruti Athale,[3] Julia H. Shin,[1] Ju Wang,[1] Bruce A. Jacobson,[1] Simeon J. Ramsey,[1] Ken Dower,[1] Tatyana Andreyeva,[1] Heng Liu,[1] Martin Hegen,[1] Bruce L. Homer,[1] Joanne Brodfuehrer,[1] Mera Tilley,[1] Steven A. Gilbert,[1] Spencer I. Danto,[1] Jean J. Beebe,[1] Betsy J. Barnes,[2] Virginia Pascual,[3] Lih-Ling Lin,[1] Iain Kilty,[1] Margaret Fleming,[1] and Vikram R. Rao[1]

Objective. To investigate the role of PF-06650833, a highly potent and selective small-molecule inhibitor of interleukin-1–associated kinase 4 (IRAK4), in autoimmune pathophysiology in vitro, in vivo, and in the clinical setting.

Methods. Rheumatoid arthritis (RA) inflammatory pathophysiology was modeled in vitro through 1) stimulation of primary human macrophages with anti–citrullinated protein antibody immune complexes (ICs), 2) RA fibroblast-like synoviocyte (FLS) cultures stimulated with Toll-like receptor (TLR) ligands, as well as 3) additional human primary cell cocultures exposed to inflammatory stimuli. Systemic lupus erythematosus (SLE) pathophysiology was simulated in human neutrophils, dendritic cells, B cells, and peripheral blood mononuclear cells stimulated with TLR ligands and SLE patient ICs. PF-06650833 was evaluated in vivo in the rat collagen-induced arthritis (CIA) model and the mouse pristane-induced and MRL/*lpr* models of lupus. Finally, RNA sequencing data generated with whole blood samples from a phase I multiple-ascending-dose clinical trial of PF-06650833 were used to test in vivo human pharmacology.

Results. In vitro, PF-06650833 inhibited human primary cell inflammatory responses to physiologically relevant stimuli generated with RA and SLE patient plasma. In vivo, PF-06650833 reduced circulating autoantibody levels in the pristane-induced and MRL/*lpr* murine models of lupus and protected against CIA in rats. In a phase I clinical trial (NCT02485769), PF-06650833 demonstrated in vivo pharmacologic action pertinent to SLE by reducing whole blood interferon gene signature expression in healthy volunteers.

Conclusion. These data demonstrate that inhibition of IRAK4 kinase activity can reduce levels of inflammation markers in humans and provide confidence in the rationale for clinical development of IRAK4 inhibitors for rheumatologic indications.

INTRODUCTION

Rheumatoid arthritis (RA) affects ~1% of the population, manifesting with joint pain and tissue destruction and characterized in seropositive cases by the presence of antibodies against post-translationally modified proteins, as well as IgM (rheumatoid factor) (1,2). Cells involved in RA inflammation include not only lymphocytes but also neutrophils, macrophages, osteoclasts, and

ClinicalTrials.gov identifier: NCT02485769.

Supported by Pfizer. Dr. Barnes' work was supported by the National Institute of Arthritis and Musculoskeletal and Skin Diseases, NIH (grant 1R21-AR-065959-01).

[1]Aaron Winkler, PhD, Weiyong Sun, MS, Aiping Jiao, MD, M. Nusrat Sharif, PhD, Peter T. Symanowicz, MS (current address: Novartis Institutes for BioMedical Research Cambridge, Massachusetts), Julia H. Shin, MS, Ju Wang, MS, Bruce A. Jacobson, PhD, Simeon J. Ramsey, PhD, Ken Dower, PhD, Tatyana Andreyeva, MS, Heng Liu, MS, Martin Hegen, PhD, Bruce L. Homer, DVM, PhD (current address: Ashburn, Virginia), Joanne Brodfuehrer, PhD, Mera Tilley, PhD (current address: Foresite Labs, Cambridge, Massachusetts), Steven A. Gilbert, PhD, Spencer I. Danto, MD, PhD, Jean J. Beebe, PhD, Lih-Ling Lin, PhD (current address: Sanofi, Cambridge, Massachusetts), Iain Kilty, PhD (current address: Sitryx Therapeutics, Oxford, UK), Margaret Fleming, PhD (current address: Novartis Institutes for BioMedical Research Cambridge, Massachusetts), Vikram R. Rao, PhD: Pfizer, Cambridge, Massachusetts; [2]Saurav De, PhD (current address: Pfizer, Cambridge, Massachusetts), Betsy J. Barnes, PhD: The Feinstein Institute, Manhasset, New York; [3]Shruti Athale, PhD (current address: Praedicare Laboratories, Dallas, Texas), Virginia Pascual, MD (current address: Weill Cornell Medicine, New York, New York): Baylor Institute for Immunology Research, Dallas, Texas.

Author disclosures are available at https://onlinelibrary.wiley.com/action/downloadSupplement?doi=10.1002%2Fart.41953&file=art41953-sup-0001-Disclosureform.pdf.

Address correspondence to Aaron Winkler, PhD, Pfizer, 1 Portland Street, Cambridge, MA 02139. Email: aaron.winkler@pfizer.com.

Submitted for publication January 25, 2021; accepted in revised form August 17, 2021.

synovial fibroblasts. Treatments for RA include small-molecule disease-modifying antirheumatic drugs as well as biologic agents (3). The rate of sustained remission over time in RA remains disappointingly low, highlighting the need for additional therapeutic mechanisms (4).

Systemic lupus erythematosus (SLE) is also a systemic disease mediated by autoantibodies, and is characterized by tissue inflammation and damage to multiple organ systems including joints, skin, and kidneys (5). Defects in the clearance of apoptotic and necrotic cells have been demonstrated, allowing access to nuclear antigens by autoantibodies (6). Resulting immune complexes activate numerous immune cell types, including dendritic cells (DCs) and B lymphocytes. Treatments for SLE include glucocorticoids and antimalarial agents, but efficacy is limited and long-term use is associated with toxicity. The BAFF-neutralizing antibody belimumab was approved in 2015, and while it provides benefit in some SLE patients, there remains a clear need for additional treatment modalities (5).

Interleukin-1 receptor–activated kinase 4 (IRAK4) is a central regulator of the innate immune response. IRAK4 transmits signals from Toll-like receptors (TLRs) and interleukin-1 receptor (IL-1R) by binding the adaptor protein myeloid differentiation factor 88 (MyD88) and inducing signaling through IRAK1 and IRAK2 (7,8). The downstream result of myddosome assembly is activation of NF-κB, interferon regulatory factor 5 (IRF-5), and MAPK (9). Deletion of IRAK4 or inactivation of IRAK4 activity in mice prevents the development of inflammation in multiple models of inflammatory disease (10–14). Cells from IRAK4-deficient humans also show no response to TLR or IL-1R family ligands that signal through MyD88 (15).

Several recent studies have highlighted the antiinflammatory efficacy of IRAK4 inhibitors in human cells and preclinical models of inflammation (16–20). However, clinical development has been hampered by debate over the role of IRAK4 kinase activity in disease, as a significant role of kinase-independent signaling by IRAK4 has been demonstrated (21,22). We have shown that inhibition of the kinase activity of IRAK4 does not significantly affect IL-1– or TLR-induced NF-κB or MAPK activation and only minimally suppresses IL-1–induced cytokines, whereas NF-κB or MAPK activation by IL-1 or TLR and production of cytokines are not observed with IRAK4-null cells (7,23). Additionally, several in vitro studies have suggested that IRAK4 inhibitors, which inhibit inflammatory responses in rodent cells, are not equally efficacious for the same activity in human cells (22,24,25). It has also been speculated that inhibition of both IRAK4 and IRAK1 kinase activities may be required for efficacy in human cells (21,22). A recent study using an IRAK4 inhibitor has confirmed the requirement for IRAK4 kinase activity in mouse and human DC and B cell activation as well as in several in vivo models of SLE (20). However, translation of in vitro antiinflammatory efficacy of IRAK4 inhibition to reduction of inflammation in humans is lacking.

We have recently developed potent and selective inhibitors of IRAK4 with little activity against IRAK1 (18). In the present study we demonstrated that PF-06650833, a small-molecule inhibitor of IRAK4, reduces responses to disease-relevant stimuli in human cells and in animal models of RA and SLE. Importantly, we showed that administration of PF-06650833 to humans resulted in the suppression of an interferon (IFN) gene signature in a phase I multiple-ascending-dose clinical trial (26). Our findings show that selective IRAK4 inhibitors reduce signals of inflammation in humans and are potential therapies for autoimmune disease.

MATERIALS AND METHODS

The identification of PF-06650833 and methods used to define its pharmacology have been described previously (18). Details on materials and experimental procedures used in the present study are provided in Supplementary Materials, on the *Arthritis & Rheumatology* website at http://onlinelibrary.wiley.com/doi/10.1002/art.41953/abstract.

In vitro cellular assays. Human, mouse, and rat whole blood collected under institutional review board (IRB)– and institutional animal care and use committee (IACUC)–approved protocols and anticoagulated with heparin, or peripheral blood mononuclear cells (PBMCs) derived from these blood samples, were incubated with PF-06650833, exposed to TLR ligands, and cytokines were assayed with Meso Scale Discovery assay kits. Occupancy of the IRAK4 ATP-binding site was quantified via blockade of covalent labeling with a biotin-labeled ATP probe, followed by immunoprecipitation and Western blotting for IRAK4.

Human macrophages were exposed to inhibitors and then incubated with anti–citrullinated protein antibody (ACPA) immune complexes (ICs), and cytokines in the supernatant were measured with Meso Scale Discovery kits. Broad antiinflammatory phenotypic profiling was performed at Eurofins Scientific (St. Charles, MO), using a BioMAP Diversity Plus Panel with protocols that have been described previously (27,28).

Human RA fibroblast-like synoviocytes (FLS) were incubated with inhibitors, and stimulatory ligands added. Supernatants were analyzed with a Meso Scale Discovery assay kit.

Neutrophils were isolated from healthy volunteers and SLE patients under IRB-approved protocols. Neutrophils from healthy volunteers were primed with IFNα2β and stimulated with R837 alone or in combination with PF-06650833. SLE patient neutrophils were cultured in media for 8–12 hours. Double-stranded DNA (dsDNA) was quantified using a Quant-iT PicoGreen kit.

PBMCs were isolated from healthy volunteers, incubated with PF-06650833, and stimulated with R848 or SLE patient sera. Nuclear localization of IRF-5 was measured using an Amnis imaging cytometer (7).

For B cell maturation assays, human B cells were isolated from Leukopaks, primed with IFNα, incubated with PF-06650833, and stimulated with R848. Supernatants were analyzed for cytokines, and the cells were assessed for plasmablast differentiation.

A

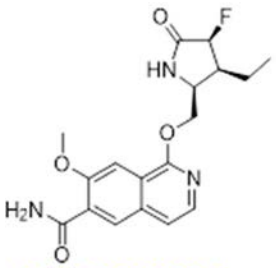

C

In vitro assay	IC50 (nM)	n
Full length Enzyme (ATP Km 600 μM)	0.23	8
PBMC (R848 induced TNF)	2.36	13
Human whole blood (R848 induced TNF) [total/free]	8.8/2.4	8
Human whole blood (R848 induced IL6) [total/free]	11.0/3.1	18
Mouse whole blood (R848 induced TNF) [total/free]	100/13	2
Rat whole blood (R848 induced TNF) [total/free]	82/23	8

B

Kinase	IC50 nM	Rank
IRAK4	0.46	1
IRAK3	72	2
CK1g2	96	3
CK1d,CK1e	150	4
PIP4K2C	150	5
NDR1	350	6
PRP4	570	7
MPSK1	660	8
LKB1	790	9
IKKe	870	10
LATS2	880	11
LRRK2	910	12
NDR2	990	13
TLK2	1200	14
MASTL	1400	15
MLKL	1500	16
TLK1	1800	17
CHK2	2600	18
AurA,AurB,AurC	2800	19
AXL	2900	20
CaMK2g	2900	21
CaMKK2	2900	22
GAK	2900	23
MAP2K6	3000	24
CaMK2d	3200	25
IRAK1	3200	26

D

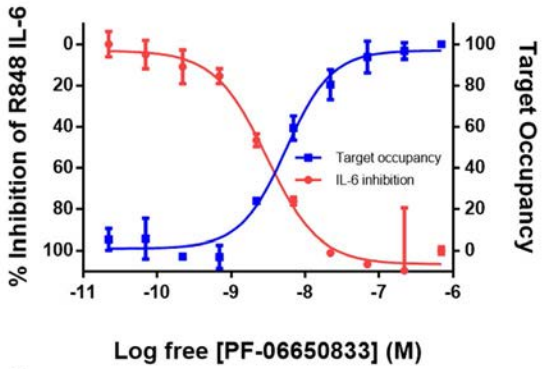

E

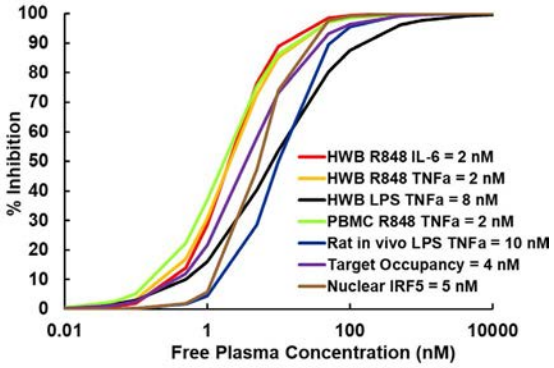

Figure 1. Pharmacologic properties of PF-06650833, an interleukin-1–associated kinase 4 (IRAK4) inhibitor. **A**, Structure of PF-06650833. **B**, Selectivity of PF-06650833 in an ActivX ATP occupancy assay using THP-1 lysates. The top 26 of >200+ kinases are shown. Fifty percent inhibition concentrations (IC_{50}) were determined using a 5-point dose-response curve (full data set shown in Supplementary Table 1, on the *Arthritis & Rheumatology* website at http://onlinelibrary.wiley.com/doi/10.1002/art.41953/abstract). **C**, Potency of PF-06650833 in enzyme and cell-based assays. IC_{50} values for enzyme and peripheral blood mononuclear cell (PBMC) assays are a single value, whereas whole blood (wb) assays for human, mouse, and rat are denoted as total concentration of compound over the non–protein-bound (free [f]) concentration of compound, calculated as (wb IC_{50} × [fu/(B/P)] = IC_{50} free, where fraction unbound [fu] = 0.22 and blood/plasma ratio [B/P] = 0.91). **D**, Demonstration of the relationship between free drug concentration, IRAK4 ATP binding site occupancy, and inhibition of downstream biology by PF-06650833 in a whole blood sample from a patient with systemic lupus erythematosus. Values are the mean ± SEM. **E**, Use of 50% maximum response concentration data from each preclinical assay to determine that 100 n*M* was the target free compound concentration required to maintain >90% IRAK4 inhibition across species and assays. CK1g2 = casein kinase 1 gamma 2; PIP_4K2C = phosphatidylinositol-5-phosphate 4-kinase 2C; NDR1 = nuclear Dbf2-related kinase 1; PRP4 = pre–mRNA processing factor 4; MPSK1 = myristoylated and palmitoylated serine/threonine kinase 1; LKB1 = liver kinase B1; LATS2 = large tumor suppressor kinase 2; LRRK2 = leucine-rich repeat kinase 2; TLK2 = tousled-like kinase 2; MASTL = microtubule-associated serine/threonine kinase–like; MLKL = mixed-lineage kinase domain–like; CHK2 = checkpoint kinase 2; AurA = aurora A kinase; AXL = AXL receptor tyrosine kinase; CAMK2g = Ca^{2+}/calmodulin-dependent protein kinase 2g; GAK = cyclin G–associated kinase; TNF = tumor necrosis factor; IL-6 = interleukin-6; HWB = human whole blood; LPS = lipopolysaccharide; IRF-5 = interferon regulatory factor 5.

The total DC fraction was obtained from healthy volunteer buffy coats, and plasmacytoid DCs (pDCs) were isolated by fluorescence-activated cell sorting and cultured with 40% SLE neutrophil supernatants with or without PF-06650833. IFNα levels were measured by enzyme-linked immunosorbent assay (ELISA).

SLE ICs were generated from patient plasma and used to stimulate human PBMCs, with or without PF-06650833. IFNα was measured by ELISA. IFN-responsive gene expression was analyzed by quantitative reverse transcription–polymerase chain reaction.

In vivo disease models. To model RA, female Lewis rats were immunized with collagen. Subsequently they were administered PF-06650833 or tofacitinib orally for 7 days. Paw volume and body weight were measured daily. All procedures were reviewed and approved by the Pfizer IACUC.

To model SLE, BALB/c mice were treated with pristane. Subsequently PF-06650833 was administered in chow at weeks 8–20, while prednisone was administered orally once daily at weeks 1–20. Serum was collected at weeks, 4, 8, 12, and 20. Anti-dsDNA, anti-SSA, and anti-RNP were quantified by ELISA. Kidney specimens were prepared as previously described (29) and evaluated by a pathologist who was blinded with regard to the treatment group.

Female lupus-prone MRL/*lpr* mice were fed standard chow with or without added PF-06650833 for 12–13 weeks. Body weights were recorded once a week, proteinuria was assessed every 2 weeks, and blood was collected every 4 weeks.

Clinical trial. The phase I studies of PF-06650833 have been described previously (26). RNA was extracted from whole blood and subjected to RNA sequencing. To assess effects on the IFN gene signature, an equally weighted 21-gene signature (30) was analyzed for percent change on day 14 compared to day 0.

RESULTS

Pharmacologic properties of PF-06650833. PF-06650833 was identified as described previously (18) (Figure 1A). The compound is selective as measured by its ability to compete with a covalent analog of ATP in monocyte cell lysates (assessed with an ActivX ATP occupancy assay) (31). Twelve kinases other than IRAK4 had 50% inhibition concentration (IC_{50}) values of <1 μ*M* (Figure 1B and Supplementary Table 1, on the *Arthritis & Rheumatology* website at http://onlinelibrary.wiley.com/doi/10.1002/art.41953/abstract), and PF-06650833 was nearly 7,000 times more selective for IRAK4 than for IRAK1 (Figure 1B). In PBMCs stimulated with the TLR-7/8 ligand R848, PF-06650833 had an IC_{50} of 2.4 n*M* for inhibition of tumor necrosis factor (TNF) release and was potent in human whole blood, with an IC_{50} of 8.8 n*M* (Figure 1C). The free IC_{50} values for PF-06650833 in rodent whole blood were determined to be 5–10-fold less potent than in human whole blood, in contrast to previous reports indicating lack of IRAK4 inhibitor activity in human cells (24,25).

Modeling of PF-06650833 IRAK4 pharmacology to select efficacious dose. Pfizer has established the "Three Pillars of Survival" concept (32) to predict clinical success based on the ability to measure candidate pharmacology. For PF-06650833, we established a system that captured all 3 pillars (free drug concentration [pillar I], target occupancy [pillar II], and downstream biologic effect [pillar III]) in an in vitro assay performed in SLE patient whole blood (Figure 1D). Increasing concentrations of PF-06650833 (pillar I) resulted in increased target occupancy (pillar II), as measured by blockade of the IRAK4 binding site from covalent modification by a probe. With a 50% maximum response concentration (EC_{50}) value very similar to the target occupancy value, R848-induced IL-6 release (pillar III) was inhibited by PF-06650833. Similar results were obtained using blood from a healthy volunteer (Supplementary Figure 1, http://onlinelibrary.wiley.com/doi/10.1002/art.41953/abstract). Thus, target occupancy and cytokine inhibition were proportional and predictable from compound concentration, allowing us to infer pillar II (target occupancy) from pillar III assay results. Using experimentally generated EC_{50}, Hill slope, and protein binding values, we then examined the relationship between free drug concentration and target inhibition in the preclinical assays (Figure 1E). The EC_{50} values for PF-06650833 varied by only 5-fold in these assays—from 2 n*M* to 10 n*M*—such that achieving >100 n*M* free drug concentration would be expected to inhibit >90% of any downstream biologic events dependent on IRAK4 kinase activity. Thus, the target efficacious concentration for preclinical experiments was set at 100 n*M*.

PF-06650833–induced inhibition of pathophysiologic processes central to RA. In seropositive RA, ACPAs are observed prior to the clinical diagnosis of RA, are a specific marker of autoimmunity, and indicate more rapid progression of disease and poorer treatment response (33,34). ACPA ICs activate macrophages to release TNF (35). Thus, we tested the ability of PF-06650833 to block ACPA IC–induced TNF in samples from 11 donors. PF-06650833 at 100 n*M* inhibited TNF release to a mean ± SEM of 57.5 ± 17.9% of that seen with DMSO treatment alone ($P = 0.003$ by paired *t*-test) (Figure 2A). As a positive control, we included a Bruton's tyrosine kinase (BTK) inhibitor, as this kinase has been previously implicated in macrophage TNF responses to both TLR and Fcγ receptor ligands (36). Results with this inhibitor were similar to those observed with IRAK inhibition.

Synovial fibroblasts from RA patients display increased inflammatory responses to TLR ligands and IL-1β (37,38). We exposed RA FLS to inflammatory stimuli in the presence or absence of 100 n*M* PF-06650833 and quantified their inflammatory response. As depicted in Figure 2B, PF-06650833 substantially reduced cytokine and matrix metalloproteinase (MMP) release in response to all ligands profiled. However, it did not

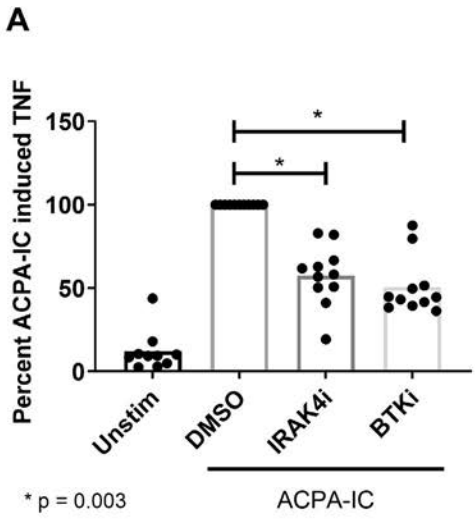

B

Stimulus	Analyte	Donor 1	Donor 2
		PF-0650833	PF-0650833
TLR1/2	IL6	15	27
TLR1/2	IL8	13	23
TLR1/2	MMP-1	33	37
TLR1/2	MMP-3	14	24
TLR4	IL6	5	20
TLR4	IL8	8	18
TLR4	MMP-1	79	44
TLR4	MMP-3	59	58
TLR5	IL6	23	35
TLR5	IL8	25	28
TLR5	MMP-1	42	57
TLR5	MMP-3	22	40
IL1b	IL6	142	131
IL1b	IL8	317	285
IL1b	MMP-1	32	26
IL1b	MMP-3	31	45

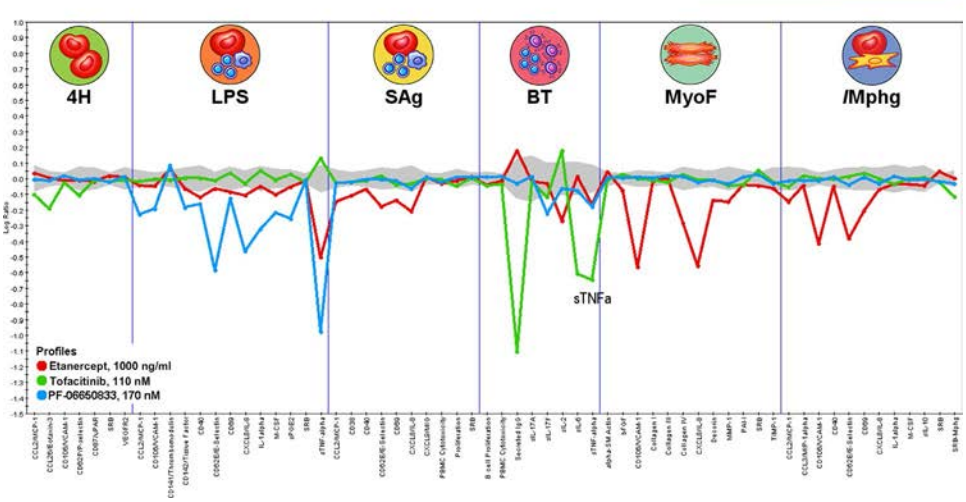

Figure 2. PF-06650833 inhibits rheumatoid arthritis (RA) pathophysiology. **A**, Human macrophages were exposed to anti–citrullinated protein antibody (ACPA) immune complexes (ICs) formed with cyclic citrullinated peptide–positive RA sera in the presence or absence of 100 n*M* interleukin-1–associated kinase 4 inhibitor (IRAK4i) (PF-06650833) or 100 n*M* Bruton's tyrosine kinase inhibitor (BTKi) (PF-303). Supernatants were analyzed by enzyme-linked immunosorbent assay for induction of tumor necrosis factor (TNF). Values are the percent in relation to DMSO treatment (set at 100). Symbols represent individual subjects (n = 11 per group); bars show the mean. **B**, Human RA fibroblast-like synoviocytes were stimulated with 10 μg/ml Pam_3Cys (Toll-like receptor 1/2 [TLR-1/2]), 10 ng/ml lipopolysaccharide (LPS) (TLR-4), 100 ng/ml flagellin (TLR-5), or 0.1 ng/ml interleukin-1β (IL-1β) in the presence or absence of 100 n*M* PF-06650833. Cytokine and matrix metalloproteinase (MMP) content in supernatants was assessed by Meso Scale Discovery assay. Values are the percent of those observed with vehicle control. **C**, Compounds at the noted concentrations were profiled with DiscoverRx on the BioMAP platform. Data represent the log ratio of values in compound-treated samples to controls, with negative values indicating inhibition and points outside of the gray shading demonstrating a statistically significant difference based on assay variability. Each point on the x-axis represents the result of a different end point in each assay system: venular endothelial cells (4H), peripheral blood mononuclear cells (PBMCs) plus venular endothelial cells stimulated with LPS (LPS), PBMCs plus venular endothelial cells stimulated with superantigen (SAg), B cells plus PBMCs (BT), lung fibroblasts (MyoF), and macrophages plus venular endothelial cells (/Mphg). Unstim = unstimulated; MCP-1 = monocyte chemotactic factor 1; VCAM-1 = vascular cell adhesin molecule 1; uPAR = urokinase-type plasminogen activator receptor; SRB = sulforhodamine B staining; VEGFR-2 = vascular endothelial growth factor receptor 2; M-CSF = macrophage colony-stimulating factor; $sPGE_2$ = soluble prostaglandin E_2; MIG = monokine induced by interferon-γ; bFGF = basic fibroblast growth factor; PAI-1 = plasminogen activator inhibitor 1; TIMP-1 = tissue inhibitor of metalloproteinases 1.

inhibit IL-1–induced cytokines in RA FLS. This is similar to our previous findings in dermal fibroblasts stimulated with IL-1β, in which cytokine release was only weakly affected by IRAK4 inhibition (8,23). Similar results were also generated using FLS from non-RA donors (n = 2), although the magnitude of inflammatory mediators released was lower (data not shown). Intriguingly, PF-06650833 was able to block MMP induction by IL-1β: the first response to IL-1β in nonhematopoietic cells we have found to be IRAK4 kinase dependent.

We next tested the ability of PF-06650833 to inhibit inflammatory processes in more physiologic tissue culture models involving multiple human primary cells, using the DiscoveRx BioMAP platform. The effect was compared to those of 2 approved RA therapies, the TNF inhibitor etanercept and the JAK inhibitor tofacitinib. As depicted in Figure 2C, PF-06650833 showed the greatest inhibition of inflammatory readouts in assays of innate immunity, notably the lipopolysaccharide (LPS)–stimulated PBMC plus endothelium assay, with modest activity in a small number of end points in the B–T cell assay. In contrast and as expected, the JAK inhibitor had no impact on assays of innate immunity (LPS, lung myofibroblasts, macrophages plus venular endothelial cells), blocking only responses in the B–T cell assay. Etanercept exhibited yet a third pattern, with predominant activity in the myofibroblast- and macrophage-containing assays, and a modest effect on some readouts in the LPS and bacterial superantigen–stimulated PBMC assays. These results indicate that an IRAK4 inhibitor would block multicellular inflammatory processes in RA in a pattern distinct from those of the approved RA treatments.

PF-06650833–induced reduction of inflammation in the rat collagen-induced arthritis (CIA) model. To profile PF-06650833 in vivo, we used the rat CIA model. Starting on the first day of disease activity (day 11–14 after collagen boost), rats with CIA were administered vehicle, 10 mg/kg tofacitinib daily, or 3 mg/kg PF-06650833 twice daily for 7 days. The kinetic disease activity data for the treatment days from a representative study (n = 10 animals per group) are presented in Figure 3, demonstrating that both PF-06650833 and tofacitinib significantly inhibited paw volume compared to that observed in vehicle-treated animals (mean ± SEM paw volume on day 7 0.786 ± 0.043 ml, 0.555 ± 0.034 ml, and 0.371 ± 0.044 ml with vehicle, PF-06650833, and tofacitinib, respectively; $P = 0.0005$, PF-06650833 versus vehicle and $P < 0.0001$, tofacitinib versus vehicle, by *t*-test). These results indicate that PF-06650833 is capable of inhibiting inflammation in vivo, even when administered weeks after the initial inflammatory insult.

PF-06650833–induced inhibition of pathophysiologic processes central to SLE. High titers of antinuclear antibodies are diagnostic for SLE, and formation of ICs contributes to the multiorgan inflammation characteristic of the disease (39). Exposure of the immune system to nuclear antigens results from impaired

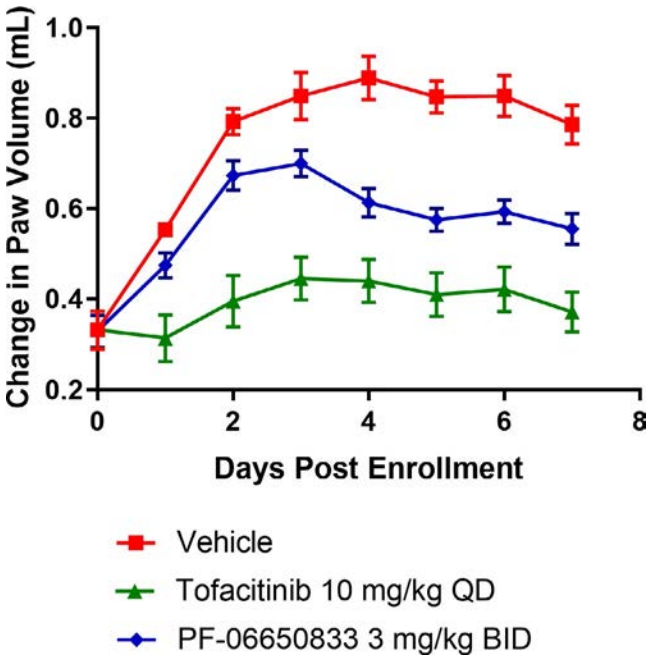

Figure 3. PF-06650833 is efficacious in rat collagen-induced arthritis (CIA). Rats with CIA were treated for 7 days with PF-06650833 3 mg/kg twice daily (bid), tofacitinib 10 mg/kg daily (qd), or vehicle, and paw volume was measured daily. Data are from a representative experiment (of 3 experiments performed). Values are the mean ± SEM.

clearance of apoptotic cells and/or enhanced release from neutrophils via NETosis (40–42). Lupus ICs can then induce cytokine release from monocytes and T cell–independent B cell maturation and can activate pDCs to release type I IFNs, resulting in the characteristic IFN gene signature of SLE (43,44). We stimulated DNA release from human neutrophils by application of the TLR-7 agonist R837 for 15 hours. DNA content in the supernatants was significantly higher than that in neutrophils incubated in medium alone (mean ± SEM 113.5 ± 10.7 ng/ml versus 43.3 ± 9.6 ng/ml; $P = 0.0001$ by paired *t*-test [n = 3 per group]), and was completely reversed by preincubation with PF-06650833 (45.83 ± 9.7 ng/ml; $P = 0.0017$ versus R837 without PF-06650833) (Figure 4A). Monocytes from SLE patients exhibit increased IRF-5 protein expression and nuclear localization (45). After confirming the ability of PF-06650833 to inhibit nuclear localization of IRF-5 stimulated by R848 (23.0 ± 13.0% versus 6.8 ± 4.4%, respectively, without versus with PF-06650833 exposure; $P = 0.012$ by two-way analysis of variance [ANOVA] [n = 3]), we demonstrated its capacity to inhibit IRF-5 nuclear localization in response to SLE patient sera (38.6 ± 18.4% versus 24.2 ± 13.0%, respectively; $P < 0.0001$ by two-way ANOVA [n = 12]) (Figure 4B).

Exposure to IFN and TLR-7 ligands results in B cell cytokine release and T cell–independent B cell maturation into plasmablasts (46,47). Incubation of human B cells with 100 n*M* PF-06650833 prior to addition of IFNα and R848 inhibited B cell IL-6 production at 24 hours to a mean ± SEM of 50.0 ± 16.7% of control ($P = 0.0045$ by paired *t*-test [n = 6 donors]), IL-10 production

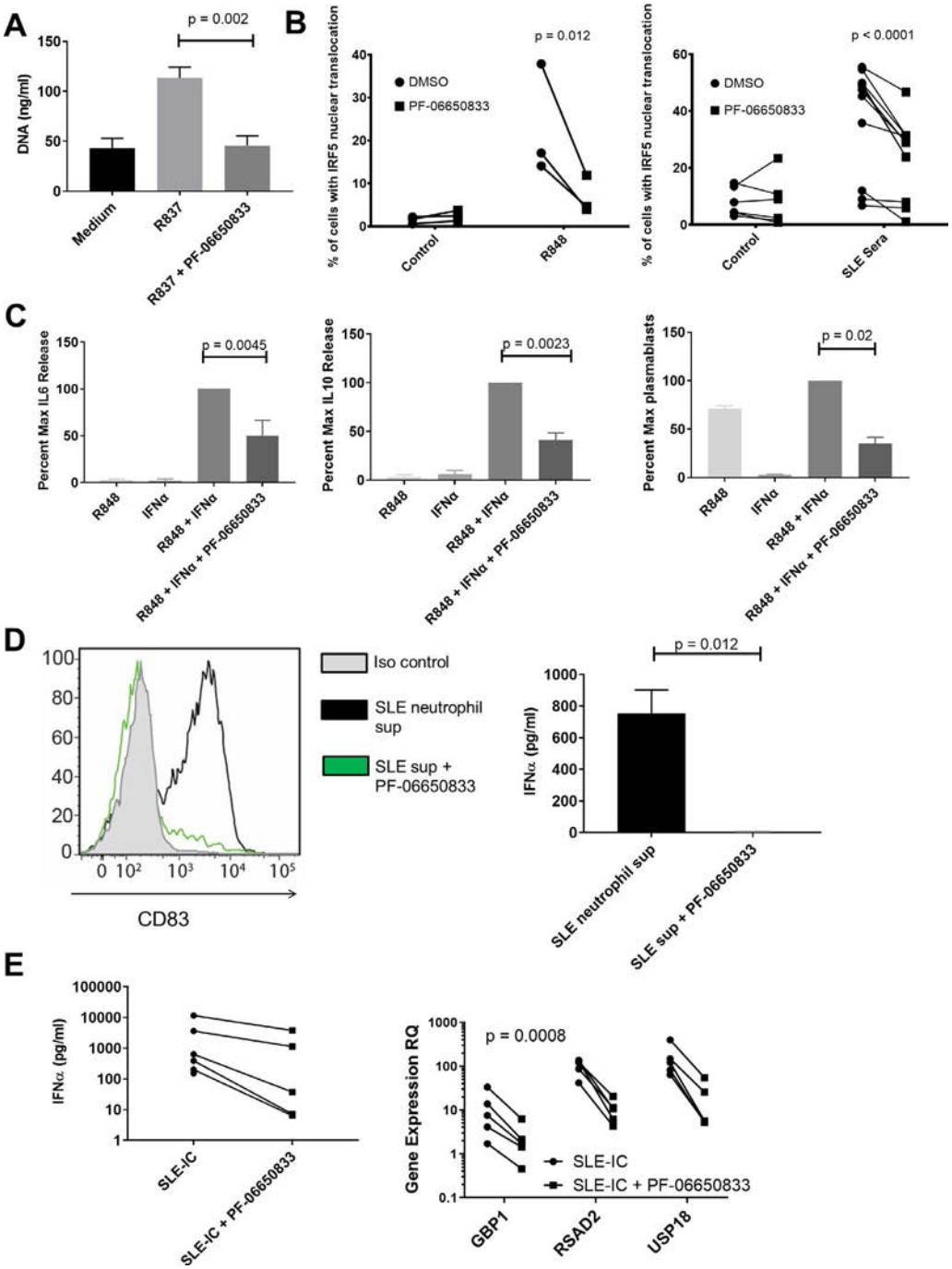

Figure 4. PF-06650833 inhibits pathophysiology in human systemic lupus erythematosus (SLE). **A**, DNA release was measured in neutrophil supernatant (sup) following exposure to R837 in the presence or absence of 100 n*M* PF-06650833. Values are the mean ± SEM (n = 3 donors). **B**, Peripheral blood mononuclear cells (PBMCs) were exposed to either R848 or SLE sera in the presence or absence of 100 n*M* PF-06650833, incubated for 2 hours at 37°C, and then interferon regulatory factor 5 (IRF-5) nuclear translocation was analyzed by Amnis imaging cytometry. **C**, B cells were exposed to interferon-α (IFNα) plus R848 in the presence or absence of 100 n*M* PF-06650833. Supernatants were harvested at 24 hours to assess interleukin-6 (IL-6) release and at 72 hours to assess IL-10 release. Plasmablasts were quantified by flow cytometry after 6 days. **D**, Neutrophils were isolated from SLE patients and NETosis induced with R837. Supernatants were used to stimulate plasmacytoid dendritic cells for 24 hours in the presence or absence of 200 n*M* PF-06650833 prior to quantification of CD83 induction by flow cytometry (n = 5) or IFNα release by enzyme-linked immunosorbent assay (ELISA) (mean ± SEM; n = 3). Iso = isotype. **E**, PBMCs were exposed to SLE immune complexes (ICs) in the presence or absence of 100 n*M* PF-06650833. After 24 hours, supernatant was analyzed by ELISA for IFNα, and IFN-induced gene expression in cells was measured by quantitative reverse transcription–polymerase chain reaction. RQ = relative quantification.

at 72 hours to 41.3 ± 7.1% of control (P = 0.0023 by paired t-test [n = 6 donors]), and CD27+CD38+ plasmablast differentiation at 7 days to 35.1 ± 6.6 % of control (P = 0.02 by paired t-test [n = 6 donors]) (Figure 4C). Although the potency of PF-06650833 (IC_{50}) for inhibiting these activities in primary human B cells (not shown) is comparable to that for inflammatory cytokine release by other cell types, inhibition is less complete than for inflammatory cytokine production by monocytes (48), suggesting IRAK4 kinase-independent signaling.

Plasmacytoid DCs are a rare population in peripheral blood, but are responsible for the majority of IFNα release (44,49). Neutrophil damage-associated molecular patterns (DAMPs) induced pDCs to up-regulate CD83, indicating maturation; this response was significantly inhibited by preincubation with 200 n*M* PF-06650833, and IFNα release from pDCs was significantly inhibited by PF-06650833 (mean ± SEM 5.7 ± 2.5 pg/ml versus 755 ± 147 pg/ml [n = 3]; P = 0.012 by paired t-test) (Figure 4D). SLE ICs formed by purifying IgG from plasma from an anti-RNP/anti-dsDNA–positive SLE patient and mixing with apoptotic cells were used to stimulate human PBMCs. PF-06650833 exposure inhibited IFNα release in all donors (n = 5), as well as the induction of 3 IFN-responsive genes (*RSAD2*, *USP18*, and *GBP1*) (P = 0.0008 by 2-way ANOVA) (Figure 4E).

Taken together, the above findings demonstrate that numerous SLE pathophysiologic processes, including neutrophil DAMP release, monocyte inflammatory cytokine response, B cell cytokine release and plasmablast differentiation, pDC maturation, and IFNα release as well as the resulting IFN gene signature, are dependent on IRAK4 kinase activity.

Therapeutic efficacy of PF-06650833 in mouse models of SLE. The pristane-induced model of SLE is dependent on TLR activation and results in an antinuclear antibody repertoire similar to that in human SLE (50). BALB/c mice were treated

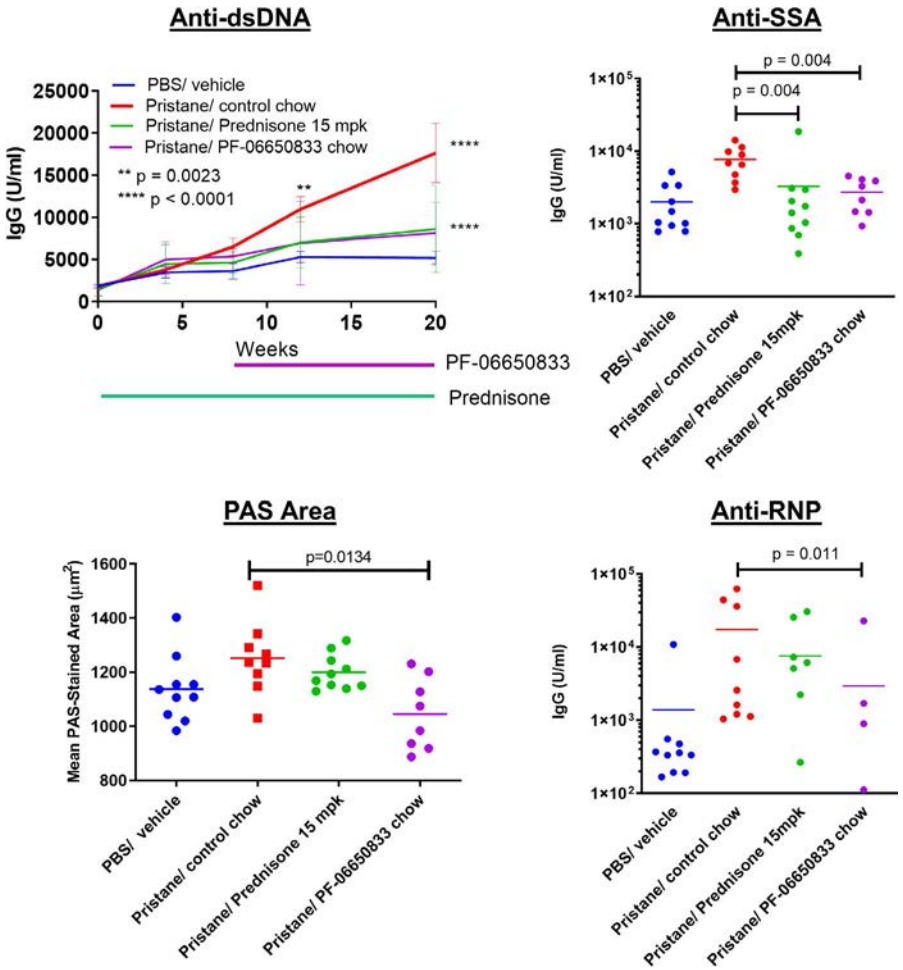

Figure 5. Effect of PF-06650833 on pristane-induced systemic lupus erythematosus. PF-06650833 was administered to BALB/c mice by chow dosing during weeks 8–20 following pristane administration. Anti–double-stranded DNA (anti-dsDNA) was quantified by enzyme-linked immunosorbent assay at weeks 4, 8, 12, and 20, and the mean ± SEM value at each of these time points is shown. Additional autoantibody titers (anti-SSA, anti-RNP) were determined, and immunohistochemical assessments (periodic acid–Schiff [PAS] staining) were performed, at week 20. Data are from a representative experiment (of 2 experiments performed). Symbols represent individual subjects; bars show the mean. PBS = phosphate buffered saline; mpk = mg/kg.

intraperitoneally with pristane to induce disease, and standard chow was replaced 8 weeks later with PF-06650833–containing chow for the remaining 12 weeks of the study. Longitudinal quantitation of antibody levels is shown in Figure 5. Anti-dsDNA titers were significantly increased in pristane-treated animals versus controls beginning at 12 weeks (mean ± SEM 10,977 ± 1,503 units/ml versus 5,294 ± 678 units/ml [n = 10 animals per group]; $P = 0.0023$ by two-way ANOVA), which persisted at week 20 (17,645 ± 3527 units/ml versus 5,103 ± 816 units/ml; $P < 0.0001$ by two-way ANOVA). At week 20, therapeutic dosing with PF-06650833 had significantly reduced anti-dsDNA titers compared to control (8,159 ± 1282 units/ml versus 17,645 ± 3,527 units/ml; $P < 0.0001$ by Mann-Whitney test), as had prednisone treatment (8,608 ± 1,637 units/ml; $P < 0.0001$). With PF-06650833 treatment, there also were significant reductions at week 20 in anti-SSA IgG (2,726 ± 494 units/ml versus 7,693 ± 1,241 units/ml; $P < 0.004$ by Mann-Whitney test) and anti-RNP IgG (3,730 ± 2,861 units/ml versus 18,127 ± 7,902 units/ml; $P = 0.011$ by Mann-Whitney test).

Kidney inflammation in the pristane-induced lupus model was mild and did not result in proteinuria. As there was no increase in renal inflammation, tubular injury, or proteinuria/cast scores in response to pristane exposure, the effects of the IRAK4 inhibitor on these end points were not evaluated. Kidneys in all groups were also evaluated by quantitative image analysis, as described previously (51), for glomerular tuft area, periodic acid–Schiff (PAS) staining area per tuft, glomerular nuclear area, IgG immunohistochemistry scores, and C3 immunohistochemistry scores. Of these, only mean glomerular tuft area was significantly increased by pristane, and only mean PAS area per tuft was significantly reduced by PF-06650833 (mean ± SEM 1,045 ± 47 μm^2, versus 1,252 ± 45 μm^2 with pristane treatment alone [n = 8 animals per group]; $P = 0.013$ by Kruskal-Wallis test) (Figure 5).

Treatment with PF-06650833 was also explored in the MRL/*lpr* mouse model of SLE. In 2 studies, PF-06650833 significantly reduced lymphadenopathy, anti–histone IgG, histologic kidney inflammation, glomerular nephropathy, and C3 and IgG deposition by immunohistochemistry, and glomerular tuft area and glomerular nuclear area by image analysis (Supplementary Figures 2 and 3, on the *Arthritis & Rheumatology* website at http://onlinelibrary.wiley.com/doi/10.1002/art.41953/abstract), while showing trends toward reductions in splenomegaly, proteinuria, anti-dsDNA, anti-SSA, and tubular injury. As BTK inhibitors have previously shown efficacy in this model (52–54) and we previously showed in vivo efficacy of the BTK inhibitor PF-06250112 in the NZB/NZW mouse model of lupus (29), it was included as a positive control. PF-06250112 significantly reduced proteinuria, autoantibody titers, and all renal histologic pathology end points other than PAS area per tuft (Supplementary Figures 2 and 3). It may be that in the pristane-induced SLE model, in which autoantibodies are induced via TLR activation, IRAK4 kinase activity is essential, while in the MRL/*lpr* model, in which autoantibody production is initiated by faulty B cell apoptosis, IRAK4 kinase activity is more important for the resulting inflammation than for the production of autoantibodies themselves.

Reduction of IFN signature genes in healthy volunteers by selective IRAK4 inhibition. We have completed 2 randomized, double-blind, sponsor-open phase I studies of the safety, pharmacokinetics, and pharmacodynamics of single- and multiple-ascending doses of PF-06650833 (26). Since the 300-mg dose of a modified-release formulation showed maximum pharmacologic effect in reducing C-reactive protein (CRP) levels on day 14 of dosing, we evaluated the effect of PF-06650833 on an IFN signature (comprising the normalized expression of 21 genes [30]) as a biomarker of systemic inflammation relevant to SLE pathogenesis at this time point, in comparison to the respective gene signature for each volunteer on day 0, prior to dosing. As shown in Figure 6, the IFN gene signature in the placebo group had changed positively by a median of 9.1%, while that in the PF-06650833–treated trial participants was reduced by

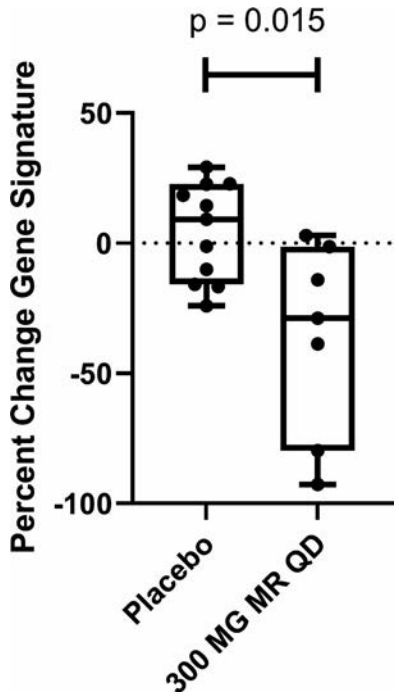

Figure 6. PF-06650833 inhibits type I interferon signature in vivo in humans. Moderate-release (MR) PF-06650833 (300 mg/day [qd]) (n = 7) or placebo (n = 11) was administered for 14 days in a phase I multiple-ascending-dose trial in healthy human volunteer subjects. Whole blood was collected in a PAXgene tube on day 0 prior to administration of the first dose and on day 14 prior to administration of the last dose, RNA extracted, and a composite gene signature calculated. The percent change in the composite gene signature for each individual participant between the 2 time points is shown. Each box represents the 25th to 75th percentiles. Lines inside the boxes represent the median. Lines outside the boxes represent the full range of values. Symbols represent individual patients.

a median of 28.8% (difference –37.9%; P = 0.015 by Wilcoxon test). The paired gene score values for each volunteer on day 0 and day 14 are also plotted in Supplementary Figure 4 (http://onlinelibrary.wiley.com/doi/10.1002/art.41953/abstract), showing minimal regulation of gene scores in placebo-treated subjects (positive change in 6 of 11 and negative change in 5 of 11), whereas the magnitude of change between day 0 and day 14 was consistently higher, and the change was negative in 6 of 7 cases, among PF-06650833–treated subjects.

Thus, we have demonstrated that in humans, an IRAK4 inhibitor reduces biomarkers of inflammation that are relevant to RA and SLE pathophysiology.

DISCUSSION

Inhibitors of innate immune signaling pathways are potential targets for treatment of autoimmune diseases (55,56). In this study, we demonstrated that PF-06650833 effectively inhibits cytokines produced by macrophages activated by ACPA ICs from RA patients as well as pDCs activated by SLE ICs. We also showed that PF-06650833 effectively inhibits cytokines induced by TLR ligands on RA FLS but is not effective against IL-1β–induced cytokines. However, PF-06650833 is effective at blocking MMPs induced by IL-1β on these cells. The reason for this difference is not known but may result from the differential effects of IRAK4 inhibition on early versus late myddosome formation and/or differential effects on transcription factor activation. Previously, investigators in our group have shown that inhibition of IRAK4 kinase activity affects IL-1β signaling by stabilizing the early form of the myddosome that signals primarily through IRAK1 and NF-κB (8,57). It is possible that IL-6/8 secretion is induced primarily by signaling via the early myddosome, whereas activation of MMPs might be mediated by the late myddosome, which signals through IRAK2 (58). Regarding transcription factors, inhibition of IRAK4 kinase activity is known to block activation of IRF-5, but not NF-κB or MAPK (7), and these effects are cell type specific (38). It is possible that in RA FLS, chromatin remodeling makes the MMP promoters more dependent on IRF-5 or other IRAK4 kinase-dependent transcription factors.

We also demonstrated that PF-06650833 is efficacious in a rat model of arthritis that did not include use of Freund's complete adjuvant (to ensure it was not driven by TLR). While it is encouraging that PF-06650833 significantly reduces severity in the rat CIA model, it is notable that the degree of inhibition was not as great as that observed with tofacitinib. It is possible that the rapid clearance of PF-06650833 from rodent species (rat $T_{½}$ = 0.6 hours [18]) resulted in transient loss of IRAK4 target inhibition in rat CIA. It has been shown previously that the efficacy of tofacitinib is driven by average target occupancy (59), while the evidence thus far suggests that minimum target occupancy is more relevant for IRAK4-mediated efficacy. Thus, the respective efficacies of PF-06650833 and tofacitinib in rat CIA may be related to target occupancy, mechanism of inhibition, or the respective contribution of each kinase to disease pathophysiology. Of greater relevance to the treatment of human RA, our group recently identified significant effects on disease activity in a phase II study of the efficacy and safety of PF-06650833 in patients with active RA and inadequate response to methotrexate (60). The rate of clinical response at 12 weeks in that study was consistent with those reported for tofacitinib, and the study itself included a cohort treated with tofacitinib. Thus, the respective efficacy of the 2 molecules will be revealed by the publication of data from this clinical trial.

We have shown here that PF-06650833 can block type I IFN induced by SLE serum and by neutrophil DAMPs in primary human pDCs. We also demonstrated that it can block plasmablast differentiation and B cell activation induced by TLR ligands and activation of the transcription factor IRF-5 by SLE serum in monocytes (61,62). Therapeutic dosing of PF-06650833 was efficacious in reducing the induction of all antinuclear antibodies tested in the pristane model of SLE, while significantly reducing only 1 of 3 reactivities assayed in the MRL/*lpr* model. Interestingly, PF-06650833 did demonstrate robust inhibition of kidney inflammatory histology in the MRL/*lpr* mouse model. It is unknown whether this difference is due to the different mechanisms of disease initiation in the 2 models or differences in ability to cover the target, as PF-06650833 is rapidly cleared from mouse circulation.

Despite lower potency in rodent cells and rapid clearance from rodent circulation, the in vitro and in vivo results generated with PF-06650833 presented here provide important insights with regard to some of the controversies concerning the relative importance of IRAK1 and IRAK4 kinase activity in various cell types in mice and humans (16,19,21,22,24,25). IRAK4 kinase activity is necessary for DAMP-induced inflammatory signaling in rodent and human leukocytes, and IRAK1 kinase activity does not provide a sufficient substitute. Findings of a recent study (20) are consistent with our data, confirming the importance of IRAK4 activity to lupus pathophysiologic signaling in DCs and B cells, and in in vivo models using an unrelated small molecule inhibitor of IRAK4. Further work is needed in the effort to understand the role of IRAK4 kinase activity in stromal cells, as well as in IL-1β–induced inflammation. We have shown that IL-1β–induced cytokines from human fibroblasts treated with an IRAK4 inhibitor were only weakly inhibited even though IRAK4 autophosphorylation was completely inhibited (8,63), while inhibition of TLR-7/8 (R848)–induced cytokine production by IRAK4 inhibition coincided with the inhibition of IRAK4 autophosphorylation in primary human monocytes (7,63). Likewise, in the results presented here, IL-1β–induced cytokines in RA FLS were not inhibited by PF-06650833, in contrast to MMPs, which were inhibited.

To demonstrate proof of pharmacologic effect in humans, we assessed markers of inflammation in a phase I clinical trial in healthy volunteers. These markers were IFN signature (increased in SLE) (44) and CRP levels (increased in RA) (64,65). Basal levels

of these markers were present in healthy volunteers, and notably, with modified-release PF-06650833 at a daily dosage of 300 mg, we observed statistically significant reductions in both end points, demonstrating that an IRAK4 inhibitor reduces markers of inflammation in humans. To our knowledge, this is the first demonstration of modulation of IFN-regulated genes in healthy volunteers. Together with the CRP data (26), the present results represent the first proof of pharmacologic effect of a selective IRAK4 inhibitor on inflammatory signaling pathways in humans. Taken together, these data strongly support the clinical utility of IRAK4 inhibitors for the treatment of multiple human inflammatory autoimmune diseases.

ACKNOWLEDGMENTS

The authors wish to thank Tatyana Souza and Varenka Rodriguez for optimizing the plasmablast differentiation assay, Jill Wright and Yanyu Zhang for human IgG purification from plasma, Alison O'Mahoney (Eurofins) for providing the DiscoverRx figure, the scientists at ActivX for performing kinase selectivity assays and at Washington Biotechnology for performing the pristane SLE model, our clinical collaborators in the phase I multiple-ascending-dose study, and especially all of the human volunteers who contributed to every phase of this work.

AUTHOR CONTRIBUTIONS

All authors were involved in drafting the article or revising it critically for important intellectual content, and all authors approved the final version to be published. Dr. Winkler had full access to all of the data in the study and takes responsibility for the integrity of the data and the accuracy of the data analysis.

Study conception and design. Winkler, Sun, De, Sharif, Athale, Jacobson, Ramsey, Dower, Hegen, Homer, Brodfuehrer, Tilley, Danto, Beebe, Barnes, Pascual, Lin, Kilty, Fleming, Rao.

Acquisition of data. Winkler, Sun, De, Jiao, Sharif, Symanowicz, Athale, Shin, Wang, Jacobson, Ramsey, Dower, Andreyeva, Liu, Homer, Danto, Beebe, Rao.

Analysis and interpretation of data. Winkler, Sun, De, Jiao, Sharif, Symanowicz, Athale, Shin, Wang, Jacobson, Ramsey, Dower, Andreyeva, Liu, Hegen, Homer, Brodfuehrer, Tilley, Gilbert, Danto, Beebe, Barnes, Pascual, Lin, Kilty, Fleming, Rao.

ROLE OF THE STUDY SPONSOR

Pfizer facilitated the study design, provided writing assistance for the manuscript, and reviewed and approved the manuscript prior to submission. The authors independently collected the data, interpreted the results, and had the final decision to submit the manuscript for publication. Publication of this article was contingent upon approval by Pfizer.

REFERENCES

1. Malmström V, Catrina AI, Klareskog L. The immunopathogenesis of seropositive rheumatoid arthritis: from triggering to targeting [review]. Nat Rev Immunol 2016;17:60–75.
2. Smolen JS, Aletaha D, Barton A, Burmester GR, Emery P, Firestein GS, et al. Rheumatoid arthritis [review]. Nat Rev Dis Primers 2018;4:18001.
3. Aletaha D, Smolen JS. Diagnosis and management of rheumatoid arthritis: a review. JAMA 2018;320:1360–72.
4. Smolen JS, Aletaha D. Rheumatoid arthritis therapy reappraisal: strategies, opportunities and challenges [review]. Nat Rev Rheumatol 2015;11:276–89.
5. Dörner T, Furie R. Novel paradigms in systemic lupus erythematosus [review]. Lancet 2019;393:2344–58.
6. Tsokos GC, Lo MS, Reis PC, Sullivan KE. New insights into the immunopathogenesis of systemic lupus erythematosus [review]. Nat Rev Rheumatol 2016;12:716–30.
7. Cushing L, Winkler A, Jelinsky SA, Lee K, Korver W, Hawtin R, et al. IRAK4 kinase activity controls Toll-like receptor–induced inflammation through the transcription factor IRF5 in primary human monocytes. J Biol Chem 2017;292:18689–98.
8. De S, Karim F, Kiessu E, Cushing L, Lin LL, Ghandil P, et al. Mechanism of dysfunction of human variants of the IRAK4 kinase and a role for its kinase activity in interleukin-1 receptor signaling. J Biol Chem 2018;293:15208–20.
9. Balka KR, De Nardo D. Understanding early TLR signaling through the Myddosome [review]. J Leukoc Biol 2019;105:339–51.
10. Suzuki N, Suzuki S, Duncan GS, Millar DG, Wada T, Mirtsos C, et al. Severe impairment of interleukin-1 and Toll-like receptor signalling in mice lacking IRAK-4. Nature 2002;416:750–6.
11. Kim TW, Staschke K, Bulek K, Yao J, Peters K, Oh KH, et al. A critical role for IRAK4 kinase activity in Toll-like receptor-mediated innate immunity. J Exp Med 2007;204:1025–36.
12. Koziczak-Holbro M, Littlewood-Evans A, Pöllinger B, Kovarik J, Dawson J, Zenke G, et al. The critical role of kinase activity of interleukin-1 receptor–associated kinase 4 in animal models of joint inflammation. Arthritis Rheum 2009;60:1661–71.
13. Nanda SK, Lopez-Pelaez M, Arthur JS, Marchesi F, Cohen P. Suppression of IRAK1 or IRAK4 catalytic activity, but not type 1 IFN signaling, prevents lupus nephritis in mice expressing a ubiquitin binding-defective mutant of ABIN1. J Immunol 2016;197:4266–73.
14. Kawagoe T, Sato S, Jung A, Yamamoto M, Matsui K, Kato H, et al. Essential role of IRAK-4 protein and its kinase activity in Toll-like receptor-mediated immune responses but not in TCR signaling. J Exp Medicine 2007;204:1013–24.
15. Picard C, Puel A, Bonnet M, Ku CL, Bustamante J, Yang K, et al. Pyogenic bacterial infections in humans with IRAK-4 deficiency. Science 2003;299:2076–9.
16. Kelly PN, Romero DL, Yang Y, Shaffer AL III, Chaudhary D, Robinson S, et al. Selective interleukin-1 receptor-associated kinase 4 inhibitors for the treatment of autoimmune disorders and lymphoid malignancy. J Exp Med 2015;212:2189–201.
17. Chaudhary D, Robinson S, Romero DL. Recent advances in the discovery of small molecule inhibitors of interleukin-1 receptor-associated kinase 4 (IRAK4) as a therapeutic target for inflammation and oncology disorders [review]. J Med Chem 2015;58:96–110.
18. Lee KL, Ambler CM, Anderson DR, Boscoe BP, Bree AG, Brodfuehrer JI, et al. Discovery of clinical candidate 1-{[(2S,3S,4S)-3-Ethyl-4-fluoro-5-oxopyrrolidin-2-yl]methoxy}-7-methoxyisoquinoline-6-carboxamide (PF-06650833), a potent, selective inhibitor of interleukin-1 receptor associated kinase 4 (IRAK4), by fragment-based drug design. J Med Chem 2017;60:5521–42.
19. Dudhgaonkar S, Ranade S, Nagar J, Subramani S, Prasad DS, Karunanithi P, et al. Selective IRAK4 inhibition attenuates disease in murine lupus models and demonstrates steroid sparing activity. J Immunol 2017;198:1308–19.
20. Corzo CA, Varfolomeev E, Setiadi AF, Francis R, Klabunde S, Senger K, et al. The kinase IRAK4 promotes endosomal TLR and immune complex signaling in B cells and plasmacytoid dendritic cells. Sci Signal 2020;13:eeaz1053.
21. Qin J, Jiang Z, Qian Y, Casanova JL, Li X. IRAK4 kinase activity is redundant for interleukin-1 (IL-1) receptor-associated kinase phosphorylation and IL-1 responsiveness. J Biol Chem 2004;279:26748–53.
22. Song KW, Talamas FX, Suttmann RT, Olson PS, Barnett JW, Lee SW, et al. The kinase activities of interleukin-1 receptor associated

kinase (IRAK)-1 and 4 are redundant in the control of inflammatory cytokine expression in human cells. Mol Immunol 2009;46:1458–66.
23. Cushing L, Stochaj W, Siegel M, Czerwinski R, Dower K, Wright Q, et al. Interleukin 1/Toll-like receptor-induced autophosphorylation activates interleukin 1 receptor-associated kinase 4 and controls cytokine induction in a cell type-specific manner. J Biol Chem 2014;289:10865–75.
24. Chiang EY, Yu X, Grogan JL. Immune complex-mediated cell activation from systemic lupus erythematosus and rheumatoid arthritis patients elaborate different requirements for IRAK1/4 kinase activity across human cell types. J Immunol 2011;186:1279–88.
25. Sun J, Li N, Oh KS, Dutta B, Vayttaden SJ, Lin B, et al. Comprehensive RNAi-based screening of human and mouse TLR pathways identifies species-specific preferences in signaling protein use. Sci Signal 2016;9:ra3.
26. Danto SI, Shojaee N, Singh RS, Li C, Gilbert SA, Manukyan Z, et al. Safety, tolerability, pharmacokinetics, and pharmacodynamics of PF-06650833, a selective interleukin-1 receptor-associated kinase 4 (IRAK4) inhibitor, in single and multiple ascending dose randomized phase 1 studies in healthy subjects. Arthritis Res Ther 2019;21:269.
27. O'Mahony A, John MR, Cho H, Hashizume M, Choy EH. Discriminating phenotypic signatures identified for tocilizumab, adalimumab, and tofacitinib monotherapy and their combinations with methotrexate. J Transl Med 2018;16:156.
28. Shah F, Stepan AF, O'Mahony A, Velichko S, Folias AE, Houle C, et al. Mechanisms of skin toxicity associated with metabotropic glutamate receptor 5 negative allosteric modulators. Cell Chem Biol 2017;24:858–69.
29. Rankin AL, Seth N, Keegan S, Andreyeva T, Cook TA, Edmonds J, et al. Selective inhibition of BTK prevents murine lupus and antibody-mediated glomerulonephritis. J Immunol 2013;191:4540–50.
30. Yao Y, Higgs BW, Richman L, White B, Jallal B. Use of type I interferon-inducible mRNAs as pharmacodynamic markers and potential diagnostic markers in trials with sifalimumab, an anti-IFNα antibody, in systemic lupus erythematosus [review]. Arthritis Res Ther 2010;12 Suppl 1:S6.
31. Patricelli MP, Nomanbhoy TK, Wu J, Brown H, Zhou D, Zhang J, et al. In situ kinase profiling reveals functionally relevant properties of native kinases. Chem Biol 2011;18:699–710.
32. Morgan P, Van Der Graaf PH, Arrowsmith J, Feltner DE, Drummond KS, Wegner CD, et al. Can the flow of medicines be improved? Fundamental pharmacokinetic and pharmacological principles toward improving Phase II survival. Drug Discov Today 2012;17:419–24.
33. Castelar-Pinheiro GR, Xavier RM. The spectrum and clinical significance of autoantibodies in rheumatoid arthritis. Front Immunol 2015;6:320.
34. Catrina AI, Svensson CI, Malmström V, Schett G, Klareskog L. Mechanisms leading from systemic autoimmunity to joint-specific disease in rheumatoid arthritis [review]. Nat Rev Rheumatol 2016;13:79–86.
35. Sokolove J, Zhao X, Chandra PE, Robinson WH. Immune complexes containing citrullinated fibrinogen costimulate macrophages via Toll-like receptor 4 and Fcγ receptor. Arthritis Rheum 2011;63:53–62.
36. Horwood NJ, Page TH, McDaid JP, Palmer CD, Campbell J, Mahon T, et al. Bruton's tyrosine kinase is required for TLR2 and TLR4-induced TNF, but not IL-6, production. J Immunol 2006;176:3635–41.
37. Falconer J, Murphy AN, Young SP, Clark AR, Tiziani S, Guma M, et al. Synovial cell metabolism and chronic inflammation in rheumatoid arthritis [review]. Arthritis Rheumatol 2018;70:984–99.
38. Doody KM, Bottini N, Firestein GS. Epigenetic alterations in rheumatoid arthritis fibroblast-like synoviocytes [review]. Epigenomics 2017;9:479–92.
39. Pisetsky DS. Anti-DNA antibodies: quintessential biomarkers of SLE [review]. Nat Rev Rheumatol 2015;12:102–10.
40. Lee KH, Kronbichler A, Park DD, Park Y, Moon H, Kim H, et al. Neutrophil extracellular traps (NETs) in autoimmune diseases: a comprehensive review. Autoimmun Rev 2017;16:1160–73.
41. Bouts YM, Wolthuis DF, Dirkx MF, Pieterse E, Simons EM, van Boekel AM, et al. Apoptosis and NET formation in the pathogenesis of SLE [review]. Autoimmunity 2012;45:597–601.
42. Mahajan A, Herrmann M, Muñoz LE. Clearance deficiency and cell death pathways: a model for the pathogenesis of SLE [review]. Front Immunol 2016;7:35.
43. Muñoz LE, Janko C, Schulze C, Schorn C, Sarter K, Schett G, et al. Autoimmunity and chronic inflammation: two clearance-related steps in the etiopathogenesis of SLE. Autoimmun Rev 2010;10:38–42.
44. Crow MK. Type I interferon in the pathogenesis of lupus [review]. J Immunol 2014;192:5459–68.
45. Stone RC, Feng D, Deng J, Singh S, Yang L, Fitzgerald-Bocarsly P, et al. Interferon regulatory factor 5 activation in monocytes of systemic lupus erythematosus patients is triggered by circulating autoantigens independent of type I interferons. Arthritis Rheum 2012;64:788–98.
46. Kiefer K, Oropallo MA, Cancro MP, Marshak-Rothstein A. Role of type I interferons in the activation of autoreactive B cells [review]. Immunol Cell Biol 2012;90:498–504.
47. Douagi I, Gujer C, Sundling C, Adams WC, Smed-Sörensen A, Seder RA, et al. Human B cell responses to TLR ligands are differentially modulated by myeloid and plasmacytoid dendritic cells. J Immunol 2009;182:1991–2001.
48. Cushing L, Winkler A, Jelinsky SA, Lee K, Korver W, Hawtin R, et al. IRAK4 kinase activity controls Toll-like receptor-induced inflammation through the transcription factor IRF5 in primary human monocytes. J Biol Chem 2017;292:18689–98.
49. Colonna M, Trinchieri G, Liu YJ. Plasmacytoid dendritic cells in immunity [review]. Nat Immunol 2004;5:1219–26.
50. Zhuang H, Szeto C, Han S, Yang L, Reeves WH. Animal models of interferon signature positive lupus [review]. Front Immunol 2015;6:291.
51. Homer BL, Dower K. 41-week study of progressive diabetic nephropathy in the ZSF1 fa/fa^{CP} rat model. Toxicol Pathol 2018;46:976–7.
52. Honigberg LA, Smith AM, Sirisawad M, Verner E, Loury D, Chang B, et al. The Bruton tyrosine kinase inhibitor PCI-32765 blocks B-cell activation and is efficacious in models of autoimmune disease and B-cell malignancy. Proc Nat Acad Sci U S A 2010;107:13075–80.
53. Kim YY, Park KT, Jang SY, Lee KH, Byun JY, Suh KH, et al. HM71224, a selective Bruton's tyrosine kinase inhibitor, attenuates the development of murine lupus. Arthritis Res Ther 2017;19:211.
54. Chalmers SA, Wen J, Doerner J, Stock A, Cuda CM, Makinde HM, et al. Highly selective inhibition of Bruton's tyrosine kinase attenuates skin and brain disease in murine lupus. Arthritis Res Ther 2018;20:10.
55. Shi FD, Ljunggren HG, Sarvetnick N. Innate immunity and autoimmunity: from self-protection to self-destruction [review]. Trends Immunol 2001;22:97–101.
56. Waldner H. The role of innate immune responses in autoimmune disease development [review]. Autoimmun Rev 2009;8:400–4.
57. De Nardo D, Balka KR, Gloria YC, Rao VR, Latz E, Masters SL. Interleukin-1 receptor–associated kinase 4 (IRAK4) plays a dual role in myddosome formation and Toll-like receptor signaling. J Biol Chem 2018;293:15195–207.
58. Pauls E, Nanda SK, Smith H, Toth R, Arthur JS, Cohen P. Two phases of inflammatory mediator production defined by the study of IRAK2 and IRAK1 knock-in mice. J Immunol 2013;191:2717–30.

59. Lamba M, Hutmacher MM, Furst DE, Dikranian A, Dowty ME, Conrado D, et al. Model-informed development and registration of a once-daily regimen of extended-release tofacitinib. Clin Pharmacol Ther 2017;101:745–53.
60. Danto SI, Shojaee N, Singh RS, Manukyan Z, Mancuso J, Peeva E, et al. Efficacy and safety of the selective interleukin-1 receptor associated kinase 4 inhibitor, PF-06650833, in patients with active rheumatoid arthritis and inadequate response to methotrexate [abstract]. Arthritis Rheumatol 2019;71 Suppl 10. URL: https://acrabstracts.org/abstract/efficacy-and-safety-of-the-selective-interleukin-1-receptor-associated-kinase-4-inhibitor-pf-06650833-in-patients-with-active-rheumatoid-arthritis-and-inadequate-response-to-methotrexate/.
61. Lazzari E, Jefferies CA. IRF5-mediated signaling and implications for SLE [review]. Clin Immunol 2014;153:343–52.
62. Ban T, Sato GR, Tamura T. Regulation and role of the transcription factor IRF5 in innate immune responses and systemic lupus erythematosus [review]. Int Immunol 2018;30:529–36.
63. Cushing L, Stochaj W, Siegel M, Czerwinski R, Dower K, Wright Q, et al. Interleukin 1/Toll-like receptor-induced autophosphorylation activates interleukin 1 receptor-associated kinase 4 and controls cytokine induction in a cell type-specific manner. J Biol Chem 2014;289:10865–75.
64. Otterness IG. The value of C-reactive protein measurement in rheumatoid arthritis [review]. Semin Arthritis Rheum 1994;24:91–104.
65. Tishler M, Caspi D, Yaron M. C-reactive protein levels in patients with rheumatoid arthritis: the impact of therapy. Clin Rheumatol 1985;4:321–4.

Arthritis & Rheumatology
Vol. 73, No. 12, December 2021, pp 2219–2228
DOI 10.1002/art.41939
© 2021, American College of Rheumatology

American College of Rheumatology
Empowering Rheumatology Professionals

Passive Smoking Throughout the Life Course and the Risk of Incident Rheumatoid Arthritis in Adulthood Among Women

Kazuki Yoshida,[1] Jiaqi Wang,[2] Susan Malspeis,[2] Nathalie Marchand,[1] Bing Lu,[1] Lauren C. Prisco,[2] Lily W. Martin,[2] Julia A. Ford,[3] Karen H. Costenbader,[1] Elizabeth W. Karlson,[1] and Jeffrey A. Sparks[1]

Objective. To investigate passive smoking throughout the life course and the risk of rheumatoid arthritis (RA), while accounting for personal smoking.

Methods. We analyzed the Nurses' Health Study II prospective cohort, using information collected via biennial questionnaires. We assessed the influence of 1) maternal smoking during pregnancy (in utero exposure), 2) childhood parental smoking, and 3) years lived with smokers since age 18. Incident RA and serostatus were determined by medical record review. Using the marginal structural model framework, we estimated the controlled direct effect of each passive smoking exposure on adult incident RA risk by serologic phenotype, controlling for early-life factors and time-updated adulthood factors including personal smoking.

Results. Among 90,923 women, we identified 532 incident RA cases (66% seropositive) during a median of 27.7 years of follow-up. Maternal smoking during pregnancy was associated with RA after adjustment for confounders, with a hazard ratio (HR) of 1.25 (95% confidence interval [95% CI] 1.03–1.52), but not after accounting for subsequent smoking exposures. Childhood parental smoking was associated with seropositive RA after adjustment for confounders (HR 1.41 [95% CI 1.08–1.83]). In the controlled direct effect analyses, childhood parental smoking was associated with seropositive RA (HR 1.75 [95% CI 1.03–2.98]) after controlling for adulthood personal smoking, and the association was accentuated among ever smokers (HR 2.18 [95% CI 1.23–3.88]). There was no significant association of adulthood passive smoking with RA (HR 1.30 for ≥20 years of living with a smoker versus none [95% CI 0.97–1.74]).

Conclusion. We found a potential direct influence of childhood parental smoking on adult-onset incident seropositive RA even after controlling for adulthood personal smoking.

INTRODUCTION

Rheumatoid arthritis (RA) is a debilitating systemic inflammatory disease characterized by prominent polyarthritis with associated morbidity and mortality (1–3). In its pathogenesis, considered an interplay of genetic and environmental exposures (4), lung inflammation is strongly implicated as an initial site of immune dysregulation and RA-related autoantibody production (5–7). Thus, smoking, personal (active) and passive, has been of interest as a major modifiable environmental risk factor for seropositive RA, which is characterized

The content of this article is solely the responsibility of the authors and does not necessarily represent the official views of the National Institutes of Health.

Supported by a Rheumatology Research Foundation R Bridge Award and the NIH (awards L30-AR-066953, K24-AR-052403, R01-AR-049880, R01-AR-057327, R01-AR-119246, R01-HL-034594, P30-AR-070253, P30-AR-072577, P30-AR-069625, UM1-CA-186107, U01-HG-008685, 1OT2-OD-026553, and R03-AR-075886). The Nurses' Health Study II was supported by the NIH (awards U01-CA-176726, R01-CA-67262, and U01-HL-145386). Dr. Yoshida's work was supported by a Rheumatology Research Foundation K Bridge Award, a Brigham and Women's Hospital Department of Medicine Fellowship Award, and the National Institute of Arthritis and Musculoskeletal and Skin Diseases, NIH (award K23-AR-076453). Dr. Sparks' work was supported by the National Institute of Arthritis and Musculoskeletal and Skin Diseases, NIH (award K23-AR-069688).

[1]Kazuki Yoshida, MD, ScD, Nathalie Marchand, ScD, Bing Lu, MD, DrPH, Karen H. Costenbader, MD, MPH, Elizabeth W. Karlson, MD, Jeffrey A. Sparks, MD, MMSc: Brigham and Women's Hospital and Harvard Medical School, Boston, Massachusetts; [2]Jiaqi Wang, MS, Susan Malspeis, MS, Lauren C. Prisco, BA, Lily W. Martin, BS: Brigham and Women's Hospital, Boston, Massachusetts; [3]Julia A. Ford, MD: University of Michigan, Ann Arbor.

Author disclosures are available at https://onlinelibrary.wiley.com/action/downloadSupplement?doi=10.1002%2Fart.41939&file=art.41939-sup-0001-Disclosureform.pdf.

Address correspondence to Kazuki Yoshida, MD, ScD, Division of Rheumatology, Inflammation, and Immunity, Brigham and Women's Hospital, 60 Fenwood Road, no. 6016Q, Boston, MA 02115 (email: kazukiyoshida@mail.harvard.edu); or to Jeffrey A. Sparks, MD, MMSc, Division of Rheumatology, Inflammation, and Immunity, Brigham and Women's Hospital, 60 Fenwood Road, no. 6016U, Boston, MA 02115 (email: jsparks@bwh.harvard.edu).

Submitted for publication April 7, 2021; accepted in revised form July 29, 2021.

by the presence of autoantibodies such as rheumatoid factor (RF) and anti–citrullinated protein antibodies (ACPAs), particularly among genetically predisposed individuals (4,8).

Personal (active) smoking is the most well-established environmental risk factor for the development of RA, as demonstrated in multiple epidemiologic studies (9–13). The potential link between passive smoking and incident RA is less established (14). This is partly due to the challenge of having a sufficiently large longitudinal database with adequately granular data to capture passive smoking and incident RA. Among the few existing cohort studies of passive smoking and RA risk are a birth cohort study of maternal smoking during pregnancy and childhood polyarthritis (15), an analysis of years living with smokers and adult incident RA in the Nurses' Health Study (NHS) (11), and a population registry–based study of childhood passive smoking and adult incident RA (16). No single study to date has provided a comprehensive view of the link between passive smoking over the life course (maternal smoking during pregnancy while in utero, childhood passive smoking, and adulthood passive smoking) and incident RA during adulthood.

Therefore, we aimed to examine the influence of passive smoking at several stages of the life course while accounting for personal smoking behavior using a framework from the life-course epidemiology literature (17). We analyzed the NHSII prospective cohort, which provided data on both passive smoking exposure spanning the participants' life course and confirmed diagnoses of adult incident RA with serostatus. We hypothesized that early-life passive smoking exposure would increase seropositive RA risk.

SUBJECTS AND METHODS

Participants and eligibility. We performed a cohort study based on the prospectively collected data in the NHSII. Briefly, the NHSII enrolled 116,429 female registered nurses ages 25–42 years in 1989. Since then, the prospective follow-up has continued every 2 years to date through mailed questionnaires, with >90% response rates. The questionnaires collect information on sociodemographic characteristics, anthropometrics, behaviors, medications, dietary intake, and health conditions. For the present study, we excluded those who self-reported prevalent RA or connective tissue diseases before the 1989 baseline questionnaire to focus on incident RA during follow-up. Subjects missing childhood parental smoking status or adulthood passive smoking information were excluded. The study protocol was approved by the institutional review board of Mass General Brigham.

Passive smoking exposure variables of interest. We examined 3 passive smoking exposures of interest: 1) maternal smoking during pregnancy as an in utero exposure, 2) parental smoking during childhood as a childhood exposure, and 3) adulthood passive smoking as an adulthood exposure. Information on all of these passive smoking variables was collected through additional smoking behavior questionnaire items in 1999, when women ranged in age from 35–52 years. Maternal smoking during pregnancy was then classified into 3 categories: yes, no, and missing/don't know. For childhood parental smoking, we compared any childhood parental smoking (either or both parents) versus no childhood parental smoking. Adulthood passive smoking was asked as years lived since age 18 with household smokers. In 1999, when the passive smoking questionnaire was administered, participants were ages 35–52 years old. We categorized the adulthood passive smoking exposure levels as 0 years, 1–19 years, or ≥20 years.

Identification of incident RA outcome. Participants who self-reported a new physician diagnosis of RA in the main NHSII questionnaires received a validated follow-up questionnaire for connective tissue disease screening (18). For participants who screened positive, medical records were requested and independently reviewed by 2 physicians to confirm the RA diagnosis and date of clinical onset based on the American College of Rheumatology (ACR) 1987 classification criteria (19) or the ACR/European Alliance of Associations for Rheumatology 2010 classification criteria (20). RA cases were further classified as seropositive (positivity for RF and/or ACPA, if available) or seronegative based on the results of clinical testing found in the medical record. RA cases were identified using all questionnaire cycles up to and including the 2017 questionnaire cycle.

Accounting for personal (active) smoking exposure in the life-course analysis framework. Our interest was in the *direct* influence of passive smoking on incident RA. Thus, we needed to adequately control for personal smoking exposure. Additionally, since personal smoking behaviors temporally occur *after* earlier-life passive smoking exposure, personal smoking may serve as a "mediator". That is, the earlier-life experience of passive smoking might have influenced the uptake of later-life personal smoking, as suggested by previous studies (21–23). Such increased uptake of personal smoking due to earlier-life experience could then affect the risk of adult incident RA (Supplementary Figure 1, available on the *Arthritis & Rheumatology* website at http://onlinelibrary.wiley.com/doi/10.1002/art.41939/abstract).

In the life-course analysis framework for early-life exposure that may influence later-life exposure as well as adulthood health outcomes, several types of hypotheses can be formed (17). On one extreme is the "social trajectory" model, which hypothesizes that early-life passive smoking is important *only* in that it promotes later-life uptake of personal smoking, and it does not cause harm by itself. The other extreme is the "cumulative exposure" model, in which passive and active cigarette smoke inhalation increases the risk of RA by cumulative dose response. The distinction can be made if we examine the "direct effect" of early-life passive smoking, controlling for later personal smoking. If such an association is observed, early-life passive smoking is demonstrated not to follow the pure "social trajectory" model. Additionally, if the early life is a particularly heightened risk period regarding smoking's link

to later-life incident RA, the direct effect may be observed even when adulthood personal smoking is absent.

We conceptualized our direct effect of interest as the "controlled direct effect" in the causal inference literature (24,25). A controlled direct effect of earlier-life passive smoking is the direct impact of earlier-life passive smoking when everybody is hypothetically forced to follow the same later-life personal smoking pattern (e.g., everybody is forced to remain never personal smokers or everybody is forced to take up personal smoking). Since everybody is controlled to have the same later-life personal smoking pattern, the direct effect of earlier-life passive smoking is isolated.

Covariates. Variables that may affect passive and/or personal smoking exposure and incident RA risks are considered confounders. A variable that lies temporally prior to a smoking exposure can be a confounder but not a mediator. However, because smoking exposures span the life course, the same covariate may be temporally ordered after an earlier smoking exposure (potential mediator), but temporally ordered before a later smoking exposure (potential confounder). Thus, from the larger set of covariates, we defined a timeline ordering the passive smoking exposures of interest, personal smoking, and additional covariates related to RA risk (Figure 1). For example, personal smoking during late adolescence could be considered a mediator occurring after the in utero smoking exposure, but be considered a confounder for the adulthood passive smoking exposure.

For the in utero passive smoking exposure of maternal smoking during pregnancy, we considered the participant's race and ethnicity, maternal and paternal education level, maternal and paternal occupation, home ownership, US state of birth, and family history of RA as confounders. For the childhood parental smoking exposure, we additionally considered preterm birth status, birth weight, breastfeeding status, and maternal smoking during pregnancy as confounders. For the adulthood passive smoking exposure, we additionally accounted for age at menarche, body mass index (BMI) at age 18, childhood parental smoking, personal smoking by age 19, and time-varying covariates up until 1999 (ascertainment of adulthood passive smoking) as confounders. Earlier exposures were considered confounders with respect to later exposures since they could be associated with later exposure and incident RA.

We additionally incorporated time-varying covariates measured during the NHSII cohort follow-up beginning in 1989, such as menopausal status and postmenopausal hormone use. Participants' personal parity and breastfeeding were self-reported. BMI was calculated as self-reported weight in kilograms/height in meters squared. Weekly hours of moderate-to-vigorous physical activity were calculated from a validated survey (26,27). Using the food-frequency questionnaires (28), we calculated the Alternate Healthy Eating Index (29,30). US residence regions were classified

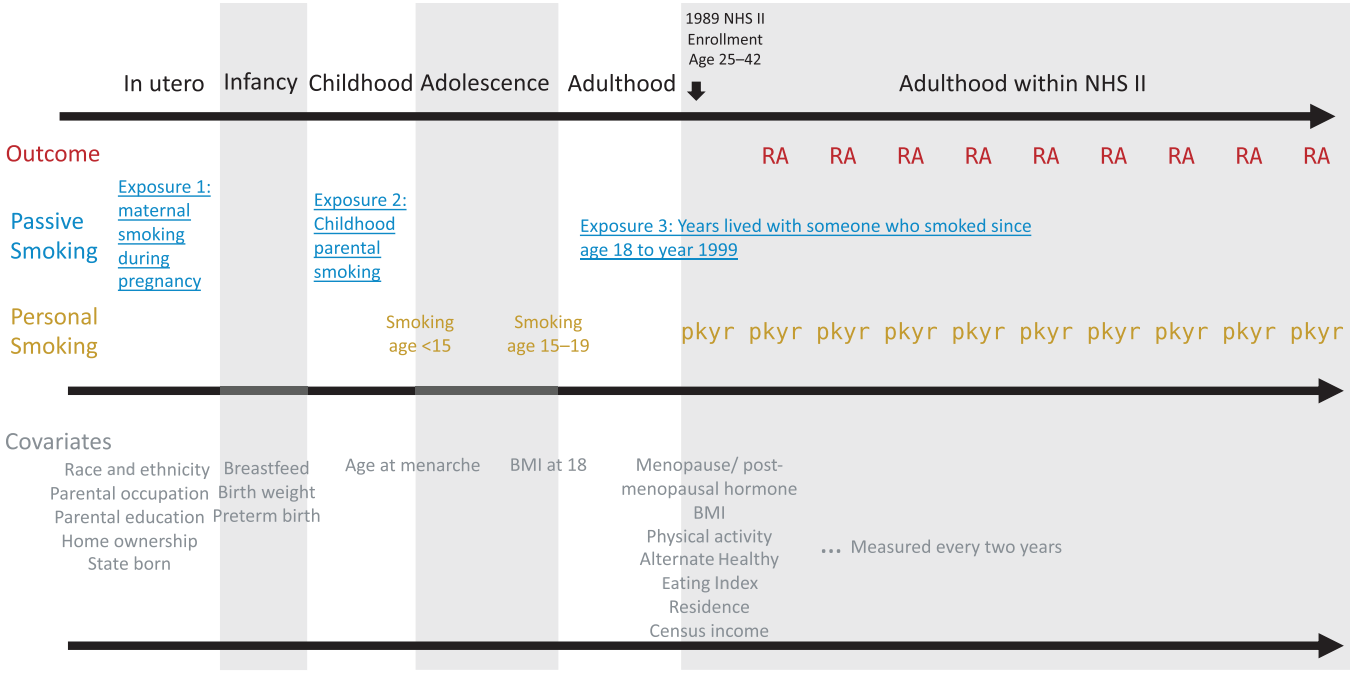

Figure 1. Time line of passive and personal smoking variables and covariates in the Nurses' Health Study II (NHSII). Exposures of interest were passive smoking exposures spanning the participants' life course: 1) maternal smoking during pregnancy (in utero passive smoking), 2) childhood parental smoking (childhood passive smoking), and 3) years lived with smokers from age 18 to 1999 (ages 35–52 years; adulthood passive smoking). In assessing the influence of passive smoking exposures on the development of rheumatoid arthritis (RA), we accounted for personal (active) smoking variables, including childhood and adolescent personal smoking and adulthood personal smoking in pack-years (pkyr). Covariates incorporated into the analyses are shown at the bottom of the figure. BMI = body mass index.

as New England, Mid-Atlantic, Midwest, South, and West based on zip code. Median household income was derived from the participant's address and US Census tract-level data by zip code.

Statistical analysis and modeling strategies. Participant characteristics at baseline, stratified by the categories in each of the 3 passive smoking exposure variables, are summarized as the mean ± SD or proportion as appropriate.

We employed several regression approaches to examine the total effect of passive smoking regardless of adulthood personal smoking and the direct effect of passive smoking accounting for adulthood personal smoking. We considered 3 separate outcomes in each analysis: all RA, seropositive RA, and seronegative RA.

First, we fit the base model using Cox proportional hazards models accounting only for the age and questionnaire cycle (calendar time). Second, we fit the confounder-adjusted models using the aforementioned passive smoking exposure–specific set of covariates that were deemed to be temporally preceding the exposure using Cox proportional hazards models. Third, we accounted for the personal smoking variables in 2 ways: using the conventional time-varying regression model (model A), and using the inverse probability–weighted controlled direct effect model (a type of marginal structural model [31]) (model B). Model B is considered less biased and is preferred for estimating the controlled direct effect, although it tends to yield a wider confidence interval. Both model A and model B adjusted for the personal smoking variables, but they accounted for the time-varying confounders of personal smoking variables differently. In model A, time-varying covariates were also included in the regression model as further adjustment variables. Model A tends to yield a more precise confidence interval, but it can result in an estimate biased toward null due to overadjustment. We fit model A with the pooled logistic

Table 1. Childhood and baseline adulthood characteristics of women in the Nurses' Health Study II (n = 90,923), according to childhood parental smoking*

	Overall (n = 90,923)	No childhood parental smoking (n = 32,064)	Any childhood parental smoking (n = 58,859)
Adulthood variables at baseline in 1989			
Age, mean ± SD years	34.47 ± 4.66	33.95 ± 4.71	34.76 ± 4.60
White race, %	92.98	91.85	93.57
Household income, %			
Quartile 1 (lowest income)	21.09	21.30	20.98
Quartile 2	34.61	35.13	34.34
Quartile 3	21.95	21.88	22.00
Quartile 4 (highest income)	22.34	21.69	22.68
BMI, mean ± SD kg/m^2	24.01 ± 4.99	23.57 ± 4.69	24.25 ± 5.12
Physical activity, %†			
<3 METs/week	14.73	14.59	14.81
≥3 METs/week	85.27	85.41	85.19
Menopausal status and PMH use, %			
Premenopausal	97.81	98.20	97.61
Postmenopausal and never used PMH	0.10	0.09	0.11
Postmenopausal and any PMH use	2.09	1.71	2.28
Smoking status, %			
Never smoker	65.88	73.67	61.65
Past smoker	21.64	18.25	23.48
Current smoker	12.47	8.08	14.87
Pack-years among ever smokers, mean ± SD	11.30 ± 8.14	9.6 ± 7.56	11.88 ± 8.2
Childhood variables			
Mother's occupation, %			
Professional	9.62	10.29	9.24
Other	70.98	71.05	70.97
Missing	19.40	18.67	19.79
Father's occupation, %			
Professional	23.08	25.83	21.55
Other	57.16	55.15	58.28
Missing	19.75	19.02	20.16
Maternal smoking during pregnancy, %			
No	64.98	94.56	48.84
Yes	24.87	1.39	37.78
Don't know/missing	10.15	4.05	13.38

* See Supplementary Table 2, available on the *Arthritis & Rheumatology* website at http://onlinelibrary.wiley.com/doi/10.1002/art.41939/abstract, for a complete list of variables. BMI = body mass index; METs = metabolic equivalents; PMH = postmenopausal hormone use.
† Data were missing for <1% of subjects.

regression approach to ensure comparability to model B. This approach approximates Cox regression with a rare outcome such as incident RA. The adulthood pack-year variable was incorporated as a 4-level ordinal time-varying covariate (0 pack-years, >0 to 10 pack-years, >10 to 20 pack-years, or >20 pack-years).

In model B, these time-varying covariates were handled through stabilized inverse probability weights (32), which aimed to eliminate their confounding upon the subsequent personal smoking variables while allowing for their mediating roles with respect to preceding passive smoking variables. We constructed stabilized inverse probability weights for each smoking variable using a weight denominator model, which included all covariates preceding the smoking variable (including those prior to birth), and a weight numerator model, which included only the covariates prior to birth. Both weight models were used to predict the probability of the smoking variable as actually observed. Adulthood personal smoking during the cohort follow-up was modeled as a pack-year ordinal variable (0 pack-years, >0 to 10 pack-years, >10 to 20 pack-years, or >20 pack-years) in ordinal logistic regression models. The final stabilized inverse probability weights were constructed as the cumulative product of the stabilized inverse probability weights over time. To avoid extreme weights, we conducted "weight truncation" at the 1st and 99th percentiles (32). We fit a weighted pooled logistic regression for the incident RA outcome using the generalized estimating equation procedure.

For both models A and B, we also conducted analyses stratified by the personal smoking status (lifelong never smoker stratum versus any personal smoking stratum) for passive smoking exposures that demonstrated associations with the incident RA outcome in the overall unstratified analyses. For the adulthood passive smoking exposure, we additionally conducted a sensitivity analysis excluding participants who were younger than 28 years in 1989, since they could not have been in the ≥20 years category. Analyses were conducted in SAS version 9.4 (33). We provided point estimates and their 95% confidence intervals (95% CIs).

RESULTS

Participants and descriptive analyses. Our analysis sample included 90,923 participants. Table 1 shows adulthood (1989 baseline questionnaire) and childhood characteristics of the participants according to childhood parental smoking. The mean ± SD age at baseline was 34.5 ± 4.7 years. The characteristics were mostly similar between those reporting no childhood parental smoking and those exposed to any childhood parental smoking. Smoking-related variables did exhibit some differences. Personal smoking at baseline was higher among those reporting any childhood parental smoking (38% were current or past smokers versus 26% of those with no childhood parental smoking). Maternal smoking during pregnancy was reported for 38% of those who reported any childhood parental smoking but only 1.4% of those who reported no childhood parental smoking. See Supplementary Tables 1–3, available on the *Arthritis & Rheumatology* website at http://

Table 2. Hazard ratios for incident RA, overall and by serologic phenotype, among women in the Nurses' Health Study II (n = 90,923), according to maternal smoking during pregnancy (in utero exposure)*

	No. of RA cases/ no. of person-years	Base model†	Confounders‡	Adulthood personal smoking and covariates (conventional model)§	Controlled direct effect model¶
All RA					
No maternal smoking	325/1,524,879	1.00 (referent)	1.00 (referent)	1.00 (referent)	1.00 (referent)
Maternal smoking	153/578,896	1.23 (1.02–1.49)#	1.25 (1.03–1.52)#	1.14 (0.92–1.41)	1.10 (0.76–1.57)
Don't know/missing	54/236,559	1.03 (0.77–1.37)	1.04 (0.78–1.39)	0.98 (0.73–1.32)	1.01 (0.64–1.58)
Seropositive RA					
No maternal smoking	209/1,523,144	1.00 (referent)	1.00 (referent)	1.00 (referent)	1.00 (referent)
Maternal smoking	104/578,180	1.31 (1.03–1.66)#	1.34 (1.06–1.70)#	1.12 (0.86–1.46)	1.04 (0.67–1.61)
Don't know/missing	39/236,345	1.16 (0.82–1.64)	1.21 (0.86–1.70)	1.07 (0.75–1.52)	1.01 (0.58–1.75)
Seronegative RA					
No maternal smoking	116/1,521,421	1.00 (referent)	1.00 (referent)	1.00 (referent)	1.00 (referent)
Maternal smoking	49/577,267	1.09 (0.78–1.53)	1.10 (0.78–1.53)	1.17 (0.79–1.72)	1.23 (0.65–2.32)
Don't know/missing	15/235,895	0.79 (0.46–1.35)	0.75 (0.44–1.30)	0.80 (0.46–1.39)	1.00 (0.47–2.14)

* Except where indicated otherwise, values are the hazard ratio (95% confidence interval).
† Adjusted for age and questionnaire cycle.
‡ Additionally adjusted for race and ethnicity, maternal and paternal education, maternal and paternal occupations, home ownership, US state of birth, and family history of rheumatoid arthritis (RA; temporally preceding confounders for the maternal smoking during pregnancy exposure).
§ Additionally adjusted for adulthood personal smoking pack-years, childhood parental smoking, adulthood passive smoking (years lived with a smoker since age 18), and temporally preceding covariates (birth weight, preterm birth, breastfeeding, age at menarche, body mass index [BMI] at age 18, menopausal status and hormone use, parity/breastfeeding, BMI, physical activity [≥3 metabolic equivalents], Alternate Healthy Eating Index, residence, and census income).
¶ Controlling for adulthood personal smoking pack-years, childhood parental smoking, adulthood passive smoking (years lived with a smoker since age 18) via conditioning and inverse probability weighting using temporally preceding covariates (birth weight, preterm birth, breastfeeding, age at menarche, BMI at age 18, menopausal status and hormone use, parity/breastfeeding, BMI, physical activity [≥3 metabolic equivalents], Alternate Healthy Eating Index, residence, and census income).
# $P < 0.05$.

Table 3. Hazard ratios for incident RA, overall and by serologic phenotype, among women in the Nurses' Health Study II (n = 90,923), according to childhood parental smoking*

	No. of RA cases/ no. of person-years	Base model†	Confounders‡	Adulthood personal smoking and covariates (conventional model)§	Controlled direct effect model¶
All RA					
No parent smoked	160/829,934	1.00 (referent)	1.00 (referent)	1.00 (referent)	1.00 (referent)
Any parent smoked	372/1,510,400	1.24 (1.03–1.49)#	1.18 (0.96–1.46)	1.11 (0.90–1.38)	1.27 (0.84–1.92)
Seropositive RA					
No parent smoked	95/829,037	1.00 (referent)	1.00 (referent)	1.00 (referent)	1.00 (referent)
Any parent smoked	257/1,508,631	1.46 (1.15–1.84)#	1.41 (1.08–1.83)#	1.30 (0.99–1.70)	1.75 (1.03–2.98)#
Seronegative RA					
No parent smoked	65/828,417	1.00 (referent)	1.00 (referent)	1.00 (referent)	1.00 (referent)
Any parent smoked	115/1,506,166	0.93 (0.68–1.26)	0.86 (0.60–1.22)	0.85 (0.60–1.21)	0.77 (0.40–1.45)

* Except where indicated otherwise, values are the hazard ratio (95% confidence interval).
† Adjusted for age and questionnaire cycle.
‡ Additionally adjusted for race and ethnicity, maternal and paternal education, maternal and paternal occupations, home ownership, US state of birth, family history of rheumatoid arthritis (RA), birth weight, preterm birth, breastfeeding, and maternal smoking during pregnancy (temporally preceding confounders for the childhood parental smoking exposure).
§ Additionally adjusted for adulthood personal smoking pack-years and adulthood passive smoking (years lived with a smoker since age 18) and temporally preceding covariates (birth weight, preterm birth, breastfeeding, age at menarche, body mass index [BMI] at age 18, menopausal status and hormone use, parity/breastfeeding, BMI, physical activity [≥3 metabolic equivalents], Alternate Healthy Eating Index, residence, and census income).
¶ Controlling for adulthood personal smoking pack-years and adulthood passive smoking (years lived with a smoker since age 18) via conditioning and inverse probability weighting using temporally preceding covariates (birth weight, preterm birth, breastfeeding, age at menarche, BMI at age 18, menopausal status and hormone use, parity/breastfeeding, BMI, physical activity [≥3 metabolic equivalents], Alternate Healthy Eating Index, residence, and census income).
# $P < 0.05$.

onlinelibrary.wiley.com/doi/10.1002/art.41939/abstract, for a full listing of characteristics stratified by each passive smoking exposure. During a median of 27.7 years of follow-up since 1989, there were a total of 532 confirmed incident RA cases. Of these, 352 incident RA cases were determined to be seropositive, whereas the remaining 180 were seronegative.

Maternal smoking during pregnancy (in utero exposure) (exposure 1). Table 2 presents the results for maternal smoking during pregnancy. This exposure was associated with all incident RA after adjustment for temporally preceding confounder variables (hazard ratio [HR] 1.25 [95% CI 1.03–1.52]). The HR was slightly higher for seropositive incident RA (HR 1.34 [95%

Table 4. Hazard ratios for incident RA, overall and by serologic phenotype, among women in the Nurses' Health Study II (n = 90,923), according to childhood parental smoking stratified by adulthood personal smoking status*

	Lifelong never personal smokers (n = 58,707)†			Ever personal smokers (n = 32,216)‡		
	No. of RA cases/no. of person-years	Adulthood covariates (conventional model)§	Controlled direct effect model¶	No. of RA cases/no. of person-years	Adulthood personal smoking and covariates (conventional model)§	Controlled direct effect model¶
All RA						
No parent smoked	115/604,161	1.00 (referent)	1.00 (referent)	45/225,773	1.00 (referent)	1.00 (referent)
Any parent smoked	188/915,414	0.99 (0.75–1.31)	0.84 (0.41–1.70)	184/594,986	1.35 (0.94–1.92)	1.43 (0.89–2.32)
Seropositive RA						
No parent smoked	67/603,473	1.00 (referent)	1.00 (referent)	28/225,565	1.00 (referent)	1.00 (referent)
Any parent smoked	128/914,492	1.15 (0.81–1.65)	0.90 (0.31–2.61)	129/594,139	1.55 (0.99–2.43)	2.18 (1.23–3.88)#
Seronegative RA						
No parent smoked	48/603,055	1.00 (referent)	1.00 (referent)	17/225,362	1.00 (referent)	1.00 (referent)
Any parent smoked	60/913,236	0.76 (0.48–1.21)	0.79 (0.43–1.45)	55/592,930	1.02 (0.56–1.84)	0.74 (0.33–1.66)

* Except where indicated otherwise, values are the hazard ratio (95% confidence interval).
† No adjustment for the level of personal smoking was required since it uniformly remained 0.
‡ Further adjustment for the level of adolescent and adulthood personal smoking was conducted.
§ Adjusted for age, questionnaire cycle, race and ethnicity, maternal and paternal education, maternal and paternal occupations, home ownership, US state of birth, family history of rheumatoid arthritis (RA), birth weight, preterm birth, breastfeeding, maternal smoking during pregnancy, adulthood personal smoking pack-years (only among adulthood personal smokers), adulthood passive smoking (years lived with a smoker since age 18), and temporally preceding covariates (menopausal status and hormone use, parity/breastfeeding, body mass index, physical activity [≥3 metabolic equivalents], Alternate Healthy Eating Index, residence, and census income).
¶ Controlling for adulthood personal smoking and adulthood passive smoking (years lived with a smoker since age 18) via conditioning and inverse probability weighting using the same covariates listed above for the conventional model.
# $P < 0.05$.

CI 1.06–1.70]). Accounting for later-life personal smoking further reduced the point estimates toward null in all incident RA and in seropositive incident RA. Estimates were similarly unremarkable for the seronegative incident RA analyses. These direct effect estimates were similar across the conventional approach (more precise) and the controlled direct effect approach (considered less biased and preferred).

Childhood parental smoking (exposure 2). Table 3 presents the results for childhood parental smoking. This exposure was associated with seropositive incident RA after adjustment for temporally preceding confounder variables (HR 1.41 [95% CI 1.08–1.83]). There was no association for all RA (1.18 [95% CI 0.96–1.46]). Accounting for later-life personal smoking by the conventional approach resulted in an HR of 1.30 for seropositive incident RA (95% CI 0.99–1.70). In contrast, the controlled direct effect analysis indicated a potential direct influence (HR 1.75 [95% CI 1.03–2.98]). Both approaches gave similar nonsignificant results for seronegative incident RA.

We further conducted analyses stratified by adulthood personal smoking status: lifelong never personal smokers (n = 58,707) and ever personal smoking at any time (n = 32,216). We conducted both the conventional and controlled direct effect analyses in these 2 strata (Table 4). Increased risk of incident RA was not detected among the lifelong never personal smokers. In contrast, controlled direct effect analysis indicated a significantly increased risk of seropositive incident RA among the adulthood personal smokers (2.18 [95% CI 1.23–3.88]), also controlling for smoking pack-years. Results of the corresponding conventional analyses were not significant.

Adulthood passive smoking (exposure 3). Table 5 presents the results for adulthood passive smoking, defined as years lived with household smokers from age 18 through 1999 (ages 35–52 years). This exposure at the level of 1–19 years had no association with all RA or seropositive RA after adjustment for temporally preceding confounder variables. At the level of ≥20 years, the point estimates were increased but were not significant. Accounting for later-life personal smoking using the conventional approach and the controlled direct effect model gave null results for both exposure levels. A sensitivity analysis that included only participants who were ≥28 years old in 1989 (n = 83,336) yielded similar results (Supplementary Table 4, available on the *Arthritis & Rheumatology* website at http://onlinelibrary.wiley.com/doi/10.1002/art.41939/abstract).

DISCUSSION

In this large cohort study of women, we found that passive smoking exposure during childhood was associated with adult-onset seropositive RA, suggesting a direct influence of early-life exposures on RA risk. We performed our study using a statistical

Table 5. Hazard ratios for incident RA, overall and by serologic phenotype, among women in the Nurses' Health Study II (n = 90,923), according to years lived with a smoker since age 18*

No. of years lived with a smoker	No. of RA cases/ no. of person-years	Base model†	Confounders‡	Adulthood personal smoking and covariates (conventional model)§	Controlled direct effect model¶
All RA					
None	267/1,314,937	1.00 (referent)	1.00 (referent)	1.00 (referent)	1.00 (referent)
1–19 years	194/821,678	1.12 (0.93–1.35)	1.00 (0.82–1.23)	0.92 (0.75–1.13)	1.00 (0.69, 1.44)
≥20 years	71/203,719	1.59 (1.22–2.08)#	1.30 (0.97–1.74)	0.99 (0.73–1.35)	1.26 (0.73–2.17)
P for trend	–	<0.001	0.10	0.91	0.40
Seropositive RA					
None	169/1,313,506	1.00 (referent)	1.00 (referent)	1.00 (referent)	1.00 (referent)
1–19 years	136/820,861	1.26 (1.00–1.58)#	1.07 (0.84–1.37)	1.00 (0.78–1.28)	1.15 (0.76–1.75)
≥20 years	47/203,301	1.74 (1.25–2.42)#	1.34 (0.94–1.93)	1.05 (0.72–1.53)	1.62 (0.84–3.15)
P for trend	–	<0.001	0.11	0.82	0.15
Seronegative RA					
None	98/1,312,174	1.00 (referent)	1.00 (referent)	1.00 (referent)	1.00 (referent)
1–19 years	58/819,399	0.89 (0.65–1.24)	0.87 (0.61–1.24)	0.79 (0.54–1.14)	0.77 (0.38–1.57)
≥20 years	24/203,011	1.36 (0.86–2.14)	1.24 (0.76–2.05)	0.89 (0.52–1.54)	0.79 (0.31–1.98)
P for trend	–	0.32	0.50	0.61	0.61

* Except where indicated otherwise, values are the hazard ratio (95% confidence interval).
† Adjusted for age and questionnaire cycle.
‡ Additionally adjusted for race and ethnicity, maternal and paternal education, maternal and paternal occupations, home ownership, US state of birth, family history of rheumatoid arthritis (RA), birth weight, preterm birth, breastfeeding, maternal smoking during pregnancy, childhood parental smoking, age at menarche, body mass index (BMI) at age 18, personal smoking by age 19, and adulthood covariates during the Nurses' Health Study II follow-up (menopause and hormone use, parity/breastfeeding, BMI, physical activity [≥3 metabolic equivalents], Alternative Healthy Eating Index, residence, and census income; all updated until 1999).
§ Additionally adjusted for adulthood personal smoking pack-years and temporally preceding covariates during the Nurses' Health Study II follow-up (fully time-updated).
¶ Controlling for adulthood personal smoking via conditioning and inverse probability weighting using the covariates listed above for the model including confounders and the conventional model.
# $P < 0.05$.

framework that accounted for the complex confounding or mediating effects of variables that occur throughout the life course. To our knowledge, ours is the first study to comprehensively apply the life-course epidemiology framework (17,25,31) to examine RA risk using a large prospective cohort with repeated measures of exposures and covariates, and lengthy follow-up. Our findings suggest that early-life inhaled exposures such as passive cigarette smoking could predispose individuals to develop RA not explained by later personal smoking behaviors. These results add to the mucosal paradigm of RA pathogenesis (5–7), where inhalants in pulmonary mucosa may trigger biologic processes that contribute to RA-related autoantibody production years before clinical RA symptoms emerge.

Personal smoking is one of the most well-established modifiable risk factors for incident RA, whereas the influence of passive smoking is less well understood (14). In a prospective cohort study utilizing the Finish Medical Birth Registry, Jaakkola and Gissler (15) examined the association of maternal smoking during pregnancy with incident RA and other polyarthritis, defined as health care utilization with relevant International Classification of Diseases, Ninth Revision codes during the first 7 years of life. They found an elevated odds ratio of developing disease (2.10 [95% CI 1.30–3.40]) for those exposed to maternal smoking during pregnancy. There was no consideration of childhood parental smoking, which could be another major source of passive smoking.

Although we did examine maternal smoking during pregnancy as one of the exposures of interest in the present study, a direct comparison to the study by Jaakkola and Gissler is difficult, since our outcome was later-life incident RA, which does not overlap with the early-life incident RA outcome used in their study. In our analysis, maternal smoking during pregnancy as an in utero exposure was almost exclusively reported by those who reported childhood parental smoking. The lack of a clear association between maternal smoking and later-life incident RA, after accounting for childhood passive smoking and personal smoking, in our study may be partly due to the strong correlation of these 2 early-life passive smoking exposures. The fact that maternal smoking during pregnancy affects the fetus through placental transfer, and not through direct inhalation, may also explain some of the differences between this passive smoking exposure and the others.

In a past study utilizing the NHS prospective cohort, Costenbader et al (11) examined the association between years lived with smokers and adult all incident RA, adjusting for variables including personal smoking pack-years. They found suggestive results for both lifelong never smokers (HR 1.46 [95% CI 0.92–2.32] for ≥30 years lived with smokers) and ever adult smokers (HR 1.59 [95% CI 0.92–2.74] for ≥30 years lived with smokers). Childhood parental smoking was not associated with incident RA using conventional analysis in that study, since personal smoking was the exposure of interest.

Since the study by Costenbader et al utilized the older NHS cohort (ages 30–55 years in 1976; ages 36–61 years at passive smoking assessment in 1982), childhood parental smoking exposure in that study occurred in the 1930s–1950s, which was different from the life experience of the more contemporary NHSII cohort, whose childhood parental smoking exposure occurred in the 1960s–1970s, when the negative health effects of smoking were more widely accepted. Such societal change may explain the difference in results between the 2 cohorts. Also, our study had a shorter possible duration of years lived with a smoker due to the earlier age at assessment of this exposure (ages 35–52 years). For the exposure "years lived with a smoker" (≥20 years category), we did find elevated point estimates in the controlled direct effect analyses (1.26 [95% CI 0.73–2.17] for all RA and 1.62 [95% CI 0.84–3.15] for seropositive RA), although they did not reach statistical significance.

Another more recently published prospective cohort study utilized the French E3N cohort, a general population cohort of 98,995 French women convened in 1990 (age range at baseline 40–65 years) (16). Seror et al examined the association of childhood and adulthood passive smoking exposures with RA, defined by self-report (collected in 2008, 2011, and 2014) with billing code confirmation. To account for adulthood personal smoking, they stratified the analyses into lifelong never smokers and ever smokers. Compared to the reference group of no passive or personal smoking exposure, the lifelong never smoker with childhood passive smoking exposure had an HR of 1.43 [95% CI 0.97–2.11]. The ever-smoker with childhood passive smoking exposure had an HR of 1.67 [95% CI 1.17–2.39], whereas the ever-smoker without childhood passive smoking exposure had an HR of 1.38 [95% CI 1.10–1.74]. Within the ever-smoker stratum, the comparison of childhood passive smoking exposure versus none should yield an HR of 1.67/1.38 = 1.21.

Similar to our results, adulthood passive smoking was not associated with RA in the study by Seror et al (16). Their results are consistent with ours, in that childhood passive smoking exposure in conjunction with adulthood personal smoking were associated with the most evidently increased risk of RA, whereas the childhood passive smoking exposure alone was less clearly associated. Our study's contribution is clarifying that the association was significant only for seropositive RA, which we ascertained through detailed medical record review, in addition to the more formal evaluation through the controlled direct effect approach.

A case–control study from the Swedish Epidemiological Investigation of Rheumatoid Arthritis examined the association of passive smoking and RA (34) among only lifelong never smokers. The authors did not find a significant association. The distinction between childhood and adulthood passive smoking was not made clearly, although a distinction was made between passive smoking within or before 10 years of the diagnosis of RA. Our findings suggest little influence of adulthood passive smoking (from age 18 years up to ages 35–52 years) on RA risk when accounting

for preceding confounding factors. Another case–control study used the Mayo Clinic Biobank repository (Minnesota and Florida) to study the association between RA outcome and several exposures, including passive smoking (35). Although the association of passive smoking and incident RA was not evident, they found that the highest pack-years of passive smoking exposure may subject individuals to an elevated risk of incident RA. Our study adds to this literature by investigating more granular passive smoking information over participants' life course using repeated measures of variables collected from a prospective cohort and using causal inference methods.

The potential biologic effects underpinning the association between early-life passive smoking exposures and adult-onset RA deserve further study. One possibility could be that passive smoking results in epigenetic modifications as a "first-hit" in individuals genetically predisposed to develop RA, and that subsequent triggers, including personal smoking, influence loss of immune tolerance and the production of RA-related autoantibodies years before clinical RA symptoms develop. Our controlled direct effect analyses are particularly appropriate for examining this possibility, because it enabled us to examine the influence of early-life passive smoking while conceptually intervening on the later-life personal smoking status.

A hypothetical, perfectly designed observational cohort study investigating the direct influence of passive smoking on incident RA would enroll participants at conception and record passive and personal smoking status as well as other covariates in granular detail as they occurred during the entire childhood and adulthood of participants. No such study exists to date, and this is unlikely to happen in the future. Our study has several limitations compared to such hypothetical perfection. One is the adult cohort nature of the NHSII, which enrolled subjects at ages 25–42 years. Since our ability to ascertain incident RA was limited to the period after enrollment, we could not study early-life RA cases. This limitation is the case for all existing studies (11,16,34,35), except one (15), which did not study adult RA cases since this would have required very lengthy surveillance. Our window of observation does capture the age range in which adult incidence of RA progressively increases (36).

One limitation of our analysis of adulthood passive smoking exposure was the time point of exposure assessment at ages 35–52 years, since the NHSII only included these questions on a single questionnaire. Longer duration of passive smoking exposure could be associated with increased RA risk. Also, postexposure enrollment poses a potential for selection or recall bias; that is, earlier exposure could theoretically bias enrollment of exposed and unexposed individuals if the exposure affects early deaths and attitudes toward participation. Since deaths attributable to passive smoking before our enrollment are likely rare and the NHSII was not initiated to study smoking (but rather to study oral contraceptives), we consider such biased enrollment to be minimal.

The determination of RA serostatus was based on medical record review of routine care laboratory data. As such, we could not conduct an analysis that distinguished patients with RF-positive RA from patients with ACPA–positive RA among those with seropositive RA, since patients diagnosed as having RA prior to the 2000s did not have ACPA checked for clinical purposes. Therefore, it is unclear whether the association of passive smoking with seropositive RA may have been different if RF and ACPA serostatus were analyzed separately.

The major strength of the NHSII is in the detailed collection of data on adulthood personal smoking (pack-years of smoking collected every 2 years) as well as other known risk factors, such as diet and BMI. This enabled us to conduct the controlled direct effect analysis that accounted for such a rich set of time-varying variables in the inverse probability weight construction. The benefit of this analytical approach appeared in the childhood parental smoking analysis, where the conventional time-varying regression model produced borderline results, likely due to overadjustment by including mediators in the model, whereas the controlled direct effect approach depicted a clearer picture of the increased risk of incident RA associated with childhood parental smoking, controlling for adulthood smoking status and pack-years. However, the potential for residual confounding still exists in our observational study.

To summarize, we found an increased risk of medical record–confirmed incident seropositive RA associated with early-life passive smoking from childhood parental smoking when combined with adulthood personal smoking, even after controlling for adulthood smoking pack-years. Our observations are most compatible with the "cumulative exposure" model in life-course epidemiology, in which both childhood parental smoking and later-life personal smoking increase the risk of adult incident seropositive RA. In particular, childhood passive smoking may be a risk factor that further amplifies the influence of adulthood personal smoking.

ACKNOWLEDGMENTS

The authors thank the participants of the NHSII for their dedicated participation in this longitudinal study, as well as the NHS staff members at the Channing Division of Network Medicine (Department of Medicine, Brigham and Women's Hospital and Harvard Medical School) for their assistance.

AUTHOR CONTRIBUTIONS

All authors were involved in drafting the article or revising it critically for important intellectual content, and all authors approved the final version to be published. Dr. Yoshida had full access to all of the data in the study and takes responsibility for the integrity of the data and the accuracy of the data analysis.

Study conception and design. Yoshida, Prisco, Martin, Sparks.

Acquisition of data. Yoshida, Wang, Malspeis, Marchand, Lu, Prisco, Martin, Ford, Costenbader, Karlson, Sparks.

Analysis and interpretation of data. Yoshida, Wang, Malspeis, Marchand, Lu, Costenbader, Karlson, Sparks.

REFERENCES

1. Benn RT, Wood PH. Mortality in rheumatoid arthritics. Br J Prev Soc Med 1972;26:60.
2. Kirwan JR. Links between radiological change, disability, and pathology in rheumatoid arthritis [review]. J Rheumatol 2001;28: 881–6.
3. Yoshida K, Lin TC, Wei MY, Malspeis S, Chu SH, Camargo CA, et al. Accrual of multimorbidity after incident rheumatoid arthritis and matched comparators using a large prospective cohort with 30 years of follow-up [abstract]. Arthritis Rheumatol 2019;71 Suppl 10. URL: https://acrabstracts.org/abstract/accrual-of-multimorbidity-after-incident-rheumatoid-arthritis-and-matched-comparators-using-a-large-prospective-cohort-with-30-years-of-follow-up/.
4. Sparks JA, Costenbader KH. Genetics, environment, and gene-environment interactions in the development of systemic rheumatic diseases [review]. Rheum Dis Clin North Am 2014;40:637–57.
5. Demoruelle MK, Solomon JJ, Fischer A, Deane KD. The lung may play a role in the pathogenesis of rheumatoid arthritis. Int J Clin Rheumatol 2014;9:295–309.
6. Sparks JA, Karlson EW. The roles of cigarette smoking and the lung in the transitions between phases of preclinical rheumatoid arthritis [review]. Curr Rheumatol Rep 2016;18:15.
7. Demoruelle MK, Wilson TM, Deane KD. Lung inflammation in the pathogenesis of rheumatoid arthritis [review]. Immunol Rev 2020;294:124–32.
8. Sparks JA, Chen CY, Jiang X, Askling J, Hiraki LT, Malspeis S, et al. Improved performance of epidemiologic and genetic risk models for rheumatoid arthritis serologic phenotypes using family history. Ann Rheum Dis 2015;74:1522–9.
9. Voigt LF, Koepsell TD, Nelson JL, Dugowson CE, Daling JR. Smoking, obesity, alcohol consumption, and the risk of rheumatoid arthritis. Epidemiology 1994;5:525–32.
10. Criswell LA, Merlino LA, Cerhan JR, Mikuls TR, Mudano AS, Burma M, et al. Cigarette smoking and the risk of rheumatoid arthritis among postmenopausal women: results from the Iowa Women's Health Study. Am J Med 2002;112:465–71.
11. Costenbader KH, Feskanich D, Mandl LA, Karlson EW. Smoking intensity, duration, and cessation, and the risk of rheumatoid arthritis in women. Am J Med 2006;119:503–11.
12. Sugiyama D, Nishimura K, Tamaki K, Tsuji G, Nakazawa T, Morinobu A, et al. Impact of smoking as a risk factor for developing rheumatoid arthritis: a meta-analysis of observational studies [review]. Ann Rheum Dis 2010;69:70–81.
13. Di Giuseppe D, Discacciati A, Orsini N, Wolk A. Cigarette smoking and risk of rheumatoid arthritis: a dose-response meta-analysis. Arthritis Res Ther 2014;16:R61.
14. Prisco LC, Martin LW, Sparks JA. Inhalants other than personal cigarette smoking and risk for developing rheumatoid arthritis [review]. Curr Opin Rheumatol 2020;32:279–88.
15. Jaakkola JJ, Gissler M. Maternal smoking in pregnancy as a determinant of rheumatoid arthritis and other inflammatory polyarthropathies during the first 7 years of life. Int J Epidemiol 2005;34:664–71.
16. Seror R, Henry J, Gusto G, Aubin HJ, Boutron-Ruault MC, Mariette X. Passive smoking in childhood increases the risk of developing rheumatoid arthritis. Rheumatology (Oxford) 2019;58:1154–62.
17. Liu S, Jones RN, Glymour MM. Implications of lifecourse epidemiology for research on determinants of adult disease [review]. Public Health Rev 2010;32:489–11.

Arthritis & Rheumatology
Vol. 73, No. 12, December 2021, pp 2229–2239
DOI 10.1002/art.41885
© 2021, American College of Rheumatology

American College of Rheumatology
Empowering Rheumatology Professionals

Prediction of the Progression of Undifferentiated Arthritis to Rheumatoid Arthritis Using DNA Methylation Profiling

Carlos de la Calle-Fabregat,[1] Ellis Niemantsverdriet,[2] Juan D. Cañete,[3] Tianlu Li,[1] Annette H. M. van der Helm-van Mil,[2] Javier Rodríguez-Ubreva,[1] and Esteban Ballestar[1]

Objective. The term "undifferentiated arthritis (UA)" is used to refer to all cases of arthritis that do not fit a specific diagnosis. A significant percentage of UA patients progress to rheumatoid arthritis (RA), others to a different definite rheumatic disease, and the rest undergo spontaneous remission. Therapeutic intervention in patients with UA can delay or halt disease progression and its long-term consequences. It is therefore of inherent interest to identify those UA patients with a high probability of progressing to RA who would benefit from early appropriate therapy. This study was undertaken to investigate whether alterations in the DNA methylation profiles of immune cells may provide information on the genetically or environmentally determined status of patients and potentially discriminate between disease subtypes.

Methods. We performed DNA methylation profiling of a UA patient cohort, in which progression to RA occurred for a significant proportion of the patients.

Results. We found differential DNA methylation in UA patients compared to healthy controls. Most importantly, our analysis identified a DNA methylation signature characteristic of those UA cases that differentiated to RA. We demonstrated that the methylome of peripheral mononuclear cells can be used to anticipate the evolution of UA to RA, and that this methylome is associated with a number of inflammatory pathways and transcription factors. Finally, we designed a machine learning strategy for DNA methylation-based classification that predicts the differentiation of UA toward RA.

Conclusion. Our findings indicate that DNA methylation profiling provides a good predictor of UA-to-RA progression to anticipate targeted treatments and improve clinical management.

INTRODUCTION

Undifferentiated arthritis (UA) is a form of early arthritis that involves joint inflammation that cannot be classified as any definite rheumatic disorder (1). Eventually, ~30% of patients with UA will develop rheumatoid arthritis (RA) or other differentiated forms of arthritis, whereas 45–55% of patients will achieve spontaneous remission (1). UA represents a unique window of opportunity to intervene during the course of the disease before more severe manifestations become established.

The ability to provide early indicators for the treatment of UA patients at high risk of developing RA is of utmost relevance for decision making regarding whether and when to start treatment with disease-modifying antirheumatic drugs (DMARDs), which usually hamper RA progression but are not recommended for UA patients who achieve eventual remission (2). To that end, prediction rules have been proven to be crucial tools to provide guidance to clinicians by estimating patient outcome probabilities. In fact, a prediction rule for UA patients, based strictly on patient clinical data, has been developed previously (3). This model accurately

Supported by Centres de Recerca de Catalunya (CERCA) Institute-Generalitat de Catalunya and the Josep Carreras Foundation. Dr. Cañete's work was supported by the Institute of Health Carlos III (FIS grant PI17/00993). Dr. Ballestar's work was supported by the Spanish Ministry of Science and Innovation (grants SAF2017-88086-R and PID2020-117212RB-I00) and the FEDER. Drs. Cañete and Ballestar's work was supported by a RETICS network grant from the Institute of Health Carlos III (RIER grant RD16/0012/0013).

[1]Carlos de la Calle-Fabregat, MSc, Tianlu Li, PhD, Javier Rodríguez-Ubreva, PhD, Esteban Ballestar, PhD: Josep Carreras Leukaemia Research Institute, Barcelona, Spain; [2]Ellis Niemantsverdriet, PhD, Annette H. M. van der Helm-van Mil, MD, PhD: Leiden University Medical Center, Leiden, The Netherlands; [3]Juan D. Cañete, MD, PhD: Hospital Clínic de Barcelona and Institut d'Investigacions Biomèdiques August Pi i Sunyer, Barcelona, Spain.

No potential conflicts of interest relevant to this article were reported.

Address correspondence to Esteban Ballestar, PhD, Epigenetics and Immune Disease Group, Josep Carreras Research Institute (IJC), Ctra de Can Ruti, Camí de les Escoles s/n, 08916 Badalona, Barcelona, Spain. Email: eballestar@carrerasresearch.org.

Submitted for publication February 10, 2021; accepted in revised form May 27, 2021.

estimates the risk of developing RA in >75% of patients with UA. However, rules based on clinical data, although easy to implement in the clinical setting, usually fail to identify a detailed biologic basis for individual phenotypic presentations of the disease, and usually do not succeed in all predictions. In this regard, approaches including "-omics" data may provide compelling alternatives or complementary tools for both improving prediction accuracy and allowing an in-depth characterization of the molecular alterations in patients (4).

Epigenetic alterations are associated with both genetic and environmentally driven determinants, which can in turn characterize pathogenic phenotypes. Specifically, DNA methylation and histone modifications, which are altered in multiple pathologic contexts, are proposed to be both a causal factor (5) and a consequence of disease (6), as well as an intermediary for genetic susceptibility (7). In all cases, the exhaustive study of these alterations using high-throughput technologies allows a detailed description and identification of novel molecular pathways that undergo alterations in a pathogenic context. DNA methylation is one of the most stable and easily comparable epigenetic modifications, and thus stands out as an ideal candidate for biomarker discovery (8).

In the present study, we characterized the DNA methylome of patients with UA in comparison to healthy controls. We also analyzed the data using different patient classification criteria, which proved to have a pivotal effect on DNA methylation profiles. In addition, we obtained the DNA methylation profiles of UA patients with known diverging future phenotypes. Moreover, we analyzed the profiles of patients with definite RA and compared them to those of patients with UA. The identification and interpretation of these data stand out as a valuable resource to delve into the molecular alterations in UA patients. Finally, we propose the use of DNA methylation data as a candidate biomarker with the ability to improve clinical prediction rules by integrating molecular insights and clinical knowledge for the prediction of patient outcomes.

PATIENTS AND METHODS

Patient cohort. A total of 72 samples from patients with UA and 8 samples from patients with RA were obtained from the Leiden Early Arthritis Clinic (EAC) cohort, which has been described previously (9). Thirteen healthy donor samples were also obtained. Patient samples were collected at the first visit (baseline). Patients had not received prior treatment with DMARDs (including glucocorticoids and antimalarial agents) and were diagnosed according to the American College of Rheumatology (ACR) 1987 criteria for RA (10). Within the group of UA patients, 39 had developed RA, while 33 remained classified as having UA, 1 year after baseline. The study was approved by the medical ethical testing committee (METC) Leiden Den Haag Delft, with cohort METC number P11.210, and the board of the Bellvitge Hospital Ethical Committee (PR275/17). The demographic and clinical characteristics of the patients and healthy donors are summarized in Supplementary Tables 1 and 2, available on the *Arthritis & Rheumatology* website at http://onlinelibrary.wiley.com/doi/10.1002/art.41885/abstract. Data on additional patient samples from the Leiden EAC cohort (with other disease subtypes) are also included in Supplementary Table 1.

DNA methylation profiling, bioinformatics analysis, and machine learning methods. Infinium HumanMethylation450K BeadChip arrays (Illumina) were used for DNA methylation analysis in the discovery cohort. By the time of the analysis of the validation cohort, 450K microarrays had been commercially discontinued; therefore, Infinium HumanMethylation EPIC

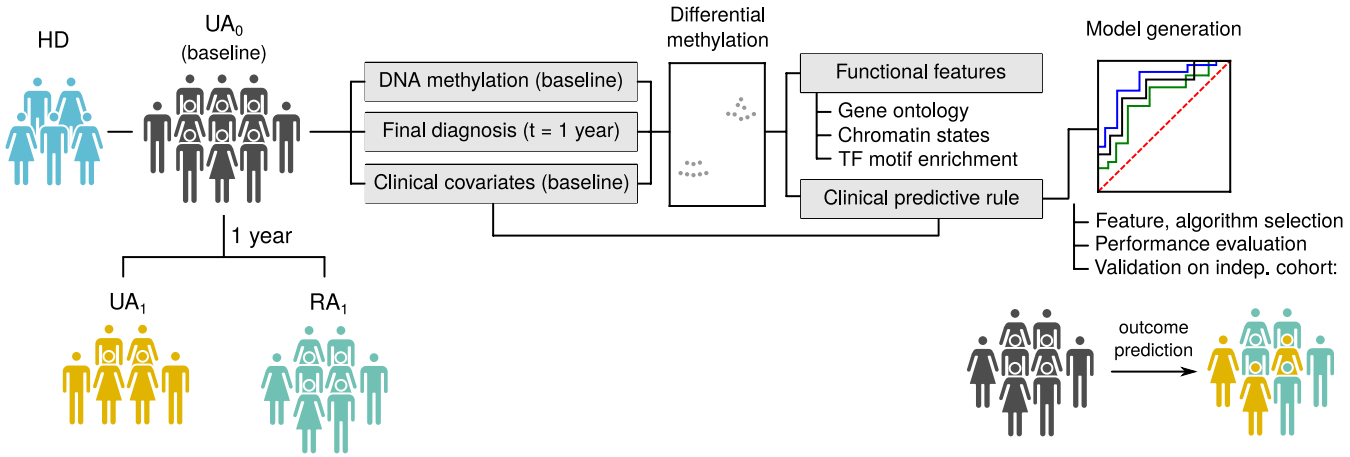

Figure 1. Flow chart of the study design, showing the conceptual and analytical workflow. Samples were obtained from healthy donors (HDs) and patients with undifferentiated arthritis at baseline (UA_0). One year after the initial visit, patients with UA at baseline were classified as continuing to have UA (UA_1) or as having developed rheumatoid arthritis (RA_1). DNA methylation profiles and clinical covariates were used to generate models to predict RA diagnosis. TF = transcription factor. Color figure can be viewed in the online issue, which is available at http://onlinelibrary.wiley.com/doi/10.1002/art.41885/abstract.

BeadChip arrays (Illumina) were used instead. Methylation array data have been deposited in the National Center for Biotechnology Information GEO database and are accessible through GEO series accession number GSE175364. Details on the bead array analysis, downstream bioinformatics methods, machine learning methods, and representation are provided in full in the Supplementary Methods, available on the *Arthritis & Rheumatology* website at http://onlinelibrary.wiley.com/doi/10.1002/art.41885/abstract.

RESULTS

Altered DNA methylome in inflammation-related genes in peripheral blood mononuclear cells (PBMCs) from patients with UA. First, we determined the DNA methylation profile of PBMCs obtained from patients in the Leiden Early Arthritis Clinic (EAC) cohort (as described in Patients and Methods). Patient demographic and clinical characteristics, including age, sex, anti–cyclic citrullinated peptide (anti-CCP) antibody status, rheumatoid factor (RF) status, and Disease Activity Score (DAS) (11) were also obtained (Supplementary Table 1). Samples from a total of 64 UA patients at the first visit (baseline), referred to as UA_0, and 13 healthy donors were analyzed. An illustrated flow chart of the study design is depicted in Figure 1. After data correction for age and sample balancing by sex and cell type proportions (Supplementary Methods and Supplementary Figure 1A, available on the *Arthritis & Rheumatology* website at http://onlinelibrary.wiley.com/doi/10.1002/art.41885/abstract), a comparison of UA_0 and healthy donor DNA methylation profiles revealed 321 hypermethylated and 3,029 hypomethylated CpG sites (Figure 2A). Of note, the differentially methylated positions (DMPs) identified did not vary significantly with regard to the different microarray chips (slide) or position within the chip (array; see Supplementary Figure 1D and the Supplementary Methods).

Gene ontology (GO) analysis of the DMPs revealed enrichment for multiple categories related to inflammatory response, immune cell activation, vitamin metabolism, and cytokine and chemokine signaling pathways in both the hypermethylated and hypomethylated clusters (Figure 2B). Among those, interleukin-1 (IL-1), IL-6, IL-12, IL-10, tumor necrosis factor (TNF), macrophage colony-stimulating factor, and chemokine CXCL2 signaling pathways were shown to be enriched within the affected regions. The hypomethylated regions were specifically enriched in categories related to antimicrobial response and type I interferon (IFN) production. Detailed examples of the methylation of CpG sites proximal to genes contained in the GO categories, showing B values in the healthy donor and UA_0 groups, are depicted in Figure 2C. Two examples of differentially methylated regions are shown in Supplementary Figure 1B. These genes were selected due to their previously reported direct involvement in rheumatic diseases and their underlying molecular pathways. For instance, we found differences between healthy donors and patients with UA at baseline (UA_0) in CpG sites located in cytokine and chemokine genes, such as *CXCR5*, *IL10*, *IL1R1*, and *IRAK2*; TNF signaling pathway genes, such as *LTA*, *TNFSF10*, and *TRAF4*; type I IFN–activated transcription factor IRF8; and others.

Analysis of transcription factor binding motifs revealed enrichment of motifs belonging to the RUNX transcription factor family in the hypermethylated cluster. Within the hypomethylated cluster, motifs of transcription factors in the basic leucine zipper and ETS families were predominantly enriched (Figure 2D).

Additionally, we performed a differentially variable position (DVP) analysis, which revealed a greater heterogeneity of DNA methylation within the UA_0 group (Figure 2E). Those DVPs exhibited <2% overlap with the previously identified DMPs, further suggesting the presence of intrinsic variance within the UA_0 group (Supplementary Figure 1C). Figure 2F depicts examples of 2 DVPs proximal to genes related to the previously identified GO categories. These data suggest the existence of an underlying epigenetic heterogeneity among UA patients, which might play a role in the diverse clinical presentation of the disease.

To ascertain the relationship between DNA methylation and genomic functional features, we calculated enrichment of the identified DMPs in 15 distinct chromatin states, defined by combinations of epigenetic modifications in PBMCs (12) (Figure 2G). DMPs in the hypermethylated cluster were enriched in regions containing gene coding sequences and transcription start sites (TSS), while hypomethylated DMPs were enriched in actively transcribed regions. Both clusters displayed an enrichment in enhancer regulatory regions, consistent with previously published studies focusing on the analysis of dynamic DNA methylation (13).

The methylome of UA patients anticipating subsequent evolution of the disease. The higher variability of methylation profiles among UA_0 samples compared to healthy individuals is consistent with the clinical heterogeneity in the UA_0 group. UA_0 was composed of 2 subgroups, one of patients who underwent subsequent differentiation to RA 1 year after the initial visit (designated as RA_1) and one of patients who remained classified as having UA 1 year after the initial visit (designated as UA_1) (Figure 1). In fact, slight clinical dissimilarities were found between these 2 groups (Supplementary Table 1). For instance, RA_1 patients had a higher frequency of seropositivity for rheumatoid factor (RF) (Figure 3A). The DAS (14) and some of the parameters included in its calculation, of note, the erythrocyte sedimentation rate and the number of swollen joints, were also higher in the RA_1 group (Figure 3B). However, technically, such differences do not allow the identification of those patients as having definite RA in the clinical setting. Therefore, we aimed to identify DNA methylation alterations that might help predict a future diagnosis in a prospective manner. In our analysis, we included the clinical features that were significantly different between the 2 groups (RF and DAS) as covariates, in order to identify methylation changes that were not due to the effect of those differences.

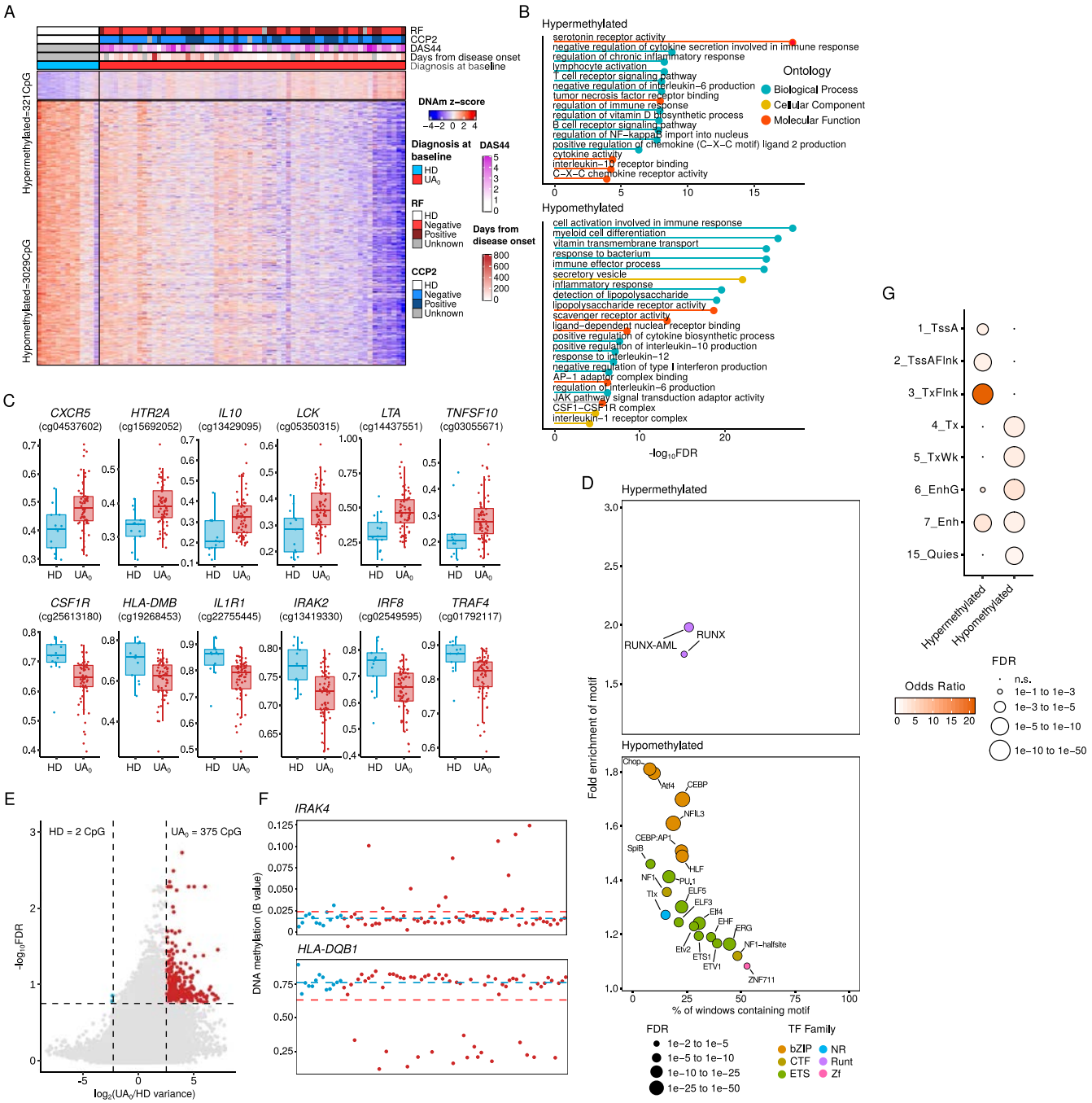

Figure 2. Characterization of the DNA methylation (DNAm) profiles of patients with undifferentiated arthritis at baseline (UA_0) compared to healthy donors (HDs). **A**, Heatmap showing differentially methylated positions (DMPs) between UA_0 and healthy donors (false discovery rate [FDR] < 0.05). Blue indicates lower methylation and red indicates higher methylation. RF = rheumatoid factor; CCP2 = anti–cyclic citrullinated peptide antibody; DAS44 = Disease Activity Score (44 joints assessed). **B**, Significant gene ontology (GO) categories in each cluster, selected by Genomic Regions Enrichment of Annotations Tool analysis of the DMPs identified. AP-1 = activator protein 1; CSF1 = colony-stimulating factor 1; CSF1R = CSF1 receptor. **C**, B values for selected significant CpG sites in the GO categories shown in **B**. Data are shown as box plots. Each box represents the 25th to 75th percentiles. Lines inside the boxes represent the median. Lines outside the boxes represent the 25th percentile minus 1.5 times the interquartile range (IQR) and the 75th percentile plus 1.5 times the IQR. Circles represent individual subjects. **D**, Significantly enriched motifs in DMPs from both clusters, analyzed by HOMER. TF = transcription factor; bZIP = basic leucine zipper; CTF = CCAAT box-binding transcription factor; NR = nuclear receptor; Zf = zinc finger domain. **E**, Variability plot depicting $\log_2$ ratio of variance (var_{UA0}:var_{HD}) for individual CpG sites by $\log_{10}$ FDR of the mean comparison *t*-test. Significant differentially variable position (DVPs) for both groups identified by the *iEVORA* package are shown in color. **F**, Two examples of DVPs, showing DNA methylation in individual healthy donors (blue) and patients with UA at baseline (red). Broken lines show the mean. **G**, Chromatin functional state enrichment in each cluster, based on public peripheral blood mononuclear cell data from the Roadmap Epigenomics Project (http://www.roadmapepigenomics.org/). TssA = active transcription start site; TssAFlnk = flanking active TSS; TxFlnk = transcript at gene 5′ and 3′; Tx = strong transcription; TxWk = weak transcription; EnhG = genic enhancers; Quies = quiescent; NS = not significant.

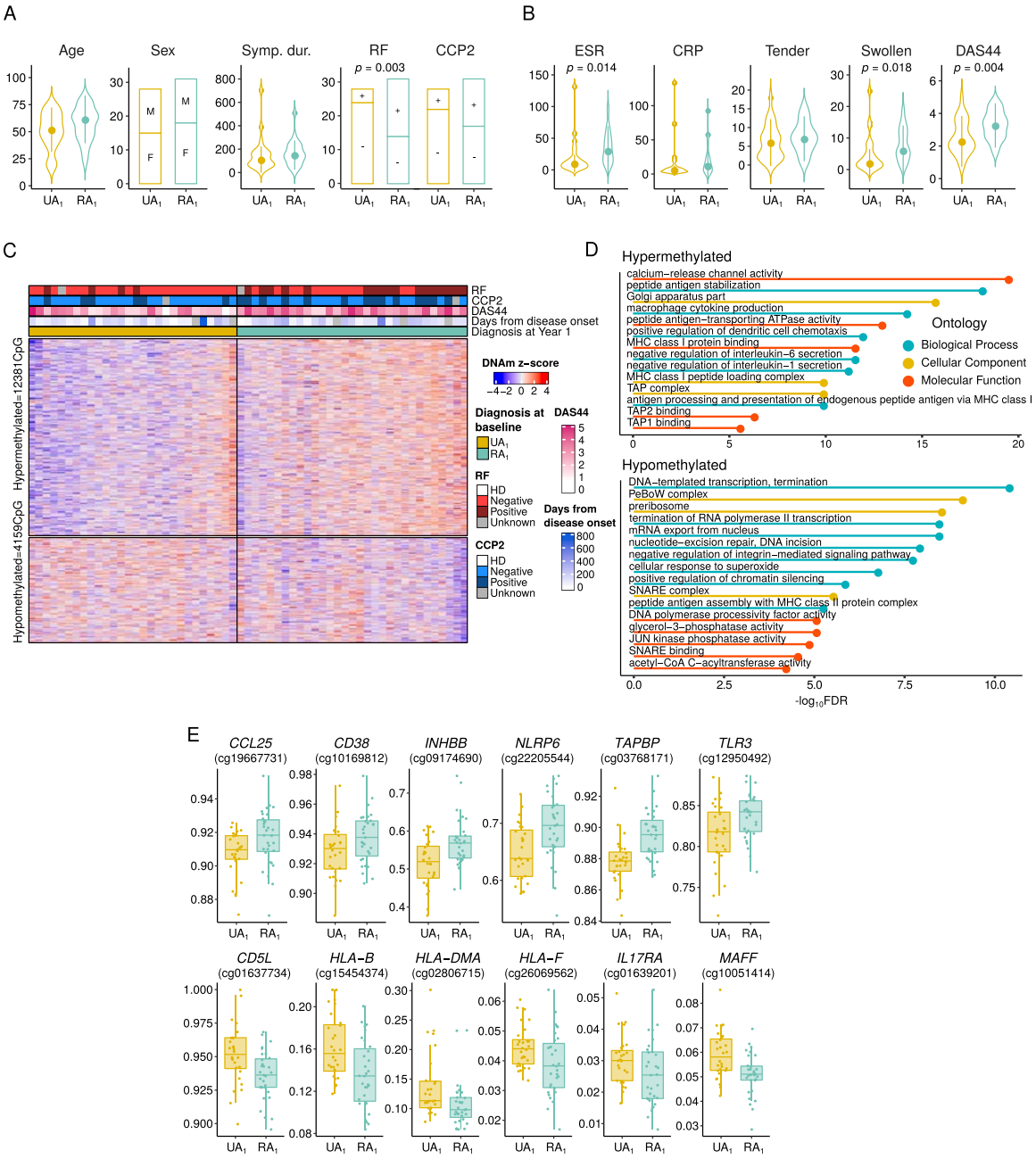

Figure 3. Characterization of the DNA methylation profiles of UA patients with diverging outcomes after 1 year. **A** and **B**, Demographic and clinical characteristics (**A**) and clinical variables included in the DAS (**B**) in patients with UA 1 year after baseline (UA_1) and patients with RA 1 year after baseline (RA_1). Violin plots show density curves; circles and vertical lines show the mean ± SD. Bars show the absolute number of patients. Significance was determined by Wilcoxon's test for numeric variables and by chi-square test for categorical variables. Symp. dur. = symptom duration in days; ESR = erythrocyte sedimentation rate; CRP = C-reactive protein. **C**, Heatmap showing DMPs between UA_1 and RA_1 ($P < 0.05$). Blue indicates lower methylation and red indicates higher methylation. **D**, Significant GO categories in each cluster, selected by Genomic Regions Enrichment of Annotations Tool analysis of the DMPs identified. MHC = major histocompatibility complex; TAP = transporter associated with antigen processing; SNARE = soluble N-ethylmaleimide–sensitive factor attachment protein receptor. **E**, B values for selected significant CpG sites in the GO categories shown in **D**. Data are shown as box plots. Each box represents the 25th to 75th percentiles. Lines inside the boxes represent the median. Lines outside the boxes represent the 25th percentile minus 1.5 times the IQR and the 75th percentile plus 1.5 times the IQR. Circles represent individual subjects. See Figure 2 for other definitions. Color figure can be viewed in the online issue, which is available at http://onlinelibrary.wiley.com/doi/10.1002/art.41885/abstract.

After verification of the similarity of cell type composition (Supplementary Figure 2A, available on the *Arthritis & Rheumatology* website at http://onlinelibrary.wiley.com/doi/10.1002/art.41885/abstract), the comparison of the DNA methylation profiles determined from baseline samples in relation to the clinical groups defined 1 year later (UA_1 versus RA_1) led to the identification of 12,381 hypermethylated CpGs and 4,159 hypomethylated CpGs (Figure 3C). These DMPs did not vary significantly with regard to slide or array (Supplementary Figure 2D).

DMPs in the hypermethylated cluster were enriched in GO categories related to antigen presentation through major histocompatibility complex (MHC) class I, as well as inflammatory cytokine signaling (such as IL-1 and IL-6). GO categories in the hypomethylated cluster were mainly related to basic cellular processes such as gene transcription, translation, and metabolism, and an additional category related to antigenic presentation through MHC class II (Figure 3D). CpG sites proximal to genes contained in the aforementioned GO categories and related to inflammatory cytokines and chemokine pathways, such as *CCL25*, *CD5L*, and *IL17RA,* were selected, and their B values in the UA_1 and RA_1 groups are depicted in Figure 3E.

Analysis of transcription factor binding motifs in the hypermethylated cluster revealed an enrichment of motifs belonging to the basic helix-loop-helix and zinc finger domain (Zf) families. The hypomethylated cluster showed enrichment of transcription factors from the ETS and Zf families (Supplementary Figure 2B). Chromatin state enrichment for the hypomethylated cluster revealed an enrichment of regions located in active and poised TSS or their flanking regions. The hypermethylated cluster showed enrichment in actively transcribed regions, enhancers, and repressed chromatin (Supplementary Figure 2C). None of the chromatin states were commonly enriched in the 2 clusters, suggesting the involvement of distinct pathways underlying the identified alterations.

Additionally, samples from patients with UA at baseline that had differentiated into other arthritis subtypes 1 year after the initial visit (psoriatic arthritis, spondyloarthritis, osteoarthritis, or reactive arthritis), labeled "other subtypes" (see Supplementary Table 1), were compared to UA_1 and RA_1. Due to the sparsity of samples of each of the other subtypes (n = 2 patients per group), we decided to identify DMPs from the UA_1 versus RA_1 comparison, and to represent the DNA methylation values of the additional samples in an unsupervised manner. In a principal components analysis (PCA), the distribution of the samples from the other subtypes group largely overlapped with the distribution of the RA_1 samples (Supplementary Figure 2E). This tendency was corroborated by inspecting the mean methylation value of the DMPs. The mean value in the other subtypes group appeared closer to that of RA_1 than to that of UA_1, in both the hypomethylated and hypermethylated CpGs (Supplementary Figure 2F).

Of note, this tendency was not reproduced individually by all of the samples, as shown by a pairwise mean comparison between the UA_1 and RA_1 groups (Supplementary Figure 2G). However, after comparing UA_1 and RA_1 to each of the samples in the group of other subtypes, we found that significant differences in the mean values occurred more frequently between the UA_1 group and the other subtypes group (6 of 8 in the hypomethylated cluster and 8 of 8 in the hypermethylated cluster) than between the RA_1 group and the other subtypes group (2 of 8 in the hypomethylated cluster and 6 of 8 in the hypermethylated cluster). Although these results need to be further confirmed, this tendency suggests the existence of an altered signature shared by patients with differentiated arthritis. Taken together, these results indicate for the first time the existence of a pre-established epigenetic signature in UA patients whose disease will evolve to RA.

Improvement of patient classification by incorporation of DNA methylation data into the clinical parameters–based model. Given our findings of DNA methylation differences between UA patient groups that had divergent diagnoses 1 year after baseline, we investigated the possibility of using DNA methylation data to obtain predictive markers of disease progression. To this end, we applied machine learning approaches to build a classification system based on DNA methylation data alone or DNA methylation data in combination with clinical data. The pipeline of the methodology included a random split of the original data into "training" and "test" sets, followed by a selection of predictor CpG sites, and a cross-validation for the internal evaluation of the model (Figure 4A). Models developed and evaluated through this procedure were constructed using logistic regression, random forest, and support vector machine (SVM) algorithms. Aiming at obtaining a relatively simple classifier, we generated models with increasing numbers of CpG sites as predictors (from 1 to 50 CpG sites). In parallel, patient clinical data (RF and DAS) were included as explanatory variables. These variables, which showed significant differences among groups, have also been included in previous studies describing classification rules that were based strictly on 9 clinical parameters (3).

The comparison of the accuracies of all models (see Supplementary Methods) showed the highest precision for SVM-generated models with RF and DAS covariates included (SVM+RF,DAS models) (Figure 4B). The top 10 most frequent CpGs (after performing 100-fold cross-validation) in the SVM+RF,-DAS model are shown in Figure 4C. Given that SVM+RF,DAS models discriminate relatively well with >10 CpGs, we selected 2 examples of models, representing a complex classifier, with 40 CpGs, and a simpler classifier, with 25 CpGs, that might potentially be implemented in the clinical setting. Finally, these models were applied to an external validation cohort (n = 8), recruited independently (Supplementary Table 2, available on the *Arthritis & Rheumatology* website at http://onlinelibrary.wiley.com/doi/10.1002/art.41885/abstract). The predicted outcome was then compared to the observed outcome 1 year after baseline for every patient (Figure 4D). For benchmarking purposes, the previously described clinical classification score (3) (named "composite score") was also used alone or along with DNA methylation in the analysis, in parallel.

Within the validation cohort, the prediction accuracy of the composite score alone was 75%, while the simplified model, which included only 2 variables (DAS and RF), showed an accuracy of 62.5% (Figure 4D). The simplified model with 25 CpGs increased the accuracy (area under the curve [AUC] 0.875) of the prediction by the clinical covariates alone (AUC 0.625). The simplified model with 40 CpGs accurately predicted the class of all 8 patients (AUC 1) (Figure 4D and Supplementary Figure 3A, available on the *Arthritis & Rheumatology* website at http://online

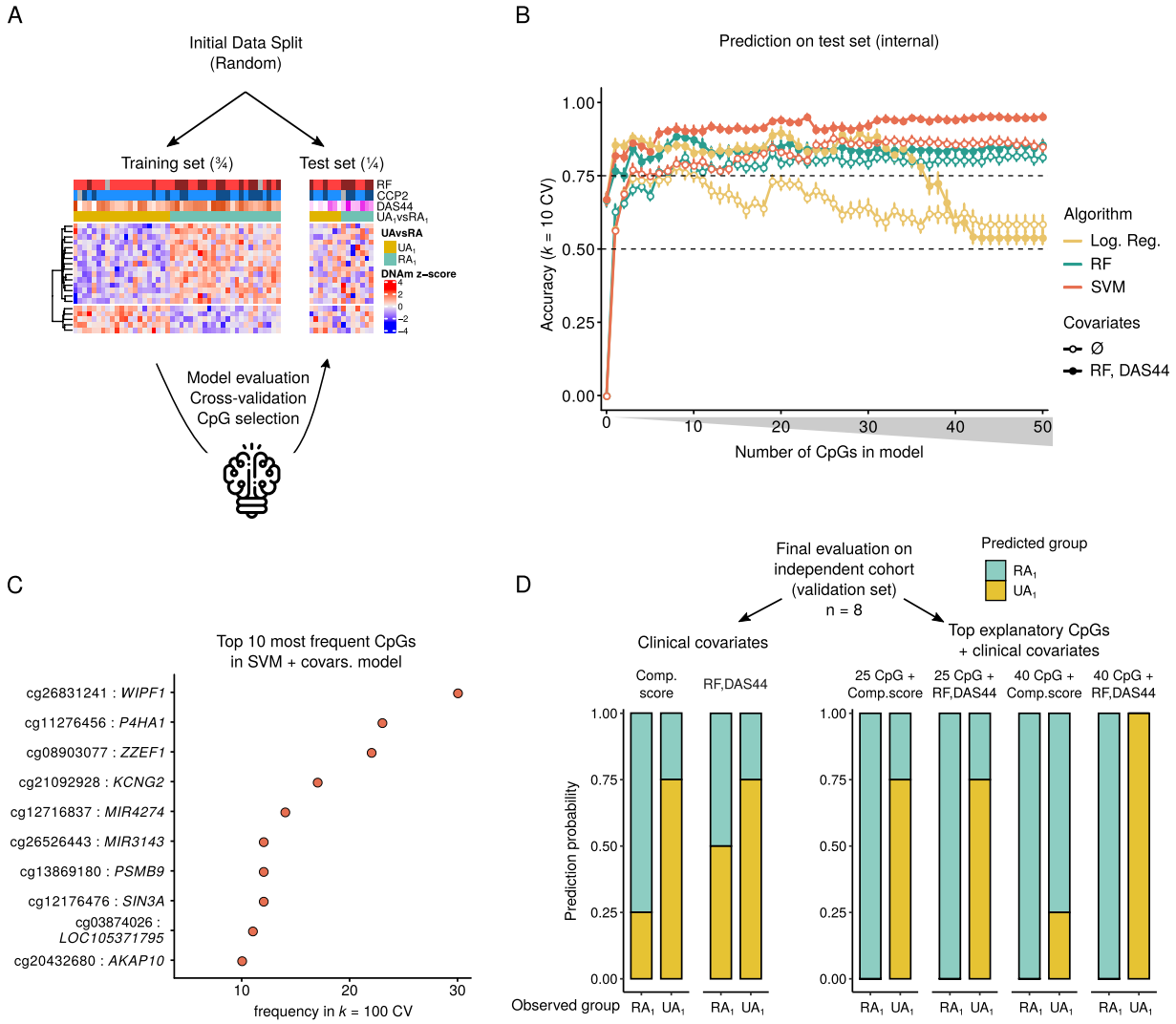

Figure 4. Development of a DNA methylation-based prediction rule by machine learning. Models were constructed to predict whether patients with UA at baseline would have RA 1 year after the initial visit (RA_1) or UA 1 year after the initial visit (UA_1). **A**, Schematic representation of the machine learning methodology, including splitting of data into training and test sets, feature (CpG) selection, evaluation of the model parameters, and cross-validation. **B**, Accuracy of the models developed using logistic regression (Log. Reg.), random forest (RF), and support vector machine (SVM) algorithms. Models included varying numbers of most frequent CpGs as explanatory variables (1–50 CpGs). Values are the mean ± SEM from 10 independent cross-validations. **C**, Top 10 most frequent CpGs after 100-fold cross-validation in the SVM model with covariates (SVM + covars). CV = cross-validation. **D**, Classification results of selected models in an independent validation cohort. Left, Prediction models based on clinical covariates only. Right, Prediction models based on the combination of DNA methylation data plus clinical covariates. Comp. score = composite score (see Figure 2 for other definitions). Color figure can be viewed in the online issue, which is available at http://onlinelibrary.wiley.com/doi/10.1002/art.41885/abstract.

library.wiley.com/doi/10.1002/art.41885/abstract). In fact, simplified models with >25 CpGs predicted future diagnosis with an average accuracy of >75%, and the addition of the CpG methylation data improved the predictive ability of clinical parameters in the majority of the models (Supplementary Figure 3B). Although the prediction accuracy of the composite score was higher than that of DAS+RF alone, after the addition of DNA methylation data, the accuracy of the simplified models was higher when compared to the composite score models, in the majority of the cases. In fact, in models with >30 CpGs, the accuracy of the models that included the composite score as a covariate dropped to random classifier levels, ~50% accuracy (Figure 4D and Supplementary Figure 3B). Taken together, these results highlight the potential of adding DNA methylation as a diagnostic predictive biomarker.

Comparison of UA and definite RA profiles, revealing progression of RA_1 status to RA status. To further characterize the UA_0 subgroups, we compared the DNA methylation profiles of UA_0 with those of patients with terminally differentiated RA (diagnosed as having RA at baseline), labeled RA_0 (Supplementary Table 2). The RA_0 group displayed the most distinct methylation profile, as shown by the greatest differences

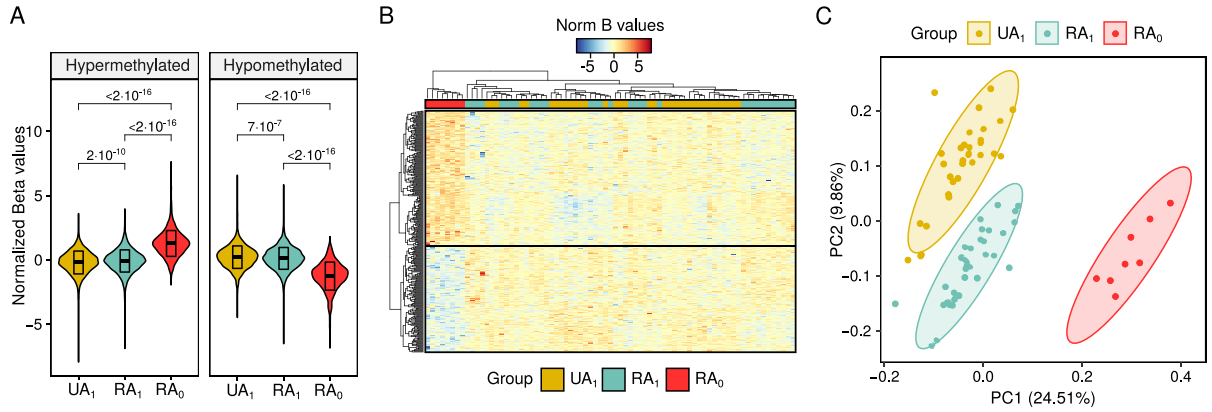

Figure 5. Comparison of the methylome profiles of patients with undifferentiated arthritis (UA) at baseline who continued to be classified as having UA 1 year after baseline (UA_1), patients with UA at baseline that progressed to RA 1 year after baseline (RA_1), and patients with RA at baseline (RA_0). **A**, Violin plots showing normalized B value distributions of differentially methylated positions (DMPs) between UA_1, RA_1 and RA_0 profiles. Boxes show the 25th to 75th percentiles. Lines inside the boxes represent the median. Values above the violin plots are *P* values. The microarray model (450k or EPIC) was included as a covariate in the *limma* model. **B**, Heatmap of the identified DMPs. Columns (samples) were clustered by a complete-linkage clustering algorithm. **C**, Principal components analysis of the DMPs. Ellipses show the 95% confidence interval for the distribution of each group. Circles represent individual patients. PC1 = principal component 1. Color figure can be viewed in the online issue, which is available at http://onlinelibrary.wiley.com/doi/10.1002/art.41885/abstract.

in mean DNA methylation when compared to both UA_1 and RA_1 (Figure 5A). We then performed unsupervised clustering of the significant DMPs among the 3 groups (RA_0, UA_1, and RA_1). We observed that all UA_1 and RA_1 samples (both subgroups of UA_0) aggregated together in the same cluster, while all RA_0 samples clustered independently (Figure 5B). Overall methylation of the identified DMPs showed significant differences among the 3 groups. In addition, these regions appeared to experience a progressive dynamic from UA_1 to RA_1 to RA_0, both for the hypermethylated and the hypomethylated clusters (Figure 5A). This tendency was further reinforced after reducing the dimensionality of the DMP data by PCA, where RA_1 patients lie in between RA_0 and UA_1, which appeared as the most extreme groups when projected in principal component 1 (PC1) and PC2 (Figure 5C).

Additionally, unsupervised K-means clustering of the DMP data revealed a total association of RA_0 in an isolated cluster (cluster 3), while UA_1 and RA_1, which were largely associated with independent clusters (clusters 1 and 2), showed a certain degree of interspersing (Supplementary Figure 4A, available on the *Arthritis & Rheumatology* website at http://onlinelibrary.wiley.com/doi/10.1002/art.41885/abstract). When samples were assigned to clusters, 5 (15.6%) of 32 UA_1 samples belonged to cluster 2 ("RA_1 cluster"), while 7 (20%) of 35 RA_1 samples belonged to cluster 1 ("UA_1 cluster"). All (100%) of the 8 RA_0 samples belonged to cluster 3 (Supplementary Figure 4B). These data reinforce the notion of a pre-existing RA-like epigenetic profile underlying UA in some patients, which reveals a progression of the disease in these patients to RA.

DISCUSSION

Our analysis of the DNA methylomes of UA patients showed a distinct signature in comparison with healthy individuals, as well as specific differences between patients whose disease subsequently evolved to RA and those whose disease remained undifferentiated. These observations prompted us to design a machine learning–based method, which improved previous classification systems (3), to predict outcomes in UA patients in our cohort. The finding that UA patients who will develop RA have a more similar DNA methylation signature to patients with well-established RA supports the notion of pre-existing epigenetic signatures that might be used to anticipate patient outcomes and, therefore, improve therapeutic decisions.

Our results show for the first time that UA patients display epigenetic alterations when compared to healthy individuals. Those alterations, which occur in regions that are functionally associated with inflammatory pathways, are common to those previously observed in other inflammatory diseases. In particular, enriched functional categories of inflammation, immune cell activation, and cytokine signaling have also been found in RA (6,15,16), SLE (17,18), asthma (19), and inflammatory bowel disease (20) in comparable studies, supporting the idea that UA shares epigenetic similarities with other inflammatory diseases and thus can be molecularly considered as such. Furthermore, the identification of vast DNA methylation differences at the TNF locus, as well as alterations at several CpGs within the HLA class II region (both at the DMP and DVP level) confirms that UA is an arthritide like RA, with which it shares clinical characteristics (7,21–23). Of note, the results of this particular analysis may be partially limited due to the exclusion of sex chromosomes and age-associated CpGs, in which UA-associated alterations could also occur.

Furthermore, we identified DNA methylation differences among UA patients based on their prospective status, namely, the diagnosis 1 year after the first visit (evolution to RA or persistent UA). After correcting for clinical features among the 2 groups, we

identified DNA methylation differences mainly localized in regions near genes related to inflammation and antigen presentation (24–27). For instance, HLA genes have been recursively linked to autoimmunity, showing both association with genetic susceptibility and epigenetic alterations in several studies (7,28,29). HLA–B, HLA–DMA, and HLA–F have further been linked to autoimmunity (30–32). Other genes, such as CD38, have been shown to be up-regulated at the protein level in UA patients, and CD38 has been proposed as a therapeutic target in UA and early arthritis (33). These observations suggest that those patients possess early biologic alterations before undergoing diverging clinical outcomes.

Identification of disease onset in the clinical setting is often preceded by the presence of unapparent molecular triggers, as previously described for RA treatment response (34) and flare outbreaks (35). Those determinants appear early in the disease course and cannot easily be detected by clinicians through non-invasive means. However, their sustained presence and effect at several levels may contribute to a specific pathologic phenotype. We believe that this study underpins the potential of using epigenetic modifications as a molecular sensor for those early disease determinants in UA, in order to improve the classification criteria for UA and prevent damage caused by sustained inflammation. However, future longitudinal studies that include data from follow-up visits would provide further insights into the mechanisms by which UA patients diverge, and their underlying epigenetic dynamics. Also, further evidence is needed to confirm whether the observed phenomenon is common to differentiated subtypes of arthritis other than RA, as suggested by the preliminary data included in this study.

Autoimmune arthritides are characterized by a high level of heterogeneity in terms of patient prognosis, joint damage, and response to treatment, for which mechanistic causality remains largely unknown (36). In this sense, the use of high-throughput technologies has enabled the development of computational methods for the processing of patient -omic data in search of novel and more precise conclusions (37–39). For instance, the implementation of machine learning algorithms in high-dimensional data analysis has previously been used to improve stratification of patients (40–42) or to predict disease activity (43,44) in RA and SLE. In the present study, we used DNA methylation in addition to clinical data on UA patients by applying machine learning approaches, fine-tuning the prediction performance of previously existing classifiers (3) in an independent validation cohort. Nevertheless, although the use of data obtained from PBMCs might limit the identification of alterations in specific cell subtypes, it simplifies the generation of data in clinical practice, avoiding the need for cell sorting. Our conclusions highlight the convenience of using both clinical and basic research data in conjunction for a complete and robust patient prognostic and therapeutic assessment. The results obtained herein are presented as a proof of concept to be further confirmed in independent studies with larger sample sizes. We hope our methodology can also be applied to other disease contexts.

The comparison of the methylation profiles of all of the UA patients included in our cohort (regardless of their prospective status at year 1, i.e., UA or RA) versus those initially classified as having RA, showed that patients with UA and those with RA displayed differential methylation profiles, further supporting the idea that these 2 groups actually belong to distinct disease entities from a molecular/epigenetic perspective. Upon exploration by unsupervised analyses, the 2 UA subgroups, UA_1 and RA_1, showed a higher resemblance to each other than either did to RA_0, suggesting that despite the existing differences among them, the 2 UA groups (UA_1 and RA_1) still behaved as an entity when compared to a differentiated group. Interestingly, UA_1 and RA_0 had the most extreme distributions, while RA_1 displayed an intermediate distribution. In all, these data suggest the pre-existence of a molecular/epigenetic signature in UA patients that develop RA in the future.

Many efforts have been devoted to promptly abort the inflammatory process and the progression of the disease to a more severe form, facilitating a rapid halt of the dysregulated inflammatory process and avoiding inflammation-associated tissue damage. Indeed, a delayed treatment of these patients is commonly associated with a worse global response to treatment, joint destruction, and impaired quality of life. In this context, our results regarding epigenetic signatures associated with distinctive UA evolution suggest that, in addition to specific clinical parameters, molecular features such as DNA methylation should be considered to be integrated into the clinic with the aim of a better classification of these patients.

ACKNOWLEDGMENTS

The authors thank all the patients who graciously donated their time and samples for arthritis research.

AUTHOR CONTRIBUTIONS

All authors were involved in drafting the article or revising it critically for important intellectual content, and all authors approved the final version to be published. Dr. Ballestar had full access to all of the data in the study and takes responsibility for the integrity of the data and the accuracy of the data analysis.

Study conception and design. de la Calle-Fabregat, van der Helm-van Mil, Ballestar.

Acquisition of data. de la Calle-Fabregat, Niemantsverdriet, van der Helm-van Mil, Rodríguez-Ubreva, Ballestar.

Analysis and interpretation of data. de la Calle-Fabregat, Cañete, Li, Rodríguez-Ubreva, Ballestar.

REFERENCES

1. Van Aken J, van Dongen H, le Cessie S, Allaart CF, Breedveld FC, Huizinga TW. Comparison of long term outcome of patients with rheumatoid arthritis presenting with undifferentiated arthritis or with rheumatoid arthritis: an observational cohort study. Ann Rheum Dis 2006;65:20–5.

2. Van Dongen H, van Aken J, Lard LR, Visser K, Ronday HK, Hulsmans HM, et al. Efficacy of methotrexate treatment in patients with probable rheumatoid arthritis: a double-blind, randomized, placebo-controlled trial. Arthritis Rheum 2007;56:1424–32.
3. Van Der Helm-van Mil AH, le Cessie S, van Dongen H, Breedveld FC, Toes RE, Huizinga TW. A prediction rule for disease outcome in patients with recent-onset undifferentiated arthritis: how to guide individual treatment decisions. Arthritis Rheum 2007;56:433–40.
4. De Maturana EL, Alonso L, Alarcón P, Martín-Antoniano IA, Pineda S, Piorno L, et al. Challenges in the integration of omics and non-omics data [review]. Genes (Basel) 2019;10:238.
5. Xu GL, Bestor TH, Bourc'his D, Hsieh CL, Tommerup N, Bugge M, et al. Chromosome instability and immunodeficiency syndrome caused by mutations in a DNA methyltransferase gene [letter]. Nature 1999;402:187–91.
6. Rodríguez-Ubreva J, de la Calle-Fabregat C, Li T, Ciudad L, Ballestar ML, Català-Moll F, et al. Inflammatory cytokines shape a changing DNA methylome in monocytes mirroring disease activity in rheumatoid arthritis. Ann Rheum Dis 2019;78:1505–16.
7. Liu Y, Aryee MJ, Padyukov L, Fallin MD, Hesselberg E, Runarsson A, et al. Epigenome-wide association data implicate DNA methylation as an intermediary of genetic risk in rheumatoid arthritis. Nat Biotechnol 2013;31:142–7.
8. Ballestar E, Sawalha AH, Lu Q. Clinical value of DNA methylation markers in autoimmune rheumatic diseases [review]. Nat Rev Rheumatol 2020;16:514–24.
9. De Rooy DP, van der Linden MP, Knevel R, Huizinga TW, van der Hel-van Mil AH. Predicting arthritis outcomes—what can be learned from the Leiden Early Arthritis Clinic? Rheumatology (Oxford) 2011;50:93–100.
10. Arnett FC, Edworthy SM, Bloch DA, McShane DJ, Fries JF, Cooper NS, et al. The American Rheumatism Association 1987 revised criteria for the classification of rheumatoid arthritis. Arthritis Rheum 1988;31:315–24.
11. Van der Heijde DM, van 't Hof MA, van Riel PL, Theunisse LM, Lubberts EW, van Leeuwen MA, et al. Judging disease activity in clinical practice in rheumatoid arthritis: first step in the development of a disease activity score. Ann Rheum Dis 1990;49:916–20.
12. Ernst J, Kellis M. ChromHMM: automating chromatin-state discovery and characterization [letter]. Nat Methods 2012;9:215–6.
13. Luo C, Hajkova P, Ecker JR. Dynamic DNA methylation: In the right place at the right time [review]. Science 2018;361:1336–40.
14. Ranganath VK, Yoon J, Khanna D, Park GS, Furst DE, Elashoff DA, et al. Comparison of composite measures of disease activity in an early seropositive rheumatoid arthritis cohort. Ann Rheum Dis 2007;66:1633–40.
15. Zhu H, Wu LF, Mo XB, Lu X, Tang H, Zhu XW, et al. Rheumatoid arthritis-associated DNA methylation sites in peripheral blood mononuclear cells. Ann Rheum Dis 2019;78:36–42.
16. Mok A, Rhead B, Holingue C, Shao X, Quach HL, Quach D, et al. Hypomethylation of CYP2E1 and DUSP22 promoters associated with disease activity and erosive disease among rheumatoid arthritis patients. Arthritis Rheumatol 2018;70:528–36.
17. Javierre BM, Fernandez AF, Richter J, Al-Shahrour F, Ignacio Martin-Subero J, Rodriguez-Ubreva J, et al. Changes in the pattern of DNA methylation associate with twin discordance in systemic lupus erythematosus. Genome Res 2010;20:170–9.
18. Lanata CM, Paranjpe I, Nititham J, Taylor KE, Gianfrancesco M, Paranjpe M, et al. A phenotypic and genomics approach in a multi-ethnic cohort to subtype systemic lupus erythematosus. Nat Commun 2019;10:3902.
19. Yang IV, Pedersen BS, Liu A, O'Connor GT, Teach SJ, Kattan M, et al. DNA methylation and childhood asthma in the inner city. J Allergy Clin Immunol 2015;136:69–80.
20. McDermott E, Ryan EJ, Tosetto M, Gibson D, Burrage J, Keegan D, et al. DNA methylation profiling in inflammatory bowel disease provides new insights into disease pathogenesis. J Crohn's Colitis 2016;10:77–86.
21. Van Steenbergen HW, Luijk R, Shoemaker R, Heijmans BT, Huizinga TW, van der Helm-van Mil AH. Differential methylation within the major histocompatibility complex region in rheumatoid arthritis: a replication study. Rheumatology (Oxford) 2014;53:2317–8.
22. Anaparti V, Agarwal P, Smolik I, Mookherjee N, El-Gabalawy H. Whole blood targeted bisulfite sequencing and differential methylation in the C6ORF10 gene of patients with rheumatoid arthritis. J Rheumatol 2020;47:1614–23.
23. Pitaksalee R, Burska AN, Ajaib S, Rogers J, Parmar R, Mydlova K, et al. Differential CpG DNA methylation in peripheral naïve CD4+ T-cells in early rheumatoid arthritis patients. Clin Epigenetics 2020;12:54.
24. Yokoyama W, Kohsaka H, Kaneko K, Walters M, Takayasu A, Fukuda S, et al. Abrogation of CC chemokine receptor 9 ameliorates collagen-induced arthritis of mice. Arthritis Res Ther 2014;16:445.
25. Wu X, Li M, Chen T, Zhong H, Lai X. Apoptosis inhibitor of macrophage/CD5L is associated with disease activity in rheumatoid arthritis. Clin Exp Rheumatol 2021;39:58–65.
26. Wang C, Yosef N, Gaublomme J, Wu C, Lee Y, Clish CB, et al. CD5L/AIM regulates lipid biosynthesis and restrains Th17 cell pathogenicity. Cell 2015;163:1413–27.
27. Van den Berg WB, Miossec P. IL-17 as a future therapeutic target for rheumatoid arthritis [review]. Nat Rev Rheumatol 2009;5:549–53.
28. Dendrou CA, Petersen J, Rossjohn J, Fugger L. HLA variation and disease [review]. Nat Rev Immunol 2018;18:325–39.
29. Kular L, Liu Y, Ruhrmann S, Zheleznyakova G, Marabita F, Gomez-Cabrero D, et al. DNA methylation as a mediator of HLA-DRB1*15:01 and a protective variant in multiple sclerosis. Nat Commun 2018;9:2397.
30. Bowness P. HLA B27 in health and disease: a double-edged sword? [review]. Rheumatology (Oxford) 2002;41:857–68.
31. Morel J, Roch-Bras F, Molinari N, Sany J, Eliaou JF, Combe B. HLA-DMA*0103 and HLA-DMB*0104 alleles as novel prognostic factors in rheumatoid arthritis. Ann Rheum Dis 2004;63:1581–6.
32. Afroz S, Giddaluru J, Vishwakarma S, Naz S, Khan AA, Khan N. A comprehensive gene expression meta-analysis identifies novel immune signatures in rheumatoid arthritis patients. Front Immunol 2017;8:74.
33. Cole S, Walsh A, Yin X, Wechalekar MD, Smith MD, Proudman SM, et al. Integrative analysis reveals CD38 as a therapeutic target for plasma cell-rich pre-disease and established rheumatoid arthritis and systemic lupus erythematosus. Arthritis Res Ther 2018;20:85.
34. Lewis MJ, Barnes MR, Blighe K, Goldmann K, Rana S, Hackney JA, et al. Molecular portraits of early rheumatoid arthritis identify clinical and treatment response phenotypes. Cell Rep 2019;28:2455–70.
35. Orange DE, Yao V, Sawicka K, Fak J, Frank MO, Parveen S, et al. RNA identification of PRIME cells predicting rheumatoid arthritis flares. N Engl J Med 2020;383:218–28.
36. Pitzalis C, Kelly S, Humby F. New learnings on the pathophysiology of RA from synovial biopsies [review]. Curr Opin Rheumatol 2013;25:334–44.
37. Donlin LT, Park SH, Giannopoulou E, Ivovic A, Park-Min KH, Siegel RM, et al. Insights into rheumatic diseases from next-generation sequencing [review]. Nat Rev Rheumatol 2019;15:327–39.
38. Lewis MJ, Barnes MR. RNA sequencing and machine learning as molecular scalpels [review]. Nat Rev Rheumatol 2018;14:388–90.
39. Stafford IS, Kellermann M, Mossotto E, Beattie RM, MacArthur BD, Ennis S. A systematic review of the applications of artificial intelligence and machine learning in autoimmune diseases [review]. NPJ Digit Med 2020;3:30.
40. Orange DE, Agius P, DiCarlo EF, Robine N, Geiger H, Szymonifka J, et al. Identification of three rheumatoid arthritis disease subtypes by

machine learning integration of synovial histologic features and RNA sequencing data. Arthritis Rheumatol 2018;70:690–701.
41. Figgett WA, Monaghan K, Ng M, Alhamdoosh M, Maraskovsky E, Wilson NJ, et al. Machine learning applied to whole-blood RNA-sequencing data uncovers distinct subsets of patients with systemic lupus erythematosus. Clin Transl Immunol 2019;8:e01093.
42. Robinson GA, Peng J, Dönnes P, Coelewij L, Naja M, Radziszewska A, et al. Disease-associated and patient-specific immune cell signatures in juvenile-onset systemic lupus erythematosus: patient stratification using a machine-learning approach. Lancet Rheumatol 2020;2:e485–96.
43. Lin C, Karlson EW, Canhao H, Miller TA, Dligach D, Chen PJ, et al. Automatic prediction of rheumatoid arthritis disease activity from the electronic medical records. PLoS One 2013;8:e69932.
44. Kegerreis B, Catalina MD, Bachali P, Geraci NS, Labonte AC, Zeng C, et al. Machine learning approaches to predict lupus disease activity from gene expression data. Sci Rep 2019;9:9617.

DOI 10.1002/art.41922

Clinical Images: Cerebral autosomal-dominant arteriopathy with subcortical infarcts and leukoencephalopathy syndrome, a central nervous system vasculitis mimic

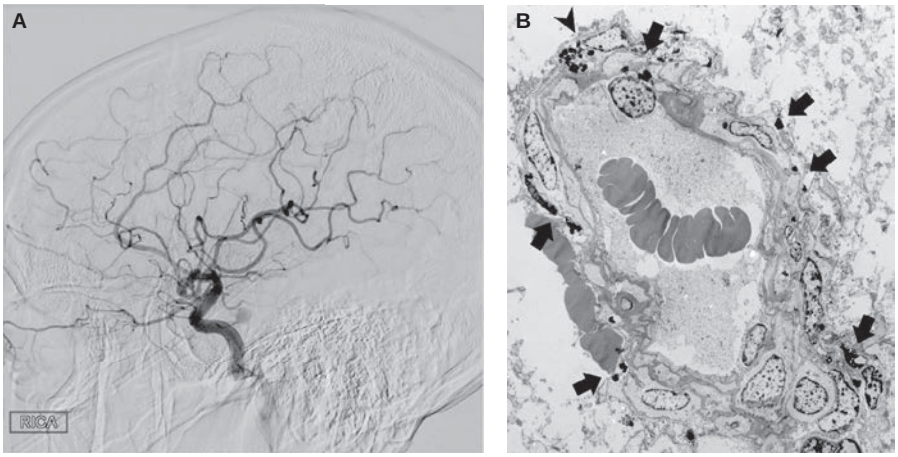

The patient, a 37-year-old man with diabetes mellitus and hypertension, presented with severe headache. Over a 1-month period, magnetic resonance imaging showed acute strokes in the right paramedian pons, left thalamus/globus pallidus/subinsula, and right corona radiata. Evaluation for primary angiitis of the central nervous system (PACNS) included lumbar puncture revealing 7 white blood cells, as well as normal protein and glucose levels. Cerebral arteriography demonstrated diffuse small vessel beading in the anterior and middle territories of the cerebral artery bilaterally (**A**). The patient was started on pulse-dose therapy with methylprednisolone empirically for PACNS. Brain biopsy did not show the expected finding of vasculitis on light microscopy, and transmission electron microscopy revealed the presence of granular osmophilic material (GOM) around smooth muscle cells in cerebral white matter arterioles. An abundance of lipofuscin in association with GOM (as indicated by **arrows** in **B** with **arrowhead** denoting a scavenger cell containing GOM and lipofuscin) suggested the presence of a degenerative process. In contrast, in patients with PACNS, brain biopsies show transmural lymphocytic vasculitis with fibrinoid necrosis (1). Given the young age of the patient, genetic testing was performed to assess for possible hereditary syndromes. The test identified a Notch homolog 3 mutation, which confirmed the diagnosis of cerebral autosomal-dominant arteriopathy with subcortical infarcts and leukoencephalopathy (CADASIL). CADASIL is the most common genetic cause of ischemic stroke, often presenting with early-onset strokes, migraines, and white matter lesions (2). Mutations in the Notch-3 gene, which encodes a transmembrane receptor expressed in arterial smooth muscle cells, result in an arteriopathy that can mimic CNS vasculitis with hypointense lesions at the cortico–subcortical junction and white matter hyperintensities in the anterior temporal lobes (1,2). The ultrastructural findings in this case could explain the beaded appearance of arterioles on arteriography, mimicking vasculitis. This case demonstrates that findings suggestive of PACNS on arteriography often lack specificity, and brain biopsy and genetic testing can be critical tools to secure the right diagnosis. Familiarity with this rare vasculitis mimic can ensure early diagnosis and avoid unnecessary immunosuppression.

Author disclosures are available at https://onlinelibrary.wiley.com/action/downloadSupplement?doi=10.1002%2Fart.41922&file=art41922-sup-0001-Disclosureform.pdf.

1. Byram K, Hajj-Ali RA, Calabrese L. CNS vasculitis: an approach to differential diagnosis and management [review]. Curr Rheumatol Rep 2018;20:37.
2. Chabriat H, Joutel A, Dichgans M, Tournier-Lasserve E, Npusser MG. Cadasil [review]. Lancet Neurol 2009;8:643–53.

Mithu Maheswaranathan, MD
Anne F. Buckley, MD, PhD
Andrew B. Cutler, MD
Lisa Criscione-Schreiber, MD, Med
Ankoor Shah, MD
Duke University School of Medicine
Durham, NC

American College of Rheumatology
Empowering Rheumatology Professionals

Arthritis & Rheumatology
Vol. 73, No. 12, December 2021, pp 2240–2248
DOI 10.1002/art.41808
© 2021, American College of Rheumatology

Subchondral Bone Length in Knee Osteoarthritis: A Deep Learning–Derived Imaging Measure and Its Association With Radiographic and Clinical Outcomes

Gary H. Chang,[1] Lisa K. Park,[1] Nina A. Le,[1] Ray S. Jhun,[1] Tejus Surendran,[1] Joseph Lai,[1] Hojoon Seo,[1] Nuwapa Promchotichai,[1] Grace Yoon,[1] Jonathan Scalera,[1] Terence D. Capellini,[2] David T. Felson,[3] and Vijaya B. Kolachalama[1]

Objective. To develop a bone shape measure that reflects the extent of cartilage loss and bone flattening in knee osteoarthritis (OA) and test it against estimates of disease severity.

Methods. A fast region-based convolutional neural network was trained to crop the knee joints in sagittal dual-echo steady-state magnetic resonance imaging sequences obtained from the Osteoarthritis Initiative (OAI). Publicly available annotations of the cartilage and menisci were used as references to annotate the tibia and the femur in 61 knees. Another deep neural network (U-Net) was developed to learn these annotations. Model predictions were compared to radiologist-driven annotations on an independent test set (27 knees). The U-Net was applied to automatically extract the knee joint structures on the larger OAI data set (n = 9,434 knees). We defined subchondral bone length (SBL), a novel shape measure characterizing the extent of overlying cartilage and bone flattening, and examined its relationship with radiographic joint space narrowing (JSN), concurrent pain and disability (according to the Western Ontario and McMaster Universities Osteoarthritis Index), as well as subsequent partial or total knee replacement. Odds ratios (ORs) and 95% confidence intervals (95% CIs) for each outcome were estimated using relative changes in SBL from the OAI data set stratified into quartiles.

Results. The mean SBL values for knees with JSN were consistently different from knees without JSN. Greater changes of SBL from baseline were associated with greater pain and disability. For knees with medial or lateral JSN, the ORs for future knee replacement between the lowest and highest quartiles corresponding to SBL changes were 5.68 (95% CI 3.90–8.27) and 7.19 (95% CI 3.71–13.95), respectively.

Conclusion. SBL quantified OA status based on JSN severity and shows promise as an imaging marker in predicting clinical and structural OA outcomes.

INTRODUCTION

Knee osteoarthritis (OA) is one of the most common debilitating conditions among older adults (1), with a burden that is expected to increase around the globe due to factors such as increasing rates of obesity (2). Because there is no effective disease-modifying therapy for knee OA, current clinical management relies in part on identification of radiographic abnormalities such as joint space narrowing (JSN) to assist in diagnosing OA and/or estimating the likelihood of progression to severe OA (3–6). Since it is important to accurately evaluate OA pathophysiology, there is a need to develop additional imaging markers, and in

Supported in part by the NIH (grants U01-AG-018820, R01-AR-070139, R21-CA-253498, R01-AG-062109, and P30-AR-072571 to Drs. Capellini, Felson, and Kolachalama). Dr. Felson's work was supported by the NIHR Manchester Biomedical Research Centre. Dr. Kolachalama's work was supported by grants from the Karen Toffler Charitable Trust, the American Heart Association (grants 17SDG33670323 and 20SFRN35460031), and the Hariri Institute for Computing and Computational Science & Engineering and Digital Health Initiative at Boston University.

[1]Gary H. Chang, PhD, Lisa K. Park, MD, Nina A. Le, BS, Ray S. Jhun, MS, Tejus Surendran, Joseph Lai, Hojoon Seo, Nuwapa Promchotichai, Grace Yoon, Jonathan Scalera, MD, Vijaya B. Kolachalama, PhD: Boston University, Boston, Massachusetts; [2]Terence D. Capellini, PhD: Harvard University and Broad Institute of MIT and Harvard, Cambridge, Massachusetts; [3]David T. Felson, MD, MPH: Boston University School of Medicine, Boston, Massachusetts, and University of Manchester, NIHR Manchester Biomedical Research Centre, Manchester University Hospitals NHS Foundation Trust, Manchester, UK.

Drs. Chang, Park, and Le contributed equally to this work. Drs. Felson and Kolachalama contributed equally to this work.

Dr. Felson has received consulting fees from Paradigm (less than $10,000 each). No other disclosures relevant to this article were reported.

Address correspondence to Vijaya B. Kolachalama, PhD, Boston University School of Medicine, 72 East Concord Street, Evans 636, Boston, MA 02118. Email: vkola@bu.edu.

Submitted for publication November 11, 2020; accepted in revised form May 6, 2021.

some cases, improve the measurement sensitivity and specificity of existing imaging markers to better predict disease progression and potential clinical outcomes.

Magnetic resonance imaging (MRI) can allow us to visually differentiate joint tissues, which facilitates accurate characterization of several imaging markers of knee OA (7). Previously, a case–control study on a subset of data from the Osteoarthritis Initiative (OAI) showed that bone shape derived from knee MRI scans predicted later onset of radiographic knee OA (8). In other studies, researchers used MRI to identify increased tibial plateau size and subchondral bone attrition during the preradiographic OA stage (9) and found variability in knee articular surface geometry in individuals with and those without OA (10). Most of these studies were performed using a small subset of individuals. While findings from these important investigations established a proof of principle, it is not trivial to extend such studies to a larger cohort due to the sheer volume of cases and the manual labor needed to precisely annotate different anatomic structures in the knee. Recently, Bowes and colleagues proposed a machine learning–driven measure of femur bone shape (defined as B-score), based on a large set of individuals from the OAI cohort (n = 4,796) (11). They showed that B-score was associated with risk of current and future pain, functional limitation, and total knee replacement (TKR). Few other studies have also attempted to characterize bone shapes in OA (8,12). A major contributor to the bone shape metric is the crust of osteophytes that arises at the margin of the cartilage plate in advanced OA. These marginal osteophytes are probably not a source of pain (13), and their size and number are poor proxies for the severity of nearby cartilage loss (14), which is the signature pathologic feature of OA.

We developed a bone shape measure defined as subchondral bone length (SBL), which did not include these marginal osteophytes but rather was driven by the extent of overlying cartilage, decreasing with cartilage denudation. Bone also flattens with increasing disease severity, increasing its area (15,16). We hypothesized that SBL variations increase with the severity of radiographic knee OA, as it accounts for the dynamic changes that occur within the subchondral region due to cartilage loss and bone flattening. We then tested whether SBL correlated with severity of knee OA defined by JSN, concurrent knee pain and disability, as well as subsequent partial knee replacement or TKR.

Table 1. Study population (n = 4,791) demographics*

Characteristic	No. (%)	Characteristic	No. (%)
Sex		*(Right knees (n = 4,727) cont'd).*	
Male	1,992 (41.58)	JSN grade, lateral	
Female	2,799 (58.42)	0	4,067 (86.0)
Age range, years		1	175 (3.7)
45–49	549 (11.46)	2	147 (3.1)
50–54	867 (18.10)	3	52 (1.1)
55–59	794 (16.57)	Data missing	286 (6.1)
60–64	763 (15.93)	K/L grade	
65–69	699 (14.59)	0	1,672 (35.4)
70–74	684 (14.28)	1	791 (16.7)
75–79	435 (9.08)	2	1,225 (25.9)
Race		3	605 (12.8)
Caucasian	3,788 (79.06)	4	148 (3.1)
African American	871 (18.18)	Data missing	286 (6.1)
Asian	82 (1.71)	Left knees (n = 4,707)	
Other	45 (0.94)	JSN grade, medial	
Data missing	5 (0.10)	0	2,922 (62.1)
BMI, kg/m^2		1	884 (16.7)
<18.5	11 (0.23)	2	517 (25.9)
18.5–24.9	1,136 (23.71)	3	103 (12.8)
25–29.9	1,874 (39.11)	Data missing	281 (6.1)
30–34.9	1,262 (26.34)	JSN grade, lateral	
35–39.9	423 (8.83)	0	4,084 (86.8)
>40	81 (1.69)	1	193 (4.1)
Data missing	4 (0.08)	2	109 (2.3)
Right knees (n = 4,727)		3	40 (0.9)
JSN grade, medial		Data missing	281 (6.0)
0	2,837 (60.0)	K/L grade	
1	1,039 (22.0)	0	1,757 (37.3)
2	469 (9.9)	1	793 (16.8)
3	96 (2.0)	2	1,121 (23.8)
Data missing	286 (6.1)	3	614 (13.0)
		4	141 (3.0)
		Data missing	281 (6.0)

* Data on subjects from the Osteoarthritis Initiative were used for this study. BMI = body mass index; JSN = joint space narrowing; K/L = Kellgren/Lawrence scale.

PATIENTS AND METHODS

Study population. Data were obtained from the OAI, an NIH-funded observational study of patients with knee OA or those at-risk for knee OA. Study subjects included men and women ranging in age from 45 to 79 years with (or at-risk for) symptomatic tibiofemoral knee OA (Table 1). Minorities made up 20.9% of the population, of whom 87.3% were African American, 4.5% were Asian, and 8.2% were in the "Other" category. Subjects with contraindications for 3T MRI (such as inflammatory arthritis) were excluded from the OAI study (Table 1). The majority of knees at baseline had a Kellgren/Lawrence (K/L) radiographic severity grade (17) of 0–3, with a K/L grade of 4 making up ~3% of the population. Note that knees with information regarding K/L grade also had data regarding JSN grade. All subjects who had both K/L and JSN grades were included in the study. The severity of JSN was based on scores read centrally ranging from 0 to 3 (0 = normal, 1 = mild, 2 = moderate, and 3 = severe) by compartments (18).

MRI acquisition and measurements. Three-dimensional (3-D) dual-echo steady-state (DESS) sagittal MR sequences of the left and right knees were available from the OAI data set at baseline (n = 9,434 knees). All scans, along with the subject-level baseline clinical data, are available on the NIH website (https://nda.nih.gov/oai/) and can be forwarded upon request. We also obtained detailed segmentation masks of the femur cartilage, lateral tibia cartilage, and medial tibia cartilage for a small portion of knees from the OAI database (n = 88), which were used to train and validate the model. The cartilage and meniscal image masks were provided by the OA Biomarkers Consortium Foundation for the

National Institutes of Health Project and performed by iMorphics (Manchester, UK). As per the OAI documentation (https://nda.nih.gov/oai/study_documentation.html), knees were chosen to represent the OAI database population (primarily moderate and severe K/L grades; n = 45 men and 43 women) and should be applicable for the validation process of our study.

DESS sequence images provide detailed definition of 3-D structures and their shapes, particularly of cartilage morphology (19,20). Imaging was performed with a 3.0 Tesla magnet using imaging sequence with a repetition time/echo time of 16.3/4.7 msec. We selected knees (4,727 right knees and 4,707 left knees) from the OAI baseline examination with DESS sequence MR images. The DESS sequence provides high in-plane and out-of-plane resolution (0.7 mm × 0.365 mm × 0.456 mm) in a time-efficient manner. The images encompassed the cartilage of the knee joint as well as the subchondral structures of the tibia and the femur.

Image preprocessing and a fast region-based convolutional neural network. Image registration and quality check were performed on all knees as previously described (21). To focus the network on the joint area, a large-sized bounding box with dimensions of 272 × 240 pixels was created to identify regions of interest (ROIs) comprising all subchondral compartments containing the manually annotated femoral and tibia cartilage. Coordinates of the ROI of each knee were subsequently used to train a fast region-based convolutional neural network (Fast R-CNN) model (22) to automatically detect the region of the knee joint (Supplementary Figure 1, available on the *Arthritis & Rheumatology* website at http://onlinelibrary.wiley.com/doi/10.1002/art.41808/abstract). The sagittal MRI slices subsequently underwent histogram equalization, and their intensity values were normalized to a range of 0–1. These slices were then used as the inputs to the neural network used to extract the knee joint structures. More details are available in the Supplementary Figures.

Image annotation pipeline. In the OAI database, 88 knee MRIs had expert-driven annotations of the cartilage. These MRIs were chosen as our primary data set for training and validating the model for both automated segmentation of cartilage and bone shape (Supplementary Figure 2, http://onlinelibrary.wiley.com/doi/10.1002/art.41808/abstract). The 88 knee MRIs were randomly split using a ratio of 7:3 for training:validation. The 61 knee images used for training (1,753 2-D sagittal slices) were passed through an image-processing pipeline based on distance-regularized level set evolution (DRLSE) to extract the bone shapes (Supplementary Figure 3, http://onlinelibrary.wiley.com/doi/10.1002/art.41808/abstract). DRLSE is an edge-based active contour model that uses the gradient information of the images to expand the segmented area until it meets the boundary (23). Once the active contour model was applied, the obtained bone shapes were further manually verified and adjusted to exclude erroneously captured soft tissues in the bone shapes. Finally, the expert-driven segmented regions of cartilage and meniscal areas were superimposed to adjust the bone shapes, where needed. The modified bone shapes from the 61 cases were then used to train a deep neural network. The remaining cases (794 2-D sagittal slices from 27 knees) were used for model validation and underwent expert-assisted manual annotation of the bone shapes as detailed below.

Annotation of the knee structures. A board-certified radiologist (JS) manually annotated bone shapes of the knee on the 27 test cases. Using a stylus on a touch-screen device, the expert outlined the cortical surface of the tibia and the femur. We traced the SBLs on both the tibia and the femur to capture the shape of the cortical bone of the femur or the tibia in contact with the cartilage.

Deep learning framework for bone and cartilage shape segmentation. All subject data reviewed by the expert radiologist were used to train a deep neural network to simultaneously extract the bone and cartilage shapes of the tibia and the femur (Supplementary Figure 4, http://onlinelibrary.wiley.com/doi/10.1002/art.41808/abstract). The neural network was based on a well-known deep learning architecture (U-Net) (24) and has the capability to learn different patterns within imaging data. More details can be found in the Supplementary Figures.

Measurement of SBL. We extracted SBLs on both the tibia and femur to capture the shape of the cortical bone of the femur or tibia that is in contact with the cartilage. Briefly, we applied a distance transform on the output of the U-Net model to detect the edge of the bone region in contact with the cartilage. The distance transform measures the distance of each pixel on the bone from its closest pixel on the cartilage. We subsequently skeletonized the detected region to a thickness of 1 pixel and calculated its arc length. If there were multiple regions detected in the femur or tibia for a specific 2-D sagittal slice, then we skeletonized each region individually and summed the arc lengths of each segment as SBL. For instance, areas denuded of cartilage would produce a gap in bone length; thus, the computed SBL would be the sum of the segments of the cartilage-covered bone. These measurements were confirmed by the radiologist.

The SBL estimates for both the femur and tibia were extracted from each 2-D sagittal slice at various locations along the frontal axis (medial to lateral side) of each knee. The knees were further stratified by JSN grade within the medial and lateral compartments on the femur and tibia.

Statistical analysis. The deep neural network used for segmenting the bone shapes was evaluated by computing the Dice coefficient between the predicted masks (generated from the U-Net model) and the bone shapes outlined by the radiologist

on the test cases (n = 27). Descriptive statistics are presented as the mean ± SD. Student's *t*-test was used to compare the mean value of 2 different groups. *P* values less than 0.05 were considered significant. To compare SBLs between knees of various sizes, we obtained the calculated SBL values from the MRI slices where cartilage was visible and interpolated the values uniformly along the frontal axis. For SBLs obtained from the *n*th location along the frontal axis, we applied a *t*-test comparing SBLs of knees with only lateral JSN (374 right knees and 342 left knees) to knees with no JSN (5,128 right and left knees) and knees with only medial JSN (1,604 right knees and 1,504 left knees) to knees with no JSN (5,128 right and left knees).

We computed mean estimates of femur-specific and tibia-specific SBL measurements at each location on the frontal axis for all the knees with a JSN grade of 0. For each knee with a JSN grade >0, we computed difference between the SBL value measured at the *n*th location and the corresponding mean SBL estimate at that location in knees with a JSN grade of 0. We then added the absolute value of these differences to create knee-specific SBL measures and divided them into quartiles. Each group (medial or lateral JSN cases) was further stratified based on clinical outcomes, which included baseline pain and disability scores (according to the Western Ontario and McMaster Universities Osteoarthritis Index [25]) and future TKR. The baseline pain and disability scores were divided by severity, such that pain scores ≥4–<8 were considered moderate, and those ≥8 were severe. Similarly, disability scores ≥20–<35 were moderate, and those ≥35 were severe (11). The criterion for future TKR was the subject having a knee replacement seen on follow-up radiography at any time during an 8-year follow-up after baseline.

We calculated odds ratios (ORs) by comparing the odds of each quartile developing the various outcomes, using quartile 1 as a reference, and 95% confidence intervals (95% CIs) were determined. ORs were calculated using a 2 × 2 contingency table with binomial outcomes for the pain and disability scores, such that 1 outcome was compared to the remaining outcomes in its corresponding category. For example, the odds of having moderate pain were compared to no pain and severe pain combined. Severe pain was compared to the combination of moderate and no pain. *P* values were calculated using Fisher's exact test. Python scripts are available on GitHub (https://github.com/vkola-lab/ar2021).

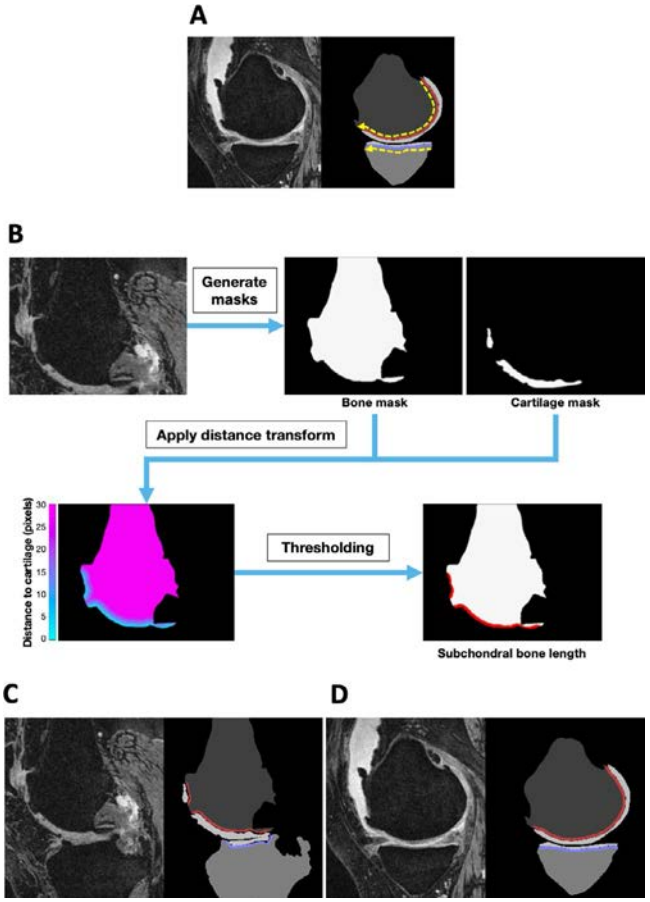

Figure 1. Subchondral bone length (SBL). **A**, A magnetic resonance imaging (MRI) slice in the sagittal plane, with traced SBLs on both the femur (red line) and tibia (blue line). Dotted lines show the direction of tracing to obtain the SBLs on the femur and tibia. **B**, Estimation of SBL by performing a distance transform using masks of the bone and cartilage. **C** and **D**, Examples of the original MRI slices (sagittal view) along with the respective masks generated by the deep learning model. Note the exclusion of the gap in cartilage coverage caused by a protruding central osteophyte in **C** and the exclusion of the anterior marginal osteophyte in **D**. SBL is shown as a red line on the femur and a blue line on the tibia.

RESULTS

Manual versus automated segmentation. Using the deep learning framework, we estimated the bone shapes defining the tibiofemoral joint (Supplementary Figure 5, http://onlinelibrary.wiley.com/doi/10.1002/art.41808/abstract). The Dice coefficients for the femur cartilage, medial tibia cartilage, and lateral tibia cartilage, using the U-Net model, were 0.903, 0.913, and 0.873, respectively. Comparison of the manual annotation and automated segmentation of the femur, tibia, and meniscus with Dice coefficients demonstrated the similarity between the predicted and expert-driven segmentations for the U-Net model. Figures 1C and D show SBLs connected with femoral and tibial cartilage. In a further comparison between the respective masks generated by the U-Net model (predicted) and the expert-driven hand-annotated images, scatter plots were generated with the measured SBL of each MRI slice of the reference estimate against predicted values (n = 27 subjects). Reference estimate versus predicted SBL of the femur generated an R^2 value of 0.922 (Supplementary Figure 6A, http://onlinelibrary.wiley.com/doi/10.1002/art.41808/abstract). Much of the discrepancy between the reference estimate from the radiologist versus predicted SBL values occurred at the extreme medial and lateral sagittal slices (SBL length <50 pixels). This pattern was consistent with the findings in tibial SBL (R^2 = 0.902) (Supplementary Figure 6B), with higher discrepancies

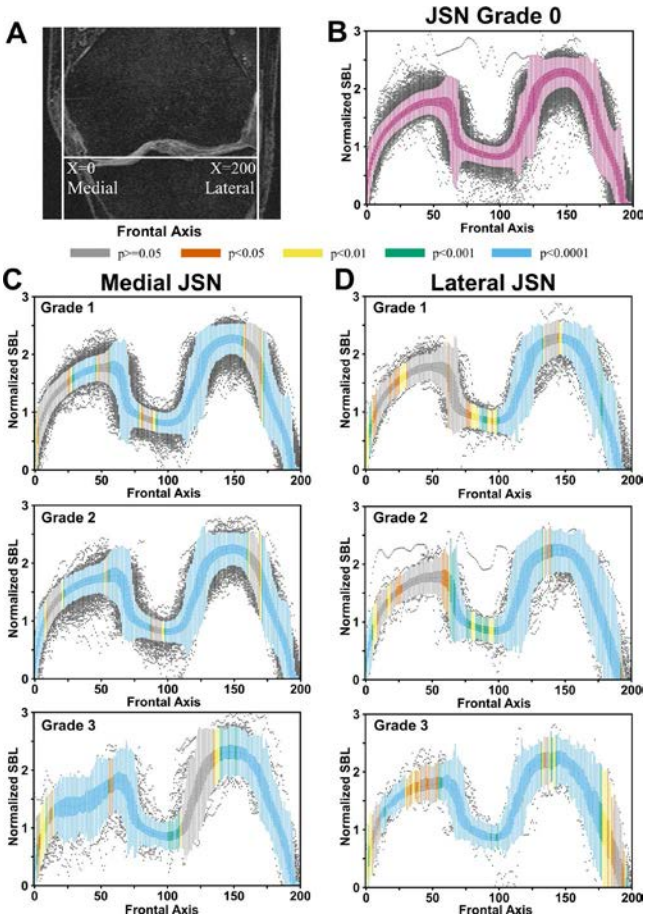

Figure 2. Distribution of subchondral bone lengths (SBLs) on the femur. **A**, Placement of the normalized x-axis on the magnetic resonance imaging (MRI) slices. For each location on the x-axis shown in the frontal axis, SBLs were computed on the sagittal slices for all knees. Two hundred total locations were chosen along the frontal axis. **B**, Normalized femoral SBL values plotted along the frontal axis for joint space narrowing (JSN) grade 0. **C**, Normalized SBL values plotted along the frontal axis for different grades of medial JSN. **D**, Normalized SBL values plotted along the frontal axis for different grades of lateral JSN. SBL normalization was performed by dividing the SBL estimated per slice by the summation of all femur and tibial SBLs for a given knee. Color coding at each location denotes the *P* value computed using the corresponding location on the JSN grade 0 plot as the reference.

seen at SBLs <25 pixels. These correspond to lateral-most and medial-most slices of the knees.

SBL in relation to joint space narrowing. Our analysis showed that most SBL values from knees with JSN grades >0 were significantly different in length than knees with no JSN for both the femur and tibia (Figures 2B–D and Figures 3B–D). This was true for knees with both medial and lateral JSN. In cases of medial JSN, on the femur we observed significant differences in SBL values for most of the medial-central, central, and lateral-most regions of the femur (Figure 2C). In the cases of lateral JSN, SBL values were significantly different from knees with grade 0 JSN in most of the lateral regions of the femur (Figure 2D), except for a few lateral-most regions for knees with grade 3 JSN. For cases with lateral JSN, statistically significant differences were not observed in most of the medial-central regions of the femur, regardless of the JSN grade (Figure 2D).

In cases of medial JSN on the tibia, we observed statistically significant differences in the medial and central regions for JSN grades >1 but only in the central regions for grade 1 JSN (Figure 3C). No significant differences were observed in the medial-central and the lateral-central regions for JSN grade 1 (Figure 3C). In cases of lateral JSN in the tibia, differences were observed in the medial-most and lateral-most regions for all JSN grades (Figure 3D). The variability in the SBL estimates seemed highest for medial-central and medial-most regions when there

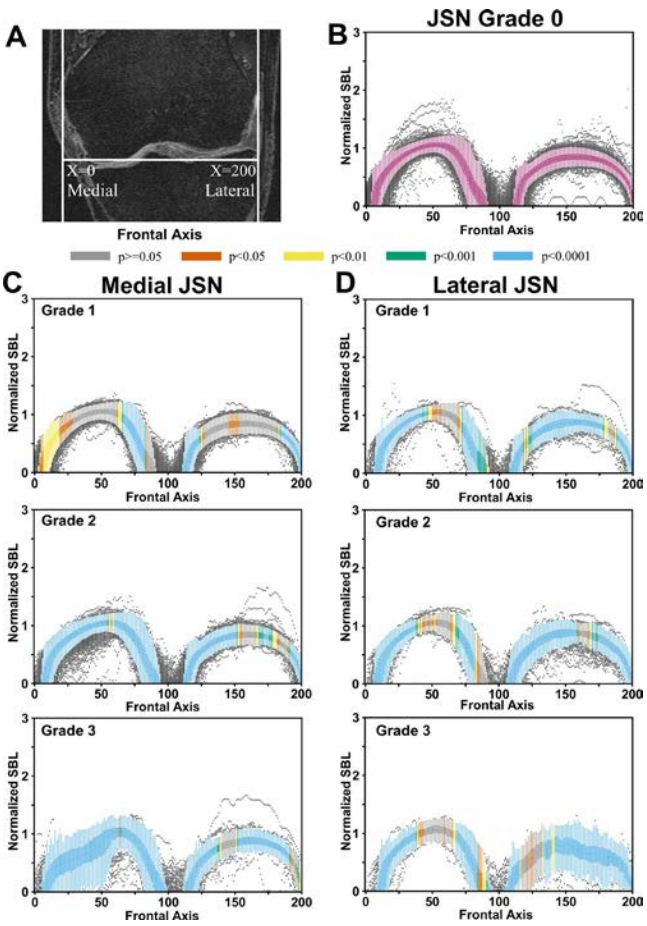

Figure 3. Distribution of SBLs on the tibia. **A**, Placement of the normalized x-axis on the MRI slices. For each location on the x-axis shown in the frontal axis, SBLs were computed on the sagittal slices for all knees. Two hundred total locations were chosen along the frontal axis. **B**, Normalized tibial SBL values plotted along the frontal axis for JSN grade 0. **C**, Normalized SBL values plotted along the frontal axis for different grades of medial JSN. **D**, Normalized SBL values plotted along the frontal axis for different grades of lateral JSN. SBL normalization was performed by dividing the SBL estimated per slice by the summation of all femur and tibial SBLs for a given knee. Color coding at each location denotes the *P* value computed using the corresponding location on the JSN grade 0 plot as the reference. See Figure 2 for definitions.

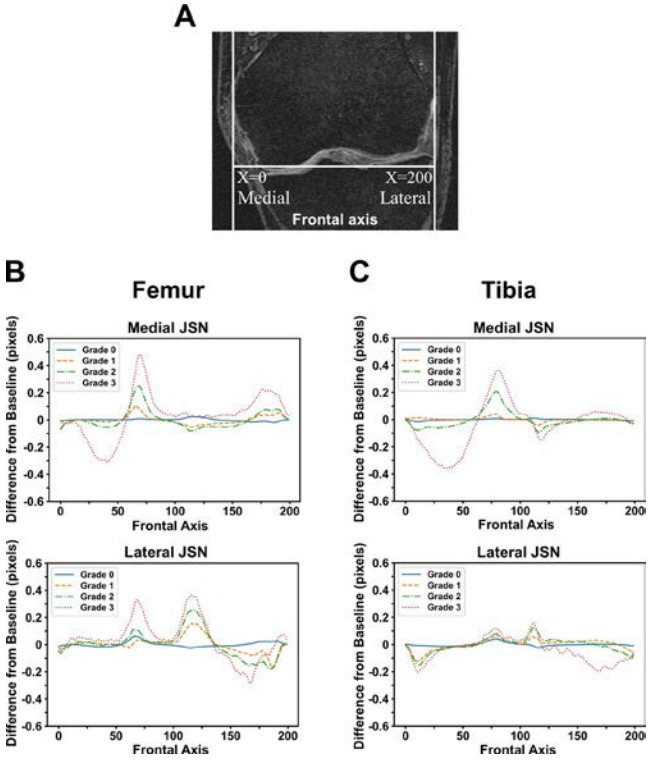

Figure 4. Differences in mean SBLs. **A**, Placement of the normalized x-axis on the MRI slices. **B**, Difference in mean femoral SBLs compared between subjects with different grades of medial or lateral JSN. **C**, Difference in mean tibial SBLs compared between subjects with different grades of medial or lateral JSN. Two hundred total locations were chosen along the frontal axis. The units of the mean SBL values plotted on the y-axis are the number of MRI pixels separating the mean SBL in knees with the given JSN grade. See Figure 2 for definitions.

was medial JSN, and in the lateral-central and lateral-most regions when there was lateral grade 3 JSN in the tibia (Figures 3C and D).

When we further examined the mean differences along the frontal axis for the femur and tibia, the variability in SBL distribution increased with JSN grade. Notably, subjects with grade 3 JSN had mean SBL values with higher peaks and troughs than JSN grades <3, regardless of the location of JSN (Figure 4). For medial grade 3 JSN in the femur and tibia, the trough was in the middle of the medial compartment, whereas for lateral grade 3 JSN, it was in the far lateral part of the lateral compartment. SBL values closer to the middle of the knee in the frontal axis showed an increase in SBL compared with grade 0 JSN (Figures 4B and C). While reductions in SBLs were seen in some locations within the affected compartments, regions near the middle of the knee often showed increased SBL lengths compared with knees that had grade 0 JSN.

SBL in relation to outcomes. In subjects with medial JSN, the ORs for moderate pain and disability were highest for knees in the highest SBL quartile (Table 2 and Supplementary Table 1, http://onlinelibrary.wiley.com/doi/10.1002/art.41808/abstract). Among knees with a medial JSN grade >0, the odds of severe pain at baseline increased with increasing quartiles of SBL, increasing about 4-fold for knees in the highest quartile (OR 4.09 [95% CI 2.88–5.79]). The ORs for severe disability showed a similar pattern. Among these knees, the odds of future TKR increased with increasing SBLs, rising to 5.68 (95% CI 3.90–8.27) for knees in the highest quartile. For knees with lateral JSN, the pattern was similar, with increasing odds of pain and disability and increased odds of TKR for knees with higher SBLs (Table 2).

DISCUSSION

In this work, we introduced a new MRI-derived bone measure, SBL, by leveraging a deep learning–based image segmentation framework and expert-driven annotations of structures comprising the knee joint. SBL depicts both tibiofemoral articular cartilage morphology and bone shape, as it reflects the cartilage-covered articular area translated to length by excluding osteophytes and denuded areas. As accurate manual segmentation of MRI studies can be highly labor-intensive, there have been several efforts to develop computational methods for automating the segmentation and measurement of knee structures, with specific focus on the cartilage and the meniscus (26–33) and other structures of the knee joint (27,34–36). We performed additional analyses to show that SBL values at different locations of the knee vary in magnitude as a function of JSN grade in both the femur and tibia. Finally, we showed that high mean SBL values identify knees with a high risk of pain and disability and with an increased risk of later TKR.

Imaging biomarkers visualized solely on MRI, such as subchondral changes, cartilage volume, and bone marrow lesions, have been found to have better correlation with symptomatic presentation in patients compared to radiographic findings such as K/L grade (37). If we measure subchondral changes on MRI at the slice level, then we can expand the range of analyses by considering how specific regions of the subchondral bone correlate with the progression and outcomes of knee OA. Our work is unique in focusing on SBL as a shape measure and provides novel insights into areas where bone length changes with increasing disease severity. There are 2 factors affecting this planar bone length measure: cartilage loss, which creates gaps in bone length and shortens it, and flattening of the bone, which can have the opposite effect, causing an increase in length. Since SBL shows shortening only with complete local loss of cartilage and not cartilage thinning, the dominant effect of disease is to cause SBL lengthening. Because of flattening, the bone lengthens in affected compartments even with removal of osteophytes (15).

We observed that mean SBL values displayed an interesting dynamic in knees with JSN grades >0 versus those with grade 0 JSN, suggesting that cartilage loss and increased bone length both drive this measure. Consistent with findings from studies in

Table 2. Association of SBL with various outcomes*

Condition and outcome	Quartile 2, OR (95% CI)	Quartile 3, OR (95% CI)	Quartile 4, OR (95% CI)
JSN grade, medial (≥1)			
Moderate pain (≥4–<8)	0.90 (0.69–1.17)	1.31 (1.02–1.68)†	1.60 (1.26–2.04)‡
Severe pain (≥8)	2.49 (1.72–3.58)‡	2.24 (1.55–3.24)‡	4.09 (2.88–5.79)‡
Moderate disability (≥20–<35)	1.10 (0.81–1.50)	1.51 (1.13–2.02)‡	1.86 (1.40–2.48)‡
Severe disability (≥35)	2.90 (1.60–5.28)‡	2.47 (1.34–4.55)‡	4.33 (2.44–7.68)‡
Future TKR	1.45 (0.93–2.24)	2.53 (1.69–3.78)‡	5.68 (3.90–8.27)‡
JSN grade, lateral (≥1)			
Moderate pain (≥4–<8)	1.29 (0.79–2.11)	1.29 (0.79–2.11)	1.49 (0.91–2.42)
Severe pain (≥8)	1.40 (0.72–2.73)	1.92 (1.02–3.62)	3.11 (1.70–5.68)‡
Moderate disability (≥20–<35)	1.17 (0.62–2.22)	1.86 (1.03–3.38)	2.51 (1.41–4.48)‡
Severe disability (≥35)	2.28 (0.78–6.70)	2.06 (0.69–6.15)	3.89 (1.41–10.72)‡
Future TKR	2.36 (1.15–4.85)†	2.15 (1.04–4.46)	7.19 (3.71–13.95)‡

* Quartiles represent change in subchondral bone length (SBL) from lowest to highest (quartile 2 to quartile 4, with quartile 1 as reference). OR = odds ratio; 95% CI = 95% confidence interval; JSN = joint space narrowing; TKR = total knee replacement.
† $P < 0.05$.
‡ $P < 0.001$.

which cartilage loss occurs with advancing OA (38), the mean SBL was shorter in the peripheral subregions of the knee. Additionally, mean SBL values followed a trend in which the peaks occurred consistently at similar locations along the frontal axis, where the magnitude of these peaks was a function of the JSN grade. We would expect, with increasing cartilage loss, that SBL would decrease but also increase due to bone flattening. Since the odds of TKR and other outcomes increased with increasing SBL, it implies that SBL changes were predominantly influenced by bone flattening. The same reasoning would apply to decreasing joint space widening based on Osteoarthritis Research International scales (3,4), such that SBL would be expected to increase in those cases as well. Nevertheless, understanding region-specific subchondral bone lengthening with developing disease may provide insights into how bone response to loading affects disease in different regions of the knee.

SBL shows promise as an imaging measure to analyze OA. It allows for feasible statistical analysis of both the amount of exposed bone from cartilage loss and the remodeling of the cortical envelope that occurs as part of the disease process. By utilizing the length instead of the subchondral surface area, it becomes straightforward to derive insights based on slice location into common regions of joint degeneration in different presentations of knee OA. Because SBL was derived by excluding marginal osteophytes, this shape measure is distinct from other published measures of bone shape dependent on the crust of the osteophytes around the edges of the articular cartilage (8). Marginal osteophytes do not appear to be related to joint pain. Furthermore, atrophic and hypertrophic forms of disease have similar levels of cartilage loss, and studies suggest that marginal osteophytes are often not in the same compartment as cartilage loss and can even occur with no loss (14). Finally, molecular stimuli of osteophyte growth often have no measurable effect on cartilage loss (39,40). SBL measurement may become more relevant because this feature could facilitate future studies related to quantifying the effects of subchondral bone changes on transarticular loading patterns across the knee and provide a better understanding of OA progression.

From the OAI database, we acquired demographic data that allowed for analysis of correlations between JSN and sex, age, race, and body mass index. Using our U-Net model, we could also apply automated segmentation to find correlations between specific knee structure changes in OA with other biomarkers. These correlations can be used to determine risk factors and individual susceptibility to develop knee OA. It would also be possible to visualize biomarker changes in relation to bone structure over time. Since the entire process is automated, these analyses can be conducted in an efficient manner.

One of the main challenges in applying deep learning to perform automated segmentation of medical imaging is the lack of high-volume expert-annotated data. To circumvent this, we adapted an efficient strategy by using the DRLSE method in combination with human verification to generate a large volume of bone annotations from the MRIs of 61 knees to train the U-Net model. The automated segmentations of bone and cartilage from the U-Net were subsequently compared to the annotation of an expert radiologist, which showed high accuracy in terms of the Dice coefficient.

There are a few limitations to our study. Our deep learning framework is based on a 2-D U-Net architecture, and recent studies have attempted to employ more advanced frameworks involving 3-D neural network architectures for image segmentation tasks (27). However, the selection of the 2-D architecture was sufficient to develop SBL as a novel 2-D shape measure. Additionally, more studies are needed to understand the distributions of mean SBL values for various grades of disease and to evaluate whether this effect is due to cartilage loss or flattening of the bone or some combination of both. There are some areas of the knee

where SBL measurement is likely to be challenging. These areas correspond to subchondral sagittal slices at the medial-most and lateral-most aspects of the knee. It is at this region that the defining border between cartilage and bone becomes unclear, thus complicating the segmentation process for radiologists as well as our automated segmentation model. Furthermore, these portions of the knee are common locations for the development of osteophytes, leading to irregular SBL that may lead to variability and poor correlation with scoring systems that utilize osteophytes as a factor.

In conclusion, our study demonstrates the ability for a deep learning framework to learn from expert-driven annotations and extend it to generating a quantitative understanding of the knee joint structures across a large cohort. Such extensions have the potential to generate statistically significant representations of knee joint shapes without having to manually process imaging data from all the cases. As an example, we identified SBL as a potentially useful measure of the subchondral bone morphology within the knee joint and showed that it varies according to JSN grade. Our findings can assist in a more detailed quantification of shape-specific risk factors of knee OA.

AUTHOR CONTRIBUTIONS

All authors were involved in drafting the article or revising it critically for important intellectual content, and all authors approved the final version to be published. Dr. Kolachalama had full access to all of the data in the study and takes responsibility for the integrity of the data and the accuracy of the data analysis.

Study conception and design. Chang, Park, Le, Felson, Kolachalama.
Acquisition of data. Chang, Park, Le, Lai, Seo, Promchotichai, Capellini, Kolachalama.
Analysis and interpretation of data. Chang, Park, Le, Jhun, Surendran, Yoon, Scalera, Felson, Kolachalama.

REFERENCES

1. Peat G, McCarney R, Croft P. Knee pain and osteoarthritis in older adults: a review of community burden and current use of primary health care [review]. Ann Rheum Dis 2001;60:91–7.
2. Sowers MR, Karvonen-Gutierrez CA. The evolving role of obesity in knee osteoarthritis [review]. Curr Opin Rheumatol 2010;22:533–7.
3. Bannuru RR, Osani MC, Vaysbrot EE, Arden NK, Bennell K, Bierma-Zeinstra SM, et al. OARSI guidelines for the non-surgical management of knee, hip, and polyarticular osteoarthritis. Osteoarthritis Cartilage 2019;27:1578–89.
4. McAlindon TE, Bannuru RR, Sullivan MC, Arden NK, Berenbaum F, Bierma-Zeinstra SM, et al. OARSI guidelines for the non-surgical management of knee osteoarthritis. Osteoarthritis Cartilage 2014;22:363–88.
5. Wolfe F, Lane NE. The longterm outcome of osteoarthritis: rates and predictors of joint space narrowing in symptomatic patients with knee osteoarthritis. J Rheumatol 2002;29:139–46.
6. Zhang W, Moskowitz RW, Nuki G, Abramson S, Altman RD, Arden N, et al. OARSI recommendations for the management of hip and knee osteoarthritis, Part II: OARSI evidence-based, expert consensus guidelines [review]. Osteoarthritis Cartilage 2008;16:137–62.
7. Roemer FW, Demehri S, Omoumi P, Link TM, Kijowski R, Saarakkala S, et al. State of the art: imaging of osteoarthritis-revisited 2020. Radiology 2020;296:5–21.
8. Neogi T, Bowes MA, Niu J, De Souza KM, Vincent GR, Goggins J, et al. Magnetic resonance imaging–based three-dimensional bone shape of the knee predicts onset of knee osteoarthritis: data from the osteoarthritis initiative. Arthritis Rheum 2013;65:2048–58.
9. Reichenbach S, Guermazi A, Niu J, Neogi T, Hunter DJ, Roemer FW, et al. Prevalence of bone attrition on knee radiographs and MRI in a community-based cohort. Osteoarthritis Cartilage 2008;16:1005–10.
10. Tummala S, Bay-Jensen AC, Karsdal MA, Dam EB. Diagnosis of osteoarthritis by cartilage surface smoothness quantified automatically from knee MRI. Cartilage 2011;2:50–9.
11. Bowes MA, Kacena K, Alabas OA, Brett AD, Dube B, Bodick N, et al. Machine-learning, MRI bone shape and important clinical outcomes in osteoarthritis: data from the Osteoarthritis Initiative. Ann Rheum Dis 2020;80:502–8.
12. Conaghan PG, Bowes MA, Kingsbury SR, Brett A, Guillard G, Rizoska B, et al. Disease-modifying effects of a novel cathepsin K inhibitor in osteoarthritis: a randomized controlled trial. Ann Intern Med 2020;172:86–95.
13. Sengupta M, Zhang YQ, Niu JB, Guermazi A, Grigorian M, Gale D, et al. High signal in knee osteophytes is not associated with knee pain. Osteoarthritis Cartilage 2006;14:413–7.
14. Markhardt BK, Li G, Kijowski R. The clinical significance of osteophytes in compartments of the knee joint with normal articular cartilage. AJR Am J Roentgenol 2018;210:W164–71.
15. Hudelmaier M, Wirth W. Differences in subchondral bone size after one year in osteoarthritic and healthy knees. Osteoarthritis Cartilage 2016;24:623–30.
16. Hunter D, Nevitt M, Lynch J, Kraus VB, Katz JN, Collins JE, et al. Longitudinal validation of periarticular bone area and 3D shape as biomarkers for knee OA progression? Data from the FNIH OA Biomarkers Consortium. Ann Rheum Dis 2016;75:1607–14.
17. Kellgren JH, Lawrence JS. Radiological assessment of osteoarthrosis. Ann Rheum Dis 1957;16:494–502.
18. Altman RD, Gold GE. Atlas of individual radiographic features in osteoarthritis, revised. Osteoarthritis Cartilage 2007;15 Suppl A:A1–56.
19. Eckstein F, Hudelmaier M, Wirth W, Kiefer B, Jackson R, Yu J, et al. Double echo steady state magnetic resonance imaging of knee articular cartilage at 3 Tesla: a pilot study for the Osteoarthritis Initiative. Ann Rheum Dis 2006;65:433–41.
20. Peterfy CG, Schneider E, Nevitt M. The osteoarthritis initiative: report on the design rationale for the magnetic resonance imaging protocol for the knee [review]. Osteoarthritis Cartilage 2008;16:1433–41.
21. Chang GH, Felson DT, Qiu S, Guermazi A, Capellini TD, Kolachalama VB. Assessment of knee pain from MR imaging using a convolutional Siamese network. Eur Radiol 2020;30:3538–48.
22. Girshick R. Fast R-CNN. December 2015. URL: https://ieeexplore.ieee.org/document/7410526.
23. Li C, Xu C, Gui C, Fox MD. Distance regularized level set evolution and its application to image segmentation. IEEE Trans Image Process 2010;19:3243–54.
24. Ronneberger O, Fischer P, Brox T. U-Net: convolutional networks for biomedical image segmentation. In: Navab N, Hornegger J, Wells W, Frangi A, editors. Medical image computing and computer-assisted intervention–MICCAI 2015. Switzerland: Springer, Cham; 2015. p. 234–41.
25. Bellamy N, Buchanan WW, Goldsmith CH, Campbell J, Stitt LW. Validation study of WOMAC: a health status instrument for measuring clinically important patient relevant outcomes to antirheumatic drug therapy in patients with osteoarthritis of the hip or knee. J Rheumatol 1988;15:1833–40.

26. Prasoon A, Petersen K, Igel C, Lauze F, Dam E, Nielsen M. Deep feature learning for knee cartilage segmentation using a triplanar convolutional neural network. Med Image Comput Comput Assist Interv 2013;16:246–53.
27. Ambellan F, Tack A, Ehlke M, Zachow S. Automated segmentation of knee bone and cartilage combining statistical shape knowledge and convolutional neural networks: data from the Osteoarthritis Initiative. Med Image Anal 2019;52:109–18.
28. Norman B, Pedoia V, Majumdar S. Use of 2D U-Net convolutional neural networks for automated cartilage and meniscus segmentation of knee MR imaging data to determine relaxometry and morphometry. Radiology 2018;288:177–85.
29. Rahman MM, Durselen L, Seitz AM. Automatic segmentation of knee menisci: a systematic review [review]. Artif Intell Med 2020;105:101849.
30. Tack A, Mukhopadhyay A, Zachow S. Knee menisci segmentation using convolutional neural networks: data from the Osteoarthritis Initiative. Osteoarthritis Cartilage 2018;26:680–8.
31. Gaj S, Yang M, Nakamura K, Li X. Automated cartilage and meniscus segmentation of knee MRI with conditional generative adversarial networks. Magn Reson Med 2020;84:437–49.
32. Ebrahimkhani S, Jaward MH, Cicuttini FM, Dharmaratne A, Wang Y, de Herrera AG. A review on segmentation of knee articular cartilage: from conventional methods towards deep learning [review]. Artif Intell Med 2020;106:101851.
33. Liu F, Zhou Z, Samsonov A, Blankenbaker D, Larison W, Kanarek A, et al. Deep learning approach for evaluating knee MR images: achieving high diagnostic performance for cartilage lesion detection. Radiology 2018;289:160–9.
34. Liu F, Zhou Z, Jang H, Samsonov A, Zhao G, Kijowski R. Deep convolutional neural network and 3D deformable approach for tissue segmentation in musculoskeletal magnetic resonance imaging. Magn Reson Med 2018;79:2379–91.
35. Martinez AM, Caliva F, Flament I, Liu F, Lee J, Cao P, et al. Learning osteoarthritis imaging biomarkers from bone surface spherical encoding. Magn Reson Med 2020;84:2190–203.
36. Zhou Z, Zhao G, Kijowski R, Liu F. Deep convolutional neural network for segmentation of knee joint anatomy. Magn Reson Med 2018;80:2759–70.
37. Wang X, Oo WM, Linklater JM. What is the role of imaging in the clinical diagnosis of osteoarthritis and disease management? [review]. Rheumatology (Oxford) 2018;57 Suppl 4:iv51–60.
38. Cotofana S, Buck R, Wirth W, Roemer F, Duryea J, Nevitt M, et al, for the Osteoarthritis Initiative Investigators Group. Cartilage thickening in early radiographic knee osteoarthritis: a within-person, between-knee comparison. Arthritis Care Res (Hoboken) 2012;64:1681–90.
39. Davidson EN, Vitters EL, Bennink MB, van Lent PL, van Caam AP, Blom AB, et al. Inducible chondrocyte-specific overexpression of BMP2 in young mice results in severe aggravation of osteophyte formation in experimental OA without altering cartilage damage. Ann Rheum Dis 2015;74:1257–64.
40. Zhou S, Wang Z, Tang J, Li W, Huang J, Xu W, et al. Exogenous fibroblast growth factor 9 attenuates cartilage degradation and aggravates osteophyte formation in post-traumatic osteoarthritis. Osteoarthritis Cartilage 2016;24:2181–92.

Arthritis & Rheumatology
Vol. 73, No. 12, December 2021, pp 2249–2260
DOI 10.1002/art.41794
© 2021, American College of Rheumatology

American College of Rheumatology
Empowering Rheumatology Professionals

Amelioration of Posttraumatic Osteoarthritis in Mice Using Intraarticular Silencing of Periostin via Nanoparticle-Based Small Interfering RNA

Xin Duan,[1] Lei Cai,[1] Christine T. N. Pham,[1] Yousef Abu-Amer,[2] Hua Pan,[3] Robert H. Brophy,[1] Samuel A. Wickline,[3] and Muhammad Farooq Rai[1]

Objective. Recent evidence delineates an emerging role of periostin in osteoarthritis (OA), since its expression after knee injury is detrimental to the articular cartilage. We undertook this study to examine whether intraarticular (IA) knockdown of periostin would ameliorate posttraumatic OA in a murine model.

Methods. Posttraumatic OA was induced in 10-week-old male C57BL/6J mice (n = 24) by destabilization of the medial meniscus (DMM), and mice were analyzed 8 weeks after surgery. Periostin expression was inhibited by small interfering RNA (siRNA) delivered IA using a novel peptide–nucleotide polyplex. Following histologic assessment of the mouse knee cartilage, the extent of cartilage degeneration was determined using Osteoarthritis Research Society International (OARSI) cartilage damage score, and severity of synovitis was also assessed. Bone changes were measured using micro–computed tomography. The effect and mechanism of periostin silencing were investigated in human chondrocytes that had been stimulated with interleukin-1β (IL-1β) with or without the IκB kinase 2 inhibitor SC-514.

Results. Periostin expression in mice with posttraumatic OA was significantly abolished using IA delivery of a peptide–siRNA nanoplatform. OARSI cartilage damage scores were significantly lower in mice receiving periostin siRNA (mean ± SEM 10.94 ± 0.66) compared to untreated mice (22.38 ± 1.30) and mice treated with scrambled siRNA (22.69 ± 0.87) (each $P = 0.002$). No differences in the severity of synovitis were observed. Subchondral bone sclerosis, bone volume/total volume, volumetric bone mineral density, and heterotopic ossification were significantly lower in mice that had received periostin siRNA treatment. Immunostaining of cartilage revealed that periostin knockdown reduced the intensity of DMM-induced matrix metalloproteinase 13 (MMP-13) expression and also diminished the phosphorylation of p65 and immunoreactivity of the aggrecan neoepitope DIPEN. Periostin knockdown also suppressed IL-1β–induced MMP-13 and ADAMTS-4 expression in chondrocytes. Mechanistically, periostin-induced MMP-13 expression was abrogated by SC-514, demonstrating a link between periostin and NF-κB.

Conclusion. IA delivery of the periostin–siRNA nanocomplex represents a promising clinical approach to mitigate the severity of joint degeneration in OA. Our findings may thus provide an unequivocal scientific rationale for longitudinal studies of this approach. Utilizing a cartilage-specific gene-knockout strategy will further illuminate the functional role of periostin in OA.

INTRODUCTION

Osteoarthritis (OA) is a painful degenerative disease that affects the diarthrodial joints and is one of the leading causes of disability and financial burden around the globe. It affects >50 million Americans, and its prevalence is projected to increase to 78 million Americans by 2040 (1). Current treatment options for OA are not optimal, and no disease-modifying OA therapy has

The content of this article is solely the responsibility of the authors and does not necessarily represent the official views of the NIH, National Institute of Arthritis and Musculoskeletal and Skin Diseases, or the Shriners Hospitals for Children.

Supported by the NIH (grants R01-AR-067491, DK-102691, P30-AR-073752, and P30-AR-074992 and National Center for Research Resources grant 1S10-RR-027552) and the Department of Orthopedic Surgery at the Washington University School of Medicine. Dr. Abu-Amer's work was supported by the NIH (grants AR-049192 and AR-072623) and the Shriners Hospitals for Children (grant 85160). Dr. Rai's work was supported by the NIH (National Institute of Arthritis and Musculoskeletal and Skin Diseases Pathway to Independence Award R00-AR-064837).

[1]Xin Duan, PhD, Lei Cai, PhD, Christine T. N. Pham, MD, Robert H. Brophy, MD, Muhammad Farooq Rai, PhD: Washington University, St. Louis, Missouri; [2]Yousef Abu-Amer, PhD: Washington University and Shriners Hospitals for Children–St. Louis, St. Louis, Missouri; [3]Hua Pan, PhD, Samuel A. Wickline, MD: University of South Florida, Tampa.

No potential conflicts of interest relevant to this article were reported.

Address correspondence to Muhammad Farooq Rai, PhD, Washington University School of Medicine at Barnes Jewish Hospital, Musculoskeletal Research Center, Department of Orthopaedic Surgery, Mail Stop 8233, 425 South Euclid Avenue, St. Louis, MO 63110. Email: rai.m@wustl.edu.

Submitted for publication October 14, 2020; accepted in revised form April 29, 2021.

successfully completed clinical trials (2). Presently, the focus of OA treatment continues to be on established, late-stage disease, which is often recalcitrant to medical therapy and generally entails costly surgical intervention, such as arthroplasty, to maintain or restore joint mobility.

We believe pharmacologic intervention represents a more cost-effective approach, but it would require targeting etiologic pathways of early, preradiographic OA, prior to irreversible structural joint damage. Posttraumatic OA—which accounts for ~12% of all OA cases—develops after joint injury and is particularly prevalent in young active adults (3). Joint injury initiates molecular changes that lead to posttraumatic OA over the course of 10–15 years (4,5). In posttraumatic OA, the nature and time of trauma is generally known (4), thus offering a unique window into the early events that are potentially reversible and amenable to disease-modifying therapy.

Recent studies have shown an emerging role of matricellular and matrix proteins, which regulate important chondrocyte functions (6). Periostin is a matricellular secretory matrix protein expressed by mesenchymal stem cells and periosteum (7,8). Emerging evidence indicates that periostin expression is increased in human OA (9–14). In addition, studies have shown that expression of periostin is increased in the cartilage matrix following knee injury in mice, suggesting it has a catabolic role in OA progression (13,15,16). We recently measured and reported on periostin expression in patients with an anterior cruciate ligament (ACL) tear—a common joint injury that often leads to posttraumatic OA. We found that expression of periostin was relatively low in the first month after injury, then increased within the first 3 months following injury, peaked at 3–6 months following injury, and then significantly declined (17). Therefore, we believe early intervention after joint injury will prevent the disease sequelae before irreversible damage occurs.

Although a complete understanding of the mechanism of action of periostin in regulating catabolic processes in the human joints remains elusive, some in vitro data indicate that periostin gain-of-function in chondrocytes increases expression of matrix metalloproteinase 13 (MMP-13). In contrast, periostin loss-of-function reduces interleukin-1β (IL-1β)–induced MMP-13 expression (15,16), which introduces the possibility that it affects NF-κB signaling. While periostin appears to be an attractive therapeutic target in joint degeneration, to date, no study has investigated the protective effects of periostin knockdown in vivo.

Given the catabolic role of periostin in OA, we hypothesized that intraarticular (IA) knockdown of periostin would reduce joint degeneration. To test this hypothesis, we examined the protective effects of periostin knockdown on cartilage degeneration in a murine model of posttraumatic OA. Moreover, we gained insights into the effects of periostin knockdown on the expression of MMP-13 and NF-κB pathways. To achieve periostin knockdown in cells and in the joint, we used RNA interference (RNAi) technology. RNAi effectively induces posttranscriptional sequence-specific gene silencing with a high degree of specificity using small interfering RNA (siRNA) (18,19). The siRNA was delivered by a nanocarrier platform (20) consisting of a peptide-based self-assembled oligonucleotide nanocomplex that penetrates cartilage to deliver siRNA to chondrocytes (21,22). The results of this study show that IA knockdown of periostin in mice ameliorates cartilage degradation and mitigates changes in the bone. Mechanistically, our findings demonstrate that suppressing periostin dampens the inflammatory NF-κB–MMP-13 signaling axis.

MATERIALS AND METHODS

Ethics statement. All animal procedures were performed following provision of ethics and statutory approval from the Washington University Institutional Animal Care and Use Committee (approval no. 20190113). All efforts were made to minimize animal suffering during this study. The institutional review board approved the use of discarded human cartilage specimens (approval no. 201104119). All patients provided written and signed informed consent prior to participation.

Mice. C57BL/6J mice were obtained from The Jackson Laboratory. Mice were housed in individually ventilated cages, with each cage containing 2–4 mice. All mice were housed in the animal husbandry facility operating at 21–22°C and were maintained on a 12-hour light/dark cycle with unrestricted food and water intake.

Generation of p5RHH–siRNA nanoparticles. We used an engineered cationic amphipathic peptide (VLTTGLPALISWIRRRHRRHC) designated p5RHH (23,24) as a vehicle for siRNAs. The p5RHH peptide that forms a polyplex with siRNAs was synthesized by GenScript. These peptide nanoparticles have been used for efficient and safe siRNA transfection in rodent joints and human articular cartilage explants (21,22,25). The periostin (product no. 162562) and scrambled siRNAs (product no. 4390846) were purchased from ThermoFisher Scientific. The p5RHH–siRNA polyplexes were prepared as described previously (21). Briefly, 10 m*M* of p5RHH peptide and 100 μ*M* of siRNA were mixed in equal volumes at a peptide:siRNA ratio of 100:1 in Hanks' balanced salt solution (HBSS). The mixture was then incubated at 37°C for 40 minutes followed by stabilization with albumin at a final siRNA concentration of 500 n*M* before IA injection.

IA delivery of p5RHH–siRNA nanoparticles. The p5RHH–siRNA nanocomplex was administered immediately after destabilization of the medial meniscus (DMM) surgery in mice, as well as at 1, 2, 4 and 6 weeks after surgery, for a total of 5 injections. The following sterile technique was used for IA injections: the knee was kept in a flexed position and 15 μl of p5RHH–siRNA nanoparticle complex was injected IA using a 30-gauge needle (21). Mice were either left untreated or received a single IA injection of one of the following treatments (n = 8 mice per group): HBSS (untreated), nontargeted scrambled siRNA, or periostin siRNA

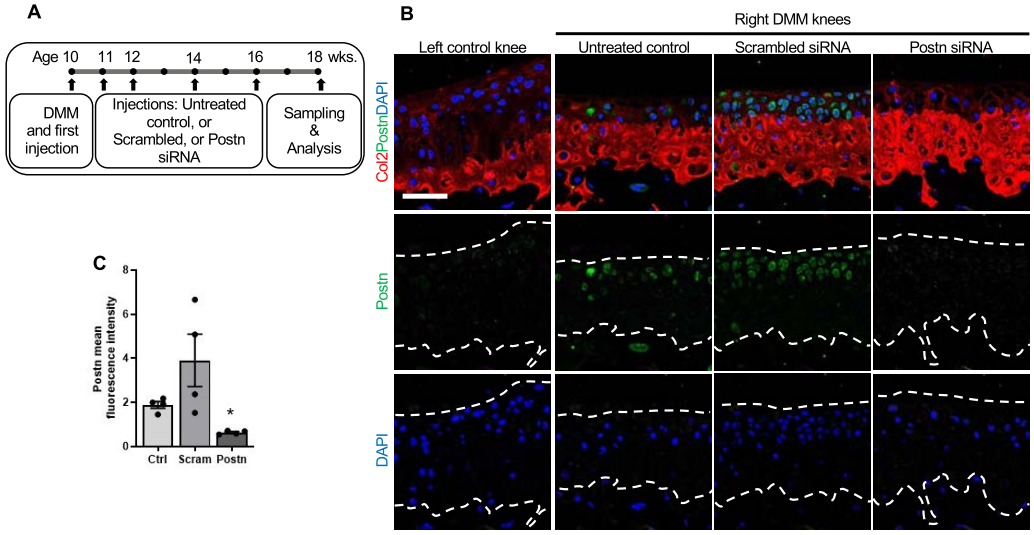

Figure 1. Suppression of up-regulated periostin (Postn) expression by gene silencing with small interfering RNA (siRNA) in the knee joints of mice following destabilization of the medial meniscus (DMM) surgery for induction of osteoarthritis (OA). **A**, DMM surgery was performed for OA induction in the knees of 10-week-old male mice, followed by intraarticular (IA) injection of periostin siRNA, nontargeted scrambled siRNA (Scram), or Hanks' balanced salt solution as an untreated control (Ctrl) (n = 8 mice per group), administered immediately after surgery and at 1, 2, 4, and 6 weeks post-DMM (5 injections total). Harvested knee joints were analyzed 8 weeks post-DMM. **B**, Immunostaining of knee cartilage revealed up-regulated expression of periostin in DMM-operated knees compared to uninjured control knees. IA administration of periostin siRNA nanoparticles suppressed the DMM-induced up-regulation of periostin. Broken white lines in middle and bottom panels delineate the area of cartilage in which type II collagen (Col2)–positive staining was detected. Scale bar = 50 μm. **C**, Quantification of periostin expression (measured as the normalized mean fluorescence intensity per chondrocyte on z-stack confocal microscopy images) shows significant differences in periostin expression between the scrambled siRNA and periostin siRNA groups. Circles represent individual samples; bars show the mean ± SEM. * = P = 0.013 versus scrambled siRNA treatment, by Kruskal-Wallis test followed by Dunn's correction for multiple comparisons.

(Figure 1A). While we did not check for any leakage of the injected contents, we have previously demonstrated that injected contents stay within the joint cavity (21).

Induction of OA in mouse knees. For OA induction, DMM surgery was performed in the right hind knee of 10-week-old mice following administration of general anesthesia (inhalation of 2.5% isoflurane in 4 liters/minute of oxygen); the surgery was carried out by transection of the anterior attachment of the medial meniscotibial ligament in the knee (26,27). To minimize pain, sustained-release buprenorphine SR (1.0 mg/kg) (SR Veterinary Technologies) was administered subcutaneously prior to surgery. The contralateral left limb was not operated on and served as an internal control. After recovering from anesthesia, all mice were weight bearing and resumed prior cage activity with normal water and food consumption.

Histologic evaluation of cartilage degeneration. Eight weeks after surgery, mice were killed in a CO_2 chamber. The knees were harvested, fixed with 10% neutral buffered formalin for 48 hours, and maintained in 70% ethyl alcohol until used. Joints were decalcified for 48 hours using Inmmunocal Decalcifier (StatLab) and then embedded in paraffin for sectioning. Serial coronal sections (5-μm thick) were cut, extending throughout the joint (26). Briefly, sections were cut at 8 levels, with each level comprising 12 sections, with 80 μm of tissue discarded between each level, thus covering >75% of the depth of the joint. Selected sections were stained with Safranin O–fast green to evaluate cartilage proteoglycans. All images were visualized with a NanoZoomer slide scanner (Hamamatsu). Cartilage damage was measured using the Osteoarthritis Research Society International (OARSI) scoring system (28). We report mean scores from 4 consecutive levels in each mouse knee and from all 4 knee compartments. The score shown is calculated based on a total possible score of 96 (6 highest scores × 4 compartments × 4 sections). OARSI scoring of cartilage damage was performed by 2 investigators (XD and LC) who were blinded with regard to sample identity, and disparities were resolved by consensus.

Histologic evaluation of synovitis. Four Safranin O–fast green–stained sections from consecutive levels of each knee were graded by researchers under blinded conditions to determine synovial pathology in the medial compartment for 2 parameters (29): enlargement of the synovial lining cell layer and synovial stroma. Scores for both synovial pathology parameters (score scale 0–6) were averaged separately, and the mean values were used for analysis.

Micro–computed tomography (micro-CT) analysis of bone. Prior to decalcification, knees were assessed by micro-CT scanning using a vivaCT 40 scanner (Scanco Medical) to analyze the 3-dimensional bone structure and to determine bone volume/

total volume (BV/TV), volumetric bone mineral density (vBMD), and heterotopic ossification (30). The medial and lateral subchondral bone parameters of each tibia were contoured separately. The relative outcome was determined by dividing the medial side measurement of the right knee by the medial side measurement of the left knee of the same mouse. This method serves as a better internal control, since it minimizes variation within each mouse.

Immunofluorescence/confocal microscopy. Paraffin-embedded sections of cartilage from the knee joints of mice were deparaffinized with xylene and rehydrated in a graded series of ethanol (70%, 50%, and 30%). Proteinase K (10 μg/ml) (Abcam) was applied to the sections for antigen retrieval for 20 minutes at 37°C. The slides were washed with phosphate buffered saline (PBS) and blocked with 10% normal goat serum. Subsequently, slides were incubated overnight at 4°C with the following primary antibodies (obtained from Abcam) diluted in 2% normal goat serum: anti-periostin (1:100 dilution), anti–phospho-p65 (1:100 dilution), anti–MMP-13 (1:200 dilution), as well as in-house anti–type II collagen (1:200 dilution). The slides were washed with PBS and incubated with the corresponding Alexa Fluor 488– or Alexa Fluor 594–conjugated secondary antibodies in 2% normal goat serum for 1 hour at room temperature and were counterstained with Fluoro-Gel II with DAPI (Electron Microscopy Sciences). All images were visualized using a confocal laser scanning microscope (Leica Biosystems). Signal intensity was quantified in 20–30 cells/section using LAS X software (Leica Biosystems).

Detection of DIPEN. Immunohistochemical analysis using antibodies against the C-terminal aggrecan neoepitope DIPEN was carried out to detect cartilage expression of DIPEN; these anti-DIPEN antibodies were generated at the aggrecan cleavage sites produced by MMP-13 (31). Briefly, sections were deparaffinized, rehydrated, and digested with proteinase K, as detailed above. Then, sections were incubated with hydrogen peroxide blocking reagent (Abcam) for 15 minutes to quench endogenous peroxidases. Sections were subsequently incubated overnight at 4°C with anti-DIPEN (1:50 dilution in 2% normal goat serum, a gift from Dr. Amanda Fosang) after blocking with 10% normal goat serum. The next day, sections were incubated with horseradish peroxidase–conjugated goat anti-rabbit secondary antibody (1:200 dilution in 2% normal goat serum) (Abcam) for 1 hour at room temperature. The signal was developed as a brown-reaction product using the peroxidase substrate diaminobenzidine (Betazoid DAB Chromogen Kit; BioCare Medical), and the sections were then counterstained with hematoxylin 560 MX (Leica Biosystems). Images were acquired with the NanoZoomer scanner.

Isolation and culture of human chondrocytes. Samples of human cartilage were obtained from patients with knee OA at the time of total knee arthroplasty. Chondrocytes were isolated through enzymatic digestion, as described previously (16). Cells were counted using a hemocytometer, and cell viability was determined using 0.4% trypan blue exclusion dye (Sigma-Aldrich). Chondrocytes were seeded at a density of 0.5×10^5 cells/well in 12-well plates and maintained at 37°C and 5% CO_2 with 95% humidity to reach 80–90% confluence. Once confluence was achieved after 2–3 days of culture, cells at passage 0 were used in subsequent experiments.

Preparation of p5RHH–siRNA nanoparticles. The p5RHH–siRNA nanoparticles were prepared for chondrocyte culture as follows: 20 m*M* of p5RHH peptide was diluted to a ratio of 1:400 (volume/volume) with Opti-MEM medium (ThermoFisher Scientific) and was vortexed for 30 seconds, followed by addition of 10 μ*M* of periostin siRNAs (product nos. S20889 and HSS116400; ThermoFisher Scientific) or nontargeting scrambled siRNA (product no. 4390846, ThermoFisher Scientific) to achieve a peptide:siRNA ratio of 100:1. The mixture was incubated at 37°C for 40 minutes with gentle shaking. The Cy5.5-labeled scrambled siRNAs were commercially obtained (Sigma-Aldrich).

Evaluation of transfection efficiency. First, 1.0×10^5 human chondrocytes were seeded onto a Lab-Tek Chamber Slide (ThermoFisher Scientific) and incubated with p5RHH-Cy5.5–labeled siRNA nanoparticles for 5 hours. Control cells were incubated with either only Opti-MEM, only peptide, or only Cy5.5-labeled siRNA. Then, the chambers were washed with PBS and cultured in complete culture medium for 72 hours. Subsequently, cells were washed in PBS and fixed with 4% paraformaldehyde for 15 minutes. Phalloidin-iFluor 488 reagent (1:1,000 dilution) (Abcam) was applied to the chamber slides. Slides were incubated for 1 hour at room temperature, washed, and mounted with Fluoro-Gel with DAPI. Images were captured using a confocal microscope.

Transfection of human chondrocytes with periostin siRNA. Human chondrocytes (n = 7) were transfected with periostin siRNA nanoparticles, scrambled siRNA nanoparticles, or Opti-MEM for only 5 hours. Then, cells were washed with PBS and cultured at 37°C for 72 hours. Thereafter, the cells were washed with PBS and 1 ng/ml of human recombinant IL-1β (R&D Systems) was added to each group. In the final step, the cells were cultured for 24 hours, washed with PBS, and used for RNA and protein extraction.

Evaluation of MMP-13 inhibition by an IKK-2 inhibitor. Next, we tested whether periostin-induced expression of MMP-13 can be suppressed by an IKK-2 inhibitor, SC-514 (product no. 354812-17-2; Sigma-Aldrich). Normal human chondrocytes were obtained from MilliporeSigma (product no. 402-05a) and were cultured as recommended by the manufacturer. Briefly, cells were cultured in a culture dish containing 10 ml of chondrocyte growth medium (MilliporeSigma) and were incubated at 37°C in a humidified incubator with 5% CO_2. Once cells reached 80% confluence, they were subcultured for the following experiments. In one experiment, 0.5×10^6 cells (n = 4) were either left untreated

(control) or treated with human recombinant IL-1β (10 ng/ml), or combined IL-1β and SC-514 (the latter was added 30 minutes before IL-1β). In another experiment, cells (n = 6) were treated exactly as above; however, human recombinant periostin (10 μg/ml) (product no. 3548-F2; R&D Systems) was instilled instead of IL-1β, and for comparison, another group of cells was treated with SC-514 alone (20 μmoles/liter). Cells were cultured at 37°C for 24 hours and then collected for RNA isolation.

Real-time quantitative polymerase chain reaction (qPCR). Total RNA was extracted using an RNeasy Mini kit (Qiagen). RNA (800 ng) was treated with DNase I (1 unit/μl) (Invitrogen) and reverse-transcribed using a High-Capacity cDNA Reverse Transcription Kit (ThermoFisher Scientific). To quantify messenger RNA (mRNA) expression of periostin, MMP-13, and IL-1β, real-time qPCR analysis was performed using custom-designed, gene-specific primers (see Supplementary Table 1, available on the *Arthritis & Rheumatology* website at http://onlinelibrary.wiley.com/doi/10.1002/art.41794/abstract) and standard methods (32). Target gene expression was normalized with respect to PPIA using the $2^{-\Delta\Delta Ct}$ method.

Western blotting. Proteins were extracted from chondrocytes using a radioimmunoprecipitation assay buffer containing a protease inhibitor cocktail (Sigma-Aldrich). The total protein concentration was determined using a protein assay kit (Bio-Rad). Next, 20 μg of total proteins diluted in sodium dodecyl sulfate sample buffer was resolved on 4–20% Mini-PROTEAN TGX Precast Protein Gels (Bio-Rad). Subsequently, proteins were electrophoretically transferred to polyvinylidene fluoride membrane (Invitrogen). Membranes were blocked with Odyssey Blocking Buffer (Li-Cor Biosciences) for 1 hour. Blots were incubated overnight at 4°C with

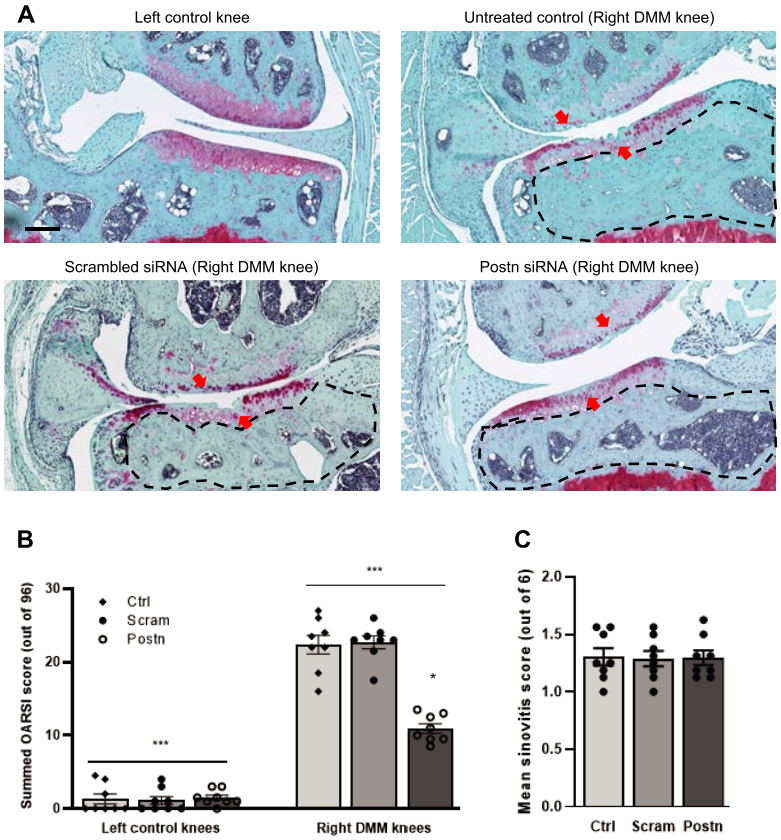

Figure 2. Attenuation of cartilage degeneration, but not synovitis, with periostin siRNA treatment in knees of mice with DMM-induced posttraumatic OA. **A**, Representative Safranin O–fast green–stained images of the knee cartilage show significantly less severe cartilage degeneration in an uninjured left knee compared to an untreated, DMM-operated right knee. Treatment with periostin siRNA resulted in reduced cartilage degeneration in the DMM-operated right knee compared to the untreated or scrambled siRNA–treated, DMM-operated right knee. In addition, more pronounced sclerosis was observed in the untreated and scrambled siRNA–treated, DMM-operated right knee as compared to the periostin siRNA–treated, DMM-operated right knee. **Arrows** indicate areas of cartilage degeneration. Broken black lines denote the subchondral bone area assessed for synovitis. Scale bar = 200 μm. **B** and **C**, Uninjured left knees and DMM-operated right knees in each treatment group were assessed for the extent of cartilage degeneration using Osteoarthritis Research Society International (OARSI) damage scores among the 4 knee compartments (**B**) and for the severity of synovitis in the knee joints (**C**). * = P = 0.002 versus untreated control or scrambled siRNA–treated, DMM-operated right knees, by Kruskal-Wallis test followed by Dunn's correction for multiple comparisons. *** = P for trend < 0.001 by two-way analysis of variance with Tukey's post hoc test for multiple comparisons. In **B** and **C**, circles represent individual samples; bars show the mean ± SEM. See Figure 1 for other definitions. Color figure can be viewed in the online issue, which is available at http://onlinelibrary.wiley.com/doi/10.1002/art.41794/abstract.

the following primary antibodies: anti-periostin (1:1,000 dilution), anti–phospho-p65 (1:1,000 dilution), anti–MMP–13 (1:4,000 dilution), or anti–total-p65 (1:1,000 dilution). The next day, membranes were washed and subsequently incubated with fluorescence-(IRDye 680RD)–labeled goat anti-rabbit IgG (Li-CoR) secondary antibody (1:20,000 dilution). For cell lysates, a housekeeping antibody, anti–β-actin (1:4,000 dilution) (Sigma-Aldrich) was used as the primary antibody, and the fluorescence (IRDye 680RD)–labeled goat anti-mouse IgG (1:20,000 dilution) was used as the secondary antibody. Blots were imaged using an Odyssey Infrared Imager, and the signal intensity was quantified using ImageJ software.

Statistical analysis. OARSI scores in DMM-operated and control mouse limbs, treated with or without periostin siRNA, were compared using two-way analysis of variance (ANOVA) with Tukey's post hoc test for multiple comparisons. A nonparametric paired *t*-test (Wilcoxon matched pairs signed rank test) was used for analysis of real-time qPCR data. For all other comparisons, we used the Kruskal-Wallis test followed by Dunn's test to correct for multiple comparisons for 3 groups and Mann-Whitney test for comparison between 2 groups. All analyses were performed with GraphPad Prism software. Data are the mean ± SEM unless indicated otherwise. *P* values less than 0.05 by 2-tailed test were considered significant.

RESULTS

Reduction in DMM-induced periostin expression following periostin siRNA treatment in mice. In knee cartilage from uninjured control mice, we observed only minimal immunofluorescence staining for periostin expression, whereas in mice subjected to DMM surgery, periostin expression was significantly increased after DMM surgery, which was consistent with our

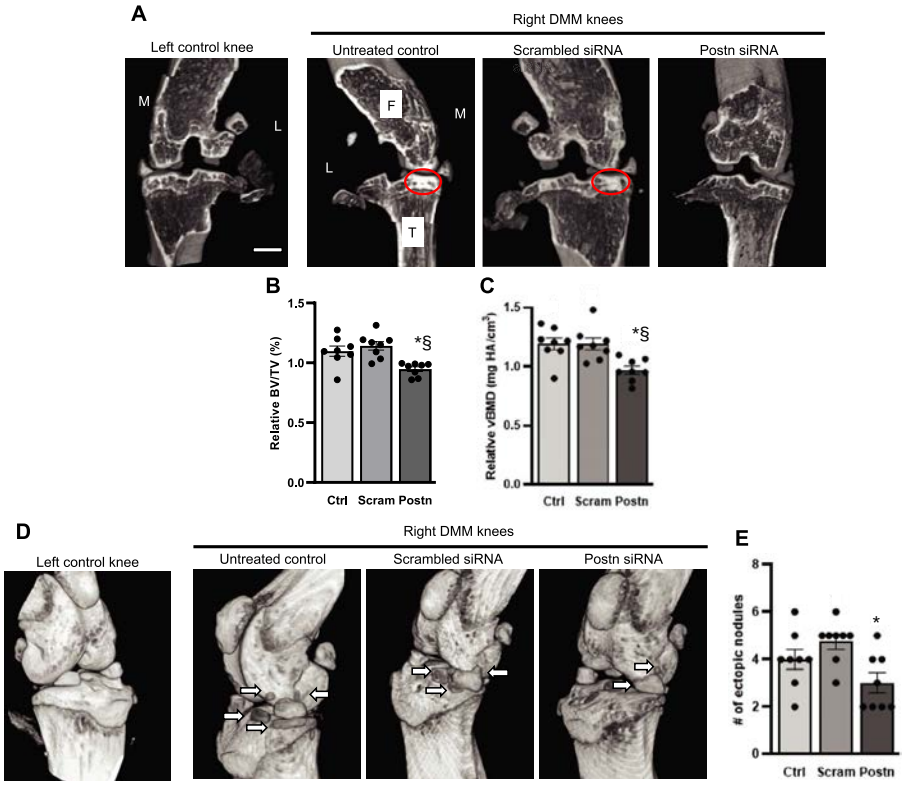

Figure 3. Blockade of DMM-induced subchondral bone changes and heterotopic ossification following treatment with periostin siRNA in knees of mice with DMM-induced OA. **A**, Three-dimensional micro–computed tomography (micro-CT) reconstructions of the knee joints show that subchondral bone sclerosis was reduced in the medial tibial compartment (circled areas) of a periostin siRNA–treated, DMM-operated knee compared to an untreated or scrambled siRNA–treated, DMM-operated knee. **M** = medial; **L** = lateral; **F** = femur; **T** = tibia. Scale bar = 1 mm. **B** and **C**, In DMM-operated right knees, bone volume/total volume (BV/TV) (**B**) and volumetric bone mineral density (vBMD) (**C**) were significantly lower in the periostin siRNA–treated mice than in the untreated or scrambled siRNA–treated controls. Values in the DMM-operated right knee were normalized to those in the uninjured left knee of the same animal to eliminate intraindividual variation. In **B**, * = *P* = 0.027 versus untreated control; § = *P* = 0.004 versus scrambled siRNA. In **C**, * = *P* = 0.01 versus untreated control; § = *P* = 0.022 versus scrambled siRNA, by Kruskal-Wallis test followed by Dunn's correction for multiple comparisons. **D**, Three-dimensional micro-CT reconstructions of mouse knee joints show heterotopic ossification (**arrows**) in the DMM-operated knees of an untreated control mouse compared to a mouse that received either periostin siRNA treatment or scrambled control siRNA. **E**, Periostin siRNA treatment reduced the number of ossified nodules in DMM-operated knees when compared to the DMM-operated knees of untreated and scrambled siRNA–treated mice. * = *P* = 0.018 versus scrambled siRNA, by Kruskal-Wallis test followed by Dunn's correction for multiple comparisons. In **B**, **C**, and **E**, circles represent individual samples; bars show the mean ± SEM. HA = hydroxyapatite (see Figure 1 for other definitions). Color figure can be viewed in the online issue, which is available at http://onlinelibrary.wiley.com/doi/10.1002/art.41794/abstract.

previous observations (16). Expression levels of periostin remained elevated in both the untreated control group and the scrambled siRNA–treated group after DMM surgery, while periostin siRNA treatment significantly suppressed expression of periostin protein in cartilage (Figure 1B). Quantification of the fluorescence intensity of signaling further confirmed that periostin expression was significantly attenuated in the periostin siRNA–treated group compared to the scrambled siRNA group (mean ± SEM fluorescence intensity units 0.63 ± 0.42 versus 3.91 ± 1.19; $P = 0.013$). Periostin expression levels were lower in the periostin siRNA group compared to the untreated control group but the difference was not statistically significant (mean ± SEM fluorescence intensity units 0.63 ± 0.42 versus 1.89 ± 0.16; $P = 0.187$). There was a slight increase in expression of periostin in the scrambled siRNA group compared to the untreated control group, but the difference was not significant (Figure 1C).

In addition to the inhibitory effects of periostin siRNA treatment in the cartilage, periostin siRNA treatment suppressed expression of periostin in the synovium of mice. The periostin protein levels were significantly lower in mice that received periostin siRNA compared to the untreated control group and the scrambled siRNA group (see Supplementary Figures 1A and B, available on the *Arthritis & Rheumatology* website at http://onlinelibrary.wiley.com/doi/10.1002/art.41794/abstract).

Mitigation of DMM-induced cartilage degeneration by periostin gene knockdown in mice. Cartilage degeneration was significantly less severe in the uninjured left knees compared to the DMM-operated right knees of mice (mean ± SEM OARSI score 1.33 ± 0.69 versus 22.38 ± 1.30; $P < 0.001$ by two-way ANOVA) at 8 weeks after surgery. We therefore examined whether periostin knockdown would convey protective effects in the mouse cartilage. We observed a reduction in the severity of cartilage degeneration in destabilized knee joints following IA treatment with periostin siRNA (Figure 2A). No difference in the severity of cartilage degeneration was observed between the untreated control group and the scrambled siRNA group.

A semiquantitative analysis of cartilage degradation using the OARSI scoring system (calculated from a total possible score

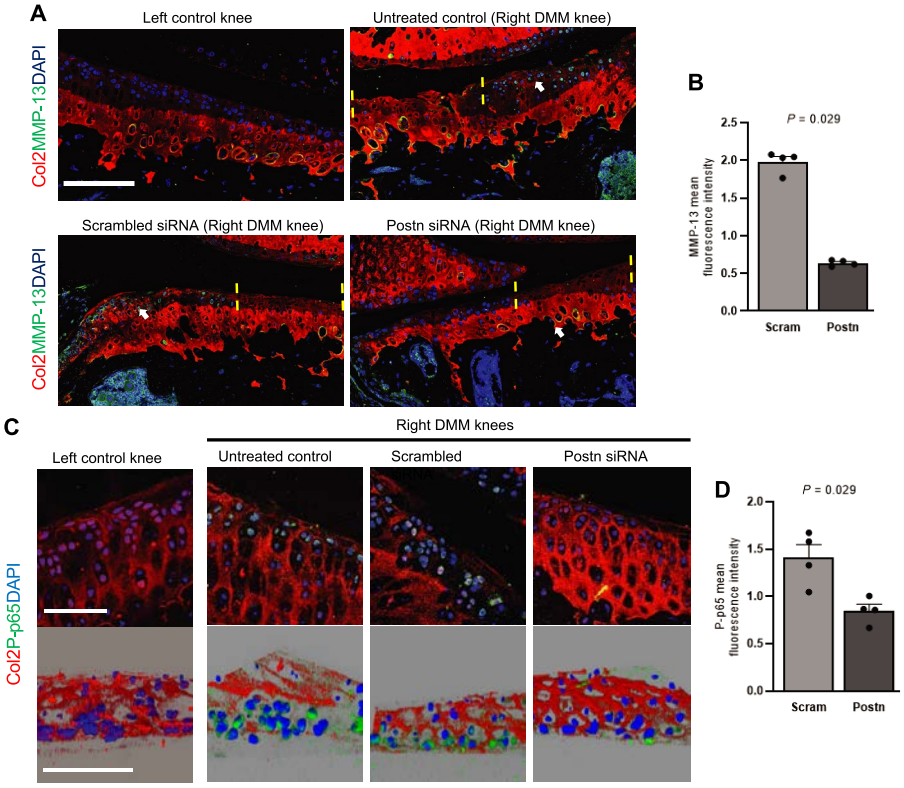

Figure 4. Abrogation of up-regulated matrix metalloproteinase 13 (MMP-13) expression and canonical NF-κB signaling following treatment with periostin siRNA in DMM-operated mouse knees. **A**, Immunofluorescence analysis of MMP-13 expression in superficial zone chondrocytes (**arrows**), in conjunction with type II collagen gene expression in cartilage, revealed higher levels of MMP-13 in untreated, DMM-operated right knees compared to uninjured left knees. Treatment with periostin siRNA reduced the MMP-13 levels around the injury site (denoted by broken vertical lines). Scale bar = 100 μm. **B** and **D**, Quantification of MMP-13 expression (**B**) and phosphorylation of p65 (**D**) shows significant differences between the scrambled siRNA– and periostin siRNA–treated DMM-operated knees. *P* values were determined by Mann-Whitney test. **C**, Immunofluorescence images of the mouse knee cartilage show 2-dimensional views (top) and 3-dimensional views (bottom), indicating localization of p-p65 subunits in the cartilage adjacent to the DMM injury site. Less colocalization of activated and phosphorylated p65 was observed in periostin siRNA–treated knees than in untreated or scrambled siRNA–treated knees. Scale bar = 50 μm. In **B** and **D**, circles represent individual samples; bars show the mean ± SEM. See Figure 1 for other definitions. Color figure can be viewed in the online issue, which is available at http://onlinelibrary.wiley.com/doi/10.1002/art.41794/abstract.

of 96) confirmed that there was no significant difference in the OARSI score of cartilage damage between the untreated control group and scrambled siRNA treatment group (mean ± SEM OARSI score 22.38 ± 1.30 versus 22.69 ± 0.87; $P = 0.999$). However, treatment with periostin siRNA significantly reduced OARSI scores compared to scores in both the untreated control group (mean ± SEM 10.94 ± 0.66 versus 22.38 ± 1.30; $P = 0.002$) and the scrambled siRNA group (10.94 ± 0.66 versus 22.69 ± 0.87; $P = 0.002$) (Figure 2B).

Lack of improvement in synovitis score with periostin knockdown in mice. There were no significant differences ($P = 0.999$ by Kruskal-Wallis test) in synovitis scores across groups (Figure 2C). The mean ± SEM synovitis score was 1.31 ± 0.08 in untreated controls, 1.29 ± 0.07 in those receiving scrambled siRNA, and 1.30 ± 0.06 in those receiving periostin siRNA.

Improvement in DMM-induced bone changes using periostin knockdown in mice. The subchondral bone plate exhibited reduced sclerosis in the subchondral bone area of the medial tibial compartment in DMM-operated, periostin siRNA–treated knees compared to knees in the untreated control group or scrambled siRNA group (Figure 3A). Moreover, a histomorphometric analysis of the knee joints revealed that BV/TV values were significantly lower in the mice treated with periostin siRNA compared to untreated control mice (13.7%; $P = 0.027$) and mice treated with scrambled siRNA (17.1%; $P = 0.004$) (Figure 3B). Similarly, vBMD was also significantly lower in periostin siRNA–treated knees compared to untreated control mice (18.5%; $P = 0.010$) and mice treated with scrambled siRNA group (18.5%; $P = 0.022$) (Figure 3C).

Findings from measurements of other bone parameters, such as the structural model index and trabecular thickness, did not reveal any significant differences across groups (data not shown). Ectopic calcified nodules (heterotopic ossification) formed

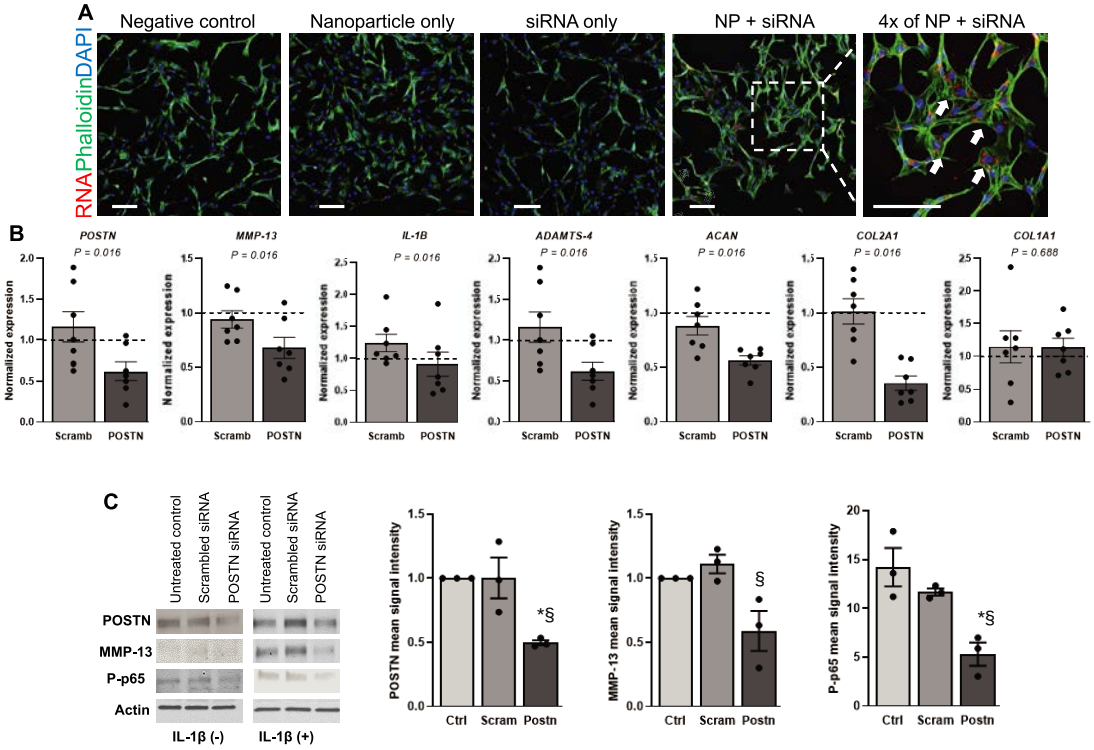

Figure 5. Attenuation of the catabolic effects of interleukin-1β (IL-1β) with periostin siRNA nanoparticle treatment in human primary chondrocytes. **A**, Human primary chondrocytes were treated with p5RHH peptide, Cy5.5-labeled siRNA, or peptide–Cy5.5-labeled siRNA. Cy5.5-labeled siRNAs delivered with nanoparticles (NPs) were effectively taken up by the human primary chondrocytes (shown in red and indicated by the **arrows**) and remained in the cells after 72 hours in culture. Scale bars in first 3 panels = 100 μm; the panel on the far right is a higher-magnification view of the boxed area to the left (scale bar = 100 μm) **B**, Real-time quantitative polymerase chain reaction analysis shows that human chondrocytes treated with IL-1β and transfected with periostin siRNA exhibit significantly lower levels of periostin, matrix metalloproteinase 13 (MMP-13), IL-1β, ADAMTS-4, ACAN, and COL2A1 mRNA. There was no effect of siRNA treatment on COL1A1 expression ($P = 0.688$ by Wilcoxon matched pairs signed rank test). **C**, First panel, Western blotting confirms that IL-1β treatment induced MMP-13 expression and activated phosphorylation of p65. Right panels, Cells treated with periostin siRNA show significantly lower levels of periostin and MMP-13 and reduced phosphorylation of p65 compared to the untreated controls and scrambled siRNA group. Second panel, * = $P = 0.025$ versus untreated control; § = $P = 0.025$ versus scrambled siRNA. Third panel, * = $P = 0.079$ versus untreated control; § = $P = 0.030$ versus scrambled siRNA. Fourth panel, * = $P = 0.010$ versus untreated control; § = $P = 0.046$ versus scrambled siRNA, by Kruskal-Wallis test followed by Dunn's correction for multiple comparisons. In **B** and **C**, circles represent individual samples; bars show the mean ± SEM. See Figure 1 for other definitions. Color figure can be viewed in the online issue, which is available at http://onlinelibrary.wiley.com/doi/10.1002/art.41794/abstract.

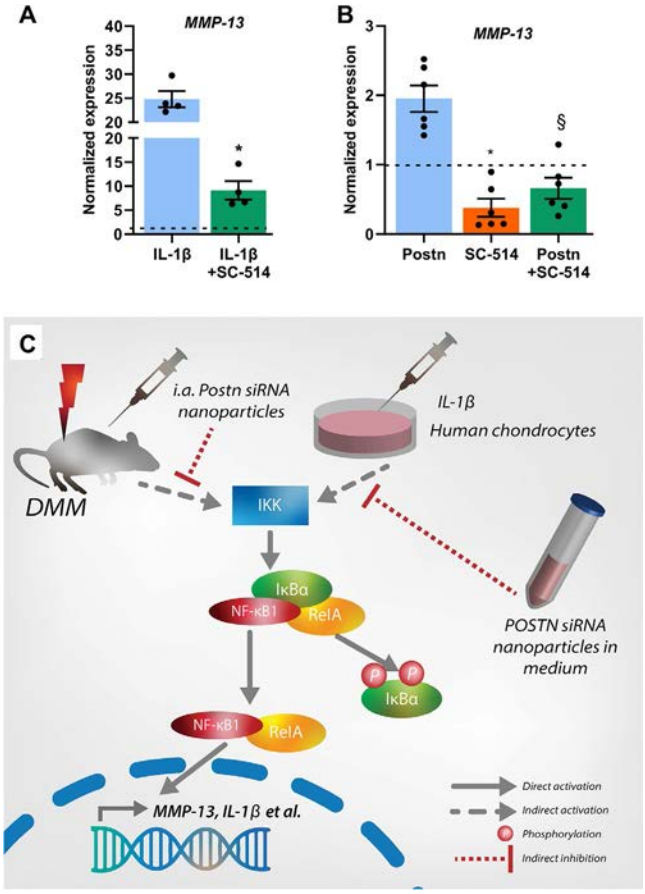

Figure 6. Pathways and mechanisms of cartilage degradation involving periostin. **A** and **B**, Expression of matrix metalloproteinase 13 (MMP-13) in human chondrocytes was assessed in the presence of interleukin-1β (IL-1β) alone or IL-1β plus the IκB kinase 2 inhibitor SC-514 (**A**) or following treatment with exogenous recombinant periostin (Postn) alone, SC-514 alone, or periostin plus SC-514 (**B**). Circles represent individual samples; bars show the mean ± SEM. In **A**, ***** = P = 0.029 versus IL-1β alone, by Wilcoxon matched pairs signed rank test. In **B**, * = P = 0.045 versus periostin alone; § = P = 0.002 versus SC-514 alone, by Kruskal-Wallis test followed by Dunn's correction for multiple comparisons. The broken horizontal line indicates untreated controls. **C**, Destabilization of the medial meniscus (DMM) surgery in mice or stimulation of human chondrocytes with IL-1β activates the NF-κB signaling pathway, as evidenced by the increased phosphorylation of p65, leading to its nuclear translocation and expression of catabolic mediators (e.g., MMP-13) that promote extracellular matrix degradation. Treatment with p5RHH–periostin (POSTN) small interfering RNA (siRNA) reduces the activation of p65, blocks the downstream catabolic effects of NF-κB signaling, and prevents progressive cartilage degradation. Color figure can be viewed in the online issue, which is available at http://onlinelibrary.wiley.com/doi/10.1002/art.41794/abstract.

in and around the synovium in DMM-operated joints (Figure 3D); however, slightly fewer of these nodules were observed in the periostin siRNA–treated group compared to the untreated control group (mean ± SEM nodule count 3.00 ± 0.42 versus 4.00 ± 0.42; P = 0.481) and the scrambled siRNA group (3.00 ± 0.42 versus 4.75 ± 0.31; P = 0.018) (Figure 3E).

Suppression of MMP-13 expression and NF-κB signaling by periostin knockdown in mice with DMM-induced OA. We observed that the intensity of MMP-13 protein expression was increased in the knee joints of mice following DMM surgery, whereas after treatment with periostin siRNA, the intensity of MMP-13 expression was significantly reduced (Figures 4A and B). These results suggest that periostin modulates MMP-13 expression in vivo. We also observed that NF-κB signaling activity was low in control knees, whereas DMM surgery significantly increased the expression of canonical (p65) NF-κB activation, evident from increased phosphorylation of p65. Furthermore, we demonstrated that periostin siRNA treatment significantly suppressed phosphorylation of p65 compared to the untreated control and scrambled siRNA groups (Figures 4C and D).

Decrease in DIPEN expression following periostin knockdown in mice with DMM-induced OA. We noted that there was no staining for the aggrecan neoepitope DIPEN in control left knees; however, there was markedly increased staining in untreated knees and scrambled siRNA–treated knees from DMM-operated mice. In contrast, we found that periostin siRNA–treated knees had reduced expression of DIPEN (see Supplementary Figure 2, available on the *Arthritis & Rheumatology* website at http://onlinelibrary.wiley.com/doi/10.1002/art.41794/abstract).

Suppression of MMP-13 and NF-κB activity following periostin knockdown in human chondrocytes. We demonstrated that Cy5.5-labeled siRNA nanoparticles were effectively taken up by human primary chondrocytes and subsequently remained in the cells (Figure 5A). As expected, naked, noncomplexed siRNA was not taken up by chondrocytes. These results further suggest that the peptide–siRNA nanoparticles are required for efficient siRNA transfection of chondrocytes.

After establishing the efficiency of siRNA delivery, we stimulated human primary chondrocytes with IL-1β to model an in vitro inflammatory condition, and then evaluated the therapeutic effects of periostin knockdown in the IL-1β–stimulated chondrocytes. We observed that exposure to IL-1β significantly increased expression levels of MMP-13 mRNA (~10-fold) and IL-1β mRNA (~5,500-fold) relative to untreated controls. We confirmed that periostin siRNA significantly knocked down expression of periostin both at the mRNA level (Figure 5B) and the protein level (Figure 5C). We observed that periostin siRNA treatment significantly suppressed mRNA expression of IL-1β (P = 0.016), MMP-13 (P = 0.016), ADAMTS-4 (P = 0.016), ACAN (P = 0.016), and COL2A1 (P = 0.016), compared to treatment with scrambled siRNA. There was no effect of treatment on COL1A1 expression (P = 0.688) (Figure 5B). Furthermore, periostin knockdown also attenuated NF-κB p65 phosphorylation and NF-κB downstream product MMP-13, as determined using Western blotting. Signal intensity was quantified using ImageJ (Figure 5C). Specifically, we noted that signal intensity of periostin (P = 0.025) and p-p65

($P = 0.010$) were significantly lower in the periostin-treated group than in the untreated control group, while MMP-13 signal intensity was borderline significant ($P = 0.079$). The signal intensity of periostin ($P = 0.025$), MMP-13 ($P = 0.030$), and p-p65 ($P = 0.046$) was significantly lower in the periostin siRNA group compared to the scrambled siRNA group. We noted subtle increases in expression of periostin and MMP-13 in the scrambled siRNA group compared to the untreated control group, which were not statistically significant.

Suppression of periostin-induced MMP-13 expression in human chondrocytes using an IKK-2 inhibitor. We observed increased expression of MMP-13 in human chondrocytes treated with IL-1β (Figure 6A) or periostin (Figure 6B). Treatment with SC-514 significantly suppressed the expression of MMP-13 (Figures 6A and B), indicating that periostin is expressed upstream of the NF-κB pathway (Figure 6C).

DISCUSSION

Despite significant advances in our understanding of the affected cellular and molecular pathways in OA, no new clinical therapeutic targets have been identified. The current study explored the intermittent local joint delivery of periostin siRNA using nanoparticles to mitigate OA pathology in a murine model of knee joint injury. Previous studies showed that periostin is expressed in human and mouse OA cartilage, where periostin levels are strongly associated with cartilage-degrading enzyme MMP-13 (15,16). Herein, we show that knockdown of periostin suppresses NF-κB and its downstream catabolic genes, including MMP-13 and IL-1β. To the best of our knowledge, this is the first study that shows the therapeutic effects of periostin knockdown in posttraumatic OA in vivo, whereas previous studies mainly focused on periostin overexpression or inhibition in vitro.

We used the peptide–siRNA nanoplatform that was previously used for IA administration of NF-κB siRNA and showed that NF-κB knockdown suppressed injury-induced chondrocyte death and early joint responses to injury (21,22). In the present study, we demonstrate, for the first time, the long-term (8-week) efficiency of this nanoparticle delivery system. These results further confirm the translational potential of this technology in the treatment of posttraumatic OA.

We noted that IA delivery of periostin siRNA mitigated several aspects of posttraumatic OA, i.e., cartilage degeneration, subchondral bone sclerosis, and heterotopic ossification, suggesting that periostin affects the whole joint, which is consistent with findings of previous studies that showed differential expression patterns of periostin in various joint tissues (13,16,33,34). Thus, periostin knockdown effectively suppressed events that lead to the structural damage characteristic of OA, in addition to suppressing cartilage degeneration. Of note, periostin siRNA treatment reversed subchondral bone changes that were mainly confined to the medial region, indicating that periostin exerts therapeutic effects in the diseased compartment. In the present study, we did not observe significant differences in synovitis scores across the various treatments. While lower periostin intensity in the periostin siRNA–injected group confirms that the injected particles localized there, a complete knockdown of periostin was not achieved, thus potentially explaining the lack of significant differences in synovitis score. Moreover, we recently found that periostin-null mice developed significantly less synovitis after DMM compared to wild-type mice, whereas 24-month-old animals did not demonstrate such differences in a model of age-induced spontaneous OA (35). These observations imply that the link between periostin expression and synovitis is context dependent and merits further investigation.

How periostin exerts its effects on these various tissues is still unclear. Periostin binding to integrin receptors (αvβ3/αvβ5 or DDR-1) in various cell types (36–38) reportedly activates intracellular signaling pathways directly (39) or indirectly (via downstream ERK signaling) (40) and leads to NF-κB activation. This in turn regulates the production of inflammatory mediators, such as MMPs. In injured joints, NF-κB activation triggers expression of a myriad of genes that promote the destruction of the articular joint and lead to changes that are characteristic of OA (21,41).

One NF-κB–dependent gene is MMP-13, which is thought to represent the major collagenase activity in OA, since its expression is up-regulated in human OA and experimental OA models (42,43). Conditional overexpression of MMP-13 in murine cartilage induces cartilage pathology and OA (44). In contrast, global knockout of MMP-13 protects against experimental OA in rodents (45). Our results showed that periostin knockdown suppressed MMP-13 expression in chondrocytes in OA patients and in an experimental posttraumatic OA mouse model. Moreover, we demonstrated that MMP-13–generated C-terminal neoepitope DIPEN was also reduced, indicating less proteolytic cleavage of aggrecan (46). In addition to MMP-13, periostin knockdown also significantly suppressed expression of ADAMTS-4 and IL-1β, which surprisingly reduced expression of matrix genes (COL2A1 and ACAN), suggesting an antiinflammatory role rather than a pro-anabolic role of periostin. To test whether periostin-mediated regulation of MMP-13 expression is NF-κB dependent, we performed pilot studies. Preliminary data revealed that periostin-induced MMP-13 expression can be abrogated by an IKK-2 inhibitor, suggesting a possible link between periostin and the NF-κB signaling pathway.

A limitation of the current investigation is the lack of multiple time points to demonstrate how periostin expression and treatment effects vary with time. With regard to the expression of periostin, we noted increased periostin signal intensity at 4 weeks after DMM (data not shown). Periostin expression remained elevated at 8 weeks (in the current study) and at 12 weeks (16). These findings, along with findings from ACL tears in humans

(16,17,34), prompted us to initiate siRNA therapy early, prior to periostin-mediated cartilage degeneration. Our study provides proof-of-concept that early intervention to knock down periostin expression after joint injury leads to significant mitigation of posttraumatic OA progression. However, intervention immediately after joint injury is not always possible. Additional longitudinal studies will be necessary to determine the therapeutic window during which periostin knockdown will still result in a protective effect.

Another limitation is that we did not analyze the role of periostin in the meniscus and ligaments. However, previous studies showed that IA administration of peptide–siRNA nanoparticle targets the whole joint (21). Future research will determine if and how periostin knockdown affects meniscal/ligament biology. It is likely that periostin modulates meniscus and ligament biology in different ways (16,34,47). Another limitation of our current study is the lack of measurements for functional tests, such as pain, gait, and behavior.

Last, we used 10-week-old mice, which falls within the standards of the field. Although some researchers believe skeletal maturity in mice is reached at ≥12 weeks of age (48,49), others recommend a minimum age of 10 weeks for the mouse to reach skeletal maturity in preclinical modes of OA, in order to gain meaningful insights into human OA (50). While growth plates do not completely close in mice, it is recommended that OA experiments in mice are conducted after the major growth spurt has occurred and when the animals are sexually mature. In our study, since siRNA treatment was administered at 10 weeks of age through 16 weeks of age and analysis was performed at 18 weeks of age, it was not clear how skeletal maturation confounds the therapeutic effects of siRNA treatment. Even if the mice are not skeletally mature, skeletal maturity does not explain the effect of treatment. In all 3 groups, mice matured at the same rate, and the differences in OA parameters were specific to periostin siRNA treatment.

In summary, we demonstrated that the IA periostin–siRNA nanocomplex represents a promising clinical approach to delay or mitigate the development of posttraumatic OA. Moreover, our data suggest that periostin knockdown suppresses the activity of NF-κB, a classical pathway implicated in OA development. Mechanistically, we show that periostin-induced MMP-13 expression was abrogated by SC-514, demonstrating a link between periostin and NF-κB. Follow-up mechanistic and cartilage-specific gene–knockout studies will further elucidate this link and the functional role of periostin in OA.

ACKNOWLEDGMENTS

We would like to thank Crystal Idleburg and Samantha Coleman (Musculoskeletal Research Center, Washington University School of Medicine) for providing technical support. We would also like to thank Dr. Ryan Nunley (Department of Orthopaedic Surgery, Washington University School of Medicine) for generously providing human cartilage samples.

AUTHOR CONTRIBUTIONS

All authors were involved in drafting the article or revising it critically for important intellectual content, and all authors approved the final version to be published. Dr. Rai had full access to all of the data in the study and takes responsibility for the integrity of the data and the accuracy of the data analysis.

Study conception and design. Duan, Rai.

Acquisition of data. Duan, Cai, Pham, Abu-Amer, Pan, Brophy, Wickline, Rai.

Analysis and interpretation of data. Duan, Cai, Pham, Abu-Amer, Pan, Brophy, Wickline, Rai.

REFERENCES

1. Hootman JM, Helmick CG, Barbour KE, Theis KA, Boring MA. Updated projected prevalence of self-reported doctor-diagnosed arthritis and arthritis-attributable activity limitation among US adults, 2015–2040. Arthritis Rheumatol 2016;68:1582–7.
2. Rai MF, Pham CT. Intra-articular drug delivery systems for joint diseases [review]. Curr Opin Pharmacol 2018;40:67–73.
3. Brown TD, Johnston RC, Saltzman CL, Marsh JL, Buckwalter JA. Posttraumatic osteoarthritis: a first estimate of incidence, prevalence, and burden of disease. J Orthop Trauma 2006;20:739–44.
4. Rai MF, Brophy RH, Sandell LJ. Osteoarthritis following meniscus and ligament injury: insights from translational studies and animal models [review]. Curr Opin Rheumatol 2019;31:70–9.
5. Roos H, Adalberth T, Dahlberg L, Lohmander LS. Osteoarthritis of the knee after injury to the anterior cruciate ligament or meniscus: the influence of time and age. Osteoarthritis Cartilage 1995;3:261–7.
6. Bornstein P, Sage EH. Matricellular proteins: extracellular modulators of cell function [review]. Curr Opin Cell Biol 2002;14:608–16.
7. Horiuchi K, Amizuka N, Takeshita S, Takamatsu H, Katsuura M, Ozawa H, et al. Identification and characterization of a novel protein, periostin, with restricted expression to periosteum and periodontal ligament and increased expression by transforming growth factor beta. J Bone Miner Res 1999;14:1239–49.
8. Coutu DL, Wu JH, Monette A, Rivard GE, Blostein MD, Galipeau J. Periostin, a member of a novel family of vitamin K-dependent proteins, is expressed by mesenchymal stromal cells. J Biol Chem 2008;283:17991–8001.
9. Lourido L, Calamia V, Mateos J, Fernández-Puente P, Fernández-Tajes J, Blanco FJ, et al. Quantitative proteomic profiling of human articular cartilage degradation in osteoarthritis. J Proteome Res 2014;13:6096–106.
10. Chijimatsu R, Kunugiza Y, Taniyama Y, Nakamura N, Tomita T, Yoshikawa H. Expression and pathological effects of periostin in human osteoarthritis cartilage. BMC Musculoskelet Disord 2015;16:215.
11. Rousseau JC, Sornay-Rendu E, Bertholon C, Garnero P, Chapurlat R. Serum periostin is associated with prevalent knee osteoarthritis and disease incidence/progression in women: the OFELY study. Osteoarthritis Cartilage 2015;23:1736–42.
12. Honsawek S, Wilairatana V, Udomsinprasert W, Sinlapavilawan P, Jirathanathornnukul N. Association of plasma and synovial fluid periostin with radiographic knee osteoarthritis: cross-sectional study. Joint Bone Spine 2015;82:352–5.
13. Loeser RF, Olex AL, McNulty MA, Carlson CS, Callahan MF, Ferguson CM, et al. Microarray analysis reveals age-related differences in gene expression during the development of osteoarthritis in mice. Arthritis Rheum 2012;64:705–17.
14. Chou CH, Wu CC, Song IW, Chuang HP, Lu LS, Chang JH, et al. Genome-wide expression profiles of subchondral bone in osteoarthritis. Arthritis Res Ther 2013;15:R190.

15. Attur M, Yang Q, Shimada K, Tachida Y, Nagase H, Mignatti P, et al. Elevated expression of periostin in human osteoarthritic cartilage and its potential role in matrix degradation via matrix metalloproteinase-13. FASEB J 2015;29:4107–21.
16. Chinzei N, Brophy RH, Duan X, Cai L, Nunley RM, Sandell LJ, et al. Molecular influence of anterior cruciate ligament tear remnants on chondrocytes: a biologic connection between injury and osteoarthritis. Osteoarthritis Cartilage 2018;26:588–99.
17. Brophy RH, Cai L, Duan X, Zhang Q, Townsend RR, Nunley RM, et al. Proteomic analysis of synovial fluid identifies periostin as a biomarker for anterior cruciate ligament injury. Osteoarthritis Cartilage 2019;27:1778–89.
18. Deng F, Chen X, Liao Z, Yan Z, Wang Z, Deng Y, et al. A simplified and versatile system for the simultaneous expression of multiple siRNAs in mammalian cells using Gibson DNA Assembly. PLoS One 2014;9:e113064.
19. Rai MF, Pan H, Yan H, Sandell LJ, Pham CT, Wickline SA. Applications of RNA interference in the treatment of arthritis [review]. Transl Res 2019;214:1–16.
20. Xin Y, Huang M, Guo WW, Huang Q, Zhang LZ, Jiang G. Nano-based delivery of RNAi in cancer therapy [review]. Mol Cancer 2017;16:134.
21. Yan H, Duan X, Pan H, Holguin N, Rai MF, Akk A, et al. Suppression of NF-κB activity via nanoparticle-based siRNA delivery alters early cartilage responses to injury. Proc Natl Acad Sci U S A 2016;113:E6199–208.
22. Yan H, Duan X, Pan H, Akk A, Sandell LJ, Wickline SA, et al. Development of a peptide-siRNA nanocomplex targeting NF- κB for efficient cartilage delivery. Sci Rep 2019;9:442.
23. Hou KK, Pan H, Ratner L, Schlesinger PH, Wickline SA. Mechanisms of nanoparticle-mediated siRNA transfection by melittin-derived peptides. ACS Nano 2013;7:8605–15.
24. Hou KK, Pan H, Lanza GM, Wickline SA. Melittin derived peptides for nanoparticle based siRNA transfection. Biomaterials 2013;34:3110–9.
25. Zhou HF, Yan H, Pan H, Hou KK, Akk A, Springer LE, et al. Peptide-siRNA nanocomplexes targeting NF-κB subunit p65 suppress nascent experimental arthritis. J Clin Invest 2014;124:4363–74.
26. Hashimoto S, Rai MF, Janiszak KL, Cheverud JM, Sandell LJ. Cartilage and bone changes during development of post-traumatic osteoarthritis in selected LGXSM recombinant inbred mice. Osteoarthritis Cartilage 2012;20:562–71.
27. Glasson SS, Blanchet TJ, Morris EA. The surgical destabilization of the medial meniscus (DMM) model of osteoarthritis in the 129/SvEv mouse. Osteoarthritis Cartilage 2007;15:1061–9.
28. Glasson SS, Chambers MG, Van Den Berg WB, Little CB. The OARSI histopathology initiative: recommendations for histological assessments of osteoarthritis in the mouse. Osteoarthritis Cartilage 2010;18 Suppl 3:S17–23.
29. Lewis JS, Hembree WC, Furman BD, Tippets L, Cattel D, Huebner JL, et al. Acute joint pathology and synovial inflammation is associated with increased intra-articular fracture severity in the mouse knee. Osteoarthritis Cartilage 2011;19:864–73.
30. Duan X, Sandell LJ, Chinzei N, Holguin N, Silva MJ, Schiavinato A, et al. Therapeutic efficacy of intra-articular hyaluronan derivative and platelet-rich plasma in mice following axial tibial loading. PLoS One 2017;12:e0175682.
31. Fosang AJ, Last K, Knauper V, Murphy G, Neame PJ. Degradation of cartilage aggrecan by collagenase-3 (MMP-13) [letter]. FEBS Lett 1996;380:17–20.
32. Brophy RH, Rai MF, Zhang Z, Torgomyan A, Sandell LJ. Molecular analysis of age and sex-related gene expression in meniscal tears with and without a concomitant anterior cruciate ligament tear. J Bone Joint Surg Am 2012;94:385–93.
33. Duchamp de Lageneste O, Julien A, Abou-Khalil R, Frangi G, Carvalho C, Cagnard N, et al. Periosteum contains skeletal stem cells with high bone regenerative potential controlled by Periostin. Nat Commun 2018;9:773.
34. Cai L, Brophy RH, Tycksen ED, Duan X, Nunley RM, Rai MF. Distinct expression pattern of periostin splice variants in chondrocytes and ligament progenitor cells. FASEB J 2019;33:8386–405.
35. Attur M, Duan X, Cai L, Han T, Zhang W, Tycksen ED, et al. Periostin loss-of-function protects mice from post-traumatic and age-related osteoarthritis. Arthritis Res Ther 2021;23:104.
36. Bao S, Ouyang G, Bai X, Huang Z, Ma C, Liu M, et al. Periostin potently promotes metastatic growth of colon cancer by augmenting cell survival via the Akt/PKB pathway. Cancer Cell 2004;5:329–39.
37. Gillan L, Matei D, Fishman DA, Gerbin CS, Karlan BY, Chang DD. Periostin secreted by epithelial ovarian carcinoma is a ligand for $\alpha_V\beta_3$ and $\alpha_V\beta_5$ integrins and promotes cell motility. Cancer Res 2002;62:5358–64.
38. Han T, Mignatti P, Abramson SB, Attur M. Periostin interaction with discoidin domain receptor-1 (DDR1) promotes cartilage degeneration. PLoS One 2020;15:e0231501.
39. Masuoka M, Shiraishi H, Ohta S, Suzuki S, Arima K, Aoki S, et al. Periostin promotes chronic allergic inflammation in response to Th2 cytokines. J Clin Invest 2012;122:2590–600.
40. Lambert AW, Wong CK, Ozturk S, Papageorgis P, Raghunathan R, Alekseyev Y, et al. Tumor cell-derived periostin regulates cytokines that maintain breast cancer stem cells. Mol Cancer Res 2016;14:103–13.
41. Marcu KB, Otero M, Olivotto E, Borzi RM, Goldring MB. NF-κB signaling: multiple angles to target OA [review]. Curr Drug Targets 2010;11:599–613.
42. Davidson EN, Remst DF, Vitters EL, van Beuningen HM, Blom AB, Goumans MJ, et al. Increase in ALK1/ALK5 ratio as a cause for elevated MMP-13 expression in osteoarthritis in humans and mice. J Immunol 2009;182:7937–45.
43. Li H, Wang D, Yuan Y, Min J. New insights on the MMP-13 regulatory network in the pathogenesis of early osteoarthritis [review]. Arthritis Res Ther 2017;19:248.
44. Neuhold LA, Killar L, Zhao W, Sung ML, Warner L, Kulik J, et al. Postnatal expression in hyaline cartilage of constitutively active human collagenase-3 (MMP-13) induces osteoarthritis in mice. J Clin Invest 2001;107:35–44.
45. Little CB, Barai A, Burkhardt D, Smith SM, Fosang AJ, Werb Z, et al. Matrix metalloproteinase 13–deficient mice are resistant to osteoarthritic cartilage erosion but not chondrocyte hypertrophy or osteophyte development. Arthritis Rheum 2009;60:3723–33.
46. Janusz MJ, Little CB, King LE, Hookfin EB, Brown KK, Heitmeyer SA, et al. Detection of aggrecanase- and MMP-generated catabolic neoepitopes in the rat iodoacetate model of cartilage degeneration. Osteoarthritis Cartilage 2004;12:720–8.
47. Brophy RH, Zhang B, Cai L, Wright RW, Sandell LJ, Rai MF. Transcriptome comparison of meniscus from patients with and without osteoarthritis. Osteoarthritis Cartilage 2018;26:422–32.
48. Fang H, Huang L, Welch I, Norley C, Holdsworth DW, Beier F, et al. Early changes of articular cartilage and subchondral bone in the DMM mouse model of osteoarthritis. Sci Rep 2018;8:2855.
49. Van der Kraan PM. Factors that influence outcome in experimental osteoarthritis [review]. Osteoarthritis Cartilage 2017;25:369–75.
50. Poole R, Blake S, Buschmann M, Goldring S, Laverty S, Lockwood S, et al. Recommendations for the use of preclinical models in the study and treatment of osteoarthritis. Osteoarthritis Cartilage 2010;18 Suppl 3:S10–6.

Arthritis & Rheumatology
Vol. 73, No. 12, December 2021, pp 2261–2270
DOI 10.1002/art.41878
Published 2021. This article is a U.S. Government work and is in the public domain in the USA.

American College of Rheumatology
Empowering Rheumatology Professionals

Osteoarthritis Care and Risk of Total Knee Arthroplasty Among Medicare Beneficiaries: A Population-Based Study of Regional Covariation

Michael M. Ward

Objective. To examine health care utilization among patients with knee osteoarthritis (OA) and assess whether utilization differs among residents of regions with high and low rates of total knee arthroplasty (TKA).

Methods. This was a retrospective cohort study of US Medicare beneficiaries with knee OA enrolled from 2005 to 2010. Health care utilization data for knee complaints, including rates of physician visits, physical therapy, knee injections, and arthroscopy, were abstracted from claims files until time of TKA or the end of the study in 2015. Utilization was compared among beneficiaries who lived in regions with high or low rates of TKA.

Results. Among 988,570 beneficiaries with knee OA, 327,499 (33.1%) underwent TKA during follow-up (median 5.6 years). Higher frequency of visits for knee complaints was associated with increased risk of TKA, whereas physical therapy, specialist care, and intraarticular treatments were associated with lower risk of TKA. Frequency of TKA varied from 26.4% in the lowest regional TKA rate quintile to 42.1% in the highest regional TKA rate quintile. Rates of physician visits, physical therapy, specialist care, and treatment with intraarticular injections varied inversely with regional TKA rate quintile. For example, 32.5% of beneficiaries in the lowest region quintile and 23.6% in the highest region quintile underwent physical therapy. Across all quintiles, physical therapy was associated with lower TKA rates.

Conclusion. Dedicated nonsurgical OA care was infrequently used to treat elderly Americans with knee OA. Nonsurgical care was more common in regions with low TKA rates, suggesting reciprocal emphasis on medical treatment compared to surgical treatment across regions.

INTRODUCTION

Forty to fifty percent of Americans will develop symptomatic knee osteoarthritis (OA) in their lifetime, often with substantial functional limitations and pain (1). Total knee arthroplasty (TKA), the most effective treatment for advanced knee OA, is the most commonly performed nonobstetric procedure in the US (2–4). In 2014, aggregate costs of TKA hospitalizations were $11.8 billion, while the overall cost of care for patients with knee OA was ~$34 billion (4,5). Rising rates of TKA are projected to strain clinical capacity, prompting efforts to develop care models to optimize knee OA treatment and increase the appropriateness of TKA (6–12). These care models emphasize patient education, weight loss, exercise and physical therapy, analgesics, and, in selected patients, orthoses and intraarticular injections, to lessen knee OA progression and the need for TKA (10–12). Based on evidence of their benefit, these interventions have also been recommended by professional societies (12,13).

The frequency of conservative care use in the US population of patients with knee OA is unknown. It is unclear how often patients are seen for knee complaints, how commonly specialists such as rheumatologists or physiatrists are consulted, and how commonly physical therapy and intraarticular medications are used. Findings from studies of selected US cohorts and data from a study population in Ontario suggest low rates of office visits, the use of intraarticular injections by fewer than one-half of patients, and infrequent use of physical therapy and visits to specialists other than orthopedists (14–18). If nonoperative measures are infrequently used, particularly among patients who later undergo TKA, it could suggest opportunities to improve the health status in patients with knee OA and potentially decrease the need for TKA (10–13). Conversely, if conservative care is already widely used, efforts to slow

The views presented in this manuscript are those of the author and do not necessarily represent those of the National Institutes of Health or the US Government.

Supported by the Intramural Research Program of the National Institute of Arthritis and Musculoskeletal and Skin Diseases, NIH (grant ZIA-AR-041153).

Michael M. Ward, MD, MPH: National Institute of Arthritis and Musculoskeletal and Skin Diseases, NIH, Bethesda, Maryland.

No potential conflicts of interest relevant to this article were reported.

Address correspondence to Michael M. Ward, MD, MPH, National Institute of Arthritis and Musculoskeletal and Skin Diseases, NIH, Building 10 CRC, Room 4-1339, 10 Center Drive, Bethesda, MD 20892. Email: wardm1@mail.nih.gov or michaelward852@gmail.com.

Submitted for publication December 2, 2020; accepted in revised form May 18, 2021.

the increase in TKA rates would need to rely more on primary prevention strategies, such as weight loss interventions.

In the US and in other countries, rates of TKA vary considerably among regions (19–22). We recently reported that TKA rates among Medicare beneficiaries varied from 61% to 182% of the national average in different regions (23). Rates were highest in the Midwest and Mountain West regions. This wide variation was observed despite adjustment for regional differences in disease burden. It is not known whether conservative care for knee OA follows similar patterns, but study of the relationship between conservative care and TKA rates would indicate whether TKA use was commensurate with the overall intensity of knee OA care in each region. If levels of conservative care and TKA rates were inversely associated, with lower use of conservative care in regions with high rates of TKA, it could suggest that high rates of TKA were partly the result of using TKA as a substitute for conservative care. In our prior study (23), TKA rates were shown to be inversely associated with the number of outpatient visits for knee complaints on the group level. The goal of this study was to investigate health care utilization among elderly patients with knee OA, determine the association between conservative care and TKA rates using patient-level data, and examine whether conservative care covaried with TKA use across regions with high and low rates of TKA.

PATIENTS AND METHODS

Data source. In this retrospective cohort study, 100% Medicare fee-for-service inpatient and outpatient claims from 2005 to 2015 were used. The study protocol was approved by the National Institute of Diabetes and Digestive and Kidney Diseases Institutional Review Board (no. 15-AR-N010), which waived the requirement for patient written informed consent because the data were deidentified.

Study cohort. The source group comprised beneficiaries who were enrolled in Medicare at age 65 years from 2005 to 2010. These years were selected so that those who were enrolled in Medicare in 2010 would have at least 5 years of follow-up, given that 2015 was the latest year of available data. From this group, those who had an outpatient or inpatient diagnosis claim of knee OA in accordance with the International Classification of Diseases, Ninth Revision, Clinical Modification (ICD-9-CM) diagnosis code (715.x6) during a face-to-face physician encounter were identified. This group was then limited to beneficiaries living in one of the 50 states or the District of Columbia and those who had valid zip codes. These restrictions were needed to assign beneficiaries to one of 306 hospital referral regions of the Dartmouth Atlas of Health Care. Hospital referral regions are defined geographic areas that reflect local referral patterns for major surgeries (24). A flow diagram of the cohort construction is presented in Supplementary Figure 1 (available on the *Arthritis & Rheumatology* website at http://onlinelibrary.wiley.com/doi/10.1002/art.41878/abstract). A single outpatient or inpatient knee OA claim has a positive predictive value of 0.82, sensitivity of 0.55, and specificity of 0.75 for the presence of knee OA (25), using the American College of Rheumatology classification criteria for knee OA as the standard (26), and has been used in previous studies of health care utilization in knee OA (5,27,28). Requiring at least 2 claims is associated with higher specificity (0.91), but much lower sensitivity (0.25) (25).

Health care utilization. Following the initial knee OA claim, all subsequent outpatient and inpatient claims for knee OA, knee pain, stiffness, or other symptoms (ICD-9 719.46, 719.56, 719.66, 719.7, 719.86, 719.96; ICD-10 M17, M25.56), knee effusion (ICD-9 719.06, 719.16, 719.26, 719.36; ICD-10 M25.46), or internal derangement (ICD-9 717, 718.46, 718.56, 718.86, 718.96; ICD-10 M23) were identified. These claims were considered to represent provider visits related to knee OA because they followed the initial claim. Claims reported by orthopedic surgeons, physiatrists, rheumatologists, or pain medicine specialists were noted. Beneficiaries who had primary TKA based on ICD-9 procedure code 81.54 or ICD-10 procedure code prefixed 0SRC or 0SRD were identified.

Codes from the Healthcare Common Procedure Coding System, along with diagnosis codes for knee complaints, were used to identify treatment by physical therapy, arthrocentesis, intraarticular glucocorticoid or hyaluronic acid (HA) injections, and arthroscopy (Supplementary Table 1, available on the *Arthritis & Rheumatology* website at http://onlinelibrary.wiley.com/doi/10.1002/art.41878/abstract). Medicare Part D data from 2006 to 2015 were used to identify beneficiaries who were prescribed oral opiates, limiting this to the time prior to TKA among those who underwent TKA (29).

Data on visits and procedures were obtained until the time of the first primary TKA, death, or the study end date of December 31, 2015. Visits that did not include diagnosis codes for knee OA or knee complaints were not included. All provider visits and treatments analyzed were covered by Medicare and would generate a claim.

Covariates. Demographic information from master beneficiary files was collected. Beneficiaries were categorized as being poor if they received subsidies for medical insurance premiums. Zip code of residence at the time of the initial knee OA claim was used to assign each beneficiary to a hospital referral region (30). The TKA rate for each region was previously indexed to the national average as an observed/expected ratio, with expected rates based on a national model adjusted for beneficiary demographics and socioeconomic characteristics, the prevalence of knee OA and knee symptom claims, area-based measures of knee OA risk factors (i.e., obesity, smoking, or occupational physical activity), and comorbidities (23). An observed/expected ratio of 1.0 represents a region with TKA rates at the national average. For this analysis, regions were categorized into quintiles of observed/expected ratios of TKA rates: 0.61–0.88, 0.89–0.96, 0.97–1.04, 1.05–1.20, and 1.21–1.82 (Supplementary Figure 2, http://onlinelibrary.wiley.com/doi/10.1002/art.41878/abstract), hereafter termed

Table 1. Characteristics of Medicare beneficiaries, overall and by regional TKA rate quintile*

	All (n = 988,570)	Quintile 1 (n = 234,027)	Quintile 2 (n = 196,705)	Quintile 3 (n = 237,416)	Quintile 4 (n = 189,138)	Quintile 5 (n = 131,284)	*P* for trend
TKA observed/expected ratio, range	–	0.61–0.88	0.89–0.96	0.97–1.04	1.05–1.20	1.21–1.82	–
Age at Medicare entry, mean ± SD years	66.5 ± 1.3	66.5 ± 1.3	66.5 ± 1.3	66.5 ± 1.3	66.5 ± 1.3	66.5 ± 1.4	0.37
Male	350,127 (35.4)	78,148 (33.4)	69,356 (35.2)	84,417 (35.6)	68,943 (36.4)	49,263 (37.5)	<0.0001
White	855,312 (86.5)	184,614 (78.9)	169,002 (85.9)	204,374 (86.1)	171,703 (90.8)	125,619 (95.7)	<0.0001
Black	80,296 (8.1)	26,219 (11.2)	18,786 (9.6)	22,973 (9.7)	10,289 (5.4)	2,029 (1.5)	–
Other race/ethnicity	52,962 (5.4)	23,194 (9.9)	8,917 (4.5)	10,069 (4.2)	7,146 (3.8)	3,636 (2.8)	–
Socioeconomic status, poor	99,952 (10.1)	39,970 (17.1)	19,929 (10.1)	20,316 (8.5)	12,777 (6.7)	6,960 (5.3)	<0.0001
Follow-up, median (IQR) years	5.62 (1.83–7.19)	5.87 (3.00–7.38)	5.68 (2.06–7.25)	5.57 (1.72–7.14)	5.48 (1.45–7.09)	5.25 (0.96–6.88)	<0.0001
Time from Medicare entry to first knee OA claim, median (IQR) years	1.27 (0.46–2.48)	1.27 (0.46–2.49)	1.25 (0.45–2.46)	1.27 (0.46–2.49)	1.26 (0.45–2.47)	1.28 (0.46–2.51)	0.12
TKA	327,499 (33.1)	61,752 (26.4)	62,376 (31.7)	79,408 (33.4)	68,628 (36.3)	55,335 (42.1)	<0.0001
Time from first knee OA claim to TKA in those with TKA, median (IQR) years	0.97 (0.17–2.98)	1.15 (0.22–3.21)	1.04 (0.19–3.06)	1.03 (0.19–3.06)	0.88 (0.15–2.82)	0.76 (0.13–2.69)	<0.0001

* Regional total knee arthroplasty (TKA) rate quintiles ranged from quintile 1 (lowest TKA rates) to quintile 5 (highest TKA rates). Except where indicated otherwise, values are the number (%).
IQR = interquartile range; OA = osteoarthritis.

regional TKA rate quintile. Data were also collected on 13 comorbidities present at the time of cohort entry that were most strongly associated with TKA risk in the previous study (23,31).

Statistical analysis. Analysis was performed in 4 steps. First, levels and types of health care use, overall and across regional TKA rate quintiles, were examined. Second, time-to-event analysis to examine the association between measures of conservative care and TKA was used. Third, in the time-to-event analysis, whether measures of conservative care were differentially associated with TKA among patients in regions with high or low rates of TKA was examined. This moderation analysis indicated whether subgroups of patients, defined by their health care use, had similar (or more disparate) risk of TKA across regions with high or low rates of TKA. Fourth, sensitivity analyses were performed.

In the first step, annual visit rates using the duration of follow-up as the denominator were calculated. Follow-up was censored if the beneficiary changed to a managed care plan or if they moved to a region in a different quintile and did not return to their original region within 6 months. Visit rates for patients who underwent TKA and those who did not undergo TKA were calculated separately and by region quintile to determine whether care varied among regions with high or low TKA rates. The proportion of beneficiaries who made any visits to physical therapists, physiatrists, rheumatologists, or pain medicine physicians and the proportion who had any intraarticular glucocorticoid injections, HA injections, or knee arthroscopy were calculated. Beneficiaries who were prescribed opiates for ≥60 days or ≥20% of follow-up were classified as being prolonged opiate users. It was hypothesized that conservative care would be more frequent in regions with lower relative rates of TKA. The Jonckheere-Terpstra test and Cochran-Armitage test were used to compare trends in median visit rates and proportions across region quintiles, respectively.

Next, time-to-event analysis was used to examine whether TKA rates varied by region quintile. Beneficiaries were followed up from the time of the first knee OA claim to TKA, death, relocation, enrollment in a managed care plan, or the end of the study, whichever occurred first. Cox proportional hazards models were used to adjust for age, sex, race, socioeconomic status, and the 13 comorbidities. For each covariate, log(-log(survival)) plots were visually examined to ensure that the proportional hazards assumption was satisfied. Given the very large sample size, hypothesis tests for this purpose were not informative. Because differences in TKA rates by region previously defined on the group level may have been confounded by a group-level third variable (23), this analysis at the individual patient level helps test whether an ecologic fallacy was present.

The association of measures of health care use with time to TKA were analyzed in the Cox proportional hazards model. These measures included visit rates for knee complaints in 4 categories (<1 visit/year, 1.0–2.9 visits/year, 3.0–5.9 visits/year, and ≥6.0 visits/year) and indicator variables for prolonged opiate use and having ever visited a physical therapist, physiatrist, rheumatologist, or pain specialist. Visit categories were based on preliminary analysis of deciles of visit rates that showed similar risks of TKA. This analysis was repeated using the annual orthopedic surgeon visit rate, and also the association of TKA risk with intraarticular glucocorticoid injections, HA injections, and arthroscopy was assessed.

In the third step, the interaction between the visit frequency category and region quintile was analyzed to determine whether higher visit rates moderated the risk of TKA across regions. In

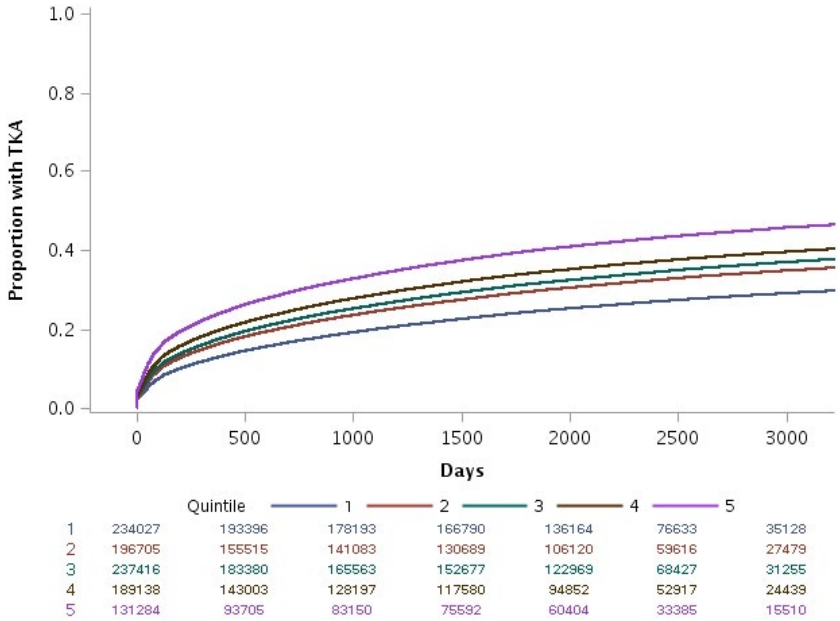

Figure 1. Cumulative incidence of total knee arthroplasty (TKA) by regional TKA rate quintile. The numbers below the graph are the number of beneficiaries under observation at each time point. Color figure can be viewed in the online issue, which is available at http://onlinelibrary.wiley.com/doi/10.1002/art.41878/abstract.

separate models, interactions between region quintile and each of the other measures of health care use were examined. Among beneficiaries who had a given intervention, less steep gradients from the lowest region quintile to the highest region quintile would indicate that the intervention was associated with less disparity in TKA use across regions. Given the large sample size, all tests of interactions were significant ($P < 0.0001$). Interpretation therefore focused on differences in adjusted hazard ratios (HRs) across region quintiles.

As one sensitivity analysis, all analyses were repeated in White Medicare beneficiaries, since racial/ethnic minorities have lower rates of TKA compared to White populations, and the racial/ethnic composition of regions varied with TKA rates. To assess the potential effects of left truncation, analyses were repeated in the subset of beneficiaries whose first knee OA claim occurred ≥2 years after entry into Medicare. Analysis was performed using SAS, version 9.4.

RESULTS

Study cohort. This cohort of 988,570 beneficiaries included mostly women (64.6%), with a mean age of 66.5 years at the time of the first knee OA visit (Table 1). The median time to first knee OA claim after entry into Medicare was 1.27 years, and median follow-up after the first knee OA visit was 5.62 years. During follow-up, 327,499 beneficiaries (33.1%) had TKA, 3,633 (0.4%) died, 45,830 (4.6%) changed to managed care coverage, and 35,949 (3.6%) changed regional TKA rate quintiles. The most common comorbidity was depression (18%) (Supplementary Table 2, http://onlinelibrary.wiley.com/doi/10.1002/art.41878/abstract). White beneficiaries comprised 78.9% of the lowest regional TKA rate quintile (quintile 1), but 95.7% of the highest regional TKA rate quintile (quintile 5) (Table 1 and Supplementary Table 3, http://onlinelibrary.wiley.com/doi/10.1002/art.41878/abstract). Overall, 3.0% of beneficiaries had a single knee OA claim, but this proportion was 8.9% in the subset who progressed to undergoing TKA.

Regional differences in TKA rates. In quintile 1, 26.4% of beneficiaries underwent TKA, and 42.1% of beneficiaries in quintile 5 underwent TKA (Figure 1). Compared to beneficiaries in quintile 3 (regions with rates at the national average), the adjusted HR for TKA was 0.80 (95% confidence interval [95% CI] 0.78–0.81) among beneficiaries in quintile 1 and 1.28 (95% CI 1.26–1.30) among beneficiaries in quintile 5 (Supplementary Table 4, http://onlinelibrary.wiley.com/doi/10.1002/art.41878/abstract). Results were similar among White Medicare beneficiaries (Supplementary Tables 3 and 4). This analysis indicates that regional differences in TKA rates previously found at the group or population level are also evident at the patient level, which excludes an ecologic fallacy (23).

Health care use overall and by region. Beneficiaries had a median of 1.8 visits/year to any provider for knee complaints (interquartile range [IQR] 0.5–5.6) and a median of 0.5 visits/year (IQR 0–2.0) to orthopedic surgeons (Table 2). Visit rates were substantially higher among those who subsequently had TKA (median 7.1 visits/year [IQR 3.1–15.6] overall and median 3.0 visits/year [IQR 0.9–7.4] to orthopedic surgeons), likely reflecting more severe knee OA. Physical therapy was used by 27.1% of beneficiaries, while smaller proportions had visits to physiatrists, rheumatologists, or pain specialists. There was little overlap in visits to different specialists (Supplementary Table 5, http://onlinelibrary.wiley.com/doi/10.1002/art.41878/abstract).

Although 26.1% of beneficiaries had ever been prescribed opiates, only 7.7% were treated with opiates regularly. Intraarticular glucocorticoid injections were received by 39.2% of beneficiaries, and HA injections were received by 18.9%. Of those without TKA, 9.9% underwent arthroscopy.

Visit rates for knee complaints were higher among beneficiaries in quintile 1 compared to those in quintile 5 (Table 2). For example, among those without TKA, median visit rates were 1.3/year in quintile 1 and 0.8/year in quintile 5. There were no clear trends in orthopedic surgeon visit rates or prolonged opiate use across quintiles. However, compared to beneficiaries in quintile 5, those in quintile 1 were more likely to have visited physical therapists, physiatrists, rheumatologists, or pain specialists and were more likely to be treated with intraarticular glucocorticoid and HA injections. In contrast, beneficiaries in quintile 5 more often underwent arthroscopy.

Results were similar in White beneficiaries and in the 233,296 beneficiaries with ≥6.0 visits/year, indicating regional differences in care even among more frequent users (Supplementary Tables 6 and 7, http://onlinelibrary.wiley.com/doi/10.1002/art.41878/abstract). Similar gradients in utilization were present among the 332,080 beneficiaries whose first knee OA claim occurred ≥2 years after Medicare entry (Supplementary Table 8, http://onlinelibrary.wiley.com/doi/10.1002/art.41878/abstract).

Health care utilization and risk of TKA. Among all beneficiaries, higher rates of knee-related visits to any provider and higher rates of orthopedic surgeon visits were associated with increased TKA rates (Table 3). In contrast, TKA rates were lower among beneficiaries who underwent physical therapy or visited physiatrists, rheumatologists, or pain specialists, those who were treated with opiates for a prolonged period of time, or those who received intraarticular treatments. While these associations may reflect clinical benefit and reduced need for TKA from these interventions, they could also represent selection of these interventions by beneficiaries more averse to TKA. These results were similar among White beneficiaries (Supplementary Table 9, http://onlinelibrary.wiley.com/doi/10.1002/art.41878/abstract).

Health care utilization and moderation analysis of differences in TKA rates across regions. Compared to the reference group (quintile 3), TKA rates were higher in region quintile 5 and lower in region quintile 1 at all frequencies of knee-related visits (Figure 2). However, the gradient in TKA rates across

Table 2. Health care utilization among Medicare beneficiaries with knee OA, stratified by TKA status and regional TKA rate quintile*

	All (n = 988,570)	Quintile 1 (n = 234,027)	Quintile 2 (n = 196,705)	Quintile 3 (n = 237,416)	Quintile 4 (n = 189,138)	Quintile 5 (n = 131,284)	Z score
Annual visits for knee complaints, median (IQR)							
All	1.8 (0.5–5.6)	1.9 (0.5–5.6)	1.7 (0.5–5.3)	1.8 (0.5–5.4)	1.8 (0.5–5.8)	1.8 (0.5–6.2)	−4.8†
TKA	7.1 (3.1–15.6)	7.6 (3.4–15.6)	7.1 (3.1–15.4)	7.0 (3.1–15.2)	7.1 (3.1–16.0)	6.8 (2.7–16.3)	−8.4†
No TKA	1.0 (0.3–2.5)	1.3 (0.4–3.1)	1.0 (0.3–2.4)	1.0 (0.3–2.4)	0.9 (0.3–2.2)	0.8 (0.3–2.0)	−69.9†
Annual orthopedic surgeon visits, median (IQR)							
All	0.5 (0–2.0)	0.4 (0–1.7)	0.5 (0–2.0)	0.5 (0–2.0)	0.5 (0–2.2)	0.4 (0–2.1)	20.4
TKA	3.0 (0.9–7.4)	3.2 (1.0–7.5)	3.2 (1.0–7.6)	3.0 (1.0–7.3)	3.0 (0.9–7.6)	2.4 (0.6–6.7)	−23.1†
No TKA	0.2 (0–0.7)	0.2 (0–0.8)	0.2 (0–0.8)	0.2 (0–0.7)	0.2 (0–0.7)	0.2 (0–0.6)	−23.7†
Physical therapy							
All	267,830 (27.1)	76,078 (32.5)	50,983 (25.9)	63,448 (26.7)	46,364 (24.5)	30,957 (23.6)	62.2
TKA	76,494 (23.4)	15,912 (25.8)	14,262 (22.9)	19,749 (24.9)	15,125 (22.0)	11,446 (20.7)	19.9
No TKA	191,336 (28.9)	60,166 (34.9)	36,721 (27.3)	43,699 (27.6)	31,239 (25.9)	19,511 (25.7)	54.8
Physiatrist visit							
All	48,160 (4.8)	20,400 (8.7)	7,271 (3.7)	10,257 (4.3)	6,756 (3.6)	3,476 (2.6)	83.0
TKA	10,428 (3.2)	3,406 (5.5)	1,608 (2.6)	2,334 (2.9)	2,016 (2.9)	1,064 (1.9)	29.9
No TKA	37,732 (5.7)	16,994 (9.9)	5,663 (4.2)	7,923 (5.0)	4,740 (3.9)	2,412 (3.2)	72.5
Rheumatologist visit							
All	83,320 (8.4)	26,727 (11.4)	17,749 (9.0)	19,040 (8.0)	12,715 (6.7)	7,089 (5.4)	70.6
TKA	20,992 (6.4)	5,884 (9.5)	4,375 (7.0)	4,938 (6.2)	3,471 (5.1)	2,324 (4.2)	40.0
No TKA	62,328 (9.4)	20,843 (12.1)	13,374 (10.0)	14,102 (8.9)	9,244 (7.7)	4,765 (6.3)	52.9
Pain specialist visit							
All	16,093 (1.6)	5,227 (2.2)	3,414 (1.7)	3,478 (1.4)	2,852 (1.5)	1,122 (0.8)	31.2
TKA	3,786 (1.2)	994 (1.6)	804 (1.3)	847 (1.1)	795 (1.2)	346 (0.6)	14.8
No TKA	12,307 (1.9)	4,233 (2.5)	2,610 (1.9)	2,631 (1.7)	2,057 (1.7)	776 (1.0)	24.6
Prolonged opiate use							
All	75,973 (7.7)	16,198 (6.9)	16,255 (8.2)	18,784 (7.9)	15,645 (8.3)	9,091 (6.9)	−4.3
TKA	15,690 (4.8)	2,862 (4.6)	3,074 (4.9)	3,927 (4.9)	3,445 (5.0)	2,382 (4.3)	1.6
No TKA	60,283 (9.1)	13,336 (7.7)	13,181 (9.8)	14,857 (9.4)	12,200 (10.1)	6,709 (8.8)	−14.6
Intraarticular glucocorticoid injection							
All	387,702 (39.2)	92,071 (39.3)	81,743 (41.5)	94,345 (39.7)	72,397 (38.3)	47,146 (35.9)	23.8
TKA	139,529 (42.6)	27,510 (44.5)	28,400 (45.5)	34,472 (43.4)	28,232 (41.1)	20,915 (37.8)	27.5
No TKA	248,173 (37.5)	64,561 (37.5)	53,343 (39.7)	59,873 (37.9)	44,165 (36.6)	26,231 (34.5)	15.8
Intraarticular HA injection							
All	187,268 (18.9)	50,439 (21.5)	36,894 (18.7)	44,566 (18.8)	33,752 (17.5)	21,617 (16.4)	38.8
TKA	73,436 (22.4)	16,364 (26.5)	14,460 (23.2)	18,247 (23.0)	14,390 (21.0)	9,975 (18.0)	35.2
No TKA	113,832 (17.2)	34,075 (19.8)	22,434 (16.7)	26,319 (16.7)	19,362 (16.1)	11,642 (15.3)	30.1
Arthroscopy							
All	94,177 (9.5)	19,790 (8.4)	19,353 (9.8)	23,104 (9.7)	18,880 (10.0)	13,050 (9.9)	−16.1
TKA	28,784 (8.8)	5,269 (8.5)	5,731 (9.2)	7,216 (9.1)	6,054 (8.8)	4,514 (8.2)	2.7
No TKA	65,393 (9.9)	14,521 (8.4)	13,622 (10.1)	15,888 (10.0)	12,826 (10.6)	8,536 (11.2)	−23.6

* Except where indicated otherwise, values are the number (%). All Z scores for trend across regional total knee arthroplasty (TKA) rate quintiles were significant ($P < 0.0001$), except for the Z score across quintiles for arthroscopy utilization among patients who underwent TKA ($P = 0.006$). OA = osteoarthritis; IQR = interquartile range; HA = hyaluronic acid.
† Negative Z scores on the Jonckheere-Terpstra test indicate a decrease in utilization rates among those in the higher regional TKA rate quintiles.

Table 3. Association of health care utilization with total knee arthroplasty rates among Medicare beneficiaries with knee osteoarthritis*

	All office visits, adjusted HR (95% CI)	Orthopedic surgeon visits, adjusted HR (95% CI)
Annual visits for knee complaints		
<1.0 visit/year	1.00 (referent)	1.00 (referent)
1.0–2.9 visits/year	2.14 (2.11–2.18)	4.34 (4.30–4.39)
3.0–5.9 visits/year	8.38 (8.27–8.50)	11.54 (11.42–11.67)
≥6.0 visits/year	32.38 (31.99–32.77)	31.97 (31.63–32.30)
Physical therapy	0.31 (0.30–0.31)	0.55 (0.54–0.56)
Physiatrist visit	0.47 (0.45–0.48)	0.75 (0.73–0.77)
Rheumatologist visit	0.50 (0.49–0.51)	0.93 (0.91–0.95)
Pain specialist visit	0.42 (0.40–0.44)	0.74 (0.71–0.76)
Prolonged opiate use	0.57 (0.55–0.58)	0.62 (0.60–0.63)
Intraarticular glucocorticoid injection	0.61 (0.60–0.62)	0.63 (0.62–0.65)
Intraarticular HA injection	0.46 (0.45–0.47)	0.44 (0.43–0.45)
Arthroscopy	0.56 (0.54–0.57)	0.54 (0.53–0.55)

* Results are the adjusted hazard ratio (HR) and 95% confidence interval (95% CI) for association of each utilization variable with total knee arthroplasty rates according to visit type (all office visits for knee complaints or visits to orthopedic surgeons). Cox proportional hazards models were used, with adjustments for age, sex, race, socioeconomic status (poor), 13 comorbidities, and region quintile. HA = hyaluronic acid.

regions was steeper among beneficiaries with low visit rates, and less steep among beneficiaries with high visit rates. For example, the adjusted HR from quintile 1 to quintile 5 ranged from 0.76 to 1.39 among beneficiaries with <1.0 visit/year, compared to a lower range (adjusted HR 0.80 to 1.21) among beneficiaries with ≥6.0 visits/year. Results were similar for orthopedic surgeon visit rates, with a gradient in adjusted HR of 0.75 to 1.59 among beneficiaries with <1.0 visit/year, compared to a gradient of 0.80 to 1.30 among those with ≥6.0 visits/year. These results indicate that the greatest disparity in TKA use across regions was among beneficiaries with the lowest frequency of knee-related visits. In the lowest TKA rate quintiles (quintiles 1 and 2), beneficiaries with low visit frequencies were somewhat less likely to undergo a TKA compared to those with higher visit frequencies, whereas in the highest TKA quintile (quintile 5), beneficiaries with low visit frequencies were more likely to undergo a TKA relative to those with higher visit frequencies.

Regardless of region, beneficiaries who received physical therapy had lower risk of TKA compared to those who did not (Figure 2). With respect to intraarticular treatments, risks for TKA were substantially lower among those in quintile 5 who received intraarticular glucocorticoid injections, HA injections, or arthroscopy. Conversely, risks for TKA were somewhat higher among beneficiaries in quintile 1 who received these treatments (i.e., closer to those of beneficiaries in quintile 3), indicating a smaller gradient in TKA risk across regions among beneficiaries who received these interventions. There was no moderation in TKA risk by physiatrist, rheumatologist, or pain specialist visits, or

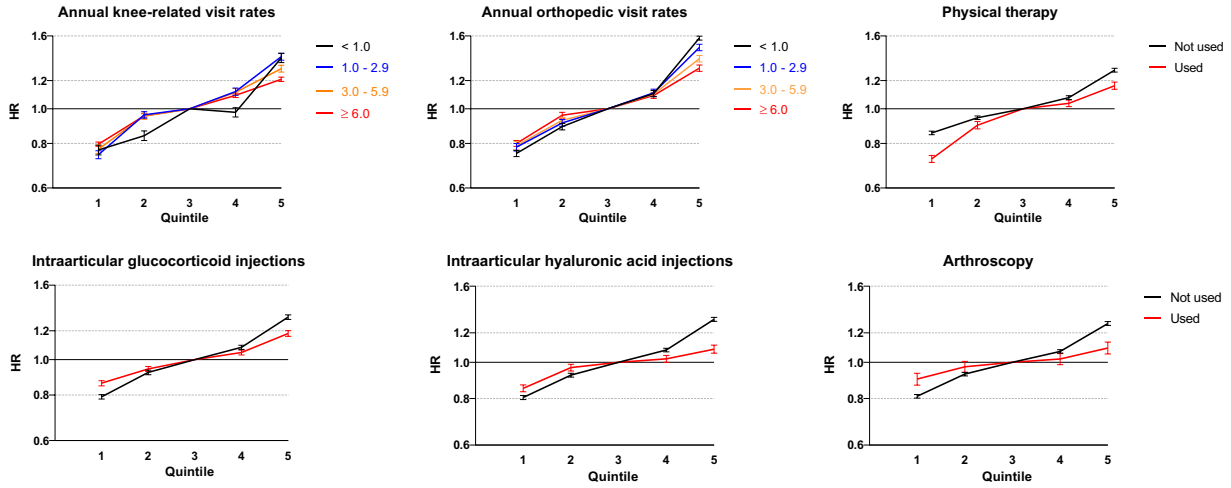

Figure 2. Rates of total knee arthroplasty (TKA) by regional TKA rate quintile in strata of health care utilization. Results are shown as adjusted hazard ratios (HRs) and 95% confidence intervals based on interactions between regional TKA rate quintiles and each measure of health care utilization, calculated using Cox proportional hazards models. Quintile 3 is the reference category for each stratum.

with prolonged treatment with opiates (Supplementary Figure 3, http://onlinelibrary.wiley.com/doi/10.1002/art.41878/abstract). Results were very similar in analyses that were limited to White beneficiaries (Supplementary Figure 4, http://onlinelibrary.wiley.com/doi/10.1002/art.41878/abstract).

DISCUSSION

This study had 3 main findings. First, dedicated nonsurgical OA care was infrequently used. Physical therapy and intraarticular treatments were used by a minority of patients, and few were treated by rheumatologists, physiatrists, or pain specialists. While this may be because many beneficiaries had mild knee OA, use of these services was also low among those who subsequently had TKA. Second, there was an inverse association between TKA rates and the use of conservative treatments across regions, including office visit rates, treatment by specialists, and receipt of intraarticular injections. Third, disparities in the risk of TKA across regions were more pronounced among beneficiaries with low office visit rates and those who did not receive prior intraarticular treatments, which are markers of less severe knee OA. Taken together, these results suggest opportunities to expand nonsurgical care for knee OA that may reduce TKA rates.

The finding of generally low use of conservative interventions in patients with knee OA is consistent with findings from a prior claims-based US study, which showed that 10.0% of patients received physical therapy prior to TKA and 25.9% received physical therapy without TKA (14). Intraarticular glucocorticoid injections (43.5% versus 16.6%) and HA injections (15.4% versus 6.3%), and arthroscopy (19.6% versus 11.5%) were more common among patients who subsequently had TKA. In other US studies that only examined health care use prior to TKA, 13–16% of patients received physical therapy, 46–63% received glucocorticoid injections, 18–24% received HA injections, and 15–35% received any opiates (32–35). In this study, prolonged opiate use was more common among those who did not ultimately undergo TKA, perhaps indicating the presence of contraindications or reservations about surgery. Other studies did not specifically examine knee OA or visit rates (36–38).

Visit rates for knee complaints and the frequency of use of physical therapy, specialists in musculoskeletal medicine, and intraarticular injections were inversely associated with TKA rates across regions. Lower use of physical therapy, physiatry, and rheumatology care in regions with high TKA rates in the upper Midwest and Northwest were not likely related to an undersupply of providers in these regions. Recent workforce studies indicate that a shortage of physical therapists is most severe in southern states, California, and Nevada, whereas supply of physiatrists is lowest in Arizona, New Mexico, and several southern states (39,40). Similarly, the supply of rheumatologists per capita is higher in the upper Midwest and Northwest regions compared to the south (41). While intraarticular glucocorticoid injections are recommended to treat knee OA, recent clinical guidelines now recommend against the use of HA injections as a general treatment approach (12,42). Although arthroscopy was associated with a lower risk of subsequent TKA in the group overall, arthroscopy was more common in regions with higher TKA rates, possibly reflecting a predisposition to surgery among beneficiaries in these regions. Visit rates to orthopedic surgeons prior to TKA were also lower in regions with higher TKA rates, consistent with faster progression to TKA in these regions. Taken together, these associations suggest that TKA is a substitution for longer periods of conservative care in regions with higher TKA rates.

The moderation analysis provides additional support that TKA was a substitution for conservative care in some regions. Risks of TKA were most disparate across regions among patients with low rates of knee-related visits (<1.0 visit/year). In most regions, patients with low visit rates had a low risk of TKA, presumably because low visit rates reflect less severe knee OA. Yet, these "low-risk" patients were at substantially higher risk if they lived in regions with high TKA rates. There was less disparity in TKA rates across regions among patients with higher office visit rates (≥6.0 visits/year), a marker of more severe knee OA, indicating more consistency across regions in the use of TKA among such patients. These associations were present for both overall visit frequency and visits specifically to orthopedic surgeons.

An alternative explanation is that regions with high TKA risks included more beneficiaries with more severe knee OA. Although opiate use is an indicator of pain severity, patient-reported measures of pain and physical function and radiographs were not available, and differences in knee OA severity could not be examined directly. However, if higher TKA risks represent more severe knee OA, higher rates of physician visits for knee OA, higher use of physical therapy and specialty care, and greater use of intraarticular glucocorticoid injections would have also been expected in these regions, yet the opposite trends were present. The moderation analysis also indicated regional differences in TKA risk among beneficiaries with the same frequency of visits and among those who received intraarticular injections or arthroscopy, which are indirect measures of knee OA severity. Additionally, TKA risks varied widely across several small geographic areas (Maine/New Hampshire/Massachusetts, the greater Chicago region, West Texas/New Mexico), which cannot be explained by differences in the clinical presentation or severity of knee OA.

The moderation analysis also provides insight into the subsets of patients for which there was more consistency in TKA use across the country. TKA rates were more consistent across regions among beneficiaries who had arthroscopy or intraarticular injections, indicating greater agreement on the need (or lack of need) for TKA among these patients. Conversely, there were greater disparities in TKA use among patients who did not receive these interventions, which may reflect a group with milder knee OA. Beneficiaries who received physical therapy had lower TKA rates relative to those who did not receive physical therapy across all regions, suggesting a true benefit in reducing TKA (43–45).

This study has some potential limitations. The population analyzed was limited to Medicare beneficiaries age ≥65 years. Associations may be different in younger patients. TKA rates in persons age <65 years are approximately one-half those among persons age ≥65 years, and differential rates of TKA among younger and older persons across regions (46) may bias the results of this study. For example, regions with high TKA rates may reflect greater postponement of TKA until Medicare eligibility, rather than higher overall use of TKA. Conversely, TKA rates might be high among young persons in the regions identified as having low rates among Medicare beneficiaries, resulting in depletion of persons eligible for TKA at older ages. There are no national studies of TKA rates by region among younger individuals. The TKA quartile map in this study corresponds with the geographic distribution of persons living with a TKA (irrespective of age at surgery), which suggests that the findings among those age ≥65 years may also apply to the whole population (47), but this could not be tested directly. It is not known what treatments were used prior to entry into Medicare. However, most beneficiaries were in Medicare for >1 year before their first knee OA claim, and results were similar in the subset whose first knee OA claim occurred after 2 years in Medicare. Willingness to undergo TKA is an important factor determining its use (48), and it is unknown whether this varies by region. There may be coding inaccuracies, but beneficiaries had multiple visits for knee complaints. A small proportion of beneficiaries had only one knee OA claim, but it was important to include these patients because they were overrepresented among those receiving a TKA. Finally, costs of care and the relative cost-effectiveness of different treatment approaches were not examined, but the costs of nonoperative care for knee OA are generally low (49).

In conclusion, physical therapy and specialist care were infrequently used by Medicare beneficiaries with knee OA, even among those who later underwent TKA. It would be important to know whether use of these services was limited by capacity constraints or underappreciation of their role in knee OA treatment. These results indicate the possibility for greater use of conservative care for knee OA, with the potential to slow rising TKA rates. The reciprocal association between TKA rates and use of nonsurgical treatments across regions suggests that TKA was a substitution for nonoperative care more often in regions with high TKA rates. Disparities in TKA use across regions were greatest among patient subgroups with indicators of less severe knee OA, for which TKA may be more discretionary. These associations raise questions about whether the appropriateness of TKA also varies by region.

AUTHOR CONTRIBUTIONS

Dr. Ward drafted the article, revised it critically for important intellectual content, approved the final version to be published, and takes responsibility for the integrity of the data and the accuracy of the data analysis.

REFERENCES

1. Murphy L, Schwartz TA, Helmick CG, Renner JB, Tudor G, Koch G, et al. Lifetime risk of symptomatic knee osteoarthritis. Arthritis Rheum 2008;59:1207–13.
2. Skou ST, Roos EM, Laursen MB, Rathleff MS, Arendt-Nielsen L, Simonsen O, et al. A randomized, controlled trial of total knee replacement. N Engl J Med 2015;373:1597–606.
3. Skou ST, Roos EM, Laursen MB, Rathleff MS, Arendt-Nielsen L, Rasmussen S, et al. Total knee replacement and non-surgical treatment of knee osteoarthritis: 2-year outcome from two parallel randomized controlled trials. Osteoarthritis Cartilage 2018;26:1170–80.
4. McDermott KW, Freeman WJ, Elixhauser A. Overview of operating room procedures during inpatient stays in U.S. hospitals, 2014: statistical brief #233. In: Healthcare Cost and Utilization Project statistical briefs. Rockville (MD): Agency for Healthcare Research and Quality; 2017. URL: https://www.ncbi.nlm.nih.gov/books/NBK487976/.
5. Chen F, Su W, Bedenbaugh AV, Oruc A. Health care resource utilization and burden of disease in a US Medicare population with a principal diagnosis of osteoarthritis of the knee. J Med Econ 2020;23:1151–8.
6. Cram P, Lu X, Kates SL, Singh JA, Li Y, Wolf BR. Total knee arthroplasty volume, utilization, and outcomes among Medicare beneficiaries, 1991–2010. JAMA 2012;308:1227–36.
7. Losina E, Thornhill TS, Rome BN, Wright J, Katz JN. The dramatic increase in total knee replacement utilization rates in the United States cannot be fully explained by growth in population size and the obesity epidemic. J Bone Joint Surg Am 2012;94:201–7.
8. Navathe AS, Troxel AB, Liao JM, Nan N, Zhu J, Zhong W, et al. Cost of joint replacement using bundled payment models. JAMA Intern Med 2017;177:214–22.
9. Riddle DL, Jiranek WA, Hayes CW. Use of a validated algorithm to judge the appropriateness of total knee arthroplasty in the United States: a multicenter longitudinal cohort study. Arthritis Rheumatol 2014;66:2134–43.
10. Allen KD, Choong PF, Davis AM, Dowsey MM, Dziedzic KS, Emery C, et al. Osteoarthritis: models for appropriate care across the disease continuum [review]. Best Pract Res Clin Rheumatol 2016;30:503–35.
11. Button K, Morgan F, Weightman AL, Jones S. Musculoskeletal care pathways for adults with hip and knee pain referred for specialist opinion: a systematic review. BMJ Open 2019;9:e027874.
12. Kolasinski SL, Neogi T, Hochberg MC, Oatis C, Guyatt G, Block J, et al. 2019 American College of Rheumatology/Arthritis Foundation guideline for the management of osteoarthritis of the hand, hip, and knee. Arthritis Rheumatol 2020;72:220–33.
13. Bannuru RR, Osani MC, Vaysbrot EE, Arden NK, Bennell K, Bierma-Zeinstra SM, et al. OARSI guidelines for the non-surgical management of knee, hip, and polyarticular osteoarthritis. Osteoarthritis Cartilage 2019;27:1578–89.
14. Dhawan A, Mather RC III, Karas V, Ellman MB, Young BB, Bach BR Jr, et al. An epidemiologic analysis of clinical practice guidelines for non-arthroplasty treatment of osteoarthritis of the knee. Arthroscopy 2014;30:65–71.
15. Allen KD, Oddone EZ, Coffman CJ, Jeffreys AS, Bosworth HB, Chatterjee R, et al. Patient, provider, and combined interventions for managing osteoarthritis in primary care: a cluster randomized trial. Ann Intern Med 2017;166:401–11.
16. Harrold LR, Yood RA, Straus W, Andrade SE, Reed JI, Cernieux J, et al. Challenges of estimating health service utilization for osteoarthritis patients on a population level. J Rheumatology 2002;29:1931–6.
17. Canizares M, Davis AM, Badley EM. The pathway to orthopaedic surgery: a population study of the role of access to primary care and

availability of orthopaedic services in Ontario, Canada. BMJ Open 2014;4:e004472.

18. MacKay C, Canizares M, Davis AM, Badley EM. Health care utilization for musculoskeletal disorders. Arthritis Care Res (Hoboken) 2010;62:161–9.
19. Judge A, Welton NJ, Sandhu J, Ben-Shlomo Y. Geographical variation in the provision of elective primary hip and knee replacement: the role of socio-demographic, hospital and distance variables. J Public Health (Oxf) 2009;31:413–22.
20. Wright JG, Hawker GA, Bombardier C, Croxford R, Dittus RS, Freund DA, et al. Physician enthusiasm as an explanation for area variation in the utilization of knee replacement surgery. Med Care 1999:946–56.
21. Schäfer T, Pritzkuleit R, Jeszenszky C, Malzahn J, Maier W, Günther KP, et al. Trends and geographical variation of primary hip and knee joint replacement in Germany. Osteoarthritis Cartilage 2013;21:279–88.
22. Birkmeyer JD, Reames BN, McCulloch P, Carr AJ, Campbell WB, Wennberg JE. Understanding of regional variation in the use of surgery [review]. Lancet 2013;382:1121–9.
23. Ward MM, Dasgupta A. Regional variation in rates of total knee arthroplasty among Medicare beneficiaries. JAMA Netw Open 2020;3:e203717.
24. The Dartmouth Institute for Health Policy and Clinical Practice. The Dartmouth Atlas of Health Care. URL: http://www.dartmouthatlas.org.
25. Rahman MM, Kopec JA, Goldsmith CH, Anis AH, Cibere J. Validation of administrative osteoarthritis diagnosis using a clinical and radiological population-based cohort. Int J Rheumatol 2016;2016:6475318.
26. Altman R, Asch E, Bloch D, Bole G, Borenstein D, Brandt K, et al. Development of criteria for the classification and reporting of osteoarthritis: classification of osteoarthritis of the knee. Arthritis Rheum 1986;29:1039–49.
27. Dominick KL, Ahern FM, Gold CH, Heller DA. Health-related quality of life and health service use among older adults with osteoarthritis. Arthritis Care Res (Hoboken) 2004;51:326–31.
28. Wright EA, Katz JN, Cisternas MG, Kessler CL, Wagenseller A, Losina E. Impact of knee osteoarthritis on health care resource utilization in a US population-based national sample. Med Care 2010;48:785–91.
29. Morden NE, Munson JC, Colla CH, Skinner JS, Bynum JP, Zhou W, et al. Prescription opioid use among disabled Medicare beneficiaries: intensity, trends and regional variation. Med Care 2014;52:852–9.
30. Centers for Medicare and Medicaid Services. Medicare geographic variation public use files. URL: https://www.cms.gov/Research-Statistics-Data-and-Systems/Statistics-Trends-and-Reports/Medicare-Geographic-Variation/GV_PUF.html.
31. Centers for Medicare and Medicaid Services. Chronic Conditions Data Warehouse: condition categories. URL: https://www.ccwdata.org/web/guest/condition-categories.
32. Bedard NA, Dowdle SB, Anthony CA, DeMik DE, McHugh MA, Bozic KJ, et al. The AAHKS Clinical Research Award: what are the costs of knee osteoarthritis in the year prior to total knee arthroplasty? J Arthroplasty 2017;32:S8–10.
33. Warwick H, O'Donnell J, Mather RC III, Jiranek W. Disparity of health services in patients with knee osteoarthritis before total knee arthroplasty. Arthroplast Today 2020;6:81–7.
34. Cohen JR, Bradley AT, Lieberman JR. Preoperative interventions and charges before total knee arthroplasty. J Arthroplasty 2016;31:2730–5.
35. Berger A, Bozic K, Stacey B, Edelsberg J, Sadosky A, Oster G. Patterns of pharmacotherapy and health care utilization and costs prior to total hip or total knee replacement in patients with osteoarthritis. Arthritis Rheum 2011;63:2268–75.
36. Gore M, Tai KS, Sadosky A, Leslie D, Stacey BR. Clinical comorbidities, treatment patterns, and direct medical costs of patients with osteoarthritis in usual care: a retrospective claims database analysis. J Med Econ 2011;14:497–507.
37. Dunn JD, Pill MW. A claims-based view of health care charges and utilization for commercially insured patients with osteoarthritis. Manag Care 2009;18:44–50.
38. White AG, Birnbaum HG, Janagap C, Buteau S, Schein J. Direct and indirect costs of pain therapy for osteoarthritis in an insured population in the United States. J Occup Environ Med 2008;50:998–1005.
39. Zimbelman JL, Juraschek SP, Zhang X, Lin VW. Physical therapy workforce in the United States: forecasting nationwide shortages. PM R 2010;2:1021–9.
40. Salsberg E, Erikson C. The changing physician workforce landscape: implications for physical medicine and rehabilitation. Am J Phys Med Rehabil 2007;86:838–44.
41. Battafarano DF, Ditmyer M, Bolster MB, Fitzgerald JD, Deal C, Bass AR, et al. 2015 American College of Rheumatology workforce study: supply and demand projections of adult rheumatology workforce, 2015–2030. Arthritis Care Res (Hoboken) 2018;70:617–26.
42. Jevsevar DS. Treatment of osteoarthritis of the knee: evidence-based guideline [review]. J Am Acad Orthop Surg 2013;21:571–6.
43. Deyle GD, Henderson NE, Matekel RL, Ryder MG, Garber MB, Allison SC. Effectiveness of manual physical therapy and exercise in osteoarthritis of the knee: a randomized, controlled trial. Ann Intern Med 2000;132:173–81.
44. Fransen M, McConnell S, Harmer AR, van der Esch M, Simic M, Bennell KL. Exercise for osteoarthritis of the knee: a Cochrane systematic review. Br J Sports Med 2015;49:1554–7.
45. Deyle GD, Allen CS, Allison SC, Gill NW, Hando BR, Petersen EJ, et al. Physical therapy versus glucocorticoid injection for osteoarthritis of the knee. N Engl J Med 2020;382:1420–9.
46. Sloan M, Premkumar A, Sheth NP. Projected volume of primary total joint arthroplasty in the U.S., 2014 to 2030. J Bone Joint Surg Am 2018;100:1455–60.
47. Kremers HM, Larson DR, Crowson CS, Kremers WK, Washington RE, Steiner CA, et al. Prevalence of total hip and knee replacement in the United States. J Bone Joint Surg Am 2015;97:1386–97.
48. Hawker GA, Wright JG, Coyte PC, Williams JI, Harvey B, Glazier R, et al. Determining the need for hip and knee arthroplasty: the role of clinical severity and patients' preferences. Med Care 2001;39:206–16.
49. Losina E, Paltiel AD, Weinstein AM, Yelin E, Hunter DJ, Chen SP, et al. Lifetime medical costs of knee osteoarthritis management in the United States: impact of extending indications for total knee arthroplasty. Arthritis Care Res (Hoboken) 2015;67:203–15.

Arthritis & Rheumatology
Vol. 73, No. 12, December 2021, pp 2271–2281
DOI 10.1002/art.41882
© 2021, American College of Rheumatology

American College of Rheumatology
Empowering Rheumatology Professionals

Targeting the CCR6/CCL20 Axis in Entheseal and Cutaneous Inflammation

Zhenrui Shi,[1] Emma Garcia-Melchor,[2] Xuesong Wu,[3] Anthony E. Getschman,[4] Mimi Nguyen,[3] Douglas J. Rowland,[3] Machelle Wilson,[3] Flavia Sunzini,[2] Moeed Akbar,[2] Mindy Huynh,[3] Timothy Law,[3] Smriti K. Raychaudhuri,[5] Siba P. Raychaudhuri,[5] Brian F. Volkman,[4] Neal L. Millar,[2] and Sam T. Hwang[3]

Objective. To assess the involvement of the CCR6/CCL20 axis in psoriatic arthritis (PsA) and psoriasis (PsO) and to evaluate its potential as a therapeutic target.

Methods. First, we quantified CCL20 levels in peripheral blood and synovial fluid from PsA patients and examined the presence of CCR6+ cells in synovial and tendon tissue. Utilizing an interleukin-23 minicircle DNA (IL-23 MC) mouse model exhibiting key features of both PsO and PsA, we investigated CCR6 and CCL20 expression as well as the preventive and therapeutic effect of CCL20 blockade. Healthy tendon stromal cells were stimulated in vitro with IL-1β to assess the production of CCL20 by quantitative polymerase chain reaction and enzyme-linked immunosorbent assay. The effect of conditioned media from stimulated tenocytes in inducing T cell migration was interrogated using a Transwell system.

Results. We observed an up-regulation of both CCR6 and CCL20 in the enthesis of IL-23 MC–treated mice, which was confirmed in human biopsy specimens. Specific targeting of the CCR6/CCL20 axis with a CCL20 locked dimer (CCL20LD) blocked entheseal inflammation, leading to profound reductions in clinical and proinflammatory markers in the joints and skin of IL-23 MC–treated mice. The stromal compartment in the tendon was the main source of CCL20 in this model and, accordingly, in vitro activated human tendon cells were able to produce this chemokine and to induce CCR6+ T cell migration, the latter of which could be blocked by CCL20LD.

Conclusion. Our study highlights the pathogenic role of the CCR6/CCL20 axis in enthesitis and introduces the prospect of a novel therapeutic approach for treating patients with PsO and PsA.

INTRODUCTION

Psoriatic arthritis (PsA) is a chronic inflammatory arthritis affecting up to one-third of individuals with psoriasis (PsO) (1). Current treatments aim to control aberrant inflammation in both skin and joints by targeting inflammatory cytokines. Blockade of tumor necrosis factor (TNF), interleukin-17A (IL-17A), and IL-23 have been remarkably successful in treating skin PsO, with ~80% of PsA patients achieving 75% improvement according to the Psoriasis Area and Severity Index (PASI) (2,3), while only 60% of patients with PsA achieve a clinically meaningful improvement according to the American College of Rheumatology 20% improvement criteria (1,4–6). Furthermore, their use is restricted by their side effect panel, with an increased susceptibility to infections (7), and the development of neutralizing antibodies (8). There is therefore a clear need for novel therapeutics targeting both skin and joint inflammation with greater selectivity, fewer side effects, and longer periods of clinical remission.

Supported by the NIH (National Institute of Arthritis and Musculoskeletal and Skin Diseases grant ROI-AR-06309101A1 to Dr. Hwang and National Center for Advancing Translational Sciences grant UL1-TR-001860 to Dr. Wilson), the National Psoriasis Foundation (Translational Research grant to Dr. Volkman and a New Investigator award to Dr. Getschman), the US Department of Defense (Small Business Innovation Research grant 1R43-AR-074363-01 to Dr. Getschman), the Group for Research and Assessment of Psoriasis and Psoriatic Arthritis (fellowship grant to Dr. Shi), the Medical Research Council, UK (grant MR/R020515/1 to Dr. Millar), and a Pfizer ASPIRE award.

[1]Zhenrui Shi, MD, PhD: University of California, Davis, Sacramento, and Sun Yat-sen Memorial Hospital and Sun Yat-sen University, Guangzhou, China; [2]Emma Garcia-Melchor, MD, PhD, Flavia Sunzini, MD, Moeed Akbar, PhD, Neal L. Millar, MD, PhD, FRCS(Ed): University of Glasgow, Glasgow, UK; [3]Xuesong Wu, MD, PhD, Mimi Nguyen, MD, Douglas J. Rowland, PhD, Machelle Wilson, PhD, Mindy Huynh, BS, Timothy Law, MD, Sam T. Hwang, MD, PhD: University of California at Davis, Sacramento; [4]Anthony E. Getschman, PhD, Brian F. Volkman, PhD: Medical College of Wisconsin, Milwaukee; [5]Smriti K. Raychaudhuri, MD, Siba P. Raychaudhuri, MD, FACP: University of California, Davis.

Drs. Shi and Garcia-Melchor contributed equally to this work.

Drs. Getschman, Volkman, and Hwang have intellectual property interest in the CCL20 locked dimer molecule and own stock or stock options in Xlock Biosciences. No other disclosures relevant to this article were reported.

Address correspondence to Neal L. Millar, PhD, FRCS(Ed), Institute of Infection, Immunity and Inflammation, College of Medicine, Veterinary and Life Sciences University of Glasgow, 120 University Ave, Glasgow G12 8TA, UK (email: neal.millar@glasgow.ac.uk); or to Samuel T. Hwang, MD, PhD, University of California Davis School of Medicine, Department of Dermatology, Suite 1400, 3301 C Street, Sacramento, CA 95816 (email: sthwang@ucdavis.edu.)

Submitted for publication July 29, 2020; accepted in revised form May 18, 2021.

Recent findings have underscored the role of the IL-23/IL-17 axis as a key player in PsO and PsA (9). In the skin, IL-23 is essential for the differentiation and maintenance of Th17 cells (10) contributing to the activation of keratinocytes (11), recruitment of neutrophils, and perpetuating dysregulated cytokine/chemokine production (12). In PsA, synovial IL-23 expression is associated with higher indexes of disease severity (13), and the neovascularity of the tissue correlates with the recruitment of pathogenic IL-23/IL-17–producing CD4+ T cells into the joints (14). Furthermore, the enthesis, an important site of inflammation in PsA that is represented by the connective tissue linking tendons and ligaments with bones, has been shown to contain populations of IL-23 receptor (IL-23R)–expressing cells capable of producing IL-17, including γδ T cells and innate lymphoid cells (ILCs) (15–17).

Chemokines represent a superfamily of immunomodulatory small protein molecules that regulate leukocyte migration to inflammatory sites through their chemoattractant properties. The CCR6/CCL20 axis is a prominent immune modulator in both innate and adaptive immune responses of a wide range of inflammatory disorders (18). CCL20 is produced by epithelial and endothelial cells, peripheral blood mononuclear cells (PBMCs), Th17 cells, and neutrophils, whereas CCR6 is expressed in Th17 and Treg cells, memory T cells, B cells, and dendritic cells (19,20). Both CCR6 and CCL20 are strongly induced by retinoic acid receptor–related orphan nuclear receptor γt (21), a critical transcription factor for Th17 differentiation. Importantly, CCR6 and CCL20 are expressed at significantly higher levels in lesional psoriatic skin, and CCR6 expression is increased on circulating PBMCs from PsO patients compared to healthy donors (22). While CCL20 synovial fluid levels have been shown to correlate with markers of PsA disease activity (13), there remains a paucity of mechanistic investigation into the CCR6/CCL20 axis in PsA and, particularly, in its role at the enthesis.

We previously manipulated the monomeric wild-type CCL20 sequence such that the resulting protein adopted a locked dimeric structure that is similar to spontaneous dimers of CCL20 that occur in nature (23). The resulting dimeric molecule, CCL20 locked dimer (CCL20LD), binds CCR6 with physiologic affinity but blocks chemotactic activity of the natural CCL20 and was able to ameliorate psoriasiform dermatitis (PsD) in an IL-23 intradermal injection mouse model.

To further explore the potential for CCR6/CCL20 as a therapeutic target for PsO and PsA, we tested the efficacy of CCL20LD in an IL-23–dependent model of skin and entheseal inflammation in the autoimmune-prone strain of B10.RIII mice (16,24). In this study, we demonstrate that CCL20LD not only reduces IL-23–mediated skin inflammation but also attenuates entheseal and synovial inflammation. Importantly, we show that the CCR6/CCL20 axis is highly enriched in tendon tissue and mediates the recruitment of inflammatory cells into the entheseal site.

PATIENTS AND METHODS

Human tissue collection and preparation. All procedures and protocols were approved by the NHS West of Scotland Ethics Committee (REC14/WS/1035). Informed consent was obtained from all patients according to standard procedures.

Tendon samples were collected from patients with PsA who were undergoing shoulder surgery. Tissues were immediately fixed in 4% formalin for a minimum of 24 hours and then embedded in paraffin. Healthy human tendon stromal cells or tenocytes were explanted from hamstring tendons of patients undergoing anterior cruciate ligament reconstruction.

Mice. The therapeutic effects of CCL20LD were examined in vivo with an IL-23 minicircle DNA (IL-23 MC) model. Female B10.RIII-H2r H2-T18b/(71NS)SnJ mice that were 8–10 weeks of age were purchased from The Jackson Laboratory (Bar Harbor, ME). Mice were acclimatized for 1 week before any treatments and housed in the same animal vivarium. All animal experiments were performed under protocols (no. 20960) approved by the Institutional Animal Care and Use Committee at the University of California, Davis.

CCL20LD treatment. CCL20LD (provided by Xlock Biosciences, LLC, Muskego, WI) was expressed and purified as previously described (23). Protein purity was determined by mass spectrometry, and biologic function was confirmed by the inhibition of wild-type CCL20–dependent migration of CCR6-transfected Jurkat cells in a Transwell chemotaxis assay.

In the therapeutic model, mice received intraperitoneal (IP) injection of 20 μg (~1 mg/kg) or 100 μg (~5 mg/kg) once daily in 200 μl phosphate buffered saline (PBS) starting on day 7 after IL-23 MC delivery. To create a preventative model, mice received IP injections of 20 μg (~1 mg/kg) CCL20LD once daily dissolved in 200 μl PBS starting on day 0. More detailed experimental procedures are described in the Supplementary Methods (available on the *Arthritis & Rheumatology* website at http://onlinelibrary.wiley.com/doi/10.1002/art.41882/abstract).

Statistical analysis. Results are expressed as the mean ± SEM for continuous variables. Data were analyzed using GraphPad Prism version 6 and SAS version 9.4. Student's unpaired 2-tailed *t*-test was used to compare 2 groups, and one-way analysis of variance (ANOVA) with Dunnett's post hoc test was used for multiple comparisons unless otherwise indicated. Given the relatively small sample size of mice, Cohen's *d* coefficient was calculated to assess the effect size before using parametric tests. Clinical associations were analyzed using Wilcoxon's rank sum test or Spearman's rank correlation test. *P* values less than 0.05 were considered significant.

RESULTS

Elevated CCR6/CCL20 expression in patients with PsA. In order to assess the contribution of CCR6 and CCL20 to PsA pathogenesis, we first measured CCL20 levels in serum and synovial fluid (SF) from PsA patients and compared them to those of healthy controls and individuals with osteoarthritis (OA). While serum CCL20 levels were comparable among healthy controls and PsA patients, SF levels were significantly increased in PsA patients compared to the OA group (Figure 1A). We also found that among PsA patients, CCL20 levels were higher in SF than in peripheral blood, with a significant correlation observed between CCL20 SF levels and bone erosions or the use of nonsteroidal antiinflammatory drugs (NSAIDs) (Supplementary Tables 1 and 2, http://onlinelibrary.wiley.com/doi/10.1002/art.41882/abstract).

We then screened for the presence of multiple chemokines and cytokines in SF. As expected, levels were higher in PsA as compared to OA patients (Figures 1B and C and Supplementary Table 3, http://onlinelibrary.wiley.com/doi/10.1002/art.41882/abstract). It was striking, however, that the fold change in CCL20 in PsA versus OA patient samples was the highest among all 17 measured chemokines (Figure 1D). Moreover, in PsA patients, the intensity of CCL20 was positively correlated with IL-6 (Figure 1E). No significant correlations were observed between the levels of CCL20 and any other cytokines/chemokines listed in Figure 1C (data not shown).

Based on the presence of high levels of CCL20 in joint fluids from PsA patients, we next assessed the presence of CCR6+ cells in synovial tissues. We observed CCR6+ cells in synovial membranes from both healthy subjects and PsA patients, with staining in vessels, infiltrating immune cells, and stromal cells (Figure 1F). Thus, both CCL20 and its receptor CCR6 are locally expressed at high levels in PsA patients, suggesting a potential role for this pathway in its pathogenesis.

Elevated CCR6/CCL20 expression in IL-23 MC–treated mice. We next investigated whether CCR6 and CCL20 expression was similarly increased in the IL-23 MC mouse model that recapitulates the clinical and immunologic features of both PsO and PsA (25,26). IL-23 MC–injected mice showed a significant elevation of IL-23 in serum as early as 24 hours after delivery (Supplementary Figure 1A, http://onlinelibrary.wiley.com/doi/10.1002/art.41882/abstract). Four days after IL-23 MC treatment, skin

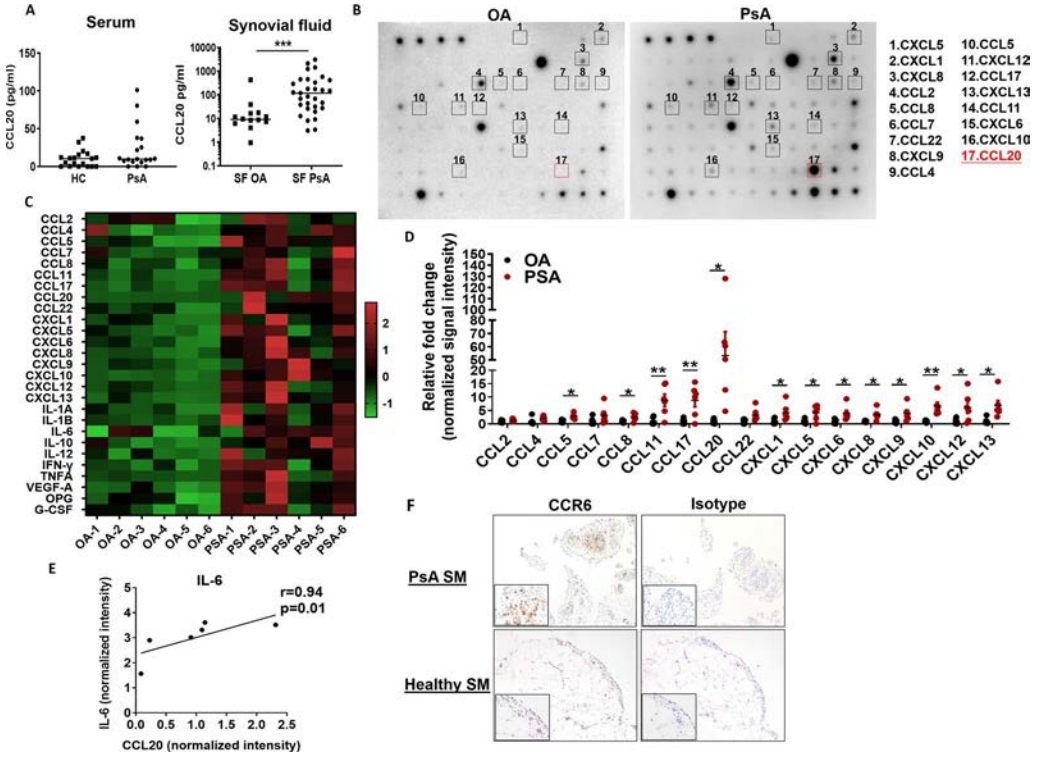

Figure 1. CCR6/CCL20 expression in patients with psoriatic arthritis (PsA). **A**, Quantification of CCL20 by enzyme-linked immunosorbent assay in serum from healthy controls (HC) (n = 19) and PsA patients (n = 19), and in synovial fluid (SF) from patients with osteoarthritis (OA) (n = 14) and those with PsA (n = 31). **B–D**, Representative image of cytokine array showing the expression profile of 80 chemokines/cytokines (**B**), heatmap showing expression of chemokines and cytokines (normalized by Z-score for each protein) (**C**), and quantification of the relative fold change in normalized signal intensity of chemokines (**D**) in SF from patients with OA and those with PsA (n = 6). In **A** and **D**, symbols represent individual subjects; horizontal lines show the mean. **E**, Analysis of correlations between the normalized signal intensity of CCL20 and interleukin-6 (IL-6) using Spearman's rho correlation coefficients. **F**, Immunohistochemical staining for CCR6 in the synovial membrane (SM) from PsA patients and healthy controls. Original magnification × 10; original magnification in insets × 40. * = $P < 0.05$; ** = $P < 0.01$; *** = $P < 0.001$, by Mann-Whitney U test for serum samples in **A**, and by Student's 2-tailed *t*-test in **D**. IFNγ = interferon-γ; TNF = tumor necrosis factor; VEGF = vascular endothelial growth factor; OPG = osteoprotegerin; G-CSF = granulocyte colony-stimulating factor.

erythema and hind paw inflammation were visible, and by day 7, both hind and front paws were involved. Typical features of PsO (scaling, redness, and edema) and PsA (swollen paws) were observed for >3 weeks (Supplementary Figures 1B and C).

Our previous study suggested that γδ T cells were the predominant cell type expressing CCR6 in murine models of PsO (27). On day 7, IL-23 MC delivery led to increased percentages and absolute numbers of γδ T cells expressing CCR6 into the ear skin, cervical skin draining lymph nodes, ankle joints, and popliteal lymph nodes (Figures 2A–E and Supplementary Figure 2A, http://onlinelibrary.wiley.com/doi/10.1002/art.41882/abstract). Consistently, γδ T cells from IL-23 MC–treated mice had higher mean fluorescence intensity of CCR6 expression (Supplementary Figure 2B, http://onlinelibrary.wiley.com/doi/10.1002/art.41882/abstract). It should be noted that there are 2 distinct subsets of γδ cells in mice skin in terms of the amount of T cell receptors present on their surface, γδ high–expressing (γδ-high) T cells (also known as dendritic epidermal T cells [DETCs]) and γδ-low T cells (28). We have previously shown that γδ-low T cells account for the majority of IL-17A production and are required for the development of maximal skin inflammation in an IL-23 injection model of psoriasiform dermatitis (29). Consistent with this, our data show that γδ-low T cells, as opposed to γδ-high T cells, were the major cell population expressing CCR6 in ear skin from IL-23 MC–injected mice.

Polymerase chain reaction analysis further confirmed significant up-regulation of *Ccr6* and *Ccl20* expression in both ear skin and hind paw tissue from IL-23 MC–treated mice (Figure 2F). Thus, systemic induction with IL-23 MC resulted in an up-regulation of CCR6 and CCL20 in both skin and joints.

Attenuation of IL-23 MC–mediated skin inflammation by CCL20LD. We then tested the efficacy of CCL20LD in preventing psoriatic inflammation in the IL-23 MC model, with daily IP injections of either 20 μg CCL20LD or vehicle being administered for 7 consecutive days (Supplementary Figure 3A, http://onlinelibrary.wiley.com/doi/10.1002/art.41882/abstract). Within 7 days of initiation, vehicle-treated mice developed remarkable erythema, desquamation, and induration (Supplementary Figure 3B), whereas CCL20LD-treated mice developed significantly less skin inflammation. This was assessed clinically, with CCL20LD-treated mice showing a nearly 50% reduction in ear thickness and Psoriasis Severity Index (PSI) score, and histologically, showing a 54% reduction in epidermal thickness and a 62% reduction in Munro microabcesses (Supplementary Figures 3C and D). In keratinocytes, CCL20LD treatment resulted in reduced nuclear

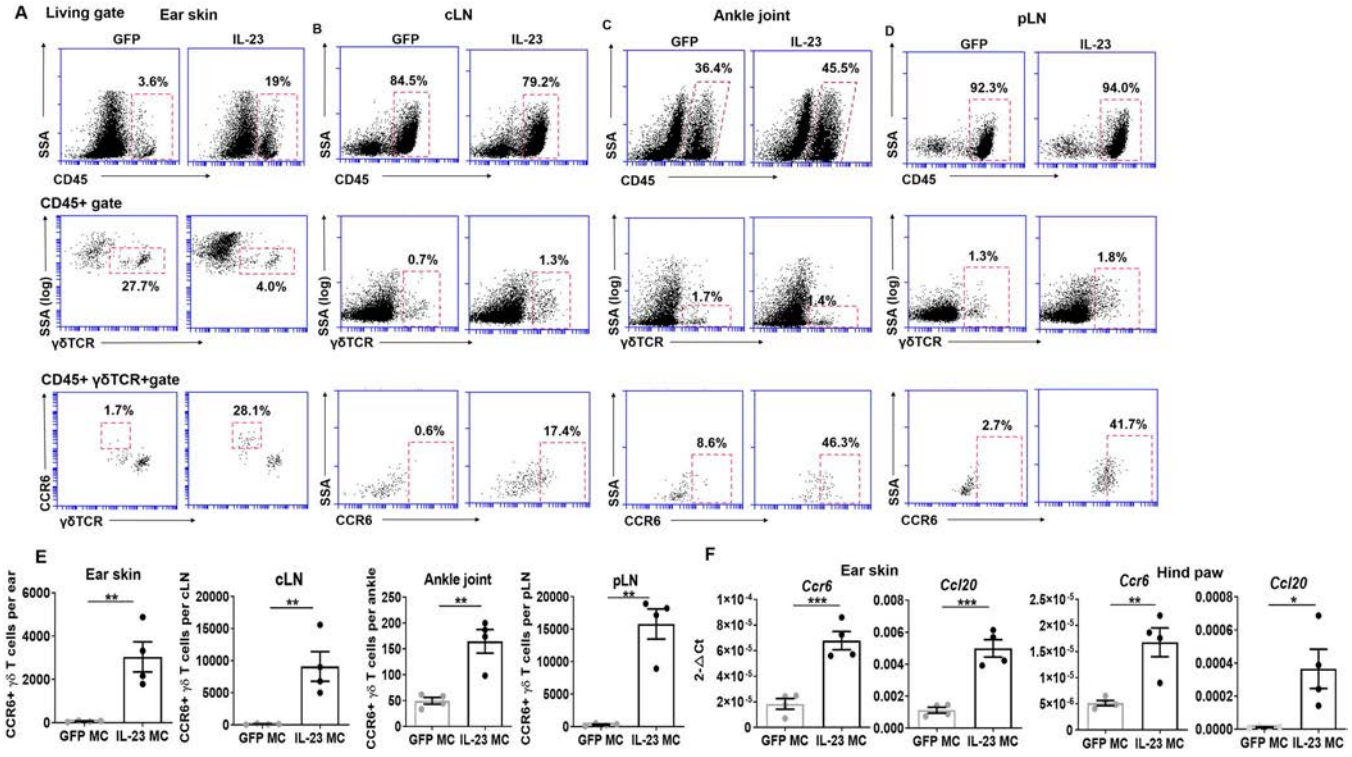

Figure 2. CCR6/CCL20 expression in interleukin-23 minicircle DNA (IL-23 MC)–treated mice. **A–D**, Representative gating strategy of flow cytometry, showing γδ-low T cells expressing CCR6 in ear skin (**A**), and γδ T cells expressing CCR6 in the cervical skin draining lymph node (cLN) (**B**), ankle joint (**C**), and popliteal lymph node (pLN) (**D**). **E**, Absolute numbers of CCR6+ γδ T cells per sample of ear skin, cervical skin draining lymph node, ankle joint, and popliteal lymph node. **F**, Expression of *Ccr6* and *Ccl20* in ear skin and hind paw tissue. Bars show the mean ± SEM (n = 4 mice per group). Data are representative of 2 independent experiments. * = $P < 0.05$; ** = $P < 0.01$; *** = $P < 0.001$, by Student's 2-tailed *t*-test. GFP = green fluorescent protein. Color figure can be viewed in the online issue, which is available at http://onlinelibrary.wiley.com/doi/10.1002/art.41882/abstract.

staining of Ki-67 and phospho-STAT3 (Supplementary Figure 3E). Flow cytometric analysis revealed marked reductions in CD45+ leukocytes, CCR6+ γδ-low T cells, and neutrophils (Supplementary Figure 3F). Gene expression of PsO-associated cytokines including *Il17a, Il17f, Il22, Il6,* and *S100a8* was also suppressed by CCL20LD (Supplementary Figure 3G).

We next assessed whether CCL20LD could block established skin disease in a therapeutic manner. Beginning on day 7 following IL-23 MC injection, mice were treated daily with vehicle alone, 20 μg of CCL20LD, or 100 μg of CCL20LD for 7 additional days (Figure 3A). Mice treated with the higher dose developed significantly less scaling and erythema (Figure 3B) and had a nearly 50% reduction in ear thickness and clinical PSI score (Figure 3C). Histologically, both CCL20LD treatment groups exhibited reductions in epidermal thickness and profoundly decreased numbers of Munro microabcesses (Figure 3D). CCL20LD treatment dampened the increased nuclear staining of Ki-67 and phospho-STAT3 in a dose-dependent manner (Figure 3E). Flow cytometric analysis showed a reduction in the infiltration of CD45+ leukocytes, CCR6+ γδ T cells, and neutrophils (Figure 3F). Although not statistically significant, mice receiving high-dose treatment exhibited down-regulation of *Ccr6* and *Ccl20* expression (Supplementary Figure 4A, http://onlinelibrary.wiley.com/doi/10.1002/art.41882/abstract). Similar trends were seen in the expression profiles of cytokine transcripts such as *Il17a*, *Cxcl1*, *Cxcl2*, *Il6*, and *S100a9*. A significant reduction was observed in the expression of *Il1b* and *S100a8* in the group with high-dose treatment (Supplementary Figure 4B). We further performed immunohistochemical staining of CD4, CD8, and F4/80. In contrast to CCR6+ γδ T cells and neutrophils, the infiltration of CD4+ T cells, CD8+ T cells, and F4/80 macrophages was not reduced by CCL20LD treatment, which may contribute to the sustained levels of some cytokines (Supplementary Figure 5, http://onlinelibrary.wiley.com/doi/10.1002/art.41882/abstract). Thus, we determined that CCL20LD suppresses the clinical, histologic, and molecular features of IL-23–mediated dermatitis in a preventative, therapeutic, and dose-dependent manner.

Attenuation of IL-23 MC–mediated joint inflammation by CCL20LD. Above, we demonstrated that IL-23 MC delivery resulted in significantly swollen hind paws by day 7 following delivery of IL-23 MC (Supplementary Figure 1, http://onlinelibrary.wiley.com/doi/10.1002/art.41882/abstract). When

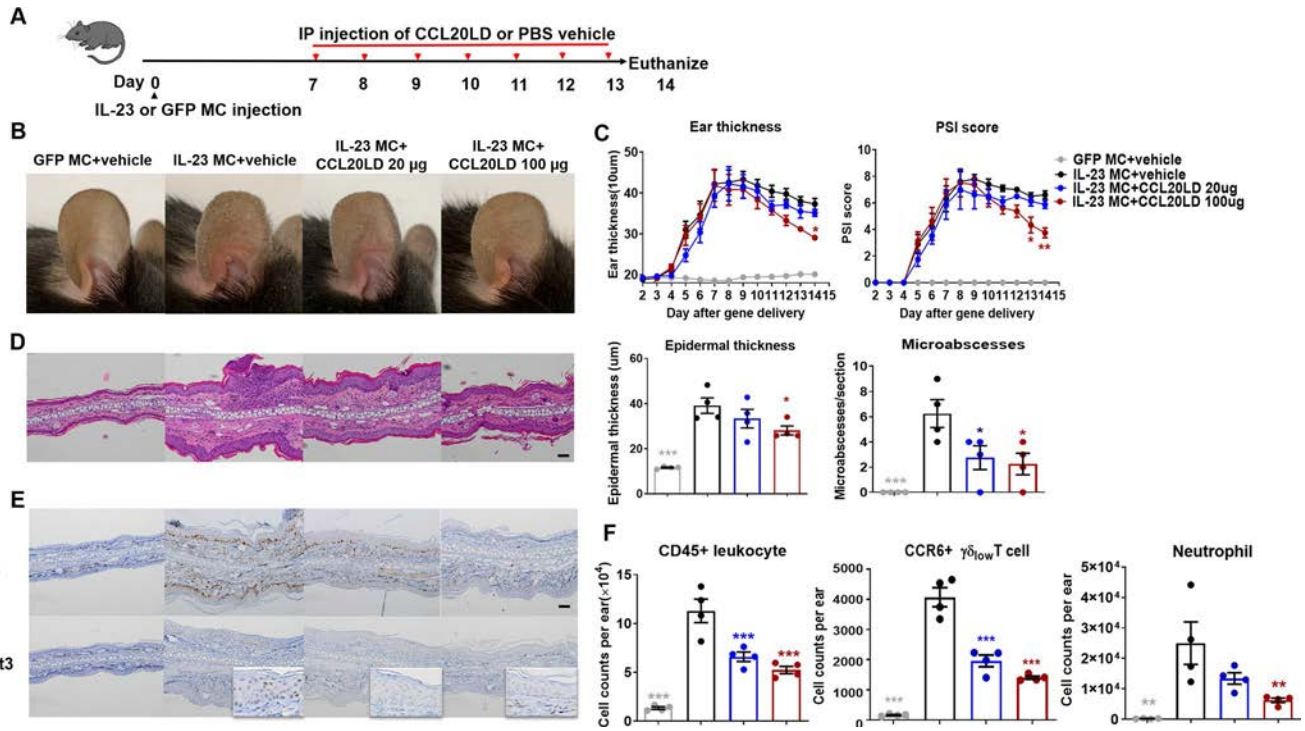

Figure 3. CCL20 locked dimer (CCL20LD) ameliorates IL-23 MC–mediated psoriasiform dermatitis in a therapeutic manner. **A**, Schematic illustration of experimental protocols. B10.RIII mice were treated with phosphate buffered saline (PBS) vehicle or CCL20LD at a dose of 20 μg or 100 μg for 7 consecutive days beginning on day 7 after MC was delivered. **B** and **C**, Photographs of the ear of a representative mouse in each treatment group (**B**) and time course of ear thickness and Psoriasis Severity Index (PSI) score (**C**). **D**, Hematoxylin and eosin–stained sections of ear tissue from a mouse in each group (bar = 50 μm) and histologic analysis of epidermal thickness and number of microabcesses. **E**, Immunohistochemical staining of Ki-67 and phospho-Stat3 in tissue sections from a mouse in each group. Bar = 50 μm; original magnification × 20. **Inset**, higher-magnification view (25:1 ratio). **F**, Absolute numbers of CD45+ leukocytes, γδ-low T cells expressing CCR6, and neutrophils as determined by flow cytometry. Bars show the mean ± SEM (n = 4 mice per group). Data are representative of 2 independent experiments. * = $P < 0.05$; ** = $P < 0.01$; *** = $P < 0.001$ versus the IL-23 MC + vehicle–treated group, by two-way analysis of variance (ANOVA) with Bonferroni correction in **C** and by one-way ANOVA with Dunnett's post hoc test in **D** and **F**. IP = intraperitoneal (see Figure 2 for other definitions).

treated with preventative administration of CCL20LD, we observed a 60% reduction in the incidence of arthritis and a 95% reduction in severity (Supplementary Figures 6A and B, http://onlinelibrary.wiley.com/doi/10.1002/art.41882/abstract). Synovial hyperplasia and inflammation were profoundly attenuated, with a reduction in synovial neutrophilic infiltration (Supplementary Figures 6C and D). The increased expression of *Tnfsf11*(*RANKL*), but not of *Tnfrsf11b* (*Opg*), in paw tissue from IL-23 MC–treated mice was also suppressed by CCL20LD (Supplementary Figure 6E). In contrast to the partial reduction in proinflammatory markers in skin, CCL20LD treatment resulted in a >75% reduction in all measured proinflammatory markers in the paw tissues, including *Il17a*, *Tnf*, *Il6*, and *Il1b* (Supplementary Figure 6F).

In the therapeutic model, mice treated with CCL20LD had clinically ameliorated joint inflammation, with greater improvement seen in the high-dose group than in the low-dose group (60% versus 50% reduction in paw swelling score) (Figures 4A and B). Histologically, IL-23–induced joint swelling was characterized by pannus formation with destruction of articular surfaces, which was milder in the low-dose group and nearly absent in the high-dose group (Figure 4C). Accordingly, a significant reduction in histologic score was observed in the CCL20LD-treated group (Figure 4D). In the paw tissue, the reduced inflammation was corroborated by a reduction in synovial neutrophilic infiltration (Supplementary Figure 7, http://onlinelibrary.wiley.com/doi/10.1002/art.41882/abstract) and decreased metabolic activity as demonstrated by lower ^{18}F-fluorodeoxyglucose uptake as observed on positron emission tomography/computed tomography scans (Figure 4E). Expression of *Ccr6* and *Ccl20* was down-regulated in mice treated with CCL20LD (Supplementary Figure 8, http://onlinelibrary.wiley.com/doi/10.1002/art.41882/abstract), and a similar trend was observed in the expression of other genes involved in bone and tissue erosion (*RANKL*, *Mmp9*, and *Ctsk*) (30) and inflammation (*Il17a, Il1b*, *Il6*, and *Tnf*) (Figure 4F).

We then compared the therapeutic effect between CCL20LD and anti–IL-17A antibody, a biologic agent that has previously demonstrated a high level of efficacy in treating PsO and PsA (2,31). Mice treated with CCL20LD at a daily dosage of 100 μg exhibited a better therapeutic effect on ear inflammation compared to those receiving 100 μg anti–IL-17A antibodies every other day, as measured by lower ear thickness, PSI score, and decreased infiltration of neutrophils and CCR6+ γδ-low T cells (Supplementary Figures 9A–D, http://onlinelibrary.wiley.com/doi/10.1002/art.41882/abstract). Treatment with CCL20LD and anti–IL-17A antibodies both resulted in significant improvement of IL-23–mediated joint inflammation, as evidenced by decreased inflammation score, less cellular infiltrates in ankle joints, and suppressed transcripts of IL-17A, IL-1β, IL-6, and TNF

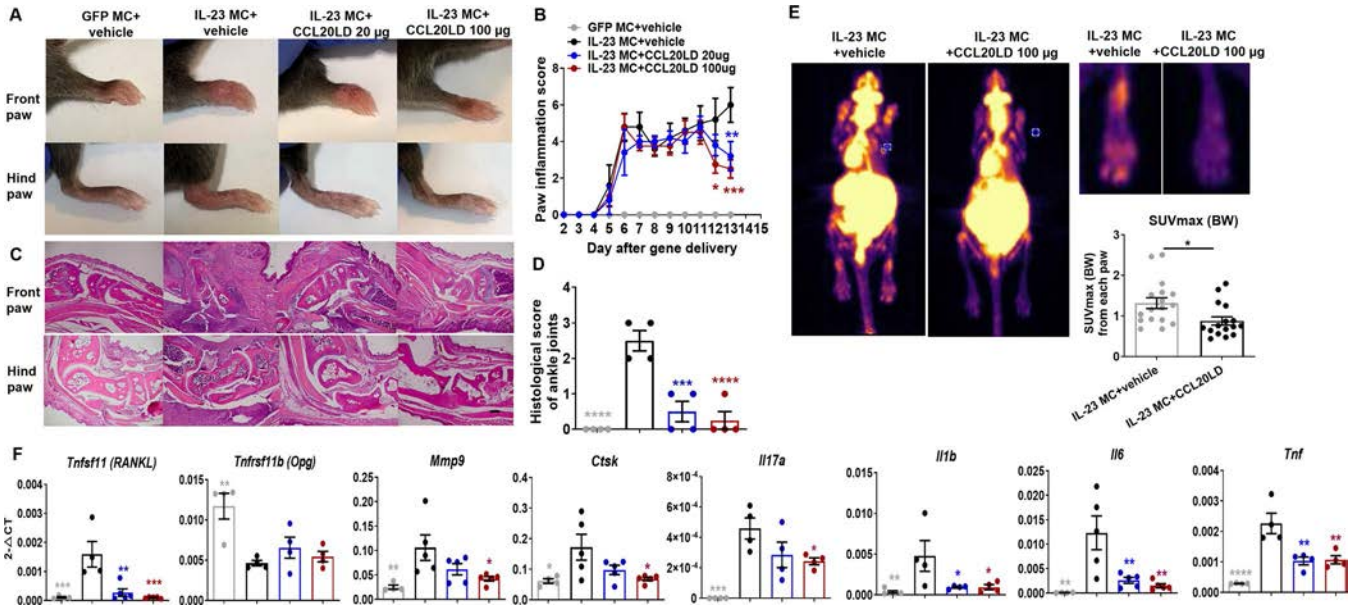

Figure 4. CCL20 locked dimer (CCL20LD) ameliorates IL-23 MC–mediated joint inflammation in a therapeutic manner. **A**, Photographs of the front and hind paw of a representative mouse in each treatment group. B10.RIII mice were treated with phosphate buffered saline (PBS) vehicle or CCL20LD at a dose of 20 μg or 100 μg for 7 consecutive days beginning on day 7 after IL-23 MC was delivered. **B**, Time course of paw inflammation score. **C**, Hematoxylin and eosin–stained sections of paw tissue for histologic evaluation of disease severity (bar = 200 μm). **D**, Histologic scores of disease severity in the ankle joints. **E**, Maximum-intensity projections of ^{18}F-fluorodeoxyglucose–positron emission tomography (^{18}F-PET) images showing a representative mouse in each treatment group (top left), with enlarged images of the hind paw of these 2 mice (top right). The pseudo-color in PET indicates higher glucose metabolism, hence the increased cellular metabolic activity. Quantification of joint disease, using the standardized uptake maximum value (SUVmax) based on body weight (BW) in the hind paw of mice in each group is shown (bottom right). **F**, Relative expression of genes for osteoclastogenesis-related markers and proinflammatory cytokines in the paw tissue. Bars show the mean ± SEM (n = 4 mice per group). * = $P < 0.05$; ** = $P < 0.01$; *** = $P < 0.001$; **** = $P < 0.0001$ versus the IL-23 MC + vehicle–treated group, by two-way ANOVA with Bonferroni correction in **D**, by Student's 2-tailed *t*-test in **E**, and by one-way ANOVA with Dunnett's post hoc test in **F**. See Figure 2 for other definitions.

(Supplementary Figures 9E–H). Collectively, our findings showed that CCL20LD treatment led to profound reductions in all measured clinical and proinflammatory markers in the joints of IL-23 MC–treated mice in both preventative and therapeutic settings.

Attenuation of IL-23–mediated enthesitis by CCL20LD. To understand the potential role of the CCR6/CCL20 axis in enthesitis, we first assessed CCR6 expression in human tendon tissue. In healthy tissue, CCR6 staining localized on vessels in the para-tendon tissue, with some tenocytes showing CCR6 cytoplasmic staining. In tendon tissue from PsA patients, CCR6 staining increased with the cell infiltrate and numerous CCR6+ cells were observed throughout the tendon (Figure 5A).

We next assessed the involvement of the enthesis in IL-23 MC–treated mice, observing an increased percentage and absolute number of CCR6+ γδ T cells in the Achilles tendon from IL-23 MC–treated mice (Figure 5B). Strikingly, 50- and 1,000-fold increases in *Ccr6* and *Ccl20* expression were found in the tendons of IL-23 MC–treated mice, respectively (Figure 5C), significantly higher than those observed in the paw tissue overall. Of note, expression of *Ccl20* in CD45– cells was 6-fold higher than in CD45+ cells (Figure 5D). The up-regulation of *Ccl20* was accompanied by dramatic elevations in several inflammatory mediators in the Achilles tendon such as *Il23r*, *Il17a*, *Il22*, *Il6*, *Il1b*, and *Tnf* (Supplementary Figure 10, http://onlinelibrary.wiley.com/doi/10.1002/art.41882/abstract). In line with these transcriptional changes, IL-23 MC–treated mice also exhibited histologic findings of enthesitis, such as the infiltration of leukocytes in and adjacent to the Achilles tendon and synovio–entheseal complex (Figure 5E and Supplementary Figure 11, http://onlinelibrary.wiley.com/doi/10.1002/art.41882/abstract).

No obvious calcaneal erosion was found in IL-23 MC–injected mice treated with vehicle or CCL20LD (Supplementary Figure 12, http://onlinelibrary.wiley.com/doi/10.1002/art.41882/abstract). These histologic changes, together with accumulation of Gr-1–positive neutrophils, were markedly attenuated by CCL20LD treatment (Supplementary Figure 13, http://onlinelibrary.wiley.com/doi/10.1002/art.41882/abstract). Consistent with

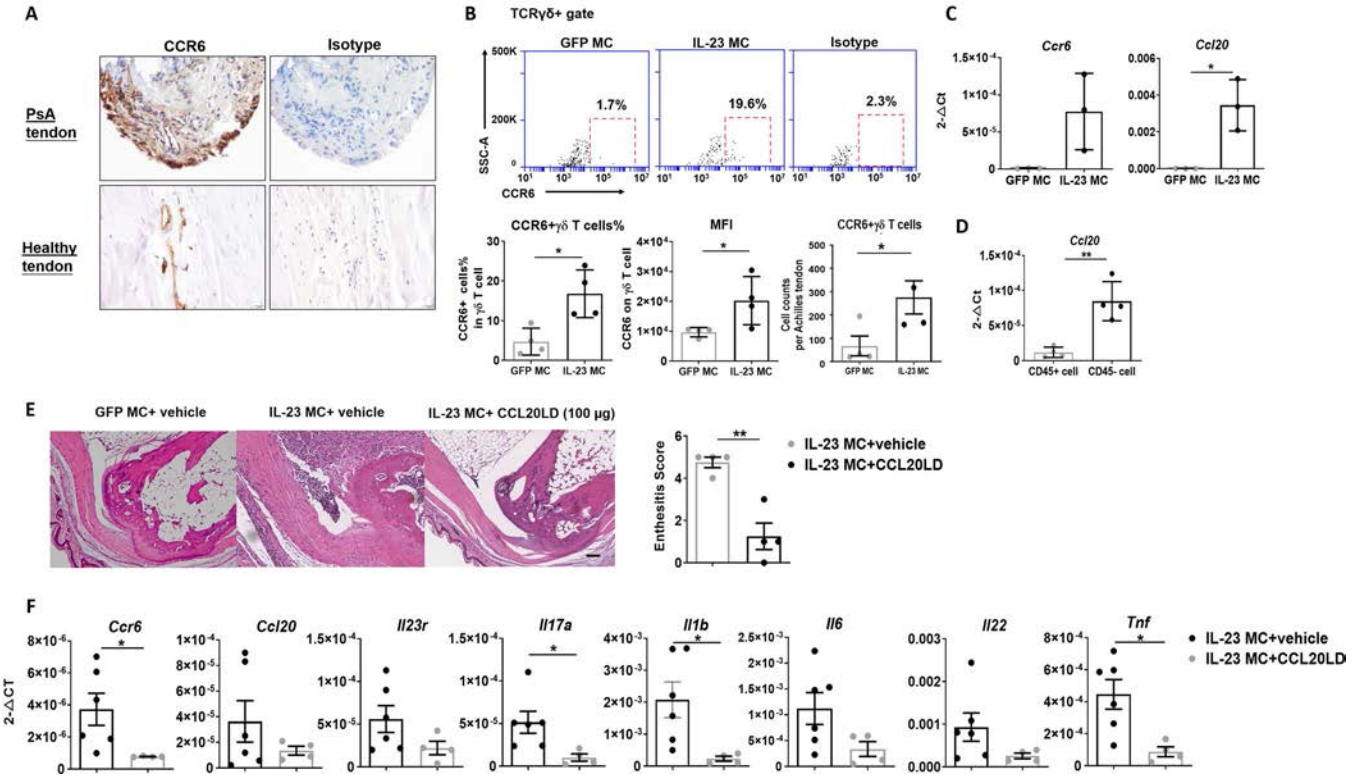

Figure 5. CCL20 locked dimer (CCL20LD) attenuates interleukin-23 minicircle DNA (IL-23 MC)–mediated enthesitis in patients with psoriatic arhritis (PsA) and in mouse models of PsA. **A**, Immunohistochemical staining for CCR6 in tendon tissue from PsA patients and healthy donors. Original magnification × 40. **B**, Representative results from intracellular staining for CCR6 in the tendon tissue from mice in each treatment group, and flow cytometry results showing the percentage and absolute counts of CCR6+ γδ T cells and mean fluorescence intensity (MFI) of staining for CCR6 on γδ T cells. **C**, Relative expression of *Ccr6* and *Ccl20* in Achilles tendons from mice treated with green fluorescent protein (GFP) MC or IL-23 MC on day 7 after gene delivery. **D**, Relative expression of *Ccl20* in CD45+ and CD45– cells in Achilles tendons from mice treated with IL-23 MC. **E**, Hematoxylin and eosin–stained sections of mouse tendon tissue showing enthesis. Mice were treated with either GFP MC + vehicle, IL-23 MC + vehicle, or IL-23 MC + 100 μg CCL20LD (bar = 100 μm), according to the same protocol as described in Figure 3A. Enthesitis scores were lower in the IL-23 MC–injected group treated with CCL20LD than in the IL-23 MC–injected group treated with vehicle. **F**, Relative expression of genes for proinflammatory markers in Achilles tendons from IL-23 MC–injected mice treated with either vehicle or CCL20LD. Bars show the mean ± SEM (n = 3–6 mice per group). * = $P < 0.05$; ** = $P < 0.01$, by Student's 2-tailed *t*-test. TCRγδ = T cell receptor γδ.

these findings, expression of *Ccr6* and *Ccl20* as well as other proinflammatory markers were suppressed in the tendons of mice therapeutically treated with CCL20LD following establishment of enthesitis (Figure 5F). These results suggest an important role of the stromal compartment in the tendon in the production of CCL20 and show that CCL20LD blockade dampens this inflammatory response in the entheses following IL-23 MC induction.

Human tenocytes produce CCL20 upon activation with IL-1β. Because our data in the IL-23 MC mouse model suggest that tendon stromal cells were the main producers of CCL20 in this model, we wondered if activated human tendon stromal cells, also known as tenocytes, could be capable of producing CCL20. To evaluate this, we stimulated healthy tenocytes with IL-1β, an inflammatory cytokine that has been involved in sterile inflammation (32) and has been shown to be increased in animal models of tendon injury and exercise (33). We observed a striking up-regulation of *CCL20* expression ($2^{-\Delta C_t}$ 3.825 × 10^{-6} ± 1.387× 10^{-6} versus 0.001701 ± 0.0004745; fold change 680.5 ± 215.2; n = 5) ($P < 0.0001$) and significant increases in CCL20 protein in supernatants of activated tenocytes (mean ± SEM 1.048 ± 0.5658 pg/ml versus 481.8 ± 84.26 pg/ml; n = 13) ($P < 0.0001$) (Figure 6A).

We next assessed the capacity of conditioned medium from tenocytes activated with IL-1β to induce the migration of T cells using a Transwell assay. After 4 hours, we observed increased migration of CCR6+ cells (mean ± SEM 20.39% ± 2.9 with medium alone, 20.56% ± 2.6 with unstimulated tenocytes, and 24.77% ± 3.1 with activated tenocytes) and increased migration of CCR6+CD161+ cells (mean ± SEM 11.1% ± 1.99 with medium alone, 11.59% ± 1.89 with unstimulated tenocytes, and 14.66%

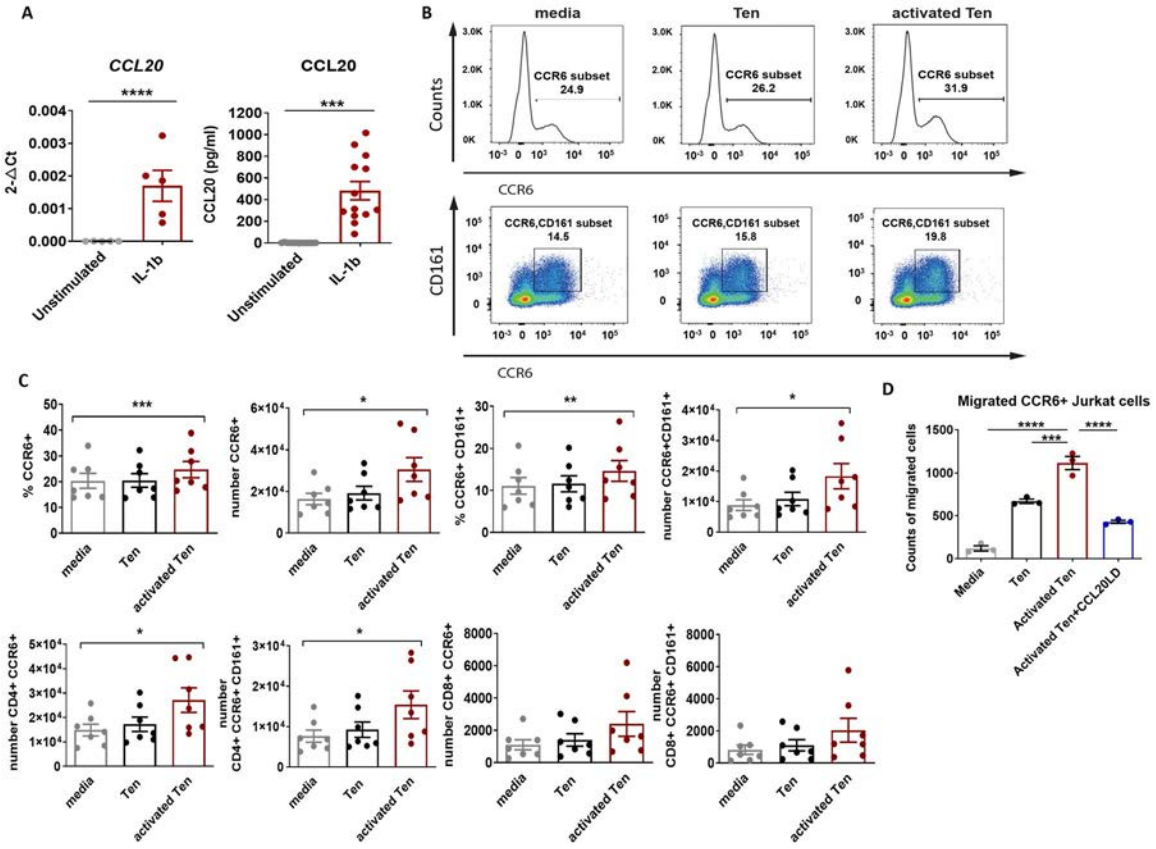

Figure 6. Human tenocytes produce CCL20 upon stimulation with IL-1β. **A**, Tendon stromal cells (Ten) from healthy donors were stimulated with IL-1β (1 ng/ml) for 4 hours for quantitative polymerase chain reaction analysis of CCL20 gene expression, or stimulated for 18 hours for analysis of CCL20 protein expression by enzyme-linked immunosorbent assay in the supernatants. **B** and **C**, CD3+ cells from peripheral blood of healthy donors were preactivated overnight with CD3 and CD28 antibodies in a Transwell system, and conditioned medium alone, conditioned medium cultured with unactivated tenocytes, or conditioned medium cultured with IL-1β–activated tenocytes was added into the Transwells. After 4 hours, cells that migrated to the lower chamber were analyzed by flow cytometry. Representative fluorescence-activated cell sorting plots show the percentage and number of CCR6+ or CCR6+CD161+ cells among total CD3+ live cells (**B**), and the percentage and number of CCR6+ or CCR6+CD161+ cells compared to other cell subsets under each Transwell condition (**C**). **D**, Migration of CCR6+ Jurkat cells toward conditioned medium alone, conditioned medium cultured with unactivated tenocytes, conditioned medium cultured with IL-1β–activated tenocytes, or conditioned medium cultured with IL-1β–stimulated tenocytes in the presence of CCL20LD (100 ng/ml) was assessed. Bars show the mean ± SEM. Data are representative of 3 independent experiments. * = $P < 0.05$; ** = $P < 0.01$; *** = $P < 0.001$; **** = $P < 0.0001$, by Student's paired *t*-test (left) or by Wilcoxon's signed rank test (right) in **A**, and by one-way analysis of variance with Dunnett's post hoc test in **C** and **D**. See Figure 5 for other definitions.

± 2.48 with activated tenocytes) toward conditioned medium from tenocytes, particularly if they had been previously activated (Figures 6B and C). While migration was not vigorous, it should be noted that ~30% of the unsorted T cells used in these assays expressed CCR6 (data not shown), thus limiting the migration response that could be detected.

We therefore performed chemotaxis assays with a human Jurkat T cell line that does not overexpress CCR6 and a retrovirally transduced CCR6-overexpressing (CCR6+) Jurkat T cell line (23) (Supplementary Figure 14A, http://onlinelibrary.wiley.com/doi/10.1002/art.41882/abstract). Only CCR6+ Jurkat cells but not nontransduced Jurkat cells responded to CCL20 in a dose-dependent manner (Supplementary Figure 14B). Compared to medium from unstimulated tenocytes, medium from stimulated tenocytes attracted more migration of CCR6+ Jurkat cells, which was totally blocked by 100 ng/ml CCL20LD (Figure 6D). Such increased chemotaxis by media from stimulated tenocytes and further inhibition by CCL20LD was not observed when using CCR6– Jurkat cells (Supplementary Figure 14C). Taken together, these findings demonstrate that stromal cells in human tendons are able to produce chemotactically active CCL20 in response to inflammatory stimuli and damage, resulting in enhanced recruitment of CCR6+ cells in vitro and, possibly, into the tendon in vivo.

DISCUSSION

Strategies to target chemokines and their respective receptors are extremely attractive to reduce the burden of chronic inflammatory diseases. Among the ~20 known chemokine receptors, the CCR6/CCL20 pair particularly has been associated with Th17-dominant immune activity (34). We have previously shown in an experimental model of human PsO involving local intradermal injection of IL-23 that CCR6 is essential for the epidermal trafficking of IL-17/22–producing cells (29) and that CCR6-deficient and anti-CCL20 monoclonal antibody–treated mice are resistant to the development of PsD (27,35). In accordance with this, treatment with CCL20LD led to a partial reduction in IL-23–mediated skin inflammation in both the preventative and therapeutic models in the current work.

In addition to PsO, where CCR6 has long been proposed as a target for therapy (34), emerging data also suggest that CCR6/CCL20 signaling is involved in the pathology of other inflammatory rheumatic diseases such as rheumatoid arthritis (RA). In patients with RA, increased numbers of CCR6+ T cells have been found in the circulation as well as in inflamed joints (36). Synoviocytes from arthritic joints of both mice and humans were found to produce large quantities of CCL20 (21). Furthermore, administration of blocking antibodies to CCL20 inhibited experimental joint inflammation in a collagen-induced arthritis model (21). Indeed, a CCL20-neutralizing antibody (GSK3050002) with a high binding affinity to human CCL20 has been used in a first-in-humans study to show selective blockade of CCR6+ cells in a suction blister model without significant safety concerns (37), suggesting that a blocking antibody–based approach may be possible in humans. In contrast to this approach to CCR6/CCL20 blockade, CCL20LD only differs by 1 internal amino acid residue from the natural chemokine, and thus is likely to be resistant to the development of antidrug antibodies that lead to loss of therapeutic efficacy with many antibody-based therapeutics (38).

In the current study, we showed that CCL20LD and anti–IL-17A antibodies had similar therapeutic effects on IL-23–mediated skin and joint inflammation. Th17 cells are important mediators of immune responses against extracellular bacteria and fungi, and, as such, play critical regulatory roles in maintaining mucosal homeostasis (39). For example, mice deficient in IL-17A or IL-17RA are more vulnerable to local infection of *Candida albicans*, but CCR6-deficient mice exhibit similar resistance to *C albicans* compared to wild-type mice (40). Further studies are warranted to evaluate CCR6-targeted therapy in terms of risk for infection.

Though the significance of Th17 cells in PsA was identified a decade ago, the cellular and molecular mechanisms of enthesitis in spondyloarthritis, including PsA, remain largely unknown (41). Recent studies have provided evidence for the role of mechanical stress in the pathogenesis of arthritis (42). Mechanical stress in the enthesis, areas where tendons and ligaments attach to bones and therefore are responsible for the transmission of mechanical forces from the muscle to the bone (43), could trigger the development of a chronic immune response in individuals with a certain genetic background. This fact, taken together with the observation of increased local levels of CCL20, prompted us to interrogate whether the stromal compartment could be the source of CCL20. In the IL-23 MC model, we found that CD45– cells exhibited higher CCL20 gene expression and that healthy human tenocytes were able to produce CCL20 in response to activation with IL-1β, as previously reported for synovial fibroblasts (21). As our in vitro experiments suggest, tenocytes can then promote the migration of CCR6+ cells, such as γδ T cells or ILCs, that populate healthy entheses (15,17,44). In sum, we propose that tenocytes likely play a critical role in both initiation and perpetuation of enthesitis by locally regulating interactions of CCL20 and CCR6.

We have previously showed that CCR6-deficient mice on the C57BL/6J strain background were resistant to IL-23–induced skin inflammation but exhibited no observed changes in the incidence or severity of relatively mild joint inflammation compared to wild-type mice (45). It is, however, well known that the standard C57BL/6J strain of mice is relatively resistant to experimental autoimmune arthritis (46), whereas others, such as the closely related B10.RIII strain, are much more prone to and have greater severity of induced arthritis (16,24). This susceptibility is associated with the major histocompatibility complex (MHC) allele, H2r, the T cell receptor V β8 chain, and other non-MHC loci (23,34). The differences in the propensity to arthritis between different mouse strains led us to conduct our follow up studies using the B10.RIII strain and CCL20LD to more conclusively evaluate the role of

the CCR6/CCL20 axis in psoriatic joint inflammation. We found that the fold change in transcripts of CCR6 and CCL20 in paw tissue was higher in B10.RIII mice than that in C57BL/6J mice after delivery of the same dose of IL-23 MC (mean ± SD fold change in C57BL/6J versus B10.RIII mice 1.59 ± 0.59 versus 3.14 ± 1.03 for *Ccr6*, 10.69 ± 6.07 versus 22.40 ± 8.12 for *Ccl20*) (45), which may contribute to the discrepancy between our studies. Given the fact that the levels of CCL20 were highly elevated in the SF from PsA patients, we suggest that the results from B10.RIII mice will probably more closely mirror the response to CCR6/CCL20 blocking treatment in human patients.

The present study had some limitations, such as small sample size and heterogeneity of the recruited patients. Further studies with an enlarged sample size are necessary to comprehensively evaluate the profile of CCL20 in SF as well as its correlation with the clinical phenotype. Also, considering the higher dosage of IL-23 MC we used (26), it is possible that the high levels of IL-23 made it difficult to reverse or improve some of the outcomes. Mouse models with different disease severity due to titration of IL-23 MC, optimal dosing, and route of administration of CCL20LD treatment need to be explored and warrant further optimization along with determination of the ability of this therapy to reverse or ameliorate bone destruction.

In summary, these data confirm the role of the CCR6/CCL20 axis in IL-23/IL-17–mediated skin and joint disease, but, perhaps most importantly, we could also bridge the role of CCR6 and CCL20 in entheseal disease as suggested by both human and murine study findings. In IL-23 MC–driven entheseal and joint inflammation, an engineered variant of CCL20 reverses the histologic and molecular signs of inflammation, offering hope that targeting this pathway may be a new avenue for treating an unmet need in treating PsA.

ACKNOWLEDGMENTS

We express our deepest gratitude to patients who donated samples for research purposes. We thank Q. Chen and H. Sugandha for technique assistance on preparing hematoxylin and eosin slides and immunohistochemical staining, Dr. Iannis E. Adamopoulos and Cuong T. Nguyen for providing GFP and IL-23 minicircle, Dr. Giacomo Cafaro for the pilot CCL20 tendon cell experiments, and Maria-Ioanna Christodoulou for providing serum samples.

AUTHOR CONTRIBUTIONS

All authors were involved in drafting the article or revising it critically for important intellectual content, and all authors approved the final version to be published. Dr. Shi had full access to all of the data in the study and takes responsibility for the integrity of the data and the accuracy of the data analysis.

Study conception and design. Shi, Garcia-Melchor, Millar, Hwang.
Acquisition of data. Shi, Garcia-Melchor, Wu, Rowland, Sunzini, Akbar, Huynh, Law, S. K. Raychaudhuri, S. P. Raychaudhuri.
Analysis and interpretation of data. Shi, Garcia-Melchor, Getschman, Nguyen, Rowland, Wilson, S. P. Raychaudhuri, Volkman, Millar, Hwang.

REFERENCES

1. Deodhar A, Gottlieb AB, Boehncke WH, Dong B, Wang Y, Zhuang Y, et al. Efficacy and safety of guselkumab in patients with active psoriatic arthritis: a randomised, double-blind, placebo-controlled, phase 2 study. Lancet 2018;391:2213–24.
2. Langley RG, Elewski BE, Lebwohl M, Reich K, Griffiths CE, Papp K, et al. Secukinumab in plaque psoriasis: results of two phase 3 trials. N Engl J Med 2014;371:326–38.
3. Papp KA, Langley RG, Lebwohl M, Krueger GG, Szapary P, Yeilding N, et al. Efficacy and safety of ustekinumab, a human interleukin-12/23 monoclonal antibody, in patients with psoriasis: 52-week results from a randomised, double-blind, placebo-controlled trial (PHOENIX 2). Lancet 2008;371:1675–84.
4. Felson DT, Anderson JJ, Boers M, Bombardier C, Furst D, Goldsmith C, et al. American College of Rheumatology preliminary definition of improvement in rheumatoid arthritis. Arthritis Rheum 1995;38:727–35.
5. McInnes IB, Kavanaugh A, Gottlieb AB, Puig L, Rahman P, Ritchlin C, et al. Efficacy and safety of ustekinumab in patients with active psoriatic arthritis: 1 year results of the phase 3, multicentre, double-blind, placebo-controlled PSUMMIT 1 trial. Lancet 2013;382:780–9.
6. McInnes IB, Mease PJ, Kirkham B, Kavanaugh A, Ritchlin CT, Rahman P, et al. Secukinumab, a human anti-interleukin-17A monoclonal antibody, in patients with psoriatic arthritis (FUTURE 2): a randomised, double-blind, placebo-controlled, phase 3 trial. Lancet 2015;386:1137–46.
7. Blauvelt A. Safety of secukinumab in the treatment of psoriasis. Expert Opin Drug Saf 2016;15:1413–20.
8. Honda H, Umezawa Y, Kikuchi S, Yanaba K, Fukuchi O, Ito T, et al. Switching of biologics in psoriasis: reasons and results. J Dermatol 2017;44:1015–9.
9. Sakkas LI, Bogdanos DP. Are psoriasis and psoriatic arthritis the same disease? The IL-23/IL-17 axis data [review]. Autoimmun Rev 2017;16:10–5.
10. Chan TC, Hawkes JE, Krueger JG. Interleukin 23 in the skin: role in psoriasis pathogenesis and selective interleukin 23 blockade as treatment. Ther Adv Chronic Dis 2018;9:111–9.
11. Speeckaert R, Lambert J, Grine L, Van Gele M, De Schepper S, van Geel N. The many faces of interleukin-17 in inflammatory skin diseases [review]. Br J Dermatol 2016;175:892–901.
12. Harper EG, Guo C, Rizzo H, Lillis JV, Kurtz SE, Skorcheva I, et al. Th17 cytokines stimulate CCL20 expression in keratinocytes in vitro and in vivo: implications for psoriasis pathogenesis. J Invest Dermatol 2009;129:2175–83.
13. Celis R, Planell N, Fernandez-Sueiro JL, Sanmarti R, Ramirez J, Gonzalez-Alvaro I, et al. Synovial cytokine expression in psoriatic arthritis and associations with lymphoid neogenesis and clinical features. Arthritis Res Ther 2012;14:R93.
14. Fiocco U, Stramare R, Martini V, Coran A, Caso F, Costa L, et al. Quantitative imaging by pixel-based contrast-enhanced ultrasound reveals a linear relationship between synovial vascular perfusion and the recruitment of pathogenic IL-17A-F$^+$IL-23$^+$ CD161$^+$ CD4$^+$ T helper cells in psoriatic arthritis joints. Clin Rheumatol 2017;36:391–9.
15. Cuthbert RJ, Fragkakis EM, Dunsmuir R, Li Z, Coles M, Marzo-Ortega H, et al. Group 3 innate lymphoid cells in human enthesis. Arthritis Rheumatol 2017;69:1816–22.
16. Sherlock JP, Joyce-Shaikh B, Turner SP, Chao CC, Sathe M, Grein J, et al. IL-23 induces spondyloarthropathy by acting on ROR-γ$^+$ CD3$^+$CD4$^-$CD8$^-$ entheseal resident T cells. Nat Med 2012;18:1069–76.
17. Reinhardt A, Yevsa T, Worbs T, Lienenklaus S, Sandrock I, Oberdörfer L, et al. Interleukin-23–dependent γ/δ T cells produce interleukin-17 and accumulate in the enthesis, aortic valve, and ciliary body in mice. Arthritis Rheumatol 2016;68:2476–86.
18. Ranasinghe R, Eri R. Pleiotropic immune functions of chemokine receptor 6 in health and disease [review]. Medicines (Basel) 2018;5:69.

19. Singh SP, Zhang HH, Foley JF, Hedrick MN, Farber JM. Human T cells that are able to produce IL-17 express the chemokine receptor CCR6. J Immunol 2008;180:214–21.
20. Lee AY, Korner H. CCR6 and CCL20: emerging players in the pathogenesis of rheumatoid arthritis [review]. Immunol Cell Biol 2014; 92:354–8.
21. Hirota K, Yoshitomi H, Hashimoto M, Maeda S, Teradaira S, Sugimoto N, et al. Preferential recruitment of CCR6-expressing Th17 cells to inflamed joints via CCL20 in rheumatoid arthritis and its animal model. J Exp Med 2007;204:2803–12.
22. Homey B, Dieu-Nosjean MC, Wiesenborn A, Massacrier C, Pin JJ, Oldham E, et al. Up-regulation of macrophage inflammatory protein-3 α/CCL20 and CC chemokine receptor 6 in psoriasis. J Immunol 2000;164:6621–32.
23. Getschman AE, Imai Y, Larsen O, Peterson FC, Wu X, Rosenkilde MM, et al. Protein engineering of the chemokine CCL20 prevents psoriasiform dermatitis in an IL-23-dependent murine model. Proc Natl Acad Sci U S A 2017;114:12460–5.
24. Nandakumar KS, Holmdahl R. A genetic contamination in MHC-congenic mouse strains reveals a locus on chromosome 10 that determines autoimmunity and arthritis susceptibility. Eur J Immunol 2005;35:1275–82.
25. Adamopoulos IE, Tessmer M, Chao CC, Adda S, Gorman D, Petro M, et al. IL-23 is critical for induction of arthritis, osteoclast formation, and maintenance of bone mass. J Immunol 2011; 187:951–9.
26. Leys L, Wang Y, Paulsboe S, Edelmayer R, Salte K, Wetter J, et al. Characterization of psoriasiform dermatitis induced by systemic injection of interleukin-23 minicircles in mice. J Dermatol 2019;46:482–97.
27. Mabuchi T, Singh TP, Takekoshi T, Jia GF, Wu X, Kao MC, et al. CCR6 is required for epidermal trafficking of γδ-T cells in an IL-23-induced model of psoriasiform dermatitis. J Invest Dermatol 2013; 133:164–71.
28. Sumaria N, Roediger B, Ng LG, Qin J, Pinto R, Cavanagh LL, et al. Cutaneous immunosurveillance by self-renewing dermal γδ T cells. J Exp Med 2011;208:505–18.
29. Mabuchi T, Takekoshi T, Hwang ST. Epidermal CCR6$^+$ γδ T cells are major producers of IL-22 and IL-17 in a murine model of psoriasiform dermatitis. J Immunol 2011;187:5026–31.
30. Boyle WJ, Simonet WS, Lacey DL. Osteoclast differentiation and activation [review]. Nature 2003;423:337–42.
31. Mease PJ, McInnes IB, Kirkham B, Kavanaugh A, Rahman P, van der Heijde D, et al. Secukinumab inhibition of interleukin-17A in patients with psoriatic arthritis. N Engl J Med 2015;373:1329–39.
32. Dinarello CA. Biologic basis for interleukin-1 in disease [review]. Blood 1996;87:2095–147.
33. Morita W, Dakin SG, Snelling SJ, Carr AJ. Cytokines in tendon disease: a systematic review. Bone Joint Res 2017;6:656–64.
34. Hedrick MN, Lonsdorf AS, Hwang ST, Farber JM. CCR6 as a possible therapeutic target in psoriasis [review]. Expert Opin Ther Targets 2010;14:911–22.
35. Hedrick MN, Lonsdorf AS, Shirakawa AK, Lee CC, Liao F, Singh SP, et al. CCR6 is required for IL-23-induced psoriasis-like inflammation in mice. J Clin Invest 2009;119:2317–29.
36. Benham H, Norris P, Goodall J, Wechalekar MD, FitzGerald O, Szentpetery A, et al. Th17 and Th22 cells in psoriatic arthritis and psoriasis. Arthritis Res Ther 2013;15:R136.
37. Bouma G, Zamuner S, Hicks K, Want A, Oliveira J, Choudhury A, et al. CCL20 neutralization by a monoclonal antibody in healthy subjects selectively inhibits recruitment of CCR6$^+$ cells in an experimental suction blister. Br J Clin Pharmacol 2017;83:1976–90.
38. Baker MP, Reynolds HM, Lumicisi B, Bryson CJ. Immunogenicity of protein therapeutics: the key causes, consequences and challenges. Self Nonself 2010;1:314–22.
39. Van Hamburg JP, Tas SW. Molecular mechanisms underpinning T helper 17 cell heterogeneity and functions in rheumatoid arthritis [review]. J Autoimmun 2018;87:69–81.
40. Verma AH, Richardson JP, Zhou C, Coleman BM, Moyes DL, Ho J, et al. Oral epithelial cells orchestrate innate type 17 responses to Candida albicans through the virulence factor candidalysin. Sci Immunol 2017;2:eaam8834.
41. Raychaudhuri SP, Raychaudhuri SK, Genovese MC. IL-17 receptor and its functional significance in psoriatic arthritis. Mol Cell Biochem 2012;359:419–29.
42. Jacques P, Lambrecht S, Verheugen E, Pauwels E, Kollias G, Armaka M, et al. Proof of concept: enthesitis and new bone formation in spondyloarthritis are driven by mechanical strain and stromal cells. Ann Rheum Dis 2014;73:437–45.
43. Gracey E, Burssens A, Cambre I, Schett G, Lories R, McInnes IB, et al. Tendon and ligament mechanical loading in the pathogenesis of inflammatory arthritis [review]. Nat Rev Rheumatol 2020;16: 193–207.
44. McGonagle DG, McInnes IB, Kirkham BW, Sherlock J, Moots R. The role of IL-17A in axial spondyloarthritis and psoriatic arthritis: recent advances and controversies [review]. Ann Rheum Dis 2019; 78:1167–78.
45. Shi Z, Garcia-Melchor E, Wu X, Yu S, Nguyen M, Rowland DJ, et al. Differential requirement for CCR6 in IL-23-mediated skin and joint inflammation. J Invest Dermatol 2020;140:2386–97.
46. Pan M, Kang I, Craft J, Yin Z. Resistance to development of collagen-induced arthritis in C57BL/6 mice is due to a defect in secondary, but not in primary, immune response. J Clin Immunol 2004; 24:481–91.

Arthritis & Rheumatology
Vol. 73, No. 12, December 2021, pp 2282–2292
DOI 10.1002/art.41796
Published 2021. This article is a U.S. Government work and is in the public domain in the USA.

American College of Rheumatology
Empowering Rheumatology Professionals

RNA Externalized by Neutrophil Extracellular Traps Promotes Inflammatory Pathways in Endothelial Cells

Luz P. Blanco,[1] Xinghao Wang,[1] Philip M. Carlucci,[1] Jose Jiram Torres-Ruiz,[1] Jorge Romo-Tena,[2] Hong-Wei Sun,[1] Markus Hafner,[1] and Mariana J. Kaplan[1]

Objective. Neutrophil extracellular traps (NETs) are extracellular lattices composed of nucleic material bound to neutrophil granule proteins. NETs may play pathogenic roles in the development and severity of autoimmune diseases such as systemic lupus erythematosus (SLE), at least in part, through induction of type I interferon (IFN) responses via externalization of oxidized immunostimulatory DNA. A distinct subset of SLE proinflammatory neutrophils (low-density granulocytes [LDGs]) displays enhanced ability to form proinflammatory NETs that damage the vasculature. We undertook this study to assess whether NET-bound RNA can contribute to inflammatory responses in endothelial cells (ECs) and the pathways that mediate this effect.

Methods. Expression of newly synthesized and total RNA was quantified in NETs from healthy controls and lupus patients. The ability of ECs to take up NET-bound RNA and downstream induction of type I IFN responses were quantified. RNAs present in NETs were sequenced and specific small RNAs were tested for induction of endothelial type I IFN pathways.

Results. NETs extruded RNA that was internalized by ECs, and this was enhanced when NET-bound nucleic acids were oxidized, particularly in lupus LDG–derived NETs. Internalization of NET-bound RNA by ECs was dependent on endosomal Toll-like receptors (TLRs) and the actin cytoskeleton and induced type I IFN–stimulated genes (ISGs). This ISG induction was dependent on NET-associated microRNA let-7b, a small RNA expressed at higher levels in LDG-derived NETs, which acted as a TLR-7 agonist.

Conclusion. These findings highlight underappreciated roles for small RNAs externalized in NETs in the induction of proinflammatory responses in vascular cells, with implications for lupus vasculopathy.

INTRODUCTION

Systemic lupus erythematosus (SLE) is an autoimmune syndrome characterized by development of autoantibodies that target nucleic acids or proteins binding to nucleic acids, pleiotropic clinical manifestations, immune complex (IC) deposition in various organs, and acute and chronic inflammation (1,2). Endogenous nucleic acids released during various forms of cell death have been considered important sources of autoantigens in SLE, leading to chronic stimulation of innate and adaptive immune responses. Recognition of self–nucleic acids by endosomal Toll-like receptors (TLRs) on various immune cells is considered an important step in the pathogenesis of SLE, promoting autoantibody and IC formation and the production of type I interferons (IFNs), with pathogenic effects (3).

In addition to apoptosis and necrosis as putative sources of externalized nuclear autoantigens, there is another form of cell death whereby extracellular traps extruded by neutrophils contain modified DNA. Dysregulation on formation and clearance of these neutrophil extracellular traps (NETs) may play important roles in generating and exposing modified autoantigens to the immune system and in amplifying inflammatory responses in SLE and other autoimmune conditions (4). SLE is characterized by the presence of a distinct subset of proinflammatory neutrophils, low-density granulocytes (LDGs), endowed with enhanced capacity to form NETs (5,6) in a mitochondrial reactive oxygen

Supported by the Intramural Research Program, National Institute of Arthritis and Musculoskeletal and Skin Diseases, NIH (grant ZIA-AR-041199).

[1]Luz P. Blanco, PhD, Xinghao Wang, BS, Philip M. Carlucci, BS, Jose Jiram Torres-Ruiz, MD, Hong-Wei Sun, PhD, Markus Hafner, PhD, Mariana J. Kaplan, MD: National Institute of Arthritis and Musculoskeletal and Skin Diseases, NIH, Bethesda, Maryland; [2]Jorge Romo-Tena, MD, MSc: National Institute of Arthritis and Musculoskeletal and Skin Diseases, NIH, Bethesda, Maryland, and Universidad Nacional Autónoma de México, Mexico City, Mexico.

No potential conflicts of interest relevant to this article were reported.

Address correspondence to Mariana J. Kaplan, MD, National Institute of Arthritis and Musculoskeletal and Skin Diseases, NIH, Systemic Autoimmunity Branch, 10 Center Drive, Room 12N248C, Bethesda, MD 20892. Email: mariana.kaplan@nih.gov.

Submitted for publication May 20, 2020; accepted in revised form April 29, 2021.

species (ROS)–dependent manner (7,8). Oxidation of genomic and mitochondrial DNA during NET formation amplifies immunogenicity of this nucleic acid and promotes type I IFN responses through engagement of the cyclic GMP-AMP synthase/stimulator of IFN genes (cGAS/STING) pathway (8,9). NETs also damage the endothelium and may play pathogenic roles in the development of vasculopathy and premature atherosclerosis characteristic of SLE (4,10).

While mitochondrial DNA and chromatin are present in NETs, it is unclear if additional nuclear components with potential immunomodulatory capabilities become externalized and modified during this process, and the role that they may play in immune dysregulation and tissue injury. RNAs, particularly small RNAs, are increasingly described for their central roles in promoting cross-talk between cells and their immunomodulatory and proinflammatory activities (11). RNAs can be delivered to other cells inside microvesicles or exosomes and, following uptake, can regulate gene expression in target cells (12). Recently, RNAs present in NETs have been associated with perpetuation of inflammation and subsequent propagation of NET formation in psoriasis skin lesions (13), while NET-bound miR-142 microRNA induces tumor necrosis factor expression by macrophages in vitro (14).

We hypothesized that NETs serve as carriers of RNAs that may regulate endothelial cell (EC) responses and that differential RNA expression in lupus NETs may induce exacerbated proinflammatory responses in the endothelium. To test this hypothesis, we assessed whether RNA present in NETs could be internalized by ECs. We also characterized differential expression of miRNAs in NETs from healthy controls and SLE patients and their effects on EC biology and type I IFN responses.

MATERIALS AND METHODS

Cell lines. Human aortic ECs (HAECs) (no. CC-2535; Lonza) and human dermal microvascular ECs (no. 2543; Lonza) were seeded over gelatin-coated (no. G1890; Sigma-Aldrich) cell culture containers in MCDB 131 medium (no. 10372019; Gibco, ThermoFisher Scientific) or EBM-2 Endothelial Cell Growth Basal Medium (no. CC-3156; Lonza), containing an EGM-2 Endothelial SingleQuots kit (no. CC-4176; Lonza). Cells were used after no more than 10 passages.

Isolation of neutrophils and NETs. Low- and normal-density neutrophils were isolated from peripheral venous blood from SLE patients and healthy controls, as previously described (8,15). SLE patients met the American College of Rheumatology revised criteria for this disease (16) and were enrolled in the study (National Institutes of Health [NIH] protocol no. 94-AR-0066). Healthy volunteers were recruited at the Blood Bank Clinical Center (NIH). All subjects provided written informed consent. Neutrophils (2×10^6 cells/ml RPMI) were allowed to form spontaneous NETs for 1.5 hours at 37°C, followed by the addition of 10 units/ml RNase-free DNase (no. 00672727; ThermoFisher Scientific). Some of the NET preparations were induced in the presence of 5 μl 5-ethynyl uridine (5-EU) reagent from a Click-It RNA Alexa Fluor 488 Imaging kit (no. C10329; ThermoFisher Scientific) to label newly synthesized RNA. NETs were collected after 30 minutes and were further separated from cells by centrifugation (5 minutes at 5,000 revolutions per minute), followed by filtering through 0.45-μm syringe filters to exclude whole cells (no. 6901-2504; GE Healthcare Life Sciences). NET aliquots were stored at –80°C until used.

Immunofluorescence microscopy. Neutrophils were seeded onto chambered coverslips (no. 155383; Lab-Tek, ThermoFisher Scientific) at a density of 100,000 cells/ml and were allowed to attach for 1.5 hours, followed by fixation in 4% paraformaldehyde overnight at 4°C. Cells were washed with phosphate buffered saline (PBS) and permeabilized with Triton X-100 0.2% for 10 minutes, and were then washed and incubated with Click-It reagent, according to the manufacturer's instructions. Cells were blocked in 0.5% gelatin for 15 minutes and then incubated with various primary nonconjugated antibodies followed by secondary fluorochrome-conjugated antibodies, after labeling with Click-It. Anti-human antibodies (all from Abcam) included LL-37 mouse monoclonal antibody (1:250 dilution; no. ab80895), neutrophil elastase rabbit polyclonal antibody (1:500 dilution; no. ab21595), histone H2A rabbit polyclonal antibody (1:250 dilution; no. ab18255), and high mobility group box chromosomal protein 1 (HMGB-1) rabbit polyclonal antibody (1:250 dilution; no. 10829-1-AP). Secondary fluorochrome-conjugated antibodies (all at 1:250 dilution and from ThermoFisher Scientific) included Alexa Fluor 488 donkey anti-mouse antibody (no. A-21202) and Alexa Fluor 555 and Alexa Fluor 488 donkey anti-rabbit antibody (nos. A-32773 and A-21206). Hoechst 33342 (no. H3570; ThermoFisher Scientific) was used at a 1:1,000 dilution to stain nuclear and extracellular DNA fibers, in conjunction with the secondary antibody.

For neutrophils and NETs, incubations were conducted overnight at 4°C for primary antibodies and for 2 hours at room temperature with the secondary antibodies and Hoechst. ProLong Gold antifade reagent (no. P36930; ThermoFisher Scientific) was used to mount the samples that were then imaged in a Zeiss LSM780 confocal microscope. Total protein measurement in NETs was performed using a BCA kit (no. 23225; ThermoFisher Scientific), with 50 μg/ml used per experiment. For ImageJ analysis of microvesicles in NETs, images were examined using Adobe Photoshop software, and the setting Photoshop>filter>stylize>find edges was applied to estimate the mean size of vesicles containing newly synthesized RNA in NETs.

Quantification of NET-bound newly synthesized and total RNA. Newly synthesized RNA in neutrophils and NETs was labeled using a Click-It RNA imaging kit after incubating cells for 1.5 hours with 5-EU (5 μl/ml), according to the manufacturer's

instructions. Additional experiments labeled NET-bound RNA using SYTO RNASelect green dye (no. S32703; ThermoFisher Scientific) or ExoGlow red dye (no. EXOR100A-1SBI; System Biosciences). SYTO RNASelect green dye (1 μl/ml) was added to NETs for the duration of the incubations. ExoGlow red dye was added to 100 μl/ml NETs for 20 minutes at 37°C, followed by the addition of 200 μl trichloroacetic acid for 40 minutes on ice. Suspensions were centrifuged for 10 minutes at 14,000 rpm, and the pellet containing labeled NETs was resuspended in 500 μl PBS and stored at –80°C. Staining of total RNA in EC lines was performed by incubating cells with SYTO RNASelect green dye (1 μl/ml media) for 1 hour at 37°C.

In vitro oxidation of NETs and determination of oxidized nucleotide content. Spontaneously formed NETs from healthy control neutrophils were oxidized in vitro following an adapted protocol (17). Briefly, 1 ml of NETs was mixed with 25 μ*M* cytochrome c (no. C2867; Sigma-Aldrich) and 1 m*M* hydrogen peroxide in HEPES (pH 7.3) for 1 hour at 37°C. The reaction was stopped with 5 m*M* EDTA, and oxidized NETs were stored at –80°C. Negative controls were defined as NETs without addition of cytochrome c and hydrogen peroxide. Oxidation of nucleic acids was confirmed by an 8-hydroxyguanosine (8-OHG) immunoblot and was also performed in LDGs without in vitro oxidation. Briefly, 5 μl of NET suspension was attached to a nitrocellulose membrane strip and allowed to dry. After blocking by incubation in 10% bovine serum albumin and successive washes in 0.05% PBS–Tween 20, the nitrocellulose membrane was incubated overnight at 4°C with anti–8-OHG mouse monoclonal antibody (1:500 dilution) (no. ab62623; Abcam), washed with 0.05% PBS–Tween 20, and incubated with donkey anti-mouse IRDye 800 CW (1:10,000 dilution) (no. 926-32212; Li-Cor). The membrane was scanned and imaged using an Odyssey CLx imager.

Assessment of NET-bound RNA uptake by ECs. EC lines were seeded onto gelatin-coated coverslips (density 25,000 cells/ml). Semiconfluent cells were incubated with 5-EU–containing NETs (50 μg/ml protein) for 3 hours, washed in PBS and fixed in 4% paraformaldehyde overnight at 4°C. To assess the uptake of NET-derived newly synthesized RNA containing 5-EU into ECs, cells were treated using the Click-It newly synthesized RNA labeling procedure, permeabilized for 10 minutes with Triton X-100 0.2%, and washed and blocked in 0.5% gelatin for 30 minutes. Immunostaining was performed using the protocol described above for neutrophils in order to quantify internalization of newly synthesized RNA. In additional experiments aimed at quantifying total RNA uptake by ECs, NETs were labeled with ExoGlow red dye and then incubated with ECs in 96-well plates in the presence or absence of the following: RNase 1 (20 units/ml; no. EN0601), RNase A (0.1 mg/ml; no. EN0531), and RNase H (50 units/ml; no. EN0201) (all from ThermoFisher Scientific); TLR-7/9 inhibitor (ODN TTAGGC) and respective control (ODN TTAGGG) at 4 μ*M* final concentration (both from InvivoGen); or chloroquine at 20 μ*M* final concentration (no. C6628) or cytochalasin D at 2 μg/ml final concentration (no. C8273; both from Sigma-Aldrich). Experiments were performed in triplicate. Cells were washed in PBS, and nuclei were stained with Hoechst to quantify cell numbers. Fluorescence (excitation/emission 460 nm/650 nm for cells and 361 nm/497 nm for nuclei) was measured using a Synergy HTX BioTek plate reader.

Isolation and sequencing of NET-bound small RNAs and use of small RNA inhibitors and mimics. NET-bound RNA was isolated using an ExoMir kit (no. 5145; Bioo Scientific). For each sample, 1 μg eluted RNA was subjected to limited alkaline hydrolysis in a 15 μl buffer of 10 m*M* Na_2CO_3 and 10 m*M* $NaHCO_3$ (pH 10.3) at 60ºC for 10 minutes. The partially hydrolyzed RNA was dephosphorylated for 1 hour with 10 units of calf intestinal phosphatase (New England Biolabs) in a 50-μl reaction of 100 m*M* NaCl, 50 m*M* Tris HCl (pH 7.9) at 25ºC, and 10 m*M* $MgCl_2$, 1 m*M* dithiothreitol, 3 m*M* Na_2CO_3, and 3 m*M* $NaHCO_3$ at 37ºC. The resulting RNA was re-phosphorylated for 1 hour with 10 units of T4 polynucleotide kinase (NEB) in a 20-μl reaction of 70 m*M* Tris HCl (pH 7.6), 10 m*M* MgCl2, 5 m*M* dithiothreitol, and 1 m*M* ATP at 37ºC.

Fragments of 19–35 nucleotides were converted into barcoded small RNA complementary DNA (cDNA) libraries, as previously described (18), and sequenced on an Illumina HiSeq 2500 instrument. Adapters were trimmed using Cutadapt (http://journal.embnet.org/index.php/embnetjournal/article/view/200/458). Alignment and annotation were performed as previously described (19). Sequencing reads were mapped to human genome hg19 with Bowtie version 0.12.8. Small RNA expression values (reads per kilobase per million) were calculated using Partek version 6.6, with genomic annotations generated using HOMER (20). Analysis of variance was performed with Partek version 6.6. The sequence data files are deposited in Gene Expression Omnibus (accession no. GSE160143).

The miRCURY LNA miRNA power inhibitor and negative control against microRNA let-7b (miR-let-7b) were from Qiagen (nos. YI04102235 and YI00199006-DCA) and were used at a final concentration of 50 n*M*. The miR-let-7b MISSION microRNA mimic was from Sigma-Aldrich (no. HMI0007) and was also used at a final concentration of 50 n*M*.

Immunoprecipitation of HMGB-1–bound miR-let-7b and quantification by quantitative polymerase chain reaction (PCR). Immunoprecipitation of NET-bound HMGB-1 was performed by incubating 1 ml of control or SLE NETs with 1 μg anti–HMGB-1–conjugated rabbit polyclonal antibody overnight at 4°C. The suspension was incubated with protein A–conjugated agarose beads (50 μl diluted 2× in PBS) (no. 17127901; GE Healthcare) for 2 hours at room temperature. After 3 washes in water, agarose pellets were stored at –80°C. Elution

of RNA from immunoprecipitated HMGB-1 was performed as previously described (21). After elution, the RNA was precipitated, and each sample was resuspended in 15 µl water. The miR-let-7b quantitative PCR was performed using an hs_let-7b_1 miScript Primer Assay (no. MS00003122; Qiagen) with HiSpec buffer, 12 µl of template for the cDNA synthesis, and following the kit instructions for quantitative PCR.

Gene expression analysis by quantitative PCR. Gene expression in HAECs was quantified using specific TaqMan primers probes (*GAPDH*, Hs02786624_g1; *IFNA5*, Hs04186137_sH; *IFI44*, Hs00951349_m1; *IRF7*, Hs01014809_g1; all from ThermoFisher Scientific) after isolation of the RNA using a Direct-zol RNA miniprep kit (no. R2050; Zymo Research). Quantitative PCR was conducted following a protocol that we previously described (22).

RESULTS

NETs express newly synthesized RNA that is internalized by ECs. The first indication that RNA was present in NETs from lupus neutrophils was obtained using NanoDrop and confirmed by Bioanalyzer quantification (Supplementary Table 1, available on the *Arthritis & Rheumatology* website at http://onlinelibrary.wiley.com/doi/10.1002/art.41796/abstract). Results showed that the amount of RNA in cells from SLE patients versus those from healthy controls was not significantly different. RNA present in NETs was predominantly small RNA; a representative Bioanalyzer electrophoretography report for RNA isolated from SLE normal-density granulocyte (NDG)–derived NETs is shown in Figure 1A. To confirm that RNA was present in NETs in a more refined manner, we used the Click-It technology (23) to label and track de novo synthesized RNA. Newly synthesized RNA in neutrophils was effectively labeled following a 2-hour incubation in the presence of modified ribonucleotide 5-EU, which is incorporated into newly synthesized RNA and can be subsequently labeled with fluorescence. Labeled newly synthesized RNA was detected in vesicle-like structures in healthy control NDGs and SLE LDGs before active NET formation (Supplementary Figures 1A and B, http://onlinelibrary.wiley.com/doi/10.1002/art.41796/abstract). Using confocal microscopy, we observed that newly synthesized RNA was present in well-defined vesicle-like structures within NETs (Figures 1B and C). The mean ± SD size of these vesicles was 1.99 ± 0.16 µm in diameter. Overall, these findings suggest that NETs externalize newly synthesized RNA.

We tracked the uptake of NET-associated newly synthesized RNA by ECs. HAECs were incubated for 2.5 hours with lupus-derived NETs carrying 5-EU–labeled RNA and permeabilized and stained to detect internalized newly synthesized RNA. Newly synthesized RNA derived from NETs was internalized by HAECs, detected in their cytoplasm in vesicle-like structures (Figures 2A–C) and colocalized with neutrophil granule proteins neutrophil elastase (Figure 2A) and neutrophil-derived LL-37 (Figure 2B).

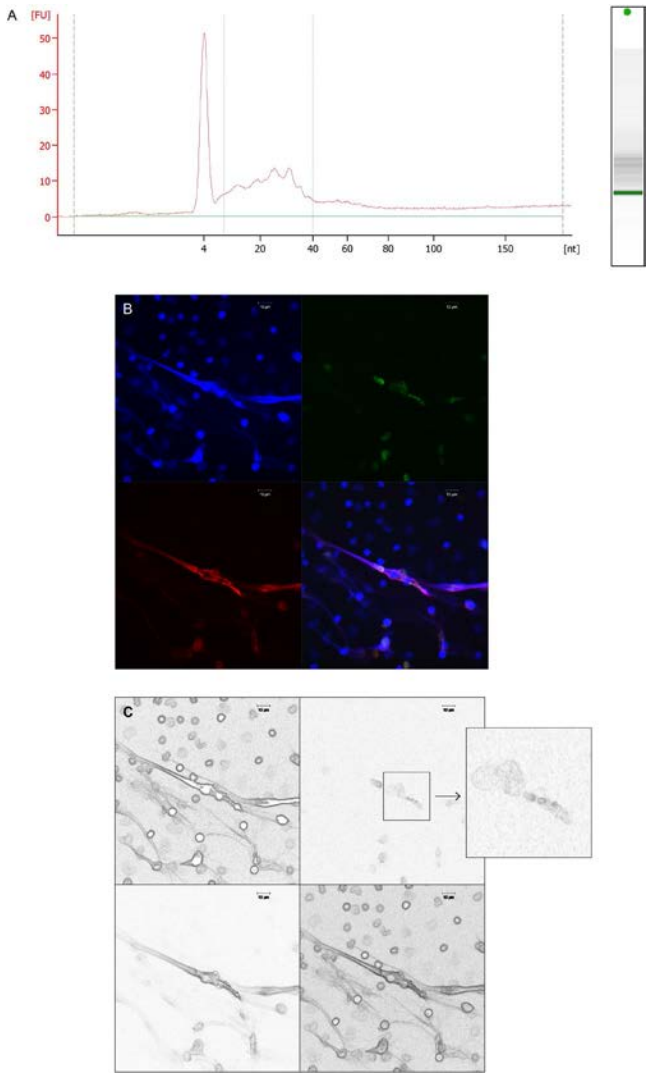

Figure 1. RNA is detected in neutrophil extracellular traps (NETs), and newly synthesized RNA in NETs colocalizes in vesicle-like structures. **A**, Bioanalyzer electrophoretography report on RNA from a representative sample of systemic lupus erythematosus (SLE) normal-density granulocyte–derived NETs, showing that small RNAs are the predominant RNA species quantified in NETs. **B**, Confocal microscopy image of SLE low-density granulocytes undergoing NET formation. The newly synthesized RNA (green) in NETs is contained in vesicle-like structures that colocalize with extracellular DNA (blue) and neutrophil elastase (red). Original magnification × 63. **C**, The image in **B**, after processing using the Photoshop>filter>stylize>find edge, and then transformation to black and white. **Inset**, Higher-magnification view of the area where the newly synthesized RNA shows a vesicle-like morphology. FU = fluorescent units; nt = nucleotides.

Both molecules were externalized during NET formation and were quantified to track colocalization of RNA with granule proteins contained within NETs. NET-derived newly synthesized RNA also trafficked into HAEC nuclei, as shown in the fluorescence profile graphs (Figure 2A). Coincubation of NETs with RNase A for the duration of the assay attenuated uptake of newly synthesized NET-bound RNA by HAECs (Figure 2C).

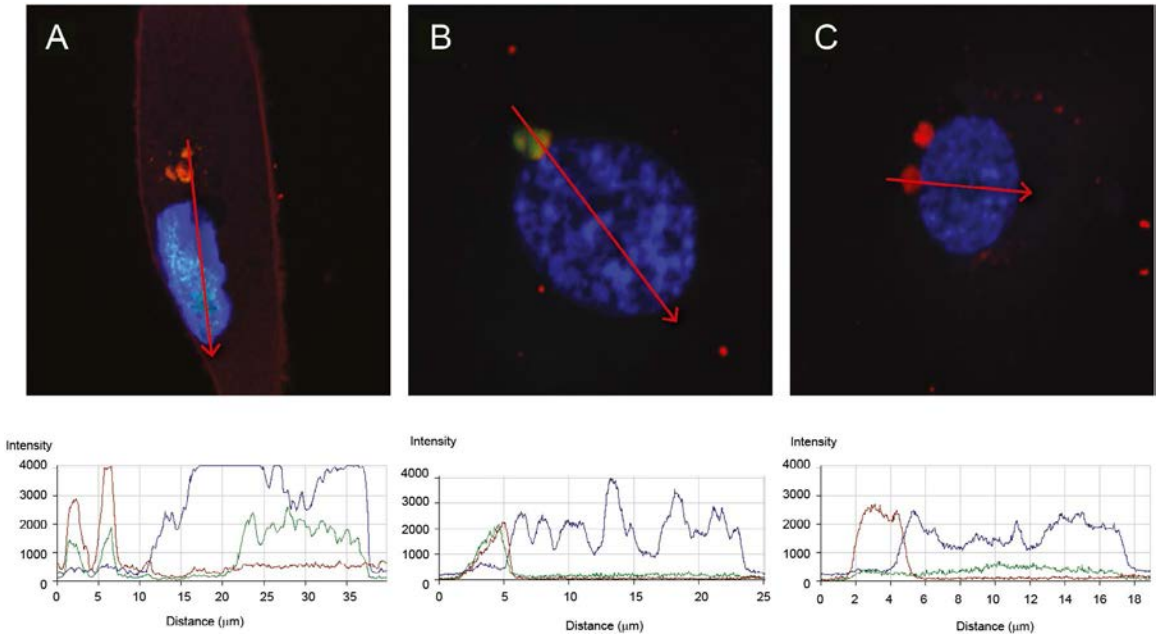

Figure 2. Newly synthesized RNA from neutrophil extracellular traps (NETs) is internalized by human aortic endothelial cells (HAECs). The uptake of newly synthesized RNA from NETs into HAECs was analyzed with laser confocal microscopy. Representative images of permeabilized HAECs with intracellular newly synthesized RNA (green), DNA/Hoechst (blue), and either neutrophil elastase (red in **A** and **C**) or LL-37 (red in **B**) are shown. In **C,** the experiment was performed in the presence of RNase A. For each profile image, the fluorescence for each fluorochrome was quantified in the region of the **arrow** displayed, and the respective fluorescence quantification is shown in the bottom graphs. The images are representative of ≥3 experiments using different systemic lupus erythematosus and healthy control samples. Original magnification × 126.

Furthermore, the DNA/protein NET scaffold appeared to be required for efficient uptake of NET-bound RNA, because naked newly synthesized RNA purified from NETs was not readily taken up by HAECs (Supplementary Figure 2A, http://onlinelibrary.wiley.com/doi/10.1002/art.41796/abstract). However, adding 1 μ*M* recombinant LL-37 (as previously used [24]) to the RNA further enhanced RNA internalization (Supplementary Figure 2B). Taken together, these results indicate that newly synthesized RNA present in NETs can be internalized by ECs. Additionally, after ImageJ analysis of several images from different experiments, the amount of internalized newly synthesized RNA from NETs was higher when using NETs derived from lupus patients compared to healthy controls (Supplementary Figure 3, http://onlinelibrary.wiley.com/doi/10.1002/art.41796/abstract).

Modulation of RNA uptake by ECs via oxidative status of NETs. Previous studies have suggested that the level of DNA oxidation in NETs modulates the induction of type I IFN responses in target cells and that lupus LDG–derived NETs contain higher amounts of oxidized nucleic acids than NETs generated by other types of stimulation (8). To explore whether oxidation status of nucleic acids present in NETs modulates the ability of target cells to internalize NET-bound newly synthesized RNA, we oxidized, in vitro, spontaneously generated NETs purified from healthy control neutrophils that were labeled with 5-EU to identify newly synthesized RNA. Following an in vitro oxidation procedure using cytochrome c (17), we confirmed by dot-blot the presence of oxidized nucleic acids using an antibody that recognizes 8-OHG. Both spontaneously formed SLE LDG–derived NETs and in vitro–oxidized spontaneously generated healthy control NETs displayed enhanced amounts of oxidized nucleic acids compared to non-oxidized healthy control NETs (Figure 3A). The degree of uptake of newly synthesized RNA by HAECs correlated with the level of nucleic acid oxidation in NETs (Figures 3B and C) and was the highest for lupus LDG–derived NETs that carried the most elevated levels of nucleic acid oxidation (Figure 3D).

To confirm these data, representative nuclei-associated green fluorescence images of internalized newly synthesized NET-associated RNA were quantified using ImageJ (Supplementary Figure 3A, http://onlinelibrary.wiley.com/doi/10.1002/art.41796/abstract). To confirm that green fluorescence detected in HAECs was due to incorporation of traces of free 5-EU carried by NETs, HAECs were incubated with free 5-EU. The faint diffuse fluorescence pattern detected with free 5-EU was different from that of newly synthesized RNA labeled in NETs (Supplementary Figure 3B). To confirm our findings, we used SYTO RNASelect green dye, another dye that stains total RNA and also labels HAEC nucleoli (Supplementary Figure 3). Internalized NET-bound newly synthesized RNA displayed enhanced localization in nucleoli. These observations indicate that the ability of NET-bound RNA to be internalized by ECs is dependent on the oxidation status of the

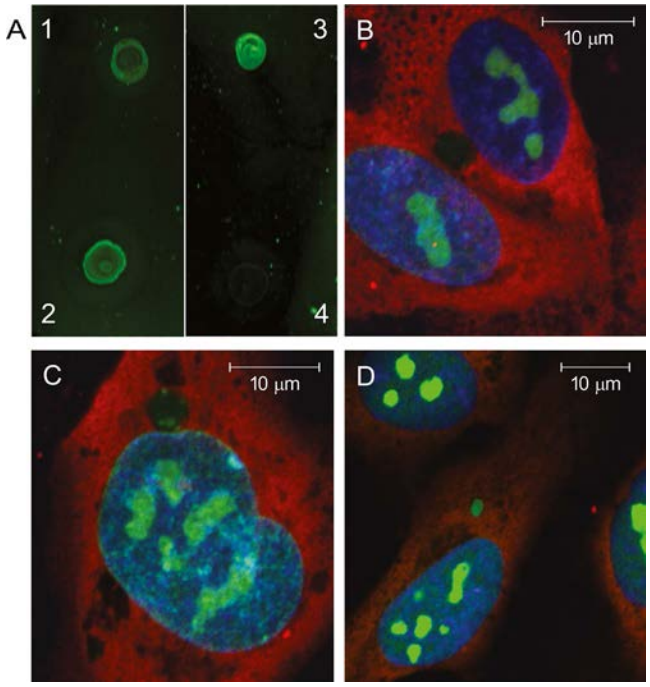

Figure 3. NET-derived newly synthesized RNA uptake by endothelial cells (ECs) increases with the degree of nucleic acid oxidation in NETs. NETs spontaneously derived from healthy control normal-density granulocytes were oxidized in vitro using cytochrome c. **A**, A dot-blot of anti–8-hydroxyguanosine was used to determine the level of nucleic acid oxidation. Healthy control NETs before (quadrant 1) and after (quadrant 2) in vitro oxidation are shown. Controls included SLE low-density granulocyte (LDG)–derived NETS without added in vitro oxidation (quadrant 3) and vehicle alone without NETs (quadrant 4). **B–D**, Human aortic ECs (HAECs) were incubated with non-oxidized control NETs (**B**), in vitro–oxidized control NETs (**C**), or non-oxidized SLE LDG–derived NETs (**D**) for 3 hours, and images of newly synthesized RNA were obtained. The confocal images display internalized newly synthesized RNA (green), DNA (blue), and neutrophil elastase (red). Images are representative of 3 independent experiments. Nuclei-associated green and blue fluorescence from **B**, **C**, **D,** and images from additional experiments were quantified using ImageJ (Supplementary Figure 2, http://onlinelibrary.wiley.com/doi/10.1002/art.41796/abstract). Original magnification × 126 in **B** and **C**; × 97 in **D**. See Figure 1 for other definitions.

nucleic acids in NETs, with RNA bound to lupus NETs being more readily internalized.

Uptake of NET-bound total RNA by ECs is dependent on actin cytoskeleton and endosomal TLRs. To characterize the mechanisms by which NET-bound RNA is internalized by ECs, we labeled total RNA in NETs with ExoGlow red dye. This dye is based on the chemistry of acridine orange designed for staining nucleic acids contained in exosomes, and it interacts with RNA and DNA but emits fluorescence in distinct wavelengths (red for RNA and green for DNA). The total RNA-labeled NETs were incubated with HAECs in a plate assay to fluorometrically quantify both total RNA uptake and the relative number of cells by staining nuclei with Hoechst. The ability of ECs to internalize NET-bound total RNA was significantly reduced by the preincubation of these cells with cytochalasin D (an inhibitor of actin cytoskeleton polymerization) and by chloroquine (an inhibitor of endosomal acidification/endosomal TLRs) (25) (Figure 4A). Uptake of RNA was also inhibited by a specific TLR-7/9 inhibitor, suggesting a role for endosomal TLRs in the internalization of NET-bound RNA and consistent with previous observations that NET internalization by other cells, such as synovial fibroblasts, is dependent on the function of these TLRs (26).

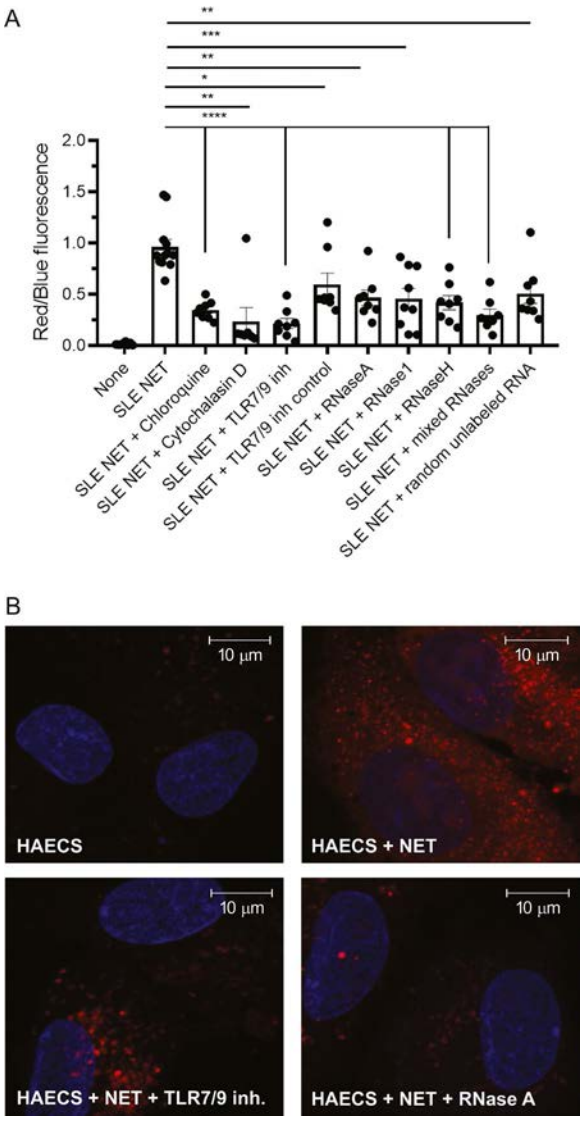

Figure 4. Uptake of NET-bound total RNA by endothelial cells (ECs) depends on the actin cytoskeleton and endosomal Toll-like receptors (TLRs). **A**, Ratio between ExoGlow red fluorescence–stained internalized total RNA derived from NETs and blue fluorescence (Hoechst)–stained DNA, quantified by plate assay and fluorometry. Bars show the mean ± SEM of 3 independent experiments; symbols represent individual samples. * = $P < 0.05$; ** = $P < 0.01$; *** = $P < 0.001$; **** = $P < 0.0001$, by Mann-Whitney U test. **B**, Representative images of human aortic ECs (HAECs) with total RNA in NETs stained with the ExoGlow red dye. Original magnification × 126. Hoechst (blue) was used to quantify the number of cells in **A** and to label nuclei in **B**. See Figure 1 for other definitions.

To further assess the type of NET-bound RNA that may be preferentially internalized by ECs, we tested different RNases (RNase H, RNase 1, and RNase A). Both RNase 1 and RNase A have been shown to act similarly on single-stranded RNAs, particularly under high-salt conditions (27). In contrast, RNase H preferentially targets RNA–DNA hybrids. The addition of either RNases or HAEC-derived non-labeled RNA to digest or compete with NET-bound RNAs, respectively, significantly decreased the uptake of NET-bound labeled RNA by HAECs (Figure 4A). Different RNases showed variable effects in reducing the ability of ECs to internalize NET-bound RNA, suggesting that NETs contain diverse types of RNAs with the potential to be internalized by HAECs. The most effective inhibitor was RNase H, followed by RNase 1 and RNase A. Representative laser confocal images are shown in Figure 4B. These findings indicate that ECs internalize RNA through mechanisms involving the actin cytoskeleton and endosomal TLRs.

Characterization of NET-bound RNAs. Identifying that some NET-associated RNAs are contained in vesicle-like structures (Figure 1) led us to characterize methods to purify the NET-bound RNA derived from healthy control and SLE neutrophils, by using a kit designed for RNA isolation from exosomes. To exclude remaining whole cells from the NET analyses, suspensions were filtered through a 0.45-μm pore-size filter before the RNA isolation procedure, as described above. We then sequenced NET-bound small RNAs (Supplementary Table 2, http://onlinelibrary.wiley.com/doi/10.1002/art.41796/abstract). Hierarchical clustering and principal components analyses revealed significant differences in small RNA expression in NETs from SLE NDGs and LDGs and healthy control NDGs (Figures 5A and B). Among the small RNAs sequenced, most of them were more abundant in spontaneous NETs from healthy control NDGs, compared to SLE-derived NETs. NETs from SLE NDGs were enriched in miR-7704 and miR-24–1, compared to NETs from control NDGs and SLE LDGs (Figure 5C and Supplementary Table 2). The most abundant small RNAs in LDG-derived NETs were miR-let-7b and miR-27b (Figure 5C), when compared to SLE and control NDG–derived NETs. Therefore, subsequent work focused on their putative role in modulating EC biology.

Promotion of type I IFN responses in ECs by NET-bound small RNA miR-let-7b. We hypothesized that small RNAs present in NETs may regulate proinflammatory responses in ECs. NETs can induce type I IFN responses in myeloid cells,

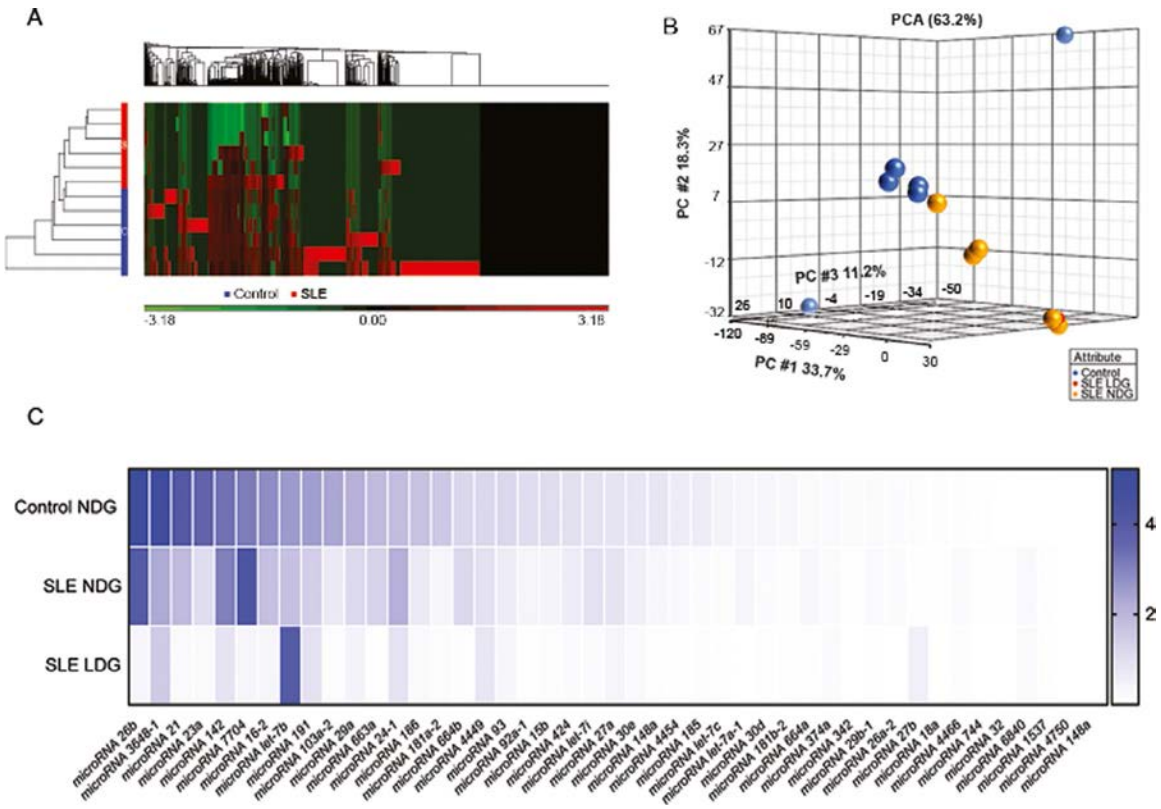

Figure 5. Small RNAs present in NETs characterized by sequencing. **A**, Hierarchical clustering after Partek analysis of small RNA sequencing. **B**, Principal components analysis (PCA) of small RNA sequences comparing NETs from healthy control normal-density granulocytes (NDGs) (blue), SLE low-density granulocytes (LDGs) (red), and SLE NDGs (yellow). **C**, Heatmap showing expression of selected small RNAs from NETs purified from control NDGs, SLE NDGs, or SLE LDGs. The gene expression in $\log_2$ (reads per kilobase per million) was normalized to the small RNA housekeeping gene *RNU6ATAC*. The small RNA sequencing analysis in NETs was performed using 12 samples (6 from SLE patients and 6 from healthy controls). See Figure 1 for other definitions.

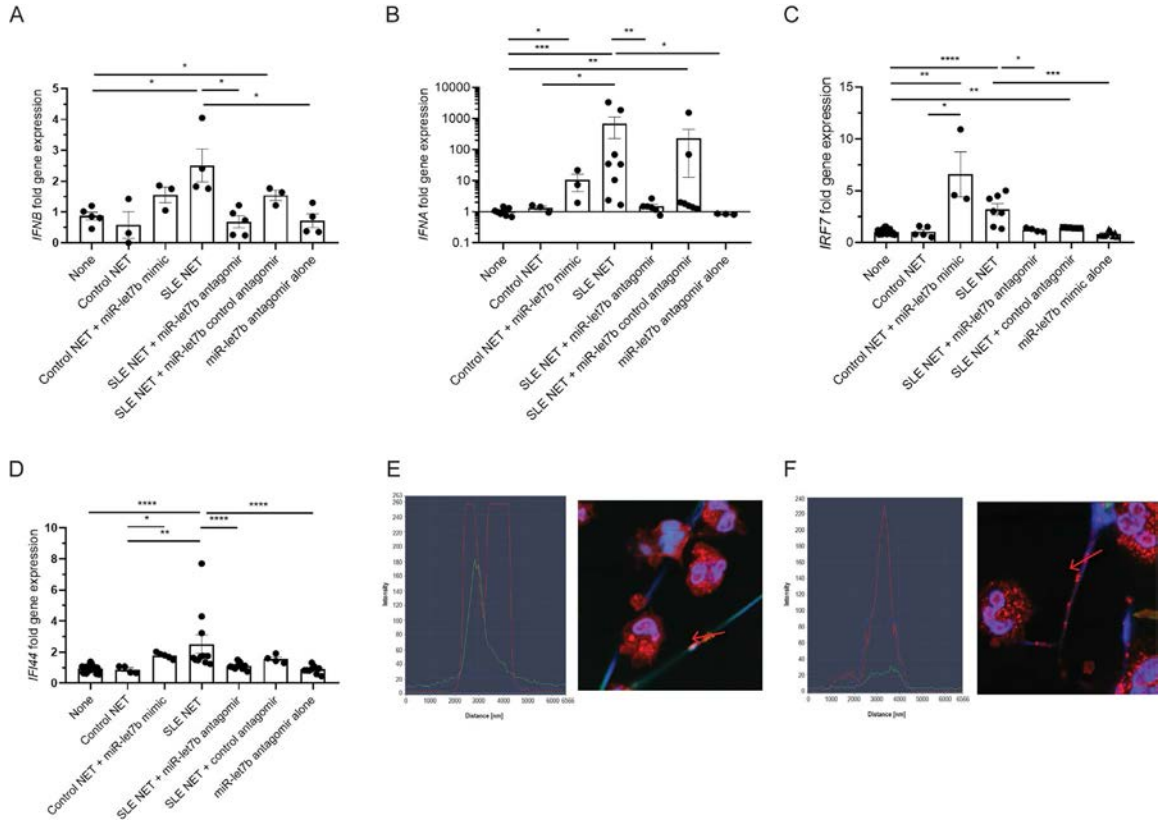

Figure 6. MicroRNA let-7b (miR-let-7b) in NETs induces type I interferon responses in endothelial cells (ECs). **A–D**, Expression levels of *IFNB* (**A**), *IFNA* (**B**), *IRF7* (**C**), and *IFI44* (**D**) in HAECs, quantified after 6 hours (**A**) and 24 hours (**B–D**) of coincubation with SLE NETs (average of low-density granulocytes [LDGs] and normal-density granulocytes [NDGs]) or healthy control NDGs (control NET) in the presence or absence of antagomir for miR-let-7b and control antagomir. Results also show the effect of a miR-let-7b mimic added to control NETs or the antagomir alone. Bars show the mean ± SEM of 3 independent experiments; symbols represent individual samples. * = $P < 0.05$; ** = $P < 0.01$; *** = $P < 0.001$; **** = $P < 0.0001$, by Mann-Whitney U test. **E** and **F**, In NETs, high mobility group box chromosomal protein 1 (HMGB-1) colocalizes with total RNA. Representative images show SLE LDG cells (**E**) or SLE NDG cells (**F**) and NETs. NETs and nuclei are stained with Hoechst (blue), and for HMGB-1 (red) and total RNA (green). The left panel in each image depicts plots of profile fluorescence quantification, with **arrows** showing the NET. See Figure 1 for other definitions.

at least in part, through oxidation of nucleic acids that trigger the cGAS/STING pathway (8). To test whether NETs promote type I IFN responses in ECs, which induces proinflammatory responses in vasculature, we incubated HAECs with spontaneously generated NETs from SLE NDGs and LDGs and from control NDGs for 6 hours (Figure 6A) or 24 hours (Figures 6B–D), and quantified type I IFN messenger RNAs and type I IFN–stimulated genes (ISGs). Only NETs derived from SLE NDGs and LDGs, but not NETs derived from control neutrophils, significantly enhanced expression of *IFNA*, *IFNB*, and the ISGs *IFI44* and *IRF7* in ECs (Figures 6A–D).

To assess whether type I IFN responses induced in ECs by lupus NETs are driven, at least in part, by specific small RNAs, we evaluated putative candidates. As mentioned above, miR-let-7b was the highest expressed small RNA in LDG-derived NETs. It was previously implicated in induction of ISGs in rheumatoid arthritis synovial macrophages and in nociceptor neurons, as it has a GU-rich sequence that directly activates TLR-7 (28,29). We incubated HAECs with NETs in the presence or absence of a specific antagomir (antisense oligonucleotide inhibitor) against miR-let-7b or a control antagomir (oligonucleotide sequence with <70% homology to any sequence in any organism in NCBI and miRBase databases), and measured *IFNB, IFNA,* and ISG expression. The miR-let-7b antagomir (but not the control antagomir) significantly inhibited expression of these IFN genes, suggesting that miR-let-7b contributes to induction of type I IFN responses in ECs triggered by lupus NETs (Figures 6A–D). To further confirm this effect, we incubated HAECs with or without control NDG–derived NETs in the presence or absence of exogenously added miR-let-7b mimic and then quantified gene expression. The miR-let-7b mimic added to control NETs significantly induced IFN gene expression in HAECs.

A putative candidate by which miR-let-7b interacts with TLR-7 is HMGB-1, a histone-like alarmin described in NETs (30) that forms complexes with miR-let-7b, leading to cell toxicity in TLR-7–dependent models (31). Indeed, total RNA colocalized with HMGB-1 in NETs, and this was enhanced in SLE LDG–derived NETs when compared with SLE NDG–derived NETs (Figures 6E

and F). Following immunoprecipitation with an antibody against HMGB-1, we assessed remnant HMGB-1–associated miR-let-7b using quantitative PCR. Indeed, HMGB-1–associated miR-let-7b was more abundant in SLE LDG–derived NETs compared to autologous NDG–derived NETs (Supplementary Figure 4, http://onlinelibrary.wiley.com/doi/10.1002/art.41796/abstract). These data suggest that small RNA miR-let-7b present in NETs promotes type I IFN responses in ECs and that this phenomenon is enhanced in lupus-derived NETs.

DISCUSSION

We have shown that NETs contain small RNAs that, upon uptake and internalization by ECs, induce type I IFN responses. This process is enhanced by NET-associated oxidized nucleotides that are significantly increased in SLE LDG–derived NETs. The resultant enhanced oxidation of nucleotides in lupus NETs correlated with the ability of ECs to internalize NET-bound RNA. Previous reports have indicated that oxidation of cell membranes increases the ability of cells to internalize extracellular cargoes by reducing lipid hydrophobicity (32). Oxidation of NETs, either in vivo through neutrophil-derived ROS or in vitro as shown in this study, may modify vesicle-associated lipids that contain RNAs and enhance their uptake by ECs.

The alarmins LL-37 and HMGB-1 have RNA binding activity and are present in NETs (6,13,33). We confirmed that ECs exposed to NETs take up LL-37 that colocalizes with neutrophil-derived newly synthesized RNA. This is consistent with previous studies that have shown that exogenous LL-37 can enter target cells and disrupt nuclear membranes during NET formation (34). Furthermore, both HMGB-1 and LL-37 have been associated with the ability of plasmacytoid dendritic cells (pDCs) to take up exogenous DNA from NETs (30,35,36) and enhance type I IFN synthesis. Also, previous evidence indicates that extracellular LL-37 can bind to extracellular self-RNA and transfer it to the endosomes of DCs to activate type I IFN responses through TLR-7/8. As such, the presence of both RNA and LL-37 in NETs may lead to the creation of stable complexes that protect RNA from degradation and promote immunomodulatory and vasculopathic activity that is enhanced in the context of SLE NETs (37,38).

Among the small RNAs contained in the NETs, miR-let-7b was shown to display interferogenic activity on pDCs (37), given its intrinsic ability to act as a natural ligand of TLR-7 (28,31). Recently, miR-let-7b was characterized as an endogenous TLR-7 agonist involved in inflammation propagation in psoriatic arthritis (39). Induction of type I IFN responses in ECs has been linked to the development of vasculopathy and atherothrombosis, particularly in SLE, through pleiotropic effects on vascular repair, inflammation, and coagulation (40–43). As such, the induction of endothelial interferogenic responses induced by small RNAs bound to NETs may be highly conducive to vascular damage. The roles of endogenous miR-let-7b in endothelial function are complex and may also involve protecting these cells from oxidation (44–47). Consequently, future studies should comprehensively address how this NET-bound small RNA modulates overall vascular health in SLE and other inflammatory diseases. Of note, other components of NETs can induce endothelial damage, including histones (48–50) and matrix metalloproteinases (10). Therefore, dissecting the precise role that these different NET components play in the overall development of vasculopathy should be characterized in future studies to define the best therapeutic target.

In conclusion, we report that NETs are a source of intracellular RNAs that impact EC biology. These effects are particularly driven by small RNAs and their interactions with NET-derived alarmins. These observations are relevant not only for vascular damage induced in SLE but also for other conditions associated with NET formation and vascular damage, such as sepsis, atherothrombosis, and cancer. Future studies should assess whether targeting specific RNAs present in NETs could have therapeutic implications in these potentially devastating conditions.

ACKNOWLEDGMENT

We are grateful to Ms Daniela Aguero for expert support in the preparation of figures.

AUTHOR CONTRIBUTIONS

All authors were involved in drafting the article or revising it critically for important intellectual content, and all authors approved the final version to be published. Dr. Kaplan had full access to all of the data in the study and takes responsibility for the integrity of the data and the accuracy of the data analysis.

Study conception and design. Blanco, Hafner, Kaplan.
Acquisition of data. Blanco, Wang, Carlucci, Torres-Ruiz, Romo-Tena.
Analysis and interpretation of data. Blanco, Sun, Hafner, Kaplan.

REFERENCES

1. Tsokos GC. Systemic lupus erythematosus [review]. N Engl J Med 2011;365:2110–21.
2. Rahman A, Isenberg DA. Systemic lupus erythematosus [review]. N Engl J Med 2008;358:929–39.
3. Barrat FJ, Crow MK, Ivashkiv LB. Interferon target-gene expression and epigenomic signatures in health and disease [review]. Nat Immunol 2019;20:1574–83.
4. Kaplan MJ. Neutrophils in the pathogenesis and manifestations of SLE [review]. Nat Rev Rheumatol 2011;7:691–9.
5. Denny MF, Yalavarthi S, Zhao W, Thacker SG, Anderson M, Sandy AR, et al. A distinct subset of proinflammatory neutrophils isolated from patients with systemic lupus erythematosus induces vascular damage and synthesizes type I IFNs. J Immunol 2010;184:3284–97.
6. Villanueva E, Yalavarthi S, Berthier CC, Hodgin JB, Khandpur R, Lin AM, et al. Netting neutrophils induce endothelial damage, infiltrate tissues, and expose immunostimulatory molecules in systemic lupus erythematosus. J Immunol 2011;187:538–52.
7. Carmona-Rivera C, Kaplan M. Low-density granulocytes: a distinct class of neutrophils in systemic autoimmunity [review]. Semin Immunopathol 2013;35:455–63.
8. Lood C, Blanco LP, Purmalek MM, Carmona-Rivera C, De Ravin SS, Smith CK, et al. Neutrophil extracellular traps enriched in oxidized

mitochondrial DNA are interferogenic and contribute to lupus-like disease. Nat Med 2016;22:146–53.
9. Gehrke N, Mertens C, Zillinger T, Wenzel J, Bald T, Zahn S, et al. Oxidative damage of DNA confers resistance to cytosolic nuclease TREX1 degradation and potentiates STING-dependent immune sensing. Immunity 2013;39:482–95.
10. Carmona-Rivera C, Zhao W, Yalavarthi S, Kaplan MJ. Neutrophil extracellular traps induce endothelial dysfunction in systemic lupus erythematosus through the activation of matrix metalloproteinase-2. Ann Rheum Dis 2015;74:1417–24.
11. Mittelbrunn M, Sánchez-Madrid F. Intercellular communication: diverse structures for exchange of genetic information [review]. Nat Rev Mol Cell Biol 2012;13:328–35.
12. Mittelbrunn M, Gutierrez-Vazquez C, Villarroya-Beltri C, Gonzalez S, Sanchez-Cabo F, Gonzalez MA, et al. Unidirectional transfer of microRNA-loaded exosomes from T cells to antigen-presenting cells. Nat Commun 2011;2:282.
13. Herster F, Bittner Z, Archer NK, Dickhöfer S, Eisel D, Eigenbrod T, et al. Neutrophil extracellular trap-associated RNA and LL37 enable self-amplifying inflammation in psoriasis. Nat Commun 2020;11:105.
14. Linhares-Lacerda L, Temerozo JR, Ribeiro-Alves M, Azevedo EP, Mojoli A, Nascimento MT, et al. Neutrophil extracellular trap-enriched supernatants carry microRNAs able to modulate TNF-α production by macrophages. Sci Rep 2020;10:2715.
15. Blanco LP, Pedersen HL, Wang X, Lightfoot YL, Seto N, Carmona-Rivera C, et al. Improved mitochondrial metabolism and reduced inflammation following attenuation of murine lupus with coenzyme Q10 analog idebenone. Arthritis Rheumatol 2020;72:454–64.
16. Hochberg MC, for the Diagnostic and Therapeutic Criteria Committee of the American College of Rheumatology. Updating the American College of Rheumatology revised criteria for the classification of systemic lupus erythematosus [letter]. Arthritis Rheum 1997;40:1725.
17. Tanaka M, Jaruga P, Küpfer PA, Leumann CJ, Dizdaroglu M, Sonntag WE, et al. RNA oxidation catalyzed by cytochrome c leads to its depurination and cross-linking, which may facilitate cytochrome c release from mitochondria. Free Radic Biol Med 2012;53:854–62.
18. Hafner M, Renwick N, Farazi TA, Mihailović A, Pena JT, Tuschl T. Barcoded cDNA library preparation for small RNA profiling by next-generation sequencing. Methods 2012;58:164–70.
19. Farazi TA, Brown M, Morozov P, ten Hoeve JJ, Ben-Dov IZ, Hovestadt V, et al. Bioinformatic analysis of barcoded cDNA libraries for small RNA profiling by next-generation sequencing. Methods 2012;58:171–87.
20. Heinz S, Benner C, Spann N, Bertolino E, Lin YC, Laslo P, et al. Simple combinations of lineage-determining transcription factors prime cis-regulatory elements required for macrophage and B cell identities. Molecular Cell 2010;38:576–89.
21. Selth LA, Gilbert C, Svejstrup JQ. RNA immunoprecipitation to determine RNA-protein associations in vivo. Cold Spring Harb Protoc 2009;2009:pdb.prot5234.
22. Goel RR, Wang X, O'Neil LJ, Nakabo S, Hasneen K, Gupta S, et al. Interferon λ promotes immune dysregulation and tissue inflammation in TLR7-induced lupus. Proc Natl Acad Sci 2020;117:5409–19.
23. Oulhen N, Foster S, Wray G, Wessel G. Identifying gene expression from single cells to single genes [review]. Methods Cell Biol 2019;151:127–58.
24. Dahl S, Cerps S, Rippe C, Swärd K, Uller L, Svensson D, et al. Human host defense peptide LL-37 facilitates double-stranded RNA pro-inflammatory signaling through up-regulation of TLR3 expression in vascular smooth muscle cells. Inflamm Res 2020;69:579–88.
25. Schrezenmeier E, Dörner T. Mechanisms of action of hydroxychloroquine and chloroquine: implications for rheumatology [review]. Nat Rev Rheumatol 2020;16:155–66.
26. Carmona-Rivera C, Carlucci PM, Moore E, Lingampalli N, Uchtenhagen H, James E, et al. Synovial fibroblast-neutrophil interactions promote pathogenic adaptive immunity in rheumatoid arthritis. Sci Immunol 2017;2:eaag3358.
27. Kawashima T, Ikari N, Kouchi T, Kowatari Y, Kubota Y, Shimojo N, et al. The molecular mechanism for activating IgA production by Pediococcus acidilactici K15 and the clinical impact in a randomized trial. Sci Rep 2018;8:5065.
28. Kim S, Chen Z, Essani AB, Elshabrawy HA, Volin MV, Volkov S, et al. Identification of a novel Toll-like receptor 7 endogenous ligand in rheumatoid arthritis synovial fluid that can provoke arthritic joint inflammation. Arthritis Rheumatol 2016;68:1099–110.
29. Park CK, Xu ZZ, Berta T, Han Q, Chen G, Liu XJ, et al. Extracellular microRNAs activate nociceptor neurons to elicit pain via TLR7 and TRPA1. Neuron 2014;82:47–54.
30. Garcia-Romo GS, Caielli S, Vega B, Connolly J, Allantaz F, Xu Z, et al. Netting neutrophils are major inducers of type I IFN production in pediatric systemic lupus erythematosus. Sci Transl Med 2011;3:73ra20.
31. Coleman LG, Zou J, Crews FT. Microglial-derived miRNA let-7 and HMGB1 contribute to ethanol-induced neurotoxicity via TLR7. J Neuroinflammation 2017;14:22.
32. Wang TY, Libardo MD, Angeles-Boza AM, Pellois JP. Membrane oxidation in cell delivery and cell killing applications [review]. ACS Chem Biol 2017;12:1170–82.
33. Kahlenberg JM, Carmona-Rivera C, Smith CK, Kaplan MJ. Neutrophil extracellular trap–associated protein activation of the NLRP3 inflammasome is enhanced in lupus macrophages. J Immunol 2013;190:1217–26.
34. Neumann A, Berends ET, Nerlich A, Molhoek EM, Gallo RL, Meerloo T, et al. The antimicrobial peptide LL-37 facilitates the formation of neutrophil extracellular traps. Biochem J 2014;464:3–11.
35. Lande R, Ganguly D, Facchinetti V, Frasca L, Conrad C, Gregorio J, et al. Neutrophils activate plasmacytoid dendritic cells by releasing self-DNA–peptide complexes in systemic lupus erythematosus. Sci Transl Med 2011;3:73ra19.
36. Chamilos G, Gregorio J, Meller S, Lande R, Kontoyiannis DP, Modlin RL, et al. Cytosolic sensing of extracellular self-DNA transported into monocytes by the antimicrobial peptide LL37. Blood 2012;120:3699–707.
37. Salvi V, Gianello V, Busatto S, Bergese P, Andreoli L, D'Oro U, et al. Exosome-delivered microRNAs promote IFN-α secretion by human plasmacytoid DCs via TLR7. JCI Insight 2018;3:e98204.
38. Ganguly D, Chamilos G, Lande R, Gregorio J, Meller S, Facchinetti V, et al. Self-RNA–antimicrobial peptide complexes activate human dendritic cells through TLR7 and TLR8. J Exp Med 2009;206:1983–94.
39. Van Raemdonck K, Umar S, Palasiewicz K, Romay B, Volkov S, Arami S, et al. TLR7 endogenous ligands remodel glycolytic macrophages and trigger skin-to-joint crosstalk in psoriatic arthritis. Eur J Immunol 2021;51:714–20.
40. Denny MF, Thacker S, Mehta H, Somers EC, Dodick T, Barrat FJ, et al. Interferon-α promotes abnormal vasculogenesis in lupus: a potential pathway for premature atherosclerosis. Blood 2007;110:2907–15.
41. Somers EC, Zhao W, Lewis EE, Wang L, Wing JJ, Sundaram B, et al. Type I interferons are associated with subclinical markers of cardiovascular disease in a cohort of systemic lupus erythematosus patients. PLoS One 2012;7:e37000.
42. Thacker SG, Berthier CC, Mattinzoli D, Rastaldi MP, Kretzler M, Kaplan MJ. The detrimental effects of IFN-α on vasculogenesis in lupus are mediated by repression of IL-1 pathways: potential role in atherogenesis and renal vascular rarefaction. J Immunol 2010;185:4457–69.
43. Thacker SG, Zhao W, Smith CK, Luo W, Wang H, Vivekanandan-Giri A, et al. Type I interferons modulate vascular function, repair,

thrombosis, and plaque progression in murine models of lupus and atherosclerosis. Arthritis Rheum 2012;64:2975–85.

44. Bao M, Zhang Y, Lou X, Cheng Y, Zhou H. Protective effects of let-7a and let-7b on oxidized low-density lipoprotein induced endothelial cell injuries. PLoS One 2014;9:e106540.
45. Beltrami C, Besnier M, Shantikumar S, Shearn AI, Rajakaruna C, Laftah A, et al. Human pericardial fluid contains exosomes enriched with cardiovascular-expressed microRNAs and promotes therapeutic angiogenesis. Mol Ther 2017;25:679–93.
46. Zhu L, Li Q, Qi D, Niu F, Li Q, Yang H, et al. Atherosclerosis-associated endothelial cell apoptosis by miRNA let7-b-mediated downregulation of HAS-2. J Cell Biochem 2020;121:3961–72.
47. Chen PY, Qin L, Barnes C, Charisse K, Yi T, Zhang X, et al. FGF regulates TGF-β signaling and endothelial-to-mesenchymal transition via control of let-7 miRNA expression. Cell Rep 2012;2:1684–96.
48. Daigo K, Takamatsu Y, Hamakubo T. The protective effect against extracellular histones afforded by long-pentraxin PTX3 as a regulator of NETs [review]. Front Immunol 2016;7:344.
49. Meegan JE, Yang X, Beard RS, Jannaway M, Chatterjee V, Taylor-Clark TE, et al. Citrullinated histone 3 causes endothelial barrier dysfunction. Biochem Biophys Res Commun 2018;503:1498–502.
50. Saffarzadeh M, Juenemann C, Queisser MA, Lochnit G, Barreto G, Galuska SP, et al. Neutrophil extracellular traps directly induce epithelial and endothelial cell death: a predominant role of histones. PLoS One 2012;7:e32366.

Arthritis & Rheumatology
Vol. 73, No. 12, December 2021, pp 2293–2302
DOI 10.1002/art.41876
© 2021, American College of Rheumatology

American College of Rheumatology
Empowering Rheumatology Professionals

Neuropsychiatric Events in Systemic Lupus Erythematosus: Predictors of Occurrence and Resolution in a Longitudinal Analysis of an International Inception Cohort

John G. Hanly,[1] Caroline Gordon,[2] Sang-Cheol Bae,[3] Juanita Romero-Diaz,[4] Jorge Sanchez-Guerrero,[4] Sasha Bernatsky,[5] Ann E. Clarke,[6] Daniel J. Wallace,[7] David A. Isenberg,[8] Anisur Rahman,[8] Joan T. Merrill,[9] Paul R. Fortin,[10] Dafna D. Gladman,[11] Murray B. Urowitz,[11] Ian N. Bruce,[12] Michelle Petri,[13] Ellen M. Ginzler,[14] M. A. Dooley,[15] Rosalind Ramsey-Goldman,[16] Susan Manzi,[17] Andreas Jonsen,[18] Graciela S. Alarcón,[19] Ronald F. van Vollenhoven,[20] Cynthia Aranow,[21] Meggan Mackay,[21] Guillermo Ruiz-Irastorza,[22] S. Sam Lim,[23] Murat Inanc,[24] Kenneth C. Kalunian,[25] Soren Jacobsen,[26] Christine A. Peschken,[27] Diane L. Kamen,[28] Anca Askanase,[29] and Vernon Farewell[30]

Objective. To determine predictors of change in neuropsychiatric (NP) event status in a large, prospective, international inception cohort of patients with systemic lupus erythematosus (SLE).

Methods. Upon enrollment and annually thereafter, NP events attributed to SLE and non-SLE causes and physician-determined resolution were documented. Factors potentially associated with the onset and resolution of NP events were determined by time-to-event analysis using a multistate modeling structure.

Results. NP events occurred in 955 (52.3%) of 1,827 patients, and 593 (31.0%) of 1,910 unique events were attributed to SLE. For SLE-associated NP (SLE NP) events, multivariate analysis revealed a positive association with male sex ($P = 0.028$), concurrent non-SLE NP events excluding headache ($P < 0.001$), active SLE ($P = 0.012$), and glucocorticoid use ($P = 0.008$). There was a negative association with Asian race ($P = 0.002$), postsecondary education ($P = 0.001$), and treatment with immunosuppressive drugs ($P = 0.019$) or antimalarial drugs ($P = 0.056$). For non-SLE NP events excluding headache, there was a positive association with concurrent SLE NP events ($P < 0.001$) and a negative association with African race ($P = 0.012$) and Asian race ($P < 0.001$). NP events attributed to SLE had a higher resolution rate than non-SLE NP events, with the exception of headache, which had comparable resolution rates. For SLE NP events, multivariate analysis revealed that resolution was more common in patients of Asian race ($P = 0.006$) and for central/focal NP events ($P < 0.001$). For non-SLE NP events, resolution was more common in patients of African race ($P = 0.017$) and less common in patients who were older at SLE diagnosis ($P < 0.001$).

Conclusion. In a large and long-term study of the occurrence and resolution of NP events in SLE, we identified subgroups with better and worse prognosis. The course of NP events differs greatly depending on their nature and attribution.

The views expressed in this article are those of the authors and not necessarily those of the NHS, the NIHR, or the UK Department of Health.

The Hopkins Lupus Cohort is supported by the NIH (grants AR-43727 and AR-69572). The Montreal General Hospital Lupus Clinic is partially supported by the Singer Family Fund for Lupus Research. Dr. Hanly's work was supported by the Canadian Institutes of Health Research (grant MOP-88526). Dr. Gordon's work was supported by Lupus UK, Sandwell and West Birmingham Hospitals NHS Trust, and the Birmingham NIHR/Wellcome Trust Clinical Research Facility. Dr. Bae's work was supported in part by the Republic of Korea (grant NRF-2017M3A9B4050335). Dr. Bernatsky holds a James McGill Research Chair. Dr. Clarke holds The Arthritis Society Chair in Rheumatic Diseases at the University of Calgary. Drs. Isenberg and Rahman's work was supported by the NIHR University College London Hospitals Biomedical Research Center. Dr. Fortin holds a tier 1 Canada Research Chair on Systemic Autoimmune Rheumatic Diseases at Université Laval. Dr. Bruce is an NIHR Senior Investigator and is supported by Versus Arthritis UK, the NIHR Manchester Biomedical Research Centre, and the NIHR Manchester Clinical Research Facility. Dr. Dooley's work was supported by the NIH (grant RR-00046). Dr. Ramsey-Goldman's work was supported by the NIH (grants 5UL1-TR-001422-02 [formerly 8UL1-TR-000150 and UL-1RR-025741], K24-AR-02318, and P30-AR-072579 [formerly P60-AR-064464 and P60-AR-48098]). Dr. Ruiz-Irastorza's work was supported by the Department of Education, Universities, and Research of the Basque Government. Dr. Jacobsen's work was supported by the Danish Rheumatism Association (grant A3865) and the Independent Research Fund Denmark (grant 0134-00473B).

[1]John G. Hanly, MD: Queen Elizabeth II Health Sciences Centre and Dalhousie University, Halifax, Nova Scotia, Canada; [2]Caroline Gordon, MD: University of Birmingham, Birmingham, UK; [3]Sang-Cheol Bae, MD, PhD, MPH: Hanyang University Hospital for Rheumatic Diseases, Seoul, Republic of Korea; [4]Juanita Romero-Diaz, MD, MSc, Jorge Sanchez-Guerrero, MD, MSc: Instituto Nacional de Ciencias Médicas y Nutrición Salvador Zubirán, Mexico City, Mexico; [5]Sasha Bernatsky, MD, PhD: McGill University, Montreal, Quebec, Canada; [6]Ann E. Clarke, MD, MSc: University of Calgary, Calgary, Alberta, Canada; [7]Daniel J. Wallace, MD: Cedars-Sinai Medical Center and University of California, Los Angeles; [8]David A. Isenberg, MD, Anisur Rahman, MD, PhD: University College London, London, UK; [9]Joan T. Merrill, MD: Oklahoma Medical Research Foundation, Oklahoma City; [10]Paul R. Fortin, MD, MPH: Centre Hospitalier Universitaire de Québec–Université Laval, Quebec City, Quebec, Canada;

INTRODUCTION

Neurologic and psychiatric clinical events resulting from abnormalities of the central, peripheral, and autonomic nervous systems occur in patients with systemic lupus erythematosus (SLE) (1,2). Recent studies suggest that ~30–50% of all neuropsychiatric (NP) events in SLE patients are attributable to SLE (3,4), although the exact proportion varies depending on the type of NP event. Prospective, observational cohort studies of SLE patients have shown differences in the outcome of NP events depending, in part, on their attribution to SLE or non-SLE causes.

In a recent study (5) using multistate modeling at the patient level, we reported the occurrence, attribution, and outcome of all NP events in SLE patients. Regardless of attribution, NP events occurred most frequently around the time of the diagnosis of SLE and had a significant negative impact on health-related quality of life. Although the majority of NP events resolved over time, patients with NP events attributed to SLE (NP SLE events) had a higher mortality rate.

To further advance the understanding of nervous system disease in SLE patients, we aimed to identify the clinical and laboratory variables associated with the development and resolution of NP events over time. The present study in a large, prospective, international inception cohort of SLE patients was performed to determine predictors of change in a patient's NP event status, based on a multistate modeling approach and attribution rules previously described (5).

PATIENTS AND METHODS

Research study network. The study was conducted by the Systemic Lupus International Collaborating Clinics (SLICC) (6), a network that currently consists of 52 investigators at 43 academic centers in 16 countries. At the initiation of the present study, patients recently diagnosed as having SLE were recruited from the then 31 SLICC sites in Europe, Asia, and North America. Data were collected per protocol at enrollment and annually, ensuring data quality, management, and security. The Nova Scotia Health Authority Central Zone Research Ethics Board and each of the participating centers' research ethics review boards approved the study.

Patients. Enrollment was permitted up to 15 months after the diagnosis of SLE, defined as when the revised American College of Rheumatology (ACR) classification criteria (7) were first recognized. Lupus-related variables included the SLE Disease Activity Index 2000 (SLEDAI-2K) (8) and SLICC/ACR Damage Index (SDI) (9).

NP events. NP events were first characterized within an enrollment window (6 months prior to the diagnosis of SLE up to the enrollment date) using ACR case definitions for 19 NP syndromes (10). Patients were reassessed annually within a 6-month window using a detailed protocol to record information on the same 19 NP syndromes (10), presence of prespecified non-SLE causes, results of appropriate investigations, medications, and outcomes. New NP events since the last study assessment and the status of previous NP events were determined at each assessment. For recurring events within an assessment period, the date of the first episode was taken as the onset of the event.

NP events were also classified into the following mutually exclusive categories: central/diffuse, central/focal, and peripheral. Central/diffuse NP events included aseptic meningitis, demyelinating syndrome, headache, acute confusional state, anxiety disorder, cognitive dysfunction, mood disorder, and psychosis. Central/focal NP events included cerebrovascular disease, movement disorder, myelopathy, and seizure disorders. Peripheral NP events included autonomic neuropathy, mononeuropathy, myasthenia gravis, Guillain-Barré syndrome, cranial neuropathy, plexopathy, and polyneuropathy.

[11]Dafna D. Gladman, MD, Murray B. Urowitz, MD: Centre for Prognosis Studies in the Rheumatic Diseases, Toronto Western Hospital, and University of Toronto, Ontario, Canada; [12]Ian N. Bruce, MD: Centre for Epidemiology Versus Arthritis, Manchester Academic Health Sciences Centre, University of Manchester, NIHR Manchester Biomedical Research Centre, and Manchester University NHS Foundation Trust, Manchester, UK; [13]Michelle Petri, MD, MPH: Johns Hopkins University School of Medicine, Baltimore, Maryland; [14]Ellen M. Ginzler, MD, MPH: State University of New York Downstate Medical Center, Brooklyn; [15]M. A. Dooley, MD, MPH: University of North Carolina, Chapel Hill; [16]Rosalind Ramsey-Goldman, MD, DrPH: Northwestern University Feinberg School of Medicine, Chicago, Illinois; [17]Susan Manzi, MD, MPH: Allegheny Health Network, Pittsburgh, Pennsylvania; [18]Andreas Jonsen, MD, PhD: Lund University, Lund, Sweden; [19]Graciela S. Alarcón, MD, MPH: University of Alabama at Birmingham; [20]Ronald F. van Vollenhoven, MD: Amsterdam University Medical Center, Amsterdam, The Netherlands; [21]Cynthia Aranow, MD, Meggan Mackay, MD: Feinstein Institute for Medical Research, Manhasset, New York; [22]Guillermo Ruiz-Irastorza, MD: Hospital Universitario Cruces and University of the Basque Country, Barakaldo, Spain; [23]S. Sam Lim, MD, MPH: Emory University, Atlanta, Georgia; [24]Murat Inanc, MD: Istanbul University, Istanbul, Turkey; [25]Kenneth C. Kalunian, MD: University of California San Diego School of Medicine, La Jolla; [26]Soren Jacobsen, MD, DMSc: Rigshospitalet, Copenhagen University Hospital, Copenhagen, Denmark; [27]Christine A. Peschken, MD: University of Manitoba, Winnipeg, Manitoba, Canada; [28]Diane L. Kamen, MD: Medical University of South Carolina, Charleston; [29]Anca Askanase, MD, MPH: NYU Langone Orthopedic Hospital, New York, New York; [30]Vernon Farewell, PhD: University of Cambridge, Cambridge, UK.

Dr. Clarke has received consulting fees from AstraZeneca, Bristol Myers Squibb, Exagen Diagnostics, and GlaxoSmithKline (less than $10,000 each). Dr. Wallace has received consulting fees from Merck, EMD Serono, Pfizer, Lilly, and Glenmark (less than $10,000 each). Dr. Bruce has received consulting fees, speaking fees, and/or honoraria from Eli Lilly, GlaxoSmithKline, AstraZeneca, UCB, and Bristol Myers Squibb (less than $10,000 each) and research support from GlaxoSmithKline. Dr. van Vollenhoven has received consulting fees, speaking fees, and/or honoraria from AbbVie, AstraZeneca, Biotest, Bristol Myers Squibb, Celgene, GlaxoSmithKline, Janssen, Lilly, Novartis, Pfizer, and UCB (less than $10,000 each) and research support from AbbVie, Bristol Myers Squibb, GlaxoSmithKline, Pfizer, and UCB. Dr. Inanc has received consulting fees from UCB and Amgen (less than $10,000 each). No other disclosures relevant to this article were reported.

Address correspondence to John G. Hanly, MD, Nova Scotia Rehabilitation Center, Division of Rheumatology, Second Floor, 1341 Summer Street, Halifax, Nova Scotia B3H 4K4, Canada. Email: john.hanly@nshealth.ca.

Submitted for publication December 11, 2020; accepted in revised form May 13, 2021.

Attribution of NP events. Factors considered in the attribution decision rules included: 1) temporal onset of NP event(s) in relation to the diagnosis of SLE; 2) concurrent non-SLE factor(s), such as potential causes ("exclusions") or contributing factors ("associations") for each NP syndrome listed in the glossary of the ACR case definitions of NP events (10); and 3) "common" NP events that are frequent in normal population controls as described by Ainiala et al (11). These common events include isolated headaches, anxiety, mild depression (mood disorders failing to meet the criteria for "major depressive-like episodes"), mild cognitive impairment (deficits in <3 of the 8 specified cognitive domains), and polyneuropathy without electrophysiologic confirmation. Two attribution decision rules of different stringency (models A and B) were designed (12,13).

Attribution model A (more stringent). NP events attributed to SLE 1) had their onset within the enrollment window or subsequently and 2) had no "exclusions" or "associations," and 3) were not one of the NP events identified by Ainiala et al (11).

Attribution model B (less stringent). NP events attributed to SLE 1) had their onset within 10 years prior to the diagnosis of SLE and were still present within the enrollment window, or occurred subsequently, and 2) had no "exclusions," and 3) were not one of the NP events identified by Ainiala et al (11).

All NP events attributed to SLE using model A were included in the NP events attributed to SLE using model B. All other events were classified as a non-SLE NP event.

Outcome of NP events. The change in NP events between onset and follow-up was compared at each follow-up assessment using a physician-generated score on a 7-point Likert scale, where 1 = patient demise, 2 = much worse, 3 = worse, 4 = no change, 5 = improved, 6 = much improved, and 7 = resolved (14). A precise date was recorded for outcomes 1 and 7.

Factors potentially associated with NP events. Variables of interest included sex; race, ethnicity, and location; age at SLE diagnosis; education level; concurrent NP events with a different attribution (updated at each assessment); and SLEDAI-2K and SDI scores (excluding NP variables); as well as medications. Central/diffuse, central/focal, and peripheral events were also considered in the analyses, as were lupus anticoagulant (LAC), IgG anticardiolipin, anti–β_2-glycoprotein I, anti–ribosomal P, and anti-NR2 glutamate receptor (anti-NR2) antibodies. The LAC assay was performed using screen-and-confirm reagents (Rainbow Scientific), and the other autoantibodies were measured by enzyme-linked immunosorbent assay at the Oklahoma Medical Research Foundation (15–18). Autoantibody levels were measured once at enrollment.

Statistical analysis. As we previously described (5), multistate patient-level models, characterized by transition rates between states, were examined, one for NP events attributed to SLE (by model B) and the other for non-SLE events (Figure 1). In the present study, an additional multistate model for non-SLE events excluding headache was examined due to the predominance of headache among the non-SLE NP events. Models for SLE NP events restricted by central/diffuse, central/focal, and peripheral events were also examined. Events other than the type being modeled were excluded when fitting each model.

The 4 states in the multistate models were as follows: state 1 = no NP event ever; state 2 = no current NP event but ≥1 event in the past, with state entry defined as the time of resolution of the last active NP event after entry into state 3; state 3 = new/ongoing NP event(s) with state entry defined as the onset of any NP event when previously in state 1 or state 2; and state 4 = death. Modeling assumed transitions could occur between and not just at assessments, and each site investigator provided the approximate dates for the onset and resolution of NP events and the precise date of death.

The time origin was 6 months before SLE diagnosis. Patients could move back and forth between state 2 (resolution of NP event) and state 3 (new/ongoing NP event). The model incorporates deaths occurring in any state from state 1 to state 3.

For the purposes of this analysis, the transition rates were estimated using Cox's semiparametric relative risk regression model. This allows explanatory (predictor) variables to influence transition rates through a regression model on the logarithm of the transition rates, while the baseline transition rate is allowed to be an arbitrary function of time since entering the state. The primary focus is on hazard ratio (HR) estimates and 95% confidence intervals (95% CIs), which are provided based on univariate (single-factor) analyses and from multivariate models. Effects are assumed to be the same on the transitions to the NP event state from both the no NP event state and the resolved state. Model estimation was implemented using the R (19) package 'survival'(20). Kaplan-Meier–like estimates of the probability of onset and probability of resolution over time were also calculated both for transitions within the multistate models and for some NP event-level analyses.

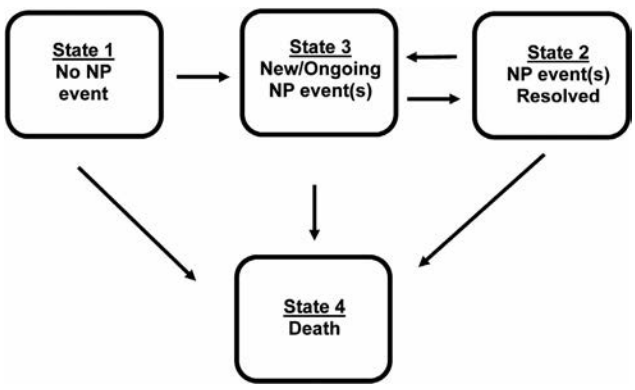

Figure 1. Multistate model of observed transitions in neuropsychiatric (NP) status in patients with systemic lupus erythematosus.

Table 1. Multivariate analysis of predictors of transitions to the NP event state for SLE NP events and for non-SLE NP events excluding headache*

	Model 1 (n = 426 transitions)		Model 2 (n = 192 transitions)	
	HR (95% CI)	*P*	HR (95% CI)	*P*
SLE NP events				
Male sex	1.35 (1.03–1.78)	0.028	1.55 (1.05–2.29)	0.026
Asian race†	0.59 (0.42–0.82)	0.002	0.60 (0.37–0.98)	0.04
Postsecondary education	0.72 (0.59–0.88)	0.001	0.73 (0.55–0.98)	0.040
Past non-SLE NP events (without headache)	1.21 (0.74–1.98)	0.434	1.16 (0.68–1.99)	0.59
Concurrent non-SLE NP events (without headache)	1.83 (1.31–2.55)	<0.001	1.79 (1.17–2.75)	0.007
SLEDAI-2K (without NP variables)	–	–	1.19 (1.04–1.36)	0.012
SDI (without NP variables)	–	–	1.05 (0.94–1.18)	0.35
Glucocorticoids	–	–	1.59 (1.12–2.34)	0.008
Antimalarial drugs	–	–	0.74 (0.54–1.01)	0.056
Immunosuppressive drugs	–	–	0.67 (0.50–0.94)	0.019
Non-SLE NP events excluding headache‡				
Non-US African race†	0.52 (0.32–0.86)	0.012	–	–
Asian race†	0.40 (0.26–0.62)	<0.001	–	–
Past SLE NP events	1.29 (0.84–2.00)	0.24	–	–
Concurrent SLE NP events	2.31 (1.66–3.21)	<0.001	–	–

* Two models were used for the multivariate analysis of predictors of transition to the neuropsychiatric (NP) event state for systemic lupus erythematosus (SLE)–associated NP (SLE NP) events. Model 1 included only time-invariant variables, or those defined at all time points. Model 2 was restricted to transitions for which there was information on all of the variables included in model 1 and additional time-varying explanatory variables, which were available only for events that occurred after the initial patient assessment. HR = hazard ratio; 95% CI = 95% confidence interval; SLEDAI-2K = SLE Disease Activity Index 2000; SDI = Systemic Lupus International Collaborating Clinics/American College of Rheumatology Damage Index.
† Other races and ethnicities were included in the analysis, but the results were not significant.
‡ n = 337 transitions.

RESULTS

Patient characteristics. Over 12 years (1999–2011), 1,827 patients were recruited into the SLICC inception cohort from 5 different geographic areas of the world, namely the US (n = 540 [29.5%]), Europe (n = 477 [26.1%]), Canada (n = 418 [22.9%]), Mexico (n = 223 [12.2%]), and Asia (n = 169 [9.3%]). Of these patients, 88.8% were women. The mean ± SD age at enrollment was 35.1 ± 13.3 years, and patients were of various races and ethnicities (Caucasian, 48.8%; African, 16.8%; Hispanic, 15.4%; Asian, 15.1%; and other, 3.9%). Study participants had a mean ± SD disease duration of 5.6 ± 4.2 months, SLEDAI-2K of 5.3 ± 5.4, and SDI of 0.32 ± 0.74. At enrollment, patients were receiving glucocorticoids (70.3%), antimalarials (67.4%), immunosuppressants (40.1%), warfarin (5.4%), low-dose aspirin (14.3%), antidepressants (10.1%), anticonvulsants (4.4%), and antipsychotic drugs (0.7%). For this analysis, the final study visit was in September 2017. Patients underwent up to 19 assessments, and the mean follow-up duration was 7.6 ± 4.6 years. During the study, there were 100 deaths (5.6%). The number of patients who died while in state 1, state 2, and state 3 were 61, 18, and 21, respectively, for the SLE NP event model and 66, 13, and 21, respectively, for the non-SLE NP event model.

NP manifestations. Of 1,827 patients, 955 (52.3%) experienced a single NP event, and 493 (27.0%) experienced ≥2 events. All 19 NP syndromes (10) were represented, with a total of 1,910 unique NP events. The majority, 1,749 (91.6%) of 1,910, involved the central nervous system, and 161 (8.4%) involved the peripheral nervous system (10). Further classification of the NP events revealed that, of the 1,910 total events, 1,479 (77.4%) were central/diffuse, 270 (14.1%) were central/focal, and 161 (8.4%) were peripheral. The proportion of NP events attributed to SLE varied from 17.9% (attribution model A) to 31.0% (attribution model B) and occurred in 13.5% (model A) to 21.2% (model B) of patients. Of the 593 events attributed to SLE by model B, 231 (39.0%), 244 (41.1%), and 118 (19.9%) were central/diffuse, central/focal, and peripheral, respectively. For the 1,317 non-SLE events, the comparable numbers were 1,248 (94.8%), 26 (2.0%), and 43 (3.2%).

Factors associated with the onset of SLE NP events. For SLE NP events, univariate analyses of transitions to the NP event state revealed a positive association with male sex (HR 1.39 [95% CI 1.07–1.81]; $P = 0.014$), SLEDAI-2K without NP variables (HR 1.13 [95% CI 1.01–1.27]; $P = 0.030$), SDI without NP variables (HR 1.12 [95% 1.01–1.24]; $P = 0.029$), glucocorticoid use (HR 1.50 [95% CI 1.13–2.01]; $P = 0.006$), and concurrent non-SLE NP events (HR 1.58 [95% CI 1.25–2.01]; $P = 0.002$). There was a negative association with Asian race (HR 0.57 [95% CI 0.41–0.79]; $P < 0.001$), postsecondary education (HR 0.71 [95% CI 0.59–0.86]; $P < 0.001$), and antimalarial drug use (HR 0.72 [95% CI 0.55–0.94]; $P = 0.014$). There was no association with anticardiolipin (HR 1.05 [95% CI 0.75–1.47]; $P = 0.766$), anti–β_2-glycoprotein I (HR 0.93 [95% CI 0.67–1.30]; $P = 0.69$), LAC (HR 1.10 [95% CI 0.84–1.45]; $P = 0.478$),

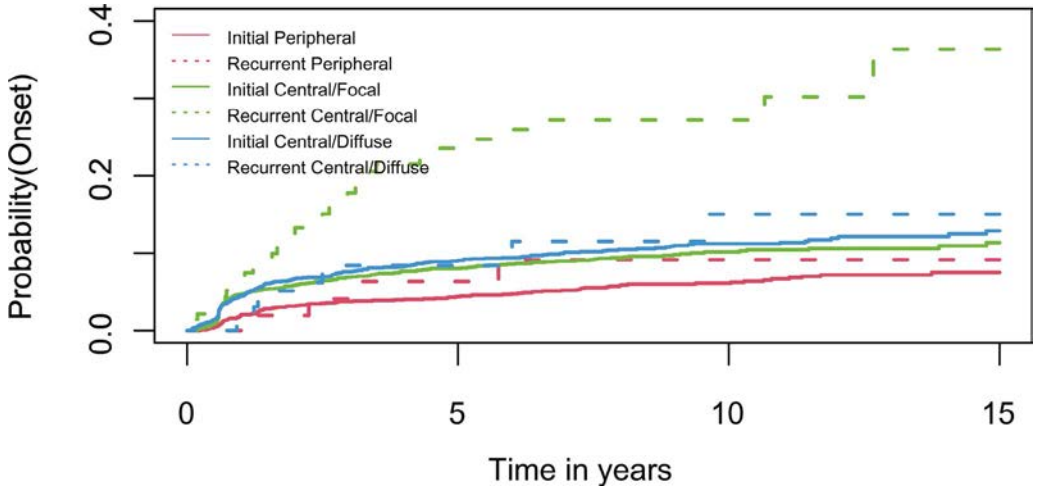

Figure 2. Probability curves for the onset and recurrence of peripheral, central/focal, and central/diffuse neuropsychiatric (NP) events attributed to systemic lupus erythematosus (SLE) using attribution model B, in which NP events were attributed to SLE if they 1) had their onset within 10 years prior to the diagnosis of SLE and were still present within the enrollment window, or occurred subsequently, and 2) had no "exclusions" (potential non-SLE causes), and 3) were not one of the common NP events identified by Ainiala et al (11).

anti–ribosomal P (HR 0.95 [95% CI 0.64–1.40]; $P = 0.781$), or anti-NR2 (HR 0.78 [95% CI 0.52–1.16]; $P = 0.216$) antibodies.

The results of multivariate analyses for SLE NP events in the multistate models are summarized in Table 1. For transitions to the NP event state (state 3) from either state 1 or state 2, two models, with associated estimated HRs and 95% CIs and *P* values, are presented. The first model includes only time-invariant variables, or those defined at all time points, and is estimated on all 492 observed transitions into state 3. (New events occurring while other events are ongoing do not represent a transition.) The second model is restricted to the 192 transitions for which there is information on all the variables in the first model and additional time-varying explanatory variables, the latter only being available for events occurring after the initial patient assessment. Results discussed are based on the first model when possible and on the second model otherwise.

For SLE NP events, there was a positive association with male sex (HR 1.35 [95% CI 1.03–1.78]; $P = 0.028$), concurrent non-SLE NP events excluding headache (HR 1.83 [95% CI 1.31–2.55]; $P < 0.001$), SLEDAI-2K without NP variables (HR 1.19 [95% CI 1.04–1.36]; $P = 0.012$), and glucocorticoid use (HR 1.59 [95% CI 1.12–2.34]; $P = 0.008$). There was a negative association with Asian race (HR 0.59 [95% CI 0.42–0.82]; $P = 0.002$), postsecondary education (HR 0.72 [95% CI 0.59–0.88]; $P = 0.001$), and immunosuppressive drug use (HR 0.67 [95% CI 0.50–0.94]; $P = 0.019$). The negative association with antimalarial drug use approached statistical significance (HR 0.74 [95% CI 0.54–1.01]; $P = 0.056$).

Factors associated with the onset of non-SLE NP events. For non-SLE NP events, univariate analyses revealed a positive association with Caucasian race at US sites (HR 1.37 [95% CI 1.14–1.65]; $P < 0.001$), glucocorticoid use (HR 1.30 [95% CI 1.09–1.55]; $P = 0.004$), and concurrent SLE NP events (HR 1.61 [95% CI 1.29–2.02]; $P < 0.001$). There was a negative association with male sex (HR 0.56 [95% CI 0.44–0.71]; $P < 0.001$), Hispanic ethnicity (HR 0.70 [95% CI 0.57–0.86]; $P \leq 0.001$), age at SLE diagnosis (HR 0.99 [95% CI 0.98–0.99]; $P < 0.001$), and immunosuppressive drug use (HR 0.78 [95% CI 0.66–0.93]; $P = 0.005$).

Since headache was a very frequent non-SLE NP event, occurring in 670 (36.7%) of the patients and accounting for 916 (69.5%) of non-SLE NP events, the univariate analysis for non-SLE NP events was repeated with headache excluded. This analysis revealed a lower number of significant associations, albeit with substantially fewer transitions, which included a positive association with concurrent SLE NP events (HR 2.37 [95% CI 1.72–3.29]; $P < 0.001$) and a negative association with African race at non-US sites (HR 0.54 [95% CI 0.32–0.89]; $P = 0.015$), Asian race (HR 0.38 [95% CI 0.28–0.58]; $P < 0.001$), and immunosuppressive drug use (HR 0.67 [95% CI 0.49–0.92]; $P < 0.001$). Complete univariate analyses for SLE NP events, non-SLE NP events, non-SLE NP events excluding headache, and headache only revealed additionally that Asian race had a positive association with headache, so that the negative association with other non-SLE events led to no demonstrable association when all non-SLE events were examined. A comprehensive analysis of predictors of headache has been published previously (21).

The results of multivariate analyses for non-SLE events excluding headache in the multistate models are summarized in Table 1. For non-SLE events, variables included in the model are defined at all time points and therefore only one model is presented. Excluding headache, there was a positive association with concurrent SLE NP events (HR 2.31 [95% CI 1.66–3.21]; $P < 0.001$) and a negative association with African race at non-US sites (HR 0.52 [95% CI 0.32–0.86]; $P = 0.012$) and Asian race (HR 0.40 [95% CI 0.26–0.62]; $P < 0.001$).

Table 2. Number of patients at risk at the indicated time points for new and recurrent NP events attributed to SLE and for resolution of NP events*

	0 years	5 years	10 years	15 years
New and recurrent SLE NP events†				
Initial peripheral	1,827	1,340	695	175
Recurrent peripheral	59	31	14	1
Initial central/focal	1,827	1,295	666	174
Recurrent central/focal	144	64	22	1
Initial central/diffuse	1,827	1,271	654	175
Recurrent central/diffuse	102	65	20	4
Resolution of all NP events‡				
Non-SLE NP events	401	109	31	6
SLE NP events	593	120	41	12
Headache	916	198	57	11
Resolution of SLE NP events‡				
Peripheral	118	34	10	5
Central/focal	244	31	12	2
Central/diffuse	231	55	19	5
Resolution of non-SLE NP events‡				
Peripheral	43	15	3	1
Central/focal	26	4	3	0
Central/diffuse	1,248	288	82	16
Resolution of non-SLE NP events with headache as separate category‡				
Peripheral	43	15	3	1
Central/focal	26	4	3	0
Central/diffuse	332	90	25	5
Headache	916	198	57	11

* Values are the number of patients at risk. See Table 1 for definitions.
† Probability curves are shown in Figure 2.
‡ Probability curves are shown in Figures 3A–D.

Onset of new SLE NP events in central/diffuse, central/focal, and peripheral groups. Estimated probability-of-onset curves and the number of patients at risk for new and recurrent SLE NP events, representing entries into multistate model state 3, are provided in Figure 2 and Table 2, respectively. The NP events are clustered into central/diffuse, central/focal, and peripheral groups, with curves based on multistate models for each group. As can be seen, the rates for new and recurrent NP events in each of these clusters are similar, with the exception of the higher rate of recurrence in the central/focal group.

An initial investigation of the potential differential effects of predictors of central/diffuse, central/focal, and peripheral SLE NP events revealed no marked variation. An approximate global test for differential effects, used to make allowance for multiple comparisons, for the factors in model 1 (shown in Table 1) generated a chi-square statistic of 21.8 with 20 degrees of freedom (df) ($P = 0.34$). The only estimated quantitative difference of note was for the effect of Hispanic ethnicity, which had a common nonsignificant estimated effect (HR 0.93 [95% CI 0.71–1.21]; $P = 0.57$) but had somewhat different estimated effects in the central/diffuse, central/focal, and peripheral groups (HR 0.50 [95% CI 0.31–0.83] [$P = 0.007$], HR 1.34 [95% CI 0.90–1.99] [$P = 0.15$], and HR 1.13 [95% CI 0.65–1.99] [$P = 0.66$], respectively).

For the additional variables in the second SLE NP events model in Table 1, a global test of differential effects generated a chi-square statistic of 18.66 with 10df ($P = 0.04$). There was some evidence that the glucocorticoid effect was more marked in the central/focal group (HR 2.42 [95% CI 1.40–4.17]; $P = 0.002$) than in the central/diffuse group (HR 1.40 [95% CI 0.84–2.33]; $P = 0.20$) or in the peripheral group (HR 1.30 [95% CI 0.69–1.46]; $P = 0.42$). There was also some evidence that the effect of antimalarial drugs was more evident in the central/focal group (HR 0.69 [95% CI 0.45–1.07]; $P = 0.09$) and central/diffuse group (HR 0.60 [95% CI 0.37–0.95]; $P = 0.03$) than in the peripheral group (HR 0.93 [95% CI 0.50–1.74]; $P = 0.83$). Multiplicity considerations suggest that these findings should be interpreted cautiously. Sample size was insufficient to address differential effects for non-SLE NP events.

We looked for an association between central/focal SLE NP events and antiphospholipid antibodies and between central/diffuse SLE NP events and generalized SLE disease activity as reflected in the SLEDAI-2K score. Neither association was identified in our analysis. Specifically, although the presence of LAC had a slightly higher HR for central/focal events, it was not significant in the univariate analysis, and there was no evidence of differential effects by event type ($P = 0.33$). The same pattern emerged when LAC was added to the multivariate model, with the test for differential effects yielding $P = 0.22$. With respect to the SLEDAI-2K, there was no clear evidence of differential effects by event type. A formal test generated $P = 0.10$, and when we looked at individual effects, the largest effect was for central/focal events, not central/diffuse events.

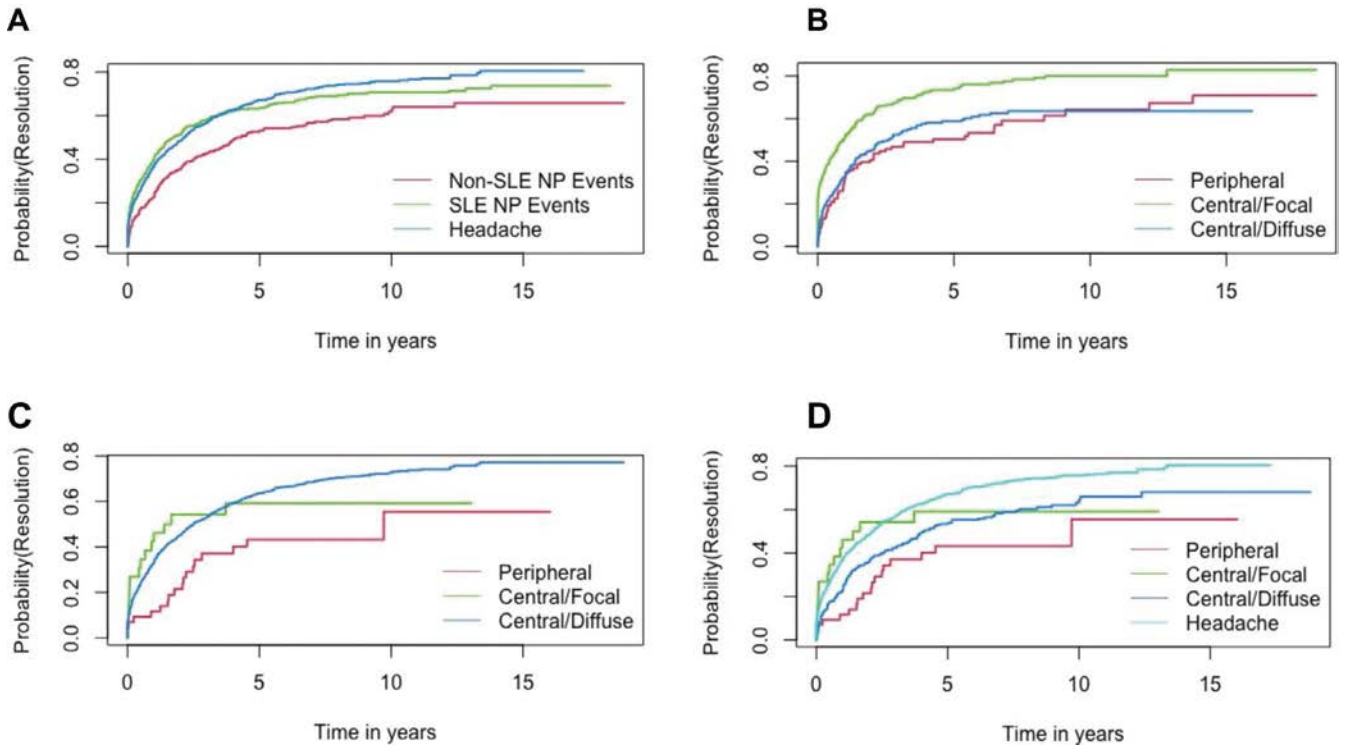

Figure 3. Probability curves for the resolution of all neuropsychiatric (NP) events (**A**), NP events attributed to systemic lupus erythematosus (SLE) (**B**), NP events not related to SLE (**C**), and NP events not related to SLE, with headache analyzed as a separate category (**D**). NP events were attributed to SLE or non-SLE causes using attribution model B, in which NP events were attributed to SLE if they 1) had their onset within 10 years prior to the diagnosis of SLE and were still present within the enrollment window, or occurred subsequently, and 2) had no "exclusions" (potential non-SLE causes), and 3) were not one of the common NP events identified by Ainiala et al (11).

Resolution of central/diffuse, central/focal, and peripheral NP events. To provide background to the development of regression models for transitions to the resolved state, probability-of-resolution curves at the event level, i.e., each event provides one observation, are presented in Figure 3, and the numbers of patients at risk are presented in Table 2. Due to the predominance of headache in the non-SLE NP event group, headache was separated from the other non-SLE NP events in this analysis. As a group, NP events attributed to SLE had a higher rate of resolution than non-SLE NP events, with the exception of headache, which had a comparable rate of resolution to SLE NP events (Figure 3A). Within the SLE NP events, the rate of resolution was highest for central/focal NP events compared to central/diffuse and peripheral NP events (Figure 3B). For the non-SLE NP events, a similar pattern of resolution was seen (Figure 3C), which was more apparent when the rate of resolution for headache was separated from the other central/diffuse NP events (Figure 3D).

Factors associated with the resolution of NP events. Since predictors of resolution of headache have been presented elsewhere (21), in this analysis, predictors of the transition to the resolved state, state 2, from the new/ongoing NP event state, state 3, were examined for SLE NP events and non-SLE events excluding headache. For these multistate models, explanatory variables were defined as binary indicators of any peripheral event in the active state and of any central/focal event in the active state because multiple types of events may be present for patients in the NP event state. The reference category for the effects associated with these indicators was all active events being central/diffuse because these events were the most frequent.

For SLE NP events, univariate analyses of transitions to the resolved NP state revealed a positive association with Asian race (HR 1.77 [95% CI 1.19–2.63]; $P = 0.004$) and any central/focal NP event (HR 1.66 [95% CI 1.29–2.15]; $P < 0.001$). For non-SLE NP events, there was a positive association with Hispanic ethnicity (HR 1.69 [95% CI 1.14–2.48]; $P = 0.008$) and with African race at non-US sites (HR 1.99 [95% CI 1.10,3.61]; $P = 0.022$).

The results of multivariate analysis are summarized in Table 3. For SLE NP events, there was a positive association with Asian race (HR 1.72 [95% CI 1.17–2.54]; $P = 0.006$) and with any central/focal NP event (HR 1.74 [95% CI 1.33–2.27]; $P < 0.001$). For non-SLE NP events there was a positive association with African race at non-US sites (HR 2.06 [95% CI 1.14–3.73]; $P = 0.017$) and a negative association with age at diagnosis of SLE (HR 0.98 [95% CI 0.96–0.99]; $P < 0.001$).

Table 3. Multivariate analysis of predictors of transitions to the resolved NP event state for SLE NP events and for non-SLE NP events excluding headache*

	HR (95% CI)	*P*
SLE NP events (n = 270 transitions)		
Asian race†	1.72 (1.17–2.54)	0.006
Any peripheral event	0.89 (0.65–1.24)	0.500
Any central/focal event	1.74 (1.33–2.27)	<0.001
All central/diffuse events	1.00	–
Past non-SLE NP events (excluding headache)	0.93 (0.59–1.47)	0.76
Concurrent non-SLE NP events (excluding headache)	0.63 (0.44–0.91)	0.12
Previous headache	0.98 (0.67–1.43)	0.93
Current headache	0.80 (0.58–1.09)	0.15
Non-SLE NP events excluding headache (n = 176 transitions)		
Hispanic ethnicity†	1.43 (0.96–2.13)	0.082
Non-US African race†	2.06 (1.14–3.73)	0.017
Age at SLE diagnosis	0.98 (0.96–0.99)	<0.001
Any peripheral event	0.76 (0.44–1.29)	0.306
Any central/focal event	1.38 (0.72–2.64)	0.328
All central/diffuse events	1.00	–

* See Table 1 for definitions.
† Other races and ethnicities were included in the analysis, but the results were not significant.

DISCUSSION

Long-term observation of a large international SLE disease inception cohort was used to identify predictors of both the occurrence and resolution of NP events with current standard of care. The inclusion of all NP events, regardless of attribution, provided insight into differences between NP events attributed to SLE and to non-SLE causes. The predominance of headache within the non-SLE NP group prompted a separate analysis of this individual event. The results of our study indicate heterogeneity in the occurrence, resolution, and recurrence of different NP events and in predictors of those events over time. As multiple NP events due to different causes may present concurrently in individual patients, the findings emphasize the importance of recognizing attribution of NP events as a determinant of clinical outcome.

The SLICC SLE disease inception cohort is well suited for the present study. Over the course of 21 years since enrollment began, this large, prospective, international cohort has provided the basis for examining several SLE manifestations and complications, including atherosclerosis (22), lupus nephritis (23), cumulative organ damage (24), frailty (25), and NP disease (4). The study of NP disease has been facilitated by standardized data collection, use of predetermined rules to identify attribution of NP events to SLE and non-SLE causes, and recruitment of patients close to the time of diagnosis of SLE. Previous studies of NP disease in the SLICC cohort have focused on individual NP manifestations (4,21,26–29), made possible by the large size of the cohort and prolonged follow-up. In the present study, using a multistate modeling approach, we examined the long-term course of all NP events in the SLICC cohort, with a particular emphasis on the factors associated with clinically meaningful change in NP status over time. NP events occur frequently in SLE patients (30,31). In the present study, more than half of the patients experienced at least a single event during the study, and more than a quarter experienced ≥2 events. There was also a wide spectrum of manifestations, and all 19 of the individual ACR case definitions for NP disease in SLE were represented. More than three-quarters of the NP events were in the central/diffuse category, and only 31% of all events were attributed to SLE.

There is a paucity of information on predictors of NP events in SLE. This is partly due to study limitations, including small cohort size, failure to determine attribution of NP events in a standardized way, and short observation period (32–34). In the present study, multivariate analysis of predictors of the onset of SLE NP events indicated a higher risk in men than in women and a reduced risk in individuals of Asian race. Of interest, the risk was also reduced in patients with postsecondary education, consistent with the findings of a study of 1,121 Korean SLE patients (30). Likewise, Asian race was also associated with a lower risk of non-SLE NP events, as was African race at non-US sites. For both types of NP events, adjustment for age at diagnosis did not alter the findings regarding race, and there was a significant association with concurrent NP events of the alternate attribution, indicating that NP events due to SLE and non-SLE causes present concurrently in many patients. As the etiology of NP events due to SLE and non-SLE causes is different, their co-occurrence emphasizes the importance of determining the correct attribution, which will direct therapy. In support of this point and consistent with the findings of other studies (30,35), the present study showed that the onset of NP events attributed to SLE was associated with SLE disease activity and glucocorticoid use. None of the lupus autoantibodies measured at enrollment predicted the onset of NP events. This finding is not surprising, given that previous autoantibody associations with SLE NP events have been restricted to specific NP manifestations, such as cerebrovascular events (26) and psychosis (27).

Previous studies have sought predictors of clinical outcome in patients with NPSLE. In a study of 32 hospitalized SLE patients (36), 14 of whom had antiphospholipid syndrome (APS), NP status improved in 69% of cases over 2 years of followup. In the same study, prior NP events and APS were associated with adverse outcomes. An increased mortality risk in SLE patients with NP disease has been demonstrated in previous studies (5,30), especially in patients with central/focal NP events (30). In the present study, there were group differences in the rate of resolution of NP events. Overall, SLE NP events were more likely to resolve compared to non-SLE NP events with the exception of headache. Resolution of SLE events was more likely in patients of Asian race and those with central/focal nervous system disease, with no effect seen for

age at diagnosis. For non-SLE NP events, African race at non-US sites and younger age at diagnosis were associated with a better outcome. There was no association between the resolution of NP events and lupus autoantibodies measured at enrollment.

The higher rate of recurrence of central/focal SLE NP events (Figure 2) likely explains the previously reported overall higher rate for SLE versus non-SLE events (5). The central/focal disease group also had the highest rate of resolution of SLE NP events (Figure 3B). This group of NP events includes transient ischemic attacks (TIAs) which, by definition, resolve within 24 hours and thus could have influenced both recurrence and resolution rates. However, this is very unlikely, as TIAs were few in number (n = 29) and the curves for both recurrence and resolution were not appreciably different when TIAs were removed from the analysis (data not shown). Overall, central/focal SLE NP events were not associated with lupus autoantibodies, although we have previously reported an association of stroke and TIAs with antiphospholipid antibodies in the SLICC cohort (26). Likewise, in the present study we found an overall association between SLE NP events and global SLE disease activity, excluding neurologic variables, but no such association was found with central/diffuse SLE NP events per se.

How can the findings of this study inform our approach to patient management? First, although nervous system events occur frequently in SLE patients, the majority are not a direct effect of a targeted autoimmune lupus response. The management of these non-SLE NP events rests primarily on the treatment of comorbid conditions and symptomatic therapies. Second, as is the case with other lupus manifestations such as nephritis (23), SLE NP events occur most frequently early in the disease course (5). Third, the presentation of SLE NP events is often associated with generalized SLE disease activity, and SLE NP events have a more favorable outcome than NP events attributed to non-SLE causes. Finally, the associations with race or ethnicity, sex, and education, and the lack of association with lupus autoantibodies, emphasizes the importance of not overlooking etiologic factors beyond the more traditional autoimmune disease paradigms for NPSLE. For example, the negative association between the onset of SLE NP events and education may be due to differences in adherence to prescribed medications (37).

There are limitations to the present study. First, the predominance of Caucasian race in the cohort may have limited the ability to find additional associations for NPSLE in racial or ethnic minorities. Second, the clustering of NP events into a limited number of categories reduced the likelihood of finding specific clinical–serologic associations, such as the association of cerebrovascular disease with antiphospholipid antibodies (26). Third, assessment of the outcome of NP events was restricted to physician determinations and did not include patient-centered perceptions, as has been done in previous studies of individual NP manifestations in the SLICC inception cohort (4,21,26–29). Finally, although the study was well suited to evaluate NP events early in the disease course when events are frequently due to SLE disease activity, the mean follow up of 7.6 years is likely insufficient for the study of later NP events, such as cerebrovascular disease attributed to accelerated atherosclerosis. Despite these limitations, the present study provides valuable data on the presentation, outcome, and predictors of NP disease in SLE patients enrolled in a long-term, international, disease inception cohort.

AUTHOR CONTRIBUTIONS

All authors were involved in drafting the article or revising it critically for important intellectual content, and all authors approved the final version to be published. Dr. Hanly had full access to all of the data in the study and takes responsibility for the integrity of the data and the accuracy of the data analysis.

Study conception and design. Hanly, Gordon, Romero-Diaz, Clarke, Merrill, Fortin, Gladman, Urowitz, Bruce, Petri, Alarcón, Askanase, Farewell.

Acquisition of data. Hanly, Gordon, Bae, Romero-Diaz, Sanchez-Guerrero, Bernatsky, Clarke, Wallace, Isenberg, Rahman, Merrill, Fortin, Gladman, Urowitz, Bruce, Petri, Ginzler, Dooley, Ramsey-Goldman, Manzi, Alarcón, van Vollenhoven, Aranow, Mackay, Ruiz-Irastorza, Lim, Inanc, Kalunian, Jacobsen, Peschken, Kamen, Askanase.

Analysis and interpretation of data. Hanly, Gordon, Romero-Diaz, Bernatsky, Clarke, Wallace, Fortin, Urowitz, Bruce, Jonsen, Alarcón, van Vollenhoven, Inanc, Askanase, Farewell.

REFERENCES

1. Schwartz N, Stock AD, Putterman C. Neuropsychiatric lupus: new mechanistic insights and future treatment directions [review]. Nat Rev Rheumatol 2019;15:137–52.
2. Hanly JG, Kozora E, Beyea SD, Birnbaum J. Nervous system disease in systemic lupus erythematosus: current status and future directions [review]. Arthritis Rheumatol 2019;71:33–42.
3. Fanouriakis A, Pamfil C, Rednic S, Sidiropoulos P, Bertsias G, Boumpas DT. Is it primary neuropsychiatric systemic lupus erythematosus? Performance of existing attribution models using physician judgment as the gold standard. Clin Exp Rheumatol 2016;34:910–7.
4. Hanly JG, Li Q, Su L, Urowitz MB, Gordon C, Bae SC, et al. Peripheral nervous system disease in systemic lupus erythematosus: results from an international inception cohort study. Arthritis Rheumatol 2020;72:67–77.
5. Hanly JG, Urowitz MB, Gordon C, Bae SC, Romero-Diaz J, Sanchez-Guerrero J, et al. Neuropsychiatric events in systemic lupus erythematosus: a longitudinal analysis of outcomes in an international inception cohort using a multistate model approach. Ann Rheum Dis 2020;79:356–62.
6. Isenberg D, Ramsey-Goldman R. Systemic Lupus International Collaborating Group—onwards and upwards? [letter]. Lupus 2006;15:606–7.
7. Hochberg MC. Updating the American College of Rheumatology revised criteria for the classification of systemic lupus erythematosus [letter]. Arthritis Rheum 1997;40:1725.
8. Gladman DD, Ibanez D, Urowitz MB. Systemic lupus erythematosus disease activity index 2000. J Rheumatol 2002;29:288–91.
9. Gladman D, Ginzler E, Goldsmith C, Fortin P, Liang M, Urowitz M, et al. The development and initial validation of the Systemic Lupus International Collaborating Clinics/American College of Rheumatology Damage Index for systemic lupus erythematosus [review]. Arthritis Rheum 1996;39:363–9.
10. ACR Ad Hoc Committee on Neuropsychiatric Lupus Nomenclature. The American College of Rheumatology nomenclature and case definitions for neuropsychiatric lupus syndromes. Arthritis Rheum 1999;42:599–608.

11. Ainiala H, Hietaharju A, Loukkola J, Peltola J, Korpela M, Metsänoja R, et al. Validity of the new American College of Rheumatology criteria for neuropsychiatric lupus syndromes: a population-based evaluation. Arthritis Rheum 2001;45:419–23.
12. Hanly JG, Urowitz MB, Su L, Sanchez-Guerrero J, Bae SC, Gordon C, et al. Short-term outcome of neuropsychiatric events in systemic lupus erythematosus upon enrollment into an international inception cohort study. Arthritis Rheum 2008;59:721–9.
13. Hanly JG, Urowitz MB, Sanchez-Guerrero J, Bae SC, Gordon C, Wallace DJ, et al. Neuropsychiatric events at the time of diagnosis of systemic lupus erythematosus: an international inception cohort study. Arthritis Rheum 2007;56:265–73.
14. Hanly JG, Urowitz MB, Jackson D, Bae SC, Gordon C, Wallace DJ, et al. SF-36 summary and subscale scores are reliable outcomes of neuropsychiatric events in systemic lupus erythematosus. Ann Rheum Dis 2011;70:961–7.
15. Merrill JT, Zhang HW, Shen C, Butman BT, Jeffries EP, Lahita RG, et al. Enhancement of protein S anticoagulant function by β2-glycoprotein I, a major target antigen of antiphospholipid antibodies: β2-glycoprotein I interferes with binding of protein S to its plasma inhibitor, C4b-binding protein. Thromb Haemost 1999;81:748–57.
16. Merrill JT, Shen C, Gugnani M, Lahita RG, Mongey AB. High prevalence of antiphospholipid antibodies in patients taking procainamide. J Rheumatol 1997;24:1083–8.
17. Erkan D, Zhang HW, Shriky RC, Merrill JT. Dual antibody reactivity to β2-glycoprotein I and protein S: increased association with thrombotic events in the antiphospholipid syndrome. Lupus 2002;11:215–20.
18. Hanly JG, Urowitz MB, Siannis F, Farewell V, Gordon C, Bae SC, et al. Autoantibodies and neuropsychiatric events at the time of systemic lupus erythematosus diagnosis: results from an international inception cohort study. Arthritis Rheum 2008;58:843–53.
19. R Core Team. R: a language and environment for statistical computing. Vienna, Austria: R Foundation for Statistical Computing. 2018. URL: https://www.R-project.org/.
20. Therneau T. A package for survival analysis in R. Version 3.2-7. 2020. URL: https://CRAN.R-project.org/package=survival.
21. Hanly JG, Urowitz MB, O'Keeffe AG, Gordon C, Bae SC, Sanchez-Guerrero J, et al. Headache in systemic lupus erythematosus: results from a prospective, international inception cohort study. Arthritis Rheum 2013;65:2887–97.
22. Urowitz MB, Gladman DD, Farewell V, Su J, Romero-Diaz J, Bae SC, et al. Accrual of atherosclerotic vascular events in a multicenter inception systemic lupus erythematosus cohort. Arthritis Rheumatol 2020;72:1734–40.
23. Hanly JG, O'Keeffe AG, Su L, Urowitz MB, Romero-Diaz J, Gordon C, et al. The frequency and outcome of lupus nephritis: results from an international inception cohort study. Rheumatology (Oxford) 2016;55:252–62.
24. Bruce IN, O'Keeffe AG, Farewell V, Hanly JG, Manzi S, Su L, et al. Factors associated with damage accrual in patients with systemic lupus erythematosus: results from the Systemic Lupus International Collaborating Clinics (SLICC) Inception Cohort. Ann Rheum Dis 2015;74:1706–13.
25. Legge A, Kirkland S, Rockwood K, Andreou P, Bae SC, Gordon C, et al. Evaluating the properties of a frailty index and its association with mortality risk among patients with systemic lupus erythematosus. Arthritis Rheumatol 2019;71:1297–307.
26. Hanly JG, Li Q, Su L, Urowitz MB, Gordon C, Bae SC, et al. Cerebrovascular events in systemic lupus erythematosus: results from an international inception cohort study. Arthritis Care Res (Hoboken) 2018;70:1478–87.
27. Hanly JG, Li Q, Su L, Urowitz MB, Gordon C, Bae SC, et al. Psychosis in systemic lupus erythematosus: results from an international inception cohort study. Arthritis Rheumatol 2019;71:281–9.
28. Hanly JG, Su L, Urowitz MB, Romero-Diaz J, Gordon C, Bae SC, et al. Mood disorders in systemic lupus erythematosus: results from an international inception cohort study. Arthritis Rheumatol 2015;67:1837–47.
29. Hanly JG, Urowitz MB, Su L, Gordon C, Bae SC, Sanchez-Guerrero J, et al. Seizure disorders in systemic lupus erythematosus results from an international, prospective, inception cohort study. Ann Rheum Dis 2012;71:1502–9.
30. Ahn GY, Kim D, Won S, Song ST, Jeong HJ, Sohn IW, et al. Prevalence, risk factors, and impact on mortality of neuropsychiatric lupus: a prospective, single-center study. Lupus 2018;27:1338–47.
31. Ainiala H, Loukkola J, Peltola J, Korpela M, Hietaharju A. The prevalence of neuropsychiatric syndromes in systemic lupus erythematosus. Neurology 2001;57:496–500.
32. McLaurin EY, Holliday SL, Williams P, Brey RL. Predictors of cognitive dysfunction in patients with systemic lupus erythematosus. Neurology 2005;64:297–303.
33. Mikdashi J, Handwerger B. Predictors of neuropsychiatric damage in systemic lupus erythematosus: data from the Maryland lupus cohort. Rheumatology (Oxford) 2004;43:1555–60.
34. Dong J, Li H, Wang JB, Yao Y, Yang QR. Predictors for neuropsychiatric development in Chinese adolescents with systemic lupus erythematosus. Rheumatol Int 2012;32:2681–6.
35. Morrison E, Carpentier S, Shaw E, Doucette S, Hanly JG. Neuropsychiatric systemic lupus erythematosus: association with global disease activity. Lupus 2014;23:370–7.
36. Karassa FB, Ioannidis JP, Boki KA, Touloumi G, Argyropoulou MI, Strigaris KA, et al. Predictors of clinical outcome and radiologic progression in patients with neuropsychiatric manifestations of systemic lupus erythematosus. Am J Med 2000;109:628–34.
37. Scalzi LV, Hollenbeak CS, Mascuilli E, Olsen N. Improvement of medication adherence in adolescents and young adults with SLE using web-based education with and without a social media intervention, a pilot study. Pediatr Rheumatol Online J 2018;16:18.

Arthritis & Rheumatology
Vol. 73, No. 12, December 2021, pp 2303–2313
DOI 10.1002/art.41799
© 2021, American College of Rheumatology

American College of Rheumatology
Empowering Rheumatology Professionals

Lupus Susceptibility Region Containing *CDKN1B* rs34330 Mechanistically Influences Expression and Function of Multiple Target Genes, Also Linked to Proliferation and Apoptosis

Bhupinder Singh,[1] Guru P. Maiti,[1] Xujie Zhou,[2] Mehdi Fazel-Najafabadi,[1] Sang-Cheol Bae,[3] Celi Sun,[1] Chikashi Terao,[4] Yukinori Okada,[5] Kek Heng Chua,[6] Yuta Kochi,[7] Joel M. Guthridge,[1] Hong Zhang,[2] Matthew Weirauch,[8] Judith A. James,[1] John B. Harley,[8] Gaurav K. Varshney,[1] Loren L. Looger,[9] and Swapan K. Nath[1]

Objective. In a recent genome-wide association study, a significant genetic association between rs34330 of *CDKN1B* and risk of systemic lupus erythematosus (SLE) in Han Chinese was identified. This study was undertaken to validate the reported association and elucidate the biochemical mechanisms underlying the effect of the variant.

Methods. We performed an allelic association analysis in patients with SLE, followed by a meta-analysis assessing genome-wide association data across 11 independent cohorts (n = 28,872). In silico bioinformatics analysis and experimental validation in SLE-relevant cell lines were applied to determine the functional consequences of rs34330.

Results. We replicated a genetic association between SLE and rs34330 (meta-analysis $P = 5.29 \times 10^{-22}$, odds ratio 0.84 [95% confidence interval 0.81–0.87]). Follow-up bioinformatics and expression quantitative trait locus analysis suggested that rs34330 is located in active chromatin and potentially regulates several target genes. Using luciferase and chromatin immunoprecipitation–real-time quantitative polymerase chain reaction, we demonstrated substantial allele-specific promoter and enhancer activity, and allele-specific binding of 3 histone marks (H3K27ac, H3K4me3, and H3K4me1), RNA polymerase II (Pol II), CCCTC-binding factor, and a critical immune transcription factor (interferon regulatory factor 1 [IRF-1]). Chromosome conformation capture revealed long-range chromatin interactions between rs34330 and the promoters of neighboring genes *APOLD1* and *DDX47*, and effects on *CDKN1B* and the other target genes were directly validated by clustered regularly interspaced short palindromic repeat (CRISPR)–based genome editing. Finally, CRISPR/dead CRISPR-associated protein 9–based epigenetic activation/silencing confirmed these results. Gene-edited cell lines also showed higher levels of proliferation and apoptosis.

Conclusion. Collectively, these findings suggest a mechanism whereby the rs34330 risk allele (C) influences the presence of histone marks, RNA Pol II, and IRF-1 transcription factor to regulate expression of several target genes linked to proliferation and apoptosis. This process could potentially underlie the association of rs34330 with SLE.

INTRODUCTION

Systemic lupus erythematosus (SLE) is an inflammatory autoimmune disease characterized by autoantibody production, complement activation, and immune complex deposition, resulting in tissue and organ damage (e.g., in the kidney, skin, and lungs, among others). SLE incidence and prevalence has a strong sex bias (ratio of women to men 9:1) primarily affecting women of childbearing age, and a strong racial/ethnic bias, with a prevalence of SLE that is 3–5-fold higher in populations of Black, Hispanic, and Asian ancestries compared to those of White ancestry (1).

Genetic influence in SLE susceptibility is well established. Several genome-wide association studies (GWAS) have identified

Supported by the NIH (grants R01-AR-060366, R01-AI-132532, and R21-AI-144829 to Dr. Nath and grant P30-AR-073750 to Dr. James) and the National Research Foundation of the Republic of Korea (grant 2017M3A9B4050335 to Dr. Bae).

[1]Bhupinder Singh, PhD, Guru P. Maiti, PhD, Mehdi Fazel-Najafabadi, PhD, Celi Sun, MS, Joel M. Guthridge, PhD, Judith A. James, MD, PhD, Gaurav K. Varshney, PhD, Swapan K. Nath, PhD: Oklahoma Medical Research Foundation, Oklahoma City; [2]Xujie Zhou, MD, PhD, Hong Zhang, MD, PhD: Peking University First Hospital, Peking University, Ministry of Health of China, Beijing, China; [3]Sang-Cheol Bae, MD, PhD, MPH: Hanyang University Hospital for Rheumatic Diseases, Seoul, Republic of Korea; [4]Chikashi Terao, MD, PhD: RIKEN Center for Integrative Medical Sciences, RIKEN Yokohama Campus, Yokohama, Japan, and University of Shizuoka, Shizuoka, Japan; [5]Yukinori Okada, MD, PhD: Osaka University, Osaka, Japan; [6]Kek Heng Chua, PhD: University of Malaya, Kuala Lumpur, Malaysia; [7]Yuta Kochi, MD, PhD: Tokyo Medical and Dental University, RIKEN Center for Integrative Medical Sciences,

genetic associations between numerous single-nucleotide polymorphisms (SNPs) and SLE susceptibility (2). Among them, rs34330 was identified as a novel SLE susceptibility locus in East Asian populations (3). This SNP is located within the 5′-untranslated region (5′-UTR) (–79 C/T) of the cyclin-dependent kinase (CDK) inhibitor 1B gene (*CDKN1B*) at 12p13. *CDKN1B* encodes $p27^{Kip1}$, an inhibitor of cyclin/CDK complexes, which are crucial for cell cycle progression and development. *CDKN1B* plays a key role in many cellular events and can act as a tumor suppressor gene (4). The primary function of this multifunctional enzyme is to pause cell cycle progression during the G_1/S transition by inhibiting cyclin A/CDK2 activity until S phase onset (5), allowing cells to repair DNA damage and replication errors. Genetic lesions at *CDKN1B* could disrupt cell cycle control and contribute to cellular damage and SLE progression. Inhibitor $p27^{Kip1}$ localizes to multiple places in the cell. Its cell cycle functions are largely performed in the nucleus, whereas in the cytoplasm, it binds to the G protein RhoA, promoting apoptosis by inhibiting both p27 and RhoA (6). *CDKN1B* is also involved in autophagy modulation and autoimmunity development (7). The roles of $p27^{Kip1}$ in T cell function are complex. It opposes the development of CD4+ T cell effector function, inhibits proliferation of thymic and mature T cells, promotes T cell anergy and immune tolerance, and is critical for autophagy and apoptosis (7). In turn, autophagy promotes T cell proliferation through T cell receptor–driven degradation of $p27^{Kip1}$ (8).

The *CDKN1B* polymorphism at rs34330 has also been associated with susceptibility to multiple cancers including breast, lung, thyroid, endometrial, and hepatocellular cancer, where T is a risk allele (9). *CDKN1B* signaling promotes apoptosis in SLE patients undergoing bone marrow mesenchymal stem cell transplantation (10).

Since the first report, no study has been conducted to replicate rs34330 association with SLE, establish rs34330 target genes, or determine specific mechanisms and downstream genes by which rs34330 contributes to SLE susceptibility. In this study, using a combination of in vitro experimental assays in 3 SLE-relevant cell lines, we extensively characterized the impact of the rs34330 risk allele on *CDKN1B* and its neighboring genes. Our findings support the notion that the risk allele elevates cell type–specific promoter and enhancer activity, influencing the expression of multiple neighboring genes. Using clustered regularly interspaced short palindromic repeat (CRISPR)–based genetic and epigenetic editing, we validated and extended the predicted effects on target gene expression, proliferation, and apoptosis.

MATERIALS AND METHODS

Study design. The overall study design and experimental steps are outlined in Figure 1. First, to assess the consistency and veracity of the genetic effect, we performed an allelic association analysis with new cohorts followed by a meta-analysis of rs34330 (*CDKN1B*) across 11 independent cohorts of Asian and European ancestries (n = 28,872). Second, we used in silico bioinformatics analysis to identify potential regulatory effects on gene expression and annotated this region with epigenetic data on histone modifications and expression quantitative trait loci (eQTLs) across multiple tissues. Third, we performed luciferase reporter assays in the cell lines HEK 293 (kidney-derived neuronal), Jurkat (T lymphocyte), U937 (monocyte), and lymphoblastoid cell lines (LCLs) (lymphoblastoid B cells) to measure allele-specific regulatory effects. Fourth, a combination of DNA pull-down, electrophoretic mobility shift assay (EMSA), Western blotting, and mass spectrometry was used to identify DNA-bound proteins followed by chromatin immunoprecipitation (ChIP)–quantitative polymerase chain reaction (qPCR) to identify allele-specific binding of interacting proteins. Fifth, using chromosome conformation capture assays, we assessed chromatin interaction between rs34330 and neighboring genes in primary B cells, T cells, HEK 293 cells, and Jurkat cells. Sixth, CRISPR-based deletion and activation/inhibition were performed to assess SNP effects on target gene expression. Finally, we compared cell growth and viability between 35 nucleotide-edited knockout (KO) and wild-type (WT) cells using proliferation and apoptosis assays.

The methods discussed below are described in further detail in Supplementary Materials and Methods, available on the *Arthritis & Rheumatology* website at http://onlinelibrary.wiley.com/doi/10.1002/art.41799/abstract.

Assessment of rs34330 association with SLE. To assess the genetic association between rs34330 and SLE, we performed a meta-analysis using METAL (11) to assess GWAS data from 11 cohorts. We used summary statistics from the original 6 cohorts (12) (Supplementary Table 1, available on the *Arthritis & Rheumatology* website at http://onlinelibrary.wiley.com/doi/10.1002/art.41799/abstract) as the discovery cohort. To replicate the association with SLE, we genotyped rs34330 in 4 independent cohorts of Beijing Han Chinese (BHC), Korean, Malayan Chinese, and European-American ancestries (Supplementary Table 1) and added genetic data from a Japanese cohort (13). Association analysis and summary statistics for the genotyped SNPs were performed using Plink (14).

RIKEN Yokohama Campus, Yokohama, Japan; [8]Matthew Weirauch, PhD, John B. Harley, MD, PhD: Cincinnati Children's Hospital Medical Center, University of Cincinnati, and Cincinnati VA Medical Center, Cincinnati, Ohio; [9]Loren L. Looger, PhD: Howard Hughes Medical Institute, Janelia Research Campus, Ashburn, Virginia.

Drs. Singh and Maiti contributed equally to this work.

No potential conflicts of interest relevant to this article were reported.

Address correspondence to Swapan K. Nath, PhD, Oklahoma Medical Research Foundation, Arthritis and Clinical Immunology Program, 825 Northeast 13th Street, Oklahoma City, OK 73104. Email: swapan-nath@omrf.org.

Submitted for publication August 26, 2020; accepted in revised form May 4, 2021.

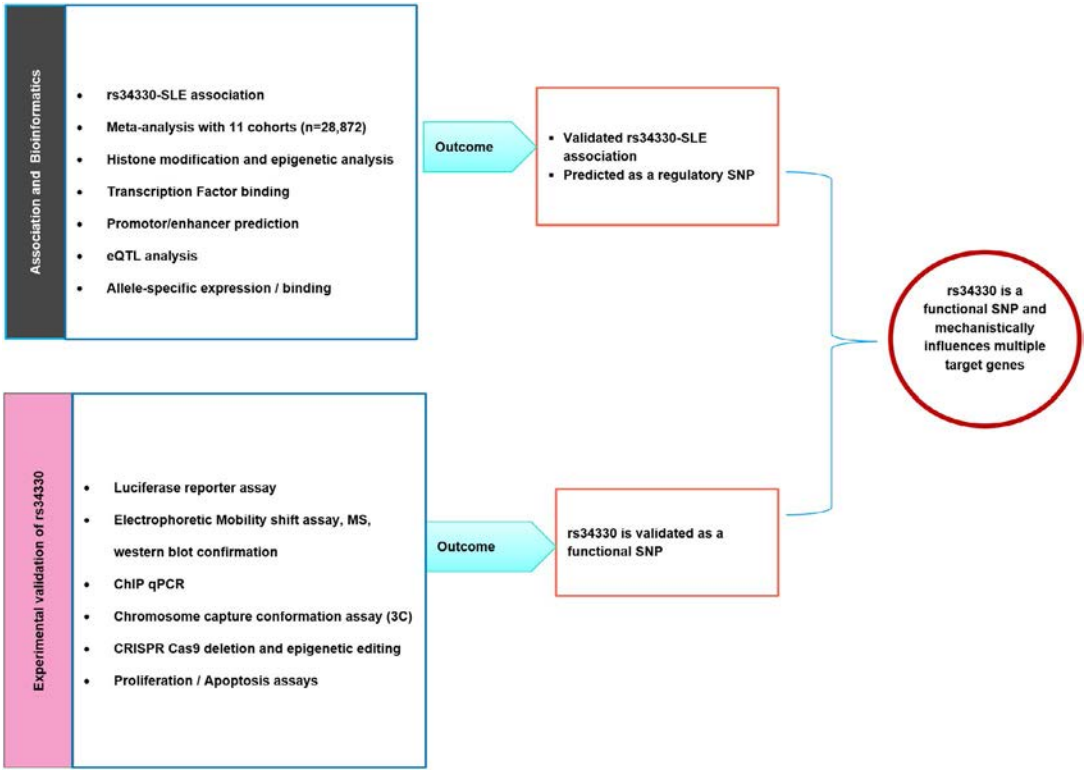

Figure 1. Overall study design and experimental steps to validate the association between rs34330 and systemic lupus erythematosus (SLE). eQTL = expression quantitative trait locus; SNP = single-nucleotide polymorphism; MS = mass spectrometry; ChIP = chromatin immunoprecipitation; qPCR = quantitative polymerase chain reaction; CRISPR = clustered regularly interspaced short palindromic repeat; Cas9 = CRISPR-associated protein 9.

Bioinformatics, transcription factor binding, and allelic imbalance analyses. To identify functional roles of the rs34330 region, we first used annotations from HaploReg-version 4.1 (15), and Bayesian functional scores from 3DSNP (16) and RegulomeDB (17). To assess chromatin context and epigenetic regulation at this locus, we identified several active histone marks (H3K27ac, H3K4me1, and H3K4me3), DNase I hypersensitivity, and RNA polymerase II (Pol II) binding for lymphoblastoid B cells (GM12878), using data from the ENCODE database (18) (Figure 2A).

Expression QTL analysis. To determine the effects of the rs34330 region on the expression of *CDKN1B* and neighboring genes, we assessed its effect in multiple tissue samples from the Genotype-Tissue Expression Project (19), LCLs from the Multiple Tissue Human Expression Resource project (18), and blood cell lines from Blood eQTL (20). We also queried whole blood–based eQTL data from the East Asian eQTL mapping project (21) and a Korean eQTL database for Crohn's disease (22). Additionally, we used a conditional eQTL database, which distinguishes between dependent and independent eQTL effects (23).

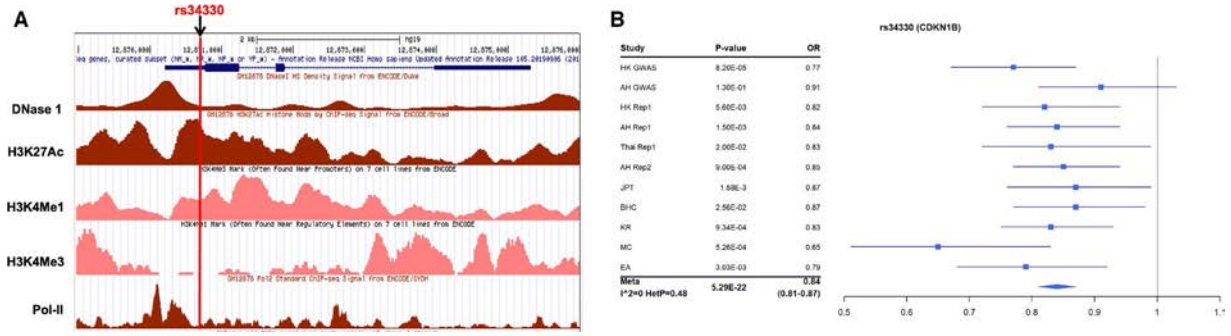

Figure 2. Genetic association between the single-nucleotide polymorphism rs34330 and systemic lupus erythematosus (SLE). **A**, ENCODE project data showing relevant histone marks, DNase I hypersensitivity, and RNA polymerase II (Pol II) binding in lymphoblastoid B cells (GM12878), with data obtained using the UCSC genome browser. **B**, Meta-analysis (Meta) and forest plots of association between rs34330 and SLE in the 11 cohorts of Asian and European ancestries. Squares represent the odds ratio (OR), and horizontal lines represent the 95% confidence interval. The elongated diamond represents the overall OR for the 11 cohorts. HK = Hong Kong; GWAS = genome-wide association study; AH = Anhui; Rep1 = replication 1; Thai = Thailand; JPT = Japanese in Tokyo; BHC = Beijing Han Chinese; KR = Korean; MC = Malayan Chinese; EA = European American.

Luciferase reporter assay. To assess the potential enhancer/promoter activity of this rs34330-containing region, we used the Dual-Luciferase Reporter Assay system (Promega). Briefly, the rs34330-containing region was cloned into the pGL4.26 vector for enhancer assay and the pGL4.14 vector for promoter assay (both from Promega). Each plasmid was transiently cotransfected with pGL4.74 (internal control) in HEK 293 cells, Jurkat cells, U937 cells, and LCLs. After 24 hours, enhancer/promoter activity was measured using a Dual-Luciferase Reporter Assay.

DNA pull-down assay. A DNA pull-down assay was performed as previously described (24). Briefly, nuclear extract from cultured Jurkat cell lines was incubated with biotin-labeled DNA (risk and non-risk alleles of rs34330) attached to Dynabeads M-280. Proteins bound to the beads were separated from unbound proteins by successive washes and later resolved with sodium dodecyl sulfate–polyacrylamide gel electrophoresis, followed by peptide mass fingerprint matrix-assisted laser desorption ionization mass spectrometry analysis of single bands.

ChIP assay. Two Coriell cell lines with the risk (CC) and non-risk (TT) genotypes for rs34330 were cultured in RPMI 1640 medium, and ChIP assays were performed using a Magnify ChIP kit (Invitrogen). Briefly, 1×10^7 cells were fixed, sonicated, and immunoprecipitated against targeted antibodies (poly[ADP-ribose] polymerase [PARP-1], interferon regulatory factor 1 [IRF-1], CCCTC-binding factor [CTCF], Pol II, H3K27ac, H3K4me3, and H3K4me1). DNA from the immunoprecipitated chromatin complexes was eluted, reverse crosslinked, purified, and later subjected to quantitative reverse transcriptase–PCR (qRT-PCR) analysis.

Chromosome conformation capture assay. Chromosome conformation capture is an important technique used to study chromatin structures that occur in living cells. Briefly, together with primary T cells and B cells, HEK 293 and Jurkat cells were fixed with formaldehyde, and crosslinked nuclei were isolated after cells were lysed. The nuclear content was digested with *Sac* I and T4 DNA ligase. The digested DNA was purified by proteinase K digestion, followed by phenol–chloroform treatment and alcohol precipitation. The purified DNA was diluted for chromosome conformation capture–PCR after quantitation.

CRISPR/CRISPR-associated protein 9 (Cas9)–based deletion of the rs34330 region. We used CRISPR/Cas9 to delete a small region (<40 bases) surrounding rs34330 in 2 different cell lines (HEK 293 and Jurkat). Briefly, to deliver the single-guide RNA (sgRNA)/Cas9 RNP complex into HEK cells, we used Lipofectamine 3000, and a Neon Electroporation system was used for Jurkat cells. After 4 days and 7 days, indel efficiency was measured using Sanger sequencing, and analyzed using TIDE and/or ICE. For downstream experiments, CRISPR-edited pooled cells were grown, harvested, and later subjected to messenger RNA isolation and quantitative PCR for *CDKN1B* and neighboring genes *DDX47*, *APOLD1*, *MANSC1*, and *GPR19*.

CRISPR-based activation and CRISPR inhibition. For CRISPR inhibition and CRISPR-based activation, plasmids SP-dCas9-VPR (no. 63798), pcDNA-dCas9-p300 (no. 61357), and dCas9-KRAB-MeCP2 (no. 110821) (all from Addgene; kind gifts from Dr. George Church, Harvard Medical School, Boston, MA) (25–27) were used. The pools of sgRNA were the same as those used for the Cas9 deletion experiment. Transfections in HEK 293 cells were performed in 24-well plates using 375 ng of respective dead Cas9 (dCas9) expression vector and 125 ng of equimolar-pooled or individual guide RNA expression vectors mixed with Lipofectamine 3000 (no. L300001; Life Technologies). Cells were harvested for RNA 72 hours post-transfection. RNA was extracted, and qPCR was performed as previously described (24).

Flow cytometric analysis of cell apoptosis. KO and WT Jurkat cells were stained with Ki-67 for proliferation assays. Apoptosis between 2 groups of cell lines (KO and WT) was also measured after cells were maintained under serum starvation conditions for 2 hours. The progression of the cell cycle was measured using propidium iodide staining.

RESULTS

Meta-analysis of rs34330 association with SLE. We used the rs34330 association results directly from the first report (3) (5,365 cases and 10,024 controls in the discovery set, with a P value for association with SLE of 5.00×10^{-13}). To replicate the genetic association of rs34330, data from 5 cohorts (4,858 cases and 8,625 controls in the replication set) were used (Supplementary Table 1, http://onlinelibrary.wiley.com/doi/10.1002/art.41799/abstract). We used direct genotyping data on rs34330 from 4 cohorts (BHC, Korean, Malayan Chinese, and European American ancestries) and augmented with summary data from a recently published report from our Japanese collaborators (13). Our results confirmed the association of rs34330 with SLE ($P = 1.71 \times 10^{-10}$) (Supplementary Table 2, http://onlinelibrary.wiley.com/doi/10.1002/art.41799/abstract).

Next, we performed a meta-analysis of the combined effect of the association of rs34330 and SLE across 11 cohorts of Asian and European ancestries (total 28,872 [10,223 cases and 18,649 controls]) (Supplementary Table 2). The results showed a strong and consistent association between rs34330 and SLE (meta-analysis $P = 5.29 \times 10^{-22}$, odds ratio 0.84 [95% confidence interval 0.81–0.87]) (Figure 2B). The odds ratios were consistent across populations with no significant heterogeneity ($I^2 = 0$, P for heterogeneity = 0.48), and the findings were confirmed to be robust when tested for publication bias, as supported by a symmetric funnel plot (Supplementary Figure 1, http://onlinelibrary.wiley.com/doi/10.1002/art.41799/abstract).

Bioinformatics prediction of rs34330 as a potential regulatory variant. Our findings of the presence of various histone marks, chromatin accessibility, and RNA Pol II occupancy all indicated that rs34330 is located within an active regulatory region (Figure 2A). Using multiple bioinformatics packages, rs34330 was scored as highly probable to be functional, based on a 3DSNP score of 163.7 (predicted as a promoter in 109 cells/tissues, 51 predicted transcription factor binding sites), a RegulomeDB score of 4 (predicted as having regulatory potential), and the presence of a ChromHMM active transcription start site (TSS).

Next, we predicted differential transcription factor binding between the risk (C) and non-risk (T) alleles of rs34330 using multiple databases, discovering several with predicted differential binding. Among these, IRFs exhibited 3–5-fold greater binding to the risk allele (Supplementary Table 3, http://onlinelibrary.wiley.com/doi/10.1002/art.41799/abstract). The transcriptional repressor CTCF bound preferentially (4–16-fold) to the non-risk allele, suggesting greater transcriptional activation at the risk allele.

Expression QTL and allele-specific expression analyses. Using several databases, we identified rs34330 as a significant eQTL, especially in immune cells (P values between 2.3×10^{-2} and $P > 1.8 \times 10^{-17}$ for several immune cell types), affecting nearby genes *APOLD1*, *DDX47*, and *GPR19* (Supplementary Table 4, http://onlinelibrary.wiley.com/doi/10.1002/art.41799/abstract). All eQTL target genes were also identified among the eQTLs assessed in Asian cohorts (21). This SNP is also an eQTL for a long noncoding RNA *RP11-59H1.4* ($P = 1.89 \times 10^{-6}$) in the whole blood of patients of Korean descent with Crohn's disease (22).

To detect allelic imbalance, we used the allele-specific expression database AlleleDB, which contains LCLs derived from individuals from the 1000 Genomes Project (28). We identified 2 heterozygous (C/T) individuals with strong allele-specific expression at rs34330. The risk allele (C)–containing *CDKN1B* transcripts were significantly greater than the non-risk allele (T)–containing transcripts in both individuals ($P = 2.15 \times 10^{-12}$ and $P = 1.22 \times 10^{-7}$, respectively).

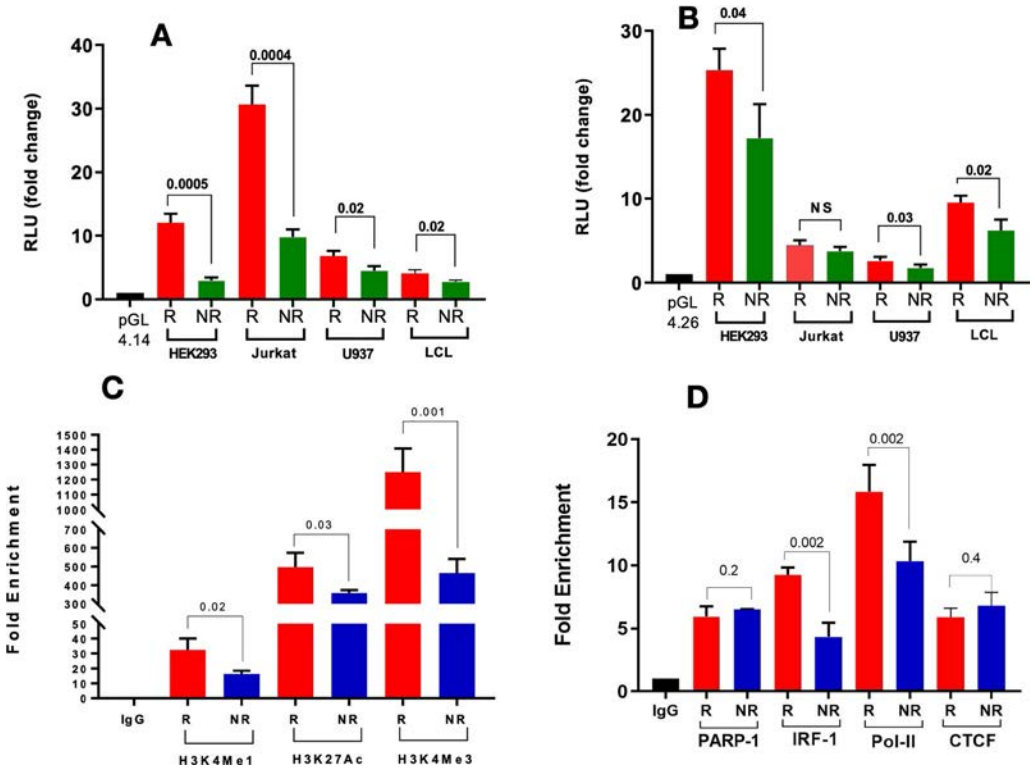

Figure 3. Results of luciferase reporter assay and chromatin immunoprecipitation (ChIP)–quantitative polymerase chain reaction (qPCR) assay for rs34330 functionality. **A**, Allele-specific promoter assays across 4 cell lines (HEK 293, Jurkat, U937, and lymphoblastoid cell lines [LCL]). **B**, Allele-specific enhancer assays across 4 cell lines (HEK 293, Jurkat, U937, and LCL). Empty vectors pGL4.14 and pGL4.26 were used as reference. **C**, ChIP-qPCR assays for determining allele-specific DNA–protein interactions with H3K4me1, H3K27ac, and H3H4me3. **D**, ChIP-qPCR assays for determining allele-specific DNA–protein interactions with poly(ADP-ribose) polymerase 1 (PARP-1), interferon regulatory factor 1 (IRF-1), RNA polymerase II (Pol II), and CCCTC-binding factor (CTCF). All analyses were conducted according to CC risk (R) and TT non-risk (NR) genotype. For each assay, the binding affinity was measured against IgG control. Bars show the mean ± SD (n = 3). Numbers above the bars are the P values, determined by Student's t-test. Primers and their sequences used for these experiments are listed in Supplementary Table 5, http://onlinelibrary.wiley.com/doi/10.1002/art.41799/abstract. RLU = relative luminescence units; NS = not significant.

Validating allele-specific regulatory effects of rs34330. To experimentally assess the allele-specific regulatory potential (promoter and enhancer) of 575-bp sequences surrounding rs34330, we used luciferase reporter assays in 4 different cell lines (HEK 293, Jurkat T lymphocytes, U937 monocytes, and LCLs [B lymphocytes]). We found marked promoter activity (up to 30-fold over empty vector) in all 4 cell lines, with the C risk allele showing significantly more activity than the T non-risk allele (~5-fold [$P = 5.0 \times 10^{-4}$] for HEK 293, ~3-fold [$P = 4.0 \times 10^{-4}$] for Jurkat, ~50% more [$P = 2.3 \times 10^{-2}$] for U937, and ~2-fold [$P = 2.0 \times 10^{-2}$] for LCLs) (Figure 3A). This is consistent with previous reports that rs34330-C exerts higher promoter activity than rs34330-T (29). Substantial enhancer activity (up to 26-fold over empty vector) was observed, using a minimal promoter plasmid (pGL4.26) with both risk-allele and non-risk allele sequence, in 3 of the 4 cell types. Sequences containing the risk allele produced significantly more reporter gene activity in HEK 293 cells (~50% more [$P = 4.15 \times 10^{-2}$]), U937 cells (~30% more [$P = 3.38 \times 10^{-2}$]), and LCLs (40% more [$P = 2.0 \times 10^{-2}$]), but not Jurkat cells ($P = 0.188$), indicating that the rs34330-C base is critical for enhancer activity in a cell type–dependent manner (Figure 3B).

Allele-specific binding of rs34330 to regulatory proteins. Since the region containing rs34330 colocalizes with strong promoter and enhancer activity, we sought to identify interacting proteins. Two Coriell cell lines with risk and non-risk genotypes were used for these experiments. First, using ChIP-grade antibodies (Abcam), we checked histone marks H3K27ac and H3K4me3, which are usually associated with active transcription near the promoter/transcription start site, and H3K4me1, which is usually associated with active transcription at an enhancer. As expected, we observed significantly more active marking with the CC genotype (risk) than the TT genotype (non-risk) (~2-fold [$P = 2.2 \times 10^{-2}$] for H3K4me1, ~1.6-fold [$P = 3.92 \times 10^{-2}$] for H3K27ac, and ~3-fold [$P = 1.4 \times 10^{-3}$] for H3K4me3) (Figure 3C), with the 2 most

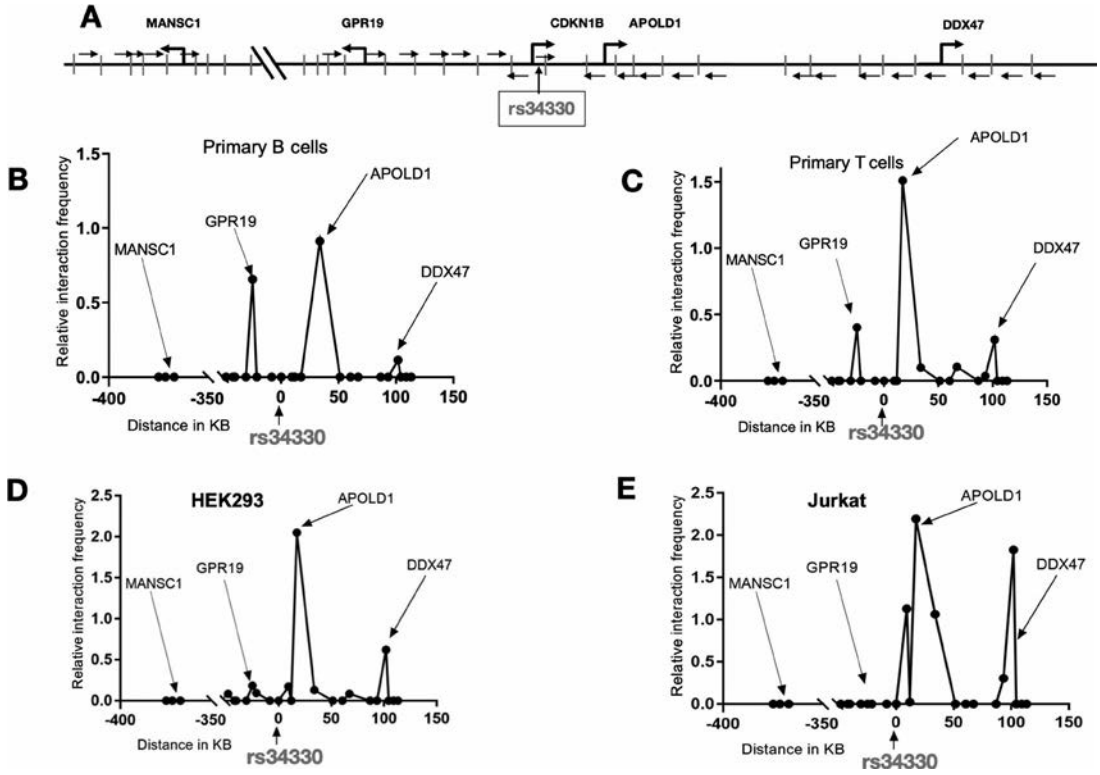

Figure 4. Long-range chromosomal interaction analysis of the rs34330 region using chromosome conformation capture. **A**, Schematic representation of the rs34330 region with primer locations for chromosome conformation capture experiments and neighboring gene regions. Vertical lines indicate the position of *Sac* I restriction enzyme sites. **Small arrows** represent the primer location with orientation. The forward primer at the rs34330 region is the common primer for all other reverse primers within the *APOLD1* and *DDX47* gene regions. Similarly, the reverse primer at the rs34330 region is the common primer for all other forward primers within the *GPR19* and *MANSC1* gene regions. **Large arrows** represent the transcriptional start site of the respective genes. **B–E**, Relative interaction of rs34330 regions with different genomic regions in primary B cell lines (**B**), primary T cell lines (**C**), HEK 293 cell lines (**D**), and Jurkat cell lines (**E**). The relative interaction frequency for each primer set represents the intensity of the polymerase chain reaction band from experimental DNA normalized to the polymerase chain reaction band intensity from bacterial artificial chromosome DNA. The x-axis shows the genomic distance of the interacting region in the forward and reverse directions from single-nucleotide polymorphism rs34330 (0 kb). Circles represent the relative interaction frequencies at the corresponding restriction sites. Primers and their sequences used for these experiments are listed in Supplementary Table 5, http://onlinelibrary.wiley.com/doi/10.1002/art.41799/abstract.

significant marks being the promoter/TSS-associated modifications (H3K4me1 and H3K4me3), consistent with the location of rs34330.

Next, we tested the differential binding of the transcription factors predicted through bioinformatics. Antibodies against Pol II bound significantly more with the risk genotype (~50% more; $P = 2.11 \times 10^{-3}$) than the non-risk genotype, consistent with greater transcriptional activity of the risk allele. As it was predicted by bioinformatics analysis that several IRF transcription factors could differentially bind to the SNP region (Supplementary Table 3, http://onlinelibrary.wiley.com/doi/10.1002/art.41799/abstract), we tested IRFs 2, 4, 5, and 8, but did not detect any binding at this region (data not shown). However, IRF-1 showed strong binding, with ~2-fold as much at the risk locus ($P = 2.5 \times 10^{-3}$). With post hoc annotation of the SNP region using ConSite (30), we identified a plausible IRF-1 site 27 bp away from the SNP (Supplementary Figure 2, http://onlinelibrary.wiley.com/doi/10.1002/art.41799/abstract). SNP effects on transcription factor binding sites that are within close proximity are routinely observed (31), manifested through mechanisms such as protein–protein interactions with the transcription factor, alteration of histone occupancy, or mediators of chromatin looping. To assess differential binding with CTCF, we tested for binding that was significantly enriched around the rs34330 region compared to IgG. Relatively greater binding was found with the non-risk allele compared to the risk allele (as suggested in the bioinformatics analysis), but the difference was not significant ($P = 0.4$) (Figure 3D).

In addition to testing the predicted transcription factors, we pursued an unbiased approach to discovering binding proteins, using a DNA pull-down assay followed by an EMSA. This revealed an ~100-kd band preferentially binding to the risk allele; mass spectrometry of this band identified PARP-1 as the binding protein (Supplementary Figure 3, http://onlinelibrary.wiley.com/doi/10.1002/art.41799/abstract). Follow-up experiments with ChIP-qPCR showed substantial binding to both the risk and non-risk alleles, with no allelic differences (Figure 3D). The source of the apparent discrepancy in findings between the 2 techniques is not known and may involve cell type–specific effects (Jurkat cells for EMSA and Coriell LCLs for ChIP-qPCR).

Long-range chromatin interactions between rs34330 and target genes. To examine interactions between the rs34330 region and neighboring promoters, we performed chromosome conformation capture experiments in primary T cells, B cells, HEK 293 cells, and Jurkat cells, using semiquantitative PCR (Figure 4A). We detected interaction between rs34330 and the *APOLD1* and *DDX47* promoters in all 4 cell lines tested

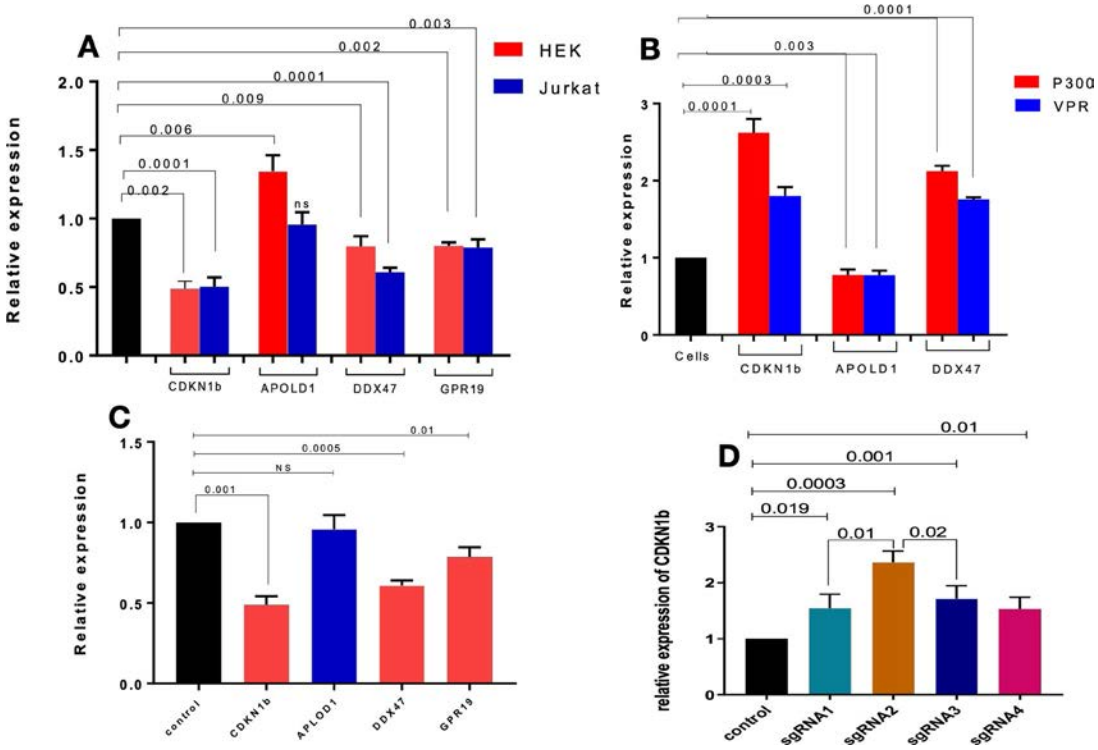

Figure 5. Effects of clustered regularly interspaced short palindromic repeat (CRISPR)–based genetic and epigenetic editing in different study models. **A**, Levels of mRNA for *CDKN1B*, *APOLD1*, and *DDX47* in pooled edited cells. **B**, Epigenetic effects of CRISPR-based activation on *CDKN1B*, *APOLD1*, and *DDX47* using dCas9-p300 and dCas9-VPR in HEK 293 cells. **C**, Epigenetic effects of CRISPR inhibition using dCas9-KRAB-MeCP2 in HEK 293 cells. **D**, Epigenetic fine-mapping of rs34330 relative to the transcriptional functional unit for *CDKN1B* expression using dCas9-p300. Numbers above the bars are the *P* values, determined by Student's *t*-test. Bars show the mean ± SD (n = 3). NS = not significant; sgRNA = single-guide RNA. Primers and their sequences used for these experiments are listed in Supplementary Table 5, http://onlinelibrary.wiley.com/doi/10.1002/art.41799/abstract.

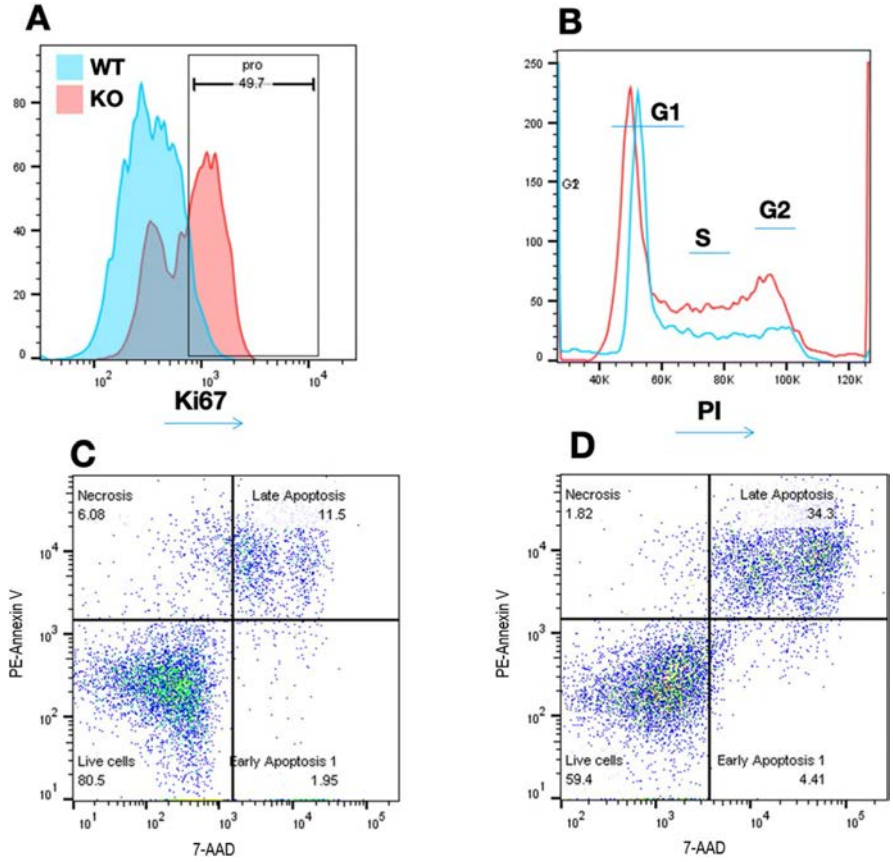

Figure 6. Flow cytometry analysis for assessing proliferation and apoptosis of clustered regularly interspaced short palindromic repeat (CRISPR)–edited Jurkat cell lines. **A**, Ki-67 staining in wild-type (WT) Jurkat cells versus CRISPR-edited knockout (KO) Jurkat cells, showing high proliferation (pro) in KO cells (red) compared to WT cells (blue). **B**, Cell cycle analysis performed with propidium iodide (PI) staining of KO cells (red) versus WT cells (blue), showing highly increased levels of S phase and G_2 phase. **C** and **D**, Flow cytometry charts showing apoptosis measured by staining with phycoerythrin (PE)–conjugated annexin V/7-aminoactinomycin D (7-AAD). The percentage of apoptotic cells was determined in WT cells (**C**) and KO cells (**D**).

(Figures 4B–E). Chromosome conformation capture cannot discriminate *CDKN1B* promoter binding, as it is only 79 bp away. Interactions with the *DDX47* promoter were higher in Jurkat cells than HEK 293 cells, indicating cell type–specific interactions or chromatin states of this region. Thus, the rs34330 region predominantly interacts with the *DDX47* and *APOLD1* promoters, consistent with the eQTL results in which these 2 genes were the most significantly modulated. While no significant interaction with the *MANSC1* promoter regions was detected in any cells, interaction with *GPR19* was detected in both primary B cells and T cells.

Validating transcriptional impacts of rs34330 on target genes using CRISPR-based genome editing. To validate the observed transcriptional effects of the rs34330 region, we deleted ~35 bases in HEK 293 and Jurkat cells with CRISPR/Cas9 (32), using a pool of 3 sgRNAs. We confirmed ~35 bp deletion by Sanger sequencing. The editing efficiency was very high: 98% for HEK 293 cells and 87% for Jurkat cells (Supplementary Figure 4, http://onlinelibrary.wiley.com/doi/10.1002/art.41799/abstract). Next, we performed qRT-PCR on WT and CRISPR/Cas9-edited (KO) HEK 293 and Jurkat cells. Levels of *CDKN1B*, *DDX47*, and *GPR19* were significantly reduced in KO cells (~50% [$P = 2.0 \times 10^{-3}$], ~25% [$P = 9.0 \times 10^{-3}$], and ~25% [$P = 2.0 \times 10^{-3}$], respectively, in HEK 293 cells and ~50% [$P = 1.0 \times 10^{-4}$], ~40% [$P = 1.0 \times 10^{-4}$], and ~25% [$P = 3.0 \times 10^{-3}$], respectively, in Jurkat cells) (Figure 5A). Interestingly, *APOLD1* was up-regulated in KO HEK 293 cells (~35% [$P = 6.0 \times 10^{-3}$]), but not in Jurkat cells ($P = 4.5 \times 10^{-1}$). These observations confirm that rs34330 has cell type–specific repressive and enhancing effects on *CDKN1B* and nearby genes.

Epigenetic modification of the rs34330 region. CRISPR/Cas9 can be converted into a targetable transcriptional activator or repressor, permitting mechanistic epigenetic studies of gene loci (25). We performed CRISPR/dCas9-based activation using 2 transcriptional modulator domains, one performing histone acetylation with a histone acetyltransferase (dCas9-p300)

and another recruiting transcription complexes to the promoter with the HIV-derived VPR activator (dCas9-VPR) (25). We also used CRISPR/dCas9-based inhibition with the hybrid repressor protein Kruppel-associated box (KRAB)–methyl-CpG binding protein 2 (MeCP-2). Epigenetic activation with P300 and VPR increased expression of *CDKN1B* ~2–3-fold, along with *DDX47* (~2-fold), in HEK 293 cells, whereas *APOLD1* expression was significantly reduced (~20%) (Figure 5B). The KRAB-MeCP-2 repressor significantly decreased *CDKN1B* expression in HEK 293 cells by ~2-fold, *DDX47* by ~40%, and *GPR19* by ~30%; *APOLD1* was unaffected (Figure 5C).

Next, to determine the importance of sgRNA position with respect to rs34330, we measured *CDKN1B* expression using sgRNA-based activation with dCas9-p300. We found that all 4 sgRNAs significantly increased *CDKN1B* expression. The greatest expression increase was from sgRNA2 (12 bases from rs34330), increasing expression ~40% more than was observed with the other sgRNAs (Figure 5D).

Impact of the rs34330 region on apoptosis and proliferation. Cyclins, CDKs, and CDK inhibitors, including CDKN1B/p27^{Kip1}, play crucial roles in the cell cycle and cellular proliferation. These proteins regulate transitions between the G_1, S, G_2, and M cell cycle phases, especially the G_1 to S phase (33). Cell cycle progression is usually inhibited by p27^{Kip1} (7), primarily by blocking CDK-2/cyclin E complex activation. We sought to determine the effect of the rs34330 region on apoptosis and proliferation, using the WT and KO cells described above. Cell cycle progression was monitored with propidium iodide staining of DNA, proliferation was assessed by immunolabeling against Ki-67, and apoptosis was investigated by staining of DNA with 7-aminoactinomycin D (7-AAD) and anti–annexin V antibodies. A substantial increase in Ki-67 staining (50%) was seen in KO Jurkat cells compared to WT Jurkat cells (Figure 6A). The number of cells at the G_1 to G_2 division dramatically increased in KO cells (Figure 6B). Upon serum starvation, KO cells showed much greater annexin V/7-AAD staining than WT cells (35% versus 11%) (Figures 6C and D). Thus, KO cells showed much higher levels of proliferation, cell cycle progression, and apoptosis than WT cells, suggesting that the rs34330 region played a prominent role in suppressing these 3 phenomena, likely through regulation of p27^{Kip1} levels.

DISCUSSION

Converting GWAS data on complex traits into mechanistic understanding of the underlying pathologic processes presents a formidable challenge (34). *CDKN1B* (i.e., p27^{Kip1} and Kip1) has been proposed as an SLE susceptibility locus in Asian populations (3). However, this association result has not yet been thoroughly studied, nor have underlying mechanisms been defined or any target gene(s) of this genetic association been proposed. In this study, we replicated a genetic association between SLE and rs34330 and established several aspects of the mechanism of its contribution to disease.

SLE is accompanied by dysregulated activation and proliferation of immune cells, primarily T cells and B cells. An intricate balance of cyclins, CDKs, and CDK inhibitors (e.g., p27^{Kip1}) regulates cell cycle progression, activation, proliferation, autophagy, and apoptosis in these cells, and genetic lesions can disrupt these pathways. Increasing evidence has shown that immune cell abnormalities, dysregulated apoptosis, and poor clearance of apoptotic and autophagic materials can contribute to SLE development and progression.

CDKN1B encodes p27^{Kip1}, an inhibitor of cyclin/CDK complexes, which are crucial for cell cycle progression and development (4,5). Dysregulated expression of p27^{Kip1} is a frequent event in several human cancers (7). *CDKN1B* has 2 paralogs in the genome, *CDKN1A* (encoding p21^{Waf1}) and *CDKN1C* (encoding p57^{Kip2}), with related functions in cell cycle regulation, proliferation, and apoptosis (35). Reduced expression of *CDKN1A* is associated with SLE susceptibility, and the 5′-UTR SNP rs762624 is linked to risk of both SLE and lupus nephritis (36). Moreover, interferon-1–mediated induction of p21^{Waf1} contributes to induction of apoptosis (37). Apoptosis is inhibited by binding of p57^{Kip2} to the stress-related kinase MAPK8. We have previously shown that rs1990760, the SLE risk allele of *IFIH1*, drove inflammatory signaling in part, leading to increased transcription of *MAPK8* (38). Autoantibodies against p57^{Kip2} are frequently observed in neonatal lupus, particularly in conjunction with anti-Ro antibodies (39). Thus, all 3 members of the *CDKN1* (also known as Cip/Kip) family have demonstrated SLE involvement.

In this study, we replicated the association of rs34330 in 4 additional Asian cohorts and in a European cohort. We also subsequently proposed and experimentally validated a potential mechanism underlying SLE pathogenicity. The rs34330 variant is located in a region of active chromatin upstream (–79 bp) of the *CDKN1B* translation start site, with potential for both promoter and enhancer activity. Our analysis supports the notion that rs34330 is an eQTL for multiple neighboring genes, *APOLD1* in particular. Luciferase reporter assays using a 575-bp sequence surrounding rs34330 confirmed allele-specific promoter (HEK 293, Jurkat, and U937) and enhancer (HEK and U937) activities, with the risk allele (C) having significantly higher promoter and enhancer activity than the non-risk allele (T). ChIP-qPCR showed allele-specific binding to IRF-1 and Pol II, as well as several active histone marks (H3K4me1, H3K27ac, and H3K4me3). IRF-1 is a critical immune transcription factor, with implications in numerous autoimmune diseases. It drives inflammasome hyperactivity in SLE, is a dendritic cell marker for SLE progression (40), and is a potent transcriptional activator of major histocompatibility complex class I genes (41), among many other targets.

We applied several approaches to identify target genes and mechanisms underlying the rs34330 association. First, we used chromosome conformation capture experiments to detect

regions of chromatin looping, bringing together promoters and enhancers. Our chromosome conformation capture experiments showed a significant interaction between the rs34330 region and *APOLD1*, *GPR19*, and *DDX47*. Second, to functionally detect target genes, we used CRISPR/Cas9 to delete ~35 bases surrounding rs34330. KO cells showed *APOLD1* up-regulation and *CDKN1B*, *GPR19*, and *DDX47* down-regulation. Third, we used CRISPR-based activation and CRISPR inhibition–based epigenetic activation and silencing. The up-regulation of *APOLD1* and down-regulation of *CDKN1B*, *DDX47*, and *GPR19* were reproduced with the two approaches. *GPR19* is similarly involved in both cell cycle progression (particularly G_2/M) (42) and apoptosis (43), and rs34330 may regulate these processes by changing levels of both $p27^{Kip1}$ and *GPR19*. *DDX47* is a DEAD box RNA helicase, many of which are involved in innate immunity, with some being known SLE risk genes, including *IFIH1/MDA5*, *RIG1/DDX58*, and *LGP2/DHX58*, as well as their adaptor mitochondrial antiviral signaling protein (44). Further studies are required to more finely dissect the effects of rs34330 on *CDKN1B*, *APOLD1*, *DDX47*, and *GPR19* contributing to SLE susceptibility.

We cannot rule out the involvement of other biochemical pathways not explored in our study. Notably, $p27^{Kip1}$ plays other roles in immune function, for instance in regulating T cell anergy (inadequate T cell costimulation despite antigen recognition) (41). Systemic autoimmunity was also inhibited by $p27^{Kip1}$ through control of Treg cell activity and differentiation (45). Deficiency of $p27^{Kip1}$ in aged C57BL/6 mice reduced the number and activity of Treg cells and induced the development of mild lupus-like abnormalities, indicating that the SLE association of *CDKN1B* may be due, at least in part, to immune phenotypes not directly queried in this study (45). However, no studies in humans have been reported.

Despite the strong genetic association of rs34330, and our experiments directly evaluating the effect of this single-basepair change on enhancer and promoter activity, gene expression, and binding of active histone marks and transcriptional activators (as well as a direct validation of the effects of the ~35-bp rs34330 region on apoptosis, proliferation, and cell cycle progression), we cannot rule out the possibility that there may be other functional SNPs in this locus. Interestingly, no SNPs with a linkage disequilibrium (LD) threshold of $r^2 = 0.6$ were found in our study populations of Asian ancestry (Supplementary Table 6, available on the *Arthritis & Rheumatology* website at http://onlinelibrary.wiley.com/doi/10.1002/art.41799/abstract). At a relaxed LD threshold, we found several SNPs around rs34330. However, the closest top and bottom SNPs were far away ($r^2 = 0.55$ [distance 759 bases] for rs36228499 and $r^2 = 0.42$ [distance 2,958 bases] for rs34324). As rs34330-deleted KO cells had many relevant phenotypes, we can at least accept the rs34330 region as a functional regulatory unit.

Taken together, our findings show that the risk rs34330 C allele exhibits increased binding with the IRF-1 transcriptional activator, and Pol II is associated with significant increases in 3 active chromatin marks, has potent promoter activity (~3–5 times more than the non-risk allele) and enhancer activity (~40% more than the non-risk allele), is physically associated with the *APOLD1* and *DDX47* promoters (in addition to being located in the *CDKN1B* promoter), and drives increased expression of *CDKN1B*, *DDX47*, and *GPR19* and decreased expression of *APOLD1*. Increased occupancy of CTCF around rs34330 supports its role, but it is unclear whether CTCF affects allele-specific gene expression through its looping. The region surrounding the SNP was also shown to negatively regulate proliferation, cell cycle progression, and apoptosis, as evidenced from studies on KO cells. This study demonstrates the effectiveness of hypothesis-driven follow-up experiments to conclusively localize GWAS association with specific SNPs and their associated mechanisms.

ACKNOWLEDGMENTS

We thank all patients with SLE and healthy controls who participated in this study. We also thank the research assistants, coordinators, and physicians who helped in the recruitment of subjects for this project.

AUTHOR CONTRIBUTIONS

All authors were involved in drafting the article or revising it critically for important intellectual content, and all authors approved the final version to be published. Dr. Singh had full access to all of the data in the study and takes responsibility for the integrity of the data and the accuracy of the data analysis.

Study conception and design. Singh, Maiti, Nath.

Acquisition of data. Singh, Maiti, Zhou, Bae, Terao, Okada, Chua, Kochi, Zhang, Nath.

Analysis and interpretation of data. Singh, Maiti, Fazel-Najafabadi, Sun, Guthridge, Weirauch, James, Harley, Varshney, Looger, Nath.

REFERENCES

1. Alarcón-Riquelme ME, Ziegler JT, Molineros J, Howard TD, Moreno-Estrada A, Sánchez-Rodríguez E, et al. Genome-wide association study in an Amerindian ancestry population reveals novel systemic lupus erythematosus risk loci and the role of European admixture. Arthritis Rheumatol 2016;68:932–43.
2. Oparina N, Martinez-Bueno M, Alarcon-Riquelme ME. An update on the genetics of systemic lupus erythematosus [review]. Curr Opin Rheumatol 2019;31:659–68.
3. Yang W, Tang H, Zhang Y, Tang X, Zhang J, Sun L, et al. Meta-analysis followed by replication identifies loci in or near CDKN1B, TET3, CD80, DRAM1, and ARID5B as associated with systemic lupus erythematosus in Asians. Am J Hum Genet 2013;92:41–51.
4. Bencivenga D, Caldarelli I, Stampone E, Mancini FP, Balestrieri ML, Della Ragione F, et al. $p27^{Kip1}$ and human cancers: a reappraisal of a still enigmatic protein [review]. Cancer Lett 2017;403:354–65.
5. Sherr CJ, Roberts JM. CDK inhibitors: positive and negative regulators of G_1-phase progression [review]. Genes Dev 1999;13:1501–12.
6. Larrea MD, Hong F, Wander SA, da Silva TG, Helfman D, Lannigan D, et al. RSK1 drives $p27^{Kip1}$ phosphorylation at T198 to promote RhoA inhibition and increase cell motility. Proc Natl Acad Sci U S A 2009;106:9268–73.
7. Yang Q, Al-Hendy A. The emerging role of p27 in development of diseases. Cancer Stud Mol Med 2018;4:e1–3.
8. Jia W, He MX, McLeod IX, Guo J, Ji D, He YW. Autophagy regulates T lymphocyte proliferation through selective degradation of the cell-cycle inhibitor CDKN1B/p27Kip1. Autophagy 2015;11:2335–45.

9. Cheng XK, Wang XJ, Li XD, Ren XQ. Genetic association between the cyclin-dependent kinase inhibitor gene p27/Kip1 polymorphism (rs34330) and cancer susceptibility: a meta-analysis. Sci Rep 2017;7:44871.
10. Tan W, Gu Z, Shen B, Jiang J, Meng Y, Da Z, et al. PTEN/Akt-p27^{kip1} signaling promote the BM-MSCs senescence and apoptosis in SLE patients. J Cell Biochem 2015;116:1583–94.
11. Willer CJ, Li Y, Abecasis GR. METAL: fast and efficient meta-analysis of genomewide association scans. Bioinformatics 2010;26:2190–1.
12. Sun C, Molineros JE, Looger LL, Zhou XJ, Kim K, Okada Y, et al. High-density genotyping of immune-related loci identifies new SLE risk variants in individuals with Asian ancestry. Nat Genet 2016;48:323–30.
13. Akizuki S, Ishigaki K, Kochi Y, Law SM, Matsuo K, Ohmura K, et al. PLD4 is a genetic determinant to systemic lupus erythematosus and involved in murine autoimmune phenotypes. Ann Rheum Dis 2019;78:509–18.
14. Purcell S, Neale B, Todd-Brown K, Thomas L, Ferreira MA, Bender D, et al. PLINK: a tool set for whole-genome association and population-based linkage analyses. Am J Hum Genet 2007;81:559–75.
15. Ward LD, Kellis M. HaploReg: a resource for exploring chromatin states, conservation, and regulatory motif alterations within sets of genetically linked variants. Nucleic Acids Res 2012;40:D930–4.
16. Lu Y, Quan C, Chen H, Bo X, Zhang C. 3DSNP: a database for linking human noncoding SNPs to their three-dimensional interacting genes. Nucleic Acids Res 2017;45:D643–9.
17. Boyle AP, Hong EL, Hariharan M, Cheng Y, Schaub MA, Kasowski M, et al. Annotation of functional variation in personal genomes using RegulomeDB. Genome Res 2012;22:1790–7.
18. Grundberg E, Small KS, Hedman AK, Nica AC, Buil A, Keildson S, et al. Mapping cis- and trans-regulatory effects across multiple tissues in twins. Nat Genet 2012;44:1084–9.
19. Carithers LJ, Moore HM. The Genotype-Tissue Expression (GTEx) project [editorial]. Biopreserv Biobank 2015;13:307–8.
20. Westra HJ, Peters MJ, Esko T, Yaghootkar H, Schurmann C, Kettunen J, et al. Systematic identification of trans eQTLs as putative drivers of known disease associations. Nat Genet 2013;45:1238–43.
21. Narahara M, Higasa K, Nakamura S, Tabara Y, Kawaguchi T, Ishii M, et al. Large-scale East-Asian eQTL mapping reveals novel candidate genes for LD mapping and the genomic landscape of transcriptional effects of sequence variants. PLoS One 2014;9:e100924.
22. Jung S, Liu W, Baek J, Moon JW, Ye BD, Lee HS, et al. Expression quantitative trait loci (eQTL), apping in Korean patients with Crohn's disease and identification of potential causal genes through integration with disease associations. Front Genet 2020;11:486.
23. Jansen R, Hottenga JJ, Nivard MG, Abdellaoui A, Laport B, de Geus EJ, et al. Conditional eQTL analysis reveals allelic heterogeneity of gene expression. Hum Mol Genet 2017;26:1444–51.
24. Molineros JE, Singh B, Terao C, Okada Y, Kaplan J, McDaniel B, et al. Mechanistic characterization of RASGRP1 variants identifies an hnRNP-K-regulated transcriptional enhancer contributing to SLE susceptibility. Front Immunol 2019;10:1066.
25. Chavez A, Scheiman J, Vora S, Pruitt BW, Tuttle M, Iyer EP, et al. Highly efficient Cas9-mediated transcriptional programming. Nat Methods 2015;12:326–8.
26. Hilton IB, D'Ippolito AM, Vockley CM, Thakore PI, Crawford GE, Reddy TE, et al. Epigenome editing by a CRISPR-Cas9-based acetyltransferase activates genes from promoters and enhancers. Nat Biotechnol 2015;33:510–7.
27. Yeo NC, Chavez A, Lance-Byrne A, Chan Y, Menn D, Milanova D, et al. An enhanced CRISPR repressor for targeted mammalian gene regulation. Nat Methods 2018;15:611–6.
28. Chen J, Rozowsky J, Galeev TR, Harmanci A, Kitchen R, Bedford J, et al. A uniform survey of allele-specific binding and expression over 1000-Genomes-Project individuals. Nature Commun 2016;7:11101.
29. Capasso M, McDaniel LD, Cimmino F, Cirino A, Formicola D, Russell MR, et al. The functional variant rs34330 of CDKN1B is associated with risk of neuroblastoma. J Cell Mol Med 2017;21:3224–30.
30. Sandelin A, Wasserman WW, Lenhard B. ConSite: web-based prediction of regulatory elements using cross-species comparison. Nucleic Acids Res 2004;32:W249–52.
31. MacQuarrie KL, Fong AP, Morse RH, Tapscott SJ. Genome-wide transcription factor binding: beyond direct target regulation [review]. Trends Genet 2011;27:141–8.
32. Mali P, Yang L, Esvelt KM, Aach J, Guell M, DiCarlo JE, et al. RNA-guided human genome engineering via Cas9. Science 2013;339:823–6.
33. Kawamata N, Morosetti R, Miller CW, Park D, Spirin KS, Nakamaki T, et al. Molecular analysis of the cyclin-dependent kinase inhibitor gene p27/Kip1 in human malignancies. Cancer Res 1995;55:2266–9.
34. Claussnitzer M, Cho JH, Collins R, Cox NJ, Dermitzakis ET, Hurles ME, et al. A brief history of human disease genetics. Nature 2020;577:179–89.
35. Wan Q, Chen H, Li X, Yan L, Sun Y, Wang J. Artesunate inhibits fibroblasts proliferation and reduces surgery-induced epidural fibrosis via the autophagy-mediated p53/p21(waf1/cip1) pathway. Eur J Pharmacol 2019;842:197–207.
36. Kim K, Sung YK, Kang CP, Choi CB, Kang C, Bae SC. A regulatory SNP at position -899 in CDKN1A is associated with systemic lupus erythematosus and lupus nephritis. Genes Immun 2009;10:482–6.
37. Papageorgiou A, Dinney CP, McConkey DJ. Interferon-α induces TRAIL expression and cell death via an IRF-1-dependent mechanism in human bladder cancer cells. Cancer Biol Ther 2007;6:872–9.
38. Molineros JE, Maiti AK, Sun C, Looger LL, Han S, Kim-Howard X, et al. Admixture mapping in lupus identifies multiple functional variants within IFIH1 associated with apoptosis, inflammation, and autoantibody production. PLoS Genet 2013;9:e1003222.
39. Niewold TB, Rivera TL, Buyon JP, Crow MK. Serum type I interferon activity is dependent on maternal diagnosis in anti-SSA/Ro–positive mothers of children with neonatal lupus. Arthritis Rheum 2008;58:541–6.
40. Wardowska A, Komorniczak M, Bułło-Piontecka B, Dębska-Ślizień MA, Pikuła M. Transcriptomic and epigenetic alterations in dendritic cells correspond with chronic kidney disease in lupus nephritis. Front Immunol 2019;10:2026.
41. Chang CH, Hammer J, Loh JE, Fodor WL, Flavell RA. The activation of major histocompatibility complex class I genes by interferon regulatory factor-1 (IRF-1). Immunogenetics 1992;35:378–84.
42. Kastner S, Voss T, Keuerleber S, Glockel C, Freissmuth M, Sommergruber W. Expression of G protein-coupled receptor 19 in human lung cancer cells is triggered by entry into S-phase and supports G(2)-M cell-cycle progression. Mol Cancer Res 2012;10:1343–58.
43. Huang L, Guo B, Liu S, Miao C, Li Y. Inhibition of the LncRNA Gpr19 attenuates ischemia-reperfusion injury after acute myocardial infarction by inhibiting apoptosis and oxidative stress via the miR-324-5p/Mtfr1 axis. IUBMB Life 2020;72:373–83.
44. Oliveira L, Sinicato NA, Postal M, Appenzeller S, Niewold TB. Dysregulation of antiviral helicase pathways in systemic lupus erythematosus [review]. Front Genet 2014;5:418.
45. Iglesias M, Postigo J, Santiuste I, González J, Buelta L, Tamayo E, et al. p27^{Kip1} inhibits systemic autoimmunity through the control of Treg cell activity and differentiation. Arthritis Rheum 2013;65:343–54.

American College of Rheumatology
Empowering Rheumatology Professionals

Arthritis & Rheumatology
Vol. 73, No. 12, December 2021, pp 2314–2326
DOI 10.1002/art.41883
© 2021, American College of Rheumatology

Inositol-Requiring Enzyme 1α–Mediated Synthesis of Monounsaturated Fatty Acids as a Driver of B Cell Differentiation and Lupus-like Autoimmune Disease

Yana Zhang,[1] Ming Gui,[2] Yajun Wang,[3] Nikita Mani,[3] Shuvam Chaudhuri,[3] Beixue Gao,[3] Huabin Li,[4] Yashpal S. Kanwar,[3] Sarah A. Lewis,[5] Sabrina N. Dumas,[5] James M. Ntambi,[5] Kezhong Zhang,[6] and Deyu Fang[3]

Objective. To explore the molecular mechanisms underlying dysregulation of lipid metabolism in the pathogenesis of systemic lupus erythematosus (SLE).

Methods. B cells in peripheral blood from patients with SLE and healthy controls were stained with BODIPY dye for detection of lipids. Mice with targeted knockout of genes for B cell–specific inositol-requiring enzyme 1α (IRE-1α) and stearoyl-coenzyme A desaturase 1 (SCD-1) were used for studying the influence of the IRE-1α/SCD-1/SCD-2 pathway on B cell differentiation and autoantibody production. The preclinical efficacy of IRE-1α suppression as a treatment for lupus was tested in MRL.Fas^{lpr} mice.

Results. In cultures with mouse IRE-1α–null B cells, supplementation with monounsaturated fatty acids largely rescued differentiation of plasma cells from B cells, indicating that the compromised capacity of B cell differentiation in the absence of IRE-1α may be attributable to a defect in monounsaturated fatty acid synthesis. Moreover, activation with IRE-1α/X-box binding protein 1 (XBP-1) was required to facilitate B cell expression of SCD-1 and SCD-2, which are 2 critical enzymes that catalyze monounsaturated fatty acid synthesis. Mice with targeted *Scd1* gene deletion displayed a phenotype that was similar to that of IRE-1α–deficient mice, with diminished B cell differentiation into plasma cells. Importantly, in B cells from patients with lupus, both IRE-1α expression and *Xbp1* messenger RNA splicing were significantly increased, and this was positively correlated with the expression of both *Scd1* and *Scd2* as well as with the amount of B cell lipid deposition. In MRL.Fas^{lpr} mice, both genetic and pharmacologic suppression of IRE-1α protected against the pathologic development and progression of lupus-like autoimmune disease.

Conclusion. The results of this study reveal a molecular link in the dysregulation of lipid metabolism in the pathogenesis of lupus, demonstrating that the IRE-1α/XBP-1 pathway controls plasma cell differentiation through SCD-1/SCD-2–mediated monounsaturated fatty acid synthesis. These findings provide a rationale for targeting IRE-1α and monounsaturated fatty acid synthesis in the treatment of patients with SLE.

INTRODUCTION

One signature of systemic lupus erythematosus (SLE) in patients is the production of self-reactive antibodies. The autoantibodies often deposit into tissues and organs, leading to impairment of their functions, including development of nephropathy, which leads to loss of kidney function. Since plasma cells, which differentiate from B cells upon recognition of self antigens,

Supported by the NIH (Center for Scientific Review grant R01-DK-60635 to Dr. Kanwar, grant R01-DK-062388 and National Institute of Diabetes and Digestive and Kidney Diseases grant DK-118093 to Dr. Ntambi, Center for Scientific Review grant DK-090313 to Dr. K. Zhang, and National Institute of Allergy and Infectious Diseases grants R01-AI-079056 and R01-AI-108634, National Institute of Arthritis and Musculoskeletal and Skin Diseases grant R01-AR-006634, and National Cancer Institute grant R01-CA-232347 to Dr. Fang).

[1]Yana Zhang, MD, PhD: The Third Affiliated Hospital of Sun Yat-sen University, Guangzhou, China, and Northwestern University Feinberg School of Medicine, Chicago, Illinois; [2]Ming Gui, MD, PhD: Third Xiangya Hospital of Central South University, Changsha, China; [3]Yajun Wang, MD, PhD, Nikita Mani, BS, Shuvam Chaudhuri, BS, Beixue Gao, MD, Yashpal S. Kanwar, MD, PhD, Deyu Fang, MD, PhD: Northwestern University Feinberg School of Medicine, Chicago, Illinois; [4]Huabin Li, MD, PhD: Affiliated Eye, Ear, Nose, and Throat Hospital, Fudan University, Shanghai, China; [5]Sarah A. Lewis, PhD, Sabrina N. Dumas, PhD, James M. Ntambi, PhD: University of Wisconsin–Madison; [6]Kezhong Zhang, PhD: Wayne State University School of Medicine, Detroit, Michigan.

No potential conflicts of interest relevant to this article were reported.

Address correspondence to Yana Zhang, MD, PhD, The Third Affiliated Hospital of Sun Yat-sen University, Department of Otorhinolaryngology-Head and Neck Surgery, Guangzhou 510630, China (email: zhangyn95@mail.sysu.edu.cn); or to Deyu Fang, MD, PhD, Northwestern University Feinberg School of Medicine, Department of Pathology, 303 East Chicago Avenue, Chicago, IL 60611 (email: fangd@northwestern.edu).

Submitted for publication January 20, 2021; accepted in revised form May 27, 2021.

are the only resource of autoimmune antibodies, suppression of B cell activation has been a focus in the development of therapeutic strategies for lupus as well as for other antibody-mediated diseases (1–3). Accumulated evidence has suggested that dysregulation of lipid metabolism is involved in the pathogenesis of human autoimmune diseases. Dramatic increases in the levels of free fatty acids, in particular the monounsaturated fatty acids oleic acid and palmitoleic acid, are positively correlated with the extent of disease activity in SLE (4–7). However, a direct connection between dysregulation of lipid metabolism and SLE has remained largely unclear.

Immune responses can also be adversely affected by abnormalities in the unfolded protein response, which could potentially contribute to the development of autoimmunity (8,9). The transition of B cells into plasma cells provokes the unfolded protein response, as indicated by observations of the inositol-requiring enzyme 1α (IRE-1α)–mediated messenger RNA (mRNA) splicing of X-box binding protein 1 (XBP-1), a transcription factor that promotes expression of endoplasmic reticulum (ER) chaperones (10). IRE-1α is an ER stress sensor which contains an ER luminal sensor domain that recognizes unfolded proteins, and a cytosolic kinase/RNase domain that regulates downstream effectors such as XBP-1 (11–14). XBP-1 up-regulates the synthesis of lipids and chaperones, contributing to the expansion of the ER and increased production of Ig in plasma cells (15–17). As the only enzyme that catalyzes this XBP-1 splicing, it is not surprising that IRE-1 is involved in regulating B cell differentiation (18–20). The IRE-1α RNase also selectively cleaves ER-bound mRNAs to alleviate ER protein load, a process known as regulated IRE-1–dependent decay (RIDD) (21). Indeed, phosphorylation of IRE-1α at S729 regulates RIDD in B cells and contributes to antibody production (18). However, the exact molecular mechanisms underlying how IRE-1α controls B cell differentiation into antibody-secreting plasma cells are not fully defined.

In the present study, we unexpectedly observed that addition of monounsaturated fatty acids to the culture medium containing IRE-1α–null B cells fully rescued plasma cell differentiation from these B cells, indicating that the compromised capacity of IRE-1α–null B cell differentiation could be attributed to a defect in monounsaturated fatty acid synthesis. Importantly, in our analysis of B cells from lupus patients, we detected a dramatic increase in IRE-1α/XBP-1 activation, which positively correlated with the up-regulation of stearoyl-CoA desaturase 1 (SCD-1) and SCD-2 expression by B cells and also with the accumulation of lipids in B cells. Similar to observations in mice with knockout of either the *Ire1α* or *Xbp1* genes, targeted deletion of the *Scd1* gene in mice largely diminished B cell differentiation into plasma cells. Ablation of the IRE-1α/XBP-1 pathway or treatment with an IRE-1α–specific inhibitor partially protected mice against the development of lupus-like autoimmunity. These findings define a previously unappreciated molecular mechanism underlying the control of B cell immunity through the IRE-1α/XBP-1 pathway, and provide a rationale for manipulation of the IRE-1α/XBP-1 pathway in combating autoimmune diseases, including the management of SLE.

MATERIALS AND METHODS

Collection of blood samples and isolation of B cells from SLE patients and healthy controls. This study was approved by the Ethics Committee at the Third Xiangya Hospital of Central South University in China (approval no. 2019-S190). All patients fulfilled the American College of Rheumatology 1982 revised criteria for the classification of SLE (22). The extent of disease activity in all patients was clinically evaluated using the SLE Disease Activity Index 2000 (SLEDAI-2K) (23). All patients with a SLEDAI-2K score of ≥6 who had not received immunosuppressive treatment, in particular with rituximab, were included in the study. Fourteen patients with active SLE and 11 healthy subjects were enrolled. Prior to study enrollment, all subjects gave their written informed consent to participate, in accordance with the Declaration of Helsinki.

Whole venous blood samples were collected from the SLE patients and healthy controls. Peripheral blood mononuclear cells (PBMCs) were isolated using Ficoll-Hypaque density-gradient centrifugation of EDTA-anticoagulated blood samples (24). B lymphocytes were isolated from the PBMCs using CD19 microbeads (catalog no. 130-050-301; Miltenyi Biotec) in accordance with the manufacturer's instructions.

Mice. *Ire1α*$^{fl/fl}$ mice (25) and CD19-Cre C57BL/6 mice (26) were backcrossed to an MRL-MpJ-Fas^{lpr}/J mouse strain (stock no. 000485; The Jackson Laboratory) for at least 10 generations. All animals used in this study were maintained under specific pathogen–free conditions, and all experiments were approved by the Institutional Animal Care and Use Committees at Northwestern University. More details are described in the Supplementary Materials and Methods (available on the *Arthritis & Rheumatology* website at http://onlinelibrary.wiley.com/doi/10.1002/art.41883/abstract).

Enzyme-linked immunosorbent assay (ELISA) and flow cytometry analyses of mouse serum. Serum titers of antinuclear antibodies and anti–double-stranded DNA (anti-dsDNA) antibodies from *Ire1α*$^{fl/fl}$ and CD19-Cre/*Ire1α*$^{fl/fl}$ MRL.Fas^{lpr} mice were measured using commercial ELISA kits (catalog no. M-5210 for antinuclear antibodies, catalog no. M-5110 for anti-dsDNA; Alpha Diagnostic). Absorbance at 450 nm was detected using a FilterMax F5 microplate reader (Molecular Devices).

For flow cytometry analyses, sera from *Ire1α*$^{fl/fl}$ and CD19-Cre *Ire1α*$^{fl/fl}$ MRL.Fas^{lpr} mice were diluted in 1% bovine serum albumin, followed by incubation with prefixed and permeabilized mouse lymphoma EL4 cells on ice for 30 minutes. Staining was performed with the appropriate fluorophore-conjugated anti-mouse Ig antibodies, followed by washing. Results were analyzed on a FACSCanto II instrument (BD Biosciences).

Statistical analysis. All results are expressed as the mean ± SD. Groups were compared using Student's 2-tailed *t*-test. The Gehan-Berslow-Wilcoxon test was used for calculation of survival curves, and the Spearman's rank correlation test was applied to assess correlations. *P* values less than or equal to 0.05 were considered significant.

RESULTS

Elevated lipid accumulation in B cells from SLE patients. It has been well documented that dramatic increases in the levels of free fatty acids, in particular monounsaturated fatty acids, are positively correlated with the extent of disease activity in SLE (4–7,27,28). We thus speculated that deposition of lipids would accumulate in B cells from lupus patients. Analysis of the culture medium with BODIPY staining revealed a significant increase in lipid volumes in B cells from lupus patients compared to healthy controls (Figure 1A). In contrast, there was only a modest increase in lipid volumes in T lymphocytes from SLE patients, with no significant difference compared to healthy controls (Supplementary Figure 1, available on the *Arthritis & Rheumatology* website at http://onlinelibrary.wiley.com/doi/10.1002/art.41883/abstract).

Further analyses of the cells with real-time reverse transcription–polymerase chain reaction (RT-PCR) detected a drastic increase in the expression of *Scd1* and *Scd2* mRNA

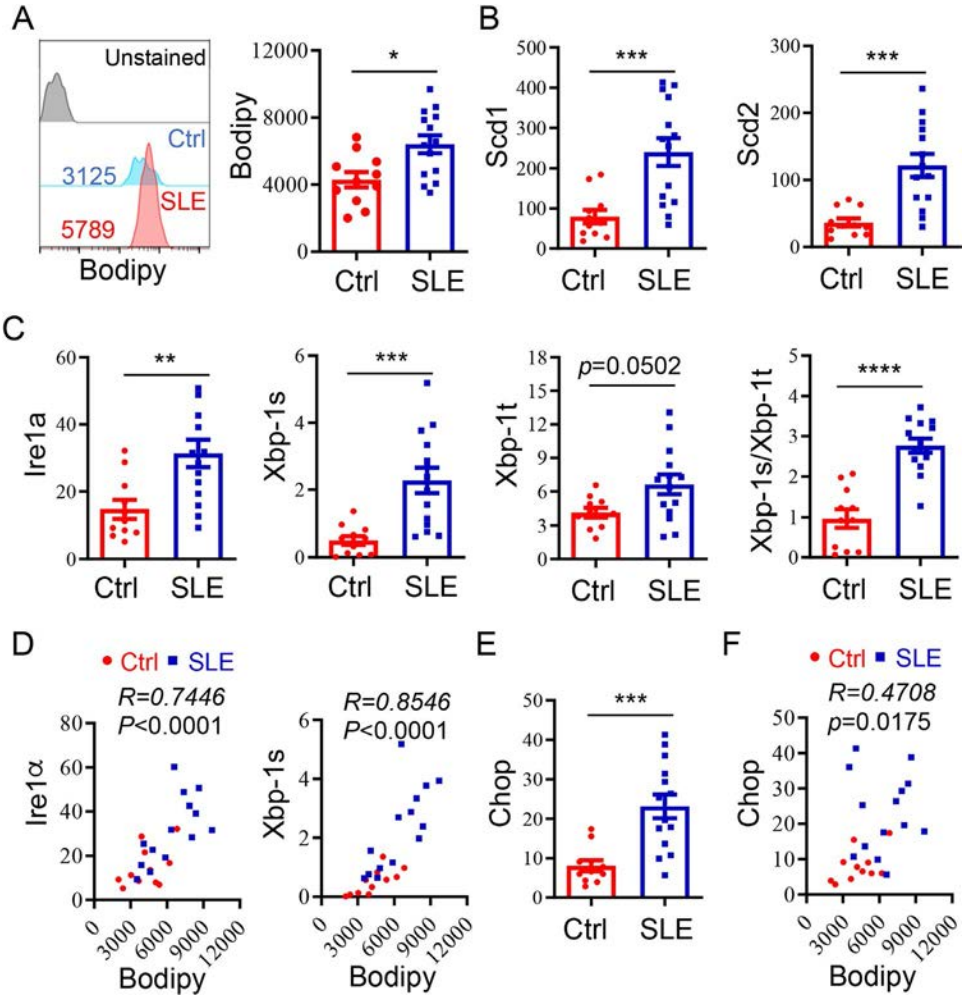

Figure 1. Increased lipid accumulation in B cells from patients with systemic lupus erythematosus (SLE) compared to healthy controls. CD19+ B cells were isolated from peripheral blood mononuclear cells from patients with active SLE (SLE Disease Activity Index score ≥6; n = 14) and healthy controls (n = 11). **A**, Intracellular lipid content in CD19+ B cells. Left, Representative flow cytometry profiles of lipid BODIPY 493/503 staining of B cells. Values are the mean quantification of lipids detected. Right, Results of lipid BODIPY staining, expressed as the mean fluorescence intensity. **B** and **C**, Reverse transcription–quantitative polymerase chain reaction (RT-qPCR) analyses of CD19+ B cells showing the relative expression of *Scd1* and *Scd2* mRNA (**B**) as well as *Ire1α*, *Xbp1s*, and *Xbp1t* mRNA and the ratio of *Xbp1s* to *Xbp1t* (**C**). **D**, Spearman's rank correlation analyses assessing correlations of intracellular lipid content with relative expression of *Ire1α* and *Xbp1s* mRNA. **E** and **F**, RT-qPCR analyses of CD19+ B cells showing the relative expression of *Chop* mRNA (**E**), and Spearman's rank correlation analyses assessing correlations of intracellular lipid content with *Chop* mRNA levels (**F**). In **A–C** and **E**, symbols represent individual samples; bars show the mean ± SD. * = $P < 0.05$; ** = $P < 0.01$; *** = $P < 0.001$; **** = $P < 0.0001$, by Student's 2-tailed *t*-test. Color figure can be viewed in the online issue, which is available at http://onlinelibrary.wiley.com/doi/10.1002/art.41883/abstract.

by B cells from patients with SLE (Figure 1B). *Scd1* and *Scd2* are critical enzymes for catalyzing the rate-limiting step in the formation of monounsaturated fatty acids (29), and therefore the observed increase in the expression of *Scd1* and *Scd2* in lupus patients suggests that both genes are involved in B cell autoimmunity.

We then analyzed whether the activation of the IRE-1α/XBP-1 pathway, which plays a critical role in the regulation of lipid metabolism (15,29), is altered in lupus B cells. Indeed, a dramatic increase in the expression of *Ire1α* was detected in B cells from patients with active lupus compared to B cells from healthy controls. As a consequence, levels of spliced *Xbp1* (*Xbp1s*) mRNA were significantly increased. In addition, we detected a modest increase in the levels of total *Xbp1* (*Xbp1t)* mRNA (Figure 1C). More importantly, the ratio of *Xbp1s* to *Xbp1t* transcripts, an indicator of IRE-1α activation, was increased almost 3-fold in B cells from lupus patients compared to B cells from healthy controls (Figure 1C). These results suggest that elevated activation of the IRE-1α/XBP-1 pathway in B cells is possibly involved in the pathogenesis of SLE.

Based on these findings showing that B cells in the SLE microenvironment exhibit a robust activation of the IRE-1α/XBP-1 pathway, leading to more lipid accumulation in lupus B cells through induction of *Scd1* and *Scd2* gene transcription, we assessed the potential correlations of these processes. Our analyses confirmed a strong positive correlation between IRE-1α/XBP-1 activation and levels of lipid accumulation in B cells from lupus patients (Figure 1D). In contrast, despite the fact that the expression of the ER stress–responsive gene *Chop* was also increased in lupus B cells, its correlation with B cell lipid levels was rather modest (Figures 1E and F).

Role of B cell–intrinsic IRE-1α in the progression of lupus-like disease and rapid mortality in mice. *Generation of IRE-1α–deficient mice.* To determine the possible pathogenic role of increased B cell IRE-1α activation in lupus-like disease, we backcrossed *Ire1α*$^{fl/fl}$/CD19-Cre mice, initially on the C57BL/6 genetic background, for at least 10 generations with MRL.Fas^{lpr} mice, a strain that develops a spontaneous lupus-like disease that resembles human SLE (30,31); this allowed us to generate *Ire1α*$^{fl/fl}$/CD19-Cre/MRL.Fas^{lpr} (*Ire1*$^{\Delta}$MRL.Fas^{lpr}) mice for this study. The expression of Cre recombinase under the CD19 promoter, which was insufficient to delete the floxed *Ire1α* gene in naive B cells, resulted in a sufficient *Ire1α* deletion upon 48-hour stimulation of B cells with lipopolysaccharide (LPS) (Supplementary Figures 2A and B, available on the *Arthritis & Rheumatology* website at http://onlinelibrary.wiley.com/doi/10.1002/art.41883/abstract). Similarly, while *Xbp1s* mRNA levels in naive B cells were indistinguishable between wild-type and *Ire1*$^{\Delta}$MRL.Fas^{lpr} mice, *Xbp1s* mRNA expression in activated B cells was largely diminished in mice with *Ire1α* deletion (see Supplementary Figure 2B). Further analyses revealed that neither the development of nor maturation of B cells was altered in *Ire1*$^{\Delta}$MRL.Fas^{lpr} mice (Supplementary Figure 2C [http://onlinelibrary.wiley.com/doi/10.1002/art.41883/abstract]), which is likely attributable to insufficient *Ire1α* gene deletion during B cell development and maturation in the mice.

Effect on mortality and kidney and lung function. Importantly, the survival of mice with lupus-like disease was dramatically improved among those with suppressed B cell IRE-1α expression as compared to littermate control mice (Figure 2A). More than 50% of MRL.Fas^{lpr} mice with B cell–specific *Ire1α* deletion survived for at least 6 months. In contrast, only 12.5% of *Ire1α*-sufficient MRL.Fas^{lpr} control mice were able to survive to the same age (Figure 2A).

Impairment of kidney function has been known to be one of the important pathogenic factors responsible for occurrence of death in lupus (32). Indeed, in our mouse model, the levels of proteinuria, a measure of kidney function, were markedly reduced in *Ire1*$^{\Delta}$MRL.Fas^{lpr} mice compared to littermate controls (Figure 2B).

Histopathologic analysis of the kidneys demonstrated that the decrease in proteinuria was associated with significantly reduced severity of glomerulonephritis in mice with *Ire1α* deletion, whereas the extent of interstitial nephritis was not significantly altered in *Ire1*$^{\Delta}$MRL.Fas^{lpr} mice (Figures 2C–E). Furthermore, histologic examination of tissue samples demonstrated a substantial reduction in both lung and liver inflammation in mice with B cell–specific *Ire1α* deletion (Figures 2F–H). However, the severity of dermatitis was indistinguishable between *Ire1*$^{\Delta}$MRL.Fas^{lpr} mice and control mice (Figure 2I), thus demonstrating that ablation of B cell *Ire1α* does not protect MRL.Fas^{lpr} mice from development of dermatitis. These data demonstrate that B cell expression of IRE-1α is responsible for multiorgan disease manifestations and rapid mortality in MRL.Fas^{lpr} mice.

Kidney failure is known to develop in the presence of high titers of autoantibodies during lupus-like autoimmunity (33). Therefore, we evaluated whether *Ire1α* deficiency in mouse B cells affected the production of autoantibodies. In a previously reported study, the autoreactive antibody levels were gradually increased with age in the serum of MRL.Fas^{lpr} mice (34). Importantly, in our study, B cell–specific IRE-1α suppression largely diminished the production of both anti-dsDNA and antinuclear antibodies (Figures 2J and K). Further analysis validated the results by showing a similar reduction in autoreactive IgG, IgG1, IgG2a, and IgA levels in the serum of *Ire1*$^{\Delta}$MRL.Fas^{lpr} mice, particularly those in later stages of the disease (Supplementary Figures 3A and B, available on the *Arthritis & Rheumatology* website at http://onlinelibrary.wiley.com/doi/10.1002/art.41883/abstract). As a consequence, the autoreactive immune complex deposition in the kidneys of MRL.Fas^{lpr} mice was largely abolished by suppression of B cell IRE-1α expression (Figures 2L and M). Collectively, our data indicate that B cell IRE-1α activation drives lupus pathogenicity, and IRE-1α suppression is a potential therapeutic strategy to treat the symptoms and severity of lupus.

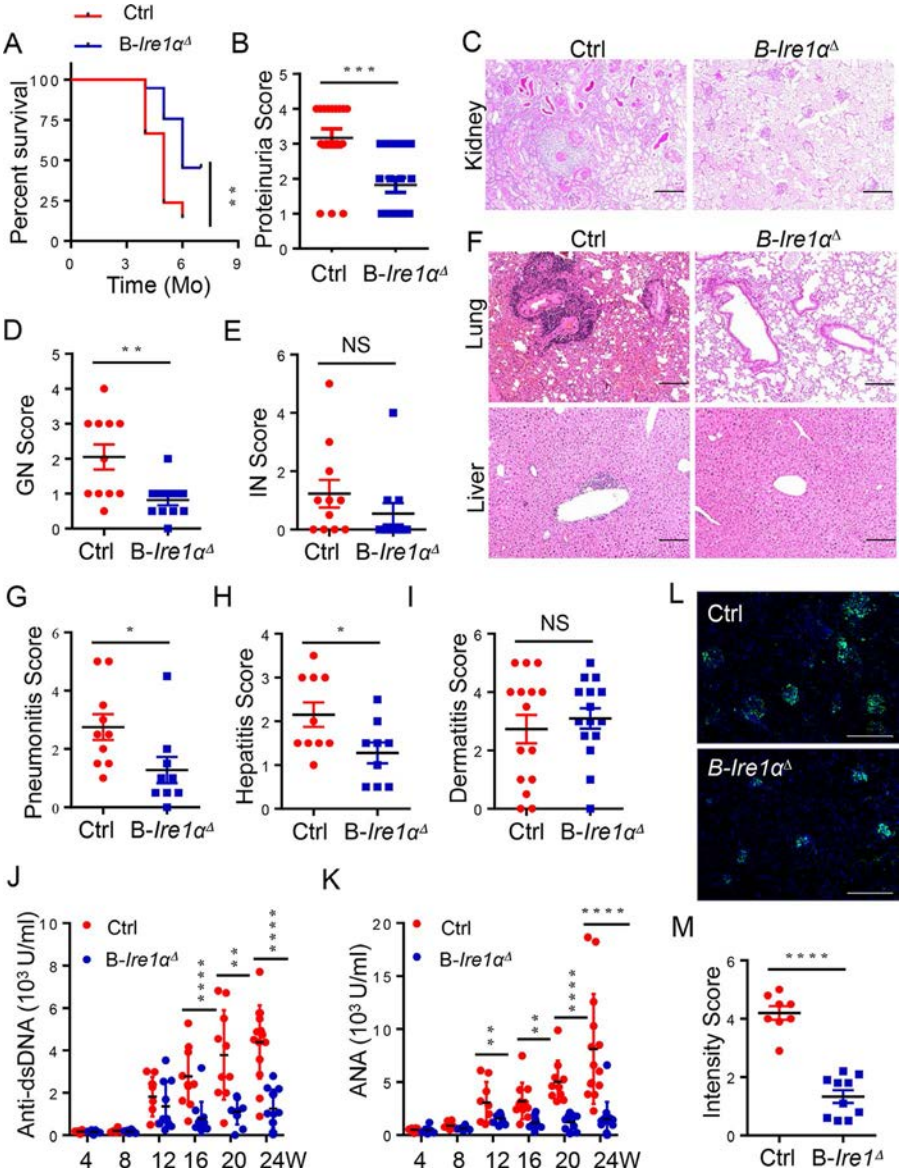

Figure 2. Role of B cell–intrinsic inositol-requiring enzyme 1α (IRE-1α) in disease progression and rapid mortality in a murine model of lupus. **A**, Survival rate over time among *Ire1*$^{\Delta}$MRL.Fas^{lpr} mice compared to littermate controls (n = 10 per group). **B**, Proteinuria scores in 16-week-old *Ire1*$^{\Delta}$MRL.Fas^{lpr} mice compared to littermate controls. **C–E**, Periodic acid–Schiff staining of kidney sections for histologic analysis (**C**; low-magnification images from a representative mouse in each group), with scoring for the severity of glomerulonephritis (GN) (**D**) and interstitial nephritis (IN) (**E**) (n = 11 per group). **F**, Hematoxylin and eosin–stained lung sections (top) and liver sections (bottom) from a representative 20-week-old mouse in each group, illustrating perivascular infiltrates in target organs. **G–I**, Scores for the severity of pneumonitis (**G**), hepatitis (**H**), and dermatitis (**I**) in *Ire1*$^{\Delta}$MRL.Fas^{lpr} mice compared to littermate controls. **J** and **K**, Enzyme-linked immunosorbent assays analyzing anti–double-stranded DNA (anti-dsDNA) (**J**) and antinuclear antibodies (ANA) (**K**) in serum from *Ire1*$^{\Delta}$MRL.Fas^{lpr} mice compared to littermate controls. **L** and **M**, Immunofluorescence staining of kidney glomeruli (**L**; images from a representative mouse in each group), and quantification of the intensity scores of anti-IgG staining in *Ire1*$^{\Delta}$MRL.Fas^{lpr} mice compared to littermate controls (**M**). In **B**, **D**, **E**, **G–I**, and **J–M**, symbols represent individual samples; bars show the mean ± SD. Scale bars in **C**, **F**, and **L** = 200 μm. * = $P < 0.05$; ** = $P < 0.01$; *** = $P < 0.001$; **** = $P < 0.0001$, by Gehan-Berslow-Wilcoxon test in **A**, and by Student's unpaired *t*-test in **B**, **D**, **E**, **G–K**, and **M**. Mo = months; NS = not significant; W = weeks.

Effect on differentiation of plasma cells. Since plasma cells are the primary sources of autoantibodies, we analyzed the differentiation of B cells into plasma cells in *Ire1α*-sufficient and *Ire1α*-deficient MRL.Fas^{lpr} mice. As expected, both the percentages and absolute numbers of B220^{intermediate}CD138+ plasma cells in the spleens and lymph nodes were markedly decreased, in an age-dependent manner, in MRL.Fas^{lpr} mice with B cell *Ire1α* ablation (Supplementary Figures 4A and B, available on the *Arthritis & Rheumatology* website at http://onlinelibrary.wiley.com/doi/10.1002/art.41883/abstract), indicating that suppression of

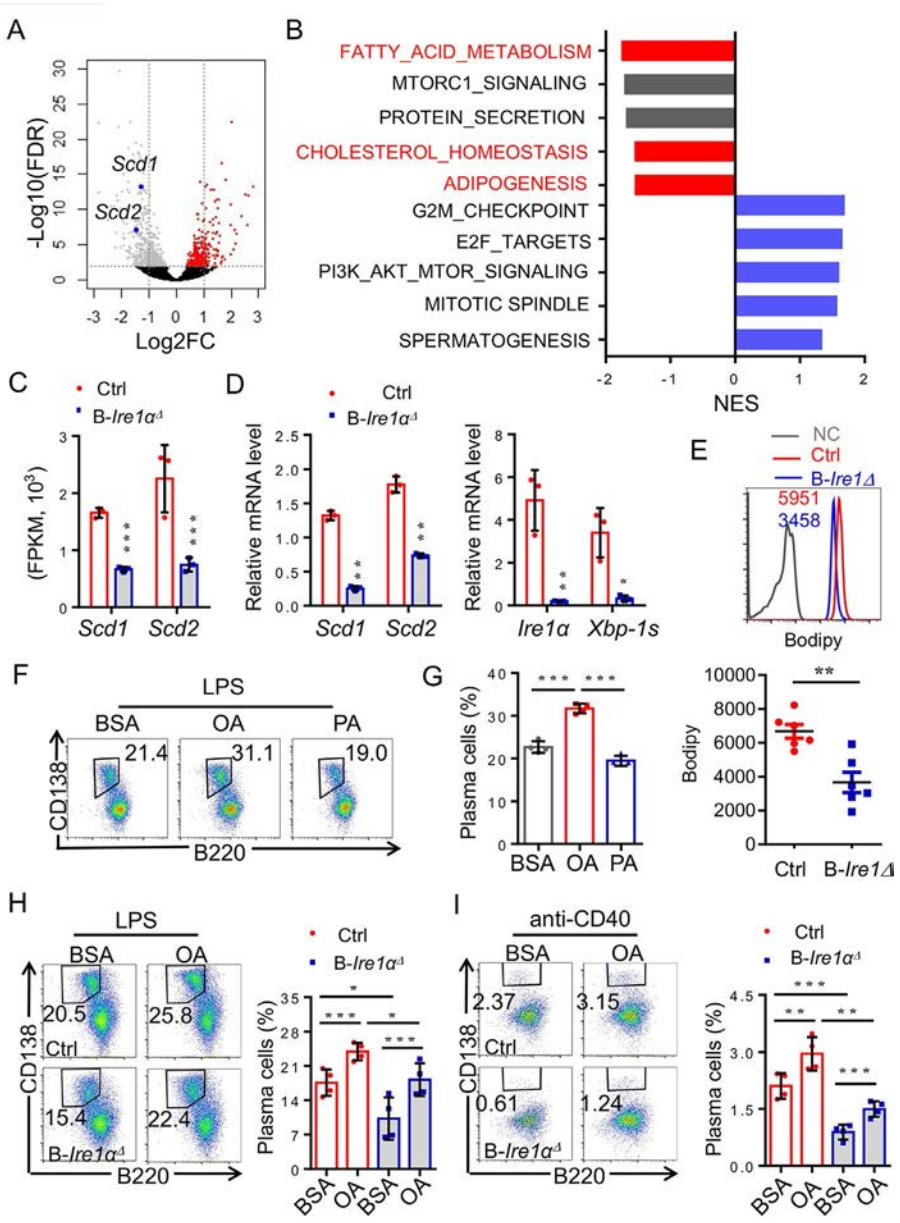

Figure 3. Effects of monounsaturated fatty acids on plasma cell differentiation from inositol-requiring enzyme 1α (IRE-1α)–null B cells in mice. **A**, Volcano plots of differential gene expression, including expression of *Scd1* and *Scd2* (blue dots), in RNA-sequencing analyses of sorted B220^{intermediate}CD138^{high} plasma cells from B cell–specific IRE-1α–deficient mice, with red scatter dots representing up-regulated genes and gray scatter dots representing down-regulated genes relative to that in littermate controls. **B**, Gene set enrichment analysis of significantly up-regulated pathways (red bars and dark gray bars) and significantly down-regulated pathways (blue bars) in plasma cells from IRE-1α–deficient mice relative to controls. The red bars are used to emphasize the lipid-associated signaling pathways. **C**, Expression of *Scd1* and *Scd2* mRNA in plasma cells from IRE-1α–deficient mice compared to controls, with results expressed as fragments per kilobase million (FPKM). **D**, Reverse transcription–quantitative polymerase chain reaction analysis of expression of *Scd1, Scd2*, *Ire1α*, and *Xbp1s* mRNA in plasma cells from *Ire1α*-deficient mice compared to controls. Results in **C** and **D** are the mean ± SD (n = 3 samples per group). **E**, BODIPY staining for detection of lipids in B cells from *Ire1α*-null mice compared to control mice; a negative control (NC) was used as reference. Graphs and values show the mean quantification of lipids detected (top), with results of BODIPY staining in each mouse group expressed as the mean ± SD (n = 6 samples per group) (bottom). **F** and **G,** Representative flow cytometry profiles (**F**) and quantification of the results (**G**), showing frequencies of B220^{intermediate}CD138^{high} plasma cells following stimulation with lipopolysaccharide (LPS) and treatment with either bovine serum albumin (BSA), oleic acid (OA), or palmitoleic acid (PA). **H** and **I**, Representative profiles of fluorescence-activated cell–sorted plasma cells (left panels) and quantification of the results (right panels), showing plasma cell differentiation from IRE-1α–null B cells upon in vitro stimulation with either LPS (**H**) or anti-CD40 (**I**) followed by treatment with BSA or OA. Results in **F–I** are the mean ± SD (n = 4 samples per group). * = $P < 0.05$; ** = $P < 0.01$; *** = $P < 0.001$, by Student's unpaired 2-tailed *t*-test. Log2FC = $\log_2$ fold change; Log10(FDR) = $\log_{10}$ false discovery rate; NES = normalized enrichment score; MTORC1 = mechanistic target of rapamycin complex 1; PI3K = phosphatidylinositol 3-kinase. Color figure can be viewed in the online issue, which is available at http://onlinelibrary.wiley.com/doi/10.1002/art.41883/abstract.

B cell–specific IRE-1α protects MRL.Fas^{lpr} mice from lupus pathogenesis via the suppression of plasma cell differentiation.

To support this finding, we further demonstrated that *Ire1α* gene deletion largely abolished B cell differentiation into plasma cells in vitro (Supplementary Figures 4C and D [http://onlinelibrary.wiley.com/doi/10.1002/art.41883/abstract]). In addition, lack of *Ire1α* expression in B cells displayed a time-dependent reduction in both viability and proliferation (Supplementary Figures 4E and F [http://onlinelibrary.wiley.com/doi/10.1002/art.41883/abstract]). Collectively, these data demonstrate a pivotal role for IRE-1α expression in promoting B cell immunity, including in regulating B cell survival, growth, and plasma cell differentiation.

Supplementation of the culture medium with monounsaturated fatty acids largely rescued the differentiation of plasma cells from IRE-1α–null B cells in mice. Since the increased activation of the IRE-1α/XBP-1 pathway was found to positively correlate both with the expression of the monounsaturated fatty acid synthetic genes *Scd1* and *Scd2* and with lipid accumulation in B cells from patients with SLE (as shown in Figure 1), we then hypothesized that IRE-1α may promote plasma cell differentiation through its facilitation of B cell lipid homeostasis. Indeed, in an unbiased genome-wide transcriptome analysis, we detected a significant reduction in the expression of lipid metabolic enzymes, including both *Scd1* and *Scd2*, in B cells from IRE-1α–deficient mice (Figures 3A and C). Furthermore, gene set enrichment analysis confirmed that, with the deletion of *Ire1α* in plasma cells from mice, the expression of genes in multiple lipid metabolic pathways, including the fatty acid metabolism pathway, was reduced (Figure 3B). In contrast, the top up-regulated genes in plasma cells from *Ire1α*-deficient mice were involved in cell cycle progression and survival (Figure 3B), thus further validating our discovery that suppression of IRE-1α attenuates the growth of plasma cells and even

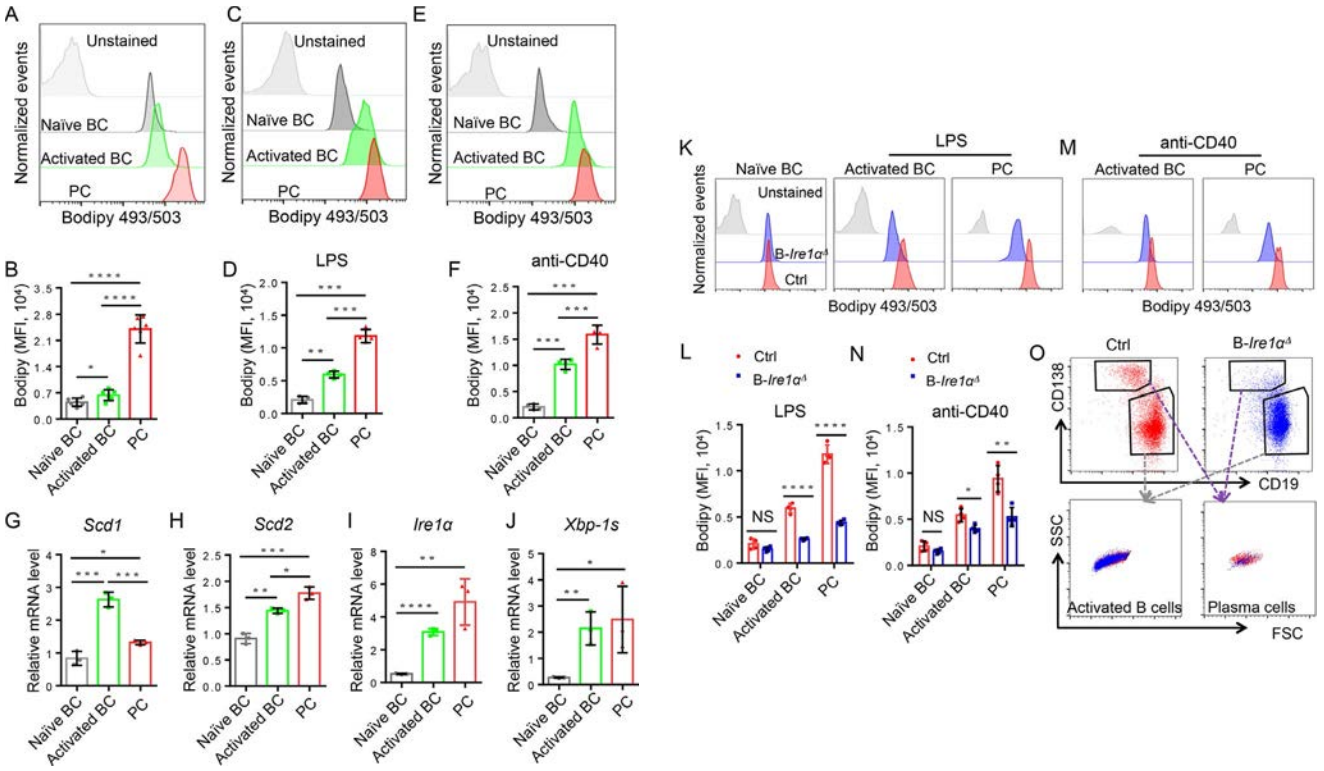

Figure 4. Inositol-requiring enzyme 1α (IRE-1α) activation promotes stearoyl-coenzyme A desaturase 1 (SCD-1)/SCD-2–mediated lipid accumulation during B cell (BC) activation and plasma cell (PC) differentiation. **A** and **B**, In vivo intracellular lipid content in naive B cells, activated B cells, and plasma cells isolated from splenocytes from *Ire1*$^{\Delta}$MRL.Fas^{lpr} mice (each n = 6) was assessed using fluorescence-activated cell sorter (FACS) analysis of lipid BODIPY 493/503 staining (representative FACS plots shown) (**A**), with results quantified as the mean fluorescence intensity (MFI) of staining (**B**). **C–F**, In vitro intracellular lipid content was assessed using FACS analysis of naive B cells, activated B cells, and plasma cells isolated from splenocytes from *Ire1*$^{\Delta}$MRL.Fas^{lpr} mice (each n = 4) (**C** and **E**). Primary naive B cells were left unstimulated or stimulated with either lipopolysaccharide (LPS) (1 mg/ml) for 2 days or anti-CD40 (4 μg/ml) for 3 days, with results quantified as the MFI of lipid BODIPY staining (**D** and **F**). **G–J**, Reverse transcription–quantitative polymerase chain reaction was used to assess expression levels of *Scd1* (**G**), *Scd2* (**H**), *Ire1α* (**I**), and *Xbp1s* (**J**) in naive B cells, activated B cells, and plasma cells (each n = 3). **K–N**, Primary B cells were isolated from 4–5-week-old *Ire1*$^{\Delta}$MRL.Fas^{lpr} mice and littermate control mice and stimulated with LPS (**K** and **L**) or anti-CD40 (**M** and **N**) in vitro for 4 days (each n = 4). Representative FACS plots are shown (**K** and **M**), with results expressed as the MFI of lipid BODIPY staining (**L** and **N**). Bars show the mean ± SD. **O**, Representative FACS plots show the proportions of activated B cells and plasma cells among splenocytes from *Ire1*$^{\Delta}$MRL.Fas^{lpr} mice and littermate controls. * = $P < 0.05$; ** = $P < 0.01$; *** = $P < 0.001$; **** = $P < 0.0001$, by Student's unpaired 2-tailed *t*-test. Color figure can be viewed in the online issue, which is available at http://onlinelibrary.wiley.com/doi/10.1002/art.41883/abstract.

promotes apoptosis of plasma cells (Supplementary Figures 4D–F [http://onlinelibrary.wiley.com/doi/10.1002/art.41883/abstract]).

Real-time RT-PCR analysis confirmed that the expression of both *Scd1* and *Scd2* in plasma cells was largely inhibited by *Ire1α* suppression (Figure 3D). A similar reduction in *Scd1* and *Scd2* gene expression was also detected in activated IRE-1α–null B cells (Supplementary Figure 5, available on the *Arthritis & Rheumatology* website at http://onlinelibrary.wiley.com/doi/10.1002/art.41883/abstract). As a consequence, the lipid volumes in B cells were dramatically decreased by *Ire1α* gene deletion (Figure 3E). These results suggest that the reduction in expression of lipid metabolic genes is possibly involved in the defect in plasma cell differentiation from IRE-1α–null B cells.

Since activation of the IRE-1α/XBP-1 pathway promotes B cell differentiation through SCD-1 and SCD-2, we examined whether the monounsaturated fatty acid products of SCD-1 and SCD-2 could facilitate plasma cell differentiation. Surprisingly, cocultivation of B cells with oleic acid significantly enhanced B cell differentiation into plasma cells in vitro (Figures 3F and G). In contrast, addition of the saturated fatty acid palmitoleic acid showed little effect (Figures 3F and G).

We then speculated whether administration of oleic acid would rescue IRE-1α–null B cell differentiation into plasma cells. As expected, *Ire1α* gene suppression dramatically impaired B cell differentiation into plasma cells upon in vitro stimulation (Figures 3H and I). Notably, supplementation with oleic acid largely rescued plasma cell differentiation from IRE-1α–null B cells (Figures 3H and I), clearly indicating that the impairment in SCD-1/SCD-2–mediated oleic acid synthesis was responsible for the defect in IRE-1α–null B cell differentiation into plasma cells. These results reveal that the IRE-1α/XBP-1/SCD-1/SCD-2 pathway is essential for optimal plasma cell differentiation.

Promotion of SCD-1/SCD-2–mediated lipid accumulation during B cell activation and plasma cell differentiation following activation of the IRE-1α/XBP-1 pathway. Our discovery that oleic acid supplementation largely rescued IRE-1α–null B cell differentiation into plasma cells suggests that IRE-1α controls plasma cell differentiation through promotion of SCD-1/SCD-2–mediated lipid synthesis. Indeed, analysis of the lipid levels in primary naive and activated B cells and plasma cells revealed a gradual increase in the intensity of lipid BODIPY staining (Figures 4A and B). This increase in lipid levels during B cell activation and differentiation was further validated following in vitro stimulation of the cells with either LPS (Figures 4C and D) or anti-CD40 (Figures 4E and F).

Consistent with the increase in lipid levels, the expression of both *Scd1* and *Scd2* was up-regulated in activated B cells and plasma cells (Figures 4G and H). Similarly, both the expression of IRE-1α and activation of IRE-1α were dramatically elevated during B cell activation and differentiation (Figures 4I and J). Taken together with the observation that *Ire1α* genetic deletion resulted in reduced expression of *Scd1* and *Scd2* in B cells, these results indicate that IRE-1α–induced SCD-1/SCD-2 expression is critical for B cell activation and plasma cell differentiation.

To further confirm this, we found that suppression of IRE-1α dramatically reduced the lipid levels in naive B cells, activated B cells, and plasma cells (Figures 4K–N). Importantly, *Ire1α* genetic suppression dramatically reduced the BODIPY signal for lipids in activated B cells and plasma cells, without showing any effect on cell size, as indicated by analysis of their forward- and side-scatter patterns (Figure 4O). Collectively, our results suggesting that IRE-1α regulates B cell differentiation through SCD-1/SCD-2–mediated lipid synthesis.

Impairment of B cell differentiation into plasma cells through genetic and pharmacologic SCD-1 suppression. For analysis of the effects of SCD-1 suppression, we first validated the critical functions of SCD-1 in B cell differentiation with a commercially available specific SCD inhibitor (SCDi), and tested its effects on plasma cell differentiation. As expected, SCDi treatment achieved a similar effect, with comparable efficacy, as that of *Ire1α* deletion, with results predominantly demonstrating diminished plasma cell differentiation in vitro following SCDi treatment (Figures 5A–C). Similar to the observations in cultures with IRE-1α–null B cells, the addition of oleic acid largely rescued plasma cell differentiation, reversing the inhibitory effects of SCDi treatment (Figures 5D–F). Therefore, our results suggest that SCD-1–mediated synthesis of oleic acid is essential for optimal B cell differentiation into plasma cells.

To provide proof-of-concept evidence to support our conclusion that SCD-1 is required for plasma cell differentiation, we determined the impact of targeted *Scd1* gene deletion on B cell differentiation. Genetic deletion of *Scd1* did not alter the frequency of B220+ B cells in the spleens of *Scd1*$^{-/-}$ mice. In contrast, both the absolute number and percentage of B220^{intermediate}CD138+ plasma cells in the spleens were remarkably reduced in *Scd1*$^{-/-}$ mice when compared with their littermate controls (Figures 5G and H), indicating that SCD-1 functions are essential for maintaining the plasma cell pool in the steady state in mice.

In addition, *Scd1* gene deletion dramatically inhibited B cell differentiation into plasma cells in vitro. More importantly, the addition of oleic acid largely rescued the plasma cell differentiation from *Scd1*$^{-/-}$ B cells (Figures 5I and J). These results clearly define a critical role of SCD-1–mediated monounsaturated fatty acid synthesis in B cell differentiation into plasma cells.

Effects of an IRE-1α–specific inhibitor as a potential therapy for lupus. We then evaluated the preclinical efficacy of an IRE-1α–specific inhibitor, BI09, in protecting MRL.Fas^{lpr} mice from lupus pathogenesis. BI09 has been shown to prevent the ability of IRE-1α to splice *Xbp1* mRNA into the activated *Xbp1* transcription factor (35). We initiated BI09 treatment in MRL.Fas^{lpr} mice from age 10 weeks, a time point after disease onset that allows

for assessment of autoimmune antibody production. Unsurprisingly, transient BI09 treatment of MRL.Fas^{lpr} mice largely protected against the progression of lupus nephropathy, as indicated by dramatic reduction in the levels of proteinuria compared to that in untreated control mice (Figure 6A).

Immunohistologic staining of the kidneys detected a trend toward reduced autoreactive antibody deposition in the kidneys of BI09-treated MRL.Fas^{lpr} mice (P = 0.054) (Figures 6B and C), which might be attributed to the effects of BI09 treatment, unlike that with targeted genetic deletion of *Ire1α*, which could only achieve partial suppression of IRE-1α activity (as shown in Figure 2). Consistent with our findings, neither the reduction in severity of kidney glomerulonephritis nor the reduction in severity of interstitial nephritis was statistically significantly different between the BI09 treatment group and the control group (Figures 6D–F). However, similar to the effects of B cell–specific IRE-1α suppression, BI09 treatment significantly reduced the infiltration of lymphocytes into the lungs and livers of mice, without any effect on skin inflammation (Figures 6D–H). These results indicate that the IRE-1α–specific inhibitor BI09 protects MRL.Fas^{lpr} mice from autoreactive antibody–mediated lupus pathogenesis. To support these findings, we analyzed serum antibody levels and found that

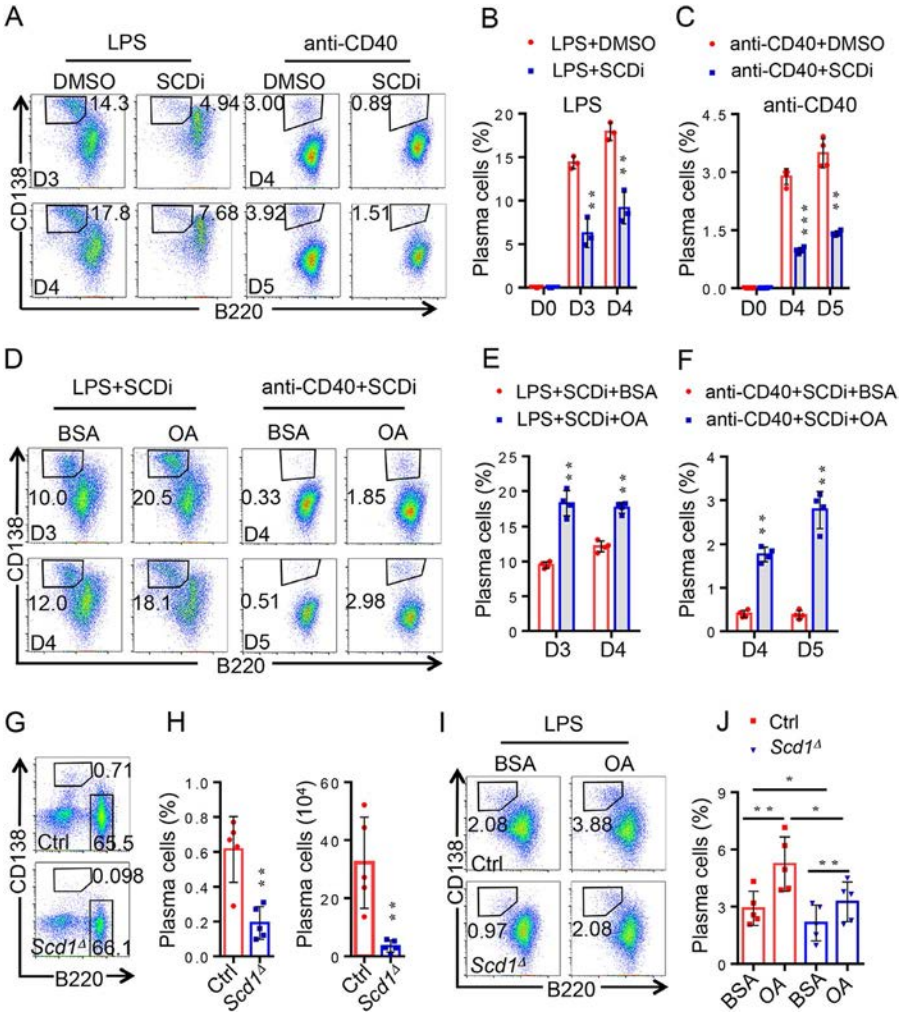

Figure 5. Genetic and pharmacologic suppression of stearoyl-coenzyme A desaturase 1 (SCD-1) impairs B cell differentiation into plasma cells. **A–C**, Representative flow cytometry profiles (**A**) and quantification of the results (**B** and **C**) show the frequencies of CD3–B220^{intermediate}CD138^{high} plasma cells after primary CD43– B cells from mouse splenocytes had been treated with an SCD inhibitor (SCDi) (0.5 μ*M*) followed by stimulation with lipopolysaccharide (LPS) (1 mg/ml) on day 3 (D3) and day 4 (**A** and **B**) or with anti-CD40 (4 μg/ml) on day 4 and day 5 (**A** and **C**) (each n = 3–4). **D–F**, Representative flow cytometry profiles (**D**) and quantification of the results (**E** and **F**) show partial rescue of plasma cell differentiation from B cells with the addition of oleic acid (OA) to the culture medium, after the cells had been treated with an SCDi and stimulated in vitro with either LPS (**D** and **E**) or anti-CD40 (**D** and **F**) (each n = 4). **G** and **H**, Representative flow cytometry profiles (**G**) and quantification of the results (**H**) show percentages and absolute numbers of CD3–B220^{intermediate}CD138^{high} plasma cells from *Scd1*-deficient mouse B cells in vivo (each n = 5). **I** and **J**, Representative flow cytometry profiles (**I**) and quantification of the results (**J**) show partial rescue of plasma cell differentiation from *Scd1*-null mouse B cells with the addition of OA to the culture medium, after the cells that had been stimulated in vitro with LPS (each n = 5). Bovine serum albumin (BSA) was used as a comparator. Symbols represent individual samples; bars show the mean ± SD. * = $P < 0.05$; ** = $P < 0.01$; *** = $P < 0.001$, by Student's 2-tailed *t*-test. Color figure can be viewed in the online issue, which is available at http://onlinelibrary.wiley.com/doi/10.1002/art.41883/abstract.

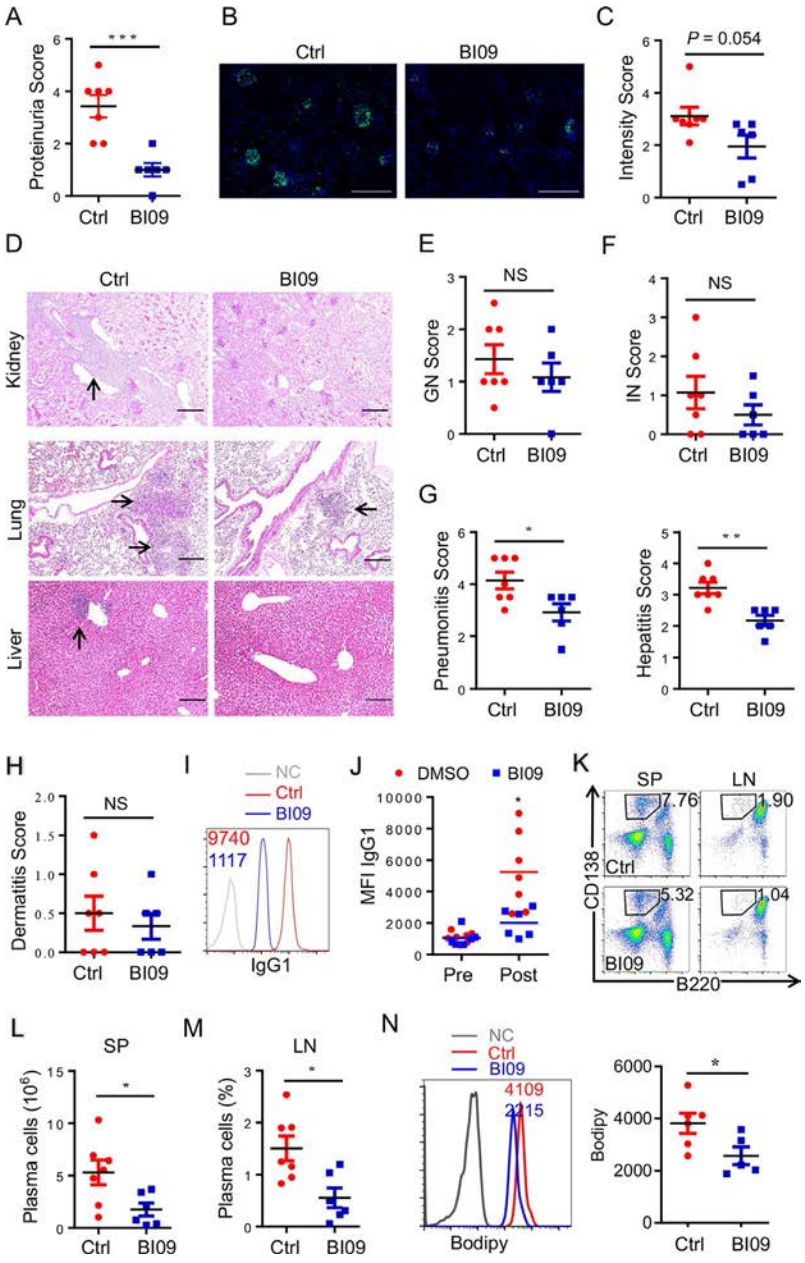

Figure 6. BI09, an inositol-requiring enzyme 1α (IRE-1α)–specific inhibitor, protects mice from lupus pathogenesis. **A**, Proteinuria scores at 3 weeks posttreatment in the kidneys of BI09-treated mice with lupus-like disease compared to DMSO controls. **B** and **C**, Immunofluorescence staining for histologic assessment of the kidney glomeruli from BI09-treated mice compared to DMSO controls (representative images are shown) (**B**), with results quantified as IgG1 staining intensity scores (**C**). **D–G**, Kidney sections from BI09-treated mice and DMSO controls were stained with periodic acid–Schiff for histologic analysis (representative images shown (**D**; top panels), and scores for the severity of glomerulonephritis (GN) (**E**) and interstitial nephritis (IN) (**F**) were assessed. In addition, lung sections (**D**; middle panels) and liver sections (**D**; bottom panels) were stained with hematoxylin and eosin, and scores for the severity of pneumonitis and hepatitis were assessed (**G**). **Arrows** indicate lymphocyte infiltration. **H**, Dermatitis scores in BI09-treated mice compared to DMSO controls. **I** and **J**, Fluorescence-activated cell sorter (FACS) analysis of autoreactive antibody profiles in the serum of BI09-treated mice compared to DMSO controls (representative FACS plots shown) (**I**), with results pre- and posttreatment quantified as the mean fluorescence intensity (MFI) of IgG1 staining (**J**). Values in **I** are the mean number of autoantibodies detected. **K–M**, Representative flow cytometry profiles (**K**) and quantification of the results (**L** and **M**), showing absolute numbers of CD3–B220^{intermediate}CD138^{high} plasma cells in splenocytes (SP) (**K** and **L**) and frequencies in lymph nodes (LN) (**K** and **M**) from BI09-treated mice compared to DMSO controls. **N**, BODIPY staining for detection of lipids in B cells from BI09-treated mice compared to DMSO controls. Values in **N** are the mean quantification of lipids detected. Symbols represent individual samples; bars show the mean ± SD. Scale bars in **B** and **D** = 200 μm. * = $P < 0.05$; ** = $P < 0.01$, by Student's unpaired 2-tailed *t*-test. NS = not significant; NC = unstained control. Color figure can be viewed in the online issue, which is available at http://onlinelibrary.wiley.com/doi/10.1002/art.41883/abstract.

the autoreactive antibody levels in the serum of BI09-treated mice were dramatically reduced when compared to those in control mice (Figures 6I and J).

Flow cytometry analysis confirmed that BI09 treatment inhibited plasma cell differentiation in MRL.Fas^{lpr} mice (Figures 6K–M). Consistent with our observation in *Ire1α*-null B cells, pharmacologic inhibition of IRE-1α resulted in a dramatic reduction in B cell lipid volumes (Figure 6N, and Supplementary Figure 6A, available on the *Arthritis & Rheumatology* website at http://onlinelibrary.wiley.com/doi/10.1002/art.41883/abstract). However, the autoimmune antibody levels rebounded back to pretreatment levels at 4 weeks after the termination of BI09 treatment (Supplementary Figure 6A), implying that pharmacologic suppression of IRE-1α, unlike that with genetic deletion, has transient effects in the treatment of lupus.

For validation of these findings, we further assessed the suppressive effects of BI09 treatment on B cell differentiation in vitro, and observed that BI09 dose-dependently inhibited CD138+ plasma cell differentiation (Supplementary Figures 6B–D [http://onlinelibrary.wiley.com/doi/10.1002/art.41883/abstract]). This reduction in plasma cell differentiation by BI09 is likely attributable to a direct inhibition of IRE-1α activation, because *Xbp1* mRNA splicing was largely inhibited by BI09 treatment (Supplementary Figure 6E [http://onlinelibrary.wiley.com/doi/10.1002/art.41883/abstract]). As a consequence, expression of *Scd1* and *Scd2* mRNA in B cells was significantly inhibited (Supplementary Figures 6F and G [http://onlinelibrary.wiley.com/doi/10.1002/art.41883/abstract]). Collectively, our data indicate that both genetic deletion and pharmacologic suppression of IRE-1α blocks B cell differentiation into plasma cells, and consequently mice are protected from the pathogenesis of B cell–mediated autoimmune disease.

DISCUSSION

Results of the present study define a previously unappreciated molecular mechanism underlying how the IRE-1α/XBP-1 pathway controls the differentiation of B cells, and our findings further provide a rationale for IRE-1α suppression as a strategy in the treatment of lupus. First, our findings demonstrate that IRE-1α suppression blocks B cell differentiation into plasma cells, which can be rescued by supplementation with monounsaturated fatty acids. Second, IRE-1α activation positively regulates the transcription of the monounsaturated fatty acid synthesis–related genes *Scd1* and *Scd2*. Third, genetic deletion and pharmacologic suppression of *Scd1* inhibits plasma cell differentiation from B cells. In addition, IRE-1α suppression largely protects mice from lupus pathogenesis. Furthermore, our studies in B cells from lupus patients show that IRE-1α/XBP-1 activation is elevated in lupus B cells, and this is positively correlated both with the increased expression of *Scd1* and *Scd2* and with lipid accumulation in B cells. Thus, taken together, these findings indicate that IRE-1α is a potential therapeutic target in the treatment of lupus and other B cell–mediated autoimmune diseases.

It has been well established that the transcription factor XBP-1 is essential for B cell differentiation into antibody-producing plasma cells (20,36). As it is the only enzyme required for *Xbp1* mRNA splicing in B cells, it is not surprising that B cell–specific IRE-1α suppression would largely diminish plasma cell differentiation and antibody secretion. XBP-1 promotes antibody production partially through induction of interleukin-6, a cytokine that is critical for B cell growth and plasma cell survival (37–39). In addition, it is speculated that in the absence of *Xbp1*, the cellular unfolded protein response is impaired, and the inefficient processing and exportation of immunoglobulin results in an accumulation of unfolded protein, which consequently leads to cell death (40). Surprisingly, we discovered that supplementation with monounsaturated fatty acids largely rescues plasma cell differentiation from B cells lacking IRE-1α, indicating that lack of monounsaturated fatty acids is at least partially responsible for the compromised capacity of IRE-1α–null B cell differentiation into plasma cells. Indeed, as was recently reported (29), we further confirmed that IRE-1α is required for the optimal expression of 2 monounsaturated fatty acid synthetic enzymes, SCD-1 and SCD-2. As proof of concept, our studies showed that genetic *Scd1* suppression impairs B cell differentiation into plasma cells. Therefore, the IRE-1α/XBP-1 pathway appears to regulate B cell differentiation into plasma cells through multiple mechanisms.

Results from our previous studies demonstrated that HRD-1, an ER-resident E3 ligase critical for degradation of misfolded proteins through the ubiquitin pathway, also catalyzes IRE-1α degradation and functions as a negative regulator of IRE-1α functions to suppress ER stress–induced cell apoptosis, all being mechanisms that are involved in the pathogenesis of arthritis and maintenance of intestinal homeostasis (41). Interestingly, as an ER stress–responsive gene, *HRD1* has been shown to be a direct target of the XBP-1 transcription factor, suggesting that a feedback loop occurs between the IRE-1α/XBP-1 pathway and HRD-1–mediated ubiquitination. In addition to our present study findings indicating the role of IRE-1α, we have previously discovered that HRD-1 protects B cells from activation-induced apoptosis by targeting the death receptor Fas (42). It will be interesting to further elucidate the effects of HRD-1–mediated IRE-1α degradation on B cell autoimmunity.

Results from the present study also define a pathogenic role for the IRE-1α/XBP-1 pathway in autoantibody-producing plasma cell differentiation through SCD-1, as well as through possibly other SCD family members such as SCD-2, which mediates monounsaturated fatty acid synthesis; these findings provide a rationale for manipulation of this pathway in lupus treatment. However, only transient efficacy could be achieved with pharmacologic suppression of IRE-1α, because the autoreactive antibody levels were restored 3 weeks after the termination of BI09 inhibitor treatment. In addition, we observed that, whereas BI09

treatment inhibited the production of autoimmune antibodies and partially protected mice from increasing severity of proteinuria, neither the reduction in kidney glomerulonephritis nor the reduction in interstitial nephritis reached statistically significant levels in the treated mice. Unlike B cell–specific targeted gene deletion, pharmacologic suppression of IRE-1α with BI09 presumably inhibits all types of cells that express IRE-1α. Indeed, suppression of IRE-1α in T cells resulted in an elevated Th2 immune response (43). Obiedat et al reported that deletion of IRE-1α or XBP-1 was sufficient to promote the expression of the NKG2D ligand, leading to an elevation in apoptosis of IRE-1α/XBP-1–knockout target cells by natural killer cells (44). Therefore, pharmacologic IRE-1α suppression is more complicated than is the B cell–specific genetic deletion of IRE-1α.

One of the most successful drugs developed as a strategy for depleting B cells is the chimeric anti-human CD20 monoclonal antibody rituximab, which has been successfully used to treat lupus and other antibody-mediated autoimmune diseases such as rheumatoid arthritis (45,46). However, in a recent review, it was reported that among 71 patients with various blistering skin diseases who were receiving rituximab, 6 deaths occurred in association with the rituximab treatment (46). Paraneoplastic pemphigus, a disease that is characteristically resistant to conventional medications and is associated with a high mortality rate, appeared to be the primary cause of death in the patients who were receiving rituximab, as 4 of the 6 deaths occurred in patients with this disease. Infectious disease, whether related to viral infections or bacterial infections, is often associated with rituximab usage (46). After binding of rituximab to CD20+ cells, the cells undergo apoptosis as a result of either a direct effect, complement- and antibody-dependent cytotoxicity, or inhibition of cell proliferation (45). Recovery of B cells begins 6–9 months after the initiation of rituximab treatment, with levels returning to normal at 1 year after treatment initiation (47). In contrast, our observations herein suggest that IRE-1α could be a better target for antibody-mediated lupus therapy, because 1) genetic suppression of IRE-1α abolishes antigen-specific antibody production without reducing B cell numbers in mice, and 2) IRE-1α suppression by its specific inhibitor, BI09, suppresses plasma cell differentiation and protects mice from lupus pathogenesis.

These are important facts to consider in drug development, because we might expect that in the case of infection occurring during treatment for lupus, termination of the IRE-1α inhibitor treatment would allow an immediate recovery of B cell functions to combat the pathogens. Moreover, a therapeutic combination of rituximab with an IRE-1α inhibitor could produce a synergistic effect in the treatment of lupus. More importantly, while rituximab suppresses autoantibody production through the depletion of B cells, presumably it has no effects on suppressing inflammatory cytokine production by myeloid cells. Based on our previous results (25) and the findings from the present study, we conclude that IRE-1α suppression has a "kill two birds with one stone" efficacy in the inhibition of the autoimmune response of both myeloid cells and B cells, which provides a rationale for targeting IRE-1α in the treatment of patients with SLE.

ACKNOWLEDGMENT

We thank staff members in Dr. Fang's laboratory for critical reading of the manuscript and providing constructive suggestions during our research.

AUTHOR CONTRIBUTIONS

All authors were involved in drafting the article or revising it critically for important intellectual content, and all authors approved the final version to be published. Drs. Y. Zhang and Fang had full access to all of the data in the study and take responsibility for the integrity of the data and the accuracy of the data analysis.

Study conception and design. Y. Zhang, Li, Ntambi, K. Zhang, Fang.
Acquisition of data. Y. Zhang, Gui, Wang, Mani, Chaudhuri, Gao, Kanwar, Lewis, Dumas, Ntambi.
Analysis and interpretation of data. Y. Zhang, Gao, Li, Kanwar, Lewis, Dumas, Fang.

REFERENCES

1. Weide R, Heymanns J, Pandort A, Koppler H. Successful long-term treatment of systemic lupus erythematosus with rituximab maintenance therapy. Lupus 2003;12:779–82.
2. Leandro MJ, Edwards JC, Cambridge G, Ehrenstein MR, Isenberg DA. An open study of B lymphocyte depletion in systemic lupus erythematosus. Arthritis Rheum 2002;46:2673–7.
3. Perrotta S, Locatelli F, La Manna A, Cennamo L, De Stefano P, Nobili B. Anti-CD20 monoclonal antibody (rituximab) for life-threatening autoimmune haemolytic anaemia in a patient with systemic lupus erythematosus. Br J Haematol 2002;116:465–7.
4. Shin TH, Kim HA, Jung JY, Baek WY, Lee HS, Park JH, et al. Analysis of the free fatty acid metabolome in the plasma of patients with systemic lupus erythematosus and fever. Metabolomics 2017;14:14.
5. Wu T, Xie C, Han J, Ye Y, Weiel J, Li Q, et al. Metabolic disturbances associated with systemic lupus erythematosus. PLoS One 2012;7:e37210.
6. Rodríguez-Carrio J, López P, Sánchez B, González S, Gueimonde M, Margolles A, et al. Intestinal dysbiosis is associated with altered short-chain fatty acids and serum-free fatty acids in systemic lupus erythematosus. Front Immunol 2017;8:23.
7. Ormseth MJ, Swift LL, Fazio S, Linton MF, Raggi P, Solus JF, et al. Free fatty acids are associated with metabolic syndrome and insulin resistance but not inflammation in systemic lupus erythematosus. Lupus 2013;22:26–33.
8. Wang J, Cheng Q, Wang X, Zu B, Xu J, Xu Y, et al. Deficiency of IRE1 and PERK signal pathways in systemic lupus erythematosus. Am J Med Sci 2014;348:465–73.
9. Todd DJ, Lee AH, Glimcher LH. The endoplasmic reticulum stress response in immunity and autoimmunity [review]. Nat Rev Immunol 2008;8:663–74.
10. Gass JN, Gifford NM, Brewer JW. Activation of an unfolded protein response during differentiation of antibody-secreting B cells. J Biol Chem 2002;277:49047–54.
11. Chen Y, Brandizzi F. IRE1: ER stress sensor and cell fate executor [review]. Trends Cell Biol 2013;23:547–55.
12. Shen X, Ellis RE, Lee K, Liu CY, Yang K, Solomon A, et al. Complementary signaling pathways regulate the unfolded protein response and are required for C. elegans development. Cell 2001;107:893–903.

13. Korennykh AV, Egea PF, Korostelev AA, Finer-Moore J, Zhang C, Shokat KM, et al. The unfolded protein response signals through high-order assembly of Ire1. Nature 2009;457:687–93.
14. Calfon M, Zeng H, Urano F, Till JH, Hubbard SR, Harding HP, et al. IRE1 couples endoplasmic reticulum load to secretory capacity by processing the XBP-1 mRNA. Nature 2002;415:92–6.
15. Cubillos-Ruiz JR, Silberman PC, Rutkowski MR, Chopra S, Perales-Puchalt A, Song M, et al. ER stress sensor XBP1 controls anti-tumor immunity by disrupting dendritic cell homeostasis. Cell 2015;161:1527–38.
16. Lee AH, Iwakoshi NN, Glimcher LH. XBP-1 regulates a subset of endoplasmic reticulum resident chaperone genes in the unfolded protein response. Mol Cell Biol 2003;23:7448–59.
17. McGehee AM, Dougan SK, Klemm EJ, Shui G, Park B, Kim YM, et al. XBP-1-deficient plasmablasts show normal protein folding but altered glycosylation and lipid synthesis. J Immunol 2009;183:3690–9.
18. Tang CH, Chang S, Paton AW, Paton JC, Gabrilovich DI, Ploegh HL, et al. Phosphorylation of IRE1 at S729 regulates RIDD in B cells and antibody production after immunization. J Cell Biol 2018;217:1739–55.
19. Zhang K, Wong HN, Song B, Miller CN, Scheuner D, Kaufman RJ, et al. The unfolded protein response sensor IRE1α is required at 2 distinct steps in B cell lymphopoiesis. J Clin Invest 2005;115:268–81.
20. Reimold AM, Iwakoshi NN, Manis J, Vallabhajosyula P, Szomolanyi-Tsuda E, Gravallese EM, et al. Plasma cell differentiation requires the transcription factor XBP-1. Nature 2001;412:300–7.
21. Hollien J, Weissman JS. Decay of endoplasmic reticulum-localized mRNAs during the unfolded protein response. Science 2006;313:104–7.
22. Tan EM, Cohen AS, Fries JF, Masi AT, McShane DJ, Rothfield NF, et al. The 1982 revised criteria for the classification of systemic lupus erythematosus. Arthritis Rheum 1982;25:1271–7.
23. Gladman DD, Ibanez D, Urowitz MB. Systemic Lupus Erythematosus Disease Activity Index 2000. J Rheumatol 2002;29:288–91.
24. Zhu YY, Su Y, Li ZG, Zhang Y. The largely normal response to Toll-like receptor 7 and 9 stimulation and the enhanced expression of SIGIRR by B cells in systemic lupus erythematosus. PLoS One 2012;7:e44131.
25. Qiu Q, Zheng Z, Chang L, Zhao YS, Tan C, Dandekar A, et al. Toll-like receptor-mediated IRE1α activation as a therapeutic target for inflammatory arthritis. EMBO J 2013;32:2477–90.
26. Rickert RC, Roes J, Rajewsky K. B lymphocyte-specific, Cre-mediated mutagenesis in mice. Nucleic Acids Res 1997;25:1317–8.
27. Huang N, Perl A. Metabolism as a target for modulation in autoimmune diseases [review]. Trends Immunol 2018;39:562–76.
28. Lo MS, Tsokos GC. Recent developments in systemic lupus erythematosus pathogenesis and applications for therapy [review]. Curr Opin Rheumatol 2018;30:222–8.
29. Xie H, Tang CH, Song JH, Mancuso A, Del Valle JR, Cao J, et al. IRE1α RNase-dependent lipid homeostasis promotes survival in Myc-transformed cancers. J Clin Invest 2018;128:1300–16.
30. Rubtsova K, Rubtsov AV, Thurman JM, Mennona JM, Kappler JW, Marrack P. B cells expressing the transcription factor T-bet drive lupus-like autoimmunity. J Clin Invest 2017;127:1392–404.
31. Papadimitraki ED, Choulaki C, Koutala E, Bertsias G, Tsatsanis C, Gergianaki I, et al. Expansion of Toll-like receptor 9–expressing B cells in active systemic lupus erythematosus: implications for the induction and maintenance of the autoimmune process. Arthritis Rheum 2006;54:3601–11.
32. Yap DY, Tang CS, Ma MK, Lam MF, Chan TM. Survival analysis and causes of mortality in patients with lupus nephritis. Nephrol Dial Transplant 2012;27:3248–54.
33. Davidson A. What is damaging the kidney in lupus nephritis? [review]. Nat Rev Rheumatol 2016;12:143–53.
34. Kinoshita K, Tesch G, Schwarting A, Maron R, Sharpe AH, Kelley VR. Costimulation by B7–1 and B7–2 is required for autoimmune disease in MRL-Faslpr mice. J Immunol 2000;164:6046–56.
35. Tang CH, Ranatunga S, Kriss CL, Cubitt CL, Tao J, Pinilla-Ibarz JA, et al. Inhibition of ER stress-associated IRE-1/XBP-1 pathway reduces leukemic cell survival. J Clin Invest 2014;124:2585–98.
36. Todd DJ, McHeyzer-Williams LJ, Kowal C, Lee AH, Volpe BT, Diamond B, et al. XBP1 governs late events in plasma cell differentiation and is not required for antigen-specific memory B cell development. J Exp Med 2009;206:2151–9.
37. Suematsu S, Matsuda T, Aozasa K, Akira S, Nakano N, Ohno S, et al. IgG1 plasmacytosis in interleukin 6 transgenic mice. Proc Natl Acad Sci U S A 1989;86:7547–51.
38. Jego G, Bataille R, Pellat-Deceunynck C. Interleukin-6 is a growth factor for nonmalignant human plasmablasts. Blood 2001;97:1817–22.
39. Iwakoshi NN, Lee AH, Vallabhajosyula P, Otipoby KL, Rajewsky K, Glimcher LH. Plasma cell differentiation and the unfolded protein response intersect at the transcription factor XBP-1. Nat Immunol 2003;4:321–9.
40. Iurlaro R, Munoz-Pinedo C. Cell death induced by endoplasmic reticulum stress [review]. FEBS J 2016;283:2640–52.
41. Sun S, Shi G, Sha H, Ji Y, Han X, Shu X, et al. IRE1α is an endogenous substrate of endoplasmic-reticulum-associated degradation. Nat Cell Biol 2015;17:1546–55.
42. Kong S, Yang Y, Xu Y, Wang Y, Zhang Y, Melo-Cardenas J, et al. Endoplasmic reticulum-resident E3 ubiquitin ligase Hrd1 controls B-cell immunity through degradation of the death receptor CD95/Fas. Proc Natl Acad Sci U S A 2016;113:10394–9.
43. Metcalfe S, Sikora K. A new marker for testicular cancer. Br J Cancer 1985;52:127–9.
44. Obiedat A, Seidel E, Mahameed M, Berhani O, Tsukerman P, Voutetakis K, et al. Transcription of the NKG2D ligand MICA is suppressed by the IRE1/XBP1 pathway of the unfolded protein response through the regulation of E2F1. FASEB J 2019;33:3481–95.
45. Kazkaz H, Isenberg D. Anti B cell therapy (rituximab) in the treatment of autoimmune diseases [review]. Curr Opin Pharmacol 2004;4:398–402.
46. Peterson JD, Chan LS. Effectiveness and side effects of anti-CD20 therapy for autoantibody-mediated blistering skin diseases: a comprehensive survey of 71 consecutive patients from the initial use to 2007. Ther Clin Risk Manag 2009;5:1–7.
47. Arin MJ, Isenberg D. Anti-CD20 monoclonal antibody (rituximab) in the treatment of pemphigus. Br J Dermatol 2005;153:620–5.

Arthritis & Rheumatology
Vol. 73, No. 12, December 2021, pp 2327–2337
DOI 10.1002/art.41887
© 2021 The Authors. *Arthritis & Rheumatology* published by Wiley Periodicals LLC on behalf of American College of Rheumatology.
This is an open access article under the terms of the Creative Commons Attribution-NonCommercial License, which permits use, distribution and reproduction in any medium, provided the original work is properly cited and is not used for commercial purposes.

American College of Rheumatology
Empowering Rheumatology Professionals

A Distinct Macrophage Subset Mediating Tissue Destruction and Neovascularization in Giant Cell Arteritis: Implication of the YKL-40/Interleukin-13 Receptor α2 Axis

Yannick van Sleen,[1] William F. Jiemy,[2] Sarah Pringle,[1] Kornelis S. M. van der Geest,[1] Wayel H. Abdulahad,[1] Maria Sandovici,[1] Elisabeth Brouwer,[1] Peter Heeringa,[1] and Annemieke M. H. Boots[1]

Objective. Macrophages mediate inflammation, angiogenesis, and tissue destruction in giant cell arteritis (GCA). Serum levels of the macrophage-associated protein YKL-40 (chitinase 3–like protein 1), previously linked to angiogenesis and tissue remodeling, remain elevated in GCA despite glucocorticoid treatment. This study was undertaken to investigate the contribution of YKL-40 to vasculopathy in GCA.

Methods. Immunohistochemistry was performed on GCA temporal artery biopsy specimens (n = 12) and aortas (n = 10) for detection of YKL-40, its receptor interleukin-13 receptor α2 (IL-13Rα2), macrophage markers PU.1 and CD206, and the tissue-destructive protein matrix metalloproteinase 9 (MMP-9). Ten noninflamed temporal artery biopsy specimens served as controls. In vitro experiments with granulocyte–macrophage colony-stimulating factor (GM-CSF)– or macrophage colony-stimulating factor (M-CSF)–skewed monocyte-derived macrophages were conducted to study the dynamics of YKL-40 production. Next, small interfering RNA–mediated knockdown of YKL-40 in GM-CSF–skewed macrophages was performed to study its effect on MMP-9 production. Finally, the angiogenic potential of YKL-40 was investigated by tube formation experiments using human microvascular endothelial cells (HMVECs).

Results. YKL-40 was abundantly expressed by a CD206+MMP-9+ macrophage subset in inflamed temporal arteries and aortas. GM-CSF–skewed macrophages from GCA patients, but not healthy controls, released significantly higher levels of YKL-40 compared to M-CSF–skewed macrophages (P = 0.039). In inflamed temporal arteries, IL-13Rα2 was expressed by macrophages and endothelial cells. Functionally, knockdown of YKL-40 led to a 10–50% reduction in MMP-9 production by macrophages, whereas exposure of HMVECS to YKL-40 led to significantly increased tube formation.

Conclusion. In GCA, a GM-CSF–skewed, CD206+MMP-9+ macrophage subset expresses high levels of YKL-40 which may stimulate tissue destruction and angiogenesis through IL-13Rα2 signaling. Targeting YKL-40 or GM-CSF may inhibit macrophages that are currently insufficiently suppressed by glucocorticoids.

INTRODUCTION

Giant cell arteritis (GCA) is an inflammatory disease that affects the medium- and large-sized arteries and has potential serious acute complications, such as blindness and stroke (1). Chronic complications can also occur, since long-term aortic inflammation is associated with the development of aneurysms and aorta dissections (2,3). GCA is commonly treated with glucocorticoids (GCs). More recently, tocilizumab (interleukin-6 [IL-6] receptor blockade) has become available as GC-sparing therapy in GCA (4). Both GCs and tocilizumab treatment suppress disease symptoms. It is less clear, however, if GCs and tocilizumab

Supported by the Dutch Arthritis Foundation "ReumaNederland" (grant RF 14-3-401). Mr. Jiemy's work was supported by a scholarship from the University Medical Center Groningen Graduate School of Medical Science and the Abel Tasman Talent Program.

[1]Yannick van Sleen, PhD, Sarah Pringle, PhD, Kornelis S. M. van der Geest, PhD, Wayel H. Abdulahad, PhD, Maria Sandovici, PhD, Elisabeth Brouwer, PhD, Peter Heeringa, PhD, Annemieke M. H. Boots, PhD: University of Groningen and University Medical Center Groningen, Groningen, The Netherlands; [2]William F. Jiemy, MSc: University of Groningen and University Medical Center Groningen, Groningen, The Netherlands, and UCSI University, Kuala Lumpur, Malaysia.

Dr. van Sleen and Mr. Jiemy contributed equally to this work. Drs. Heeringa and Boots contributed equally to this work.

Dr. van der Geest has received consulting fees, speaking fees, and/or honoraria paid to his institution from Roche (less than $10,000). Dr. Brouwer has received consulting fees, speaking fees, and/or honoraria paid to her institution from Roche (less than $10,000). No other disclosures relevant to this article were reported.

Address correspondence to Yannick van Sleen, PhD, University Medical Center Groningen, Department of Rheumatology and Clinical Immunology, Hanzeplein 1, 9700RB, Groningen, The Netherlands. Email: y.van.sleen@umcg.nl.

Submitted for publication November 9, 2020; accepted in revised form May 27, 2021.

suppress smoldering vascular inflammation, which is likely associated with relapses and chronic complications of GCA (5–9).

The inflamed vessel wall in GCA patients is characterized by a granulomatous tissue reaction involving mainly T cells and macrophages (1). Besides promoting ongoing inflammation, macrophages release factors leading to myofibroblast proliferation (e.g., platelet-derived growth factor), angiogenesis (e.g., vascular endothelial growth factor [VEGF]), and tissue destruction (e.g., matrix metalloproteinase 9 [MMP-9]) (10,11). These processes are responsible for the pathologic changes associated with the serious complications of GCA, such as vascular occlusion due to intima hyperplasia and aneurysms due to media degradation. Importantly, several studies have shown that even with treatment, macrophage activity persists in GCA patients, indicating that currently available treatments do not sufficiently suppress the local inflammatory response (6,12). Therefore, new strategies and targets are needed to adequately halt inflammation and destruction of the vessel wall.

We recently described functionally heterogeneous macrophage subsets in GCA lesions, likely due to local signals involving granulocyte–macrophage colony-stimulating factor (GM-CSF) (13). We demonstrated the presence of a specific macrophage subset in and around the media layer that lacked folate receptor β expression but showed high expression of the mannose receptor CD206. Importantly, these CD206+ macrophages exclusively expressed MMP-9, indicating that these cells are likely to be important in media destruction. Moreover, others reported MMP-9 to be an important mediator of endothelial cell migration and neoangiogenesis, thus facilitating T cell and macrophage recruitment to the vessel wall, processes crucial in the pathogenesis of GCA (11). Subsequent in vitro experiments demonstrated that the CD206+ macrophage phenotype can be induced by culturing macrophages with GM-CSF, a growth factor abundantly expressed in GCA lesions (13). Our findings on functional macrophage heterogeneity in GCA lesions, along with additional recent studies on GM-CSF signaling in GCA (12), prompted us to investigate the phenotype and functioning of the CD206+ macrophage subset in GCA in more detail. To this end, we took clues from the field of cancer immunology on tumor-associated macrophages.

Tumor-associated macrophages promote tumor growth and are associated with poor survival (14). Prior studies indicated an important role for YKL-40 (also known as chitinase 3–like protein 1) produced by tumor-associated macrophages in various inflammatory and tissue remodeling processes, including angiogenesis and tissue destruction. Furthermore, YKL-40 has been implicated as an upstream signal for MMP-9 production (15). Although early reports described elevated serum levels of YKL-40 in autoinflammatory conditions, including GCA (16), less is known about the role of YKL-40 in the immunopathology of GCA. YKL-40 is a chitinase-like protein, meaning that it is able to bind to chitin but does not cleave it, owing to the lack of enzymatic activity of YKL-40 (14). YKL-40 production by innate immune cells, including macrophages, is induced by various stimuli, including the cytokines IL-6, IL-1β, and interferon-γ (IFNγ) (17).

Interestingly, we previously showed that serum levels of YKL-40 are elevated in GCA patients at diagnosis, but do not normalize after GC treatment. In contrast, acute-phase markers such as C-reactive protein are strongly suppressed by treatment with GCs and tocilizumab, since their levels are highly dependent on IL-6 in GCA (7,18). Moreover, abundant expression of YKL-40 has been documented in GCA temporal artery biopsy specimens (7,16). However, it is yet unknown which specific cell type(s) produce YKL-40 and what the role of YKL-40 is in the immunopathogenesis of GCA.

IL-13 receptor α2 (IL-13Rα2), a high-affinity receptor for IL-13 that is distinct from IL-13Rα1, was previously thought to be a decoy receptor for IL-13 due to the lack of a signal transducing cytoplasmic tail (19,20). However, recent studies demonstrated the activation of MAPK, Akt, ERK, and STAT3 pathways in intestinal epithelial cells, nasal epithelial cells, glioblastoma cells, dendritic cells, and macrophages upon binding of either IL-13 or YKL-40 to IL-13Rα2 (21–25). The expression of this receptor in the context of GCA has so far not been reported.

In this study, we aimed to determine the cellular source of YKL-40 and to investigate its contribution to vascular pathology in GCA. Using immunohistochemistry (IHC) and immunofluorescence, we identified the subset of CD206+ macrophages as the main cellular source of YKL-40 in inflamed temporal arteries and in the aorta. In the same tissues, we next examined the expression of IL-13Rα2 to establish whether YKL-40 can signal at the site of inflammation. To assess whether YKL-40 is an upstream modulator of the tissue-destructive MMP-9, we performed in vitro experiments with monocyte-derived macrophages on the dynamics of YKL-40 and MMP-9 expression. Finally, we confirmed the angiogenic potential of YKL-40 in vitro in a tube formation assay. Our data support an important role for the YKL-40/IL-13Rα2 axis in tissue destruction and neovascularization in GCA.

PATIENTS AND METHODS

For more details on the methods, see the Supplementary Methods, available on the *Arthritis & Rheumatology* website at http://onlinelibrary.wiley.com/doi/10.1002/art.41887/abstract.

Patients. Twelve inflamed temporal artery tissue samples from treatment-naive patients with histologically proven GCA were studied. The diagnosis of GCA was based on a pathologist's assessment of the temporal artery biopsy sample as positive for panarteritis. Ten inflamed aorta tissue samples from patients with an untreated GCA-related aneurysm were also included (13). Ten noninflamed temporal artery biopsy specimens were included as controls. These noninflamed temporal artery biopsy specimens were obtained from patients with positron emission tomography (PET)–proven GCA (skip lesions; n = 3), patients with isolated polymyalgia rheumatica (PMR; n = 5), and individuals who had neither GCA nor

PMR (n = 2). The study was approved by the institutional review board of the University Medical Center Groningen (METc2010/222), and written informed consent was obtained. All procedures were conducted in compliance with the Declaration of Helsinki.

Serum and frozen peripheral blood mononuclear cells (PBMCs) from treatment-naive GCA patients and age- and sex-matched healthy controls were used for Luminex assay and in vitro studies. (Baseline characteristics of the patients and controls are shown in Supplementary Table 1, available on the *Arthritis & Rheumatology* website at http://onlinelibrary.wiley.com/doi/10.1002/art.41887/abstract.) GCA diagnoses were confirmed by temporal artery biopsy and/or PET. Healthy controls were screened by health assessment questionnaires, physical examination, and laboratory tests for past and current morbidities and were excluded if they were not healthy. Follow-up serum samples were obtained from GCA patients 1 year after the start of treatment and at treatment-free remission for the Luminex analysis. Patients were considered to be in treatment-free remission if it had been ≥2 years since the start of treatment, ≥3 months since the last treatment, and they did not have a relapse for ≥6 months after the sample was obtained.

IHC and triple fluorescence multispectral imaging. Formalin-fixed, paraffin-embedded tissue sections (3 μm) were deparaffinized and rehydrated, followed by antigen retrieval. For single staining IHC, tissues were stained with antibodies targeting YKL-40 and IL-13Rα2. Double staining for YKL-40 and the macrophage transcription factor PU.1 was performed to confirm the expression of YKL-40 by macrophages. Temporal artery biopsy specimens from GCA patients were semiquantitatively scored as previously described (26). Briefly, samples were scored on a 5-point semiquantitative scale of 0–4, where 0 = no positive cells, 1 = occasional positive cells (0–1% estimated positive), 2 = small numbers of positive cells (>1–20%), 3 = moderate numbers of positive cells (>20–50%), and 4 = large numbers of positive cells (>50%). Scores represent the average of the scores of 2 independent investigators (YvS and WFJ).

For colocalization study, triple fluorescence stainings of CD206, YKL-40, and MMP-9 were performed (n = 5). Colocalization of all 3 fluorophores was assigned the color cyan. For lists of antibodies used in IHC and immunofluorescence staining, see the Supplementary Methods and Supplementary Tables 2 and 3, available on the *Arthritis & Rheumatology* website at http://onlinelibrary.wiley.com/doi/10.1002/art.41887/abstract.

Monocyte-derived macrophages. Monocytes were isolated from thawed PBMCs from GCA patients and healthy controls using an EasySep monocyte enrichment kit without CD16 depletion (StemCell Technologies). Isolated monocytes were cultured in the presence of GM-CSF or macrophage colony-stimulating factor (M-CSF) to generate GM-CSF–skewed or M-CSF–skewed macrophages. Supernatants were collected for Luminex assay or enzyme-linked immunosorbent assay (ELISA) (see the Supplementary Methods for details on the Luminex assay and ELISA methods). For the assessment of YKL-40 levels, macrophages were activated by the addition of lipopolysaccharide (LPS) on day 5, and the supernatants were collected on day 7. Assessment of IL-6 was included as stimulation control. For YKL-40 and MMP-9 kinetics experiments, GM-CSF–skewed macrophages were generated and the supernatants were collected every 48 hours, with the final collection on day 8 for ELISAs.

Small interfering RNA (siRNA) knockdown of YKL-40. Monocyte-derived macrophages were generated in the presence of GM-CSF. On day 6, macrophages were harvested and transfected with YKL-40 siRNA (assay ID s2999, Silencer Select; ThermoFisher) or nontargeting control siRNA (catalog no. 4390843, Silencer Select; ThermoFisher) using INTERFERin (Polyplus Transfection). After 24 hours, the medium was replaced with fresh complete medium containing GM-CSF and incubated for 24 hours. The medium was then refreshed with complete medium containing GM-CSF with or without LPS. After 24 hours, medium was collected for ELISA and cells were lysed for RNA extraction and quantitative polymerase chain reaction analysis.

Tube formation assay. Human microvascular endothelial cells (HMVECs; Lonza) were treated with medium only, 150 ng/ml YKL-40 (Organon; MSD), 1,500 ng/ml YKL-40, or 20 ng/ml VEGF (PeproTech) in triplicate. HMVECs were cultured for 16 hours and then scanned on a TissueFAXS system (TissueGnostics). Tube formation was assessed by counting the number of visible enclosed fields in a blinded manner.

Flow cytometric analysis. HMVECs were stained for expression of endothelial cell marker CD31, IL-13Rα2, and VEGF receptor (VEGFR) (all from Miltenyi Biotec). Three technical replicates containing the 3 markers were compared to "fluorescence minus one" controls, in which either IL-13α2 or VEGFR antibody was omitted.

Statistical analysis. To analyze the differences between YKL-40 expression in different layers of the vessel wall and the results for GM-CSF–skewed macrophages and M-CSF–skewed macrophages from the same donor, the paired Wilcoxon signed rank test was used. Correlation analyses were performed with Spearman's correlation. To analyze the difference between groups in the tube formation assay, one-way analysis of variance with Tukey's post hoc test was used.

RESULTS

Elevation of serum levels of YKL-40 in GCA patients, without normalization of YKL-40 levels after GC treatment. To unravel the dynamics of YKL-40 in GCA patients over time, we first examined serum levels of YKL-40. In this expansion of our previous work (7), serum YKL-40 levels were confirmed to

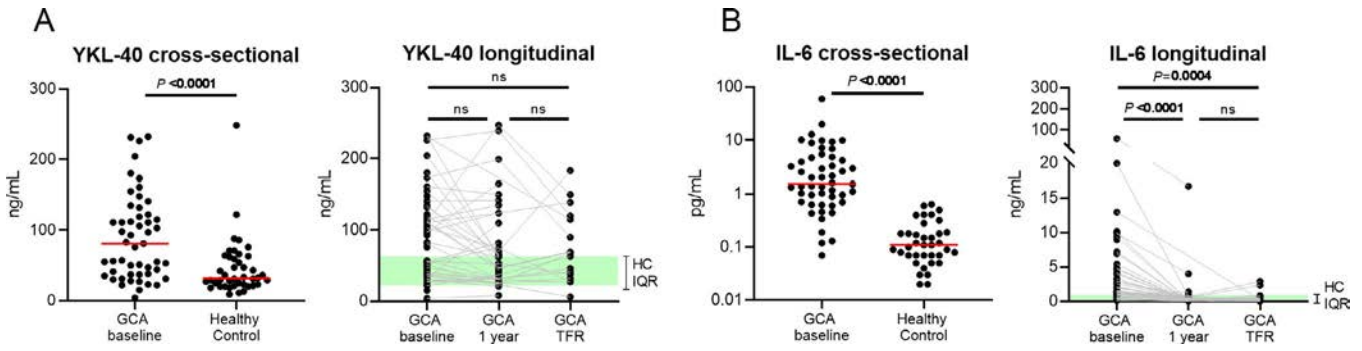

Figure 1. Serum levels of YKL-40 and interleukin-6 (IL-6) in patients with giant cell arteritis (GCA) and healthy controls (HCs). A cross-sectional analysis of serum levels of YKL-40 (**A**) and IL-6 (**B**) was conducted in treatment-naive GCA patients (n = 51) and healthy controls (n = 42), and a longitudinal analysis of serum levels of YKL-40 (**A**) and IL-6 (**B**) was conducted in matched samples from GCA patients at baseline (n = 51), 1 year after the start of glucocorticoid treatment (n = 42), and at the time of treatment-free remission (TFR; n = 17). Shading indicates the interquartile range (IQR) in healthy controls. Symbols represent individual subjects; horizontal lines show the median. In the cross-sectional analysis, *P* values were determined by Mann-Whitney U test. In the longitudinal analysis, *P* values were determined by Wilcoxon's signed rank test. NS = not significant. Color figure can be viewed in the online issue, which is available at http://onlinelibrary.wiley.com/doi/10.1002/art.41887/abstract.

be elevated in treatment-naive GCA patients when compared to age-matched healthy controls ($P < 0.0001$) (Figure 1A). Treatment with GCs for 1 year did not significantly decrease YKL-40 levels. Moreover, even GCA patients in treatment-free remission had elevated YKL-40 levels. In contrast, the high levels of IL-6 observed at baseline decreased significantly after 1 year of treatment with GCs and in treatment-free remission (Figure 1B).

Production of YKL-40 by a distinct subset of CD206+MMP-9+ macrophages in inflamed temporal arteries and aortas from GCA patients. IHC for the detection of YKL-40 in inflamed temporal artery biopsy specimens from GCA patients (n = 12) revealed a distinct staining pattern characterized by abundant expression primarily at the intima-media border (Figure 2A) (see Supplementary Figure 1, available on the *Arthritis & Rheumatology* website at http://onlinelibrary.wiley.com/doi/10.1002/art.41887/abstract, for isotype control staining). Double staining for YKL-40 and the transcription factor PU.1, which is highly expressed by macrophages, revealed that YKL-40 was expressed predominantly by macrophages (Figure 2B). Interestingly, not all PU.1-positive cells expressed YKL-40, suggesting that YKL-40 is produced by a specific subset of macrophages. Consecutive staining of YKL-40 revealed a pattern similar to that of CD206 and MMP-9 expression, suggesting that YKL-40 is predominantly produced by tissue-destructive CD206+MMP-9+ macrophages (Figure 2A). Expression of YKL-40 was not detected in noninflamed temporal arteries (Supplementary Figure 2, available on the *Arthritis & Rheumatology* website at http://onlinelibrary.wiley.com/doi/10.1002/art.41887/abstract).

YKL-40 expression was also observed in the aortas of patients with a GCA-related aortic aneurysm (n = 10) (Figure 2C). In these aortas, YKL-40 expression was mainly detected in areas of granulomatous inflammation in the media, a region containing CD206+MMP-9+ macrophages (Figure 2C). Semiquantitative scoring indeed revealed an interesting spatial distribution of YKL-40–expressing cells in inflamed temporal arteries, with the highest expression in the intima-media region (Figure 2D). To formally prove expression of YKL-40 by the CD206+MMP-9+ macrophage subset, we performed triple fluorescence staining for these markers. These data confirmed expression of YKL-40 by CD206+MMP-9+ macrophages in the inflamed temporal artery biopsy specimens (Figures 2E–G; for single immunofluorescence staining of each marker, see Supplementary Figure 3, available on the *Arthritis & Rheumatology* website at http://onlinelibrary.wiley.com/doi/10.1002/art.41887/abstract). Taken together, our results indicate that in GCA lesions, YKL-40 is highly expressed primarily by a subset of CD206+MMP-9+ tissue-destructive macrophages located in the media and at its borders.

Production of higher levels of YKL-40 by GM-CSF–skewed macrophages than by M-CSF–skewed macrophages from GCA patients. Previously, we demonstrated that GM-CSF skews macrophages into a CD206+ phenotype (13). To determine whether GM-CSF–skewed macrophages produce YKL-40, monocytes from GCA patients (n = 8) were differentiated into macrophages in the presence of GM-CSF or M-CSF for 7 days. During the last 2 days of culture, cells were stimulated with LPS (Figure 3A). Higher levels of YKL-40 were detected in the supernatants of GM-CSF–skewed macrophages than in the supernatants of M-CSF–skewed macrophages from GCA patients ($P = 0.0391$) (Figure 3B). This finding is consistent with the coexpression of CD206 and YKL-40 observed in GCA temporal artery biopsy specimens. Interestingly, no significant difference in YKL-40 levels was detected in the culture supernatant when comparing GM-CSF–skewed macrophages and M-CSF–skewed macrophages from healthy controls (n = 7).

Assessment of IL-6 levels as stimulation control revealed significant up-regulation of IL-6 production by GM-CSF–skewed

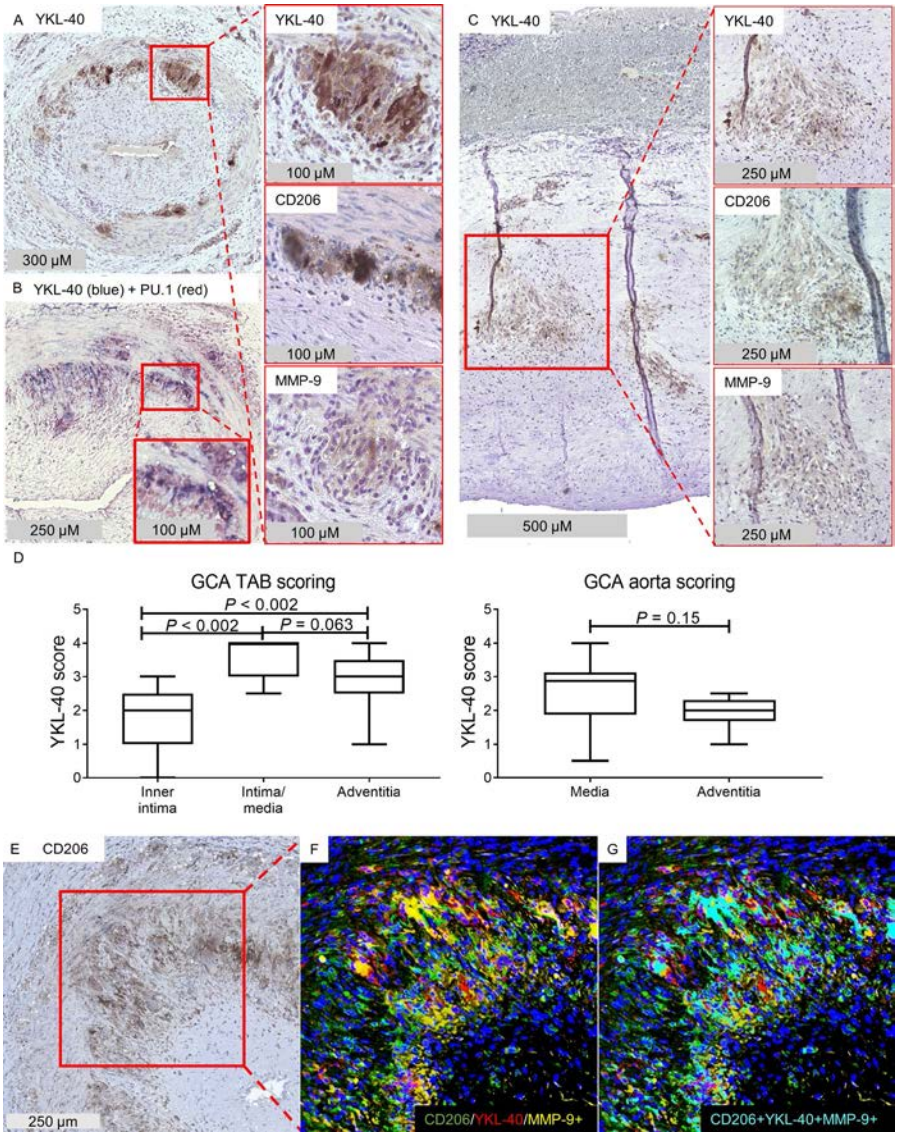

Figure 2. YKL-40 expression in CD206+MMP-9+ macrophage-rich areas in inflamed medium- and large-sized arteries from patients with giant cell arteritis (GCA). **A**, Temporal artery biopsy (TAB) specimens from treatment-naive GCA patients were stained for detection of YKL-40 by immunohistochemistry (IHC). Right panels are higher-magnification views of the boxed area, showing expression of YKL-40, CD206, and matrix metalloproteinase 9 (MMP-9) within the same region of the temporal artery biopsy. **B**, Double staining for YKL-40 and the transcription factor PU.1, which is predominantly expressed by macrophages, indicated that YKL-40 was mainly expressed by macrophages. The bottom boxed area is a higher-magnification view of the top boxed area, showing YKL-40 staining in macrophages. **C**, Aortas from patients with GCA-related aortic aneurysm were stained for detection of YKL-40 by IHC. Right panels are higher-magnification views of the boxed area, showing expression of YKL-40, CD206, and MMP-9. A pattern of YKL-40 production similar to that shown in **A** was observed within the region of CD206-expressing cells, located at the site of the granuloma in the media of inflamed aortas. **D**, YKL-40 expression in GCA temporal artery biopsy specimens and aortas was scored semiquantitatively. Expression of YKL-40 was higher in the intima-media region of temporal artery biopsy specimens, but no significant differences were found between layers in the aortas. The intima was not scored in GCA aortas due to a lack of infiltrate. Data are shown as Tukey box plots. Each box represents the 25th to 75th percentiles. Lines inside the boxes represent the median. Lines outside the boxes represent the 75th percentile plus 1.5 times the interquartile range. *P* values were determined by Wilcoxon's signed rank test. **E**–**G**, IHC staining of GCA temporal artery biopsy specimens was performed. Single staining IHC for CD206 (**E**), a merged image of triple immunofluorescence staining for CD206, YKL-40, and MMP-9 (**F**), and overlapping pixels (cyan) indicating colocalization of CD206, YKL-40, and MMP-9 (**G**) are shown. Results are representative of 12 samples in **A** and **B**, 10 samples in **C**, and 5 samples in **E**–**G**.

macrophages compared to M-CSF–skewed macrophages (Supplementary Figure 4, available on the *Arthritis & Rheumatology* website at http://onlinelibrary.wiley.com/doi/10.1002/art.41887/abstract), consistent with previous studies (27,28), in both GCA patients and healthy controls. Our data suggest an altered GM-CSF/M-CSF signaling sensitivity in monocyte/macrophages from GCA patients compared to healthy controls.

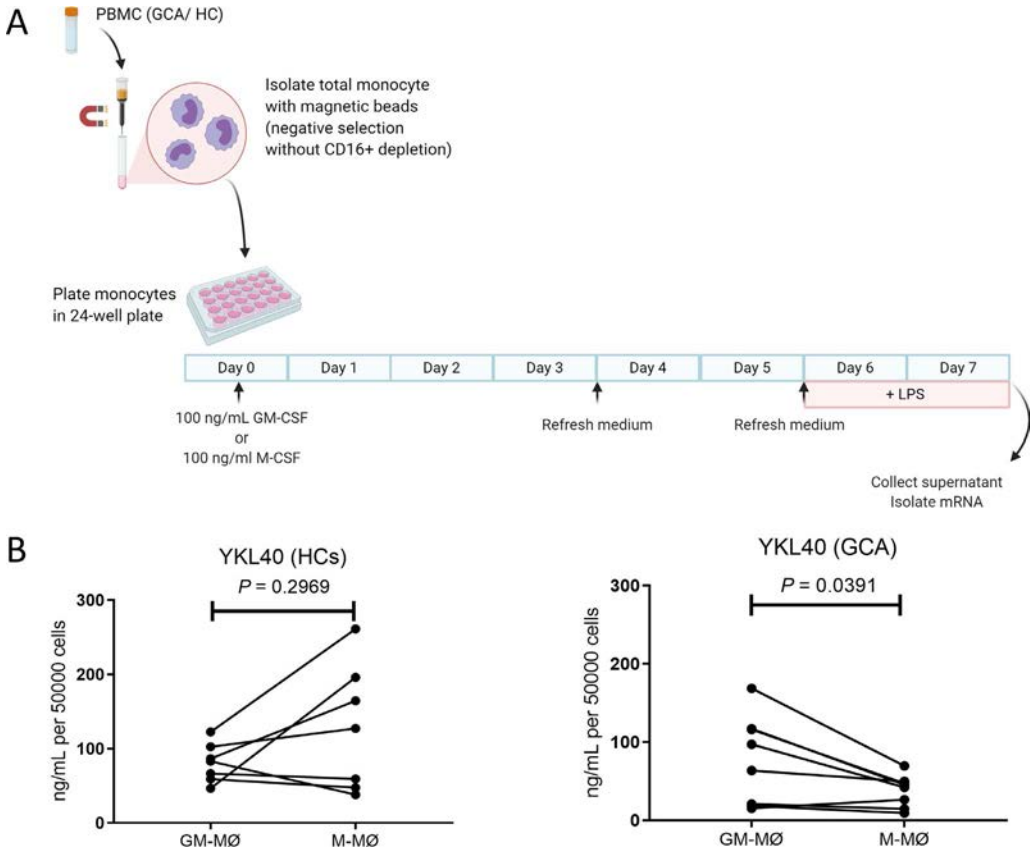

Figure 3. Elevated levels of YKL-40 in granulocyte–macrophage colony-stimulating factor (GM-CSF)–skewed macrophages from patients with giant cell arteritis (GCA). **A**, Monocytes from peripheral blood mononuclear cells (PBMCs) from healthy controls (HCs; n = 7) and GCA patients (n = 8) were differentiated into macrophages and subsequently activated for 48 hours with lipopolysaccharide (LPS). **B**, YKL-40 concentrations in the supernatants of GM-CSF–skewed macrophages (GM-MØ) and macrophage colony-stimulating factor (M-CSF)–skewed macrophages (M-MØ) from healthy controls and GCA patients were determined by Luminex assay. YKL-40 concentrations were significantly higher in GM-CSF–skewed macrophages than in M-CSF–skewed macrophages from GCA patients. *P* values were determined by Wilcoxon's signed rank test. Color figure can be viewed in the online issue, which is available at http://onlinelibrary.wiley.com/doi/10.1002/art.41887/abstract.

Strong expression of IL-13Rα2, the receptor for YKL-40, in GCA lesions. Since YKL-40 is highly expressed in GCA lesions, we next investigated the expression of IL-13Rα2, a confirmed receptor for YKL-40 (24,25), in inflamed temporal artery biopsy specimens from GCA patients (n = 12). IHC detection revealed high expression of IL-13Rα2 by endothelial cells, infiltrating leukocytes, vascular smooth muscle cells, and fibroblasts (Figure 4A), which is consistent with previous reports in the literature (19,25,29–31). Semiquantitative scoring of IL-13Rα2 staining demonstrated high expression levels in all 3 layers of the vessel wall, most prominently in the adventitia and media-intima borders (Figure 4B).

Interestingly, when analyzing the expression of IL-13Rα2 in noninflamed temporal arteries with no or few infiltrating cells, a more restricted staining was seen. IL-13Rα2 was only weakly expressed by endothelium and vascular smooth muscle layers in noninflamed temporal artery biopsy specimens from individuals without GCA or PMR (Figure 4C), while IL-13Rα2 was strongly expressed by endothelial cells, vascular smooth muscle cells, and fibroblasts in noninflamed temporal artery biopsy specimens from patients with PET-proven GCA (skip lesions) (Figure 4D) and patients with isolated PMR (Supplementary Figure 5, available on the *Arthritis & Rheumatology* website at http://onlinelibrary.wiley.com/doi/10.1002/art.41887/abstract). Taken together, our data suggest a role for the YKL-40/IL-13Rα2 signaling axis in GCA lesions.

YKL-40 as an upstream modulator of macrophage MMP-9 production. To assess if YKL-40 is an upstream modulator of the tissue-destructive MMP-9, we studied the kinetics of YKL-40 and MMP-9 production by differentiating monocytes from healthy controls (n = 8) into macrophages in the presence of 20 ng/ml or 100 ng/ml of GM-CSF (Supplementary Figures 6A and B, available on the *Arthritis & Rheumatology* website at http://onlinelibrary.wiley.com/doi/10.1002/art.41887/abstract). Both concentrations of GM-CSF equally induced the up-regulation of YKL-40 and MMP-9 as the monocytes differentiated into macrophages. Interestingly, the increase in YKL-40 levels preceded the up-regulation of MMP-9 by 2–4 days. Moreover, the increase in YKL-40 production from day 6 to day 8 strongly correlated with

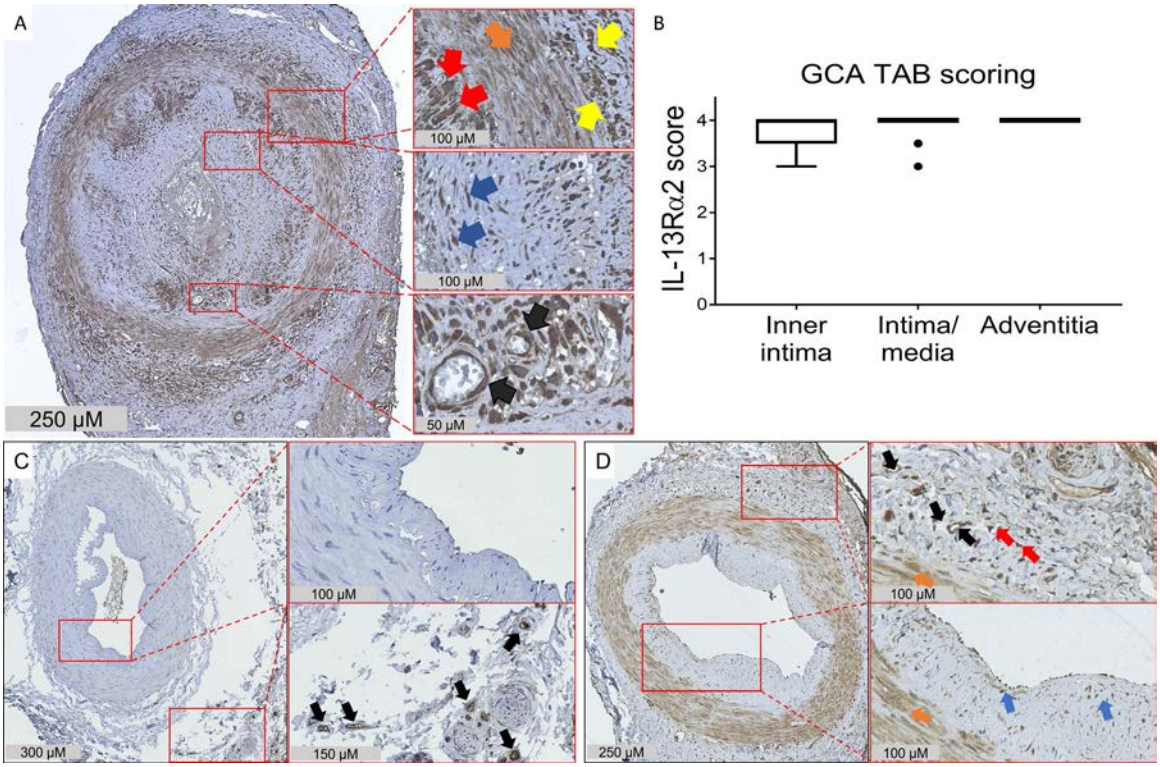

Figure 4. Elevated expression of interleukin-13 receptor α2 (IL-13Rα2) in the inflamed temporal arteries of patients with giant cell arteritis (GCA). **A**, Temporal artery biopsy (TAB) specimens from treatment-naive GCA patients were stained for IL-13Rα2. Expression of IL-13Rα2 was detected in all 3 layers of the vessel wall. Right panels are higher-magnification views of the boxed areas, showing expression of IL-13Rα2 by macrophages (**red arrows**), vascular smooth muscle cells (**orange arrow**), infiltrating leukocytes (**yellow arrows**), fibroblasts (**blue arrows**), and endothelial cells (**black arrows**). **B**, IL-13Rα2 expression in the vessel layers of GCA temporal artery biopsy specimens was scored semiquantitatively. The box represents the 25th to 75th percentiles. The line outside the box represents the 75th percentile plus 1.5 times the interquartile range (IQR). Horizontal lines represent the median. Circles indicate points outside the 25th or 75th percentile plus 1.5 times the IQR. **C**, Temporal artery biopsy specimens from individuals without GCA or polymyalgia rheumatica were stained for IL-13Rα2. Right panels are higher-magnification views of the boxed areas, showing minimal expression of IL-13Rα2 in the medial vascular smooth muscle layer and the lumen, and stronger expression in the vasa vasorum endothelial cells (**black arrows**). **D**, Temporal artery biopsy specimens from patients with positron emission tomography–proven GCA were stained for IL-13Rα2. Strong expression of IL-13Rα2 was detected in all 3 layers of the vessel wall. Right panels are higher-magnification views of the boxed areas, showing expression of IL-13Rα2 by endothelial cells (**black arrows**), vascular smooth muscle cells (**orange arrows**), and presumably resident dendritic cells (**red arrows**) and fibroblasts (**blue arrows**). Results are representative of 12 samples in **A**, 2 samples in **C**, and 3 samples in **D**.

the increase in MMP-9 production (Supplementary Figure 6C), suggesting that YKL-40 could be an upstream modulator of MMP-9 production.

To confirm the potential role of YKL-40 as an upstream signal for MMP-9 production in macrophages, we performed siRNA-mediated knockdown of YKL-40 using monocyte-derived macrophages from healthy controls and GCA patients (n = 3 each), demonstrating a knockdown efficiency of 80–95% for YKL-40 mRNA (Supplementary Figure 7, available on the *Arthritis & Rheumatology* website at http://onlinelibrary.wiley.com/doi/10.1002/art.41887/abstract). This knockdown in turn led to an 80–95% reduction in YKL-40 protein levels compared to nonbinding siRNA control (Figure 5A). Interestingly, YKL-40 knockdown reduced MMP-9 protein levels by 10–50% when compared to siRNA control (Figure 5B), suggesting that (autocrine/paracrine) MMP-9 secretion by macrophages is partially dependent on YKL-40.

Promotion of endothelial tube formation by YKL-40. YKL-40 and VEGF likely stimulate neovascularization by interacting with their respective receptors, IL-13Rα2 and VEGFR, both of which are abundantly expressed by HMVECs (Figure 6A). We aimed to confirm the proangiogenic potential of YKL-40 by performing a tube formation assay, which is often used to measure the ability of endothelial cells to form capillary-like structures. Previously, it has been demonstrated that YKL-40 has high angiogenic potential, performing equally as well as VEGF in stimulating HMVEC tube formation (32). Indeed, we demonstrated potentiation of tube formation in the presence of YKL-40 when compared to unstimulated HMVECs (Figures 6B and C). Moreover, the higher

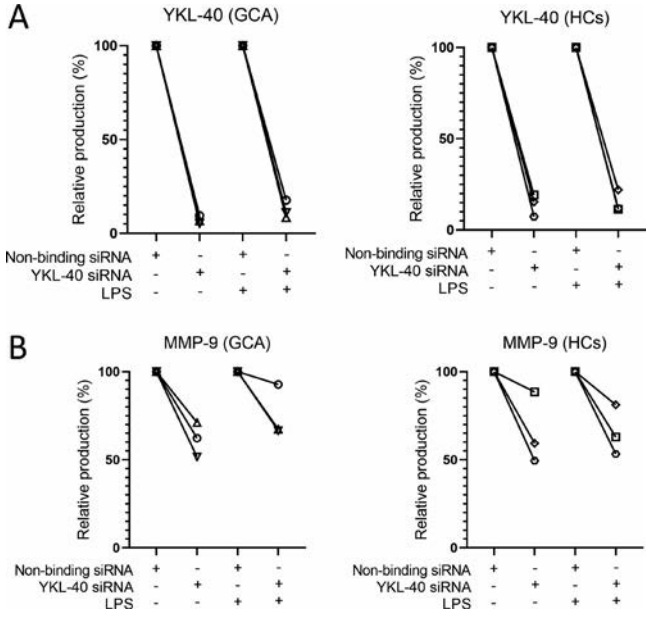

Figure 5. Reduction in macrophage YKL-40 and matrix metalloproteinase 9 (MMP-9) protein secretion upon small interfering RNA (siRNA)–mediated knockdown of YKL-40 mRNA. **A**, YKL-40 secretion in culture supernatants was reduced by 80–95% after siRNA-mediated knockdown in macrophages from both patients with giant cell arteritis (GCA) and healthy controls (HCs), left unstimulated or stimulated with lipopolysaccharide (LPS; n = 3 per group). **B**, MMP-9 secretion was reduced by 10–50% after siRNA-mediated knockdown in macrophages from both GCA patients and healthy controls, left unstimulated or stimulated with LPS (n = 3 per group).

concentration of YKL-40 had a stimulation potential equal to that of VEGF. Additionally, YKL-40 and VEGF combined induced even higher tube formation. Taken together, these results further implicate YKL-40 as playing a role in the inflammatory process in GCA by enhancing MMP-9 production and promoting angiogenesis.

DISCUSSION

Whereas the presence of macrophages in GCA lesions is well established, their functional heterogeneity and associated role in GCA pathology is less well described. In this study, we identified a specific CD206+MMP-9+ subset of macrophages that abundantly produces YKL-40 in the GCA lesions. Moreover, in vitro studies revealed that YKL-40 acts as an upstream signal that contributes to macrophage MMP-9 production and exerts potent proangiogenic effects. Taken together, our results provide strong evidence that YKL-40, secreted by CD206+MMP-9+ macrophages and giant cells, mediates vascular pathology in GCA through its ability to stimulate MMP-9 secretion and neoangiogenesis.

The presence of YKL-40 in GCA lesions was first reported in 1999 (16), when expression of YKL-40 by CD68+ macrophages located in the media borders was demonstrated. Our data confirm and extend those findings by revealing abundant expression of YKL-40 predominantly by a specific CD206+MMP-9+ subset of macrophages in the inflamed vessel walls. As recently described by our group, CD206+MMP-9+ macrophages, likely induced by local GM-CSF production, are mainly located in the media and its borders near sites of medial destruction (13). Hence, local GM-CSF production is likely important in skewing this macrophage subset toward YKL-40 production in GCA lesions as well.

Indeed, it has been reported previously that GM-CSF–skewed macrophages derived from healthy donors produce higher levels of YKL-40 than their M-CSF–skewed counterparts (33). In this study, we also found higher YKL-40 levels in GM-CSF–skewed macrophages (compared to M-CSF–skewed macrophages) derived from monocytes from GCA patients, but not in those from healthy controls. Although the exact reason for this apparent discrepancy is not known, it may relate to shifts in monocyte subset composition in conjunction with altered responsiveness to GM-CSF stimulation. With aging, the proportion of classic monocytes decreases (34), whereas this subset is expanded in GCA patients (35). Since classic monocytes have the highest GM-CSF receptor expression (13), these shifts in monocyte subset composition may underlie a heightened sensitivity to GM-CSF skewing in GCA patients. Supporting this notion, monocyte-derived macrophages from GCA patients also express higher levels of CD206, a marker of GM-CSF skewing (13). Currently, the efficacy of mavrilimumab, a GM-CSF receptor antagonist, is being evaluated for the treatment of GCA (ClinicalTrials.gov identifier: NCT03827018). The first encouraging results of this phase II trial have recently been reported, showing a 62% lower risk of flare by week 26 compared to placebo treatment. It is highly likely that mavrilimumab targets the YKL-40–producing macrophage subset, a concept which warrants further investigation.

Our data further extend the notion that YKL-40 is one of the upstream signals for MMP-9 production by macrophages. Our experiments show that YKL-40 and MMP-9 are produced by the same subset of macrophages in GCA lesions and that knocking down YKL-40 in in vitro differentiated macrophages substantially reduces their MMP-9 production. Previously, YKL-40 was found to enhance production of CCL2 and MMP-9, while YKL-40 gene silencing decreased the expression of these proteins in macrophages in mouse models bearing mammary tumors (15). In these mouse models, neutralization of YKL-40 by administering chitin decreased serum YKL-40 levels and decreased MMP-9 production by isolated splenic T cells and macrophages. MMP-9 is likely an important factor in the pathogenesis of GCA, not only in the context of medial destruction, but also as a mediator of T cell and monocyte invasion into the vessel wall (11). Taken together, our data implicate GM-CSF–skewed CD206+ macrophages in GCA lesions in the production of high levels of YKL-40 that could boost MMP-9 expression in an autocrine or paracrine manner.

This is the first study to demonstrate that IL-13Rα2, a confirmed receptor for YKL-40 (24,25), is highly expressed in GCA lesions. Previous studies have shown that the interaction of

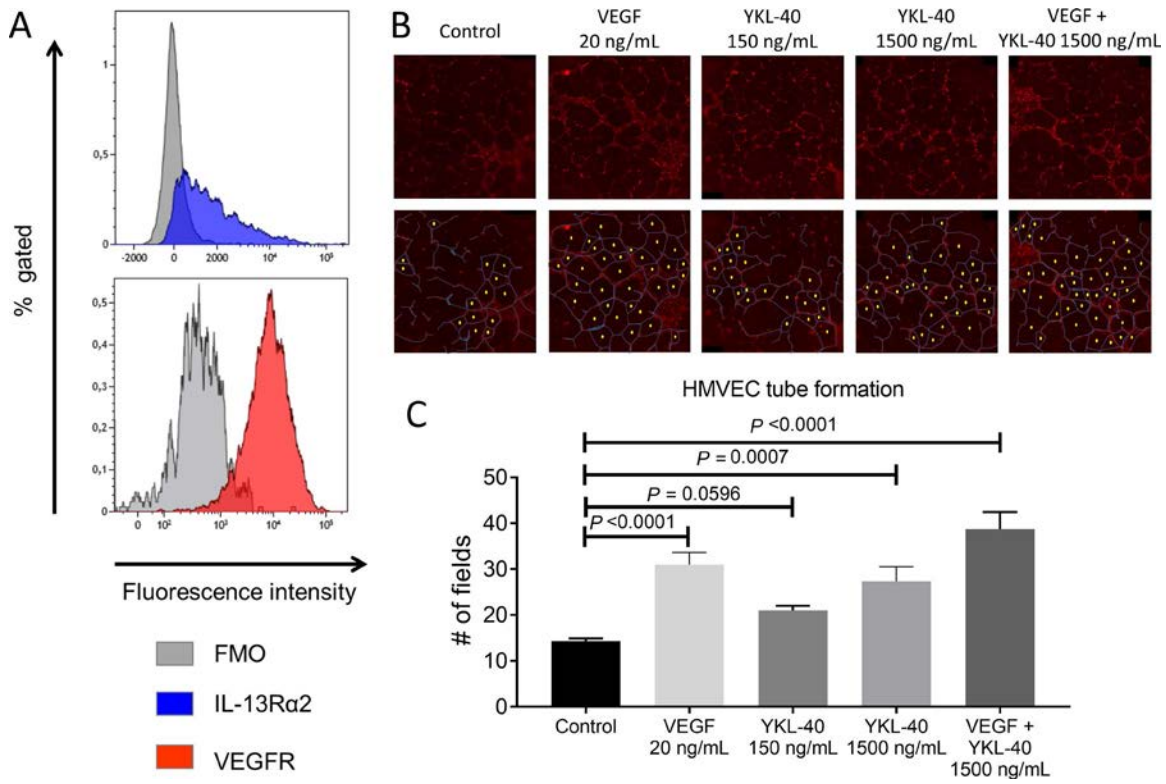

Figure 6. YKL-40 promotion of human microvascular endothelial cell (HMVEC) tube formation. **A**, Flow cytometry staining of CD31+ HMVECs showed abundant expression of interleukin-13 receptor α2 (IL-13Rα2) and vascular endothelial growth factor receptor (VEGFR). Three technical replicates are shown, comparing IL-13Rα2 and VEGFR stainings with "fluorescence minus one" (FMO) controls. **B**, HMVECs were treated with medium only (control) or the indicated concentrations of VEGF alone, YKL-40 alone, or VEGF and YKL-40. Representative images of tube formation are shown (top). Tube formation was assessed by counting the number of enclosed fields (bottom). The visible HMVEC membranes are indicated in blue, and the enclosed fields are marked with a yellow dot. **C**, Treatment of HMVECs with a higher concentration of YKL-40 induced more tube formation. Bars show the mean ± SD number of enclosed fields formed by HMVEC tube formation (triplicate experiments). *P* values were determined by analysis of variance with Tukey's post hoc test.

YKL-40 with IL-13Rα2 activates the Akt and ERK pathways, both required for MMP-9 expression (36–39). Although IL-13Rα2 was also found to be expressed by endothelial cells, smooth muscle cells, and fibroblasts in the vessel walls of individuals without GCA, its expression was highly increased in active GCA lesions, predominantly by infiltrating leukocytes. Interestingly, we found that IL-13Rα2 was only weakly expressed in temporal artery biopsy specimens from individuals without GCA or PMR (n = 2), indicating that up-regulation of IL-13Rα2 in vessel walls could be GCA/PMR specific. Further studies with more artery samples from individuals without GCA are warranted to confirm these findings.

Our data also suggest that YKL-40 may be an important mediator of neovascularization in GCA, a process that fuels the inflammatory response. The inflamed arteries of GCA patients show an expanded vasa vasorum, extending into the media and intima layers (40). YKL-40 may be one of the main instigators of this process, together with other proangiogenic molecules such as VEGF and angiopoietin 2 (10). Our tube formation assay confirms previous reports on the proangiogenic capacity of YKL-40 alone and in combination with VEGF, which is also highly expressed in GCA lesions (10,32). YKL-40 is also produced by tumor-associated macrophages, and likely plays a role in tumor angiogenesis and progression (14). Studies by Shao et al and Francescone et al showed increased CD31+ endothelial cell density in conjunction with increased expression of YKL-40 in breast cancer and glioblastoma tumors, respectively (32,41). Moreover, those studies also showed a significant reduction in CD31+ endothelial cell infiltration in tumors in mice treated with YKL-40 siRNA and YKL-40 neutralizing antibody. This tumor-supportive effect is reflected by an association of YKL-40 serum levels with a poor outcome in cancer patients. Consistent with these findings, we previously reported that high serum levels of YKL-40 in baseline GCA patients predicted a longer time to discontinuation of GC treatment (7).

Our data suggest an involvement of YKL-40 in tissue destruction and neoangiogenesis. YKL-40 may signal via IL-13Rα2, a known receptor for YKL-40, which we found to be expressed by endothelial cells at the site of inflammation in GCA. Efforts to silence this receptor using siRNA in vitro led to reduced transcript levels, but unfortunately did not suppress cell surface protein expression, suggesting a long half-life of this receptor (data not shown). Thus, we cannot exclude the possibility that the proangiogenic effects

of YKL-40 are mediated via another, not yet identified, receptor (32,41). Further studies are required to definitely prove a role for the YKL-40/IL-13Rα2 axis in neovascularization in GCA.

Although YKL-40 is becoming recognized as an important biomarker of inflammation, few mechanistic studies have been performed to investigate its role in autoinflammatory diseases such as GCA. In this study, we used a variety of approaches to identify the cellular source of YKL-40 and its function. Given the substantial effects of GCs on inflammatory processes, it is important to emphasize that we used tissues and cells from treatment-naive patients. Although our in vitro studies with cultured macrophages have elucidated YKL-40–mediated effects on MMP-9 production, the tissue microenvironment may interfere with these effects in more complex ways. Hence, further studies are required, in particular using in vivo or ex vivo models to improve our understanding of the role of YKL-40 in GCA pathogenesis.

Given its implication in various pathologic pathways, YKL-40 could be a promising target for treatment in macrophage-driven diseases. A neutralizing antibody targeting YKL-40 has shown potential in reducing angiogenesis and tumor progression (42). Blocking YKL-40 or IL-13Rα2 could also prove to be beneficial for the treatment of GCA. GCs, as well as new treatment options such as tocilizumab, may be able to temporarily repress symptoms in GCA patients (4). However, more emerging evidence has indicated that asymptomatic vessel wall inflammation persists, ultimately leading to relapses in a substantial subset of patients (6–9). The persistently high YKL-40 levels in spite of GC treatment, observed in our previous study (7) and confirmed in this study, suggest ongoing vascular inflammation and remodeling. This may be explained by the notion that YKL-40 expression is driven by a multitude of cytokines, including IL-6, GM-CS, and IFNγ (17,33). While IL-6 signaling may be terminated specifically by treatment with tocilizumab and partially by GC treatment, it appears that GM-CSF and IFNγ production are resistant to both drugs (12,43,44). Moreover, a study by Kunz et al revealed little effect of GC treatment on macrophage YKL-40 expression (33). Taken together, these observations are consistent with the persistence of YKL-40–mediated pathology in the vessel wall.

In conclusion, our findings show that a distinct subset of YKL-40–producing CD206+ macrophages is a characteristic feature of the vasculopathy in GCA. These macrophages may fuel media destruction, vasa vasorum neovascularization, and leukocyte invasion into the vessel wall. This process, likely mediated by the YKL-40/IL-13Rα2 axis, initiates a positive forward loop of proinflammatory and tissue remodeling processes via MMP-9 overexpression. Given its potential to promote several mechanisms involved in vessel wall injury, neutralizing YKL-40 or its upstream pathways may prove to be an interesting treatment option for GCA.

AUTHOR CONTRIBUTIONS

All authors were involved in drafting the article or revising it critically for important intellectual content, and all authors approved the final version to be published. Dr. van Sleen had full access to all of the data in the study and takes responsibility for the integrity of the data and the accuracy of the data analysis.

Study conception and design. van Sleen, Jiemy, Pringle, Brouwer, Heeringa, Boots.

Acquisition of data. van Sleen, Jiemy, Pringle.

Analysis and interpretation of data. van Sleen, Jiemy, van der Geest, Abdulahad, Sandovici, Brouwer, Heeringa, Boots.

REFERENCES

1. Samson M, Corbera-Bellalta M, Audia S, Planas-Rigol E, Martin L, Cid MC, et al. Recent advances in our understanding of giant cell arteritis pathogenesis [review]. Autoimmun Rev 2017;16:833–44.
2. Gonzalez-Gay MA, Garcia-Porrua C, Piñeiro A, Pego-Reigosa R, Llorca J, Hunder GG. Aortic aneurysm and dissection in patients with biopsy-proven giant cell arteritis from northwestern Spain: a population-based study. Medicine (Baltimore) 2004;83:335–41.
3. Nuenninghoff DM, Hunder GG, Christianson TJ, McClelland RL, Matteson EL. Incidence and predictors of large-artery complication (aortic aneurysm, aortic dissection, and/or large-artery stenosis) in patients with giant cell arteritis: a population-based study over 50 years. Arthritis Rheum 2003;48:3522–31.
4. Stone JH, Tuckwell K, Dimonaco S, Klearman M, Aringer M, Blockmans D, et al. Trial of tocilizumab in giant-cell arteritis. N Engl J Med 2017;377:317–28.
5. Schmidt WA. Ultrasound in the diagnosis and management of giant cell arteritis [review]. Rheumatology (Oxford) 2018;57 Suppl 2:ii22–31.
6. Maleszewski JJ, Younge BR, Fritzlen JT, Hunder GG, Goronzy JJ, Warrington KJ, et al. Clinical and pathological evolution of giant cell arteritis: a prospective study of follow-up temporal artery biopsies in 40 treated patients. Mod Pathol 2017;30:788–96.
7. Van Sleen Y, Sandovici M, Abdulahad W, Bijzet J, van der Geest K, Boots AM, et al. Markers of angiogenesis and macrophage products for predicting disease course and monitoring vascular inflammation in giant cell arteritis. Rheumatology (Oxford) 2019;58:1383–92.
8. Gloor AD, Yerly D, Adler S, Reichenbach S, Kuchen S, Seitz M, et al. Immuno-monitoring reveals an extended subclinical disease activity in tocilizumab-treated giant cell arteritis. Rheumatology (Oxford) 2018;57:1795–801.
9. Reichenbach S, Adler S, Bonel H, Cullmann JL, Kuchen S, Bütikofer L, et al. Magnetic resonance angiography in giant cell arteritis: results of a randomized controlled trial of tocilizumab in giant cell arteritis. Rheumatology (Oxford) 2018;57:982–6.
10. Kaiser M, Younge B, Björnsson J, Goronzy JJ, Weyand CM. Formation of new vasa vasorum in vasculitis: production of angiogenic cytokines by multinucleated giant cells. Am J Pathol 1999;155:765–74.
11. Watanabe R, Maeda T, Zhang H, Berry GJ, Zeisbrich M, Brockett R, et al. MMP (matrix metalloprotease)-9-producing monocytes enable T cells to invade the vessel wall and cause vasculitis. Circ Res 2018;31;123:700–15.
12. Cid M, Muralidharan S, Corbera-Bellalta M, Espigol-Frigole G, Hernandez JM, Denuc A, et al. Fri0010 GM-CSFR pathway is implicated in pathogenic inflammatory mechanisms in giant cell arteritis. Ann Rheum Dis 2020;79:576.
13. Jiemy WF, van Sleen Y, van der Geest KS, Ten Berge HA, Abdulahad WH, Sandovici M, et al. Distinct macrophage phenotypes skewed by local granulocyte macrophage colony-stimulating factor (GM-CSF) and macrophage colony-stimulating factor (M-CSF) are associated with tissue destruction and intimal hyperplasia in giant cell arteritis. Clin Transl Immunology 2020;27;9:e1164.
14. Libreros S, Iragavarapu-Charyulu V. YKL-40/CHI3L1 drives inflammation on the road of tumor progression [review]. J Leukoc Biol 2015;98:931–6.

15. Libreros S, Garcia-Areas R, Shibata Y, Carrio R, Torroella-Kouri M, Iragavarapu-Charyulu V. Induction of proinflammatory mediators by CHI3L1 is reduced by chitin treatment: decreased tumor metastasis in a breast cancer model. Int J Cancer 2012;15;131:377–86.
16. Johansen JS, Baslund B, Garbarsch C, Hansen M, Stoltenberg M, Lorenzen I, et al. YKL-40 in giant cells and macrophages from patients with giant cell arteritis. Arthritis Rheum 1999;42:2624–30.
17. Kzhyshkowska J, Mamidi S, Gratchev A, Kremmer E, Schmuttermaier C, Krusell L, et al. Novel stabilin-1 interacting chitinase-like protein (SI-CLP) is up-regulated in alternatively activated macrophages and secreted via lysosomal pathway. Blood 2006;15;107:3221–8.
18. Stone JH, Tuckwell K, Dimonaco S, Klearman M, Aringer M, Blockmans D, et al. Glucocorticoid dosages and acute-phase reactant levels at giant cell arteritis flare in a randomized trial of tocilizumab. Arthritis Rheumatol 2019;71:1329–38.
19. Fichtner-Feigl S, Strober W, Kawakami K, Puri RK, Kitani A. IL-13 signaling through the IL-13α 2 receptor is involved in induction of TGF-β 1 production and fibrosis. Nat Med 2006;12:99–106.
20. Lupardus PJ, Birnbaum ME, Garcia KC. Molecular basis for shared cytokine recognition revealed in the structure of an unusually high affinity complex between IL-13 and IL-13Rα2. Structure 2010;18:332–42.
21. Liu J, Li Y, Andiappan A, Yan Y, Tan K, Ong H, et al. Role of IL-13Rα2 in modulating IL-13-induced MUC 5 AC and ciliary changes in healthy and CRS w NP mucosa. Allergy 2018;73:1673–85.
22. Bhardwaj R, Suzuki A, Leland P, Joshi BH, Puri RK. Identification of a novel role of IL-13Rα2 in human Glioblastoma multiforme: interleukin-13 mediates signal transduction through AP-1 pathway. J Transl Med 2018;20;16:369.
23. Roy S, Liu H, Jaeson MI, Deimel LP, Ranasinghe C. Unique IL-13Rα2/STAT3 mediated IL-13 regulation detected in lung conventional dendritic cells, 24 h post viral vector vaccination. Sci Rep 2020;10:1017.
24. He CH, Lee CG, Cruz CS, Lee C, Zhou Y, Ahangari F, et al. Chitinase 3-like 1 regulates cellular and tissue responses via IL-13 receptor α2. Cell Rep 2013;4:830–41.
25. Xu N, Bo Q, Shao R, Liang J, Zhai Y, Yang S, et al. Chitinase-3-like-1 promotes M2 macrophage differentiation and induces choroidal neovascularization in neovascular age-related macular degeneration. Invest Ophthalmol Vis Sci 2019;60:4596–605.
26. Van der Geest KS, Abdulahad WH, Chalan P, Rutgers A, Horst G, Huitema MG, et al. Disturbed B cell homeostasis in newly diagnosed giant cell arteritis and polymyalgia rheumatica. Arthritis Rheumatol 2014;66:1927–38.
27. Samaniego R, Palacios BS, Domiguez-Soto Á, Vidal C, Salas A, Matsuyama T, et al. Macrophage uptake and accumulation of folates are polarization-dependent in vitro and in vivo and are regulated by activin A. J Leukoc Biol 2014;95:797–808.
28. Lukic A, Larssen P, Fauland A, Samuelsson B, Wheelock CE, Gabrielsson S, et al. GM-CSF–and M-CSF–primed macrophages present similar resolving but distinct inflammatory lipid mediator signatures. FASEB J 2017;31:4370–81.
29. Paquin-Proulx D, Greenspun BC, Pasquet L, Strunz B, Aleman S, Falconer K, et al. IL13Rα2 expression identifies tissue-resident IL-22-producing PLZF innate T cells in the human liver. Eur J Immunol 2018;48:1329–35.
30. Badalyan V, Thompson R, Addo K, Borthwick LA, Fisher AJ, Ort T, et al. TNF-α/IL-17 synergy inhibits IL-13 bioactivity via IL-13Rα2 induction. J Allergy Clin Immunol 2014;134:975–8.
31. Hecker M, Zasłona Z, Kwapiszewska G, Niess G, Zakrzewicz A, Hergenreider E, et al. Dysregulation of the IL-13 receptor system: a novel pathomechanism in pulmonary arterial hypertension. Am J Respir Crit Care Med 2010;182:805–18.
32. Shao R, Hamel K, Petersen L, Cao Q, Arenas RB, Bigelow C, et al. YKL-40, a secreted glycoprotein, promotes tumor angiogenesis. Oncogene 2009;28:4456.
33. Kunz LI, van't Wout EF, van Schadewijk A, Postma DS, Kerstjens HA, Sterk PJ, et al. Regulation of YKL-40 expression by corticosteroids: effect on pro-inflammatory macrophages in vitro and its modulation in COPD in vivo. Respir Res 2015;16:154.
34. Seidler S, Zimmermann HW, Bartneck M, Trautwein C, Tacke F. Age-dependent alterations of monocyte subsets and monocyte-related chemokine pathways in healthy adults. BMC Immunol 2010;11:30.
35. Van Sleen Y, Wang Q, van der Geest KS, Westra J, Abdulahad WH, Heeringa P, et al. Involvement of monocyte subsets in the immunopathology of giant cell arteritis. Sci Rep 2017;7:6553.
36. Ruhul Amin A, Senga T, Oo ML, Thant AA, Hamaguchi M. Secretion of matrix metalloproteinase-9 by the proinflammatory cytokine, IL-1β: a role for the dual signalling pathways, Akt and Erk. Genes Cells 2003;8:515–23.
37. Lee SJ, Lee YS, Seo KW, Bae JU, Kim GH, Park SY, et al. Homocysteine enhances MMP-9 production in murine macrophages via ERK and Akt signaling pathways. Toxicol Appl Pharmacol 2012;260:89–94.
38. Shim Y, Kang B, Jeon H, Park I, Lee K, Lee I, et al. Clusterin induces matrix metalloproteinase-9 expression via ERK1/2 and PI3K/Akt/NF-κB pathways in monocytes/macrophages. J Leukoc Biol 2011;90:761–9.
39. Lee Y, Tran HT, Van Ta Q. Regulation of expression of matrix metalloproteinase-9 by JNK in Raw 264.7 cells: presence of inhibitory factor (s) suppressing MMP-9 induction in serum and conditioned media. Exp Mol Med 2009;41:259–68.
40. Cid MC, Hernández-Rodríguez J, Esteban M, Cebrián M, Gho YS, Font C, et al. Tissue and serum angiogenic activity is associated with low prevalence of ischemic complications in patients with giant-cell arteritis. Circulation 2002;106:1664–71.
41. Francescone RA, Scully S, Faibish M, Taylor SL, Oh D, Moral L, et al. Role of YKL-40 in the angiogenesis, radioresistance, and progression of glioblastoma. J Biol Chem 2011;286:15332–43.
42. Faibish M, Francescone R, Bentley B, Yan W, Shao R. A YKL-40–neutralizing antibody blocks tumor angiogenesis and progression: a potential therapeutic agent in cancers. Mol Cancer Ther 2011;10:742–51.
43. Weyand CM, Hicok KC, Hunder GG, Goronzy JJ. Tissue cytokine patterns in patients with polymyalgia rheumatica and giant cell arteritis. Ann Intern Med 1994;121:484–91.
44. Deng J, Younge BR, Olshen RA, Goronzy JJ, Weyand CM. Th17 and Th1 T-cell responses in giant cell arteritis. Circulation 2010;23;121:906–15.

Arthritis & Rheumatology
Vol. 73, No. 12, December 2021, pp 2338–2347
DOI 10.1002/art.41814
© 2021 The Authors. *Arthritis & Rheumatology* published by Wiley Periodicals LLC on behalf of American College of Rheumatology.
This is an open access article under the terms of the Creative Commons Attribution-NonCommercial License, which permits use, distribution and reproduction in any medium, provided the original work is properly cited and is not used for commercial purposes.

American College of Rheumatology
Empowering Rheumatology Professionals

Anticentromere Antibody Levels and Isotypes and the Development of Systemic Sclerosis

Nina M. van Leeuwen,[1] Maaike Boonstra,[1] Jaap A. Bakker,[1] Annette Grummels,[1] Suzana Jordan,[2] Sophie Liem,[1] Oliver Distler,[2] Anna-Maria Hoffmann-Vold,[3] Karin Melsens,[4] Vanessa Smith,[4] Marie-Elise Truchetet,[5] Hans U. Scherer,[1] René Toes,[1] Tom W. J. Huizinga,[1] and Jeska K. de Vries-Bouwstra[1]

Objective. Little is known on the disease course of very early systemic sclerosis (SSc). Among the information yet to be elucidated is whether anticentromere antibody (ACA) isotype levels can serve as biomarkers for future SSc development and for organ involvement. This study was undertaken to evaluate whether IgG, IgM, and IgA ACA levels in IgG ACA–positive patients are associated with disease severity and/or progression from very early SSc to definite SSc.

Methods. IgG ACA–positive patients from 5 different cohorts who had very early SSc or SSc fulfilling the American College of Rheumatology (ACR)/European Alliance of Associations for Rheumatology (EULAR) 2013 criteria were included. A diagnosis of very early SSc was based on the presence of IgG ACAs and Raynaud's phenomenon, and/or puffy fingers and/or abnormal nailfold capillaroscopy, but not fulfilling the ACR/EULAR 2013 criteria for SSc. Multivariable regression analyses were performed to determine the association between baseline ACA isotype levels and progression to definite SSc with organ involvement.

Results. Six hundred twenty-five IgG ACA–positive patients were included, of whom 138 (22%) fulfilled the criteria for very early SSc and 487 (78%) had definite SSc. Levels of IgG ACAs (odds ratio 2.5 [95% confidence interval 1.8–3.7]) and IgM ACAs (odds ratio 1.8 [95% confidence interval 1.3–2.3]) were significantly higher in patients with definite SSc. Of 115 patients with very early SSc with follow-up, progression to definite SSc occurred within 5 years in 48 (42%). Progression to definite SSc was associated with higher IgG ACA levels at baseline (odds ratio 4.3 [95% confidence interval 1.7–10.7]).

Conclusion. ACA isotype levels may serve as biomarkers to identify patients with very early SSc who are at risk for disease progression to definite SSc.

INTRODUCTION

Systemic sclerosis (SSc) is a heterogeneous autoimmune disease with high mortality and morbidity (1,2). As early intervention has been shown to improve disease course and outcome, it is very important to detect SSc at an early stage, when therapeutic interventions can prevent progression of organ damage (3,4). The American College of Rheumatology (ACR)/European Alliance of Associations for Rheumatology (EULAR) 2013 criteria for SSc have a high sensitivity for accurately classifying patients as having SSc (5). However, there are still patients who do not fulfill these criteria, despite exhibiting early signs of SSc (6). Currently, there are no biomarkers to identify which patients with signs of very early SSc will progress to having definite SSc. Identification of this subgroup of patients with very early SSc, with more precise insights into

Dr. Smith is a Senior Clinical Investigator of the Research Foundation, Flanders Belgium (FWO 1.8.029.20N).

[1]Nina M. van Leeuwen, MD, Maaike Boonstra, MD, Jaap A. Bakker, PhD, Annette Grummels, BSc, Sophie Liem, MD, Hans U. Scherer, MD, PhD, René Toes, PhD, Tom W. J. Huizinga, MD, Jeska K. de Vries-Bouwstra, MD, PhD: Leiden University Medical Center, Leiden, The Netherlands; [2]Suzana Jordan, PhD, Oliver Distler, MD: University Hospital Zurich, Zurich, Switzerland; [3]Anna-Maria Hoffmann-Vold, MD, PhD: Oslo University Hospital and Rikshospitalet, Oslo, Norway; [4]Karin Melsens, MD, Vanessa Smith, MD: Ghent University, Ghent University Hospital, and VIB-UGent Center for Inflammation Research, Ghent, Belgium; [5]Marie-Elise Truchetet, MD, PhD: Bordeaux University Hospital, Bordeaux, France.

Dr. Distler has received consulting fees, speaking fees, and/or honoraria from AbbVie, Actelion, Acceleron, Amgen, AnaMar, Beacon Discovery, Blade Therapeutics, Bayer, Boehringer Ingelheim, Catenion, Competitive Corpus, Drug Development International, CSL Behring, Chemomab, ErgoNex, Galápagos, Glenmark, GlaxoSmithKline, Horizon, Inventiva, Italfarmaco, iQone, IQVIA, Kymera, Lilly, Medac, Medscape, Mitsubishi Tanabe Pharma, MSD, Novartis, Pfizer, Roche, Sanofi, Target BioScience, and UCB (less than $10,000 each) and holds a patent for miR-29 in the treatment of systemic sclerosis (US8247389, EP2331143). No other disclosures relevant to this article were reported.

Address correspondence to Nina M. van Leeuwen, MD, Sint Franciscus Hospital, Kleiweg 500, 3045 PM Rotterdam, The Netherlands. Email: n.vanleeuwen91@gmail.com.

Submitted for publication August 13, 2020; accepted in revised form May 11, 2021.

their potential disease course, is crucial for early therapeutic interventions (7).

SSc-specific antinuclear autoantibodies (ANAs) are commonly used for disease and risk stratification. Anti–topoisomerase I antibodies and anticentromere antibodies (ACAs) are the most prevalent autoantibodies in SSc (8). The presence of ACAs is associated with limited skin involvement, higher prevalence of calcinosis, and gastrointestinal (GI) involvement (9–11). Compared to most other SSc-associated autoantibodies, the presence of ACAs generally carries a better prognosis with respect to survival (10,12). The major reactive antigen of ACAs has been identified as CENP-B, which has therefore been suggested as the primary target driving a selected B cell response characterized by IgG ACA production (13,14). Based on the observation that the generation of disease-specific ANAs is closely linked to disease development and clinical phenotype, it has been hypothesized that ANAs are implicated in disease pathogenesis (15–17). However, the exact role of these disease-specific ANAs and their underlying antigen triggers in SSc remains unclear.

In rheumatoid arthritis (RA), an autoimmune disease characterized by polyarthritis and the presence of rheumatoid factor and anti–citrullinated protein antibodies (ACPAs), an extended ACPA repertoire has been shown to be associated with disease development and disease severity, while the effector function of ACPAs is still not elucidated (18–20). At present, little information is available regarding ACA isotype levels in SSc. Detailed information on the ACA isotype distribution in ACA-positive patients with SSc can contribute to a better understanding of the characteristics and dynamics of the underlying autoreactive B cell response. Consistent with findings in RA, we hypothesize that in IgG ACA–positive SSc, the expansion of specific ACA isotype responses is associated with SSc development and severity, as reflected by organ involvement.

By taking advantage of the prospective and comprehensive clinical data available from 5 independent and well-described SSc cohorts (Leiden, Oslo, Zurich, Ghent, and Bordeaux), we aimed to evaluate whether individual ACA isotype levels are associated with disease severity in IgG ACA–positive patients with SSc. We also investigated whether these levels can identify subjects with very early SSc whose condition will progress to definite SSc.

PATIENTS AND METHODS

Patient population. The SSc cohorts in Leiden, Oslo, Zurich, Ghent, and Bordeaux are prospective cohorts including all consecutive patients with SSc (21–26). Patients in these cohorts undergo annual extensive screening, which includes a complete physical examination, laboratory testing, pulmonary function testing, transthoracic echocardiography, high-resolution computed tomography (HRCT), 24-hour electrocardiography, nailfold capillaroscopy (NFC) evaluation, and an optional cardiopulmonary exercise test. At every visit, blood samples are collected and stored in respective biobanks (27).

IgG ACA–positive patients who were included had to fulfill either the ACR/EULAR 2013 criteria for SSc (5) or criteria for very early SSc (28,29). Patients were classified as having very early SSc if they were IgG ACA positive and had Raynaud's phenomenon (RP) and/or puffy fingers and/or abnormal NFC, but did not fulfill the ACR/EULAR 2013 criteria for SSc (5,28,29). In this study, we used a prospectively collected data set from routine practices with post hoc analyses. Patients entering the cohorts before March 2019 were selected for the present study. Detailed information on all of the cohorts has been previously reported (21,23–25,30–32).

Ethics approval. Collection of biomaterials and analysis of their clinical associations was approved by the local ethics committees in Leiden (CME no. B16.037), Switzerland (no. PB 2016-02014 02014 and BASEC-Nr. 2018-01873), Norway (no. 2006/119), Ghent (no. 2008/385), and Bordeaux (no. 2012-A00081-42). All participants provided written informed consent.

Clinical characteristics. At the baseline visit, clinical data and blood samples (including samples obtained for autoantibody testing) were collected from all patients. Baseline was defined as the first visit in the SSc care pathway, which included screening for SSc. Patients were involved in the development of the SSc care pathway. Patients with SSc who fulfilled the ACR/EULAR 2013 criteria were categorized as having definite SSc either without organ involvement or with organ involvement, as described below.

For analyses, patients were categorized as having 1) very early SSc, 2) definite SSc without organ involvement, or 3) definite SSc with organ involvement. Follow-up data were collected only for the very early SSc group, as data from this group of patients were of particular interest due to the possibility of intervention early in their disease course. Follow-up consisted of an annual assessment in the SSc care pathway to monitor the course of the disease, including evaluations of the organ systems (skin, lung, heart, GI, renal, and musculoskeletal). Follow-up duration was defined as the time calculated from the baseline visit to the most recent visit. Disease duration was defined as the time from RP onset, since among patients with very early SSc, data on the time from onset of the first non-RP symptom were missing in those who did not have puffy fingers. We recorded the clinical characteristics required to evaluate the disease status of the patients (very early SSc, SSc with organ involvement, or SSc without organ involvement). The modified Rodnan skin thickness score (MRSS) (33), sclerodactyly, puffy fingers, peripheral vascular involvement including pitting scars, digital ulcers, and telangiectasia were evaluated and reported by the physician during evaluation. The NFC result was considered

abnormal if a scleroderma pattern was present, in accordance with the definitions approved by the EULAR Study Group on Microcirculation in Rheumatic Diseases and Scleroderma Clinical Trials Consortium (34,35). Use of immunosuppressive treatment at baseline, including hydroxychloroquine, mycophenolate mofetil, methotrexate, cyclophosphamide, azathioprine, and glucocorticoids, was recorded. Only ~0.5% of the patients were receiving biologic treatment at baseline; therefore, this was not considered.

Organ involvement. Digital ulcers were defined as areas with visually discernible depth and a loss of continuity of epithelial coverage and included both ischemic and traumatic ulcers. Interstitial lung disease (ILD) was considered to be present when evidenced on HRCT imaging. Myocardial involvement was assessed using a modified Medsger severity scale (36), which consists of at least 2 of the following: arrhythmias (>2% supraventricular and ventricular extrasystoles, or atrial fibrillation), conduction problems (bundle branch block), decreased left ventricular ejection fraction <54%, diastolic/systolic dysfunction, pericarditis, or pericardial effusion.

Pulmonary arterial hypertension (PAH) was defined as an increase in mean pulmonary arterial pressure of ≥25 mm Hg at rest as assessed by right heart catheterization, including the presence of precapillary pulmonary hypertension (PH), defined by a pulmonary capillary wedge pressure of ≤15 mm Hg and a pulmonary vascular resistance of >3 Wood units, in the absence of other causes of precapillary PH (i.e., PH due to lung diseases, chronic thromboembolic PH, or other rare diseases) (37). Renal crisis was defined based on clinical data (including an increase in blood pressure, increase in creatinine level, and oligo/anuric renal failure). GI involvement was defined based on a composite variable: presence of confirmed gastric antral vascular ectasia (GAVE) (data available for all patients), presence of fecal incontinence (data available for 413 of 625 patients), and/or malabsorption syndrome (data available for 317 of 625 patients), and/or weight loss >10% in 1 year (data available for 309 of 625 patients). Patients with very early SSc were considered to be progressors to definite SSc if they developed ILD, digital ulcers, PAH, renal crisis, myocardial involvement, or GI involvement and if they met the ACR/EULAR 2013 criteria during follow-up.

Anticentromere assay and measurement. Blood samples were stored, collected, and processed in accordance with the European Scleroderma Trials and Research biobank recommendations (27). All baseline samples were assessed in the clinical chemistry department of the Leiden University Medical Center. Total IgG, IgA, and IgM ACA levels (CENP-B) in all samples were measured by one of the authors (JAB) with an enzyme immunoassay (FEIA) using a Phadia 250 system (ThermoFisher Scientific). Immunofluorescence (IF) patterns were evaluated at baseline, and centromere ANA patterns (speckled) were found. IgG ACA levels (IgG CENP-B) were usually measured at commercial laboratories. The cutoff level for IgG ACA positivity was set at 7 units/ml, according to the manufacturer's instructions. IgM and IgA ACAs levels were defined as research-only parameters by the manufacturer. To define cutoff values for these parameters, levels in sera from 50 healthy subjects were measured, and the cutoff values for the presence of IgM and IgA were defined as 2 SD above the mean in these serum samples. The cutoff value for IgA ACAs was 37 arbitrary units (AU)/ml, and the cutoff value for IgM ACAs was 13 AU/ml.

Statistical analysis. Analyses were performed using IBM SPSS version 23, and graphs were created using GraphPad Prism 7 software. Descriptive statistics were used to summarize clinical and serologic features. To compare continuous independent variables, the Mann-Whitney U test was used for 2 groups, and the Kruskal-Wallis test with correction for multiple comparisons was used for >2 groups. Categorical variables were compared using the chi-square test. To evaluate cross-sectional associations between isotype levels and disease status, we used binary logistic regression with adjustment for age and disease duration (isotype levels [continuous; each isotype tested in a separate model] as predictor, and disease status [very early SSc, definite SSc without organ involvement, or definite SSc with organ involvement] as outcome measure).

Longitudinal analyses included the clinical evaluation of patients with very early SSc over time and progression of organ involvement in patients with definite SSc. To compare the clinical differences between progressors and nonprogressors, the Mann-Whitney U test and chi-square test were used. Multivariable logistic regression was used to assess the independent association between isotype levels and disease progression (isotype levels [continuous; each isotype tested in a separate model] as predictor, and disease progression [yes/no] as outcome measure), and receiver operating characteristic (ROC) curves were evaluated (Supplementary Figure 1 available on the *Arthritis & Rheumatology* website at http://onlinelibrary.wiley.com/doi/10.1002/art.41814/abstract). The possibility of predicting disease progression to definite SSc based on IgG ACA level was evaluated. Data from the previous evaluation were carried forward and applied if follow-up data on ILD, PAH, and ejection fraction were missing (generally occurring if disease was clinically stable with stable pulmonary function test results, meaning additional testing was not performed). As data on the individual components of the composite GI involvement variable were not complete for all patients, the validity of this parameter was verified in a sensitivity analysis using the subgroup with complete data (Supplementary Table 1, http://onlinelibrary.wiley.com/doi/10.1002/art.41814/abstract).

Data availability. All data relevant to this study are available in the manuscript, supplementary data files, and upon request from the corresponding author.

RESULTS

Clinical characteristics. In total, 625 IgG ACA–positive patients were included. Ninety percent (n = 558) were women, with a mean age of 58 years and a median disease duration since the first non-RP symptom of 6 years (interquartile range 2–9). Baseline characteristics of the 3 clinical groups are shown in Table 1. One hundred thirty-eight patients (22%) had very early SSc, 240 (38%) had SSc without organ involvement, and 247 (40%) had SSc with organ involvement.

IgG, IgM, and IgA ACA levels. Among all IgG ACA–positive subjects, 437 (76%) were also IgA ACA positive at baseline and 522 (89%) were also IgM ACA positive at baseline. A noncutaneous disease subset was more common in patients who were positive for both IgG and IgA ACAs compared to patients who were positive for IgG and IgM ACAs and patients who were positive for all 3 isotypes (47% versus 33% versus 27%, respectively). No other clinical differences were observed between subgroups defined by numbers of expressed isotypes (data not shown). Among patients in the very early SSc group, IgG and IgM ACA levels were significantly lower compared to patients in the definite SSc group (Figure 1 and Supplementary Figure 2, available on the *Arthritis & Rheumatology* website at http://onlinelibrary.wiley.com/doi/10.1002/art.41814/abstract). Using logistic regression with adjustment for age and disease duration since the first RP symptom, we found a significant association of IgG ACA levels (odds ratio 2.54 [95% confidence interval 1.75–3.69]) and IgM ACA levels (odds ratio 1.77 [95% confidence interval 1.34–2.34]) with disease status, with higher levels in patients with SSc (with and without organ involvement combined) compared to those with very early SSc. No significant associations were found between IgG, IgM, or IgA ACA isotype levels and definite SSc with or without organ involvement (Table 2). Findings confirming the same trend across all SSc centers are shown in Supplementary Table 2 and Supplementary Figures 3 and 4 (http://onlinelibrary.wiley.com/doi/10.1002/art.41814/abstract).

To assess a possible effect of immunomodulatory treatment on ACA isotype levels, we performed a logistic regression analysis. No significant associations were found between use of immunosuppressive treatment and IgG ACA levels (odds ratio 1.4 [95% confidence interval 0.91–2.10]), IgM ACA levels (odds ratio 0.91

Table 1. Baseline characteristics and ACA isotype expression and levels in patients with very early SSc and patients with SSc without or with organ involvement*

Characteristic (n with data available)	Patients with very early SSc (n = 138)	Patients with SSc without organ involvement (n = 240)	Patients with SSc with organ involvement (n = 247)
Female (n = 625)	125 (91)	225 (91)	208 (87)
Age, median (IQR) years (n = 625)	52 (40–62)	57 (49–66)	62 (52–69)
Time since RP onset, median (IQR) years (n = 622)	5 (1–12)	10 (3–19)	8 (2–18)
Time since non-RP onset, median (IQR) years (n = 465)	NA	5 (2–11)	6 (2–12)
lcSSc (n = 482)	NA	202 (84)	187 (78)
dcSSc (n = 482)	NA	14 (6)	27 (11)
MRSS, median (IQR) (n = 589)	0 (0–0)	3 (0–5)	4 (0–6)
Digital ulcers (n = 616)	0	0	81 (33)
FVC % predicted, mean ± SD (n = 585)	107 (17)	107 (17)	107 (19)
DLco % predicted, mean ± SD (n = 596)	81 (15)	74 (14)	67 (18)
ILD on HRCT (n = 625)	0	0	86 (36)
PAH (n = 625)	0	0	52 (21)
Myocardial involvement (n = 563)	0	0	42 (22)
Renal crisis (n = 625)	0	0	3 (1)
GI involvement (n = 625)	0	0	120 (49)
Puffy fingers (n = 548)	21 (16)	71 (39)	36 (23)
Abnormal NFC (n = 488)	69 (55)	160 (84)	149 (86)
Immunosuppressive treatment (n = 625)	25 (18)†	48 (20)	112 (46)
ACA characteristics			
IgA positivity (n = 617)	88 (72)	177 (78)	172 (75)
IgM positivity (n = 617)	106 (86)	209 (91)	207 (90)
IgG level, median (IQR) units/ml (n = 617)	274 (93–662)	480 (197–990)	619 (263–1,077)
IgM level, median (IQR) AU/ml (n = 617)	101 (41–363)	183 (55–907)	251 (63–965)
IgA level, median (IQR) AU/ml (n = 617)	69 (35–103)	78 (39–166)	86 (37–187)

* Except where indicated otherwise, values are the number (%). ACA = anticentromere antibody; SSc = systemic sclerosis; IQR = interquartile range; RP = Raynaud's phenomenon; NA = not applicable; lcSSc = limited cutaneous SSc; dcSSc = diffuse cutaneous SSc; MRSS = modified Rodnan skin thickness score; FVC = forced vital capacity; DLco = diffusing capacity for carbon monoxide; ILD = interstitial lung disease; HRCT = high-resolution computed tomography; PAH = pulmonary arterial hypertension; GI = gastrointestinal; NFC = nailfold capillaroscopy.
† Eight patients were treated with glucocorticoids, 12 with methotrexate, and 5 with hydroxychloroquine.

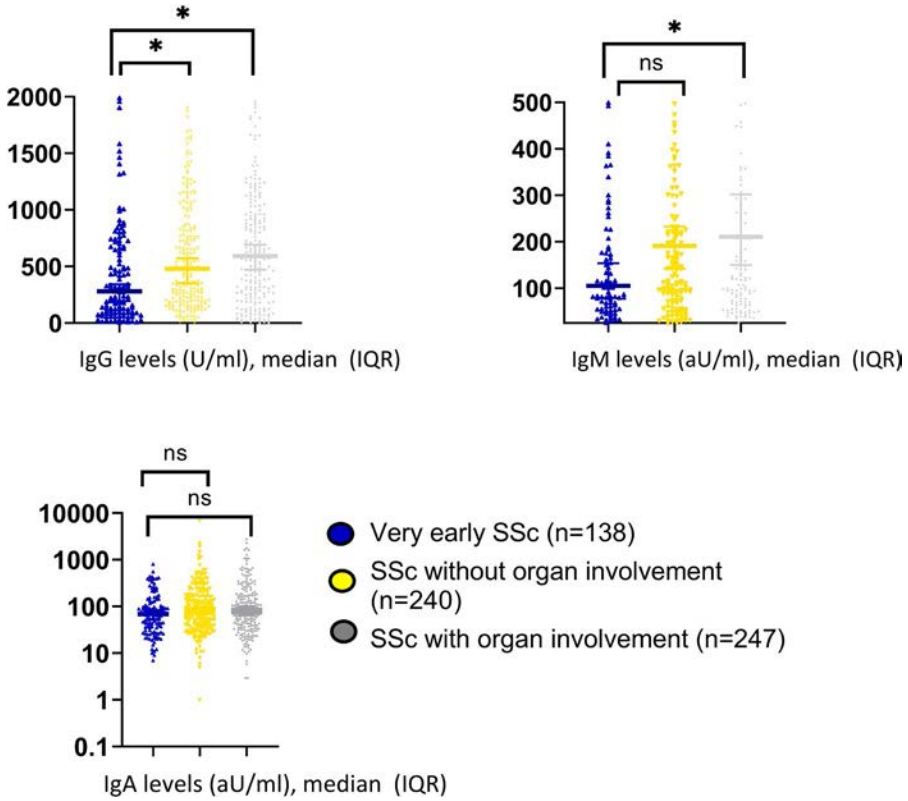

Figure 1. Anticentromere antibody (ACA) isotype levels in patients with very early systemic sclerosis (SSc), those with definite SSc without organ involvement, and those with definite SSc with organ involvement. Levels of IgG, IgM, and IgA ACAs in each group are shown. IgG and IgM ACA levels were significantly higher in patients with definite SSc with organ involvement compared to those with very early SSc; IgG ACA levels were also significantly higher in patients with definite SSc without organ involvement compared to those with very early SSc. Symbols represent individual patients; bars show the median and interquartile range (IQR). * = $P < 0.05$. NS = not significant.

[95% confidence interval 0.68–1.22]), or IgA ACA levels (odds ratio 0.74 [95% confidence interval 0.43–1.29]).

Evolution of very early SSc to definite SSc. Of the 138 patients classified as having very early SSc, 23 were lost to follow-up (Supplementary Table 3, http://onlinelibrary.wiley.com/doi/10.1002/art.41814/abstract). In total, 48 (42%) experienced disease progression to definite SSc during a median follow-up period of 2 years (range 1–4). Of these progressors, 22 (46%) developed vital organ involvement, which consisted of ILD (n = 10; 21%), cardiac involvement (n = 5; 10%), or GI involvement (n = 7; 16%). Seventy-seven percent of progressors developed skin involvement, including an increase based on the minimum clinically important difference in MRSS (n = 11; 23%) (38), development of telangiectasia (n = 31; 65%), or sclerodactyly (n = 18; 38%). Both digital ulcers and pitting scars occurred in 17% of progressors. The remaining 67 patients did not develop organ involvement and their disease did not progress to fulfilling the ACR/EULAR 2013 criteria for SSc after a median follow-up of 2 years (range 1–5).

Compared to patients considered to be nonprogressors, those who were considered to be progressors were older and had a longer median follow-up duration (Table 3). IgG ACA levels were significantly higher in progressors compared to nonprogressors at baseline and also after adjustment for follow-up duration

Table 2. Association of IgG and IgM ACA levels with baseline disease status and progression to definite SSc*

	SSc vs. very early SSc, OR (95% CI)	SSc with organ involvement vs. SSc without organ involvement, OR (95% CI)	Very early SSc progression to definite SSc, OR (95% CI)
IgG ACA units/ml	2.54 (1.75–3.69)	1.09 (0.77–1.53)	4.27 (1.70–10.71)
IgM ACA AU/ml	1.77 (1.34–2.34)	1.11 (0.83–1.26)	1.75 (0.97–3.14)
IgA ACA AU/ml	1.40 (0.90–2.17)	0.96 (0.67–1.38)	1.36 (0.47–3.96)

* Odds ratios (ORs) were adjusted for age and disease duration. IgG, IgM, and IgA anticentromere antibody (ACA) levels were $\log_2$-transformed to overcome skewness in the data. Data on ACA isotype levels were available for 115 patients with very early systemic sclerosis (SSc). 95% CI = 95% confidence interval.

Table 3. Demographic and clinical characteristics of the patients with very early SSc whose disease progressed (progressors) and patients with very early SSc whose disease did not progress (nonprogressors) at follow-up*

	Progressor group (n = 48)	Nonprogressor group (n = 67)	*P*
Demographic characteristics			
Female	43 (90)	61 (91)	0.52
Age, mean ± SD years	53 (15)†	48 (13)	0.03
Disease duration since RP onset, median (IQR) years	5 (2–11)	6 (2–14)	0.69
Follow-up duration, median (IQR) years	5 (3–7)‡	2 (1–5)	<0.001
Clinical features			
Puffy fingers§	7 (15)	8 (12)	0.55
Abnormal NFC¶	26 (54)	34 (51)	0.45
ACA isotype#			
IgM positivity	36 (86)	51 (81)	0.36
IgA positivity	31 (76)	43 (68)	0.28

* Except where indicated otherwise, values are the number (%). No clinical follow-up data were available for 23 patients with very early systemic sclerosis (SSc). RP = Raynaud's phenomenon; IQR = interquartile range; NFC = nailfold capillaroscopy; ACA = anticentromere antibody.
† $P = 0.03$ versus nonprogressor group.
‡ $P < 0.001$ versus nonprogressor group.
§ Missing data for 10 patients.
¶ Missing data for 2 patients.
# Missing data for 9 patients (5 in the progressor group and 4 in the nonprogressor group).

(Figure 2). In logistic regression analyses with correction for age and follow-up duration, IgG ACA levels were significantly associated with disease progression to definite SSc (odds ratio 4.27 [95% confidence interval 1.70–10.71]) (Table 2). Puffy fingers were a significant predictor of progression to definite SSc in the univariable analysis (odds ratio 2.95 [95% confidence interval 1.31–6.62]),

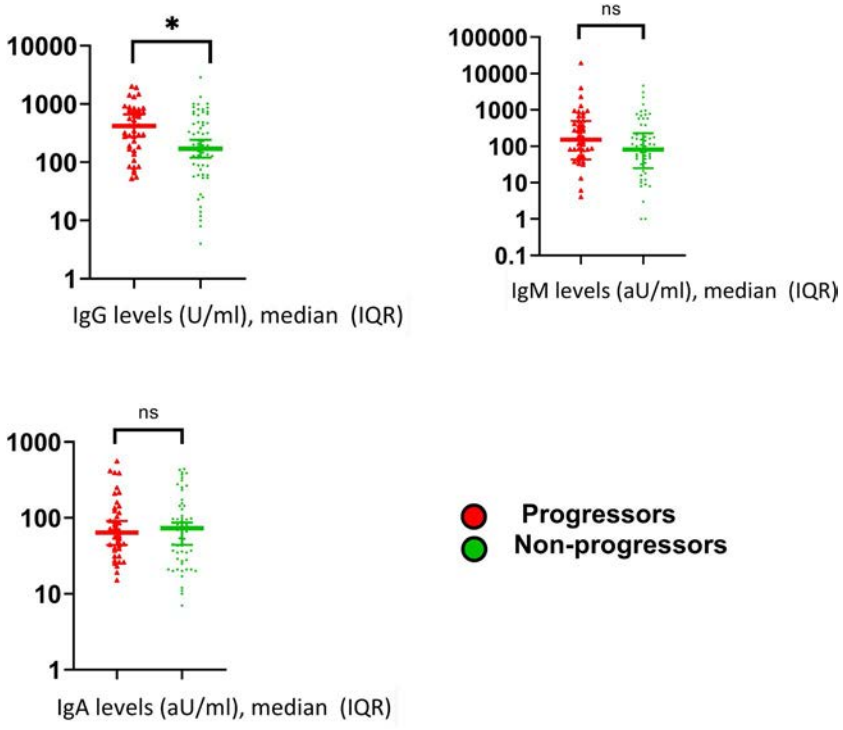

Figure 2. Anticentromere antibody (ACA) isotype levels in progressors and nonprogressors in the very early systemic sclerosis (SSc) group. IgG ACA levels were higher in patients with very early SSc whose condition progressed to definite SSc compared to nonprogressors. Symbols represent individual patients; bars show the median and interquartile range (IQR). * = $P < 0.05$. NS = not significant. Color figure can be viewed in the online issue, which is available at http://onlinelibrary.wiley.com/doi/10.1002/art.41814/abstract.

whereas abnormal NFC did not show a significant association with progression to definite SSc (Supplementary Table 4, http://onlinelibrary.wiley.com/doi/10.1002/art.41814/abstract). The ROC curves for progression to definite SSc in association with levels of IgG and IgM ACAs are shown in Supplementary Figures 1 and 5, with performance characteristics shown in Supplementary Tables 5 and 6 (http://onlinelibrary.wiley.com/doi/10.1002/art.41814/abstract). When we applied a threshold for the optimal sensitivity and negative predictive value for prediction of progression to definite SSc, we identified an IgG ACA level of 81 units/ml together with the presence of puffy fingers as having predictive capacity at baseline (Supplementary Figure 7). With this cutoff, 84% of progressors and 49% of nonprogressors were classified correctly at baseline. To further evaluate the predictive value of ACA isotype levels in SSc progression, we assessed their association with disease progression in patients with definite SSc at baseline and complete clinical data available at follow-up (n = 93) (Supplementary Table 5, http://onlinelibrary.wiley.com/doi/10.1002/art.41814/abstract). In this subgroup, levels of IgG ACAs (odds ratio 2.79 [95% confidence interval 1.08–7.26]) and levels of IgM ACAs (odds ratio 2.06 [95% confidence interval 1.18–3.61]) were independently associated with disease progression.

DISCUSSION

In this study, we analyzed ACA isotype levels in patients with very early SSc and in patients with definite SSc to evaluate whether disease severity within ACA-positive patients is associated with characteristics of the ACA immune response. Secondly, we evaluated the clinical course of patients with very early SSc and assessed whether ACA isotype levels can identify subjects whose condition will progress to definite SSc. We demonstrated that patients with definite SSc have higher levels of IgG and IgM ACAs compared to patients with very early SSc. Moreover, we showed that in patients with very early SSc, higher levels of IgG ACAs are associated with disease progression to definite SSc within 2 years.

The lower IgG and IgM ACA levels in the very early SSc group might indicate a less pronounced immune response compared to the definite SSc group. We identified the highest levels of IgG, IgM, and IgA ACAs to be present in patients with SSc with organ involvement, and in patients with definite SSc, baseline IgG and IgM ACA levels were associated with future disease progression. These findings are consistent with our hypothesis that the immune response in patients with very early SSc is less pronounced compared to patients with definite SSc.

As shown by our data and by other study findings (30), although the classification might suggest short disease duration, some patients classified as having very early SSc showed similar disease duration as patients with definite SSc. This indicates that patients who fulfill the classification criteria for very early SSc are a heterogeneous group, in which the condition will eventually progress to definite SSc in some and will continue to only meet criteria for very early SSc in others (30). Our data show that the levels of ACA-specific immune response discriminate between those 2 subgroups (Supplementary Figure 1, http://onlinelibrary.wiley.com/doi/10.1002/art.41814/abstract). Similar findings have been observed in other rheumatic diseases, including RA (18,39). The observation that IgG ACA levels are numerically higher in patients with SSc who are positive for ACAs with organ involvement compared to patients with SSc who are positive for ACAs without organ involvement is consistent with our hypothesis. However, in this comparison, the differences observed were not statistically significant. We presume that the absence of broadly validated outcome measures for SSc might at least partially explain this lack of significance. Moreover, commonly accepted definitions of severe organ involvement such as ILD and diffuse skin involvement might be less sensitive in ACA-positive SSc, as severe fibrotic disease complications are less frequent in patients with ACAs than in anti–topoisomerase I–positive patients.

To date, the effects of disease duration on isotype levels are not fully understood. One could hypothesize that isotype levels decrease over time as antigen triggering diminishes (40). Whether ACA-specific immune response occurs before clinical disease development, and for how long, is unknown. One study showed that in patients with early SSc, the median duration from the time of RP onset to definite SSc was 4.6 years (41). There were no data reported regarding the first instance of specific antibody expression or different autoantibodies in that study. In our very early SSc group, 48 patients (42%) developed definite SSc over a median time period of 5 years.

We observed the strongest association between IgG ACA levels and disease subset (very early SSc versus definite SSc). Consistent with our hypothesis, it is tempting to speculate that either IgG ACAs and/or B cell responses underlying ACA production are involved in the disease pathogenesis. Since both microangiopathy (clinically shown by RP) and dysregulated immunity (reflected by the presence of specific ANAs) are among the earliest features of SSc, it could be speculated that specifically IgG and IgM ACAs contribute to endothelial cell damage, possibly by complement activation. Indeed, ACA-positive sera have been shown to affect endothelial cells (42). In the Leiden cohort, we recently demonstrated an association between ACA-specific immune response and degree of microangiopathy (43).

Finally, there are a number of possible implications of an association between both IgM and IgG ACAs and disease progression. In adaptive immune responses, IgM is the first isotype to appear after a vaccination or an infection. In normal adaptive immune responses, IgM disappears rapidly due to isotype switching with IgG taking over, and antibodies of the IgM isotype have a short lifespan (T½ = 8 days). The ongoing presence of IgM ACAs along with the association of levels of IgG ACAs with disease progression in the present study indicate ongoing immune activation accompanied by continuous production of IgM, which is most likely caused by recently activated B cells. Since there

is no evidence regarding the natural origin of IgA ACAs in SSc pathogenesis, we can only speculate about the implication of the high prevalence of IgA ACAs that was also observed. IgA is mostly found in mucous membranes, particularly the respiratory tract and the GI tract; as such, expression of disease-specific IgA ACAs might implicate involvement of these mucous membranes in SSc pathogenesis. Frequent pulmonary and GI involvement in patients with SSc supports this hypothesis, but how and where IgA ACAs are triggered is currently unknown.

Puffy fingers or abnormal NFC were found to be predictive of the diagnosis of very early SSc in a population with RP who had not yet received a diagnosis of very early SSc (28). Randone et al (44) identified SSc-specific autoantibodies, puffy fingers, and NFC abnormalities as predictors of disease progression in patients with RP and/or ANA positivity. We identified ACA characteristics to be predictive of disease progression; however, we were not able to confirm the association between abnormal NFC and disease progression. One explanation could be differences between the patient groups studied. In our study, the majority of the patients with very early SSc already had 8 points according to the ACR/EULAR 2013 classification criteria. In the study by Randone et al, the majority of the patients scored <6 points at baseline according to the ACR/EULAR 2013 classification criteria. Interestingly, disease progression rates between patients with 8 points and patients with <8 points were comparable. Secondly, we only included ACA-positive patients, whereas Randone and colleagues included patients with RP who could be negative for ANAs or positive for ANAs with different specificities. Strikingly, the number of patients who were considered to be progressors among those with very early SSc was comparable between the 2 studies (41% versus 42%), which highlights the necessity of biomarkers to adequately identify the patients at risk. Although not within the scope of the present study, evaluating the IgG ACA level as a possible predictive biomarker in clinical practice showed that, in combination with pulmonary fibrosis, 84% of progressors and 49% of nonprogressors could be accurately identified at baseline. However, this finding needs to be further evaluated and confirmed in independent cohorts.

Previous results on the association between disease severity and ACA-specific responses have been conflicting. Two longitudinal studies with a small sample size (n = 13 and n = 15) did not provide conclusive results on the associations between clinical characteristics and ACA isotypes; however, fluctuating levels of ACA isotypes over time were observed (45,46). These studies were limited by small sample sizes, the use of nonvalidated outcome measures, and older techniques to measure specific isotypes.

To our knowledge, our study is the first to perform complete evaluation of ACA isotype responses in patients with SSc, and specifically to evaluate ACA isotype response in association with clinical progression to SSc in the very early SSc group. Our results provide an answer to one of Witebsky's postulates (47), offering evidence that may be useful in further investigations into a possible pathogenetic role of ACAs in the SSc disease course. We believe that ACA isotypes can be seen as biomarkers for the underlying immune response, and the presence and levels of the different isotypes can be used as markers for the breadth of the immune response. In addition, we hypothesize that the breadth of the immune response is a proxy for the intensity of the immune response, i.e., continuous expression of more isotypes indicates more active triggering of the adaptive immune response, which is also supported by data in other autoimmune diseases (18,19,48).

This study has some limitations. We included patients who were positive for IgG ACAs at baseline, and cannot completely exclude the possibility that patients who were positive only for IgM or IgA ACAs were missed. However, as a sensitivity check, we additionally measured expression of IgA and IgM ACAs in 46 patients with SSc of various durations who were negative for IgG ACAs (negative both by Phadia FEIA and by IF assay), which confirmed that clear expression of IgM and IgA ACAs in patients who are negative for IgG ACAs is very rare (results not shown). Likewise, no conclusions can be drawn with regard to other antibody subgroups in SSc. Since samples were not analyzed longitudinally, the effect of starting or discontinuing immunosuppressive treatment remains unclear, although we did not find an association between immunosuppressive treatment and ACA isotype levels. Another limitation is the difference in follow-up duration among patients in the very early SSc group. However, we performed 2 additional sensitivity checks: 1) including patients with long follow-up duration and 2) including patients with short disease duration, both of which confirmed the significant association between levels of IgG ACAs and progression to definite SSc (Supplementary Tables 8 and 9, http://onlinelibrary.wiley.com/doi/10.1002/art.41814/abstract). GI involvement was assessed based on available parameters including GAVE. This could have led to underestimating the prevalence of GI involvement, and therefore we performed a sensitivity check in a subgroup with additional data available (Supplementary Table 1, http://onlinelibrary.wiley.com/doi/10.1002/art.41814/abstract). Even with this broader definition of GI involvement, patients with organ involvement still showed the highest levels of IgG and IgM ACAs. To strengthen these results, the next step would be to evaluate ACA isotypes longitudinally and at the time of disease progression.

In conclusion, we have shown, to our knowledge for the first time and in a large multicenter ACA-positive SSc cohort, that IgG and IgM ACA levels are significantly higher in patients with definite SSc compared to patients with very early SSc. Moreover, we showed that in 42% of ACA-positive patients with very early SSc, disease progressed to definite SSc within 5 years and was associated with higher IgG ACA levels. Both observations indicate that CENP-B–specific IgG levels may be novel biomarkers in SSc and can potentially contribute to disease development.

AUTHOR CONTRIBUTIONS

All authors were involved in drafting the article or revising it critically for important intellectual content, and all authors approved the final version

to be published. Dr. van Leeuwen had full access to all of the data in the study and takes responsibility for the integrity of the data and the accuracy of the data analysis.

Study conception and design. van Leeuwen, Boonstra, Scherer, Toes, Huizinga, de Vries-Bouwstra.

Acquisition of data. van Leeuwen, Boonstra, Bakker, Grummels, Jordan, Liem, Distler, Hoffmann-Vold, Melsens, Smith, Truchetet, Scherer, Toes, Huizinga, de Vries-Bouwstra.

Analysis and interpretation of data. van Leeuwen, Boonstra, Bakker, Grummels, Jordan, Liem, Distler, Hoffmann-Vold, Melsens, Smith, Truchetet, Scherer, Toes, Huizinga, de Vries-Bouwstra.

REFERENCES

1. Steen VD, Medsger TA Jr. Severe organ involvement in systemic sclerosis with diffuse scleroderma. Arthritis Rheum 2000;43:2437–44.
2. Elhai M, Meune C, Avouac J, Kahan A, Allanore Y. Trends in mortality in patients with systemic sclerosis over 40 years: a systematic review and meta-analysis of cohort studies [review]. Rheumatology (Oxford) 2012;51:1017–26.
3. Tyndall AJ, Bannert B, Vonk M, Airo P, Cozzi F, Carreira PE, et al. Causes and risk factors for death in systemic sclerosis: a study from the EULAR Scleroderma Trials and Research (EUSTAR) database. Ann Rheum Dis 2010;69:1809–15.
4. Nihtyanova SI, Tang EC, Coghlan JG, Wells AU, Black CM, Denton CP. Improved survival in systemic sclerosis is associated with better ascertainment of internal organ disease: a retrospective cohort study. QJM 2010;103:109–15.
5. Van den Hoogen F, Khanna D, Fransen J, Johnson SR, Baron M, Tyndall A, et al. 2013 classification criteria for systemic sclerosis: an American College of Rheumatology/European League Against Rheumatism collaborative initiative. Arthritis Rheum 2013;65: 2737–47.
6. Jordan S, Maurer B, Toniolo M, Michel B, Distler O. Performance of the new ACR/EULAR classification criteria for systemic sclerosis in clinical practice. Rheumatology (Oxford) 2015;54:1454–8.
7. Bellando-Randone S, Matucci-Cerinic M. Very early systemic sclerosis and pre-systemic sclerosis: definition, recognition, clinical relevance and future directions [review]. Curr Rheumatol Rep 2017;19:65.
8. Allanore Y, Simms R, Distler O, Trojanowska M, Pope J, Denton CP, et al. Systemic sclerosis [review]. Nat Rev Dis Primers 2015;1:15002.
9. Steen VD. Autoantibodies in systemic sclerosis. Semin Arthritis Rheum 2005;35:35–42.
10. Ho KT, Reveille JD. The clinical relevance of autoantibodies in scleroderma [review]. Arthritis Res Ther 2003;5:80–93.
11. Liaskos C, Marou E, Simopoulou T, Barmakoudi M, Efthymiou G, Scheper T, et al. Disease-related autoantibody profile in patients with systemic sclerosis. Autoimmunity 2017;50:414–21.
12. Hao Y, Hudson M, Baron M, Carreira P, Stevens W, Rabusa C, et al. Early mortality in a multinational systemic sclerosis inception cohort. Arthritis Rheumatol 2017;69:1067–77.
13. Earnshaw W, Bordwell B, Marino C, Rothfield N. Three human chromosomal autoantigens are recognized by sera from patients with anti-centromere antibodies. J Clin Investig 1986;77:426–30.
14. Hildebrandt S, Weiner E, Senécal JL, Noell S, Daniels L, Earnshaw WC, et al. The IgG, IgM, and IgA isotypes of anti–topoisomerase I and anticentromere autoantibodies. Arthritis Rheum 1990;33:724–7.
15. Kayser C, Fritzler MJ. Autoantibodies in systemic sclerosis: unanswered questions [review]. Front Immunol 2015;6:167.
16. Hénault J, Tremblay M, Clément I, Raymond Y, Senécal JL. Direct binding of anti–DNA topoisomerase I autoantibodies to the cell surface of fibroblasts in patients with systemic sclerosis. Arthritis Rheum 2004;50:3265–74.
17. Senécal JL, Hénault J, Raymond Y. The pathogenic role of autoantibodies to nuclear autoantigens in systemic sclerosis (scleroderma). J Rheumatol 2005;32:1643–9.
18. Verpoort KN, Jol-van der Zijde CM, Papendrecht-van der Voort EA, Ioan-Facsinay A, Drijfhout JW, van Tol MJ, et al. Isotype distribution of anti–cyclic citrullinated peptide antibodies in undifferentiated arthritis and rheumatoid arthritis reflects an ongoing immune response. Arthritis Rheum 2006;54:3799–808.
19. Van der Woude D, Syversen SW, van der Voort EI, Verpoort KN, Goll GL, van der Linden MP, et al. The ACPA isotype profile reflects long-term radiographic progression in rheumatoid arthritis. Ann Rheum Dis 2010;69:1110–6.
20. Van de Stadt LA, van der Horst AR, de Koning MH, Bos WH, Wolbink GJ, van de Stadt RJ, et al. The extent of the anti-citrullinated protein antibody repertoire is associated with arthritis development in patients with seropositive arthralgia. Ann Rheum Dis 2011;70:128–33.
21. Meijs J, Schouffoer AA, Marsan NA, Kroft LJ, Stijnen T, Ninaber MK, et al. Therapeutic and diagnostic outcomes of a standardised, comprehensive care pathway for patients with systemic sclerosis. RMD Open 2016;2:e000159.
22. Hoffmann-Vold AM, Midtvedt O, Molberg O, Garen T, Gran JT. Prevalence of systemic sclerosis in south-east Norway. Rheumatology (Oxford) 2012;51:1600–5.
23. Vanthuyne M, Smith V, De Langhe E, Van Praet J, Arat S, Depresseux G, et al. The Belgian Systemic Sclerosis Cohort: correlations between disease severity scores, cutaneous subsets, and autoantibody profile. J Rheumatol 2012;39:2127–33.
24. Smith V, Scire CA, Talarico R, Airo P, Alexander T, Allanore Y, et al. Systemic sclerosis: state of the art on clinical practice guidelines. RMD Open 2018;4:e000782.
25. Frauenfelder T, Winklehner A, Nguyen TD, Dobrota R, Baumueller S, Maurer B, et al. Screening for interstitial lung disease in systemic sclerosis: performance of high-resolution CT with limited number of slices: a prospective study. Ann Rheum Dis 2014;73: 2069–73.
26. Truchetet ME, Demoures B, Guimaraes JE, Bertrand A, Laurent P, Jolivel V, et al. Platelets induce thymic stromal lymphopoietin production by endothelial cells: contribution to fibrosis in human systemic sclerosis. Arthritis Rheum 2016;68:2784–94.
27. Beyer C, Distler JH, Allanore Y, Aringer M, Avouac J, Czirják L, et al. EUSTAR biobanking: recommendations for the collection, storage and distribution of biospecimens in scleroderma research. Ann Rheum Dis 2011;70:1178–82.
28. Minier T, Guiducci S, Bellando-Randone S, Bruni C, Lepri G, Czirjak L, et al. Preliminary analysis of the very early diagnosis of systemic sclerosis (VEDOSS) EUSTAR multicentre study: evidence for puffy fingers as a pivotal sign for suspicion of systemic sclerosis. Ann Rheum Dis 2014;73:2087–93.
29. Avouac J, Fransen J, Walker UA, Riccieri V, Smith V, Muller C, et al. Preliminary criteria for the very early diagnosis of systemic sclerosis: results of a Delphi Consensus Study from EULAR Scleroderma Trials and Research Group. Ann Rheum Dis 2011;70:476–81.
30. Blaja E, Jordan S, Mihai CM, Dobrota R, Becker MO, Maurer B, et al. The challenge of very early systemic sclerosis: a combination of mild and early disease? J Rheumatol 2021;48:82–6.
31. Fretheim H, Halse AK, Seip M, Bitter H, Wallenius M, Garen T, et al. Multidimensional tracking of phenotypes and organ involvement in a complete nationwide systemic sclerosis cohort. Rheumatology (Oxford) 2020;59:2920–9.
32. Hoffmann-Vold AM, Fretheim H, Halse AK, Seip M, Bitter H, Wallenius M, et al. Tracking impact of interstitial lung disease in systemic sclerosis in a complete nationwide cohort. Am J Respir Crit Care Med 2019;200:1258–66.

33. Clements PJ, Lachenbruch PA, Ng SC, Simmons M, Sterz M, Furst DE. Skin score: a semiquantitative measure of cutaneous involvement that improves prediction of prognosis in systemic sclerosis. Arthritis Rheum 1990;33:1256–63.
34. Smith V, Beeckman S, Herrick AL, Decuman S, Deschepper E, De Keyser F, et al. An EULAR study group pilot study on reliability of simple capillaroscopic definitions to describe capillary morphology in rheumatic diseases. Rheumatology (Oxford) 2016;55:883–90.
35. Smith V, Herrick AL, Ingegnoli F, Damjanov N, De Angelis R, Denton CP, et al. Standardisation of nailfold capillaroscopy for the assessment of patients with Raynaud's phenomenon and systemic sclerosis [review]. Autoimmun Rev 2020;19:102458.
36. Medsger TA Jr, Silman AJ, Steen VD, Black CM, Akesson A, Bacon PA, et al. A disease severity scale for systemic sclerosis: development and testing. J Rheumatol 1999;26:2159–67.
37. Coghlan JG, Denton CP, Grunig E, Bonderman D, Distler O, Khanna D, et al. Evidence-based detection of pulmonary arterial hypertension in systemic sclerosis: the DETECT study. Ann Rheum Dis 2014;73:1340–9.
38. Khanna D, Clements PJ, Volkmann ER, Wilhalme H, Tseng CH, Furst DE, et al. Minimal clinically important differences for the modified Rodnan skin score: results from the Scleroderma Lung Studies (SLS-I and SLS-II). Arthritis Res Ther 2019;21:23.
39. Kastbom A, Ljungberg KR, Ziegelasch M, Wetterö J, Skogh T, Martinsson K. Changes in anti-citrullinated protein antibody isotype levels in relation to disease activity and response to treatment in early rheumatoid arthritis. Clin Exp Immunol 2018;194:391–9.
40. Brinkman DM, Jol-van der Zijde CM, ten Dam MM, Vossen JM, Osterhaus AD, Kroon FP, et al. Vaccination with rabies to study the humoral and cellular immune response to a T-cell dependent neoantigen in man. J Clin Immunol 2003;23:528–38.
41. Koenig M, Joyal F, Fritzler MJ, Roussin A, Abrahamowicz M, Boire G, et al. Autoantibodies and microvascular damage are independent predictive factors for the progression of Raynaud's phenomenon to systemic sclerosis: a twenty-year prospective study of 586 patients, with validation of proposed criteria for early systemic sclerosis. Arthritis Rheum 2008;58:3902–12.
42. Shen CY, Li KJ, Lai PH, Yu CL, Hsieh SC. Anti-CENP-B and anti-TOPO-1-containing sera from systemic sclerosis-related diseases with Raynaud's phenomenon induce vascular endothelial cell senescence not via classical p53–p21 pathway. Clin Rheumatol 2018;37:749–56.
43. van Leeuwen NM, Wortel CM, Fehres CM, Bakker JA, Scherer HU, Toes RE, et al. Association between centromere and topoisomerase specific immune responses and the degree of microangiopathy in systemic sclerosis. J Rheumatol 2021;48:402–9.
44. Randone SB, Lepri G, Husher D, Minier T, Guiducci S, Bruni C, et al. OP0065 The very early diagnosis of systemic sclerosis (VEDOSS) project: predictors to develop definite disease from an international multicentre study. Ann Rheum Dis 2019;78:104–5.
45. Tramposch HD, Smith CD, Senecal JL, Rothfield N. A long-term longitudinal study of anticentromere antibodies. Arthritis Rheum 1984;27:121–4.
46. Vazquez-Abad D, Russell CA, Cusick SM, Earnshaw WC, Rothfield NF. Longitudinal study of anticentromere and antitopoisomerase-I isotypes. Clin Immunol Immunopathol 1995;74:257–70.
47. Rose NR, Bona C. Defining criteria for autoimmune diseases (Witebsky's postulates revisited) [review]. Immunol Today 1993;14:426–30.
48. Van der Woude D, Rantapaa-Dahlqvist S, Ioan-Facsinay A, Onnekink C, Schwarte CM, Verpoort KN, et al. Epitope spreading of the anti-citrullinated protein antibody response occurs before disease onset and is associated with the disease course of early arthritis. Ann Rheum Dis 2010;69:1554–61.

American College of Rheumatology
Empowering Rheumatology Professionals

Arthritis & Rheumatology
Vol. 73, No. 12, December 2021, pp 2348–2355
© 2021, American College of Rheumatology

LETTERS

DOI 10.1002/art.41886

Addressing immeasurable time bias in an observational study: comment on the article by Suissa et al

To the Editor:

We read with great interest the article by Dr. Suissa and colleagues that reviewed observational studies of the association between allopurinol and mortality in individuals with gout (1). The authors describe immeasurable time bias as time periods during which prescription medication records are not available (e.g., hospitalizations), leading to at-risk time being potentially misclassified as unexposed time. Suissa and colleagues recommend accounting for the possibility of immeasurable time bias by evaluating hospitalizations during follow-up or using an analytic approach that is weighted by measurable time (2). Of the 12 studies included in the analysis, 3 were described as affected by immeasurable time bias, including ours (3). We wholeheartedly agree that immeasurable time bias is an important consideration in observational studies. We thought it would be useful to inform readers of how we sought to address immeasurable time bias in our study.

We evaluated hospitalizations and their possible impact on the study results in detail. Approximately 80% of individuals in our cohort experienced at least 1 hospitalization between the index date and end of follow-up. We examined the median length of admission for all hospitalizations, which was 6 days (interquartile range [IQR] 3–12). We extended each allopurinol-exposed period by a grace period of 14 days, such that, contrary to the immeasurable time periods depicted in Figure 4B in the Suissa et al study, the majority of hospitalizations would not have been susceptible to exposure misclassification. Furthermore, the median prescription duration in the cohort was 78 days (IQR 31.3–92.2), making it unlikely that brief hospitalizations would have affected refill patterns substantially and increasing our confidence that hospitalizations were not resulting in substantial exposure misclassification. Despite this, one-third of the individuals in our cohort who discontinued allopurinol had a hospitalization within 3 months of allopurinol discontinuation. This led us to conclude that our results could have had residual healthy user bias, as was discussed in our article.

To examine the possibility of healthy user bias in greater detail, we evaluated the characteristics of individuals in our cohort by allopurinol persistence and adherence. We found that those who persisted in continuing their allopurinol treatment and had the highest adherence to the treatment (i.e., highest number of days covered) also had greater comorbidity, reflected by higher weighted Johns Hopkins Aggregated Diagnosis Groups scores (mean ± SD 8.85 ± 13 versus 6.96 ± 12.9) and higher rates of cardiovascular disease, chronic kidney disease, and prior hospitalization, among other risk factors (4). The association between higher allopurinol adherence and greater comorbidity has been consistently demonstrated (5). Thus, unlike for many other medications, individuals with the greatest mortality risk are most adherent to allopurinol, and therefore less likely to be misclassified as unexposed despite brief hospitalizations.

Finally, we note that the 9 studies avoiding immeasurable time bias all did so by using intent-to-treat analyses. This is particularly problematic in studies of allopurinol as adherence is known to be poor and results would thus be biased toward the null hypothesis (5).

We thank Dr. Suissa and colleagues for raising this important methodologic issue. We are grateful to have the opportunity to provide additional useful information about how the issue of immeasurable time bias can be investigated in a specific clinical context.

Alanna Weisman, MD, PhD
University of Toronto
Institute for Clinical Evaluative Sciences
Women's College Hospital
and Mount Sinai Hospital
Gillian A. Hawker, MD, MSc
University of Toronto
Institute for Clinical Evaluative Sciences
and Women's College Hospital
George A. Tomlinson, PhD
University of Toronto
Mount Sinai Hospital
and University Health Network
Toronto, Ontario, Canada

1. Suissa S, Suissa K, Hudson M. Effectiveness of allopurinol on reducing mortality: time-related biases in observational studies. Arthritis Rheumatol 2021;73:1749–57.
2. Suissa S. Immeasurable time bias in observational studies of drug effects on mortality. Am J Epidemiol 2008;168:329–35.
3. Weisman A, Tomlinson GA, Lipscombe LL, Perkins BA, Hawker GA. Association between allopurinol and cardiovascular outcomes and all-cause mortality in diabetes: a retrospective, population-based cohort study. Diabetes Obes Metab 2019;21:1322–9.

4. Weisman A. Associations between allopurinol and cardiovascular and renal outcomes in diabetes [dissertation]. Toronto (ON): University of Toronto; 2020.
5. Scheepers L, van Onna M, Stehouwer CD, Singh JA, Arts IC, Boonen A. Medication adherence among patients with gout: a systematic review and meta-analysis. Semin Arthritis Rheum 2018;47:689–702.

DOI 10.1002/art.41884

Reply

To the Editor:

We thank Dr. Weisman and colleagues for their letter regarding our article reviewing observational studies reporting on the effectiveness of allopurinol for reducing mortality and particularly those studies that were affected by immeasurable time bias. Indeed, our review explained that immeasurable time bias can be an important complexity in observational studies where the outcome is death and hospitalizations are frequent (1).

We appreciate the clarifications of Weisman and colleagues regarding the patterns of hospitalizations in the elderly cohort used in their study (2). In particular, it is relevant to this potential bias that 80% of the cohort subjects were hospitalized at least once during the median 4.7 years of follow-up. Moreover, the likelihood of immeasurable time bias is increased as one-third of those who discontinued allopurinol had a hospitalization within 3 months of allopurinol discontinuation. With respect to this bias, however, it would be more informative to examine the patterns of hospitalizations and prescription durations in greater detail, more specifically during the period preceding death (perhaps 90 or 180 days). Thus, the uncertainties and variations in prescription durations, along with the timing and high frequency of hospitalizations, cannot preclude the possibility that immeasurable time bias may have contributed to the findings of a protective effect of allopurinol on mortality in the study by Weisman and colleagues.

The issue of healthy user bias addresses confounding bias which we did not discuss in our report. On the other hand, intent-to-treat (ITT) analyses are important, at least as sensitivity analyses. While these ITT analyses can attenuate the effects of a treatment, limiting the follow-up period to a relatively short time will help to reduce the impact of this attenuation. Unfortunately, the "all exposed" cohort design that includes only patients exposed to allopurinol, used in the study by Weisman and colleagues, does not permit ITT sensitivity analyses.

In conclusion, observational studies provide useful evidence of real-world medication effects, though time-related biases can introduce important errors. In particular, immeasurable time bias can affect observational studies of the effects of medications on the outcome of mortality in chronic diseases (1). This bias tends to exaggerate the potential benefit of treatments. Our goal was to draw attention to this potential bias in the important arena of real-world evidence research and suggest ways to avoid it. We appreciate the opportunity to do this once more.

Samy Suissa, PhD
Jewish General Hospital and McGill University
Montreal, Quebec, Canada
Karine Suissa, PhD
Brigham and Women's Hospital and Harvard Medical School
Boston, Massachusetts
Marie Hudson, MD
Jewish General Hospital and McGill University
Montreal, Quebec, Canada

1. Suissa S. Immeasurable time bias in observational studies of drug effects on mortality. Am J Epidemiol 2008;168:329–35.
2. Weisman A, Tomlinson GA, Lipscombe LL, Perkins BA, Hawker GA. Association between allopurinol and cardiovascular outcomes and all-cause mortality in diabetes: a retrospective, population-based cohort study. Diabetes Obes Metab 2019;21:1322–9.

DOI 10.1002/art.41909

Hypoxia-induced synovial fibroblast activation in inflammatory arthritis and the role of Notch-1 and Notch-3 signaling: comment on the article by Chen et al

To the Editor:

Rheumatoid arthritis (RA) is a chronic systemic autoimmune disease with local systemic inflammation, such as persistent synovial inflammation. The interaction of immune cells and inflammatory mediators results in amplification and perpetuation of the inflammation-induced joint remodeling process. RA is characterized by joint swelling, redness, and arthralgia. In their recent study, Dr. Chen and colleagues showed that Notch-1 and Notch-3 intracellular domain (N1ICD and N3ICD, respectively) was expressed in the synovial tissue of RA patients, and hypoxia-inducible factor 1α (HIF-1α) regulated expression of Notch-1 and Notch-3 (1). Hypoxia-induced N1ICD and N3ICD expression in RA synovial fibroblasts (RASFs) was inhibited by knocking out HIF-1α. In turn, knocking out Notch-1 or Notch-3 suppressed hypoxia-induced RASF invasion and angiogenesis. Moreover, Notch-1 regulated RASF migration and epithelial–mesenchymal transition under hypoxia, and inhibition of N1ICD/N2ICD slowed the progression of arthritis in rats. Chen and colleagues' findings suggest that Notch-1 and Notch-3 may regulate RASFs via interaction with HIF-1α, and that targeting Notch-1 and Notch-3 in the treatment of RA may be beneficial (1).

Notch is a multifaceted transmembrane protein. This family of proteins comprises 4 receptors (Notch-1, Notch-2,

Notch-3, and Notch-4) and 5 ligands (Jagged-1 and Jagged-2 and delta-like proteins 1, 3, and 4). Their signaling not only regulates basic cellular processes such as cell growth, differentiation, proliferation, and death, but also can play an active role in hematopoiesis and angiogenesis. Previously published studies have shown that in patients with active RA there was elevated expression of Notch-3 in T helper cells and especially in activated T cells (2). Similarly, Notch-1 and Notch-3 were highly expressed in synovium from RA patients as compared to synovium from controls (3,4). Interestingly, abrogation of Notch-1 signaling inhibited Freund's complete adjuvant–induced inflammatory arthritis, as indicated by the reduction in the progression and severity of arthritis (assessed using radiologic and histologic analyses) (5). Antisense Notch-1 oligonucleotides inhibited the proliferation of RA synoviocytes (3), and stimulation of RA synoviocytes with γ-secretase inhibitor, which blocks the production of N1ICD and N3ICD, also suppressed proliferation of synoviocytes (3). Gao et al demonstrated that N1ICD expression was elevated in synovial tissue from RA patients (6). Dimethyloxalylglycine induced N1ICD expression and Notch-1 knockdown suppressed hypoxia-induced HIF-1α expression (6). Angiogenesis and the migration and invasion of endothelial cells induced under conditions of hypoxia (3% oxygen) were inhibited following knockdown of Notch-1 or treatment with a γ-secretase inhibitor (6).

Together, Notch-1 and Notch-3 may interact with HIF-1α and then mediate hypoxia-induced RASF invasion and angiogenesis in inflammatory arthritis. However, several questions need to be addressed in the future, such as whether Notch-1 first interacts with Notch-3 and then affects HIF-1α, and how Notch-1 and/or Notch-3 affects HIF-1α and by what mechanism.

Supported by the National Natural Science Foundation of China (grant 81701606). Author disclosures are available at https://onlinelibrary.wiley.com/action/downloadSupplement?doi=10.1002%2Fart.41909&file=art41909-sup-0001-Disclosureform.doc.

Wang-Dong Xu, MD
Southwest Medical University
An-Fang Huang, MMed
Affiliated Hospital of Southwest Medical University
Luzhou, China

1. Chen J, Cheng W, Li J, Wang Y, Chen J, Shen X, et al. Notch-1 and Notch-3 mediate hypoxia-induced activation of synovial fibroblasts in rheumatoid arthritis. Arthritis Rheumatol 2021;73:1810–19.
2. Jiao Z, Wang W, Guo M, Zhang T, Chen L, Wang Y, et al. Expression analysis of Notch-related molecules in peripheral blood T helper cells of patients with rheumatoid arthritis. Scand J Rheumatol 2010;39:26–32.
3. Nakazawa M, Ishii H, Aono H, Takai M, Honda T, Aratani S, et al. Role of Notch-1 intracellular domain in activation of rheumatoid synoviocytes. Arthritis Rheum 2001;44:1545–54.
4. Ishii H, Nakazawa M, Yoshino S, Nakamura H, Nishioka K, Nakajima T. Expression of notch homologues in the synovium of rheumatoid arthritis and osteoarthritis patients. Rheumatol Int 2001;21:10–4.
5. Anchi P, Swamy V, Godugu C. Nimbolide exerts protective effects in complete Freund's adjuvant induced inflammatory arthritis via abrogation of STAT-3/NF-κB/Notch-1 signaling. Life Sci 2021;266:118911.
6. Gao W, Sweeney C, Connolly M, Kennedy A, Ng CT, McCormick J, et al. Notch-1 mediates hypoxia-induced angiogenesis in rheumatoid arthritis. Arthritis Rheum 2012;64:2104–13.

DOI 10.1002/art.41904

Reply

To the Editor:

We appreciate the comments from Dr. Xu and colleagues regarding our recently published article on hypoxia-induced activation of synovial fibroblasts in RA. It has been confirmed that HIF-1α regulates the expression of Notch-1 in RASFs under hypoxic conditions (1). Furthermore, our study shows that HIF-1α directly regulates the expression of Notch-1 and Notch-3 in the hypoxic microenvironment. However, in order for cells to be able to adapt to the hypoxic microenvironment, interaction of the regulatory functions of HIF-1α and regulatory functions of Notch signal transduction is required.

To adapt to hypoxia, HIF-1α first becomes stable and directly activates the transcription of downstream genes. In addition to this canonical response, there is another response involving Notch signal integration. It was shown in a study by Zheng et al that the affinity of factor-inhibiting HIF-1α (FIH-1) to NICD is higher than that of HIF-1α (2). Thus, when the Notch signal is activated, the NICD first combines with FIH-1, which leads to the activation of HIF-1α. This mechanism may also be stably related to HIF-1α under normoxic conditions, such as in von Hippel-Lindau syndrome (3). Taken together, the research data on the role of FIH-1 in Notch signal regulation reveal the dynamic and complex relationship between Notch signaling and hypoxia, which indicates that the signal outputs of these 2 mechanisms need to be fine-tuned in order to regulate cell response to hypoxia.

Accumulating evidence supports the hypothesis that repeated periods of hypoxia first cause HIF-1α stability and then activate Notch-1 and Notch-3 in RASFs (1,4). Although hypoxia has been implicated in the pathogenesis of RA through both direct and indirect effects via activation of hypoxia-induced Notch signaling, the way in which hypoxia maintains cells in an undifferentiated state remains unknown. Thus, elucidating the impact of Notch-1 and/or Notch-3 on hypoxia within joints affected by RA will allow better understanding of the activation of Notch-1 and Notch-3 and the mechanisms by which they affect RASFs and contribute to RA development and progression. Next, studies can be designed to examine whether overexpression of N1ICD and N3ICD in normoxic and hypoxic environments has an effect on HIF-1α, and chromatin immunoprecipitation assays can

be used to determine whether the regulatory functions of HIF-1α are either direct or indirect.

Supported by the National Key Research and Development Program of China (grant 2018YFC1705205), the Chinese Academy of Sciences Foreign Cooperation Project (grant GJHZ2063), the National Natural Science Foundation of China (grant 92068117), the Guangdong Basic and Applied Basic Research Fund (grant 2020B1515120052), the Shenzhen Science and Technology Innovation Fund (grants JCYJ20170818153602439 and JCYJ20180302150101316), the Sanming Project of Medicine in Shenzhen (grant SZSM201808072), the Shenzhen Municipality Development and Reform Commission (grant XMHT20190106001), and the Shenzhen Double Chain Project for Innovation and Development Industry supported by the Shenzhen Bureau of Industry and Information Technology (grant 201908141541). Author disclosures are available at https://onlinelibrary.wiley.com/action/downloadSupplement?doi=10.1002%2Fart.41904&file=art41904-sup-0001-Disclosureform.pdf.

Jianhai Chen, PhD
Antonia Sun, PhD
Jian Li, PhD
Wenxiang Cheng, PhD
Peng Zhang, MD
Center for Translational Medicine Research and Development
Shenzhen Institutes of Advanced Technology and Chinese Academy of Sciences
Shenzhen, China

1. Gao W, Sweeney C, Connolly M, Kennedy A, Ng CT, McCormick J, et al. Notch-1 mediates hypoxia-induced angiogenesis in rheumatoid arthritis. Arthritis Rheum 2012;64:2104–13.
2. Zheng X, Linke S, Dias JM, Zheng X, Gradin K, Wallis TP, et al. Interaction with factor inhibiting HIF-1 defines an additional mode of cross-coupling between the Notch and hypoxia signaling pathways. Proc Natl Acad Sci U S A 2008;105:3368–73.
3. Kaelin WG. Von Hippel-Lindau disease [review]. Annu Rev Pathol 2007;2:145–73.
4. Meunier A, Flores AN, McDermott N, Rivera-Figueroa K, Perry A, Lynch T, et al. Hypoxia regulates Notch-3 mRNA and receptor activation in prostate cancer cells. Heliyon 2016;2:e00104.

DOI 10.1002/art.41905

Disease activity assessment in nonradiographic axial spondyloarthritis: is it time to move beyond the Bath Ankylosing Spondylitis Disease Activity Index or Ankylosing Spondylitis Disease Activity Score? Comment on the article by Rusman et al

To the Editor:

We read with great interest the article by Dr. Rusman and colleagues on the efficacy of treatment with etanercept in patients with suspected nonradiographic axial spondyloarthritis (SpA) (1). The study conducted by Rusman and colleagues had an interesting design: patients with nonradiographic axial SpA were randomized to receive either etanercept or placebo for 16 weeks based on clinical disease activity according to the Bath Ankylosing Spondylitis Disease Activity Index (BASDAI) (2). The results of this study raise many doubts concerning the methods currently used to assess disease activity in axial SpA, and in nonradiographic axial SpA in particular.

Among patients with clinically active disease (BASDAI ≥4) in the study by Rusman et al, only 13% had C-reactive protein (CRP) levels exceeding the upper limit of normal. Similarly, active inflammation in the sacroiliac (SI) joint (according to Spondyloarthritis Research Consortium of Canada SI structural lesion score) (3) was seen in only 23% of patients at baseline. It would be interesting to know the distribution of patients according to Ankylosing Spondylitis Disease Activity Score (ASDAS) (4). Three questions from the ASDAS are borrowed from the BASDAI, and it is possible that patients who achieved remission or low disease activity according to the ASDAS score may have overestimated the extent of their disease activity on the BASDAI questionnaire. The median CRP level was 2.5 mg/liter, but the mean ASDAS-CRP score was 2.8, indicating that the extent of disease activity may have been overestimated based on the scoring of some of the components on the ASDAS.

Another striking point is the predominance of female patients in the study population (64%) and the high prevalence of peripheral joint involvement (53%) or high Maastricht Ankylosing Spondylitis Enthesitis Score (mean 7.9) (5). Although none of the joints were considered to be swollen, being instead deemed tender joints, this feature could nevertheless have contributed to an increase in the BASDAI or ASDAS score. It would be pertinent to conduct other objective assessments such as power Doppler ultrasound to look for synovial hypertrophy in such joints or entheses before considering them as actively inflamed. Also, other confounding comorbidities such as hypothyroidism (6), fibromyalgia (7), or hypovitaminosis D (8), all of which are common features in patients with SpA (specifically in female patients), could have affected BASDAI responses.

At baseline, ~30% of patients were not taking nonsteroidal antiinflammatory drugs (NSAIDs) (only 11% were taking other disease-modifying antirheumatic drugs and no patients were taking biologics). Although patients receiving etanercept and those receiving placebo showed no differences in objective treatment responses at 16 weeks, the data on percentage of patients still receiving full doses of NSAIDs or who were able to have their NSAID doses reduced by at least 50% at weeks 16 and 24 would clarify the proportion of patients who were continuing to rely on NSAID treatment, given that none actually restarted etanercept or another biologic during the 16–24-week follow-up.

On conventional radiography, there was a marked discrepancy between the Bath Ankylosing Spondylitis Radiology Index (BASRI) (9) and modified Stoke Ankylosing Spondylitis Spine

Score (mSASSS) (10) (only 3% of patients had a BASRI spine score of ≥2, whereas 60% of patients had an mSASSS score of ≥2). Explaining this discrepancy would also help to delineate high BASDAI scores in this study population.

Taking these points into consideration, it seems fallacious to use the BASDAI or ASDAS (although it is more objective) for the assessment of disease activity in nonradiographic axial SpA. We strongly agree with the authors that these measures are not validated in this specific population and that they measure "level of symptoms" more than disease activity. Thus, initiation of treatment with biologics (considering cost of therapy and risk of infections) in this specific study group (with more subjective than objective evidence) seems irrational and harmful. Even in the study conducted by Rusman and colleagues, adverse events were noted in 39.5% of patients in the etanercept group while 16.7% of patients achieved an Assessment of SpondyloArthritis international Society 20 response (more risk than benefit). Comorbidities, as mentioned above, should be ruled out before introducing treatment with etanercept.

There is a need for more objective disease activity measures, as nonradiographic axial SpA is being diagnosed more frequently. Apart from CRP levels, imaging parameters of active disease (e.g., bone marrow edema, enthesitis, capsulitis, or synovitis), swollen joint counts, and modified Schober test of spinal mobility (among other measurements) should be utilized in order to increase the robustness of disease activity assessment in the setting of nonradiographic axial SpA.

Author disclosures are available at https://onlinelibrary.wiley.com/action/downloadSupplement?doi=10.1002%2Fart.41905&file=art41905-sup-0001-Disclosureform.pdf.

Debashish Mishra, MD, DM
B. V. Harish, MD
Sudhish Gadde, MD
Pradeepta S. Patro, MD, DM
Institute of Medical Sciences and Sum Hospital Bhubaneswar, India

1. Rusman T, van der Weijden MA, Nurmohamed MT, Landewé RB, de Winter JJ, Boden BJ, et al. Is treatment in patients with suspected nonradiographic axial spondyloarthritis effective? Six-month results of a placebo-controlled trial. Arthritis Rheumatol 2021;73:806–15.
2. Garrett S, Jenkinson T, Kennedy LG, Whitelock H, Gaisford P, Calin A. A new approach to defining disease status in ankylosing spondylitis: the Bath Ankylosing Spondylitis Disease Activity Index. J Rheumatol 1994;21:2286–91.
3. Maksymowych WP, Inman RD, Salonen D, Dhillon SS, Williams M, Stone M, et al. Spondyloarthritis Research Consortium of Canada Magnetic Resonance Imaging Index for assessment of sacroiliac joint inflammation in ankylosing spondylitis. Arthritis Rheum 2005;53:703–9.
4. Lukas C, Landewé R, Sieper J, Dougados M, Davis J, Braun J, et al, for the Assessment of SpondyloArthritis international Society. Development of an ASAS-endorsed disease activity score (ASDAS) in patients with ankylosing spondylitis. Ann Rheum Dis 2009;68:18–24.
5. Heuft-Dorenbosch L, Spoorenberg A, van Tubergen A, Landewé R, van der Tempel H, Mielants H, et al. Assessment of enthesitis in ankylosing spondylitis. Ann Rheum Dis 2003;62:127–32.
6. Emmungil H, Erdogan M, Kalfa M, Karabulut G, Kocanaogullari H, Inal V, et al. Autoimmune thyroid disease in ankylosing spondylitis. Clin Rheumatol 2014;33:955–61.
7. Jones GT, Mallawaarachchi B, Shim J, Lock J, Macfarlane GJ. The prevalence of fibromyalgia in axial spondyloarthritis. Rheumatol Int 2020;40:1581–91.
8. Zhao SZ, Thong D, Duffield S, Goodson N. Vitamin D deficiency in axial spondyloarthritis is associated with higher disease activity. Arch Rheumatol 2017;32:209–15.
9. MacKay K, Mack C, Brophy S, Calin A. The Bath Ankylosing Spondylitis Radiology Index (BASRI): a new validated approach to disease assessment. Arthritis Rheum 1998;41:2263–70.
10. Creemers MC, Franssen MJ, van't Hof MA, Gribnau FW, van de Putte LB, van Riel PL. Assessment of outcome in ankylosing spondylitis: an extended radiographic scoring system. Ann Rheum Dis 2005;64:127–9.

DOI 10.1002/art.41908

Reply

To the Editor:

We would like to thank Dr. Mishra and colleagues for their comments on our article on the efficacy of treatment with etanercept in patients with suspected nonradiographic axial SpA. One of their suggestions was that the patients included were misdiagnosed, but we can confirm that the patients in our study did not have any of the comorbidities as suggested by the authors.

The main point of concern of Mishra and colleagues is that patients with a suspected diagnosis of axial SpA on the basis of the presence of several risk factors, such as inflammatory back pain plus at least 2 SpA features as well as high patient-reported disease activity (BASDAI ≥4) (1), as in our study, may not respond well to treatment with tumor necrosis factor inhibitors (TNFi) because objective signs of inflammation are lacking. As we have discussed in our article, we agree with the statement that the threshold for starting TNFi therapy, even in patients in whom a diagnosis of nonradiographic axial SpA is suspected but who have not been diagnosed as having nonradiographic axial SpA, is often too low. This, of course, may result in overtreatment and an increase in health care costs.

However, despite CRP being an attractive objective parameter for inflammation, many patients with axial SpA simply do not have raised levels of this inflammation marker, while they may have many severe manifestations of radiographic axial SpA. In addition, MRI of the sacroiliac joints can show bone marrow edema due to local inflammation, but these phenomena are also present occasionally in healthy individuals who actively participate in sports or in women who have recently given birth (2,3). As the authors undoubtedly know, the other suggestions for objective disease parameters, such as swollen joint counts and abnormal findings on the modified Schober test of spinal mobility, are not

suitable for evaluation of disease activity in axial SpA; arthritis is often absent, and results of the Schober test, most often found to be normal in patients with early disease, are not sensitive to change after treatment.

Our group therefore has developed a very interesting new tool based on physical performance measurements, the Ankylosing Spondylitis Physical Performance-based Index (ASPI), which is reliable, feasible for daily practice, and sensitive to change by treatment. We have recently published the Spanish translation, in addition to the English guidelines, which makes this new tool available for many rheumatologists around the globe (4).

Supported by an unrestricted grant from Pfizer and ReumaNederland.

Tamara Rusman, MSc
Mignon A. C. van der Weijden, MD, PhD
Michael T. Nurmohamed, MD, PhD
Carmella M. A. van der Bijl, MD
Conny J. van der Laken, MD, PhD
Pierre M. Bet, PhD
VU University Medical Center
Robert B. M. Landewé, MD, PhD
Janneke J. H. de Winter, MD, PhD
AMC University Medical Center
Bouke J. H. Boden, MD
Onze Lieve Vrouwe Gasthuis (OLVG)
Irene E. van der Horst-Bruinsma, MD, PhD
VU University Medical Center
Amsterdam, The Netherlands

1. Garrett S, Jenkinson T, Kennedy LG, Whitelock H, Gaisford P, Calin A. A new approach to defining disease status in ankylosing spondylitis: the Bath Ankylosing Spondylitis Disease Activity Index. J Rheumatol 1994;21:2286–91.
2. De Winter J, de Hooge M, van de Sande M, de Jong H, van Hoeven L, de Koning A, et al. Magnetic resonance imaging of the sacroiliac joints indicating sacroiliitis according to the Assessment of SpondyloArthritis international Society definition in healthy individuals, runners, and women with postpartum back pain. Arthritis Rheumatol 2018;70:1042–8.
3. Rusman T, John MB, van der Weijden MA, Boden BJ, van der Bijl CM, Bruijnen ST, et al. Presence of active MRI lesions in patients suspected of non-radiographic axial spondyloarthritis with high disease activity and chance at conversion after a 6-month follow-up period. Clin Rheumatol 2020;39:1521–9.
4. Van Bentum RE, Vodnizza SE, de la Fuente MP, Aldridge FV, Navarro-Compán V, Rusman TR, et al. The Ankylosing Spondylitis Performance Index: reliability and feasibility of an objective test for physical functioning. J Rheumatol 2020;47:1475–82.

DOI 10.1002/art.41893

Clinical and methodologic considerations with regard to a trial of nintedanib in patients with systemic sclerosis–associated interstitial lung disease: comment on the reanalysis by Maher et al

To the Editor:

I read with interest the reanalysis of the results of the SENSCIS trial by Dr. Maher et al (1). The extended findings in Maher and colleagues' study may represent an advance in the knowledge of the effects of nintedanib in systemic sclerosis–associated interstitial lung disease (SSc-ILD), but some aspects of the trial require additional commentary.

The success of treatment blinding in the SENSCIS trial was not assessed by Maher and colleagues, but it seems difficult to guarantee blinding with a drug that has been shown to cause diarrhea in ~44% of the patients who receive this treatment (2). Furthermore, the attributable risk of experiencing at least some change in bowel habits or new gastrointestinal symptoms with nintedanib must be even larger than the risk of diarrhea. Knowing that one is receiving an active intervention may encourage attitudes toward better health (e.g., diet to promote weight loss for those overweight, or physical exercise) that can improve forced vital capacity (FVC).

Maher and colleagues report that data imputation was performed using the worst observation carried forward (WOCF) approach. This method may perhaps be valid when data are missing completely at random; however, this is probably not the case in the SENSCIS trial. As SSc-ILD tends to progress over time, worse FVC results are more likely with longer follow-up, and so the data are probably not missing at random (i.e., the fact that the data are missing is related to the value of the outcome variable itself). The use of WOCF, as with other single imputation methods, is inadequate in this context because it can artificially reduce data variability, producing spuriously low *P* values, and may favor the nintedanib group (which has a higher dropout rate) due to the more frequent use of FVC measures recorded before week 52.

FVC is accepted as a primary outcome measure in randomized controlled trials (RCTs) because it is associated with survival in patients with SSc-ILD. However, the results of spirometry should not be analyzed outside the context of other clinical outcomes. The data released publicly by the manufacturer of nintedanib in June 2019 (3) provide additional information on this subject. In our analysis of the results presented in Table 36 of the advisory committee briefing materials, there was statistically significant worsening in limitations in daily activities due to Raynaud's phenomenon ($P = 0.002$), in the Functional Assessment of Chronic Illness Therapy functional limitations score ($P = 0.013$), and in the physician global visual analog scale score ($P = 0.026$) in the group receiving nintedanib compared with those receiving placebo (based on the numbers provided by the manufacturer, using Student's 2-tailed *t*-test, not adjusted for multiplicity).

Further studies are necessary before nintedanib can be considered an effective treatment for SSc-ILD since no evidence to date has indicated that the reduction in loss of FVC will translate into better quality of life, fewer respiratory symptoms, or prolonged survival. Perhaps another RCT with a run-in period and with selection of patients who have demonstrated adequate tolerance to treatment with nintedanib might help to answer these questions.

Markus Bredemeier, MD, MSc, PhD
Hospital Nossa Senhora da Conceição, Conceição Hospital Group
Porto Alegre, Brazil

1. Maher TM, Mayes MD, Kreuter M, Volkmann ER, Aringer M, Castellvi I, et al. Effect of nintedanib on lung function in patients with systemic sclerosis–associated interstitial lung disease: further analyses of a randomized, double-blind, placebo-controlled trial. Arthritis Rheumatol 2021;73:671–6.
2. Distler O, Highland KB, Gahlemann M, Azuma A, Fischer A, Mayes MD, et al. Nintedanib for systemic sclerosis–associated interstitial lung disease. N Engl J Med 2019;380:2518–28.
3. Boehringer Ingelheim. Arthritis Advisory Committee briefing materials: nintedanib soft capsules–indication: treatment of systemic sclerosis-associated interstitial lung disease. June 2019. URL: https://www.fda.gov/media/129233/download.

DOI 10.1002/art.41895

Reply

To the Editor:

Following the publication of further analyses of the effects of nintedanib in patients with SSc-ILD in the SENSCIS trial, Dr. Bredemeier has queried whether the occurrence of gastrointestinal adverse events in subjects treated with nintedanib may have reduced the effectiveness of treatment blinding and so introduced bias. The SENSCIS trial followed standard procedures for masking the study drug in randomized controlled trials. While it is true that a greater proportion of subjects treated with nintedanib versus placebo experienced gastrointestinal adverse events (1), the subjects in this trial may also have experienced gastrointestinal complications related to SSc or to concurrent medications, and we have no reason to believe that the results of the trial were influenced by a reduction in the effectiveness of blinding.

Dr. Bredemeier queries the use of a WOCF approach in our analyses of changes in FVC. While we are aware of the limitations of single imputation methods, this approach was chosen because it avoids some of the limitations inherent in the originally planned approach of nonresponse imputation, in which missing data at week 52 are categorized as indicative of worsening, ignoring observed FVC data. In contrast, the WOCF approach considers all of the available FVC assessments and uses the worst value. We regard this as a reasonable approach to data from the SENSCIS trial as very few subjects (2% [n = 12]) discontinued due to disease worsening and >50% of subjects received assessments until at least week 36. A reanalysis based on multiple imputation yielded a similar magnitude of risk estimates (odds ratios) and nominal *P* values of <0.05 for the same outcomes. Our conclusions are further supported by the consistency between the analyses based on imputation and the reported time-to-event analyses (which do not depend on imputation).

We acknowledge that in the SENSCIS trial, nintedanib did not have beneficial effects on patient-reported outcomes assessing quality of life. The changes in patient-reported outcomes observed over 52 weeks in the 2 treatment groups, and the differences between them, were small and we do not believe them to be of clinical relevance. In contrast, we believe that the reduced rate of decline in FVC observed in subjects treated with nintedanib compared with placebo is of high clinical relevance given the association between FVC decline and mortality demonstrated in patients with SSc-ILD (2–4) and other fibrosing ILDs (5,6). In summary, we believe that the results of the SENSCIS trial provide strong evidence that nintedanib has a clinically relevant benefit in slowing the progression of SSc-ILD.

Dr. Maher has received consulting fees, speaking fees, and/or honoraria from AstraZeneca, Blade Therapeutics, Boehringer Ingelheim, Bristol Myers Squibb, Galápagos, GlaxoSmithKline, Indalo, Pliant, Respivant, Roche, and Theravance (less than $10,000 each). Dr. Mayes has received consulting fees, speaking fees, and/or honoraria from Boehringer Ingelheim, Corbus, Eicos Sciences, Galápagos, and Mitsubishi Tanabe (less than $10,000 each). Drs. Stock and Alves are employees of Boehringer Ingelheim.

Toby M. Maher, MD
National Heart and Lung Institute
Imperial College London
National Institute for Health Research Clinical Research Facility
Royal Brompton Hospital
London, UK
and Keck School of Medicine
University of Southern California
Los Angeles, CA
Maureen D. Mayes, MD
University of Texas McGovern Medical School
Houston, TX
Christian Stock, PhD
Boehringer Ingelheim Pharma GmbH & Co. KG
Ingelheim, Germany
Margarida Alves, MD
Boehringer Ingelheim International GmbH
Ingelheim, Germany

1. Distler O, Highland KB, Gahlemann M, Azuma A, Fischer A, Mayes MD, et al. Nintedanib for systemic sclerosis–associated interstitial lung disease. N Engl J Med 2019;380:2518–28.
2. Goh NS, Hoyles RK, Denton CP, Hansell DM, Renzoni EA, Maher TM, et al. Short-term pulmonary function trends are predictive of mortality in interstitial lung disease associated with systemic sclerosis. Arthritis Rheumatol 2017;69:1670–8.
3. Hoffmann-Vold AM, Fretheim H, Halse AK, Seip M, Bitter H, Wallenius M, et al. Tracking impact of interstitial lung disease in systemic sclerosis in a complete nationwide cohort. Am J Respir Crit Care Med 2019;200:1258–66.
4. Volkmann ER, Tashkin DP, Sim M, Li N, Goldmuntz E, Keyes-Elstein L, et al. Short-term progression of interstitial lung disease in systemic sclerosis predicts long-term survival in two independent clinical trial cohorts. Ann Rheum Dis 2019;78:122–30.
5. Paterniti MO, Youwei B, Rekić D, Wang Y, Karimi-Shah BA, Chowdhury BA. Acute exacerbation and decline in forced vital

capacity are associated with increased mortality in idiopathic pulmonary fibrosis. Ann Am Thorac Soc 2017;14:1395–402.
6. Solomon JJ, Chung JH, Cosgrove GP, Demoruelle MK, Fernandez-Perez ER, Fischer A, et al. Predictors of mortality in rheumatoid arthritis-associated interstitial lung disease. Eur Respir J 2016;47:588–96.

DOI 10.1002/art.41889

Suggested considerations for the treatment of rheumatic diseases in adult patients with COVID-19: comment on the article by Mikuls et al

To the Editor:

We read with great interest the latest American College of Rheumatology (ACR) consensus-based guidance for managing rheumatic diseases in adult patients with COVID-19, as presented by Dr. Mikuls and colleagues (1). We would first like to note that our nationwide retrospective cohort studies have shown that hydroxychloroquine treatment not only presents no increased risk of cardiac arrythmia in multiple rheumatic diseases (2), but also likely provides cardiovascular protection (3). Therefore, we believe the task force should reconsider the implications of halting hydroxychloroquine treatment in the context of SARS–CoV-2 infection.

Furthermore, we would like to emphasize the potential role of the JAK inhibitor baricitinib in limiting the damage of SARS–CoV-2 infection (4). A recent randomized controlled trial of hospitalized adults with COVID-19 demonstrated that combination therapy with baricitinib and remdesivir was more effective than remdesivir alone in terms of recovery time and clinical improvement (5). Since there was no apparent increase in rates of infection and venous thromboembolism with the addition of baricitinib, the optimal protocol for continuing baricitinib use in the treatment of rheumatic diseases could be discussed in the context of confirmed or presumptive COVID-19 infection.

Finally, we would like to highlight the need for the ACR guidance to stratify based on sex and age. A recent cohort study by Avouac et al demonstrated an association between rituximab treatment and poorer COVID-19 outcomes (6). However, older men were specifically more likely to be treated with rituximab, further confounding the potential causes of this association. Another study highlighted lower risks of hospitalizations for rheumatic disease patients within a predominantly older cohort of female patients treated with disease-modifying antirheumatic drugs or JAK inhibitors (7). These potential differences in age- and sex-related disease outcomes in rheumatic diseases and COVID-19 calls attention to the need for guidelines that address the risk/benefit ratio of rheumatologic treatments at an age- and sex-specific level.

Mr. Hsu and Dr. Liu contributed equally to this work.

Jeffrey Hsu, BS
University of Virginia School of Medicine
Charlottesville, VA
Chin-Hsiu Liu, MD, PhD
China Medical University Hospital
and China Medical University
Taichung, Taiwan
James C. Wei, MD, PhD
Chung Shan Medical University Hospital
Chung Shan Medical University
and China Medical University
Taichung, Taiwan

1. Mikuls TR, Johnson SR, Fraenkel L, Arasaratnam RJ, Baden LR, Bermas BL, et al. American College of Rheumatology guidance for the management of rheumatic disease in adult patients during the COVID-19 pandemic: version 3. Arthritis Rheumatol 2021;73:e1–12.
2. Lo CH, Wei JC, Wang YH, Tsai CF, Chan KC, Li LC, et al. Hydroxychloroquine does not increase the risk of cardiac arrhythmia in common rheumatic diseases: a nationwide population-based cohort study. Front Immunol 2021;12:631869.
3. Yang DH, Wang YH, Pan LF, Wei JC. Cardiovascular protection of hydroxychloroquine in patients with Sjögren's syndrome. J Clin Med 2020;9:3469.
4. Stebbing J, Nievas GS, Falcone M, Youhanna S, Richardson P, Ottaviani S, et al. JAK inhibition reduces SARS-CoV-2 liver infectivity and modulates inflammatory responses to reduce morbidity and mortality. Sci Adv 2021;7:eabe4724.
5. Kalil AC, Patterson TF, Mehta AK, Tomashek KM, Wolfe CR, Ghazaryan V, et al. Baricitinib plus remdesivir for hospitalized adults with Covid-19. N Engl J Med 2021;384:795–807.
6. Avouac J, Drumez E, Hachulla E, Seror R, Georgin-Lavialle S, El Mahou S, et al. COVID-19 outcomes in patients with inflammatory rheumatic and musculoskeletal diseases treated with rituximab: a cohort study. Lancet Rheumatol 2021;3:e419–26.
7. Stradner MH, Dejaco C, Zwerina J, Fritsch-Stork RD. Rheumatic musculoskeletal diseases and COVID-19 a review of the first 6 months of the pandemic. Front Med (Lausanne) 2020;7:562142.

American College of Rheumatology
Empowering Rheumatology Professionals

Arthritis & Rheumatology
Vol. 73, No. 12, December 2021, p 2356
DOI 10.1002/art.42019
© 2021, American College of Rheumatology

Erratum

In the article by Atisha-Fregoso et al in the January 2021 issue of *Arthritis & Rheumatology* (Phase II Randomized Trial of Rituximab Plus Cyclophosphamide Followed by Belimumab for the Treatment of Lupus Nephritis [pages 121–131]), the frequency of belimumab infusions in the patients randomized to receive rituximab and cyclophosphamide followed by belimumab infusions (RCB group) was incorrectly reported in several instances. The first sentence of the Methods paragraph of the abstract should have read "In a multicenter, randomized, open-label clinical trial, 43 patients with recurrent or refractory LN were treated with rituximab, cyclophosphamide (CYC), and glucocorticoids followed by belimumab infusions at weeks 4, 6, and 8 and every 4 weeks thereafter through week 48 (RCB group) or with rituximab and CYC but no belimumab infusions (RC group)." The first sentence of the third paragraph of Patients and Methods (right column on page 122) should have read "At week 4, trial participants were randomized to receive rituximab and CYC followed by belimumab infusions (RCB group), or to receive rituximab and CYC but no belimumab infusions (RC group)." In the footnotes of Tables 1–3 and the legend of Figure 1, RCB should have been defined as "treatment with rituximab, cyclophosphamide, and glucocorticoids followed by belimumab infusions at weeks 4, 6, and 8 and every 4 weeks thereafter through week 48."

We regret the errors.

Arthritis & Rheumatology
Vol. 73, No. 12, December 2021, pp 2357–2360
DOI 10.1002/art.42006
© 2021, American College of Rheumatology

American College of Rheumatology
Empowering Rheumatology Professionals

Reviewers

The individuals who served as reviewers for *Arthritis & Rheumatology* in 2021 are listed below. The Editorial Board is very grateful to our reviewers for the time and expertise they have devoted to the journal. Through their thoughtful and insightful critiques they have provided an invaluable service to the journal, our authors, and the discipline of rheumatology.

Daniel H. Solomon, MD, MPH, Editor-in-Chief

Abbott, J. H.
Abhishek, Abhishek
Abreu, Candida
Adamopoulos, Iannis E.
Aghayev, Ayaz
Ahmed, Salahuddin
Akbari, Omid
Aksentijevich, Ivona
Alarcón, Graciela
Allanore, Yannick
Amato, Anthony
Amoura, Zahir
Amulic, Borko
Andrade, Felipe
Anguera, Montserrat
Appenzeller, Simone
Appleton, Thomas
Araujo, Elizabeth
Aringer, Martin
Arkema, Elizabeth
Arriens, Cristina
Artlett, Carol
Ascherman, Dana
Askling, Johan*
Assassi, Shervin*
Atamas, Sergei
Attur, Mukundan
Bacon, Kathryn
Bagavant, Harini
Baker, Joshua F.
Balevic, Stephen
Baraliakos, Xenofon
Bartoloni, Elena
Barturen, Guillermo
Bathon, Joan
Bauer Ventura, Iazsmin
Baugh, John
Becker, Mara
Beier, Frank
Bengtsson, Karin
Bennell, Kim
Benveniste, Olivier
Berard, Roberta
Berenbaum, Francis
Berger, Christoph
Bermas, Bonnie
Bernhagen, Jurgen
Beukelman, Timothy
Bhattacharyya, Swati
Bierma-Zeinstra, Sita M. A.
Bind, Marie Abele
Blanco, Patrick
Block, Joel A.
Boackle, Susan
Boer, Cindy G.
Boers, Maarten
Boilard, Eric
Bolster, Marcy
Bonassar, Larry
Bortoluzzi, Alessandra
Bossini-Castillo, Lara
Bou-Gharios, George
Bowman, Simon J.
Bozec, Aline
Brahn, Ernest
Braun, Jürgen
Broder, Anna
Brouwer, Elisabeth
Brunner, Hermine
Buckley, Lenore
Bugatti, Serena
Bujor, Andreea
Bukhari, Marwan
Calabrese, Leonard
Cañete, Juan
Canna, Scott
Cappelli, Laura
Carette, Simon
Caricchio, Roberto
Carlson, Cathy
Carmona, Loreto
Carruthers, Mollie
Chakravarty, Eliza
Chandran, Vinod
Charles, J. F.
Charles, Julia
Chen, Qian
Chizzolini, Carlo
Cho, M-La
Choi, Hyon
Choi, May
Christensen, Robin
Chu, Cong-Qiu
Chung, Lorinda
Ciccia, Francesco
Ciurea, Adrian
Clauw, Daniel
Clegg, Peter
Coates, Laura
Coghlan, J. Gerry
Cohen, Stanley
Colbert, Robert
Collins, Jamie*
Corr, Maripat
Cosmi, Lorenzo
Costedoat-Chalumeau, Nathalie
Criado, Gabriel
Croft, Adam
Cron, Randy
Crow, Mary
Crowson, Cynthia
Cuda, Carla
Cullen, Breda
Cunin, Pierre
Curtis, Jeffrey
Cush, Jack
Darrah, Erika
Datta, Syamal K.
Davis III, John
Day, Richard
D'Cruz, David
De Benedetti, Fabrizio
Deane, Kevin D.
Decker, Patrice
Dees, Clara
Demoruelle, M.
Denton, Christopher*
Desai, Sonali
Dessein, Patrick
Devauchelle-Pensec, Valérie
Dhaun, Neeraj
Diamantopoulos, Andreas
Diamond, Betty*
Diekman, Brian
Ding, Changhai
Distler, Jörg
Dixon, William
Dong, Xuemei
Dooms, Hans
Dorner, Thomas
Duncan, Emma
Dutz, Jan
Edwards, Larry
Ehrenstein, Michael R.
Eleftheriou, Despina
Elewaut, Dirk
Elkon, Keith B.
Eloranta, Maija-Leena
England, Bryant
Englund, Martin

*Each of these individuals reviewed at least 4 manuscripts.

Enomoto-Iwamoto, Motomi
Erkan, Doruk
Ermann, Joerg
Escudero, Alejandro
Fagerli, Karen M.
Fahmi, Hassan
Falk, Ronald
Farris, Amy
Fautrel, Bruno
Favazzo, Lacey
Fearon, Ursula
Feghali-Bostwick, Carol
Feldman, Candace
Ferguson, Ian
Ferguson, Polly
Filkova, Maria
Finckh, Axel
Fiorentino, David
FitzGerald, John
Flannery, Carl
Fleischmann, Roy M.
Foell, Dirk
Fonseca, João
Ford, Julia
Fox, David
Franks, Jennifer
Frech, Tracy
Frenkel, Joost
Fritzler, Marvin
Fu, Shu Man
Fujimoto, Manabu
Fujio, Keishi
Furer, Victoria
Furst, Daniel
Gaffney, Patrick
Gaffo, Angelo
Galloway, James
Gasparyan, Armen Yuri
Gattorno, Marco
Geha, Paul
George, Michael
Georgel, Philippe
Georges, George
Geurts, Jeroen
Geusens, Piet
Giacomelli, Roberto
Gianfrancesco, Milena
Giles, Jon
Gilkeson, Gary
Ginzler, Ellen
Gladman, Dafna
Goldring, Mary
Gonzalez-Gay, Miguel
Gracey, Eric
Grainger, Rebecca
Grayson, Peter
Grieshaber-Bouyer, Ricardo
Griffin, Timothy
Grom, Alexei
Guma, Monica
Gupta, Sarthak
Gutekunst, David
Haavardsholm, Espen
Hachulla, Eric
Haemel, Anna
Hahn, Bevra H.
Haqqi, Tariq
Haroon, Nigil
Harper, Lorraine
Harris, James
Hasegawa, Minoru
Hatemi, Gulen
Hawker, Gillian
Hedrich, Christian
Helfgott, Simon
Henderson, Lauren*
Hiepe, Falk
Hill, Catherine
Hoffmann-Vold, Anna-Maria
Hojo, Hironori
Hong, Chuan
Hsiao, Betty
Huang, Steven
Huizinga, Tom
Hummers, Laura
Humphrey, Mary Beth
Idborg, Helena
Imgenberg-Kreuz, Juliana
Inman, Robert
Inoue, Katsuhisa
Isenberg, David
Ishigaki, Kazuyoshi
Itoh, Yoshifumi
Izmirly, Peter
Jackson, Shaun
Jadon, Deepak
Jafarzadeh, S. Reza
Jeffries, Matlock
Jiang, Xia
Jinin, Masatoshi
Jog, Neelakshi
Johnson, William Evan
Jones, Graeme
Jonsson, A. Helena
Jorge, April
Kalliolias, George
Kalunian, Kenneth
Kameda, Hideto
Kang, Insoo
Kaplan, Chelsea
Kapoor, Mohit
Karp, David
Katz, Jeffrey N.
Kawasaki, Aya
Khanna, Dinesh
Khatiwada, Aastha
Khosroshahi, Arezou
Kim, Kwangwoo
Kim, Seoyoung*
Kim, Wan-Uk
King, Jennifer
Klareskog, Lars
Kloppenburg, Margreet
Klotsche, Jens
Knevel, Rachel
Knight, Jason
Koeleman, Bobby
Kolachalama, Vijaya
Kono, Dwight H.
Koopman, Jacob
Kottyan, Leah
Kramer, Jill
Krebs, Christian
Kremer, Joel
Krieg, Thomas
Kriegel, Martin
Kronbichler, Andreas
Krueger, Elke
Kuhn, Kristine
Kuwana, Masataka*
Kvien, Tore
Kwok, Seung-ki
Kyttaris, Vasileios*
La Cava, Antonio
Lam, Christina
Lamprecht, Peter
Lane, Joseph
Langdahl, Bente
Langefeld, Carl*
Laslett, Laura
LaValley, Michael
Laxer, Ronald M.*
Layne, Matthew
Leask, Andrew
Lee, Alfred
Lee, Eun Bong
Lee, Pui
Lefebvre, Veronique
Lei, Guang-hua
Leonard, Dag
Lessard, Christopher
Li, Xiaojuan
Li, Zhixiu
Liew, Jean
Lillegraven, Siri
Lim, S. Sam
Lin, Jianhao
Liossis, Stamatis-Nick
Little, Christopher
Little, Dianne
Little, Mark
Liu-Bryan, Ru
Lo, Grace
Lo, Mindy
Lockshin, Michael
Loggia, Marco
Longobardi, Lara
Looney, Richard J.
Lopez-Pedrera, Chary
Lopez-Sola, Marina
Lories, Rik
Losina, Elena
Lotz, Martin
Loughlin, John
Love, Thorvardur Jon
Lovell, Daniel
Lu, Liangjing
Lu, QianJin
Lu, Theresa
Lubberts, Erik
Lundberg, Ingrid E.
Luppi, Fabrizio
Lyons, Karen
Lyons, Paul
Machado, Pedro
Mahr, Alfred

*Each of these individuals reviewed at least 4 manuscripts.

Maksymowych, Walter P.
Malkiel, Susan
Malmström, Vivianne
Mammen, Andrew
Manetti, Mirko
Manzo, Antonio
Marino, Eliana
Marmor, Michael
Márquez, Ana
Martín, Javier
Massarotti, Elena
Mathai, Stephen
Matsumoto, Isao
Matthews, Brya
McAdoo, Stephen
McAlinden, Audrey
McAlindon, Timothy
McCarthy, Geraldine
McCormick, Natalie
McCoy, Sara
McCune, W. Joseph
McGonagle, Dennis
McMahan, Zsuzsanna
Mecoli, Christopher
Meffre, Eric
Mehta, Jay
Merkel, Peter
Merrill, Joan T.
Merriman, Tony
Meulenbelt, Ingrid
Michaud, Kaleb
Migliorini, Paola
Mikuls, Ted
Miller, Gary
Miller, Rachel
Minden, Kirsten
Miossec, Pierre
Miyamoto, Takeshi
Mócsai, Attila
Mohan, Chandra
Mok, C. C.
Molberg, Øyvind
Molloy, Eamonn
Monach, Paul
Montecucco, Carlomaurizio
Mooney, Robert
Morand, Eric
Morel, Laurence
Moreland, Larry
Morgan, Esi
Moriyama, Masafumi
Mosca, Marta
Moudgil, Kamal
Mount, David
Moutsopoulos, Haralampos
Moutsopoulos, Niki
Mukherjee, Monica
Munroe, Melissa
Muscal, Eyal
Mustelin, Tomas
Myasoedova, Elena
Nagy, György
Nash, Peter
Neogi, Tuhina*
Nguyen, Cuong
Nielen, Johannes
Niewold, Timothy
Nordmark, Gunnel
Nowling, Tamara
Nutt, Stephen
Oates, Jim
O'Connor, Kevin
Oddis, Chester
O'Dell, James R.
Okazaki, Kazuichi
Ombrello, Michael
O'Neil, Liam
O'Neill, Terence
Orange, Dana
Orbai, Ana-Maria
Ormseth, Michelle
Ospelt, Caroline
Otero, Miguel
Padyukov, Leonid
Pagnoux, Christian
Pascart, Tristan
Passo, Murray
Pericleous, Charis
Perl, Andras*
Peters, James
Peterson, Erik
Peterson, Jennifer
Petri, Michelle
Pham, Tho
Piette, Jean-Charles
Pillinger, Michael
Prahalad, Sampath
Price, Christina
Pringle, Sarah
Provan, Sella
Puéchal, Xavier
Radic, Marko Z.
Radner, Helga
Rahman, Ziaur
Rai, Muhammad Farooq
Ramming, Andreas
Ramos, Paula
Rantapää Dahlqvist, Solbritt
Rao, Deepak
Ravelli, Angelo
Reed, Ann
Reeves, Westley
Rice, Sarah
Richette, Pascal
Richez, Christophe
Risbano, Michael
Robinson, Philip*
Roemer, Frank
Rogge, Lars
Romberg, Neil
Rosenbaum, James
Rosenthal, Ann K.
Rossjohn, Jamie
Rovin, Brad
Rubinstein, Tamar
Ruderman, Eric
Ruiz-Irastorza, Guillermo
Ruperto, Nicolino
Ruscitti, Piero
Saadoun, David
Sacitharan, Pradeep Kumar
Salama, Alan
Salvarani, Carlo
Sammaritano, Lisa
Sampaio Maia, Benedita
Sandovici, Maria
Sauler, Maor
Savic, Sinisa
Sawalha, Amr*
Scanzello, Carla
Schaible, Hans-Georg
Scheel-Toellner, Dagmar
Scher, Jose
Scherer, Hans
Schiphof, Dieuwke
Schmajuk, Gabriela
Schneider, Stefan
Schulert, Grant
Schwartzman-Morris, Julie
Scofield, R.
Sellam, Jeremie
Selva-O'Callaghan, Albert
Sendi, Parham
Seneko, Naoki
Seo, Philip
Sepriano, Alexandre
Sfikakis, Petros
Sharma, Aman
Shelef, Miriam
Shen, Nan*
Shin, Junghee
Shmerling, Robert H.
Shoda, Hirofumi
Sieper, Joachim
Silver, Richard M.*
Silverman, Gregg J.
Simms, Robert
Simon, Lee
Smith, Judith
Smith, Kenneth
Smith, Rona
Smolen, Josef
So, Alexander
Sobanski, Vincent
Sokolove, Jeremy*
Soni, Anushka
Souto-Carneiro, Margarida
Sparks, Jeffrey
Specks, Ulrich
Spiera, Robert
Steen, Virginia
Stohl, William
Stojanovich, Ljudmila
Stoll, Matthew
Strand, Vibeke
Su, Laura
Sun, Lingyun
Svensson, Mattias
Svenungsson, Elisabet
Takayanagi, Hiroshi
Takeuchi, Tsutomu
Tam, Lai-Shan
Tanaka, Yoshiya

*Each of these individuals reviewed at least 4 manuscripts.

Tas, Sander
Taylor, Peter
Tedeschi, Sara*
Terao, Chikashi
Terkeltaub, Robert
Tesarz, Jonas
Thakkar, Vivek
Thiele, Geoffrey
Thomas, Ranjeny
Toes, Rene
Top, Karina
Toprover, Michael
Toro-Dominguez, Daniel
Touma, Zahi
Trouw, Leendert
Tsou, Pei-Suen
Turk, Matthew
Turkiewicz, Aleksandra
Tzioufas, Athanasios
Uderhardt, Stefan
Vaglio, Augusto
van der Heijde, Désirée
van der Woude, Diane
van Meurs, Joyce
van Royen-Kerkhof, Annet
Vastert, Sebastiaan
Veale, Douglas
Vecellio, Matteo Luca
Venables, Patrick
Vencovský, Jiří
Viatte, Sebastien
Vincent, Tonia
Vital, Edward
Vogel, Tiphanie
Volkmann, Elizabeth
Volpe, Bruce
Vyse, Tomothy
Wallace, Daniel
Wallace, Graham
Wallace, Zachary
Walsh, David
Watt, Fiona
Watts, Richard
Weber-Schoendorfer, Corinna
Wedderburn, Lucy
Wei, Kevin
Wei, Lei
Weinblatt, Michael
Weisman, Michael
Weiss, Pamela
Wells, Athol
Werth, Victoria
White, Daniel
Whysall, Khasia
Wilkinson, J. Mark
Williams, Jessica
Wilson, Anthony Gerard
Winchester, Robert
Winter, Deborah
Wirth, Wolfgang
Wittoek, Ruth
Woodruff, Matthew
Woolley, Ann
Wright, Helen
Wu, Chialung
Wu, Minghua
Xavier, Ricardo
Xu, Hanshi
Yamaoka, Kunihiro
Yammani, Raghunatha
Yang, Tao
Yang, Wanling
Yau, Michelle
Yazdany, Jinoos
Yelin, Edward
Yeung, Rae
Yoshida, Kazuki
You, Sungyong
Yu, Di
Zakaria, Sammy
Zaki, Sanaa
Zhang, Xuan
Zhang, Yuqing
Zhao, Sizheng Steven

*Each of these individuals reviewed at least 4 manuscripts.

VOLUME 73 TABLE OF CONTENTS

VOLUME 73 • January 2021 • NO.1

In This Issue A9

Journal Club A10

Clinical Connections A11

Special Articles

Editorial: Challenges and Opportunities: Using Omics to Generate Testable Insights Into Pathogenic Mechanisms in Preclinical Seropositive Rheumatoid Arthritis
V. Michael Holers 1

Editorial: Would a 'Rosendo' by Another Name Smell as Sweet? Gender Disparity in Academic Rank and Publications in Rheumatology
Janet E. Pope 5

Notes From the Field: Treat-to-Target From the Patient Perspective Is Bowling for a Perfect Strike
Casper G. Schoemaker and Maarten P. T. de Wit 9

Clinical Practice Guidelines by the Infectious Diseases Society of America (IDSA), American Academy of Neurology (AAN), and American College of Rheumatology (ACR): 2020 Guidelines for the Prevention, Diagnosis, and Treatment of Lyme Disease
Paul M. Lantos, Jeffrey Rumbaugh, Linda K. Bockenstedt, Yngve T. Falck-Ytter, Maria E. Aguero-Rosenfeld, Paul G. Auwaerter, Kelly Baldwin, Raveendhara R. Bannuru, Kiran K. Belani, William R. Bowie, John A. Branda, David B. Clifford, Francis J. DiMario Jr., John J. Halperin, Peter J. Krause, Valery Lavergne, Matthew H. Liang, H. Cody Meissner, Lise E. Nigrovic, James (Jay) J. Nocton, Mikala C. Osani, Amy A. Pruitt, Jane Rips, Lynda E. Rosenfeld, Margot L. Savoy, Sunil K. Sood, Allen C. Steere, Franc Strle, Robert Sundel, Jean Tsao, Elizaveta E. Vaysbrot, Gary P. Wormser, and Lawrence S. Zemel 12

Winners of the 2020 American College of Rheumatology Annual Image Competition
American College of Rheumatology Image Library Subcommittee 21

Review: The Longitudinal Immune Response to Coronavirus Disease 2019: Chasing the Cytokine Storm
Alice S. Chau, Andrew G. Weber, Naomi I. Maria, Sonali Narain, Audrey Liu, Negin Hajizadeh, Prashant Malhotra, Ona Bloom, Galina Marder, and Blanka Kaplan 23

COVID-19

Antirheumatic Disease Therapies for the Treatment of COVID-19: A Systematic Review and Meta-Analysis
Michael Putman, Yu Pei Eugenia Chock, Herman Tam, Alfred H. J. Kim, Sebastian E. Sattui, Francis Berenbaum, Maria I. Danila, Peter Korsten, Catalina Sanchez-Alvarez, Jeffrey A. Sparks, Laura C. Coates, Candace Palmerlee, Andrea Peirce, Arundathi Jayatilleke, Sindhu R. Johnson, Adam Kilian, Jean Liew, Larry J. Prokop, M. Hassan Murad, Rebecca Grainger, Zachary S. Wallace, and Alí Duarte-García, on behalf of the COVID-19 Global Rheumatology Alliance 36

Brief Report: Susceptibility to COVID-19 in Patients Treated With Antimalarials: A Population-Based Study in Emilia-Romagna, Northern Italy
Carlo Salvarani, Pamela Mancuso, Federica Gradellini, Nilla Viani, Paolo Pandolfi, Massimo Reta, Giuliano Carrozzi, Gilda Sandri, Gianluigi Bajocchi, Elena Galli, Francesco Muratore, Luigi Boiardi, Nicolò Pipitone, Giulia Cassone, Stefania Croci, Anna Maria Marata, Massimo Costantini, and Paolo Giorgi Rossi 48

Errata

Omitted Author Affiliation in the Article by Xu et al (Arthritis Rheumatol, August 2020) 52

Errors in Two Sentences in the Letter by Bertin et al (Arthritis Rheumatol, November 2020) 52

Rheumatoid Arthritis

Improvements in Fatigue Lag Behind Disease Remission in Early Rheumatoid Arthritis: Results From the Canadian Early Arthritis Cohort
Melissa Holdren, Orit Schieir, Susan J. Bartlett, Louis Bessette, Gilles Boire, Glen Hazlewood, Carol A. Hitchon, Edward Keystone, Diane Tin, Carter Thorne, Vivian P. Bykerk, and Janet E. Pope, on behalf of the Canadian Early Arthritis Cohort Investigators 53

Respiratory Diseases as Risk Factors for Seropositive and Seronegative Rheumatoid Arthritis and in Relation to Smoking
Vanessa L. Kronzer, Helga Westerlind, Lars Alfredsson, Cynthia S. Crowson, Fredrik Nyberg, Göran Tornling, Lars Klareskog, Marie Holmqvist, and Johan Askling 61

Mediterranean Diet and Risk of Rheumatoid Arthritis: Findings From the French E3N-EPIC Cohort Study
Yann Nguyen, Carine Salliot, Amandine Gelot, Juliette Gambaretti, Xavier Mariette, Marie-Christine Boutron-Ruault, and Raphaèle Seror 69

Association of a Serum Protein Signature With Rheumatoid Arthritis Development
Liam J. O'Neil, Victor Spicer, Irene Smolik, Xiaobo Meng, Rishi R. Goel, Vidyanand Anaparti, John Wilkins, and Hani S. El-Gabalawy 78

Osteoarthritis

Synergistic Roles of Macrophages and Neutrophils in Osteoarthritis Progression
Ming-Feng Hsueh, Xin Zhang, Samuel S. Wellman, Michael P. Bolognesi, and Virginia B. Kraus 89

Multi-Tissue Epigenetic and Gene Expression Analysis Combined With Epigenome Modulation Identifies *RWDD2B* as a Target of Osteoarthritis Susceptibility
Eleanor Parker, Ines M. J. Hofer, Sarah J. Rice, Lucy Earl, Sami A. Anjum, David J. Deehan, and John Loughlin 100

Spondyloarthritis

Improvement of Signs and Symptoms of Nonradiographic Axial Spondyloarthritis in Patients Treated With Secukinumab: Primary Results of a Randomized, Placebo-Controlled Phase III Study
Atul Deodhar, Ricardo Blanco, Eva Dokoupilová, Stephen Hall, Hideto Kameda, Alan J. Kivitz, Denis Poddubnyy, Marleen van de Sande, Anna S. Wiksten, Brian O. Porter, Hanno B. Richards, Sibylle Haemmerle, and Jürgen Braun 110

Systemic Lupus Erythematosus

Phase II Randomized Trial of Rituximab Plus Cyclophosphamide Followed by Belimumab for the Treatment of Lupus Nephritis
Yemil Atisha-Fregoso, Susan Malkiel, Kristina M. Harris, Margie Byron, Linna Ding, Sai Kanaparthi, William T. Barry, Wendy Gao, Kristin Ryker, Patti Tosta, Anca D. Askanase, Susan A. Boackle, W. Winn Chatham, Diane L. Kamen, David R. Karp, Kyriakos A. Kirou, S. Sam Lim, Bradley Marder, Maureen McMahon, Samir V. Parikh, William F. Pendergraft III, Amber S. Podoll, Amit Saxena, David Wofsy, Betty Diamond, Dawn E. Smilek, Cynthia Aranow, and Maria Dall'Era 121
Conversion of T Follicular Helper Cells to T Follicular Regulatory Cells by Interleukin-2 Through Transcriptional Regulation in Systemic Lupus Erythematosus
He Hao, Shingo Nakayamada, Kaoru Yamagata, Naoaki Ohkubo, Shigeru Iwata, Yoshino Inoue, Mingzeng Zhang, Tong Zhang, Yurie Kanda Satoh, Yu Shan, Takashi Otsuka, and Yoshiya Tanaka 132

Sjögren's Syndrome

Improvement of Severe Fatigue Following Nuclease Therapy in Patients With Primary Sjögren's Syndrome: A Randomized Clinical Trial
James Posada, Saba Valadkhan, Daniel Burge, Kristen Davies, Jessica Tarn, John Casement, Kerry Jobling, Peter Gallagher, Douglas Wilson, Francesca Barone, Benjamin A. Fisher, and Wan-Fai Ng 143

Pediatric Rheumatology

Phase II Open-Label Study of Anakinra in Intravenous Immunoglobulin–Resistant Kawasaki Disease
Isabelle Koné-Paut, Stéphanie Tellier, Alexandre Belot, Karine Brochard, Corinne Guitton, Isabelle Marie, Ulrich Meinzer, Bilade Cherqaoui, Caroline Galeotti, Nadja Boukhedouni, Helene Agostini, Moshe Arditi, Virginie Lambert, and Céline Piedvache 151

Rheumatology Workforce

Representation of Women as Authors of Rheumatology Research Articles
Ekta Bagga, Sarah Stewart, Gregory D. Gamble, Janine Hill, Andrew Grey, and Nicola Dalbeth 162
Brief Report: The Association Between Physician Gender and Career Advancement Among Academic Rheumatologists in the United States
April Jorge, Marcy Bolster, Xiaoqing Fu, Daniel M. Blumenthal, Nate Gross, Kimberly G. Blumenthal, and Zachary Wallace 168

Letters

Reality Check on Antiphospholipid Antibodies in COVID-19–Associated Coagulopathy
Elena Gkrouzman, Medha Barbhaiya, Doruk Erkan, and Michael D. Lockshin 173
Determinants of Morning Stiffness in Rheumatoid Arthritis: Comment on the Article by Orange et al
Siddharth Jain, Debashish Mishra, and Varun Dhir 174
Reply
Dana E. Orange, Nathalie E. Blachere, Mayu O. Frank, Salina Parveen, Edward F. DiCarlo, Serene Mirza, Tania Pannellini, Caroline S. Jiang, Mark P. Figgie, Vivian P. Bykerk, Ellen M. Gravallese, Ana-Maria Orbai, Sarah L. Mackie, and Susan M. Goodman 175
Examining the Role of NF-E2–Related Factor 2 in Lupus: Comment on the Article by Han et al
Wang-Dong Xu and An-Fang Huang 176
Reply
Shuhong Han, Haoyang Zhuang, Mingjia Li, Lijun Yang, Pui Y. Lee, Peter A. Nigrovic, and Westley H. Reeves 176
Dipeptidylpeptidase 4 as a Marker of Fibrosis in Systemic Sclerosis: Comment on the Article by Soare et al
Michael R. Liebling 178
Reply
Alina Soare and Jörg H. W. Distler 179

Clinical Images

Erosive Costovertebral Joint Arthritis—An Uncommon Manifestation of Ankylosing Spondylitis
Tal Gazitt, Najwan Nassrallah, and Devy Zisman 180

VOLUME 73 • February 2021 • NO.2

In This Issue A17

Journal Club A18

Clinical Connections A19

Special Articles

Review: Rheumatoid Arthritis Pathogenesis, Prediction, and Prevention: An Emerging Paradigm Shift
Kevin D. Deane and V. Michael Holers 181

Editorial: Urinary Biomarkers in Lupus Nephritis: Are We There Yet?
Chi Chiu Mok and Chandra Mohan 194

Online-Only Special Article

American College of Rheumatology Guidance for the Management of Rheumatic Disease in Adult Patients During the COVID-19 Pandemic: Version 3
Ted R. Mikuls, Sindhu R. Johnson, Liana Fraenkel, Reuben J. Arasaratnam, Lindsey R. Baden, Bonnie L. Bermas, Winn Chatham, Stanley Cohen, Karen Costenbader, Ellen M. Gravallese, Andre C. Kalil, Michael E. Weinblatt, Kevin Winthrop, Amy S. Mudano, Amy Turner, and Kenneth G. Saag e1

Rheumatoid Arthritis

Health Assessment Questionnaire at One Year Predicts All-Cause Mortality in Patients With Early Rheumatoid Arthritis
Safoora Fatima, O. Schieir, M. F. Valois, S. J. Bartlett, L. Bessette, G. Boire, G. Hazlewood, C. Hitchon, E. C. Keystone, D. Tin, C. Thorne, V. P. Bykerk, and J. E. Pope, on behalf of the CATCH Investigators 197

Obesity-Related Traits and the Development of Rheumatoid Arthritis: Evidence From Genetic Data
Bowen Tang, Huwenbo Shi, Lars Alfredsson, Lars Klareskog, Leonid Padyukov, and Xia Jiang 203

Multiomics and Machine Learning Accurately Predict Clinical Response to Adalimumab and Etanercept Therapy in Patients With Rheumatoid Arthritis
Weiyang Tao, Arno N. Concepcion, Marieke Vianen, Anne C. A. Marijnissen, Floris P. G. J. Lafeber, Timothy R. D. J. Radstake, and Aridaman Pandit 212

Osteoarthritis

Patients' Preoperative Expectations of Total Knee Arthroplasty and Satisfaction With Outcomes at One Year: A Prospective Cohort Study
Gillian A. Hawker, Barbara L. Conner-Spady, Eric Bohm, Michael J. Dunbar, C. Allyson Jones, Bheeshma Ravi, Tom Noseworthy, Donald Dick, James Powell, Paulose Paul, and Deborah A. Marshall, on behalf of the BEST-Knee Study Team 223

Clinical Images

Repair of Bone Erosion With Effective Urate-Lowering Therapy in a Patient With Tophaceous Gout
Shota Sakaguchi 231

Systemic Lupus Erythematosus

An Autoimmunogenic and Proinflammatory Profile Defined by the Gut Microbiota of Patients With Untreated Systemic Lupus Erythematosus
Bei-di Chen, Xin-miao Jia, Jia-yue Xu, Li-dan Zhao, Jun-yi Ji, Bing-xuan Wu, Yue Ma, Hao Li, Xiao-xia Zuo, Wen-you Pan, Xiao-han Wang, Shuang Ye, George C. Tsokos, Jun Wang, and Xuan Zhang 232

Association Between Urinary Epidermal Growth Factor and Renal Prognosis in Lupus Nephritis
Juan M. Mejia-Vilet, John P. Shapiro, Xiaolan L. Zhang, Cristino Cruz, Grant Zimmerman, R. Angélica Méndez-Pérez, Mayra L. Cano-Verduzco, Samir V. Parikh, Haikady N. Nagaraja, Luis E. Morales-Buenrostro, and Brad H. Rovin 244

Effects of BAFF Neutralization on Atherosclerosis Associated With Systemic Lupus Erythematosus
Fanny Saidoune, Guillaume Even, Yasmine Lamri, Julie Chezel, Anh-Thu Gaston, Brigitte Escoubet, Thomas Papo, Nicolas Charles, Antonino Nicoletti, and Karim Sacre 255

Association of Urinary Matrix Metalloproteinase 7 Levels With Incident Renal Flare in Lupus Nephritis
Guobao Wang, Liling Wu, Huanjuan Su, Xiaodan Feng, Meng Shi, Lingwei Jin, Manqiu Yang, Zhanmei Zhou, Cailing Su, Bihui Yang, Yajing Li, and Wei Cao 265

Vasculitis

Deficiency of Adenosine Deaminase 2 in Adults and Children: Experience From India
Aman Sharma, GSRSNK Naidu, Vikas Sharma, Saket Jha, Aaadhar Dhooria, Varun Dhir, Prateek Bhatia, Vishal Sharma, Sagar Bhattad, K. G. Chengappa, Vikas Gupta, Durga Prasanna Misra, Pallavi Pimpale Chavan, Sourabh Malaviya, Rajkiran Dudam, Banwari Sharma, Sathish Kumar, Rajesh Bhojwani, Pankaj Gupta, Vikas Agarwal, Kusum Sharma, Manphool Singhal, Manish Rathi, Ritambhra Nada, Ranjana W. Minz, Ved Chaturvedi, Amita Aggarwal, Rohini Handa, Alice Grossi, Marco Gattorno, Zhengping Huang, Jun Wang, Ramesh Jois, V. S. Negi, Raju Khubchandani, Sanjay Jain, Juan I. Arostegui, Eugene P. Chambers, Michael S. Hershfield, Ivona Aksentijevich, Qing Zhou, and Pui Y. Lee 276

Temporal Arteritis Revealing Antineutrophil Cytoplasmic Antibody–Associated Vasculitides: A Case–Control Study
Laure Delaval, Maxime Samson, Flora Schein, Christian Agard, Ludovic Tréfond, Alban Deroux, Henry Dupuy, Cyril Garrouste, Pascal Godmer, Cédric Landron, François Maurier, Guillaume le Guenno, Virginie Rieu, Julien Desblache, Cécile-Audrey Durel, Laurence Jousselin-Mahr, Hassan Kassem, Grégory Pugnet, Vivane Queyrel, Laure Swiader, Daniel Blockmans, Karim Sacré, Estibaliz Lazaro, Luc Mouthon, Olivier Aumaître, Pascal Cathébras, Loic Guillevin, and Benjamin Terrier, on behalf of the French Vasculitis Study Group and French Study Group for Giant Cell Arteritis 286

Clinical Images

Spondylitis as a Rare Manifestation of Granulomatosis With Polyangiitis
Matthias H. Busch, Joop P. Aendekerk, Astrid M. L. Oude Lashof, and Pieter van Paassen 294

Systemic Sclerosis

Hemodynamic Response to Treatment and Outcomes in Pulmonary Hypertension Associated With Interstitial Lung Disease Versus Pulmonary Arterial Hypertension in Systemic Sclerosis: Data From a Study Identifying Prognostic Factors in Pulmonary Hypertension Associated With Interstitial Lung Disease
Louis Chauvelot, Delphine Gamondes, Julien Berthiller, Ana Nieves, Sébastien Renard, Judith Catella-Chatron, Kais Ahmad, Laurent Bertoletti, Boubou Camara, Emmanuel Gomez, David Launay, David Montani, Jean-François Mornex, Grégoire Prévot, Olivier Sanchez, Anne-Marie Schott, Fabien Subtil, Julie Traclet, Ségolène Turquier, Sabrina Zeghmar, Gilbert Habib, Martine Reynaud-Gaubert, Marc Humbert, Vincent Cottin, The French Network for Pulmonary Arterial Hypertension, and The French Network for Rare Pulmonary Diseases (OrphaLung) 295
Association of Autologous Hematopoietic Stem Cell Transplantation in Systemic Sclerosis With Marked Improvement in Health-Related Quality of Life
Nancy Maltez, Mathieu Puyade, Mianbo Wang, Pauline Lansiaux, Zora Marjanovic, Catney Charles, Russell Steele, Murray Baron, Ines Colmegna, Marie Hudson, and Dominique Farge, for the Canadian Scleroderma Research Group and the MATHEC-SFGMTC Network 305
Cancer in Systemic Sclerosis: Analysis of Antibodies Against Components of the Th/To Complex
Christopher A. Mecoli, Brittany L. Adler, Qingyuan Yang, Laura K. Hummers, Antony Rosen, Livia Casciola-Rosen, and Ami A. Shah 315

Gout

Brief Report: Calcium Pyrophosphate Dihydrate Crystal Deposition in Gouty Tophi
Hang-Korng Ea, Alan Gauffenic, Quang Dinh Nguyen, Nhu G. Pham, Océane Olivier, Vincent Frochot, Dominique Bazin, Nghia H. Le, Caroline Marty, Agnès Ostertag, Martine Cohen-Solal, Jean-Denis Laredo, Pascal Richette, and Thomas Bardin 324

Pediatric Rheumatology

Imaging-Based Uveitis Surveillance in Juvenile Idiopathic Arthritis: Feasibility, Acceptability, and Diagnostic Performance
Saira Akbarali, Jugnoo S. Rahi, Andrew D. Dick, Kiren Parkash, Katie Etherton, Clive Edelsten, Xiaoxuan Liu, and Ameenat L. Solebo 330
Tapering Canakinumab Monotherapy in Patients With Systemic Juvenile Idiopathic Arthritis in Clinical Remission: Results From a Phase IIIb/IV Open-Label, Randomized Study
Pierre Quartier, Ekaterina Alexeeva, Tamàs Constantin, Vyacheslav Chasnyk, Nico Wulffraat, Karin Palmblad, Carine Wouters, Hermine I. Brunner, Katherine Marzan, Rayfel Schneider, Gerd Horneff, Alberto Martini, Jordi Anton, Xiaoling Wei, Alan Slade, Nicolino Ruperto, and Ken Abrams, in collaboration with the Paediatric Rheumatology International Trials Organisation and the Pediatric Rheumatology Collaborative Study Group 336

Autoimmune Disease

Incidence, Clinical Features, and Outcomes of Late-Onset Neutropenia From Rituximab for Autoimmune Disease
Reza Zonozi, Zachary S. Wallace, Karen Laliberte, Noah R. Huizenga, Jillian M. Rosenthal, Eugene P. Rhee, Frank B. Cortazar, and John L. Niles 347

Letters

High Prevalence of New-Onset or Worsening Hepatitis C Virus–Related Musculoskeletal Symptoms After Beginning Direct-Acting Antiviral Therapy: A Challenging Novel Observation
Muhammad Haroon, Khurram Anis, Zara Khan, and Naila Nawaz 355
Morning Stiffness and Neutrophil Circadian Disarming: Comment on the Article by Orange et al
Omer Nuri Pamuk and Sarfaraz Hasni 356
Reply
Dana E. Orange, Nathalie E. Blachere, Mayu O. Frank, Salina Parveen, Edward F. DiCarlo, Serene Mirza, Tania Pannellini, Mark P. Figgie, Vivian P. Bykerk, Caroline S. Jiang, Ellen M. Gravallese, Ana-Maria Orbai, Sarah L. Mackie, and Susan M. Goodman 357
Early-Onset Hydroxychloroquine Retinopathy and a Possible Relationship to Blood Levels: Comment on the Article by Petri et al
Naoto Yokogawa, Akiko Ohno-Tanaka, Masayuki Hashiguchi, Mikiko Shimizu, Hiroko Ozawa, Shinji Ueno, Kei Shinoda, and David J. Browning 358
Reply
Michelle Petri, Marwa Elkhalifa, Laurence S. Magder, Jessica Li, and Daniel W. Goldman 359
To Switch or Not Switch Febuxostat: Comment on the Article by FitzGerald et al
Chuanhui Xu 359

VOLUME 73 • March 2021 • NO.3

In This Issue A17

Journal Club A18

Clinical Connections A19

Special Articles

Review: New Therapeutic Targets in Antineutrophil Cytoplasm Antibody–Associated Vasculitis
Maria Prendecki and Stephen P. McAdoo 361

Editorial: Acupuncture and Knee Osteoarthritis: Does Dose Matter?
David J. Hunter and Richard E. Harris 371

COVID-19

Association of Race and Ethnicity With COVID-19 Outcomes in Rheumatic Disease: Data From the COVID-19 Global Rheumatology Alliance Physician Registry
Milena A. Gianfrancesco, Liza A. Leykina, Zara Izadi, Tiffany Taylor, Jeffrey A. Sparks, Carly Harrison, Laura Trupin, Stephanie Rush, Gabriela Schmajuk, Patricia Katz, Lindsay Jacobsohn, Tiffany Y. Hsu, Kristin M. D'Silva, Naomi Serling-Boyd, Rachel Wallwork, Derrick J. Todd, Suleman Bhana, Wendy Costello, Rebecca Grainger, Jonathan S. Hausmann, Jean W. Liew, Emily Sirotich, Paul Sufka, Zachary S. Wallace, Pedro M. Machado, Philip C. Robinson, and Jinoos Yazdany, on behalf of the COVID-19 GlobalRheumatology Alliance 374

Rheumatoid Arthritis

Allele-Specific Quantification of HLA–DRB1 Transcripts Reveals Imbalanced Allelic Expression That Modifies the Amino Acid Effects in HLA–DRβ1
Sehwan Chun, So-Young Bang, Eunji Ha, Jing Cui, Ki-Nam Gu, Hye-Soon Lee, Kwangwoo Kim, and Sang-Cheol Bae 381

Association of Agricultural, Occupational, and Military Inhalants With Autoantibodies and Disease Features in US Veterans With Rheumatoid Arthritis
Ariadne V. Ebel, Gabrielle Lutt, Jill A. Poole, Geoffrey M. Thiele, Joshua F. Baker, Grant W. Cannon, Angelo Gaffo, Gail S. Kerr, Andreas Reimold, Pascale Schwab, Namrata Singh, J. Steuart Richards, Dana P. Ascherman, Ted R. Mikuls, and Bryant R. England 392

Profiling of Serum Oxylipins During the Earliest Stages of Rheumatoid Arthritis
Javier Rodríguez-Carrio, Roxana Coras, Mercedes Alperi-López, Patricia López, Catalina Ulloa, Francisco Javier Ballina-García, Aaron M. Armando, Oswald Quehenberger, Mónica Guma, and Ana Suárez 401

Erratum

Error in Statement on Carbonated Beverage Consumption in the Article by FitzGerald et al (Arthritis Rheumatol, June 2020) 413

Osteoarthritis

Mechanosensitive Control of Articular Cartilage and Subchondral Bone Homeostasis in Mice Requires Osteocytic Transforming Growth Factor β Signaling
Karsyn N. Bailey, Jeffrey Nguyen, Cristal S. Yee, Neha S. Dole, Alexis Dang, and Tamara Alliston 414

MicroRNA-34a-5p Promotes Joint Destruction During Osteoarthritis
Helal Endisha, Poulami Datta, Anirudh Sharma, Sayaka Nakamura, Evgeny Rossomacha, Carolen Younan, Shabana A. Ali, Ghazaleh Tavallaee, Starlee Lively, Pratibha Potla, Konstantin Shestopaloff, Jason S. Rockel, Roman Krawetz, Nizar N. Mahomed, Igor Jurisica, Rajiv Gandhi, and Mohit Kapoor 426

Familial Clustering of Erosive Hand Osteoarthritis in a Large Statewide Cohort
Nikolas H. Kazmers, Huong D. Meeks, Kendra A. Novak, Zhe Yu, Gail L. Fulde, Joy L. Thomas, Tyler Barker, and Michael J. Jurynec 440

Efficacy of Intensive Acupuncture Versus Sham Acupuncture in Knee Osteoarthritis: A Randomized Controlled Trial
Jian-Feng Tu, Jing-Wen Yang, Guang-Xia Shi, Zhang-Sheng Yu, Jin-Ling Li, Lu-Lu Lin, Yu-Zheng Du, Xiao-Gang Yu, Hui Hu, Zhi-Shun Liu, Chun-Sheng Jia, Li-Qiong Wang, Jing-Jie Zhao, Jun Wang, Tong Wang, Yang Wang, Tian-Qi Wang, Na Zhang, Xuan Zou, Yu Wang, Jia-Kai Shao, and Cun-Zhi Liu 448

Systemic Lupus Erythematosus

Modulation of Cardiometabolic Disease Markers by Type I Interferon Inhibition in Systemic Lupus Erythematosus
Kerry A. Casey, Michael A. Smith, Dominic Sinibaldi, Nickie L. Seto, Martin P. Playford, Xinghao Wang, Philip M. Carlucci, Liangwei Wang, Gabor Illei, Binbing Yu, Shiliang Wang, Alan T. Remaley, Nehal N. Mehta, Mariana J. Kaplan, and Wendy I. White 459

Brief Report: Suppression of Serum Interferon-γ Levels as a Potential Measure of Response to Ustekinumab Treatment in Patients With Systemic Lupus Erythematosus
Matteo Cesaroni, Loqmane Seridi, Matthew J. Loza, Jessica Schreiter, Kristen Sweet, Carol Franks, Keying Ma, Ashley Orillion, Kim Campbell, Robert M. Gordon, Patrick Branigan, Peter Lipsky, Ronald van Vollenhoven, Bevra H. Hahn, George C. Tsokos, Marc Chevrier, Shawn Rose, Frédéric Baribaud, and Jarrat Jordan 472

Type I Interferon–Activated STAT4 Regulation of Follicular Helper T Cell–Dependent Cytokine and Immunoglobulin Production in Lupus
Xuemei Dong, Olivia Q. Antao, Wenzhi Song, Gina M. Sanchez, Krzysztof Zembrzuski, Fotios Koumpouras, Alexander Lemenze, Joe Craft, and Jason S. Weinstein 478

Vasculitis

Brief Report: A Novel *RELA* Truncating Mutation in a Familial Behçet's Disease–like Mucocutaneous Ulcerative Condition
Fahd Adeeb, Emma R. Dorris, Niamh E. Morgan, Dylan Lawless, Aqeel Maqsood, Wan Lin Ng, Orla Killeen, Eoin P. Cummins, Cormac T. Taylor, Sinisa Savic, Anthony G. Wilson, and Alexander Fraser 490
Brief Report: Use of Biologics to Treat Relapsing and/or Refractory Eosinophilic Granulomatosis With Polyangiitis: Data From a European Collaborative Study
Alice Canzian, Nils Venhoff, Maria Letizia Urban, Silvia Sartorelli, Anne-Marie Ruppert, Matthieu Groh, Nicolas Girszyn, Camille Taillé, François Maurier, Vincent Cottin, Claire de Moreuil, Vincent Germain, Maxime Samson, Marie Jachiet, Laure Denis, Virginie Rieu, Perrine Smets, Grégory Pugnet, Alban Deroux, Cécile-Audrey Durel, Achille Aouba, Pascal Cathébras, Christophe Deligny, Stanislas Faguer, Helder Gil, Bertrand Godeau, François Lifermann, Sophie Phin-Huynh, Marc Ruivard, Philippe Bonniaud, Xavier Puéchal, Jean-Emmanuel Kahn, Jens Thiel, Lorenzo Dagna, Loïc Guillevin, Augusto Vaglio, Giacomo Emmi, and Benjamin Terrier, for the French Vasculitis Study Group and the European EGPA Study Group 498
Cardiovascular and Renal Morbidity in Takayasu Arteritis: A Population-Based Retrospective Cohort Study From the United Kingdom
Ruchika Goel, Joht Singh Chandan, Rasiah Thayakaran, Nicola J. Adderley, Krishnarajah Nirantharakumar, and Lorraine Harper 504
Brief Report: Sequence-Based Screening of Patients With Idiopathic Polyarteritis Nodosa, Granulomatosis With Polyangiitis, and Microscopic Polyangiitis for Deleterious Genetic Variants in *ADA2*
Oskar Schnappauf, Natalia Sampaio Moura, Ivona Aksentijevich, Monique Stoffels, Amanda K. Ombrello, Patrycja Hoffmann, Karyl Barron, Elaine F. Remmers, Michael Hershfield, Susan J. Kelly, NISC Comparative Sequencing Program, David Cuthbertson, Simon Carette, Sharon A. Chung, Lindsy Forbess, Nader A. Khalidi, Curry L. Koening, Carol A. Langford, Carol A. McAlear, Paul A. Monach, Larry Moreland, Christian Pagnoux, Philip Seo, Jason M. Springer, Antoine G. Sreih, Kenneth J. Warrington, Steven R. Ytterberg, Daniel L. Kastner, Peter C. Grayson, and Peter A. Merkel, for the Vasculitis Clinical Research Consortium 512

Systemic Sclerosis

Dissecting the Cellular Mechanism of Prostacyclin Analog Iloprost in Reversing Vascular Dysfunction in Scleroderma
Pei-Suen Tsou, Pamela J. Palisoc, Nicholas A. Flavahan, and Dinesh Khanna 520

Pediatric Rheumatology

Efficacy and Safety of Tocilizumab for Polyarticular-Course Juvenile Idiopathic Arthritis in the Open-Label Two-Year Extension of a Phase III Trial
Hermine I. Brunner, Nicolino Ruperto, Zbigniew Zuber, Rubén Cuttica, Vladimir Keltsev, Ricardo M. Xavier, Ruben Burgos-Vargas, Inmaculada Calvo Penades, Earl D. Silverman, Graciela Espada, Manuel Ferrandiz Zavaler, Yukiko Kimura, Carolina Duarte, Chantal Job-Deslandre, Rik Joos, Wendy Douglass, Sunethra Wimalasundera, Kamal N. Bharucha, Chris Wells, Daniel J. Lovell, Alberto Martini, and Fabrizio de Benedetti, for the Paediatric Rheumatology International Trials Organisation (PRINTO) and the Pediatric Rheumatology Collaborative Study Group (PRCSG) 530

Clinical Images

An Unusual Case of Proximal Limb Muscle Weakness
Despina Michailidou, Sarah Chung, James S. Andrews, Gordon A. Starkebaum, Felix S. Chew, and Caitlin S. Latimer 541

Letters

Trends in Utilization of Urate-Lowering Therapies Following the US Food and Drug Administration's Boxed Warning on Febuxostat
Seoyoung C. Kim, Tuhina Neogi, Erin Kim, Joyce Lii, and Rishi J. Desai 542
Treat-to-Target in Gout Management? Comment on the Article by FitzGerald et al
Michael R. Kolber and Joey Ton 543
Reply
Tuhina Neogi, Nicola Dalbeth, Ted R. Mikuls, Amy S. Turner, and John D. FitzGerald 544
Anti-Th/To Antibodies: Association With Lung Disease and Potential Protection From Systemic Sclerosis–Related Cancer? Comment on the Article by Mecoli et al
Michael Mahler, Minoru Satoh, and Marvin Fritzler 545
Further Investigation of Representation of Women as Authors of Rheumatology Articles From 2005 to 2020: Comment on the Article by Bagga et al
Jennifer Velasco, Shikha Singla, Michael Putman, Abigail A. Thorgerson, Elizabeth Suelzer, and Courtney B. Crayne 546
Use of Apremilast in Patients With Psoriatic Arthritis During the COVID-19 Pandemic: Comment on the Article by Mikuls et al
Pankaj Bansal, Amandeep Goyal, Austin Cusick, and Fawad Aslam 547
Reply
Ted R. Mikuls, Liana Fraenkel, Ellen Gravallese, Sindhu R. Johnson, Amy Turner, and Kenneth G. Saag 548
Anakinra in COVID-19—How to Interpret Elevations of Serum Liver Enzymes: Comment on the Article by Navarro-Millán et al
Giulio Cavalli and Lorenzo Dagna 549
Reply
Iris Navarro-Millán and Mary K. Crow 549

VOLUME 73 • April 2021 • NO.4

In This Issue A15

Journal Club A16

Clinical Connections A17

Special Articles

In Memoriam: Raphael J. DeHoratius, MD, 1942–2020
Lawrence H. Brent 551

Expert Perspectives on Clinical Challenges: Expert Perspective: Immune Checkpoint Inhibitors and Rheumatologic Complications
Laura C. Cappelli and Clifton O. Bingham III 553

American College of Rheumatology Clinical Guidance for Multisystem Inflammatory Syndrome in Children Associated With SARS–CoV-2 and Hyperinflammation in Pediatric COVID-19: Version 2
Lauren A. Henderson, Scott W. Canna, Kevin G. Friedman, Mark Gorelik, Sivia K. Lapidus, Hamid Bassiri, Edward M. Behrens, Anne Ferris, Kate F. Kernan, Grant S. Schulert, Philip Seo, Mary Beth F. Son, Adriana H. Tremoulet, Rae S. M. Yeung, Amy S. Mudano, Amy S. Turner, David R. Karp, and Jay J. Mehta e13

Editorial: Consequences of a Great Crisis on Chronic Diseases: How Childhood Exposures May Shape Future Health
Jason J. Lee and Zumin Shi 566

Rheumatoid Arthritis

Associations of Antibodies Targeting Periodontal Pathogens With Subclinical Coronary, Carotid, and Peripheral Arterial Atherosclerosis in Rheumatoid Arthritis
Jon T. Giles, Jesper Reinholdt, Felipe Andrade, and Maximilian F. Konig 568

Distinct Expression of Coinhibitory Molecules on Alveolar T Cells in Patients With Rheumatoid Arthritis–Associated and Idiopathic Inflammatory Myopathy–Associated Interstitial Lung Disease
Maho Nakazawa, Katsuya Suzuki, Masaru Takeshita, Jun Inamo, Hirofumi Kamata, Makoto Ishii, Yoshitaka Oyamada, Hisaji Oshima, and Tsutomu Takeuchi 576

Efficacy and Safety of E6011, an Anti-Fractalkine Monoclonal Antibody, in Patients With Active Rheumatoid Arthritis With Inadequate Response to Methotrexate: Results of a Randomized, Double-Blind, Placebo-Controlled Phase II Study
Yoshiya Tanaka, Tsutomu Takeuchi, Hisashi Yamanaka, Toshihiro Nanki, Hisanori Umehara, Nobuyuki Yasuda, Fumitoshi Tago, Yasumi Kitahara, Makoto Kawakubo, Kentaro Torii, Seiichiro Hojo, Tetsu Kawano, and Toshio Imai 587

In Utero and Early Life Exposure to the Great Chinese Famine and Risk of Rheumatoid Arthritis in Adulthood
Hannah VanEvery, Wen-hao Yang, Nancy Olsen, Xinyuan Zhang, Rong Shu, Bing Lu, Shouling Wu, Liufu Cui, and Xiang Gao 596

Psoriatic Arthritis

Efficacy and Safety of Guselkumab, an Interleukin-23p19–Specific Monoclonal Antibody, Through One Year in Biologic-Naive Patients With Psoriatic Arthritis
Iain B. McInnes, Proton Rahman, Alice B. Gottlieb, Elizabeth C. Hsia, Alexa P. Kollmeier, Soumya D. Chakravarty, Xie L. Xu, Ramanand A. Subramanian, Prasheen Agarwal, Shihong Sheng, Yusang Jiang, Bei Zhou, Yanli Zhuang, Désirée van der Heijde, and Philip J. Mease 604

Systemic Lupus Erythematosus

Hospitalized Infections in Lupus: A Nationwide Study of Types of Infections, Time Trends, Health Care Utilization, and In-Hospital Mortality
Jasvinder A. Singh and John D. Cleveland 617

Clinical Images

Wong-Type Dermatomyositis in an African American Patient
Christina E. Bax, Madison Grinnell, Josef Symon S. Concha, and Victoria P. Werth 630

Sjögren's Syndrome

Interleukin-7/Interferon Axis Drives T Cell and Salivary Gland Epithelial Cell Interactions in Sjögren's Syndrome
Elodie Rivière, Juliette Pascaud, Alexandre Virone, Anastasia Dupré, Bineta Ly, Audrey Paoletti, Raphaèle Seror, Nicolas Tchitchek, Michael Mingueneau, Nikaïa Smith, Darragh Duffy, Lydie Cassard, Nathalie Chaput, Sabrina Pengam, Vanessa Gauttier, Nicolas Poirier, Xavier Mariette, and Gaetane Nocturne 631

Vasculitis

Sustained Remission of Granulomatosis With Polyangiitis After Discontinuation of Glucocorticoids and Immunosuppressant Therapy: Data From the French Vasculitis Study Group Registry
Xavier Puéchal, Michele Iudici, Christian Pagnoux, Alexandre Karras, Pascal Cohen, François Maurier, Thomas Quéméneur, François Lifermann, Mohamed Hamidou, Luc Mouthon, Benjamin Terrier, and Loïc Guillevin, for the French Vasculitis Study Group 641

Multimorbidity in Antineutrophil Cytoplasmic Antibody–Associated Vasculitis: Results From a Longitudinal, Multicenter Data Linkage Study
Shifa H. Sarica, Peter J. Gallacher, Neeraj Dhaun, Jan Sznajd, John Harvie, John McLaren, Lucy McGeoch, Vinod Kumar, Nicole Amft, Lars Erwig, Angharad Marks, Laura Bruno, York Zöllner, Corri Black, and Neil Basu 651

Systemic Sclerosis
Large-Scale Characterization of Systemic Sclerosis Serum Protein Profile: Comparison to Peripheral Blood Cell Transcriptome and Correlations With Skin/Lung Fibrosis
Chiara Bellocchi, Jun Ying, Ellen A. Goldmuntz, Lynette Keyes-Elstein, John Varga, Monique E. Hinchcliff, Marka A. Lyons, Peter McSweeney, Daniel E. Furst, Richard Nash, Leslie J. Crofford, Beverly Welch, Jonathan G. Goldin, Ashley Pinckney, Maureen D. Mayes, Keith M. Sullivan, and Shervin Assassi 660
Effect of Nintedanib on Lung Function in Patients With Systemic Sclerosis–Associated Interstitial Lung Disease: Further Analyses of a Randomized, Double-Blind, Placebo-Controlled Trial
Toby M. Maher, Maureen D. Mayes, Michael Kreuter, Elizabeth R. Volkmann, Martin Aringer, Ivan Castellvi, Maurizio Cutolo, Christian Stock, Nils Schoof, Margarida Alves, and Ganesh Raghu, on behalf of the SENSCIS Trial Investigators 671

Dermatomyositis
Risk Prediction Modeling Based on a Combination of Initial Serum Biomarker Levels in Polymyositis/Dermatomyositis–Associated Interstitial Lung Disease
Takahisa Gono, Kenichi Masui, Naoshi Nishina, Yasushi Kawaguchi, Atsushi Kawakami, Kei Ikeda, Yohei Kirino, Yumiko Sugiyama, Yoshinori Tanino, Takahiro Nunokawa, Yuko Kaneko, Shinji Sato, Katsuaki Asakawa, Taro Ukichi, Shinjiro Kaieda, Taio Naniwa, Yutaka Okano, Masataka Kuwana, and the Multicenter Retrospective Cohort of Japanese Patients with Myositis-Associated ILD (JAMI) Investigators 677

Pseudogout
Brief Report: Can Dual-Energy Computed Tomography Be Used to Identify Early Calcium Crystal Deposition in the Knees of Patients With Calcium Pyrophosphate Deposition?
Jean-François Budzik, Claire Marzin, Julie Legrand, Laurène Norberciak, Fabio Becce, and Tristan Pascart 687

Pediatric Rheumatology
Platelet Glycoprotein Ib α-Chain as a Putative Therapeutic Target for Juvenile Idiopathic Arthritis: A Mendelian Randomization Study
Shan Luo, Sarah L. N. Clarke, Athimalaipet V. Ramanan, Susan D. Thompson, Carl D. Langefeld, Miranda C. Marion, Alexei A. Grom, C. Mary Schooling, Tom R. Gaunt, Shiu Lun Au Yeung, and Jie Zheng 693

Corrigendum
Errors in Figure 6B of the Article by Ciccia et al (Arthritis Rheumatol, December 2018) 701

Health Outcomes
Prevalence, Deaths, and Disability-Adjusted Life Years Due to Musculoskeletal Disorders for 195 Countries and Territories 1990–2017
Saeid Safiri, Ali-Asghar Kolahi, Marita Cross, Catherine Hill, Emma Smith, Kristin Carson-Chahhoud, Mohammad Ali Mansournia, Amir Almasi-Hashiani, Ahad Ashrafi-Asgarabad, Jay Kaufman, Mahdi Sepidarkish, Seyed Kazem Shakouri, Damian Hoy, Anthony D. Woolf, Lyn March, Gary Collins, and Rachelle Buchbinder 702

Letters
Different Control Populations May Lead to Different Understanding of Hydroxychloroquine Blood Levels as a Risk Factor for Retinopathy: Comment on the Article by Petri et al
Tiphaine Lenfant, Gaëlle Leroux, and Nathalie Costedoat-Chalumeau 715
Lenabasum for Systemic Sclerosis—Are Cannabinoids the Missing Link? Comment on the Article by Spiera et al
Sakshi Mittal and Shefali Sharma 715
Reply
Robert Spiera, Lorinda Chung, Tracy Frech, Robyn Domsic, Vivien Hsu, Daniel E. Furst, Robert Simms, Maureen Mayes, Viktor Martyanov, Michael L. Whitfield, Nancy Dgetluck, Quinn Dinh, and Barbara White 716
Should the Biopsychosocial Model Be Considered in Systemic Autoimmune Diseases? Comment on the Article by Posada et al
Laurent Chiche, Noémie Jourde-Chiche, and Divi Cornec 717
Reply
James Posada, Benjamin A. Fisher, and Wan-Fai Ng 718
Recognition of Rare, Atypical Manifestations Is Important for Diagnosis and Management of Antineutrophil Cytoplasmic Antibody–Associated Vasculitis: Comment on the Article by Delaval et al
Mitsuhiro Akiyama 719
Reply
Laure Delaval and Benjamin Terrier 719

Erratum
Omitted Author in the Article by Bernstein et al (Arthritis Rheumatol, November 2020) 720

ACR Announcements A19

VOLUME 73 • May 2021 • NO.5

In This Issue A11

Journal Club A12

Clinical Connections A13

Special Articles

Notes From the Field: Reassessing the Cardiovascular Safety of Febuxostat: Implications of the Febuxostat versus Allopurinol Streamlined Trial
Hyon K. Choi, Tuhina Neogi, Lisa K. Stamp, Robert Terkeltaub, and Nicola Dalbeth 721

Editorial: Combining Data Sets as Well as Therapies Shows Improved Outcome in Connective Tissue Disease–Associated Pulmonary Hypertension
Christopher P. Denton and Julia Spierings 725

Editorial: Could Compensatory Autoantibody Production Affect Rheumatoid Arthritis Etiopathogenesis?
Gregg J. Silverman 728

COVID-19

Nonsteroidal Antiinflammatory Drugs and Susceptibility to COVID-19
Joht Singh Chandan, Dawit Tefra Zemedikun, Rasiah Thayakaran, Nathan Byne, Samir Dhalla, Dionisio Acosta-Mena, Krishna M. Gokhale, Tom Thomas, Christopher Sainsbury, Anuradhaa Subramanian, Jennifer Cooper, Astha Anand, Kelvin O. Okoth, Jingya Wang, Nicola J. Adderley, Thomas Taverner, Alastair K. Denniston, Janet Lord, G. Neil Thomas, Christopher D. Buckley, Karim Raza, Neeraj Bhala, Krishnarajah Nirantharakumar, and Shamil Haroon 731

Rheumatoid Arthritis

Expansion of Alternative Autoantibodies Does Not Follow the Evolution of Anti–Citrullinated Protein Antibodies in Preclinical Rheumatoid Arthritis: An Analysis in At-Risk First-Degree Relatives
Vidyanand Anaparti, Irene Smolik, Xiaobo Meng, Liam O'Neil, Mackenzie A. Jantz, Marvin J. Fritzler, and Hani El-Gabalawy 740

Lifetime Risks, Life Expectancy, and Health Care Expenditures for Rheumatoid Arthritis: A Nationwide Cohort Followed Up From 2003 to 2016
Ying-Ming Chiu, Yi-Peng Lu, Joung-Liang Lan, Der-Yuan Chen, and Jung-Der Wang 750

Etanercept or Methotrexate Withdrawal in Rheumatoid Arthritis Patients in Sustained Remission
Jeffrey R. Curtis, Paul Emery, Elaine Karis, Boulos Haraoui, Vivian Bykerk, Priscilla K. Yen, Greg Kricorian, and James B. Chung 759

Suppression of Rheumatoid Arthritis by Enhanced Lymph Node Trafficking of Engineered Interleukin-10 in Murine Models
Eiji Yuba, Erica Budina, Kiyomitsu Katsumata, Ako Ishihara, Aslan Mansurov, Aaron T. Alpar, Elyse A. Watkins, Peyman Hosseinchi, Joseph W. Reda, Abigail L. Lauterbach, Mindy Nguyen, Ani Solanki, Takahiro Kageyama, Melody A. Swartz, Jun Ishihara, and Jeffrey A. Hubbell 769

Venous Thromboembolism Risk With JAK Inhibitors: A Meta-Analysis
Mark Yates, Amanda Mootoo, Maryam Adas, Katie Bechman, Sanketh Rampes, Vishit Patel, Sumera Qureshi, Andrew P. Cope, Sam Norton, and James B. Galloway 779

Osteoarthritis

RNA Sequencing Reveals Interacting Key Determinants of Osteoarthritis Acting in Subchondral Bone and Articular Cartilage: Identification of *IL11* and *CHADL* as Attractive Treatment Targets
Margo Tuerlings, Marcella van Hoolwerff, Evelyn Houtman, Eka H. E. D. Suchiman, Nico Lakenberg, Hailiang Mei, Enrike H. M. J. van der Linden, Rob R. G. H. H. Nelissen, Yolande Y. F. M. Ramos, Rodrigo Coutinho de Almeida, and Ingrid Meulenbelt 789

Errata

Incorrect Academic Degree and/or Affiliation Information for Two Authors in the Article by Rodríguez-Carrio et al (Arthritis Rheumatol, March 2021) 799

Error in Figure 2B of the Article by Kolasinski et al (Arthritis Rheumatol, February 2020) 799

Spondyloarthritis

Which Magnetic Resonance Imaging Lesions in the Sacroiliac Joints Are Most Relevant for Diagnosing Axial Spondyloarthritis? A Prospective Study Comparing Rheumatologists' Evaluations With Radiologists' Findings
X. Baraliakos, A. Ghadir, M. Fruth, U. Kiltz, I. Reddeker, and J. Braun 800

Is Treatment in Patients With Suspected Nonradiographic Axial Spondyloarthritis Effective? Six-Month Results of a Placebo-Controlled Trial
Tamara Rusman, Mignon A. C. van der Weijden, Michael T. Nurmohamed, Robert B. M. Landewé, Janneke J. H. de Winter, Bouke J. H. Boden, Pierre M. Bet, Carmella M. A. van der Bijl, Conny van der Laken, and Irene E. van der Horst-Bruinsma 806

Systemic Lupus Erythematosus

Long-Term Safety and Efficacy of Anifrolumab in Adults With Systemic Lupus Erythematosus: Results of a Phase II Open-Label Extension Study
W. Winn Chatham, Richard Furie, Amit Saxena, Philip Brohawn, Erik Schwetje, Gabriel Abreu, and Raj Tummala 816

The Type II Anti-CD20 Antibody Obinutuzumab (GA101) Is More Effective Than Rituximab at Depleting B Cells and Treating Disease in a Murine Lupus Model
Anthony D. Marinov, Haowei Wang, Sheldon I. Bastacky, Erwin van Puijenbroek, Thomas Schindler, Dario Speziale, Mario Perro, Christian Klein, Kevin M. Nickerson, and Mark J. Shlomchik 826

Systemic Sclerosis
Long-Term Outcomes in Patients With Connective Tissue Disease–Associated Pulmonary Arterial Hypertension in the Modern Treatment Era: Meta-Analyses of Randomized, Controlled Trials and Observational Registries
Dinesh Khanna, Carol Zhao, Rajan Saggar, Stephen C. Mathai, Lorinda Chung, J. Gerry Coghlan, Mehul Shah, John Hartney, and Vallerie McLaughlin 837

Myositis
Eccentric Resistance Training Ameliorates Muscle Weakness in a Mouse Model of Idiopathic Inflammatory Myopathies
Koichi Himori, Yuki Ashida, Daisuke Tatebayashi, Masami Abe, Yuki Saito, Takako Chikenji, Håkan Westerblad, Daniel C. Andersson, and Takashi Yamada 848
Study of Tofacitinib in Refractory Dermatomyositis: An Open-Label Pilot Study of Ten Patients
Julie J. Paik, Livia Casciola-Rosen, Joseph Yusup Shin, Jemima Albayda, Eleni Tiniakou, Doris G. Leung, Laura Gutierrez-Alamillo, Jamie Perin, Liliana Florea, Corina Antonescu, Sherry G. Leung, Grazyna Purwin, Andrew Koenig, and Lisa Christopher-Stine 858
Inflammatory Myositis in Cancer Patients Receiving Immune Checkpoint Inhibitors
Jeffrey Aldrich, Xerxes Pundole, Sudhakar Tummala, Nicolas Palaskas, Clark R. Andersen, Mahran Shoukier, Noha Abdel-Wahab, Anita Deswal, and Maria E. Suarez-Almazor 866

Pediatric Rheumatology
Synovial Fluid Neutrophils From Patients With Juvenile Idiopathic Arthritis Display a Hyperactivated Phenotype
Mieke Metzemaekers, Bert Malengier-Devlies, Karen Yu, Sofie Vandendriessche, Jonas Yserbyt, Patrick Matthys, Lien De Somer, Carine Wouters, and Paul Proost 875
Amelioration of Murine Macrophage Activation Syndrome by Monomethyl Fumarate in Both a Heme Oxygenase 1–Dependent and Heme Oxygenase 1–Independent Manner
Chhanda Biswas, Niansheng Chu, Thomas N. Burn, Portia A. Kreiger, and Edward M. Behrens 885

Letters
Regulatory Action to Protect Access to Hydroxychloroquine for Approved Rheumatic Indications During COVID-19 in New Zealand
Eamon Duffy, Nicola Arroll, Richard Beasley, and Thomas Hills 896
Antiphospholipid Autoantibodies and Thrombosis in Patients With COVID-19: Comment on the Article by Bertin et al
T. Frapard, S. Hue, C. Rial, N. de Prost, and A. Mekontso Dessap 897
Reply
Daniel Bertin, Alexandre Brodovitch, Abdelouahab Beziane, Jean Louis Mege, Xavier Heim, and Nathalie Bardin 899
The Importance of Establishing a Suitable Study Population in Osteoarthritis Studies: Comment on the Article by MacFarlane et al
Duygu Tecer, Muhammet Cinar, and Sedat Yilmaz 900
Reply
Lindsey A. MacFarlane, I-Min Lee, Jeffrey N. Katz, JoAnn E. Manson, and Karen H. Costenbader 901

Clinical Images
An Unusual Presentation of Erosive Gout
Fadi Kharouf, Yusef Azraq, Yaakov Applbaum, and Hagit Peleg 902

ACR Announcements A24

VOLUME 73 • June 2021 • NO.6

In This Issue A19

Journal Club A20

Clinical Connections A21

Special Articles
ACR Presidential Address: Rheumatology During a Pandemic: Science and Resilience
Ellen M. Gravallese 903
American College of Rheumatology, American Academy of Dermatology, Rheumatologic Dermatology Society, and American Academy of Ophthalmology 2020 Joint Statement on Hydroxychloroquine Use With Respect to Retinal Toxicity
James T. Rosenbaum, Karen H. Costenbader, Julianna Desmarais, Ellen M. Ginzler, Nicole Fett, Susan M. Goodman, James R. O'Dell, Gabriela Schmajuk, Victoria P. Werth, Ronald B. Melles, and Michael F. Marmor 908
Editorial: A Picture Is Worth a Thousand Words, But Only If It Is a Good Picture
Daniel H. Solomon, Bryce A. Binstadt, David T. Felson, and Peter A. Nigrovic 912

COVID-19
Brief Report: COVID-19 Outcomes in Patients With Systemic Autoimmune Rheumatic Diseases Compared to the General Population: A US Multicenter, Comparative Cohort Study
Kristin M. D'Silva, April Jorge, Andrew Cohen, Natalie McCormick, Yuqing Zhang, Zachary S. Wallace, and Hyon K. Choi 914

Rheumatoid Arthritis

Association Between Bone Mineral Density and Autoantibodies in Patients With Rheumatoid Arthritis
Josephine A. M. P. Amkreutz, Emma C. de Moel, Lisa Theander, Minna Willim, Lotte Heimans, Jan-Åke Nilsson, Magnus K. Karlsson, Tom W. J. Huizinga, Kristina E. Åkesson, Lennart T. H. Jacobsson, Cornelia F. Allaart, Carl Turesson, and Diane van der Woude 921
The Pretreatment Gut Microbiome Is Associated With Lack of Response to Methotrexate in New-Onset Rheumatoid Arthritis
Alejandro Artacho, Sandrine Isaac, Renuka Nayak, Alejandra Flor-Duro, Margaret Alexander, Imhoi Koo, Julia Manasson, Philip B. Smith, Pamela Rosenthal, Yamen Homsi, Percio Gulko, Javier Pons, Leonor Puchades-Carrasco, Peter Izmirly, Andrew Patterson, Steven B. Abramson, Antonio Pineda-Lucena, Peter J. Turnbaugh, Carles Ubeda, and Jose U. Scher 931
Regulation of Synovial Inflammation and Tissue Destruction by Guanylate Binding Protein 5 in Synovial Fibroblasts From Patients With Rheumatoid Arthritis and Rats With Adjuvant-Induced Arthritis
Mahamudul Haque, Anil K. Singh, Madhu M. Ouseph, and Salahuddin Ahmed 943
Association of Lipid Mediators With Development of Future Incident Inflammatory Arthritis in an Anti–Citrullinated Protein Antibody–Positive Population
Kristen J. Polinski, Elizabeth A. Bemis, Fan Yang, Tessa Crume, M. Kristen Demoruelle, Marie Feser, Jennifer Seifert, James R. O'Dell, Ted R. Mikuls, Michael H. Weisman, Peter K. Gregersen, Richard M. Keating, Jane Buckner, Nichole Reisdorph, Kevin D. Deane, Michael Clare-Salzler, V. Michael Holers, and Jill M. Norris 955
Brief Report: *HLA–B*08* Identified as the Most Prominently Associated Major Histocompatibility Complex Locus for Anti–Carbamylated Protein Antibody–Positive/Anti–Cyclic Citrullinated Peptide–Negative Rheumatoid Arthritis
Cristina Regueiro, Desire Casares-Marfil, Karin Lundberg, Rachel Knevel, Marialbert Acosta-Herrera, Luis Rodriguez-Rodriguez, Raquel Lopez-Mejias, Eva Perez-Pampin, Ana Triguero-Martinez, Laura Nuño, Ivan Ferraz-Amaro, Javier Rodriguez-Carrio, Rosario Lopez-Pedrera, Montse Robustillo-Villarino, Santos Castañeda, Sara Remuzgo-Martinez, Mercedes Alperi, Juan J. Alegre-Sancho, Alejandro Balsa, Isidoro Gonzalez-Alvaro, Antonio Mera, Benjamin Fernandez-Gutierrez, Miguel A. Gonzalez-Gay, Leendert A. Trouw, Caroline Grönwall, Leonid Padyukov, Javier Martin, and Antonio Gonzalez 963
Divergence of Cardiovascular Biomarkers of Lipids and Subclinical Myocardial Injury Among Rheumatoid Arthritis Patients With Increased Inflammation
Brittany Weber, Zeling He, Nicole Yang, Martin P. Playford, Dana Weisenfeld, Christine Iannaccone, Jonathan Coblyn, Michael Weinblatt, Nancy Shadick, Marcelo Di Carli, Nehal N. Mehta, Jorge Plutzky, and Katherine P. Liao 970

Spondyloarthritis

Functional Genomic Analysis of a *RUNX3* Polymorphism Associated With Ankylosing Spondylitis
Matteo Vecellio, Liye Chen, Carla J. Cohen, Adrian Cortes, Yan Li, Sarah Bonham, Carlo Selmi, Matthew A. Brown, Roman Fischer, Julian C. Knight, and B. Paul Wordsworth 980

Systemic Lupus Erythematosus

Prevalence of Systemic Lupus Erythematosus in the United States: Estimates From a Meta-Analysis of the Centers for Disease Control and Prevention National Lupus Registries
Peter M. Izmirly, Hilary Parton, Lu Wang, W. Joseph McCune, S. Sam Lim, Cristina Drenkard, Elizabeth D. Ferucci, Maria Dall'Era, Caroline Gordon, Charles G. Helmick, and Emily C. Somers 991
Association of Higher Hydroxychloroquine Blood Levels With Reduced Thrombosis Risk in Systemic Lupus Erythematosus
Michelle Petri, Maximilian F. Konig, Jessica Li, and Daniel W. Goldman 997

Clinical Images

Lindsay's Nails in Early Limited Cutaneous Systemic Sclerosis With Severe Digital Vasculopathy
Jessica C. Ellis and John D. Pauling 1004

Systemic Sclerosis

Predictive Significance of Serum Interferon-Inducible Protein Score for Response to Treatment in Systemic Sclerosis–Related Interstitial Lung Disease
Shervin Assassi, Ning Li, Elizabeth R. Volkmann, Maureen D. Mayes, Dennis Rünger, Jun Ying, Michael D. Roth, Monique Hinchcliff, Dinesh Khanna, Tracy Frech, Philip J. Clements, Daniel E. Furst, Jonathan Goldin, Elana J. Bernstein, Flavia V. Castelino, Robyn T. Domsic, Jessica K. Gordon, Faye N. Hant, Ami A. Shah, Victoria K. Shanmugam, Virginia D. Steen, Robert M. Elashoff, and Donald P. Tashkin 1005

Gout

Effects of Dietary Patterns on Serum Urate: Results From a Randomized Trial of the Effects of Diet on Hypertension
Stephen P. Juraschek, Chio Yokose, Natalie McCormick, Edgar R. Miller III, Lawrence J. Appel, and Hyon K. Choi 1014

Autoinflammatory Disease

Novel Majeed Syndrome–Causing *LPIN2* Mutations Link Bone Inflammation to Inflammatory M2 Macrophages and Accelerated Osteoclastogenesis
Farzana Bhuyan, Adriana A. de Jesus, Jacob Mitchell, Evgenia Leikina, Rachel VanTries, Ronit Herzog, Karen B. Onel, Andrew Oler, Gina A. Montealegre Sanchez, Kim A. Johnson, Lena Bichell, Bernadette Marrero, Luis Fernandez De Castro, Yan Huang, Katherine R. Calvo, Michael T. Collins, Sundar Ganesan, Leonid V. Chernomordik, Polly J. Ferguson, and Raphaela Goldbach-Mansky 1021
Association of the Leukocyte Immunoglobulin-like Receptor A3 Gene With Neutrophil Activation and Disease Susceptibility in Adult-Onset Still's Disease
Mengyan Wang, Mengru Liu, Jinchao Jia, Hui Shi, Jialin Teng, Honglei Liu, Yue Sun, Xiaobing Cheng, Junna Ye, Yutong Su, Huihui Chi, Tingting Liu, Zhihong Wang, Liyan Wan, Jianfen Meng, Yuning Ma, Chengde Yang, and Qiongyi Hu 1033

Pediatric Rheumatology

From Diagnosis to Prognosis: Revisiting the Meaning of Muscle *ISG15* Overexpression in Juvenile Inflammatory Myopathies
Cyrielle Hou, Chloé Durrleman, Baptiste Periou, Christine Barnerias, Christine Bodemer, Isabelle Desguerre, Pierre Quartier, Isabelle Melki, Gillian I. Rice, Mathieu P. Rodero, Jean-Luc Charuel, Fréderic Relaix, Brigitte Bader-Meunier, François Jérôme Authier, and Cyril Gitiaux 1044
Early Treatment and *IL1RN* Single-Nucleotide Polymorphisms Affect Response to Anakinra in Systemic Juvenile Idiopathic Arthritis
Manuela Pardeo, Marianna Nicoletta Rossi, Denise Pires Marafon, Emanuela Sacco, Claudia Bracaglia, Chiara Passarelli, Ivan Caiello, Giulia Marucci, Antonella Insalaco, Chiara Perrone, Anna Tulone, Giusi Prencipe, and Fabrizio De Benedetti 1053
Comparison of Lesional Juvenile Myositis and Lupus Skin Reveals Overlapping Yet Unique Disease Pathophysiology
Jessica L. Turnier, Lauren M. Pachman, Lori Lowe, Lam C. Tsoi, Sultan Elhaj, Rajasree Menon, Maria C. Amoruso, Gabrielle A. Morgan, Johann E. Gudjonsson, Celine C. Berthier, and J. Michelle Kahlenberg 1062

Autoimmunity

Integrative Analysis Reveals a Molecular Stratification of Systemic Autoimmune Diseases
Guillermo Barturen, Sepideh Babaei, Francesc Català-Moll, Manuel Martínez-Bueno, Zuzanna Makowska, Jordi Martorell-Marugán, Pedro Carmona-Sáez, Daniel Toro-Domínguez, Elena Carnero-Montoro, María Teruel, Martin Kerick, Marialbert Acosta-Herrera, Lucas Le Lann, Christophe Jamin, Javier Rodríguez-Ubreva, Antonio García-Gómez, Jorge Kageyama, Anne Buttgereit, Sikander Hayat, Joerg Mueller, Ralf Lesche, Maria Hernandez-Fuentes, Maria Juarez, Tania Rowley, Ian White, Concepción Marañón, Tania Gomes Anjos, Nieves Varela, Rocío Aguilar-Quesada, Francisco Javier Garrancho, Antonio López-Berrio, Manuel Rodriguez Maresca, Héctor Navarro-Linares, Isabel Almeida, Nancy Azevedo, Mariana Brandão, Ana Campar, Raquel Faria, Fátima Farinha, António Marinho, Esmeralda Neves, Ana Tavares, Carlos Vasconcelos, Elena Trombetta, Gaia Montanelli, Barbara Vigone, Damiana Alvarez-Errico, Tianlu Li, Divya Thiagaran, Ricardo Blanco Alonso, Alfonso Corrales Martínez, Fernanda Genre, Raquel López Mejías, Miguel A. Gonzalez-Gay, Sara Remuzgo, Begoña Ubilla Garcia, Ricard Cervera, Gerard Espinosa, Ignasi Rodríguez-Pintó, Ellen De Langhe, Jonathan Cremer, Rik Lories, Doreen Belz, Nicolas Hunzelmann, Niklas Baerlecken, Katja Kniesch, Torsten Witte, Michaela Lehner, Georg Stummvoll, Michael Zauner, Maria Angeles Aguirre-Zamorano, Nuria Barbarroja, Maria Carmen Castro-Villegas, Eduardo Collantes-Estevez, Enrique de Ramon, Isabel Díaz Quintero, Alejandro Escudero-Contreras, María Concepción Fernández Roldán, Yolanda Jiménez Gómez, Inmaculada Jiménez Moleón, Rosario Lopez-Pedrera, Rafaela Ortega-Castro, Norberto Ortego, Enrique Raya, Carolina Artusi, Maria Gerosa, Pier Luigi Meroni, Tommaso Schioppo, Aurélie De Groof, Julie Ducreux, Bernard Lauwerys, Anne-Lise Maudoux, Divi Cornec, Valérie Devauchelle-Pensec, Sandrine Jousse-Joulin, Pierre-Emmanuel Jouve, Bénédicte Rouvière, Alain Saraux, Quentin Simon, Montserrat Alvarez, Carlo Chizzolini, Aleksandra Dufour, Donatienne Wynar, Attila Balog, Márta Bocskai, Magdolna Deák, Sonja Dulic, Gabriella Kádár, László Kovács, Qingyu Cheng, Velia Gerl, Falk Hiepe, Laleh Khodadadi, Silvia Thiel, Emanuele de Rinaldis, Sambasiva Rao, Robert J. Benschop, Chris Chamberlain, Ernst R. Dow, Yiannis Ioannou, Laurence Laigle, Jacqueline Marovac, Jerome Wojcik, Yves Renaudineau, Maria Orietta Borghi, Johan Frostegård, Javier Martín, Lorenzo Beretta, Esteban Ballestar, Fiona McDonald, Jacques-Olivier Pers, and Marta E. Alarcón-Riquelme 1073

Concise Communication

Validation of a Bioassay for Predicting Response to Tumor Necrosis Factor Inhibitors in Rheumatoid Arthritis
Ching-Huang Ho, Andrea A. Silva, Jon T. Giles, Joan M. Bathon, Daniel H. Solomon, Katherine P. Liao, and I-Cheng Ho 1086

Letters

Panniculitis As the First Clinical Manifestation of Myeloperoxidase–Positive Perinuclear Antineutrophil Cytoplasmic Antibody–Associated Vasculitis: Comment on the Article by Micheletti et al
D. Deleersnijder, P. De Haes, L. Peperstraete, J. Buelens, A. Betrains, and D. Blockmans 1088
Reply
Robert G. Micheletti, Zelma Chiesa Fuxench, Anthea Craven, Raashid A. Luqmani, Richard A. Watts, and Peter A. Merkel 1089
Who Has the Final Say on the Dose of Acupuncture? Comment on the Article by Tu et al
Yong Ming Li 1089
Reply
Jian-Feng Tu, Guang-Xia Shi, Jing-Wen Yang, Li-Qiong Wang, Shi-Yan Yan, and Cun-Zhi Liu 1090
COVID-19 Reinfection in a Patient Receiving Immunosuppressive Treatment for Antineutrophil Cytoplasmic Antibody–Associated Vasculitis
Kavita Gulati, Maria Prendecki, Candice Clarke, Michelle Willicombe, and Stephen McAdoo 1091

VOLUME 73 • July 2021 • NO.7

In This Issue....A9

Journal Club....A10

Clinical Connections....A11

Special Articles

American College of Rheumatology Guidance for COVID-19 Vaccination in Patients With Rheumatic and Musculoskeletal Diseases: Version 1
Jeffrey R. Curtis, Sindhu R. Johnson, Donald D. Anthony, Reuben J. Arasaratnam, Lindsey R. Baden, Anne R. Bass, Cassandra Calabrese, Ellen M. Gravallese, Rafael Harpaz, Rebecca E. Sadun, Amy S. Turner, Eleanor Anderson Williams, and Ted R. Mikuls....1093

2021 American College of Rheumatology Guideline for the Treatment of Rheumatoid Arthritis
Liana Fraenkel, Joan M. Bathon, Bryant R. England, E. William St.Clair, Thurayya Arayssi, Kristine Carandang, Kevin D. Deane, Mark Genovese, Kent Kwas Huston, Gail Kerr, Joel Kremer, Mary C. Nakamura, Linda A. Russell, Jasvinder A. Singh, Benjamin J. Smith, Jeffrey A. Sparks, Shilpa Venkatachalam, Michael E. Weinblatt, Mounir Al-Gibbawi, Joshua F. Baker, Kamil E. Barbour, Jennifer L. Barton, Laura Cappelli, Fatimah Chamseddine, Michael George, Sindhu R. Johnson, Lara Kahale, Basil S. Karam, Assem M. Khamis, Iris Navarro-Millán, Reza Mirza, Pascale Schwab, Namrata Singh, Marat Turgunbaev, Amy S. Turner, Sally Yaacoub, and Elie A. Akl....1108

Editorial: Current Treatment Strategies in Rheumatoid Arthritis After Methotrexate Are Not Enough to Maintain Sustained Remission: There Is No Holy Grail!
Janet E. Pope, Peter Nash, and Roy Fleischmann....1124

Editorial: A Good Detective Never Misses a Clue: Why the Epidemiology of Scleritis Deserves Our Attention
Matthew A. Turk and James T. Rosenbaum....1127

COVID-19

Brief Report: Risk Factors for COVID-19 and Rheumatic Disease Flare in a US Cohort of Latino Patients
Alice Fike, Julia Hartman, Christopher Redmond, Sandra G. Williams, Yanira Ruiz-Perdomo, Jun Chu, Sarfaraz Hasni, Michael M. Ward, James D. Katz, and Pravitt Gourh....1129

Rheumatoid Arthritis

Sustained Remission in Patients With Rheumatoid Arthritis Receiving Triple Therapy Compared to Biologic Therapy: A Swedish Nationwide Register Study
Hanna Källmark, Jon T. Einarsson, Jan-Åke Nilsson, Tor Olofsson, Tore Saxne, Pierre Geborek, and Meliha C. Kapetanovic....1135

Characterization and Function of Tumor Necrosis Factor and Interleukin-6–Induced Osteoclasts in Rheumatoid Arthritis
Kazuhiro Yokota, Kojiro Sato, Takashi Miyazaki, Yoshimi Aizaki, Shinya Tanaka, Miyoko Sekikawa, Noritsune Kozu, Yuho Kadono, Hiromi Oda, and Toshihide Mimura....1145

Contribution of a European-Prevalent Variant near *CD83* and an East Asian–Prevalent Variant near *IL17RB* to Herpes Zoster Risk in Tofacitinib Treatment: Results of Genome-Wide Association Study Meta-Analyses
Nan Bing, Huanyu Zhou, Xing Chen, Tomohiro Hirose, Yuta Kochi, Yumi Tsuchida, Kazuyoshi Ishigaki, Shuji Sumitomo, Keishi Fujio, Baohong Zhang, Hernan Valdez, Michael S. Vincent, David Martin, and James D. Clark....1155

Osteoarthritis

Long-Term Safety and Efficacy of Subcutaneous Tanezumab Versus Nonsteroidal Antiinflammatory Drugs for Hip or Knee Osteoarthritis: A Randomized Trial
Marc C. Hochberg, John A. Carrino, Thomas J. Schnitzer, Ali Guermazi, David A. Walsh, Alexander White, Satoru Nakajo, Robert J. Fountaine, Anne Hickman, Glenn Pixton, Lars Viktrup, Mark T. Brown, Christine R. West, and Kenneth M. Verburg....1167

Global Deletion of Pannexin 3 Resulting in Accelerated Development of Aging-Induced Osteoarthritis in Mice
P. M. Moon, Z. Y. Shao, G. Wambiekele, C. T. G. Appleton, D. W. Laird, S. Penuela, and F. Beier....1178

Spondyloarthritis

Inflammasome Activation in Ankylosing Spondylitis Is Associated With Gut Dysbiosis
Giuliana Guggino, Daniele Mauro, Aroldo Rizzo, Riccardo Alessandro, Stefania Raimondo, Anne-Sophie Bergot, M. Arifur Rahman,Jonathan J. Ellis, Simon Milling, Rik Lories, Dirk Elewaut, Matthew A. Brown, Ranjeny Thomas, and Francesco Ciccia....1189

Mediation of Interleukin-23 and Tumor Necrosis Factor–Driven Reactive Arthritis by *Chlamydia*-Infected Macrophages in SKG Mice
Xavier Romand, Xiao Liu, M. Arifur Rahman, Zaied Ahmed Bhuyan, Claire Douillard, Reena Arora Kedia, Nathan Stone, Dominique Roest, Zi Huai Chew, Amy J. Cameron, Linda M. Rehaume, Aurélie Bozon, Mohammed Habib, Charles W. Armitage, Minh Vu Chuong Nguyen, Bertrand Favier, Kenneth Beagley, Max Maurin, Philippe Gaudin, Ranjeny Thomas, Timothy J. Wells, and Athan Baillet....1200

Tumor Necrosis Factor Inhibitors Reduce Spinal Radiographic Progression in Patients With Radiographic Axial Spondyloarthritis: A Longitudinal Analysis From the Alberta Prospective Cohort
Alexandre Sepriano, Sofia Ramiro, Stephanie Wichuk, Praveena Chiowchanwisawakit, Joel Paschke, Désirée van der Heijde, Robert Landewé, and Walter P. Maksymowych 1211

Psoriatic Arthritis

Tissue-Resident Memory CD8+ T Cells From Skin Differentiate Psoriatic Arthritis From Psoriasis
Emmerik F. Leijten, Tessa S. van Kempen, Michel A. Olde Nordkamp, Juliette N. Pouw, Nienke J. Kleinrensink, Nanette L. Vincken, Jorre Mertens, Deepak M. W. Balak, Fleurieke H. Verhagen, Sarita A. Hartgring, Erik Lubberts, Janneke Tekstra, Aridaman Pandit, Timothy R. Radstake, and Marianne Boes 1220

Vasculitis

Specific Follicular Helper T Cell Signature in Takayasu Arteritis
A. C. Desbois, P. Régnier, V. Quiniou, A. Lejoncour, A. Maciejewski-Duval, C. Comarmond, H. Vallet, M. Rosenzwag, G. Darrasse-Jèze, N. Derian, J. Pouchot, M. Samson, B. Bienvenu, P. Fouret, F. Koskas, M. Garrido, D. Sène, P. Bruneval, P. Cacoub, D. Klatzmann, and D. Saadoun 1233
Genetic Association of a Gain-of-Function *IFNGR1* Polymorphism and the Intergenic Region *LNCAROD/DKK1* With Behçet's Disease
Lourdes Ortiz Fernández, Patrick Coit, Vuslat Yilmaz, Sibel P. Yentür, Fatma Alibaz-Oner, Kenan Aksu, Eren Erken, Nursen Düzgün, Gokhan Keser, Ayse Cefle, Ayten Yazici, Andac Ergen, Erkan Alpsoy, Carlo Salvarani, Bruno Casali, Bünyamin Kısacık, Ina Kötter, Jörg Henes, Muhammet Çınar, Arne Schaefer, Rahime M. Nohutcu, Alexandra Zhernakova, Cisca Wijmenga, Fujio Takeuchi, Shinji Harihara, Toshikatsu Kaburaki, Meriam Messedi, Yeong-Wook Song, Timuçin Kaşifoğlu, F. David Carmona, Joel M. Guthridge, Judith A. James, Javier Martin, María Francisca González Escribano, Güher Saruhan-Direskeneli, Haner Direskeneli, and Amr H. Sawalha 1244
The Vasculopathy of Juvenile Dermatomyositis: Endothelial Injury, Hypercoagulability, and Increased Arterial Stiffness
Charalampia Papadopoulou, Ying Hong, Petra Krol, Muthana Al Obaidi, Clarissa Pilkington, Lucy R. Wedderburn, Paul A. Brogan, and Despina Eleftheriou 1253
Epidemiology of Scleritis in the United Kingdom From 1997 to 2018: Population-Based Analysis of 11 Million Patients and Association Between Scleritis and Infectious and Immune-Mediated Inflammatory Disease
Tasanee Braithwaite, Nicola J. Adderley, Anuradhaa Subramanian, James Galloway, John H. Kempen, Krishna Gokhale, Andrew P. Cope, Andrew D. Dick, Krishnarajah Nirantharakumar, and Alastair K. Denniston 1267

Systemic Sclerosis

Association of Lymphangiogenic Factors With Pulmonary Arterial Hypertension in Systemic Sclerosis
Henriette Didriksen, Øyvind Molberg, Håvard Fretheim, Einar Gude, Suzana Jordan, Cathrine Brunborg, Vyacheslav Palchevskiy, Torhild Garen, Øyvind Midtvedt, Arne K. Andreassen, Oliver Distler, John Belperio, and Anna-Maria Hoffmann-Vold 1277
Expression Quantitative Trait Locus Analysis in Systemic Sclerosis Identifies New Candidate Genes Associated With Multiple Aspects of Disease Pathology
Martin Kerick, David González-Serna, Elena Carnero-Montoro, Maria Teruel, Marialbert Acosta-Herrera, Zuzanna Makowska, Anne Buttgereit, Sepideh Babaei, Guillermo Barturen, Elena López-Isac, PRECISESADS Clinical Consortium, Ralf Lesche, Lorenzo Beretta, Marta E. Alarcon-Riquelme, and Javier Martin 1288
Tocilizumab Prevents Progression of Early Systemic Sclerosis–Associated Interstitial Lung Disease
David Roofeh, Celia J. F. Lin, Jonathan Goldin, Grace Hyun Kim, Daniel E. Furst, Christopher P. Denton, Suiyuan Huang, and Dinesh Khanna, on behalf of the focuSSced Investigators 1301
Brief Report: Dysfunctional Keratinocytes Increase Dermal Inflammation in Systemic Sclerosis: Results From Studies Using Tissue-Engineered Scleroderma Epidermis
Barbara Russo, Julia Borowczyk, Wolf-Henning Boehncke, Marie-Elise Truchetet, Ali Modarressi, Nicolò C. Brembilla, and Carlo Chizzolini 1311

Fibromyalgia

Greater Somatosensory Afference With Acupuncture Increases Primary Somatosensory Connectivity and Alleviates Fibromyalgia Pain via Insular γ-Aminobutyric Acid: A Randomized Neuroimaging Trial
Ishtiaq Mawla, Eric Ichesco, Helge J. Zöllner, Richard A. E. Edden, Thomas Chenevert, Henry Buchtel, Meagan D. Bretz, Heather Sloan, Chelsea M. Kaplan, Steven E. Harte, George A. Mashour, Daniel J. Clauw, Vitaly Napadow, and Richard E. Harris 1318

Clinical Images

Giant Iliopsoas Bursitis in Systemic Juvenile Idiopathic Arthritis
Asami Shimbo, Yuko Akutsu, Susumu Yamazaki, Masaki Shimizu, and Masaaki Mori 1328

Pediatric Rheumatology

Brief Report: Anti–Cytosolic 5'-Nucleotidase 1A Autoantibodies Are Absent in Juvenile Dermatomyositis
Anke Rietveld, Judith Wienke, Eline Visser, Wilma Vree Egberts, Wolfgang Schlumberger, Baziel van Engelen, Annet van Royen-Kerkhof, Hui Lu, Lucy Wedderburn, Christiaan Saris, Sarah Tansley, and Ger Pruijn, on behalf of the Juvenile Dermatomyositis Research Group and the Dutch Myositis Consortium 1329
Brief Report: Distinct Gene Expression Signatures Characterize Strong Clinical Responders Versus Nonresponders to Canakinumab in Children With Systemic Juvenile Idiopathic Arthritis
Emely L. Verweyen, Alex Pickering, Alexei A. Grom, and Grant S. Schulert 1334

Letters

Prophylactic Anticoagulation Therapy: Comment on the Article by Henderson et al
Barbara Faganel Kotnik, Mojca Zajc Avramovič, Lidija Kitanovski, and Tadej Avčin....1341
Reply
Lauren A. Henderson, Kevin G. Friedman, Mary Beth F. Son, Kate F. Kernan, Scott W. Canna, Mark Gorelik, Sivia K. Lapidus, Anne Ferris, Grant S. Schulert, Philip Seo, Adriana H. Tremoulet, Rae S. M. Yeung, David R. Karp, Hamid Bassiri, Edward M. Behrens, and Jay J. Mehta....1342
Understanding the Relationships Between Type I Interferon, STAT4, and the Production of Interleukin-21 and Interferon-γ by Follicular Helper T Cells in Lupus: Comment on the Article by Dong et al
Caiqun Chen, Yan Liang, and Zaixing Yang....1343
Reply
Joe Craft and Jason Weinstein....1344
Temporal Arteritis Revealing Antineutrophil Cytoplasmic Antibody–Associated Vasculitides: Are the Visual Outcomes Different From Giant Cell Arteritis? Comment on the Article by Delaval et al
Joydeep Samanta, GSRSNK Naidu, Sakshi Mittal, Ritambhra Nada, Amanjit Bal, Ramandeep Singh, Vishali Gupta, Amod Gupta, Aman Sharma, and Benzeeta Pinto....1345
Biologics for Eosinophilic Granulomatosis With Polyangiitis—One Size Does Not Fit All: Comment on the Article by Canzian et al
Marco Caminati, Alessandro Giollo, Gianenrico Senna, and Claudio Lunardi....1346
Sjögren's Disease, Not Syndrome
Alan N. Baer and Katherine M. Hammitt....1347

VOLUME 73 • August 2021 • NO.8

In This Issue....A15

Journal Club....A16

Clinical Connections....A17

Online-Only Special Articles
American College of Rheumatology Guidance for COVID-19 Vaccination in Patients With Rheumatic and Musculoskeletal Diseases: Version 2
Jeffrey R. Curtis, Sindhu R. Johnson, Donald D. Anthony, Reuben J. Arasaratnam, Lindsey R. Baden, Anne R. Bass, Cassandra Calabrese, Ellen M. Gravallese, Rafael Harpaz, Andrew Kroger, Rebecca E. Sadun, Amy S. Turner, Eleanor Anderson Williams, and Ted R. Mikuls....e30
American College of Rheumatology Guidance for the Management of Pediatric Rheumatic Disease During the COVID-19 Pandemic: Version 2
Dawn M. Wahezi, Mindy S. Lo, Tamar B. Rubinstein, Sarah Ringold, Stacy P. Ardoin, Kevin J. Downes, Karla B. Jones, Ronald M. Laxer, Rebecca Pellet Madan, Amy S. Mudano, Amy S. Turner, David R. Karp, and Jay J. Mehta....e46

Special Articles
2021 American College of Rheumatology/Vasculitis Foundation Guideline for the Management of Giant Cell Arteritis and Takayasu Arteritis
Mehrdad Maz, Sharon A. Chung, Andy Abril, Carol A. Langford, Mark Gorelik, Gordon Guyatt, Amy M. Archer, Doyt L. Conn, Kathy A. Full, Peter C. Grayson, Maria F. Ibarra, Lisa F. Imundo, Susan Kim, Peter A. Merkel, Rennie L. Rhee, Philip Seo, John H. Stone, Sangeeta Sule, Robert P. Sundel, Omar I. Vitobaldi, Ann Warner, Kevin Byram, Anisha B. Dua, Nedaa Husainat, Karen E. James, Mohamad A. Kalot, Yih Chang Lin, Jason M. Springer, Marat Turgunbaev, Alexandra Villa-Forte, Amy S. Turner, and Reem A. Mustafa....1349
2021 American College of Rheumatology/Vasculitis Foundation Guideline for the Management of Antineutrophil Cytoplasmic Antibody–Associated Vasculitis
Sharon A. Chung, Carol A. Langford, Mehrdad Maz, Andy Abril, Mark Gorelik, Gordon Guyatt, Amy M. Archer, Doyt L. Conn, Kathy A. Full, Peter C. Grayson, Maria F. Ibarra, Lisa F. Imundo, Susan Kim, Peter A. Merkel, Rennie L. Rhee, Philip Seo, John H. Stone, Sangeeta Sule, Robert P. Sundel, Omar I. Vitobaldi, Ann Warner, Kevin Byram, Anisha B. Dua, Nedaa Husainat, Karen E. James, Mohamad A. Kalot, Yih Chang Lin, Jason M. Springer, Marat Turgunbaev, Alexandra Villa-Forte, Amy S. Turner, and Reem A. Mustafa....1366
2021 American College of Rheumatology/Vasculitis Foundation Guideline for the Management of Polyarteritis Nodosa
Sharon A. Chung, Mark Gorelik, Carol A. Langford, Mehrdad Maz, Andy Abril, Gordon Guyatt, Amy M. Archer, Doyt L. Conn, Kathy A. Full, Peter C. Grayson, Maria F. Ibarra, Lisa F. Imundo, Susan Kim, Peter A. Merkel, Rennie L. Rhee, Philip Seo, John H. Stone, Sangeeta Sule, Robert P. Sundel, Omar I. Vitobaldi, Ann Warner, Kevin Byram, Anisha B. Dua, Nedaa Husainat, Karen E. James, Mohamad Kalot, Yih Chang Lin, Jason M. Springer, Marat Turgunbaev, Alexandra Villa-Forte, Amy S. Turner, and Reem A. Mustafa....1384
Expert Perspectives on Clinical Challenges: Expert Perspective: Management of Refractory Inflammatory Myopathy
Ingrid E. Lundberg....1394
Editorial: Urate Lowering for Blood Pressure Control in Adults: Another Nail in the Coffin?
Edward Roddy and Nicola Dalbeth....1408

Rheumatoid Arthritis

Epicardial Adipose Tissue Volume As a Marker of Subclinical Coronary Atherosclerosis in Rheumatoid Arthritis
George A. Karpouzas, Panteha Rezaeian, Sarah R. Ormseth, Ivana Hollan, and Matthew J. Budoff 1412
Outcomes of a Mobile App to Monitor Patient-Reported Outcomes in Rheumatoid Arthritis: A Randomized Controlled Trial
Yvonne C. Lee, Fengxin Lu, Joshua Colls, Dee Luo, Penny Wang, Dorothy D. Dunlop, Lutfiyya N. Muhammad, Jing Song, Kaleb Michaud, and Daniel H. Solomon 1421
Protective Role of Collectin 11 in a Mouse Model of Rheumatoid Arthritis
Na Wang, Weiju Wu, Cui Qiang, Ning Ma, Kunyi Wu, Dan Liu, Jia-Xing Wang, Xiao Yang, Li Xue, Teng-Yue Diao, Jia-Yu Liu, Ang Li, Baojun Zhang, Zong-Fang Li, Conrad A. Farrar, Nirmal K. Banda, Rafael Bayarri-Olmos, Peter Garred, Wuding Zhou, and Ke Li 1430

Osteoarthritis

Involvement of Transient Receptor Potential Vanilloid Channel 2 in the Induction of Lubricin and Suppression of Ectopic Endochondral Ossification in Mouse Articular Cartilage
Hideki Nakamoto, Yuki Katanosaka, Ryota Chijimatsu, Daisuke Mori, Fengjun Xuan, Fumiko Yano, Yasunori Omata, Yuji Maenohara, Yasutaka Murahashi, Kohei Kawaguchi, Ryota Yamagami, Hiroshi Inui, Shuji Taketomi, Yuki Taniguchi, Motoi Kanagawa, Keiji Naruse, Sakae Tanaka, and Taku Saito 1441
Lipopolysaccharide Binding Protein and CD14, Cofactors of Toll-like Receptors, Are Essential for Low-Grade Inflammation–Induced Exacerbation of Cartilage Damage in Mouse Models of Posttraumatic Osteoarthritis
Yoonkyung Won, Jeong-In Yang, Seulki Park, and Jang-Soo Chun 1451

Systemic Lupus Erythematosus

Brief Report: Molecular Signatures of Kidney Antibody–Secreting Cells in Lupus Patients With Active Nephritis Upon Immunosuppressive Therapy
Etienne Crickx, Farah Tamirou, Tessa Huscenot, Nathalie Costedoat-Chalumeau, Marion Rabant, Alexandre Karras, Ailsa Robbins, Tatiana Fadeev, Véronique Le Guern, Philippe Remy, Aurélie Hummel, Selda Aydin, Bernard Lauwerys, Jean-Claude Weill, Claude-Agnès Reynaud, Frédéric Houssiau, and Matthieu Mahévas 1461
Aim2 Couples With *Ube2i* for Sumoylation-Mediated Repression of Interferon Signatures in Systemic Lupus Erythematosus
Ailing Lu, Shuxian Wu, Junling Niu, Mengmeng Cui, Mengdan Chen, William L. Clapp, Betsy J. Barnes, and Guangxun Meng 1467
Camptothecin and Topotecan, Inhibitors of Transcription Factor Fli-1 and Topoisomerase, Markedly Ameliorate Lupus Nephritis in (NZB × NZW)F1 Mice and Reduce the Production of Inflammatory Mediators in Human Renal Cells
Xuan Wang, Jim C. Oates, Kristi L. Helke, Gary S. Gilkeson, and Xian K. Zhang 1478
Retinoic Acid Receptor–Related Orphan Nuclear Receptor γt Licenses the Differentiation and Function of a Unique Subset of Follicular Helper T Cells in Response to Immunogenic Self-DNA in Systemic Lupus Erythematosus
Zhenke Wen, Lin Xu, Wei Xu, and Sidong Xiong 1489

Systemic Sclerosis

Genome-Wide Reduction in Chromatin Accessibility and Unique Transcription Factor Footprints in Endothelial Cells and Fibroblasts in Scleroderma Skin
Pei-Suen Tsou, Pamela J. Palisoc, Mustafa Ali, Dinesh Khanna, and Amr H. Sawalha 1501

Gout

Effect of Serum Urate Lowering With Allopurinol on Blood Pressure in Young Adults: A Randomized, Controlled, Crossover Trial
Angelo L. Gaffo, David A. Calhoun, Elizabeth J. Rahn, Suzanne Oparil, Peng Li, Tanja Dudenbostel, Daniel I. Feig, David T. Redden, Paul Muntner, Phillip J. Foster, Stephanie R. Biggers-Clark, Amy Mudano, Sebastian E. Sattui, Michael B. Saddekni, S. Louis Bridges Jr., and Kenneth G. Saag 1514
Reducing Immunogenicity of Pegloticase With Concomitant Use of Mycophenolate Mofetil in Patients With Refractory Gout: A Phase II, Randomized, Double-Blind, Placebo-Controlled Trial
Puja P. Khanna, Dinesh Khanna, Gary Cutter, Jeff Foster, Joshua Melnick, Sara Jaafar, Stephanie Biggers, A. K. M. Fazlur Rahman, Hui-Chien Kuo, Michelle Feese, Alan Kivitz, Charles King, William Shergy, Jeff Kent, Paul M. Peloso, Maria I. Danila, and Kenneth G. Saag 1523
A Randomized, Phase II Study Evaluating the Efficacy and Safety of Anakinra in the Treatment of Gout Flares
Kenneth G. Saag, Puja P. Khanna, Robert T. Keenan, Sven Ohlman, Lisa Osterling Koskinen, Erik Sparve, Ann-Charlotte Åkerblad, Margareta Wikén, Alexander So, Michael H. Pillinger, and Robert Terkeltaub 1533

Clinical Images

Acute Digital Necrosis Due to Interferon-α–Induced Antineutrophil Cytoplasmic Antibody–Associated Vasculitis
Yoshinori Taniguchi, Takahito Kimata, and Shigeto Kobayashi 1542

Pseudogout

Brief Report: Effects of the TNFRSF11B Mutation Associated With Calcium Pyrophosphate Deposition Disease in Osteoclastogenesis in a Murine Model
Elizabeth Mitton-Fitzgerald, Claudia M. Gohr, Charlene J. Williams, Amaryllis Ortiz, Gabriel Mbalaviele, and Ann K. Rosenthal 1543

Clinical Images

Bilateral Calf Hypertrophy With Increased Muscle Enzyme Levels
Juhi Dixit, Rasmi Ranjan Sahoo, Hardeep Singh Malhotra, Anupam Wakhlu, and Kiran Preet Malhotra 1549

Autoimmunity

A Proinflammatory Cytokine Network Profile in Th1/Type 1 Effector B Cells Delineates a Common Group of Patients in Four Systemic Autoimmune Diseases
Quentin Simon, Alexis Grasseau, Marina Boudigou, Laëtitia Le Pottier, Eléonore Bettachioli, Divi Cornec, Bénédicte Rouvière, Christophe Jamin, Lucas Le Lann, PRECISESADS Clinical Consortium, PRECISESADS Flow Cytometry Study Group, Maria Orietta Borghi, Rocio Aguilar-Quesada, Yves Renaudineau, Marta E. Alarcón-Riquelme, Jacques-Olivier Pers, and Sophie Hillion 1550

Letters

COVID-19 Disease in Patients With Recurrent Pericarditis During Treatment With Anakinra: Comment on the Article by Navarro-Millán et al
Enrica Negro, Lucia Trotta, Massimo Pancrazi, Emanuele Bizzi, Martino Brenna, Vartan Mardigyan, Massimo Imazio, and Antonio Brucato 1562
Significance of Antistriational Antibodies for Immune Checkpoint Inhibitor–Related Myositis: Comment on the Article by Aldrich et al
Shigeaki Suzuki 1563
Reply
Sudhakar Tummala, Xerxes Pundole, Jeffrey Aldrich, and Maria E. Suarez-Almazor 1564
Myositis-Specific Autoantibodies as Relevant Adjusting Variables in Myositis Research: Comment on the Article by Hou et al
Iago Pinal-Fernandez and Andrew L. Mammen 1564
Reply
Cyrielle Hou, François J. Authier, and Cyril Gitiaux 1566
Use of Precision Medicine to Guide Treatment of Patients With Rheumatoid Arthritis: Comment on the Article by Tao et al
Stanley B. Cohen, Theodore Mellors, and Martin J. Bergman 1567
Reply
Weiyang Tao, Timothy R. D. J. Radstake, and Aridaman Pandit 1569

Corrigendum

Adverse Events of Special Interest Incorrectly Referred to As Serious Adverse Events of Special Interest in the Article by Chatham et al (Arthritis Rheumatol, May 2021) 1570

VOLUME 73 • September 2021 • NO.9

In This Issue A9

Journal Club A10

Clinical Connections A11

Special Articles

Few Adverse Cardiovascular Events Among Patients With Rheumatoid Arthritis Receiving Hydroxychloroquine: Are We Reassured?
Candace H. Feldman and Mark S. Link 1571
Moving the Goalpost Toward Remission: The Case for Combination Immunomodulatory Therapies in Psoriatic Arthritis
Jose U. Scher, Alexis Ogdie, Joseph F. Merola, and Christopher Ritchlin 1574

Rheumatoid Arthritis

Semaphorins: From Angiogenesis to Inflammation in Rheumatoid Arthritis
Jérôme Avouac, Sonia Pezet, Eloïse Vandebeuque, Cindy Orvain, Virginie Gonzalez, Grégory Marin, Gaël Mouterde, Claire Daïen, and Yannick Allanore 1579
Cardiovascular Safety of Hydroxychloroquine in US Veterans With Rheumatoid Arthritis
Charles Faselis, Qing Zeng-Treitler, Yan Cheng, Gail S. Kerr, David J. Nashel, Angelike P. Liappis, Amy C. Weintrob, Pamela E. Karasik, Cherinne Arundel, Denise Boehm, Michael S. Heimall, Lawrence B. Connell, Daniel D. Taub, Yijun Shao, Douglas F. Redd, Helen M. Sheriff, Sijian Zhang, Ross D. Fletcher, Gregg C. Fonarow, Hans J. Moore, and Ali Ahmed 1589
Inclusion of Synovial Tissue–Derived Characteristics in a Nomogram for the Prediction of Treatment Response in Treatment-Naive Rheumatoid Arthritis Patients
Stefano Alivernini, Barbara Tolusso, Marco Gessi, Maria Rita Gigante, Alice Mannocci, Luca Petricca, Simone Perniola, Clara Di Mario, Laura Bui, Anna Laura Fedele, Annunziata Capacci, Dario Bruno, Giusy Peluso, Giuseppe La Torre, Francesco Federico, Gianfranco Ferraccioli, and Elisa Gremese 1601

Neutrophil Phospholipase Cγ2 Drives Autoantibody-Induced Arthritis Through the Generation of the Inflammatory Microenvironment
Krisztina Futosi, Orsolya Kása, Kata P. Szilveszter, and Attila Mócsai....1614

Systemic Lupus Erythematosus

Stratification of Patients With Sjögren's Syndrome and Patients With Systemic Lupus Erythematosus According to Two Shared Immune Cell Signatures, With Potential Therapeutic Implications
Lucia Martin-Gutierrez, Junjie Peng, Nicolyn L. Thompson, George A. Robinson, Meena Naja, Hannah Peckham, WingHan Wu, Hajar J'bari, Nyarko Ahwireng, Kirsty E. Waddington, Claire M. Bradford, Giulia Varnier, Akash Gandhi, Rebecca Radmore, Vivek Gupta, David A. Isenberg, Elizabeth C. Jury, and Coziana Ciurtin....1626

Osteoarthritis

Association of Machine Learning–Based Predictions of Medial Knee Contact Force With Cartilage Loss Over 2.5 Years in Knee Osteoarthritis
Nicholas M. Brisson, Anthony A. Gatti, Philipp Damm, Georg N. Duda, and Monica R. Maly....1638
Efficacy and Safety of Diclofenac–Hyaluronate Conjugate (Diclofenac Etalhyaluronate) for Knee Osteoarthritis: A Randomized Phase III Trial in Japan
Yoshihiro Nishida, Kazuyuki Kano, Yuji Nobuoka, and Takayuki Seo....1646
Brief Report: Association Between Gut Microbiota and Symptomatic Hand Osteoarthritis: Data From the Xiangya Osteoarthritis Study
Jie Wei, Chenhong Zhang, Yuqing Zhang, Weiya Zhang, Michael Doherty, Tuo Yang, Guangju Zhai, Abasiama D. Obotiba, Houchen Lyu, Chao Zeng, and Guanghua Lei....1656

Psoriatic Arthritis

Withdrawing Ixekizumab in Patients With Psoriatic Arthritis Who Achieved Minimal Disease Activity: Results From a Randomized, Double-Blind Withdrawal Study
Laura C. Coates, Sreekumar G. Pillai, Hasan Tahir, Ivo Valter, Vinod Chandran, Hideto Kameda, Masato Okada, Lisa Kerr, Denise Alves, So Young Park, David H. Adams, Gaia Gallo, Matthew M. Hufford, Maja Hojnik, Philip J. Mease, and Arthur Kavanaugh, for the SPIRIT-P3 Study Group....1663

Vasculitis

Mycophenolate Mofetil Versus Cyclophosphamide for Remission Induction in Childhood Polyarteritis Nodosa: An Open-Label, Randomized, Bayesian Noninferiority Trial
Paul A. Brogan, Barbara Arch, Helen Hickey, Jordi Anton, Este Iglesias, Eileen Baildam, Kamran Mahmood, Gavin Cleary, Elena Moraitis, Charalampia Papadopoulou, Michael W. Beresford, Phil Riley, Selcan Demir, Seza Ozen, Giovanna Culeddu, Dyfrig A. Hughes, Pavla Dolezalova, Lisa V. Hampson, John Whitehead, David Jayne, Nicola Ruperto, Catrin Tudur-Smith, and Despina Eleftheriou....1673
Eosinophil ETosis–Mediated Release of Galectin-10 in Eosinophilic Granulomatosis With Polyangiitis
Mineyo Fukuchi, Yosuke Kamide, Shigeharu Ueki, Yui Miyabe, Yasunori Konno, Nobuyuki Oka, Hiroki Takeuchi, Souichi Koyota, Makoto Hirokawa, Takechiyo Yamada, Rossana C. N. Melo, Peter F. Weller, and Masami Taniguchi....1683
Occupational Exposures and Smoking in Eosinophilic Granulomatosis With Polyangiitis: A Case–Control Study
Federica Maritati, Francesco Peyronel, Paride Fenaroli, Francesco Pegoraro, Vieri Lastrucci, Giuseppe D. Benigno, Alessandra Palmisano, Giovanni M. Rossi, Maria L. Urban, Federico Alberici, Paolo Fraticelli, Giacomo Emmi, Massimo Corradi, and Augusto Vaglio....1694
Dynamic Changes in the Nasal Microbiome Associated With Disease Activity in Patients With Granulomatosis With Polyangiitis
Rennie L. Rhee, Jiarui Lu, Kyle Bittinger, Jung-Jin Lee, Lisa M. Mattei, Antoine G. Sreih, Sherry Chou, Jonathan J. Miner, Noam A. Cohen, Brendan J. Kelly, Hongzhe Lee, Peter C. Grayson, Ronald G. Collman, and Peter A. Merkel....1703
Risk Factors for Severe Outcomes in Patients With Systemic Vasculitis and COVID-19: A Binational, Registry-Based Cohort Study
Matthew A. Rutherford, Jennifer Scott, Maira Karabayas, Marilina Antonelou, Seerapani Gopaluni, David Gray, Joe Barrett, Silke R. Brix, Neeraj Dhaun, Stephen P. McAdoo, Rona M. Smith, Colin C. Geddes, David Jayne, Raashid Luqmani, Alan D. Salama, Mark A. Little, and Neil Basu, on behalf of the UK and Ireland Vasculitis Rare Disease Group (UKIVAS)....1713

Systemic Sclerosis

Regulation of Monocyte Adhesion and Type I Interferon Signaling by CD52 in Patients With Systemic Sclerosis
Michał Rudnik, Filip Rolski, Suzana Jordan, Tonja Mertelj, Mara Stellato, Oliver Distler, Przemysław Blyszczuk, and Gabriela Kania....1720
Brief Report: Performance of the DETECT Algorithm for Pulmonary Hypertension Screening in a Systemic Sclerosis Cohort
Amber Young, Victor M. Moles, Sara Jaafar, Scott Visovatti, Suiyuan Huang, Dharshan Vummidi, Vivek Nagaraja, Vallerie McLaughlin, and Dinesh Khanna....1731

Clinical Images

Clinical Images: Multiple Pulmonary Artery Aneurysms in Hughes-Stovin Syndrome
Nichanametla Sravani, Krishnan Nagarajan, and Veer S. Negi....1737

Gout

Serum Metabolomics Identifies Dysregulated Pathways and Potential Metabolic Biomarkers for Hyperuricemia and Gout
Xia Shen, Can Wang, Ningning Liang, Zhen Liu, Xinde Li, Zheng-Jiang Zhu, Tony R. Merriman, Nicola Dalbeth, Robert Terkeltaub, Changgui Li, and Huiyong Yin 1738

Effectiveness of Allopurinol in Reducing Mortality: Time-Related Biases in Observational Studies
Samy Suissa, Karine Suissa, and Marie Hudson 1749

Elevated Urate Levels Do Not Alter Bone Turnover Markers: Randomized Controlled Trial of Inosine Supplementation in Postmenopausal Women
Nicola Dalbeth, Anne Horne, Borislav Mihov, Angela Stewart, Gregory D. Gamble, Tony R. Merriman, Lisa K. Stamp, and Ian R. Reid 1758

Letters

Prophylaxis Against COVID-19 With Hydroxychloroquine and Chloroquine: Comment on the Article by Putman et al
Wei Tang, Yevgeniya Gartshteyn, Cathy Guo, Tommy Chen, Jon Giles, and Anca Askanase 1765

Reply
Michael Putman, Sebastian E. Sattui, Jeffrey A. Sparks, Jean W. Liew, Rebecca Grainger, and Alí Duarte-García 1767

Use of Tofacitinib in the Context of COVID-19 Vaccination: Comment on the American College of Rheumatology Clinical Guidance for COVID-19 Vaccination in Patients With Rheumatic and Musculoskeletal Diseases
Mahta Mortezavi, Sujatha Menon, Kristen Lee, and Jose Rivas 1768

Reply
Jeffrey R. Curtis, Sindhu R. Johnson, Donald D. Anthony, Reuben J. Arasaratnam, Lindsey R. Baden, Ellen M. Gravallese, Anne R. Bass, Cassandra Calabrese, Rafael Harpaz, Andrew Kroger, Rebecca E. Sadun, Amy S. Turner, Eleanor Anderson Williams, and Ted R. Mikuls 1769

Are There Thresholds of Conflict of Interest With Gifts From Industry? Comment on the Article by Wayant et al
John D. FitzGerald 1770

Etanercept or Methotrexate Withdrawal in Rheumatoid Arthritis Patients Receiving Combination Therapy: Comment on the Article by Curtis et al
Rashmi Roongta, Sumantro Mondal, and Alakendu Ghosh 1771

Reply
Jeffrey R. Curtis, Elaine Karis, Priscilla K. Yen, Greg Kricorian, and James B. Chung 1771

VOLUME 73 • SEPTEMBER SUPPLEMENT 2021 • NO. S9

ACR Convergence 2021 ..... S1

VOLUME 73 • October 2021 • NO.10

In This Issue A15

Journal Club A16

Clinical Connections A17

Online-Only Special Article

American College of Rheumatology Guidance for COVID-19 Vaccination in Patients With Rheumatic and Musculoskeletal Diseases: Version 3
Jeffrey R. Curtis, Sindhu R. Johnson, Donald D. Anthony, Reuben J. Arasaratnam, Lindsey R. Baden, Anne R. Bass, Cassandra Calabrese, Ellen M. Gravallese, Rafael Harpaz, Andrew Kroger, Rebecca E. Sadun, Amy S. Turner, Eleanor Anderson Williams, and Ted R. Mikuls e60

Special Articles

Editorial: What Did Not Work: The Drug or the Trial?
Joan T. Merrill 1773

Editorial: "To Randomize, or Not to Randomize, That is the Question"
Nicolino Ruperto, Alberto Martini, and Angela Pistorio, for the Paediatric Rheumatology International Trials Organisation 1776

Expert Perspectives on Clinical Challenges: Management of Microvascular and Catastrophic Antiphospholipid Syndrome
Doruk Erkan 1780

COVID-19

Brief Report: Discrimination of COVID-19 From Inflammation-Induced Cytokine Storm Syndromes Using Disease-Related Blood Biomarkers
Christoph Kessel, Richard Vollenberg, Katja Masjosthusmann, Claas Hinze, Helmut Wittkowski, France Debaugnies, Carole Nagant, Francis Corazza, Frédéric Vély, Gilles Kaplanski, Charlotte Girard-Guyonvarc'h, Cem Gabay, Hartmut Schmidt, Dirk Foell, and Phil-Robin Tepasse 1791

Rheumatoid Arthritis

Nonserious Infections in Patients With Rheumatoid Arthritis: Results From the British Society for Rheumatology Biologics Register for Rheumatoid Arthritis
Katie Bechman, Kapil Halai, Mark Yates, Sam Norton, Andrew P. Cope, the British Society for Rheumatology Biologics Register for Rheumatoid Arthritis Contributors Group, Kimme L. Hyrich, and James B. Galloway 1800
Notch-1 and Notch-3 Mediate Hypoxia-Induced Activation of Synovial Fibroblasts in Rheumatoid Arthritis
Jianhai Chen, Wenxiang Cheng, Jian Li, Yan Wang, Jingqin Chen, Xin Shen, Ailing Su, Donghao Gan, Liqing Ke, Gang Liu, Jietao Lin, Liang Li, Xueling Bai, and Peng Zhang 1810
Pim Kinases as Therapeutic Targets in Early Rheumatoid Arthritis
Nicola J. Maney, Henrique Lemos, Ben Barron-Millar, Christopher Carey, Ian Herron, Amy E. Anderson, Andrew L. Mellor, John D. Isaacs, and Arthur G. Pratt 1820

Spondyloarthritis

Brief Report: Down-Regulation of Dkk-1 in Platelets of Patients With Axial Spondyloarthritis
Marcin Czepiel, Małgorzata Stec, Mariusz Korkosz, Zofia Guła, Przemysław Błyszczuk, Jarosław Baran, and Maciej Siedlar 1831

Systemic Lupus Erythematosus

Efficacy, Safety, and Pharmacodynamic Effects of the Bruton's Tyrosine Kinase Inhibitor Fenebrutinib (GDC-0853) in Systemic Lupus Erythematosus: Results of a Phase II, Randomized, Double-Blind, Placebo-Controlled Trial
David Isenberg, Richard Furie, Nicholas S. Jones, Pascal Guibord, Joshua Galanter, Chin Lee, Anna McGregor, Balazs Toth, Julie Rae, Olivia Hwang, Rupal Desai, Armend Lokku, Nandhini Ramamoorthi, Jason A. Hackney, Pedro Miranda, Viviane A. de Souza, Juan J. Jaller-Raad, Anna Maura Fernandes, Rodrigo Garcia Salinas, Leslie W. Chinn, Michael J. Townsend, Alyssa M. Morimoto, and Katie Tuckwell 1835
Predicting the Risk of Pulmonary Arterial Hypertension in Systemic Lupus Erythematosus: A Chinese Systemic Lupus Erythematosus Treatment and Research Group Cohort Study
Jingge Qu, Mengtao Li, Yanhong Wang, Xinwang Duan, Hui Luo, Cheng Zhao, Feng Zhan, Zhenbiao Wu, Hongbin Li, Min Yang, Jian Xu, Wei Wei, Lijun Wu, Yongtai Liu, Hanxiao You, Juyan Qian, Xiaoxi Yang, Can Huang, Jiuliang Zhao, Qian Wang, Xiaomei Leng, Xinping Tian, Yan Zhao, and Xiaofeng Zeng 1847

Osteoarthritis

Genetic and Epigenetic Interplay Within a *COLGALT2* Enhancer Associated With Osteoarthritis
Yulia S. Kehayova, Emily Watson, J. Mark Wilkinson, John Loughlin, and Sarah J. Rice 1856
Genetic and Epigenetic Fine-Tuning of *TGFB1* Expression Within the Human Osteoarthritic Joint
Sarah J. Rice, Jack B. Roberts, Maria Tselepi, Abby Brumwell, Julia Falk, Charlotte Steven, and John Loughlin 1866

Psoriatic Arthritis

The Epidemiology of Psoriatic Arthritis Over Five Decades: A Population-Based Study
Paras Karmacharya, Cynthia S. Crowson, Delamo Bekele, Sara J. Achenbach, John M. Davis III, Alexis Ogdie, Alí Duarte-García, Floranne C. Ernste, Hilal Maradit-Kremers, Megha M. Tollefson, and Kerry Wright 1878

Polychondritis

Somatic Mutations in *UBA1* Define a Distinct Subset of Relapsing Polychondritis Patients With VEXAS
Marcela A. Ferrada, Keith A. Sikora, Yiming Luo, Kristina V. Wells, Bhavisha Patel, Emma M. Groarke, Daniela Ospina Cardona, Emily Rominger, Patrycja Hoffmann, Mimi T. Le, Zuoming Deng, Kaitlin A. Quinn, Emily Rose, Wanxia L. Tsai, Gustaf Wigerblad, Wendy Goodspeed, Anne Jones, Lorena Wilson, Oskar Schnappauf, Ryan S. Laird, Jeff Kim, Clint Allen, Arlene Sirajuddin, Marcus Chen, Massimo Gadina, Katherine R. Calvo, Mariana J. Kaplan, Robert A. Colbert, Ivona Aksentijevich, Neal S. Young, Sinisa Savic, Daniel L. Kastner, Amanda K. Ombrello, David B. Beck, and Peter C. Grayson 1886

Clinical Images

Extensive Multiple Organ Involvement in VEXAS Syndrome
Noriyuki Takahashi, Takuya Takeichi, Tetsuya Nishida, Juichi Sato, Yasuhiro Takahashi, Masahiro Yamamura, Tomoo Ogi, and Masashi Akiyama 1896

Pediatric Rheumatology

Optimizing the Start Time of Biologics in Polyarticular Juvenile Idiopathic Arthritis: A Comparative Effectiveness Study of Childhood Arthritis and Rheumatology Research Alliance Consensus Treatment Plans
Yukiko Kimura, Laura E. Schanberg, George A. Tomlinson, Mary Ellen Riordan, Anne C. Dennos, Vincent Del Gaizo, Katherine L. Murphy, Pamela F. Weiss, Marc D. Natter, Brian M. Feldman, Sarah Ringold, and the CARRA STOP-JIA Investigators 1898
Improved Disease Course Associated With Early Initiation of Biologics in Polyarticular Juvenile Idiopathic Arthritis: Trajectory Analysis of a Childhood Arthritis and Rheumatology Research Alliance Consensus Treatment Plans Study
Mei Sing Ong, Sarah Ringold, Yukiko Kimura, Laura E. Schanberg, George A. Tomlinson, Marc D. Natter, and the CARRA Registry Investigators 1910
Transcriptomic Evaluation of Juvenile Localized Scleroderma Skin With Histologic and Clinical Correlation
Christina Schutt, Emily Mirizio, Claudia Salgado, Miguel Reyes-Mugica, Xinjun Wang, Wei Chen, Lorelei Grunwaldt, Kaila L. Schollaert, and Kathryn S. Torok 1921

Autoimmune Disease
ICBP90 Regulates *MIF* Expression, Glucocorticoid Sensitivity, and Apoptosis at the *MIF* Immune Susceptibility Locus
Jie Yao, Lin Leng, Weiling Fu, Jia Li, Christian Bronner, and Richard Bucala 1931

Letters
Body Fat Composition and Risk of Rheumatoid Arthritis: Mendelian Randomization Study
Sizheng S. Zhao, Cristina Maglio, David M. Hughes, and James P. Cook 1943
Reply
Bowen Tang, Lars Alfredsson, Lars Klareskog, Leonid Padyukov, Huwenbo Shi, and Xia Jiang 1944
Immuno-Autonomics as a Complement to Precision Medicine Guiding Treatment of Patients With Rheumatoid Arthritis: Comment on the Article by Tao et al
Andrew J. Holman 1945
Concerns Regarding *P* Value–Based Variable Selection of Exposure Variables and Confounding Factors: Comment on the Article by Hawker et al
Takahisa Ogawa, Yoshie Yamada, Ryo Momosaki, Junya Katayanagi, and Takashi Yoshioka 1946
Reply
Gillian A. Hawker, Bheeshma Ravi, Eric Bohm, Michael J. Dunbar, C. Allyson Jones, Donald Dick, Paulose Paul, Barbara L. Conner-Spady, Tom Noseworthy, Peter Faris, James Powell, and Deborah A. Marshall On behalf of the BEST- Knee Study Team 1947
Concerns Regarding the Analysis of a Takayasu Arteritis Cohort: Comment on the Article by Goel et al
Hasan Yazici, Mert Oztas, and Yusuf Yazici 1948
Reply
Ruchika Goel, Joht Singh Chandan, Rasiah Thayakaran, Nicola J. Adderley, Krishnarajah Nirantharakumar, and Lorraine Harper 1948

VOLUME 73 • November 2021 • NO.11

In This Issue .... Axx

Journal Club .... Axx

Clinical Connections .... Axx

Special Articles
Editorial: Industry Payments to Rheumatologists Ought to Be Going Down, Not Up
Aaron P. Mitchell 1951
Review: Is There a Place for Chimeric Antigen Receptor–T Cells in the Treatment of Chronic Autoimmune Rheumatic Diseases?
Cindy Orvain, Morgane Boulch, Philippe Bousso, Yannick Allanore, and Jérôme Avouac 1954
Definition and Validation of the American College of Rheumatology 2021 Juvenile Arthritis Disease Activity Score Cutoffs for Disease Activity States in Juvenile Idiopathic Arthritis
Chiara Trincianti, Evert Hendrik Pieter Van Dijkhuizen, Alessandra Alongi, Marta Mazzoni, Joost F. Swart, Irina Nikishina, Pekka Lahdenne, Lidia Rutkowska-Sak, Tadej Avcin, Pierre Quartier, Violeta Panaviene, Yosef Uziel, Chris Pruunsild, Veronika Vargova, Soamarat Vilaiyuk, Pavla Dolezalova, Sarah Ringold, Marco Garrone, Nicolino Ruperto, Angelo Ravelli, and Alessandro Consolaro, for the Paediatric Rheumatology International Trials Organisation 1966

COVID-19
Lupus Anticoagulant Single Positivity During the Acute Phase of COVID-19 Is Not Associated With Venous Thromboembolism or In-Hospital Mortality
Nicolas Gendron, Marie-Agnès Dragon-Durey, Richard Chocron, Luc Darnige, Georges Jourdi, Aurélien Philippe, Camille Chenevier-Gobeaux, Jérôme Hadjadj, Jérôme Duchemin, Lina Khider, Nader Yatim, Guillaume Goudot, Daphné Krzisch, Benjamin Debuc, Laetitia Mauge, Françoise Levavasseur, Frédéric Pene, Jeremy Boussier, Elise Sourdeau, Julie Brichet, Nadège Ochat, Claire Goulvestre, Christophe Peronino, Tali-Anne Szwebel, Franck Pages, Pascale Gaussem, Charles-Marc Samama, Cherifa Cheurfa, Benjamin Planquette, Olivier Sanchez, Jean-Luc Diehl, Tristan Mirault, Michaela Fontenay, Benjamin Terrier, and David M. Smadja 1976

Rheumatoid Arthritis
Differences in the Oral Microbiome in Patients With Early Rheumatoid Arthritis and Individuals at Risk of Rheumatoid Arthritis Compared to Healthy Individuals
Johanna M. Kroese, Bernd W. Brandt, Mark J. Buijs, Wim Crielaard, Frank Lobbezoo, Bruno G. Loos, Laurette van Boheemen, Dirkjan van Schaardenburg, Egija Zaura, and Catherine M. C. Volgenant 1986
Relationship Between Rheumatoid Arthritis and Pulmonary Function Measures on Spirometry in the UK Biobank
Lauren Prisco, Matthew Moll, Jiaqi Wang, Brian D. Hobbs, Weixing Huang, Lily W. Martin, Vanessa L. Kronzer, Sicong Huang, Edwin K. Silverman, Tracy J. Doyle, Michael H. Cho, and Jeffrey A. Sparks 1994
Interleukin-34 Reprograms Glycolytic and Osteoclastic Rheumatoid Arthritis Macrophages via Syndecan 1 and Macrophage Colony-Stimulating Factor Receptor
Katrien Van Raemdonck, Sadiq Umar, Karol Palasiewicz, Michael V. Volin, Hatem A. Elshabrawy, Bianca Romay, Chandana Tetali, Azam Ahmed, M. Asif Amin, Ryan K. Zomorrodi, Nadera Sweiss, and Shiva Shahrara 2003

Osteoarthritis

Erosive Hand Osteoarthritis: Incidence and Predictive Characteristics Among Participants in the Osteoarthritis Initiative
Timothy E. McAlindon, Jeffrey B. Driban, Mary B. Roberts, Jeffrey Duryea, Ida K. Haugen, Lena F. Schaefer, Stacy E. Smith, Alexander Mathiessen, and Charles Eaton 2015

The CRTAC1 Protein in Plasma Is Associated With Osteoarthritis and Predicts Progression to Joint Replacement: A Large-Scale Proteomics Scan in Iceland
Unnur Styrkarsdottir, Sigrun H. Lund, Saedis Saevarsdottir, Magnus I. Magnusson, Kristbjorg Gunnarsdottir, Gudmundur L. Norddahl, Michael L. Frigge, Erna V. Ivarsdottir, Gyda Bjornsdottir, Hilma Holm, Gudmundur Thorgeirsson, Thorunn Rafnar, Ingileif Jonsdottir, Thorvaldur Ingvarsson, Helgi Jonsson, Patrick Sulem, Unnur Thorsteinsdottir, Daniel Gudbjartsson, and Kari Stefansson 2025

Effect of Atorvastatin on Knee Cartilage Volume in Patients With Symptomatic Knee Osteoarthritis: Results From a Randomized Placebo-Controlled Trial
Yuanyuan Wang, Graeme Jones, Catherine Hill, Anita E. Wluka, Andrew B. Forbes, Andrew Tonkin, Sultana Monira Hussain, Changhai Ding, and Flavia M. Cicuttini 2035

Errata

Incorrect Versions of Supplementary Tables 4 and 5 and Errors in Safety Data and in Table 1 in the Article by Merrill et al (Arthritis Rheumatol, February 2018) 2043

Minus Signs Inadvertently Inserted for Two 95% Confidence Interval Values in the Article by Steen Pettersen et al (Arthritis Rheumatol, July 2019) 2043

Spondyloarthritis

The Value of Magnetic Resonance Imaging for Assessing Disease Extent and Prediction of Relapse in Early Peripheral Spondyloarthritis
Thomas Renson, Philippe Carron, Ann-Sophie De Craemer, Liselotte Deroo, Manouk de Hooge, Simon Krabbe, Lennart Jans, Mikkel Østergaard, Dirk Elewaut, and Filip Van den Bosch 2044

Clinical Images

Progressive Pseudorheumatoid Dysplasia—Radiographic Evolution Over Twenty Years
Jacopo Ciaffi, Giancarlo Facchini, Marco Miceli, Elena Borlandelli, Riccardo Meliconi, and Francesco Ursini 2051

Systemic Lupus Erythematosus

Brief Report: Estrogen-Induced hsa-miR-10b-5p Is Elevated in T Cells From Patients With Systemic Lupus Erythematosus and Down-Regulates Serine/Arginine-Rich Splicing Factor 1
Suruchi A. Ramanujan, Elena N. Cravens, Suzanne M. Krishfield, Vasileios C. Kyttaris, and Vaishali R. Moulton 2052

What Does It Mean to Be a British Isles Lupus Assessment Group–Based Composite Lupus Assessment Responder? Post Hoc Analysis of Two Phase III Trials
Richard Furie, Eric F. Morand, Ian N. Bruce, David Isenberg, Ronald van Vollenhoven, Gabriel Abreu, Lilia Pineda, and Raj Tummala 2059

Protein Mannosylation as a Diagnostic and Prognostic Biomarker of Lupus Nephritis: An Unusual Glycan Neoepitope in Systemic Lupus Erythematosus
Inês Alves, Beatriz Santos-Pereira, Hans Dalebout, Sofia Santos, Manuel M. Vicente, Ana Campar, Michel Thepaut, Franck Fieschi, Sabine Strahl, Fanny Boyaval, Ramon Vizcaíno, Roberto Silva, Stephanie Holst-Bernal, Carlos Vasconcelos, Lélita Santos, Manfred Wuhrer, António Marinho, Bram Heijs, and Salomé S. Pinho 2069

Clinical Images

Rice Bodies in Cinematic Rendering
Jian Liu, Xinge Cheng, Rongpin Wang, and Xianchun Zeng 2077

Vasculitis

Prevalence of Antineutrophil Cytoplasmic Antibody–Associated Vasculitis and Spatial Association With Quarries in a Region of Northeastern France: A Capture–Recapture and Geospatial Analysis
Stéphane Giorgiutti, Yannick Dieudonne, Olivier Hinschberger, Benoît Nespola, Julien Campagne, Hanta Nirina Rakotoarivelo, Thierry Hannedouche, Bruno Moulin, Gilles Blaison, Jean-Christophe Weber, Marie-Caroline Dalmas, Frédéric De Blay, Dan Lipsker, François Chantrel, Jacques-Eric Gottenberg, Yves Dimitrov, Olivier Imhoff, Pierre-Edouard Gavand, Emmanuel Andres, Christian Debry, Yves Hansmann, Alexandre Klein, Caroline Lohmann, François Mathiaux, Aurélien Guffroy, Vincent Poindron, Thierry Martin, Anne-Sophie Korganow, and Laurent Arnaud 2078

Systemic Sclerosis

B Cell Depletion Inhibits Fibrosis via Suppression of Profibrotic Macrophage Differentiation in a Mouse Model of Systemic Sclerosis
Hiroko Numajiri, Ai Kuzumi, Takemichi Fukasawa, Satoshi Ebata, Asako Yoshizaki-Ogawa, Yoshihide Asano, Yutaka Kazoe, Kazuma Mawatari, Takehiko Kitamori, Ayumi Yoshizaki, and Shinichi Sato 2086

Gout

Assessing the Causal Relationships Between Insulin Resistance and Hyperuricemia and Gout Using Bidirectional Mendelian Randomization
Natalie McCormick, Mark J. O'Connor, Chio Yokose, Tony R. Merriman, David B. Mount, Aaron Leong, and Hyon K. Choi 2096

Autoinflammatory Disease
Augmentation of Stimulator of Interferon Genes–Induced Type I Interferon Production in COPA Syndrome
Takashi Kato, Masaki Yamamoto, Yoshitaka Honda, Takashi Orimo, Izumi Sasaki, Kohei Murakami, Hiroaki Hemmi, Yuri Fukuda-Ohta, Kyoichi Isono, Saki Takayama, Hidenori Nakamura, Yoshiro Otsuki, Toshiaki Miyamoto, Junko Takita, Takahiro Yasumi, Ryuta Nishikomori, Tadashi Matsubayashi, Kazushi Izawa, and Tsuneyasu Kaisho 2105
Pyrin Inflammasome Activation Abrogates Interleukin-1 Receptor Antagonist, Suggesting a New Mechanism Underlying Familial Mediterranean Fever Pathogenesis
Sussi B. Mortensen, Ann-Brit E. Hansen, Trine H. Mogensen, Marianne A. Jakobsen, Hans C. Beck, Eva B. Harvald, Kate L. Lambertsen, Isik S. Johansen, and Ditte C. Andersen 2116

Fibromyalgia
Prediction of Differential Pharmacologic Response in Chronic Pain Using Functional Neuroimaging Biomarkers and a Support Vector Machine Algorithm: An Exploratory Study
Eric Ichesco, Scott J. Peltier, Ishtiaq Mawla, Daniel E. Harper, Lynne Pauer, Steven E. Harte, Daniel J. Clauw, and Richard E. Harris 2127

Rheumatology Workforce
Industry Payments to Practicing US Rheumatologists, 2014–2019
Michael S. Putman, Jay E. Goldsher, Cynthia S. Crowson, and Alí Duarte-García 2138

Letters
Cardiovascular and Renal Morbidity in Takayasu Arteritis: Comment on the Article by Goel et al
Hsuan-Hsien Liu, Hao-Hung Tsai, and James Cheng-Chung Wei 2145
Reply
Ruchika Goel, Joht Singh Chandan, Rasiah Thayakaran, Nicola J. Adderley, Krishnarajah Nirantharakumar, and Lorraine Harper 2145
Noncoding RNAs, Osteoarthritis, and the Microbiome: New Therapeutic Targets? Comment on the Article by Wei et al
Maddalena Sirufo, Lia Ginaldi, and Massimo De Martinis 2146
Reply
Jie Wei, Yuqing Zhang, Chao Zeng, and Guanghua Lei 2146
Outcomes and Western Ontario and McMaster Universities Osteoarthritis Index Score Reporting in a Trial of the Efficacy and Safety of Diclofenac–Hyaluronate Conjugate: Comment on the Article by Nishida et al
Daniel L. Riddle 2147
Reply
Yoshihiro Nishida, Kazuyuki Kano, Yuji Nobuoka, and Takayuki Seo 2148
More Steps Forward to Optimize the Dosing of Hydroxychloroquine: Comment on the Article by Petri et al
Jui-Hung Kao, Ting-Yuan Lan, and Ko-Jen Li 2149
Reply
Michelle Petri and Laurence S. Magder 2149

VOLUME 73 • December 2021 • NO.12

In This Issue A15
Journal Club A16
Clinical Connections A17
ACR Announcements A29

Special Articles
American College of Rheumatology White Paper on Antimalarial Cardiac Toxicity
Julianna Desmarais, James T. Rosenbaum, Karen H. Costenbader, Ellen M. Ginzler, Nicole Fett, Susan Goodman, James O'Dell, Christian A. Pineau, Gabriela Schmajuk, Victoria P. Werth, Mark S. Link, and Richard Kovacs 2151
Editorial: Where There's Smoke, There's a Joint: Passive Smoking and Rheumatoid Arthritis
Milena A. Gianfrancesco, and Cynthia S. Crowson 2161
Editorial: Targeting the Myddosome in Systemic Autoimmunity: Ready for Prime Time?
Mariana J. Kaplan 2163
Review: A Decade of JAK Inhibitors: What Have We Learned and What May Be the Future?
Christine Liu, Jacqueline Kieltyka, Roy Fleischmann, Massimo Gadina, and John J. O'Shea 2166

COVID-19
Risk of COVID-19 in Rheumatoid Arthritis: A National Veterans Affairs Matched Cohort Study in At-Risk Individuals
Bryant R. England, Punyasha Roul, Yangyuna Yang, Andre C. Kalil, Kaleb Michaud, Geoffrey M. Thiele, Brian C. Sauer, Joshua F. Baker, and Ted R. Mikuls 2179

Clinical Images

Leukocytoclastic Vasculitis After Vaccination With a SARS–CoV-2 Vaccine
Anne Erler, John Fiedler, Anna Koch, Alexander Schütz, and Frank Heldmann....2188

Rheumatoid Arthritis

Incident Rheumatoid Arthritis in HIV Infection: Epidemiology and Treatment
Jennifer S. Hanberg, Evelyn Hsieh, Kathleen M. Akgün, Erica Weinstein, Liana Fraenkel, Amy C. Justice, and the VACS Project Team....2189
Brief Report: Identification of Novel, Immunogenic HLA–DR-Presented *Prevotella copri* Peptides in Patients With Rheumatoid Arthritis
Annalisa Pianta, Geena Chiumento, Kristina Ramsden, Qi Wang, Klemen Strle, Sheila Arvikar, Catherine E. Costello, and Allen C. Steere....2200
The Interleukin-1 Receptor–Associated Kinase 4 Inhibitor PF-06650833 Blocks Inflammation in Preclinical Models of Rheumatic Disease and in Humans Enrolled in a Randomized Clinical Trial
Aaron Winkler, Weiyong Sun, Saurav De, Aiping Jiao, M. Nusrat Sharif, Peter T. Symanowicz, Shruti Athale, Julia H. Shin, Ju Wang, Bruce A. Jacobson, Simeon J. Ramsey, Ken Dower, Tatyana Andreyeva, Heng Liu, Martin Hegen, Bruce L. Homer, Joanne Brodfuehrer, Mera Tilley, Steven A. Gilbert, Spencer I. Danto, Jean J. Beebe, Betsy J. Barnes, Virginia Pascual, Lih-Ling Lin, Iain Kilty, Margaret Fleming, and Vikram R. Rao....2206
Passive Smoking Throughout the Life Course and the Risk of Incident Rheumatoid Arthritis in Adulthood Among Women
Kazuki Yoshida, Jiaqi Wang, Susan Malspeis, Nathalie Marchand, Bing Lu, Lauren C. Prisco, Lily W. Martin, Julia A. Ford, Karen H. Costenbader, Elizabeth W. Karlson, and Jeffrey A. Sparks....2219
Prediction of the Progression of Undifferentiated Arthritis to Rheumatoid Arthritis Using DNA Methylation Profiling
Carlos de la Calle-Fabregat, Ellis Niemantsverdriet, Juan D. Cañete, Tianlu Li, Annette H. M. van der Helm-van Mil, Javier Rodríguez-Ubreva, and Esteban Ballestar....2229

Clinical Images

Cerebral Autosomal-Dominant Arteriopathy With Subcortical Infarcts and Leukoencephalopathy Syndrome, a Central Nervous System Vasculitis Mimic
Mithu Maheswaranathan, Anne F. Buckley, Andrew B. Cutler, Lisa Criscione-Schreiber, and Ankoor Shah....2239

Osteoarthritis

Subchondral Bone Length in Knee Osteoarthritis: A Deep Learning–Derived Imaging Measure and Its Association With Radiographic and Clinical Outcomes
Gary H. Chang, Lisa K. Park, Nina A. Le, Ray S. Jhun, Tejus Surendran, Joseph Lai, Hojoon Seo, Nuwapa Promchotichai, Grace Yoon, Jonathan Scalera, Terence D. Capellini, David T. Felson, and Vijaya B. Kolachalama....2240
Amelioration of Posttraumatic Osteoarthritis in Mice Using Intraarticular Silencing of Periostin via Nanoparticle-Based Small Interfering RNA
Xin Duan, Lei Cai, Christine T. N. Pham, Yousef Abu-Amer, Hua Pan, Robert H. Brophy, Samuel A. Wickline, and Muhammad Farooq Rai....2249
Osteoarthritis Care and Risk of Total Knee Arthroplasty Among Medicare Beneficiaries: A Population-Based Study of Regional Covariation
Michael M. Ward....2261

Psoriatic Arthritis

Targeting the CCR6/CCL20 Axis in Entheseal and Cutaneous Inflammation
Zhenrui Shi, Emma Garcia-Melchor, Xuesong Wu, Anthony E. Getschman, Mimi Nguyen, Douglas J. Rowland, Machelle Wilson, Flavia Sunzini, Moeed Akbar, Mindy Huynh, Timothy Law, Smriti K. Raychaudhuri, Siba P. Raychaudhuri, Brian F. Volkman, Neal L. Millar, and Sam T. Hwang....2271

Systemic Lupus Erythematosus

RNA Externalized by Neutrophil Extracellular Traps Promotes Inflammatory Pathways in Endothelial Cells
Luz P. Blanco, Xinghao Wang, Philip M. Carlucci, Jose Jiram Torres-Ruiz, Jorge Romo-Tena, Hong-Wei Sun, Markus Hafner, and Mariana J. Kaplan....2282
Neuropsychiatric Events in Systemic Lupus Erythematosus: Predictors of Occurrence and Resolution in a Longitudinal Analysis of an International Inception Cohort
John G. Hanly, Caroline Gordon, Sang-Cheol Bae, Juanita Romero-Diaz, Jorge Sanchez-Guerrero, Sasha Bernatsky, Ann E. Clarke, Daniel J. Wallace, David A. Isenberg, Anisur Rahman, Joan T. Merrill, Paul R. Fortin, Dafna D. Gladman, Murray B. Urowitz, Ian N. Bruce, Michelle Petri, Ellen M. Ginzler, M. A. Dooley, Rosalind Ramsey-Goldman, Susan Manzi, Andreas Jonsen, Graciela S. Alarcón, Ronald F. van Vollenhoven, Cynthia Aranow, Meggan Mackay, Guillermo Ruiz-Irastorza, S. Sam Lim, Murat Inanc, Kenneth C. Kalunian, Soren Jacobsen, Christine A. Peschken, Diane L. Kamen, Anca Askanase, and Vernon Farewell....2293
Lupus Susceptibility Region Containing *CDKN1B* rs34330 Mechanistically Influences Expression and Function of Multiple Target Genes, Also Linked to Proliferation and Apoptosis
Bhupinder Singh, Guru P. Maiti, Xujie Zhou, Mehdi Fazel-Najafabadi, Sang-Cheol Bae, Celi Sun, Chikashi Terao, Yukinori Okada, Kek Heng Chua, Yuta Kochi, Joel M. Guthridge, Hong Zhang, Matthew Weirauch, Judith A. James, John B. Harley, Gaurav K. Varshney, Loren L. Looger, and Swapan K. Nath....2303

Inositol-Requiring Enzyme 1α–Mediated Synthesis of Monounsaturated Fatty Acids as a Driver of B Cell Differentiation and Lupus-like Autoimmune Disease
Yana Zhang, Ming Gui, Yajun Wang, Nikita Mani, Shuvam Chaudhuri, Beixue Gao, Huabin Li, Yashpal S. Kanwar, Sarah A. Lewis, Sabrina N. Dumas, James M. Ntambi, Kezhong Zhang, and Deyu Fang 2314

Vasculitis

A Distinct Macrophage Subset Mediating Tissue Destruction and Neovascularization in Giant Cell Arteritis: Implication of the YKL-40/Interleukin-13 Receptor α2 Axis
Yannick van Sleen, William F. Jiemy, Sarah Pringle, Kornelis S. M. van der Geest, Wayel H. Abdulahad, Maria Sandovici, Elisabeth Brouwer, Peter Heeringa, and Annemieke M. H. Boots 2327

Systemic Sclerosis

Anticentromere Antibody Levels and Isotypes and the Development of Systemic Sclerosis
Nina M. van Leeuwen, Maaike Boonstra, Jaap A. Bakker, Annette Grummels, Suzana Jordan, Sophie Liem, Oliver Distler, Anna-Maria Hoffmann-Vold, Karin Melsens, Vanessa Smith, Marie-Elise Truchetet, Hans U. Scherer, René Toes, Tom W. J. Huizinga, and Jeska K. de Vries-Bouwstra 2338

Letters

Addressing Immeasurable Time Bias in an Observational Study: Comment on the Article by Suissa et al
Alanna Weisman, Gillian A. Hawker, and George A. Tomlinson 2348

Reply
Samy Suissa, Karine Suissa, and Marie Hudson 2349

Hypoxia-Induced Synovial Fibroblast Activation in Inflammatory Arthritis and the Role of Notch-1 and Notch-3 Signaling: Comment on the Article by Chen et al
Wang-Dong Xu and An-Fang Huang 2349

Reply
Jianhai Chen, Antonia Sun, Jian Li, Wenxiang Cheng, and Peng Zhang 2350

Disease Activity Assessment in Nonradiographic Axial Spondyloarthritis: Is It Time to Move Beyond the Bath Ankylosing Spondylitis Disease Activity Index or Ankylosing Spondylitis Disease Activity Score? Comment on the Article by Rusman et al
Debashish Mishra, B. V. Harish, Sudhish Gadde, and Pradeepta S. Patro 2351

Reply
Tamara Rusman, Mignon A. C. van der Weijden, Michael T. Nurmohamed, Carmella M. A. van der Bijl, Conny J. van der Laken, Pierre M. Bet, Robert B. M. Landewé, Janneke J. H. de Winter, Bouke J. H. Boden, and Irene E. van der Horst-Bruinsma 2352

Clinical and Methodologic Considerations With Regard to a Trial of Nintedanib in Patients With Systemic Sclerosis–Associated Interstitial Lung Disease: Comment on the Reanalysis by Maher et al
Markus Bredemeier 2353

Reply
Toby M. Maher, Maureen D. Mayes, Christian Stock, and Margarida Alves 2354

Suggested Considerations for the Treatment of Rheumatic Diseases in Adult Patients With COVID-19: Comment on the Article by Mikuls et al
Jeffrey Hsu, Chin-Hsiu Liu, and James C. Wei 2355

Erratum

Incorrect Frequency of Belimumab Infusions Reported in the Article by Atisha-Fregoso et al (Arthritis Rheumatol, January 2021) 2356

Reviewers 2357

Volume 73 Table of Contents 2361